

CIVIL ENGINEERING STUDIES

STRUCTURAL RESEARCH SERIES NO. 346



10
129A
SRS 346
Vol. 2

Copy. 1

STRENGTH AND BEHAVIOR OF PRESTRESSED CONCRETE VESSELS FOR NUCLEAR REACTORS-VOLUME II

by

S. L. Paul, Alan Zimmer, H. L. Gotschall, R. H. Matson
B. I. Karlsson, B. Mohraz, W. C. Schnobrich, M. A. Sozen

Subcontract No. 2906
Contract No. W-7405-eng-26

Meta Reference Room
Civil Engineering Department
B106 C. E. Building
University of Illinois
Urbana, Illinois 61801

A REPORT ON AN INVESTIGATION CARRIED OUT AS
PART OF THE PRESTRESSED CONCRETE REACTOR VESSEL
PROGRAM OF THE OAK RIDGE NATIONAL LABORATORY
OPERATED BY UNION CARBIDE CORPORATION
FOR THE U. S. ATOMIC ENERGY COMMISSION

UNIVERSITY OF ILLINOIS
URBANA, ILLINOIS
JULY, 1969

*Metz Reference Room
Civil Engineering Department
Block C. E. Building
University of Illinois
Urbana, Illinois 61801*

CIVIL ENGINEERING STUDIES
STRUCTURAL RESEARCH SERIES NO. 346

STRENGTH AND BEHAVIOR OF PRESTRESSED CONCRETE VESSELS
FOR NUCLEAR REACTORS-VOLUME II

by

S. L. Paul, A. Zimmer, H. L. Gotschall, R. H. Matson, B. I. Karlsson,
B. Mohraz, M. A. Sozen, W. C. Schnobrich

July 1969

Subcontract No. 2906
Under Contract No. W-7405-eng-26

A Report on an Investigation
carried out as part of the
Prestressed Concrete Reactor Vessel Program
of the
Oak Ridge National Laboratory

Operated by
Union Carbide Corporation
for the
U. S. Atomic Energy Commission

University of Illinois
Urbana, Illinois

CONTENTS

STRENGTH AND BEHAVIOR OF PRESTRESSED CONCRETE VESSELS FOR NUCLEAR REACTORS VOLUME II

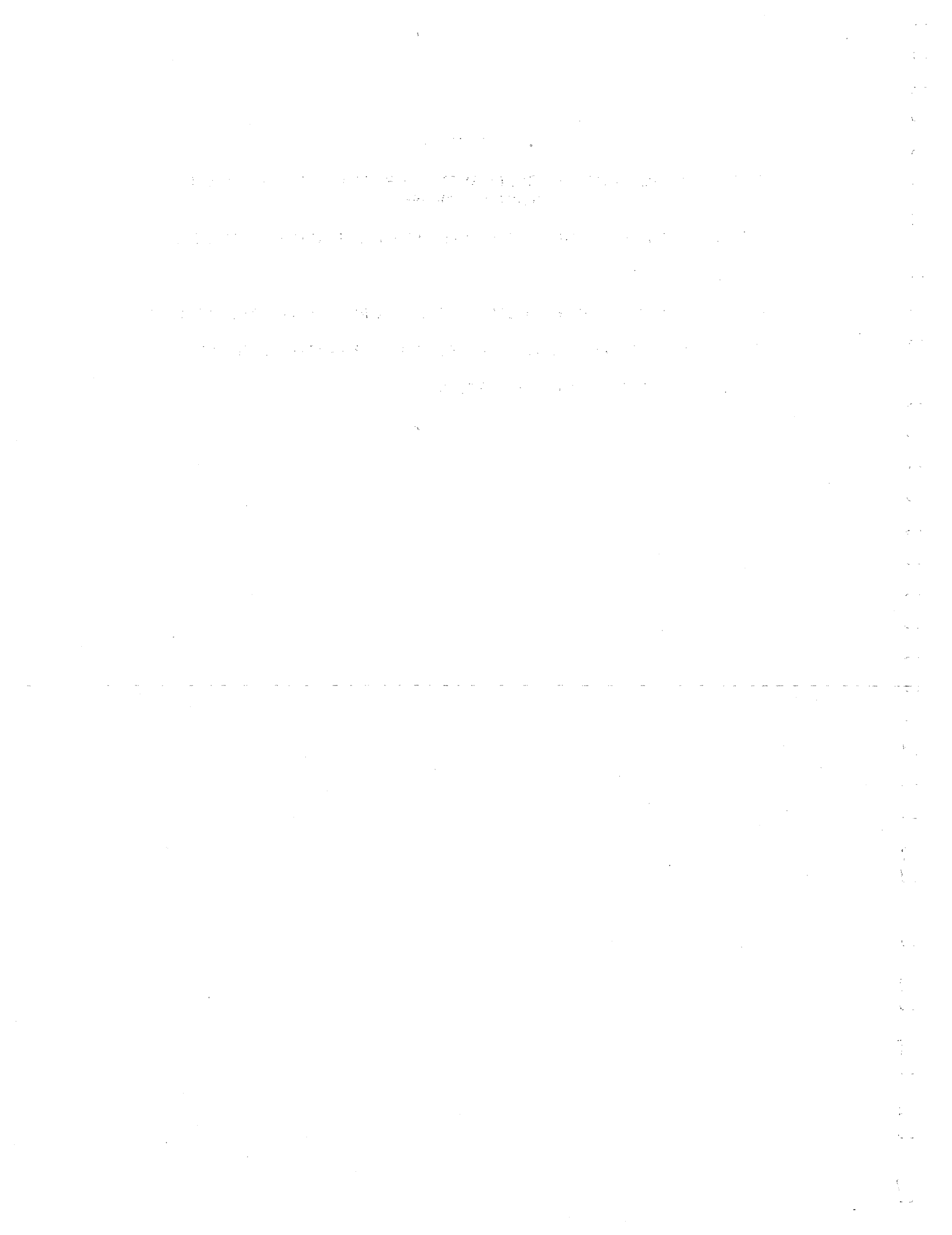
APPENDIX A MATERIAL PROPERTIES, SPECIMEN FABRICATION, TEST SETUP

APPENDIX B TEST DATA

APPENDIX C STRAIN DISTRIBUTION IN THE CIRCUMFERENTIAL REINFORCEMENT

APPENDIX D STIFFNESS MATRIX FOR THE LUMPED-PARAMETER ELEMENT

APPENDIX E COMPUTER PROGRAM LISTING



APPENDIX A

MATERIAL PROPERTIES, SPECIMEN FABRICATION, TEST SETUP

Appendix A

A1 MATERIALS

A1.1 Concrete

Test vessels PV1 and PV2 were cast from ready-mix concrete obtained from a local plant. The mix was specified to contain pea gravel aggregate and seven bags of type I cement per cubic yard of concrete.

Test vessels PV3 through PV14 were cast from concrete mixed in the laboratory. The proportions by weight of cement:sand:gravel were 1.00:3.51:3.40. Type III cement was used with a water cement ratio of 0.74. The aggregates were crushed limestone with a maximum particle size of one in. and Wabash River sand.

The concrete for vessel PV15 contained pea gravel aggregate and Wabash River sand with type III cement. The proportions by weight of cement:sand:gravel were 1.00:2.77:3.07 and the water cement ratio was 0.56. The end slab and top two inches of the skirt of vessel PV16 were cast from the same mix used for vessels PV3 through PV14. The remainder of the skirt was cast with the mix used for vessel PV15.

Table A1 gives the properties of the concrete used in the end slabs of the vessels. Two batches of concrete were required to cast vessels PV3 through PV10. Vessels PV11 through PV16 required three batches of concrete. Compression tests were conducted on five 6x12-in. cylinders from each batch. Five 6x6-in. cylinders were cast from the batch used in the end slab for use in the split cylinder test. Figure A1a shows the range of the modulus of elasticity measurements. Figure A1b is a plot of the results of the individual splitting-strength tests versus the average compressive strength in each vessel.

Two creep racks were assembled as shown in Figure A2. The results of the creep and shrinkage determinations are presented in Fig. A3. Each curve represents the average of readings from three cylinders. The 6x12-in. cylinders used for creep and shrinkage measurements were cast from concrete with the same proportions as the concrete in the vessels. The concrete in Batch I was left in the cylinder forms for two days, cured under wet burlap for seven days, and loaded to 1000 psi on 9 February 1968 at the age of eleven days. The concrete in Batch II was left in the forms for two days, cured under wet burlap for six days, and loaded to 1000 psi on 16 February 1968 at the age of ten days. Three ten-in. gage lines were established on each cylinder for measurement of deformations. Companion cylinders for each creep rack were also equipped with gage lines and stored in the laboratory for shrinkage measurements. All measurements were taken with a 0.0001-in. Whittemore gage over a ten-in. gage length. The environmental control in the laboratory is set at 50 percent relative humidity and 72°F.

A1.2 Longitudinal Reinforcement

Vessels PV1 and PV11 through PV16 were prestressed with 0.775-in. diameter Stressteel rods. Vessels PV2 through PV10 were prestressed with 1/2-in. diameter seven-wire strand.

The results of a tensile test of a 30-in. Stressteel rod are plotted in Fig. A4. The strain was measured using an eight-in. extensometer. The ultimate stress in the rod, which had a measured cross-sectional area of 0.471 sq. in. was 140 ksi.

The apparatus used to determine the "spring factor" of the 1/2-in. strand is shown in Fig. A5. The length of strand between strandvises is approximately the same as the length between the vises in the test setup. The load on the strand was cycled six times between zero and thirty kips. The load deformation characteristics of the strand under these testing conditions are presented for the first three loadings in Fig. A6. By the third loading cycle the stiffness of the strand was constant. The stiffness of the strand depended on the torsional fixity of the strandvises and on the slippage of the outer wires relative to the central wire. The nominal area of the strand was 0.151 sq. in.

A1.3 Circumferential Reinforcement

The wire that was used to prestress the vessels circumferentially was obtained from INTERPACE. Tests conducted on samples cut from the unstressed coil before prestressing and cut from the wire on the vessels after pressure testing showed no significant difference in stress-strain response. Typical stress-strain curves for each size wire used are shown in Fig. A7.

The wire used on vessels PV1 through PV10 had a diameter of 0.192 in. and a computed area of 0.0290 sq. in. Deformations to about two percent were measured with a two-in. electrical extensometer. The strain at failure was obtained from measuring the change in length of a five-in. gage length etched into the wire before the test.

The wire used on vessels PV11 through PV16 had a diameter of 0.250-in. and a computed area of 0.0491 sq. in. The wire was tested on a

Baldwin testing machine. Tests were made using a two-in. electrical extensometer to measure deformations. Another set of tests was made using a portable strain indicator to read strain from two BLH HE121 strain gages. The two strain gages were mounted on opposite sides of the wire and wired in series in order to average the strain readings.

A1.4 Liner Materials

The neoprene used to seal the pressure vessels was purchased in 200-lb. rolls. The sheets were 72 in. wide and 1/16 in. thick. It was specified as "60 Durometer Shore A Black neoprene Sheeting, Type #260".

The O-ring material was obtained in 200-ft lengths. The diameters of the 3/16-in. and 3/4-in. O-ring stock were 0.210 ± 0.010 -in. and 0.750 ± 0.010 -in. respectively. The material was specified as "70 Durometer Shore A Extruded Buna N O-ring cord stock".

The caulking used to complete the seal at the end slab was General Electric Silicone Caulking.

Sheets of aluminum with a thickness of 0.017-in. were used on the sides and end slabs of some of the vessels. Sheets of 16-oz. soft copper were used on vessels PV12 through PV16 in addition to the aluminum sheets.

Metz Reference Room
Civil Engineering Department
B106 C. E. Building
University of Illinois
Urbana, Illinois 61801

A2.1 Casting and Curing

The pressure vessels were cast in the steel form shown in Fig. A8. The same outer form was used for all sixteen vessels. This form was rolled from 5/16-in. steel plate and reinforced with rolled 2x2x1/4 in. angles. The inner form, which was a closed cylinder, and the outer form are bolted to a 1/2-in. thick base plate. The inner form for vessels PV1 through PV10, thirty-in. inside diameter, was rolled from 3/16-in. plate. Both forms used the same five-piece construction. Holes were drilled into the base plate to receive 7/8-in. diameter rods which formed ducts for the longitudinal prestressing. For vessels PV15 and PV16 which had two rows of longitudinal prestressing., 1-in. round electrical conduit was used to form the ducts for the second row of prestressing. The tops of the rods and sections of conduit were secured by a template of 1/2-in. steel plate which was supported by sections of 4-in. wide channel attached to the sides of the form. The center of the template plate was cut out to permit access to the form for the concrete and to facilitate finishing the surface of the concrete.

Vessels PV1 and PV2 were cast continuously from ready-mix concrete. All other specimens were cast in either two or three batches as noted previously. The batches were proportioned so that the end slab and at least 2-in. of the skirt were cast from a single batch. The concrete was vibrated internally with an electric vibrator during casting. Five 6x12-in. cylinders were cast from each batch. Five 6x6-in. cylinders were also cast from the end slab batch for use in the splitting test. The side walls of vessels PV11 through PV16 were reinforced with No. 4 bars to have a reinforcement

ratio of one percent. The bars were placed longitudinally about 1/2-in. from the outside surface of the concrete.

When the concrete had begun to set, usually about three hours after casting, the greased rods and conduit sections were manually extracted and the top of the vessel was trowelled to a smooth finish. The vessels were then covered with polyethylene film until the form was struck on the second day after casting. The vessels were cured under wet burlap for one week in the laboratory which had environmental control set at 70°F and 50 percent relative humidity.

A2.2 Circumferential Prestressing

The INTERPACE plant at South Beloit, Illinois, made their facilities available for applying the circumferential prestressing wire. A mandrel and end fittings as shown in Fig. A9 were designed to adapt the vessels to the equipment at INTERPACE, which is normally used to wrap concrete pipe. The vessels were transported to and from South Beloit by truck.

Anchors for the prestressing wire were cast into the vessels. An anchor is shown bolted to the form in Fig. A10a. Figure A10b shows a closeup of the anchor. A steel block about 3/4 x 3/4 x 1-1/4 in. is grooved and stamped, forming a toothed channel to grasp the wire. The block is then welded to a 3/8-in. diameter rod that has been bent into a U-shape to provide anchorage. The block and rod are hardened as a unit. The anchors were provided by INTERPACE and performed very well throughout the test series.

The prestressing operation was started by securing the wire in the anchor at the closed end. This was done by driving the wire into the toothed channel with a hammer. The first wrap of prestress was applied at a slightly reduced load. Subsequent wraps of the 0.192-in. diameter wire were applied at a tension of 4800 lb. Tension in subsequent wraps of the 0.250-in. diameter wire were applied at a tension of 7,800 lb.

A schematic diagram of the machine at INTERPACE is shown in Fig. A11. When the mandrel and vessels were in place, an axial load of about 20,000 lb was applied to create a friction force between the end fittings and the rubber bearing surfaces on the turning heads. The turning heads were rotated by a motor mounted at one end of the frame. The prestressing wire passed through a straight duct about 50 ft long from an uncoiling area to a friction wheel. The wire then passed through a load cell above the friction wheel and travelled overhead to the spacing apparatus which ran on a track above the mandrel and vessels. The spacing apparatus could advance automatically at a rate proportional to rotation of the turning heads or be adjusted by an operator. Tension was developed in the wire at the friction wheel by a D. C. motor which supplied a resisting torque. The load cell, which is located above the friction wheel, gave an account of the tension in the wire. Deviation from the desired load could be compensated by adjusting the torque transmitted by the D. C. motor. The load cell was calibrated to indicate the tension in the wire at the turning heads.

Approximately five minutes were required to prestress a vessel. Figure A12 contains two plots showing the variation of the load in the wire

as wrapping proceeded from the end slab of the vessel toward the open end. The data for Fig. A12 were obtained from recording equipment at INTERPACE which showed a plot of load versus time.

The force in the wire as it was being wrapped around the specimen was known. To obtain the effective prestress at the time of the test, the following procedure was used. All calculations referred to the prestress around the end slab. The initial prestress was assumed to be the force in the wire less the calculated effect of the reduction in diameter of the vessel due to elastic deformation of the concrete. The time-dependent losses were estimated using the creep and shrinkage data given in Fig. A3. Relaxation of the prestress wire, estimated to be less than four percent in most cases, was ignored because of lack of directly relevant data and because the scatter in the time-dependent properties of the concrete was expected to be much larger. The increase in circumferential prestress caused by longitudinal prestressing was calculated by assuming that the Poisson's ratio for concrete was 0.15.

A2.3 Longitudinal Prestressing

Vessel PV1 was prestressed longitudinally with ten 0.775-in. diameter Stressteel bolts. Vessels PV2 through PV10 were prestressed with seven-wire, 0.5-in. diameter strand. The use of strand was more economical and permitted the longitudinal restraining force of the prestressing tendons to be more evenly distributed about the periphery of the vessel. With the higher pressure required for vessels PV11 through PV16, it was necessary to use Stressteel bolts for prestressing in order to develop the necessary clamping force at the base.

Strain gages were placed on some of the Stressteel bolts, and these bolts were calibrated in the laboratory. Loading of the bolts was accomplished with a 30 ton Simplex jack with the scheme shown in Fig. A13. The jack chair permitted a nut to be tightened against a 3x3x1-in. steel bearing plate so that the load in the jack could be transferred with a minimum loss. For vessels PV13 through PV16 where sixty bolts were used for the prestressing, a continuous steel plate 1 1/4-in. thick was used for the bearing plate rather than the individual plates. The load in the bolts after the jack was released varied from 40 to 45 kips. The average load in the bolts after prestressing was completed, was less than 40 kips since the loading of a bolt adjacent to an already loaded bolt tended to reduce the load carried by the loaded bolt. The effect was increased as the number of bolts used for the prestressing was increased.

Figure A14 shows the method of prestressing the strand. The applied load was monitored either by a load cell between the jack and the top strandvise or by measuring the oil pressure in the line to the Simplex jack. Those strands that were to be monitored during the test were equipped with a load cell between the four-in. plate at the open end of the vessel and the bottom strandvise. After a load of 24 kips was applied, the jaws of the strandvises were set either by driving slotted wedges between the bearing plate and the strandvise or by driving the jaws down the strand with an implement designed to fit around the strand and inside the body of the vise. Those strands equipped with load cells under the four-in. plate carried an average load of about 20 kips after the jack was released.

The force in the strand for vessels PV2 through PV10 and in the Stressteel bolts for PV1 was monitored immediately after prestressing. To obtain the effective prestress at the time of the test, the time-dependent losses were estimated using the creep and shrinkage data given in Fig. A3 and subtracted from the initial prestress. The force in the Stressteel bolts for vessels PV11 through PV16 was monitored immediately after prestressing and immediately before the test so that the vertical prestressing force was known at the time of the test.

A2.4 Liner

A detail of the liner in each vessel is provided in Appendix B. The scheme for sealing vessels PV1 through PV5 was as follows. After cleaning the inside and filling the voids with Hydrocal, successive layers of 1/16-in. neoprene, 18 gage sheet metal, and 1/16-in. neoprene were placed on the inside surface of the end slab, using contact cement to hold them in place. A six-in. wide strip of 20-gage sheet metal was cemented to the side wall just below the end slab (Fig. B1.2).

The connection between the concrete and the steel sealing ring was achieved by welding an eight-in. wide strip of sheet metal to the ring. The neoprene sheet placed on the side wall butted the seal on the end slab and lapped over the sheet metal at the sealing ring. Contact cement was used to secure the neoprene to all surfaces except to the sheet metal at the sealing ring where rubber cement was used. Rubber cement was also used at the lapped joint in the neoprene. All surfaces to be cemented were carefully cleaned with benzene.

The seal at the junction of the end slab and side wall was made by embedding a 3/4-in. O-ring in General Electric Silicone Caulking. The seal between the steel base plate and the sealing ring was made by compressing a 3/16-in. O-ring into the groove in the base plate (Fig. A15).

Difficulties were encountered with this method of sealing at higher pressures. The details of the seal were changed for vessels PV6 through PV12. These changes are reported in Appendix B. The seal for vessel PV12 proved to be satisfactory for high pressures and was used without change for the remaining vessels.

The seal used for vessel PV12 through PV16 consisted of lining the wall and end slab with a sheet of 0.017-in. thick aluminum bonded to the concrete with rubber cement (Fig. B12.1). Next, a liner of 16-oz. soft copper was placed over the aluminum. The copper-aluminum interface was greased so that the copper would not develop large stress concentrations during deformation. The copper sheet used on the end slab had a one-in. lip which was soldered to the copper sheet on the wall. The lap in the copper wall sheet was also soldered as was the copper-steel joint at the one-in. steel base ring. The vessels were then lightly prestressed longitudinally and pressurized to 50 psi gas pressure to deform the metal liners to the contours of the concrete and to check for any major leaks in the liner. A layer of 1/16-in. thick neoprene was placed over the copper and secured with rubber cement. A 3/4-in. neoprene O-ring was also installed at the junction of the end slab and the side wall.

A3 TEST SETUP

The test shed was erected on the grounds of the Structural Dynamics Laboratory which is situated in farmland about three miles south of the university campus (Fig. A16a). The shed is a wooden enclosure built on a twelve-ft square slab-on-grade floor. It features a 5 by 5 ft steel test chamber in its center which extends from the floor through a hole in the roof. The test chamber was constructed of four 4 x 4 x 3/8 in. angles which extend vertically from the corners of the opening to the floor with 0.5 in. steel plate on the four sides. Figure A16b shows vessel PV8 inside the test chamber after the test. A hatch was provided to cover the hole in the roof when the shed was not in use. During tests the hole was covered with layers of wire mesh to impede concrete projectiles. For vessels PV11 through PV16, three layers of wire blast mats were used to cover the hole. The blast mats were anchored with 3/8-in. cable fastened to ground anchors at the sides of the shed.

After the liner and one-in. steel ring were in place (see Section A2.3 on the assembly of the liner) the vessel was placed on a four-in. thick circular steel plate shown in Fig. A15. A 3/16-in. O-ring was compressed between the one-in. ring and the four-in. closure plate to complete the seal. In vessels PV1 through PV8 a ten cubic-ft block-out was provided to fill part of the void inside the vessel and reduce the quantity of compressed gas that would be released when failure occurred. The block-out was a closed cylinder filled with vermiculite concrete for the first three tests. On the third test a leak in the block-out permitted it to become filled with gas,

causing the block-out to burst when the vessel failed. In subsequent vessels up to PV8 the block-out was filled with water. In vessels PV9 through PV16 the entire vessel was filled with water to within approximately 1/2-in. of the end slab.

Figure A17 shows the gas supply and pressure regulating scheme used to pressurize the vessels. Nitrogen gas was admitted to the vessels in the test shed through a 1/4-in. copper line from a series of gas supply bottles. The pressure within the vessel was monitored by a Bourdon test gage with 1/4 percent accuracy which was connected by a second 1/4-in. copper line to the vessel. This second line for pressure measurement eliminated error in the pressure reading due to gas flow in the line. The gas supply line and pressure monitoring line were connected through the steel base plate on the vessel.

Vessels PV9 and PV10 were exceptions to the general test setup in that they were tested using oil pressure and were tested inside the Structural Dynamics Laboratory. The remote monitoring of the tests was not necessary since compressed gas was not used in the test and the failure did not result in a violent release of energy.

A4 INSTRUMENTATION AND TEST PROCEDURE

In general the instrumentation consisted of deflection measurements across one diameter of the head and down the side on a line at one end of this diameter, strain measurements on the concrete on the inside face of the end slab on four diameters 45 degrees apart and on the outside face on two diameters, strain measurements on the circumferential prestressing steel, and change in force in the load cells on some of the longitudinal prestressing tendons. The diameter on the outside of the end slab on which deflections were measured was offset 3 degrees from one of the diameters on which strains were measured. The strain gages on the circumferential steel reinforcement were placed after the steel was wrapped so that only the change in strain during the test was measured. The load cells on the longitudinal prestressing were monitored during the prestressing operation and during the test so that the total load could be calculated. The Stressteel bolts were gaged with BLH A-19 strain gages and calibrated in a testing machine, thus eliminating the need for external load cells for the bolts. The actual number of measurements of each type and their locations are shown in Appendix B for each test.

The strain gages used on the concrete were BLH type A12 which have a one-in. gage length and are flat wound wire gages with paper backing. These gages were applied with Eastman 910 cement. There was some concern that the strain gages located on the inside of the head would be affected by the normal pressure on the gage grid. This problem has been the subject of several investigations one of which is reported in Ref. A1. These studies show that gages which are properly applied have a response resulting from

normal pressure sufficiently small that it could not be distinguished from the scatter in the strain measurements for these tests. On the inside of the head the gages were applied by first sanding the concrete to a smooth finish and then placing a layer of cement on the concrete and allowing it to set. The gages were then cemented to this prepared surface with Eastman 910 cement and a soft rubbery protective coating placed over the gage. After the protective coating had set, a 1/16 in. sheet of neoprene was glued over the gages to provide further protection and assure that the applied pressure was uniformly distributed over the gage. In vessels PV7 through PV16, the end slab was covered with a 1/4-in. thick layer of Hydrocal. Conductors from the inside strain gages were glued to the inside wall of the test vessel from the gages to the corner where the head and wall meet. At this point a hole was drilled through the wall and the leads run through this hole which was then resealed with epoxy. The entire inside surface of the end slab was then covered with a 1/4-in. thick layer of hydrocal. The neoprene gas seal was then placed over the hydrocal which covered the wires and the hole in the wall. On vessels PV11 through PV16, the gage wires were run down the inside of the vessel and out between the concrete and the one-in. steel ring. Channels 1 in. wide by 1/4-in. deep were cast in the concrete to accommodate the gage wires. On the outer surface of the concrete the strain gages were applied in the same manner, but no protective coating was used on them. The strain gages used to measure change in strain of the circumferential reinforcement were BLH type A19 which is a flat grid wire gage with a gage length of 1/16 in. and temperature compensation for steel. These gages were applied with Eastman 910 cement following standard procedures.

The load cells used to measure load in the longitudinal strand consisted of 6-in.-long aluminum cylinders 1 3/8 in. in diameter with a 5/8 in. longitudinal hole drilled through it. The aluminum in these cylinders was a soft bar stock of 2014 alloy and was heat treated in our laboratory to meet specifications for 2014-T6 temper. Four strain gages were cemented to the outside of these cylinders and wired into a full bridge. The strand was threaded into these cylinders at the lower end of the test specimen, and the change in strain monitored as the load changed in the strand. Before they were used, the load cells were calibrated in a testing machine by applying a direct compression to them. Different numbers of load cells were used in the various tests as indicated in Appendix B.

All the tests except PV9 and PV10, were performed in the test shed which was about 100 ft from the Structural Dynamics Laboratory. Approximately 135 ft of cable was required to reach the area where readings were taken in the main laboratory. A 4-conductor cable with heavy rubber coating passing through an overhead metal cable tray was used between the two buildings. This cable is Belden 8424 and contains 20 gage conductors. Several of the tests were performed during the winter so a heater was placed in the test shed to keep it warm enough for men to work. It was not possible to maintain room temperature at all times with this heater but temperature compensating strain gages were placed in the test chamber with the test specimen. The specimen was then left in the test shed for sufficient time to allow the temperature to stabilize.

Strains on the first 5 specimens were read with two BLH portable strain indicators model number 120 C in the main laboratory at the end of

the 135 ft lead wires. This strain indicator is designed to excite the bridge with an alternating square wave in order to reduce the effects of capacitance in the leads to the strain gages. However, since the leads were rather long in this case special precautions were taken. For each type of bridge used on the test vessel the effect of a given shunt was read with the indicator at the bridge. Then, with the strain indicator connected to the bridge through the long leads, the gage factor was adjusted so that the same shunt had the same effect on the bridge. This slightly adjusted gage factor was then used when the strains were read during the test. During tests PV6, PV7, and PV8 strains were read with an automatic device assembled from components in our own laboratory. An automatic stepping switch was used to switch gages, the voltage difference across two corners of the bridge was read with a digital volt meter, and the resulting voltage was printed on a paper tape with a line printer. The device was calibrated by applying shunts of known value to the bridges and the compensation for long leads was made in a manner similar to that used for the portable strain indicator. Strains read with the portable strain indicator have an accuracy of the order of $\pm 5 \mu \text{ in./in.}$ while those read with the automatic reading device were somewhat more erratic and have an accuracy of approximately $\pm 20 \mu \text{ in./in.}$. The portable strain indicators used for tests PV1 through PV5 were used for tests PV9 through PV16.

Deflections across the head of the specimen and down the outside wall were measured with 0.001 in. Ames dial gages located within the test shed but outside the test specimen enclosure. The dial gages were connected

to piano wires which were strung over ball bearing pulleys and attached to metal tabs glued to the specimen. Tension springs connected to the back end of the dial gage plunger kept the piano wire taut. The pulleys over the top of the specimen were attached to an arm which was broken off by the flying debris each time a specimen failed. The dial gages were read with a closed circuit television hookup with the receiver in the main laboratory. The television camera was located inside the test shed but outside the test specimen enclosure, had a telephoto lens so that the dial gage face almost filled the television receiver screen, and was mounted on a system of two television antenna rotors so that it could be adjusted in direction for each gage. This arrangement proved quite satisfactory for this purpose, though some of the gages were damaged by the sudden tension on the piano wire at failure of the specimen. A second television camera was set up outside the test specimen enclosure and aimed through a hole in the enclosure at a mirror to observe crack development on the end slab of the vessels.

Pressure was applied to the inside of the specimen with bottled nitrogen through a regulator. With this regulator in the line, a pressure could be set and maintained in the specimen though there was a small leak, because more gas would be supplied through the regulator as soon as the pressure dropped below the set value. Pressure within the specimen was monitored with a Bourdon pressure gage. During a test the gas pressure was increased in increments and once the pressure was set and became stable all measurements were taken. Approximately 10 to 15 minutes were usually

required to take all the readings. The size of pressure increments varied between tests depending on the anticipated maximum pressure. In general the size of the increments was reduced as failure approached.

TABLE A1
CONCRETE PROPERTIES

| Mark | Age at Test days | Slump in. | Modulus of Elasticity psi $\times 10^6$ | Splitting Strength 6x6-in. cylinder psi | Compressive Strength 6x12-in. cylinder psi |
|------|------------------|-----------|---|---|--|
| PV1 | 71 | 3 1/2 | 4.2 | 432 | 5680 |
| PV2 | 105 | 5 | 3.5 | 398 | 4955 |
| PV3 | 36 | 1 | 4.2 | 450 | 6250 |
| PV4 | 38 | 1 3/4 | 4.2 | 380 | 5680 |
| PV5 | 32 | 3/4 | 4.1 | 439 | 6250 |
| PV6 | 42 | 1 | 4.1 | 398 | 5805 |
| PV7 | 54 | 1 | 4.6 | 506 | 6720 |
| PV8 | 78 | 1 1/4 | 4.8 | 443 | 7230 |
| PV9 | 71 | 1 1/2 | 4.3 | 446 | 7140 |
| PV10 | 54 | 1 1/2 | 4.0 | 394 | 7005 |
| PV11 | 64 | 1 | 4.5 | 514 | 6830 |
| PV12 | 89 | 3 | 4.4 | 456 | 5860 |
| PV13 | 84 | 1 1/4 | 4.2 | 490 | 6750 |
| PV14 | 107 | 2 1/4 | 4.3 | 465 | 6880 |
| PV15 | 39 | 1 1/2 | 4.2 | 531 | 7340 |
| PV16 | 79 | 2 | 4.0 | 518 | 7450 |

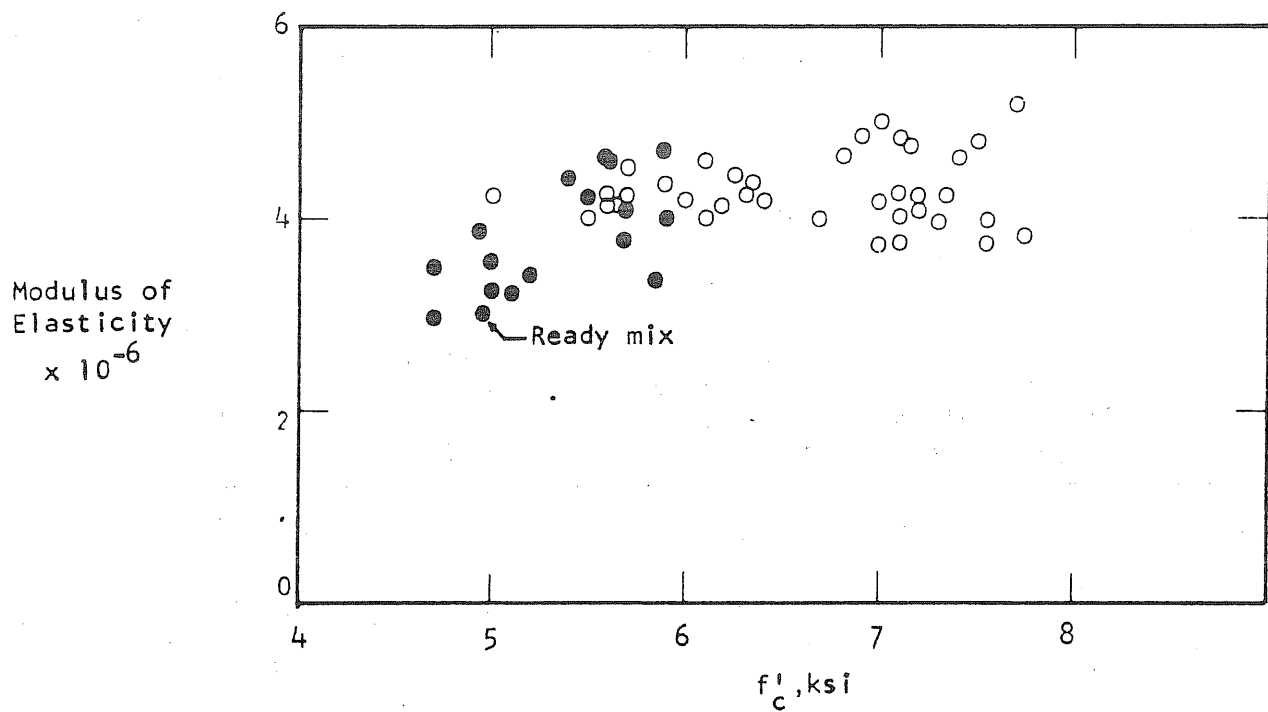


FIG. A1a MODULUS OF ELASTICITY vs COMPRESSIVE STRENGTH

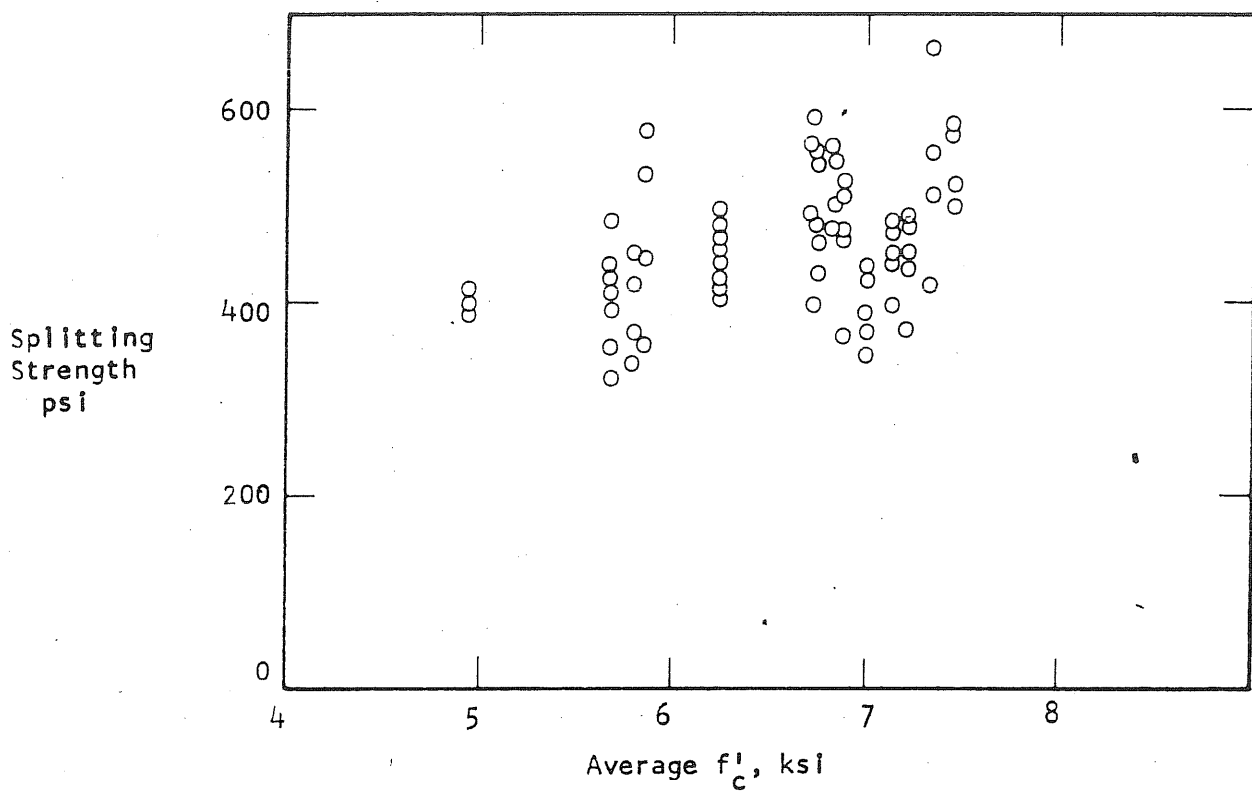


FIG. A1b SLITTING STRENGTH vs AVERAGE COMPRESSIVE STRENGTH

A 21

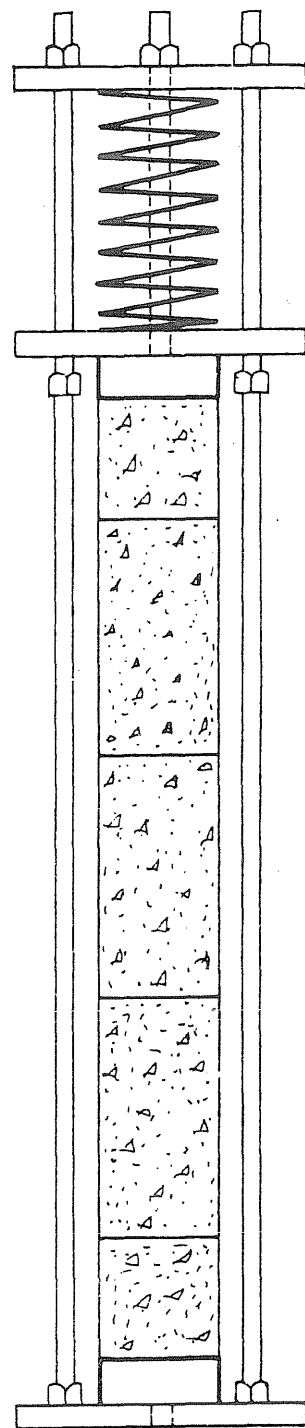


FIG. A2 CREEF RACK

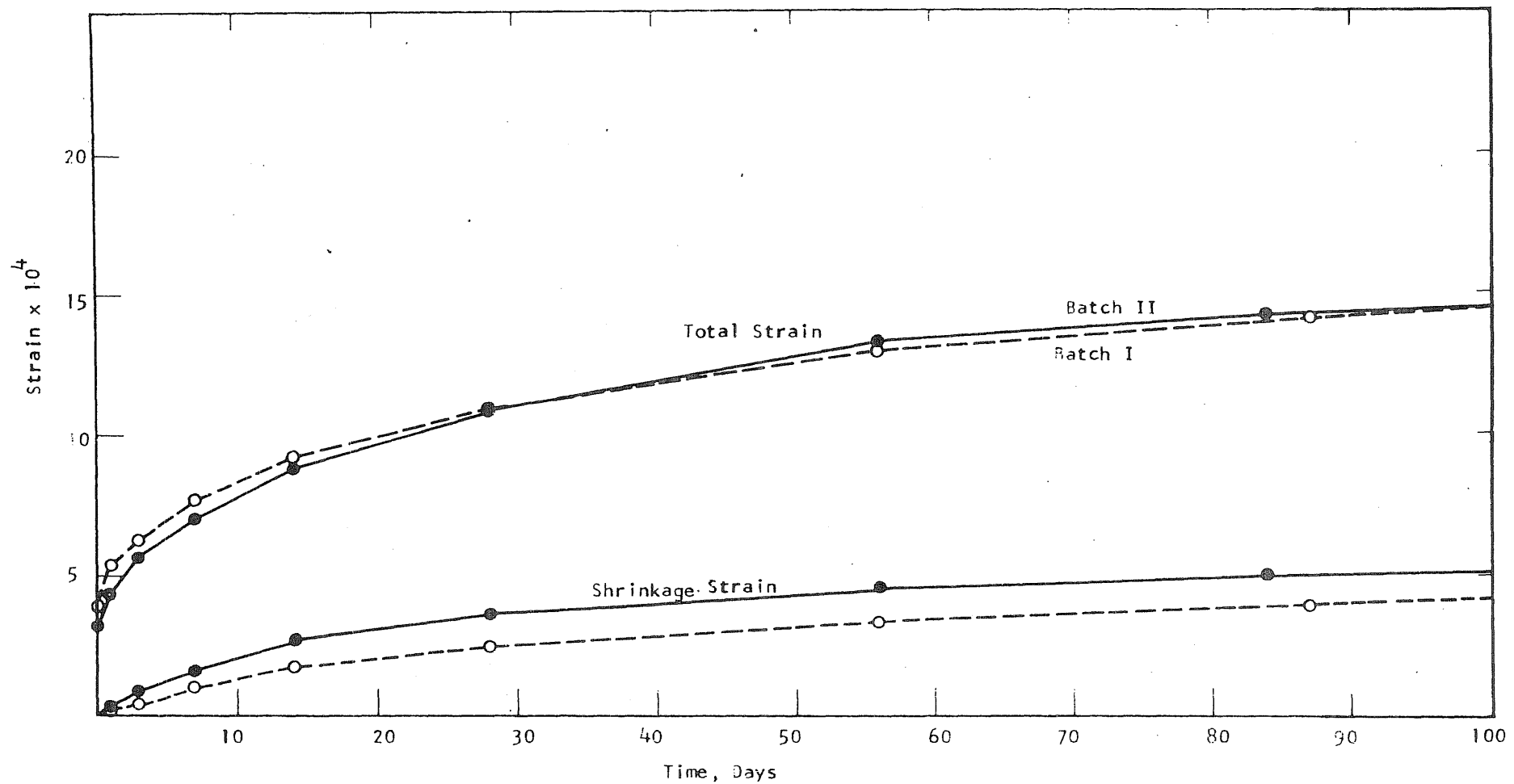


FIG. A3 SHRINKAGE STRAIN AND TOTAL STRAIN FOR 6x12-in. CYLINDER UNDER 1000 psi COMPRESSION

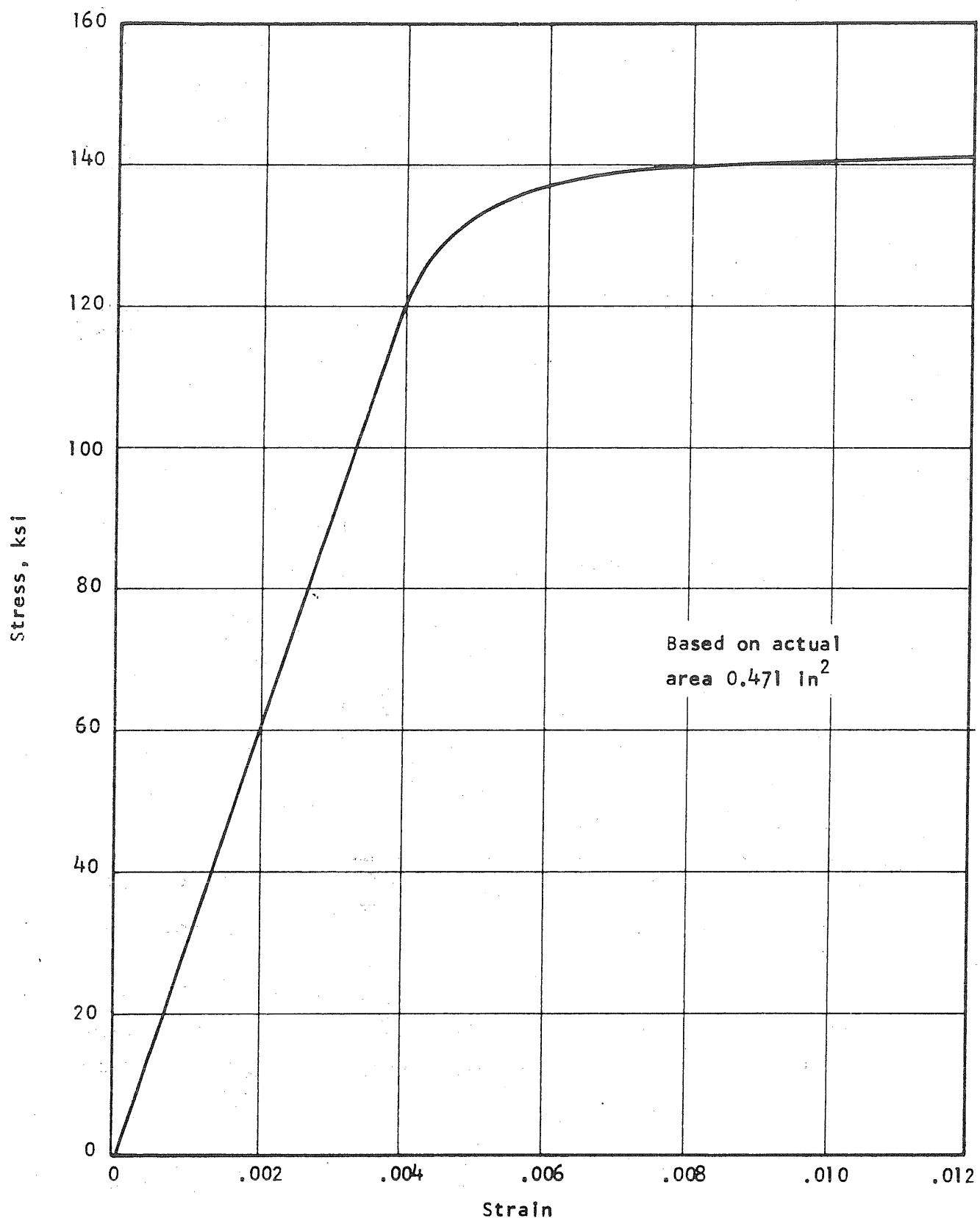


FIG. A4 STRESS-STRAIN CURVE FOR STRESSTEEL RODS

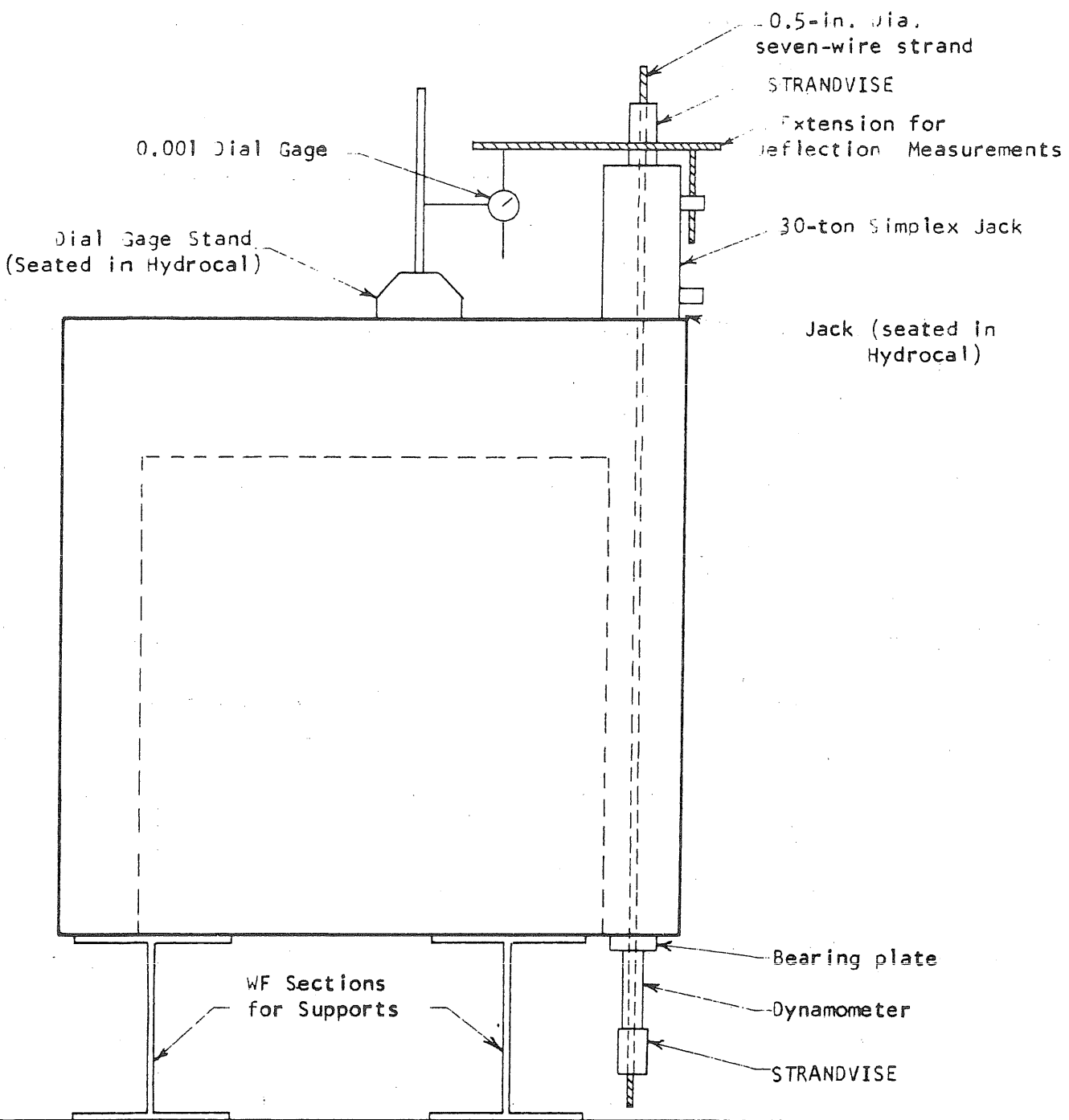


FIG. A5 APPARATUS FOR LOAD-DEFLECTION TEST ON SEVEN-WIRE STRAND

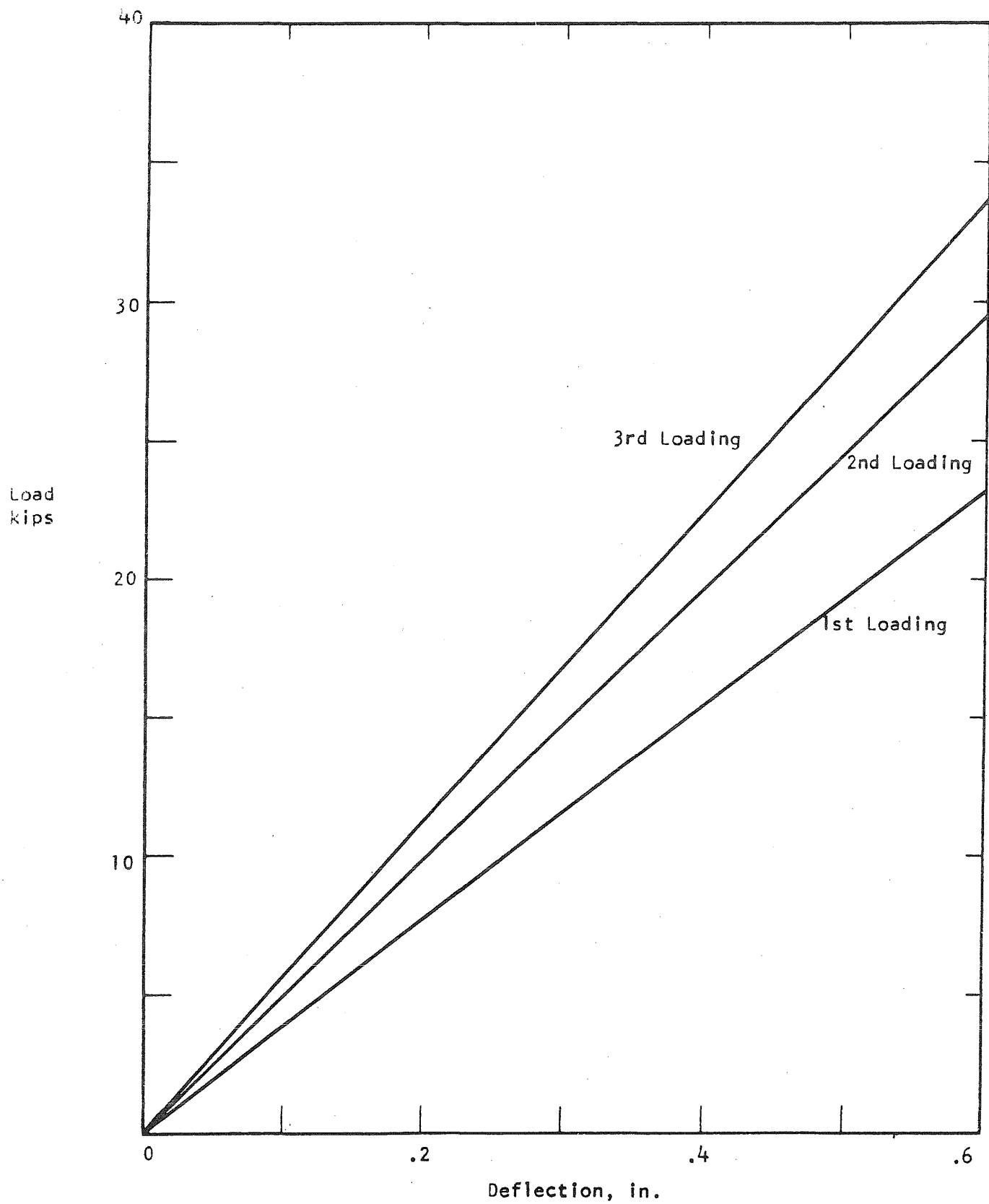


FIG. A6 LOAD VS DEFLECTION CURVES FOR SEVEN-WIRE STRAND

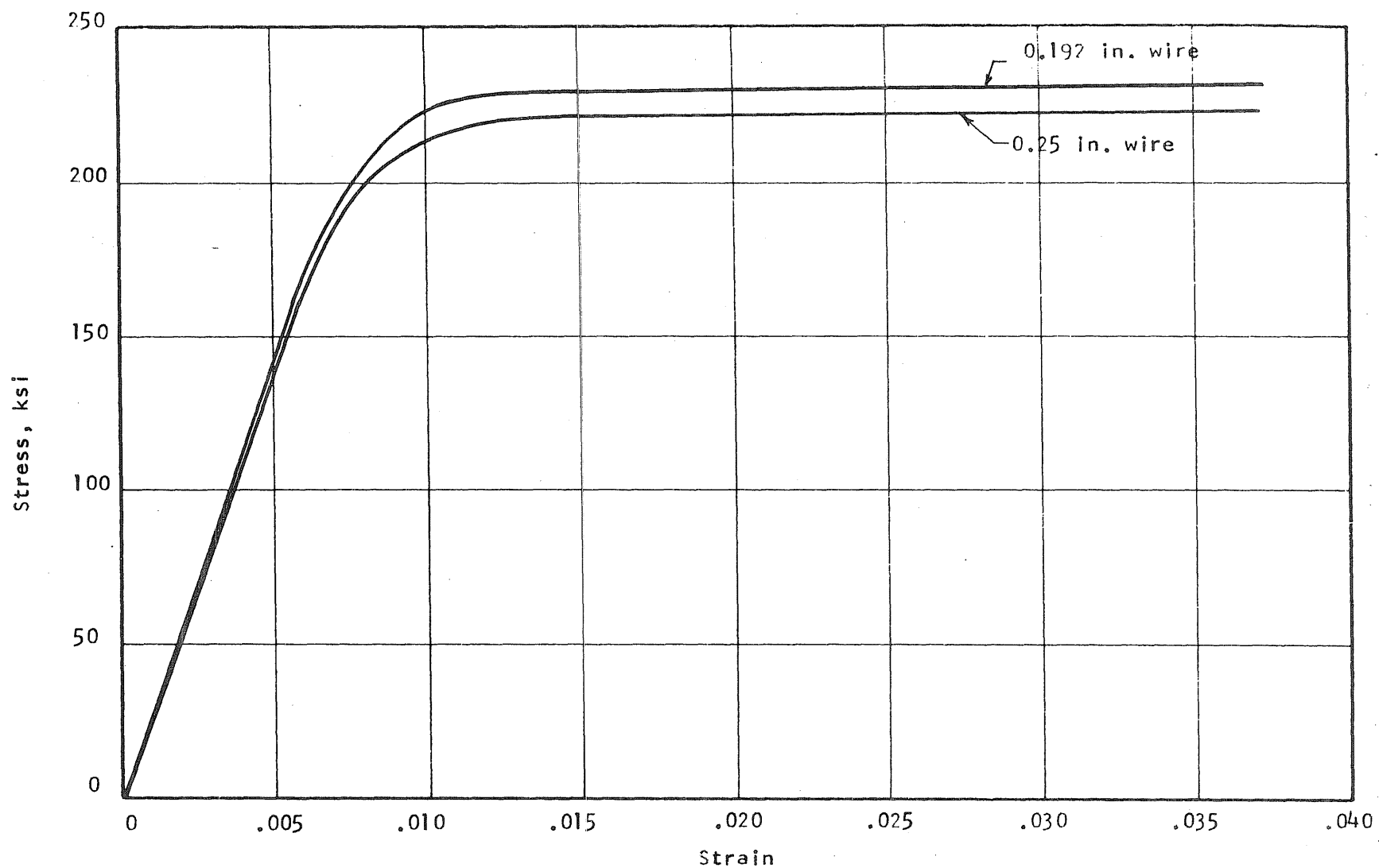


FIG A7 STRESS-STRAIN CURVE FOR PRESTRESSING WIRE

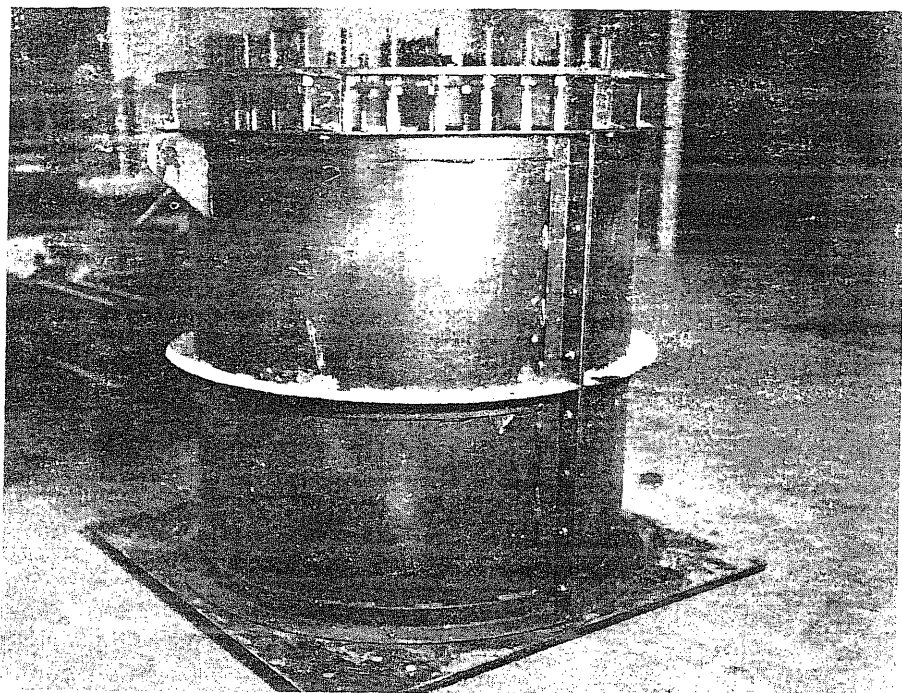


FIG. A8a PICTURE OF STEEL FORMS SHOWING TEMPLATE

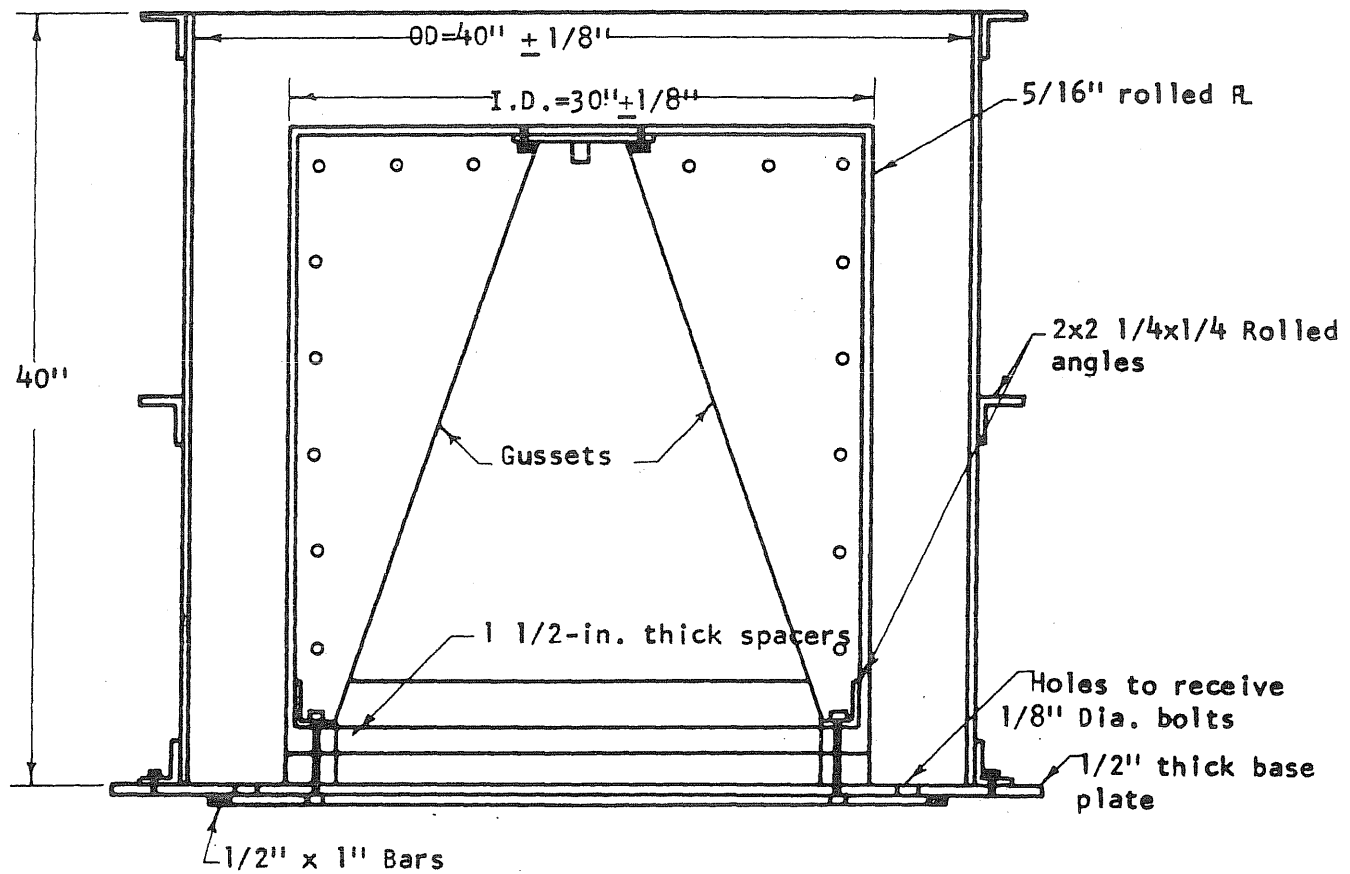


FIG. A8b DETAIL OF THE STEEL FORMS USED TO CAST PRESSURE VESSELS

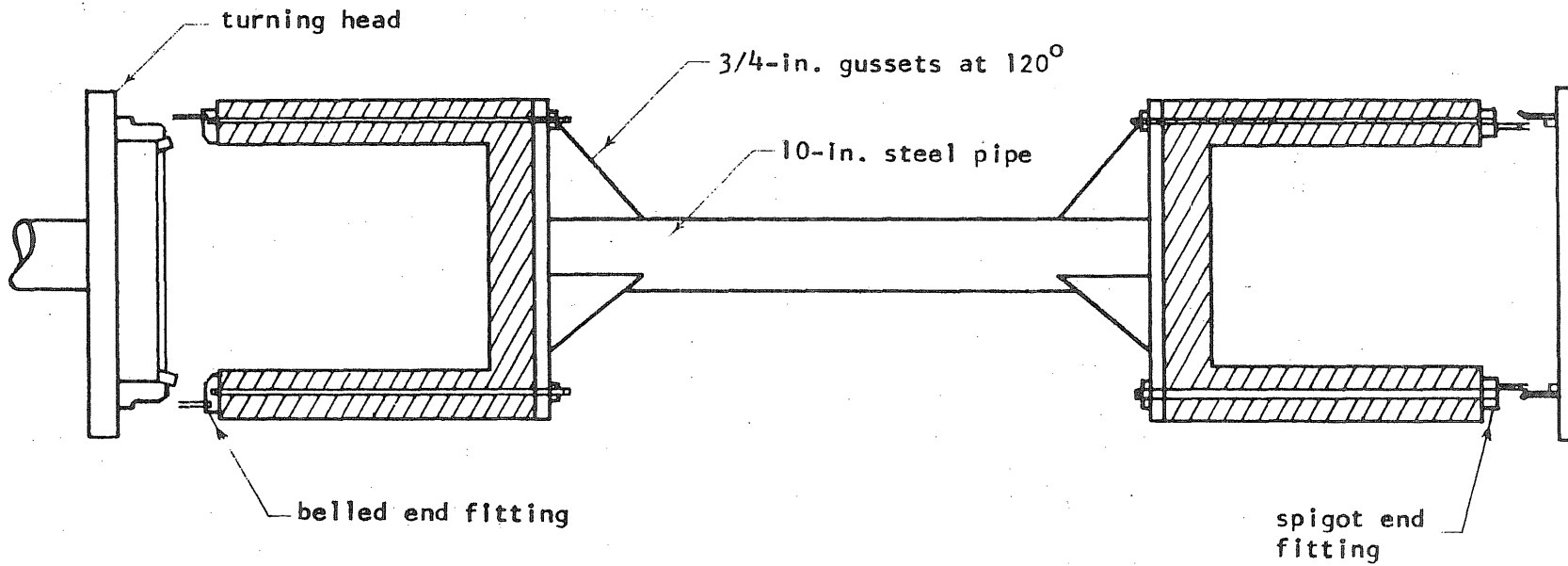


FIG. A9 SETUP FOR CIRCUMFERENTIAL PRESTRESSING

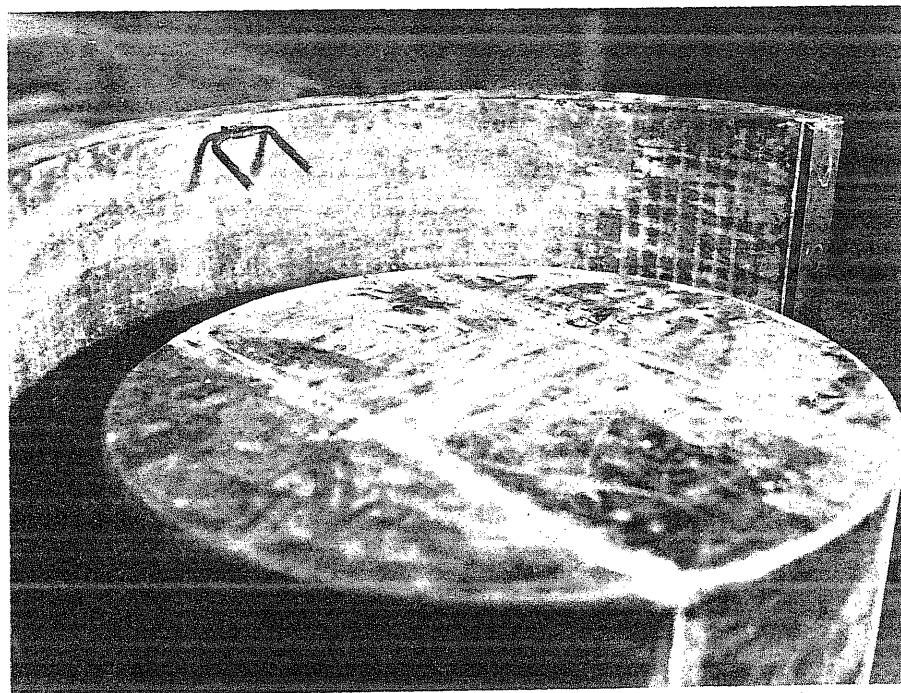


FIG. A10a ANCHOR BOLTED TO FORM

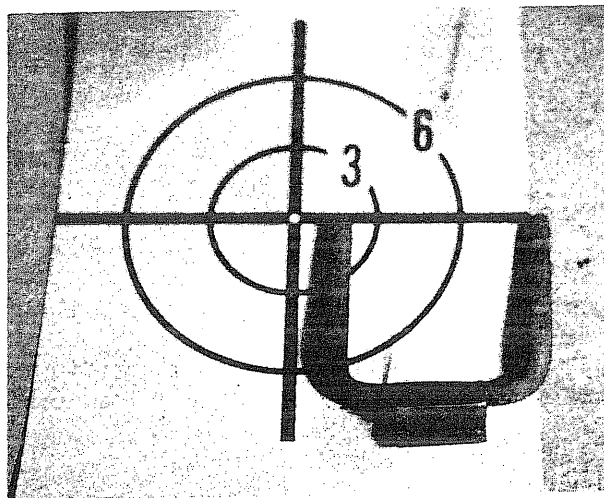


FIG. A10b CLOSEUP OF A TYPICAL ANCHOR

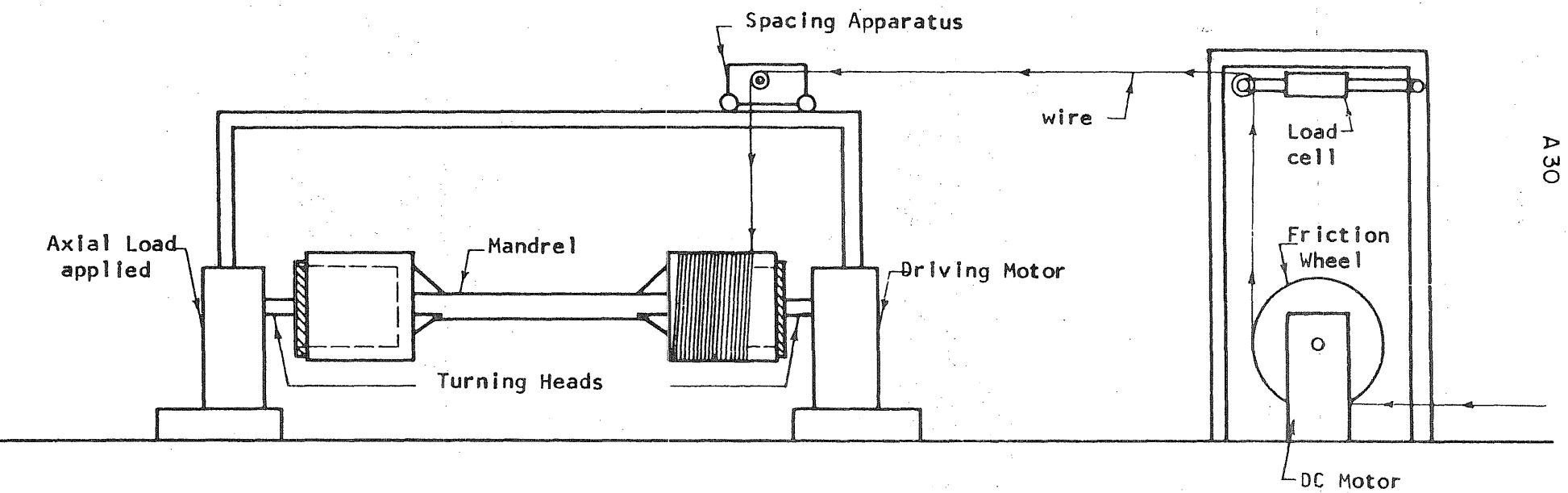


FIG. A11 SCHEMATIC DIAGRAM OF THE EQUIPMENT AT INTERPACE USED TO PRESTRESS THE PRESSURE VESSELS

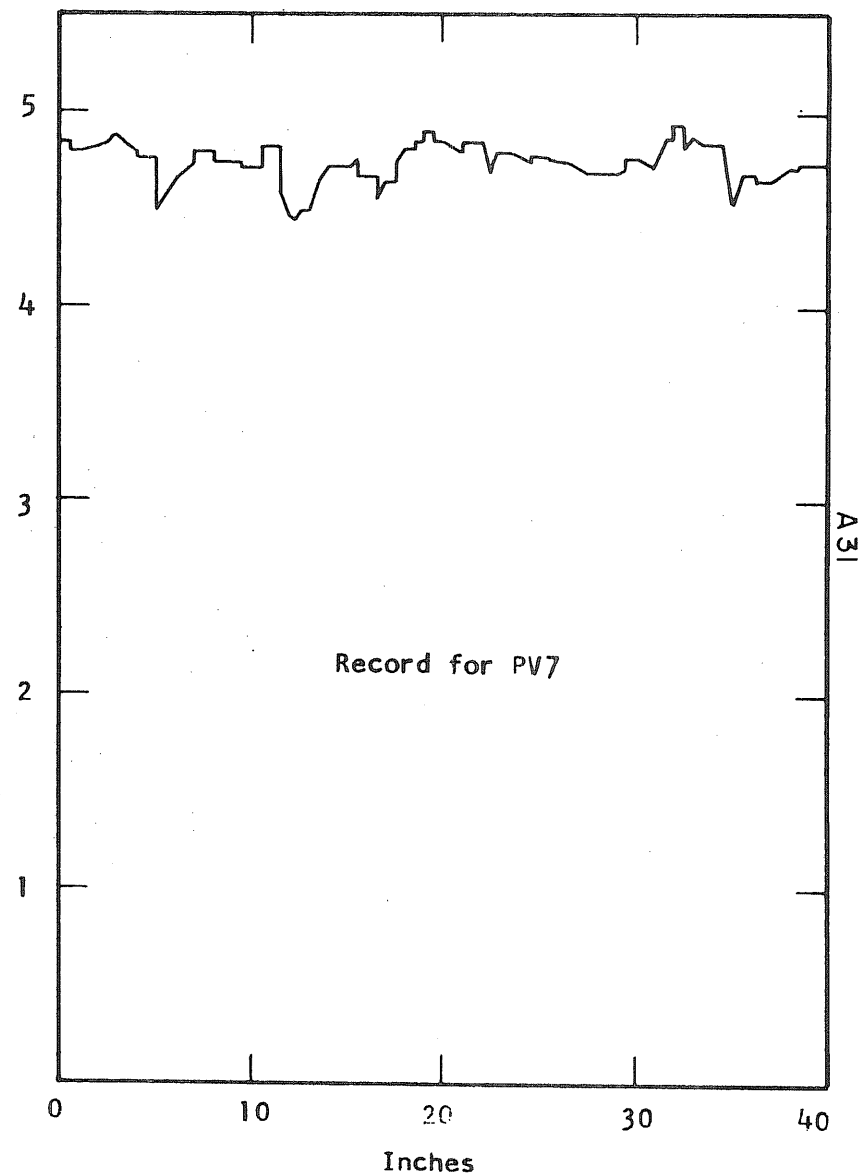
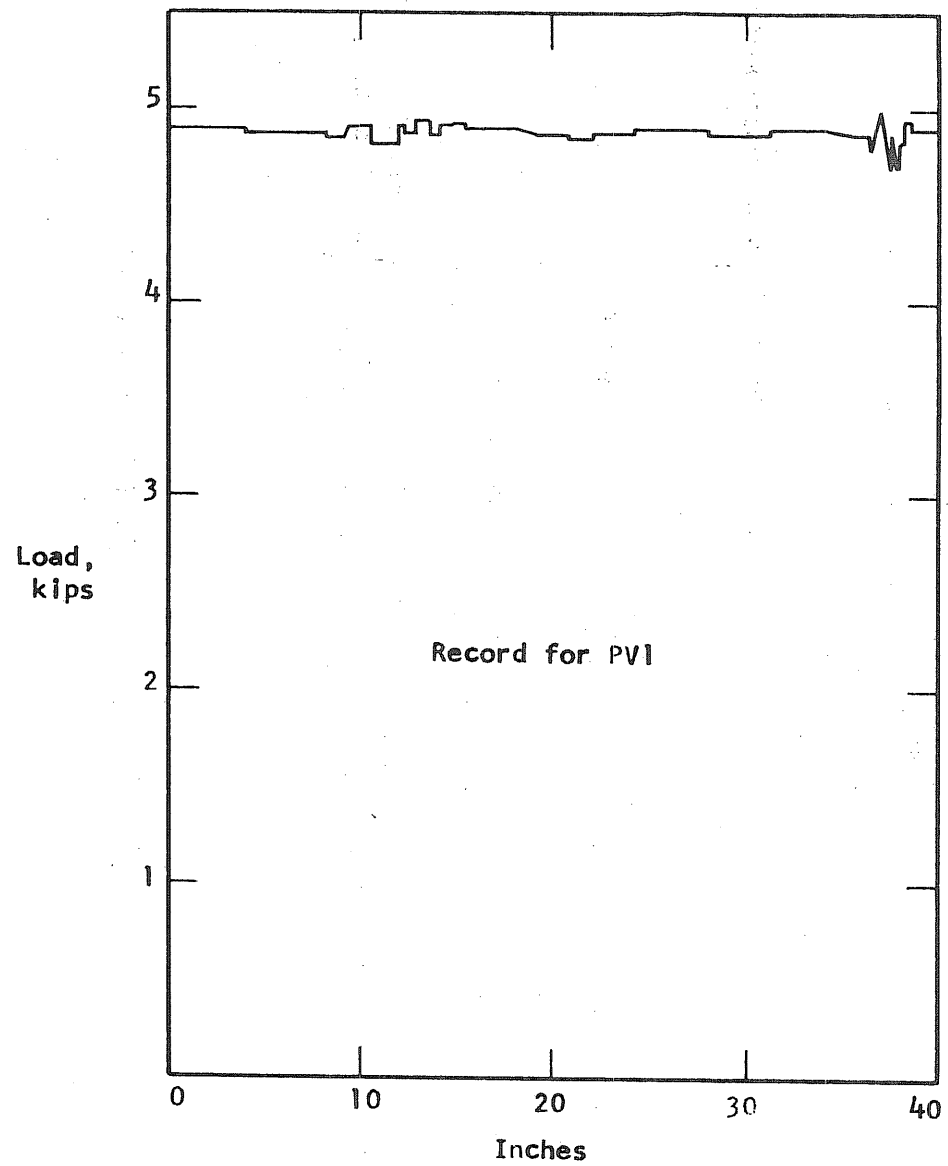


FIG. A12 LOAD IN WIRE vs DISTANCE FROM THE OUTSIDE OF THE END SLAB FOR PV1 AND PV7

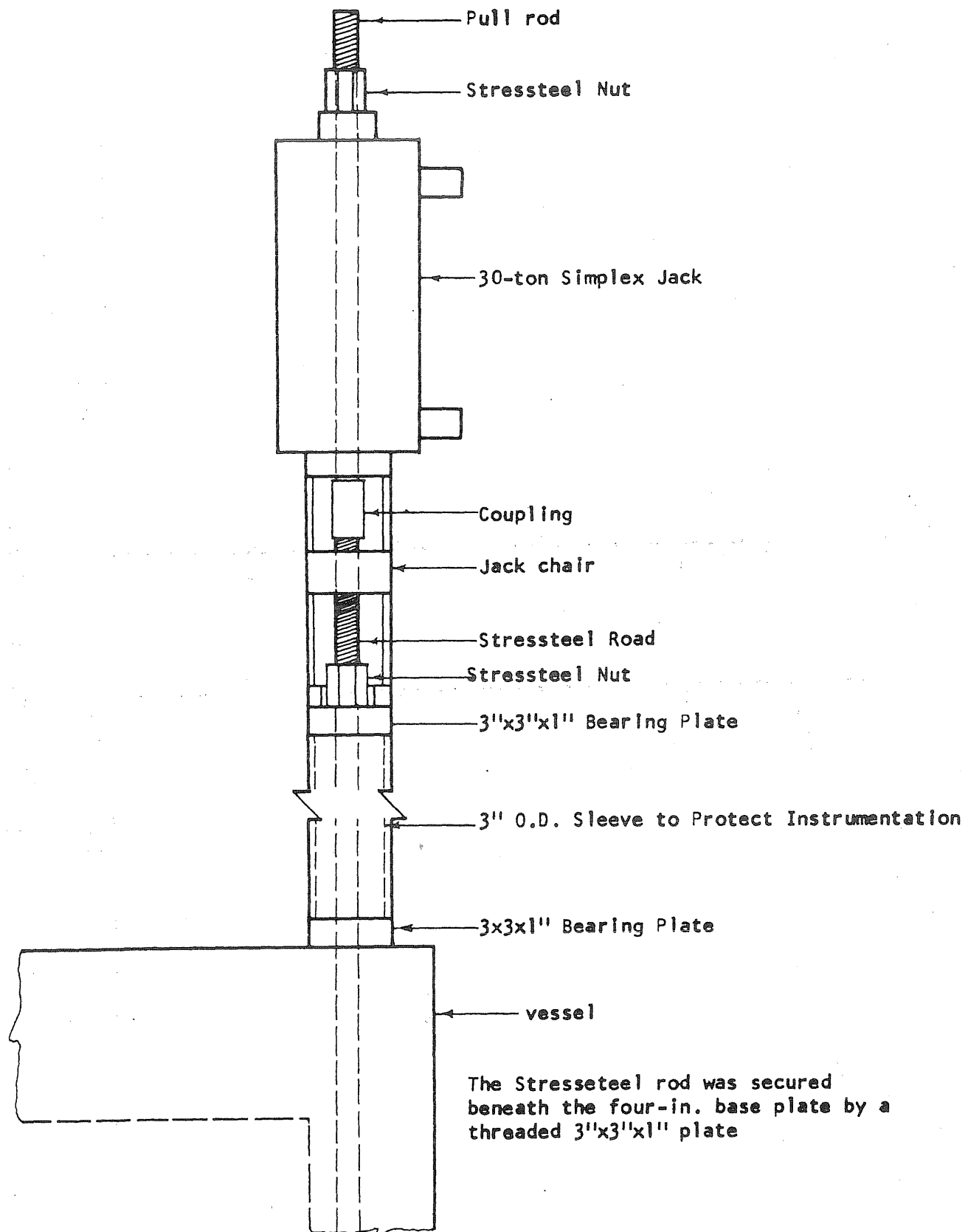


FIG. A13 APPARATUS USED TO PRESTRESS STRESSTEEL RODS

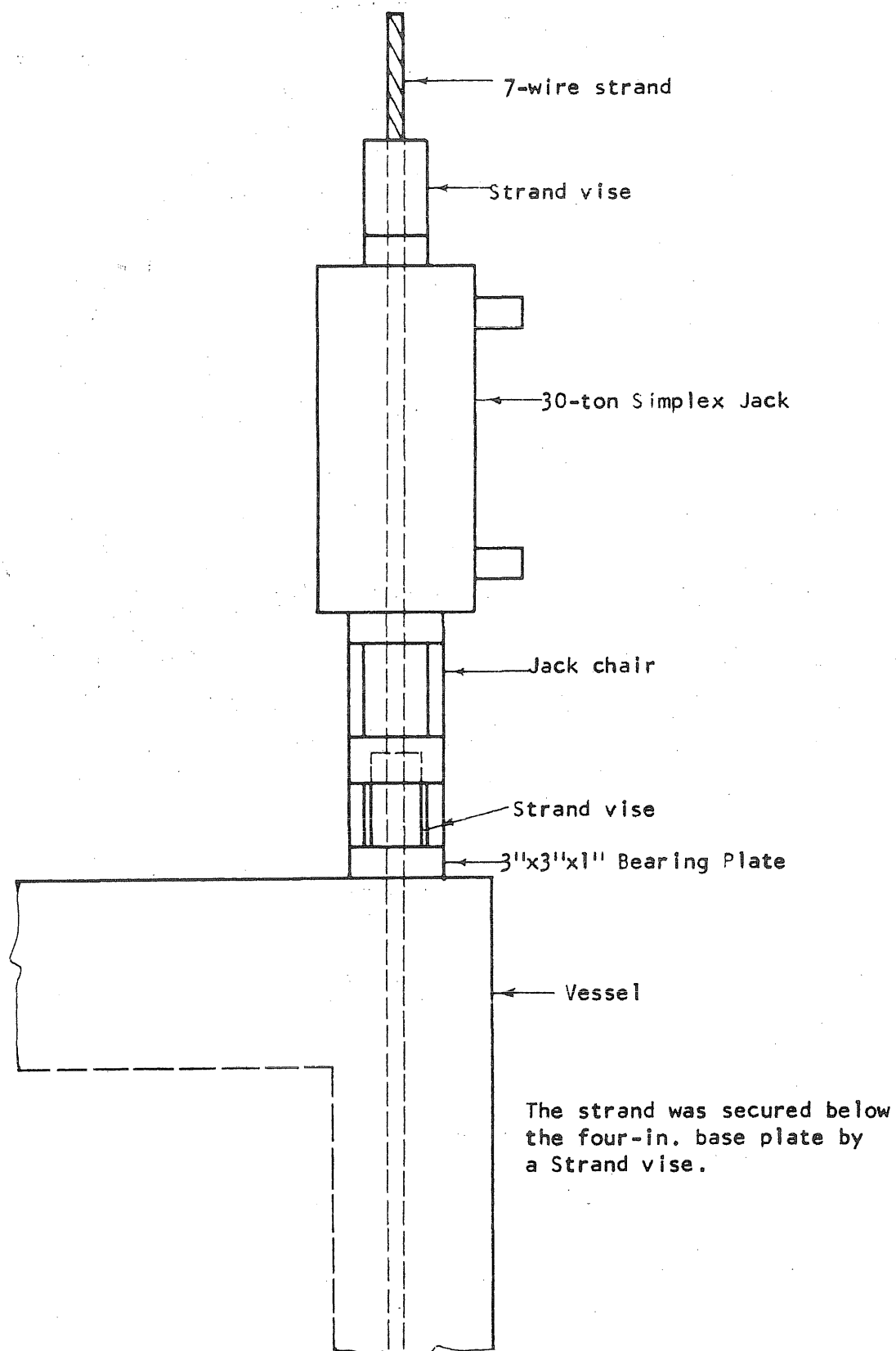
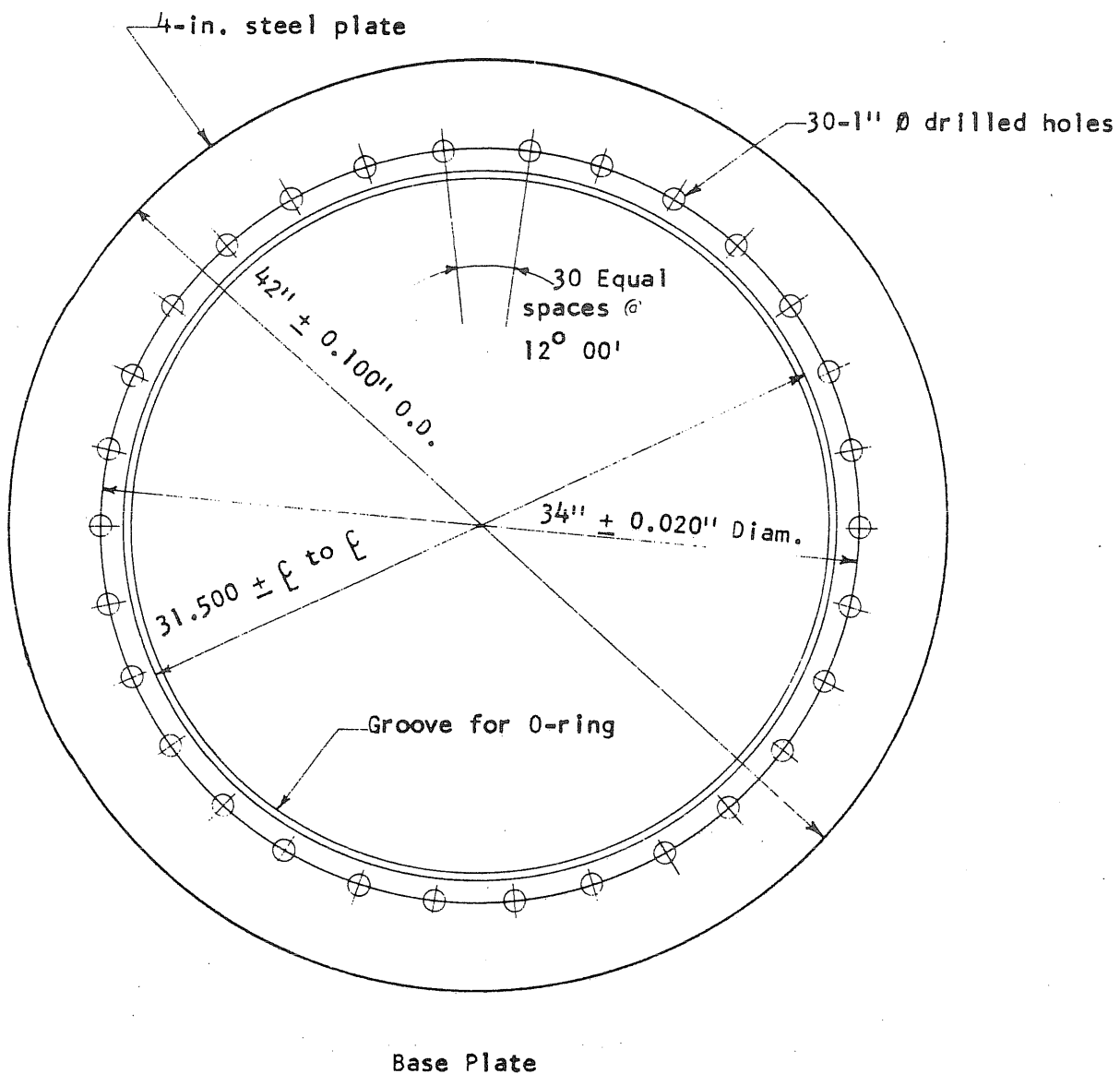
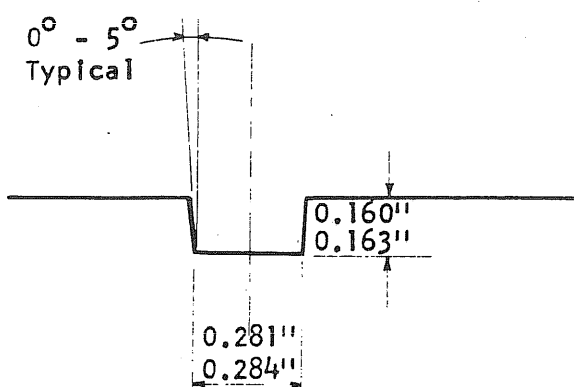


FIG. A14 APPARATUS USED TO PRESTRESS THE STRAND

A34

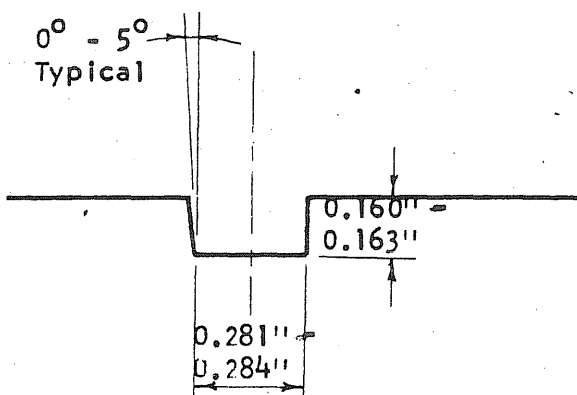
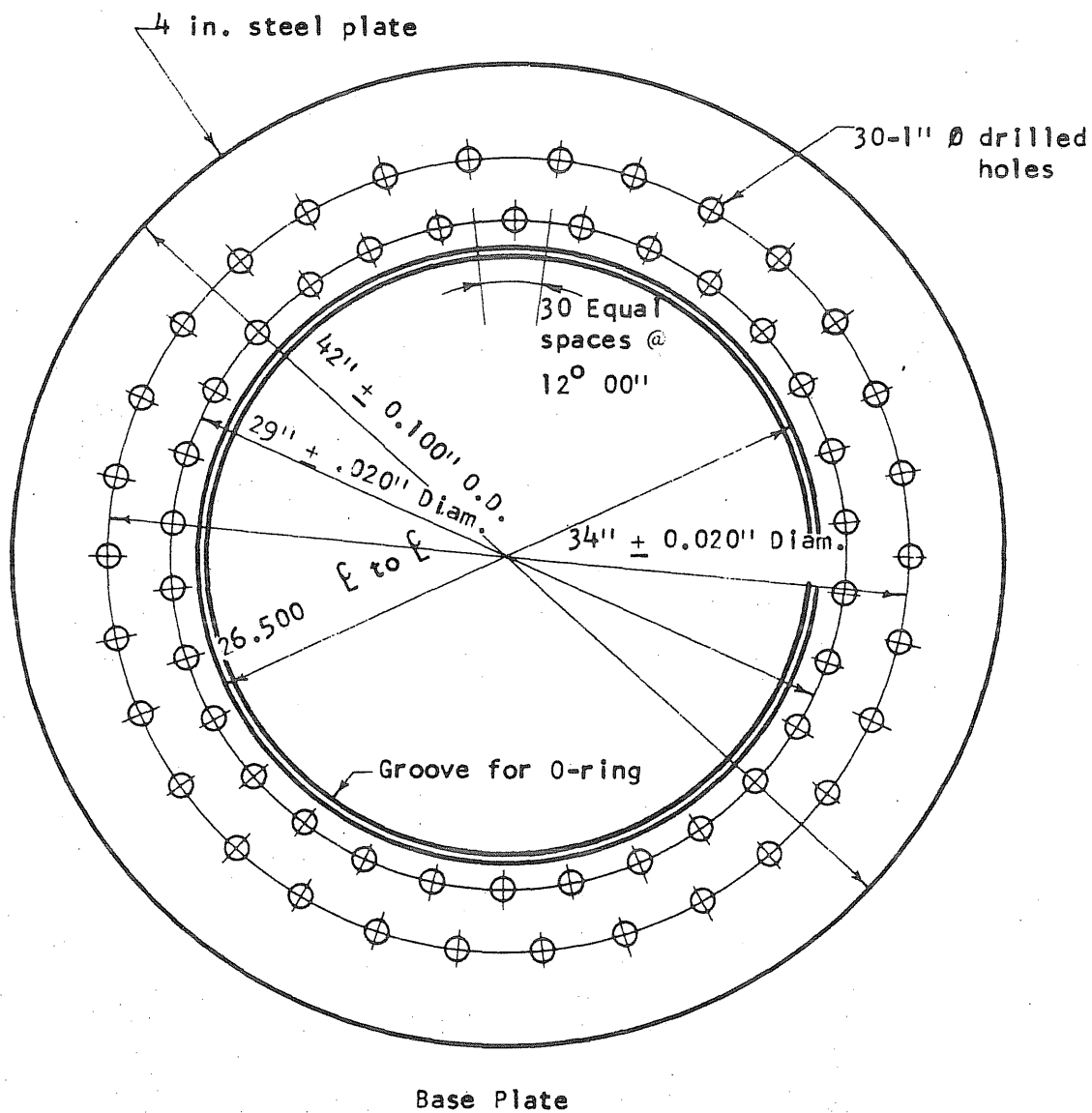


Base Plate



Detail of Groove

FIG. A15a BASE PLATE



Detail of Groove

FIG. A15b Base Plate

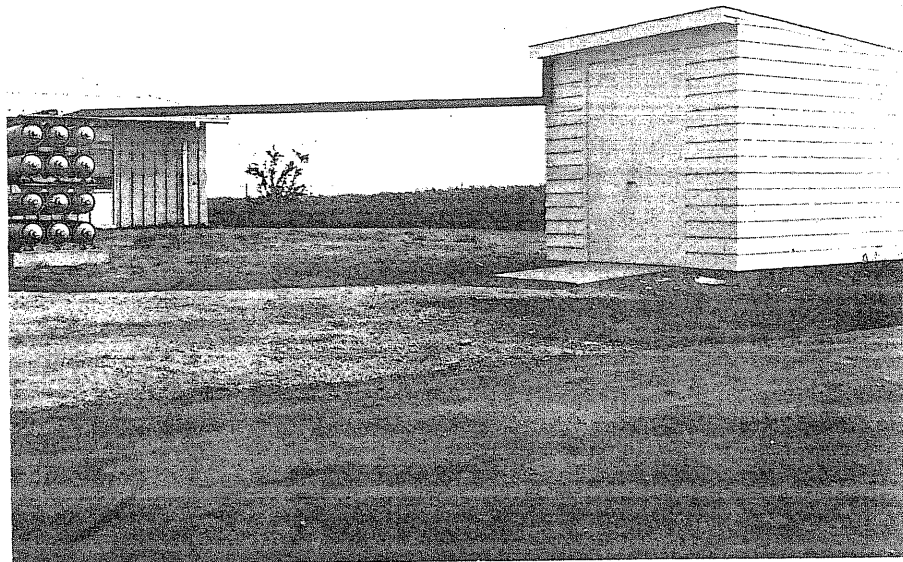


FIG. A16a THE TESTING SHED

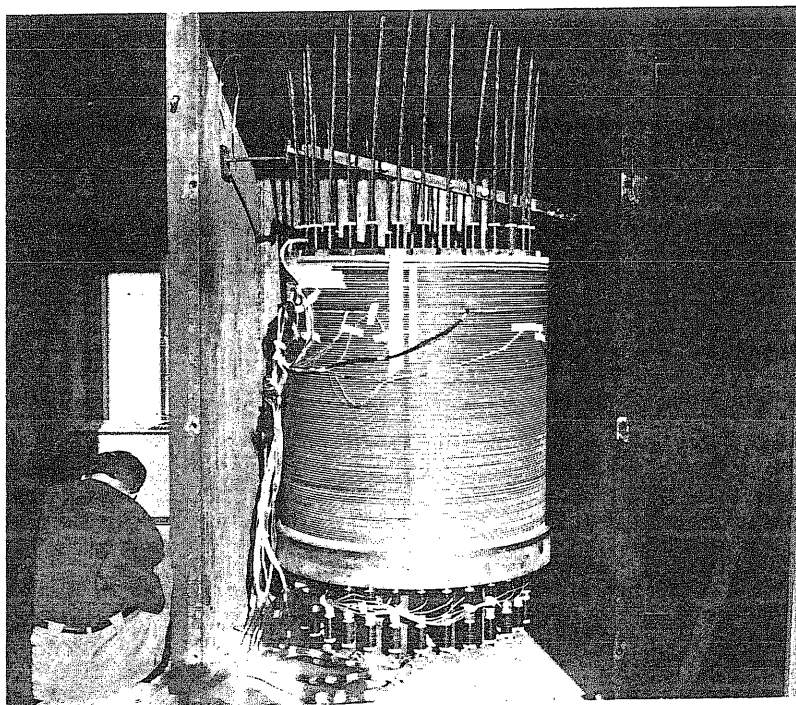


FIG. A16b PV8 IN THE TEST CHAMBER

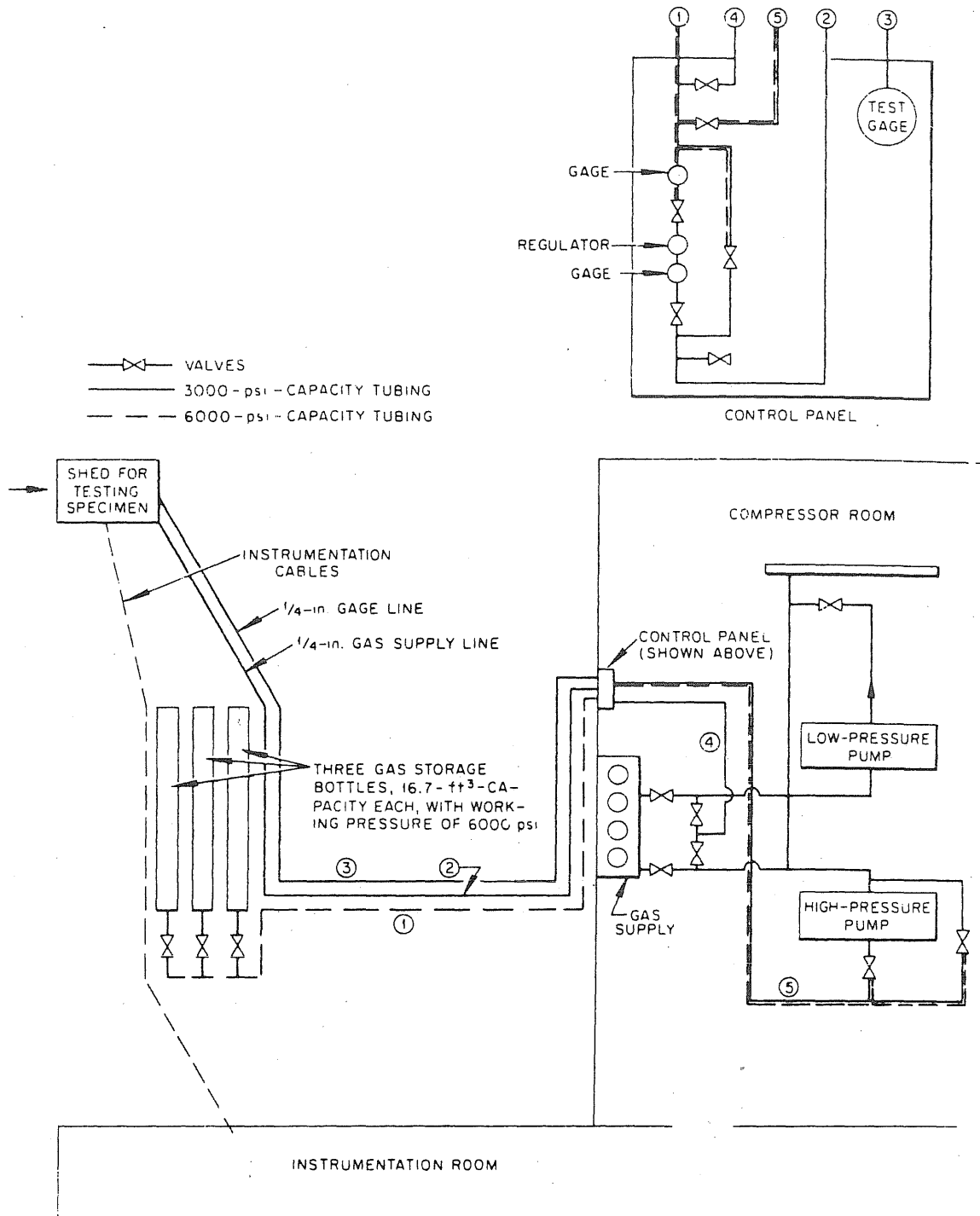


FIG. A17 SCHEMATIC DRAWING OF GAS SUPPLY AND CONTROL SYSTEMS FOR TESTS OF PRESTRESSED-CONCRETE VESSELS

APPENDIX B
TEST DATA

APPENDIX B

TEST DATA

INTRODUCTION

This appendix contains test descriptions and data for each of the 16 vessel tests. The dates of casting, prestressing, and testing of each specimen is recorded in Table B1. Vessel dimensions, prestress data, concrete strength, type of failure, and failure pressure are summarized in Tables 2.1 and 2.2 of the first volume of this report. For convenient reference these tables are repeated as Tables B2 and B3 in this appendix.

The numerical designation of each section corresponds to the designation of the vessel which it describes. Each section consists of a description of the test and descriptive information concerning the vessel and instrumentation, followed by the data resulting from the test in graphic form. The nominal thickness and wire spacing, designated t and s respectively, are given in the captions for each section. Those data which were obviously in error were discarded in order to reduce the volume of material. Some editing of data was performed where it was apparent that the zero for strain shifted, or that an error was made in a reading. The data consists first of deflection information and then concrete strains, circumferential reinforcement strains, and changes in longitudinal reinforcement force. The strain and force measurements presented were started after prestress was completed, and therefore are the result of application of internal pressure.

Development of leaks prevented completion of tests PV6, PV8, and PV11 on the first try. These vessels were resealed and retested; a third attempt was required for PV6 and a fourth for PV11 before failure

was attained. For these three vessels complete data for only the first tests are presented. The sealing details, center deflection of the end slab, and change in load in the longitudinal reinforcement are presented for the final test as well.

The same general arrangement of instrumentation was used for tests PV1 through PV5. A different but consistent arrangement of strain gage locations was used for tests PV6 through PV16 except for PV14 which was different from the other two arrangements. The locations of the gages for each test vessel are shown in the appendix and minor changes in instrumentation may be detected in the descriptive material.

TABLE B1

CHRONOLOGY

| Mark | Casting | Circumferential Prestressing | Longitudinal Prestressing | Testing |
|--------|----------|---------------------------------|------------------------------|----------|
| PV1 | 8-17-67 | 9-23-67 | 10-16-67 | 10-27-67 |
| PV2 | 8-23-67 | 9-23-67 | 12-1-67 | 12-6-67 |
| PV3 | 11-16-67 | 12-15-67 | 12-19-67 | 12-22-67 |
| PV4 | 11-29-67 | 12-15-67 | 1-2-68 | 1-5-68 |
| PV5 | 12-18-67 | 1-9-68 | 1-16-68 | 1-19-68 |
| PV6 | 12-22-67 | 1-9-68 | 1-29-68 | 2-2-68 |
| PV6.1 | -- | -- | 2-6-68 | 2-8-68 |
| PV6.2 | -- | -- | 2-8-68 | 2-8-68 |
| PV7 | 1-4-68 | 1-22-68 | 2-22-68 | 2-27-68 |
| PV8 | 1-10-68 | 1-22-68 | 3-20-68 | 3-26-68 |
| PV8.1 | -- | -- | 3-27-68 | 3-28-68 |
| PV9 | 4-17-68 | 5-2-68 | 6-26-68 | 6-27-68 |
| PV10 | 4-24-68 | 5-2-68 | 6-17-68 | 6-18-68 |
| PV11 | 7-15-68 | 7-31-68 | 9-11-68 | 9-17-68 |
| PV11.1 | -- | -- | 9-23-68 | 9-25-68 |
| PV11.2 | -- | -- | | |
| PV11.3 | -- | -- | | |
| PV12 | 7-19-68 | 7-31-68 | 10-10-68 | 10-16-68 |
| PV13 | 8-14-68 | 9-4-68 | 11-1-68 | 11-6-68 |
| PV14 | 8-19-68 | 9-4-68 | 11-21-68 12-2-68 | 12-4-68 |
| PV15 | 11-7-68 | 11-26-68 | 12-13-68 | 12-16-68 |
| PV16 | 11-12-68 | 11-26-68 | 1-3-69 1-24-69 | 1-28-69 |

TABLE B2

PROPERTIES OF THE TEST VESSELS

| Slab Mark | Thickness in. | Wall Thickness in. | Circum. Prestress | | | Long. Prestress | | | Concrete | | |
|--------------|------------------|--------------------------|-------------------|------------------------|---------------------------|---------------------------------------|------------------------|--------------------------|--------------------------|-----------------------|-----|
| | | | Wire Dia. | Wire Spacing in. | Force per Wire kips | Tendon Number Type ^a | Total Force kips | Comp. Strength psi | Tens. Strength psi | Young's 10^6 psi | |
| PV1 | 6 | 5 | 0.192 | 1.0 | 4.55 | Rod | 10 | 388 | 5680 | 432 | 4.2 |
| PV2 | 6 | 5 | 0.192 | 1.0 | 4.45 | Strand | 24 | 388 | 4955 | 398 | 3.5 |
| PV3 | 7.5 | 5 | 0.192 | 1.0 | 4.68 | Strand | 24 | 392 | 6250 | 450 | 4.2 |
| PV4 | 6 | 5 | 0.102 | 0.67 | 4.49 | Strand | 24 | 583 | 5680 | 380 | 4.2 |
| PV5 | 7.5 | 5 | 0.192 | 0.67 | 4.59 | Strand | 24 | 524 | 6250 | 439 | 4.1 |
| PV6 | 9 | 5 | 0.192 | 0.67 | 4.51 | Strand | 30 | 606 | 5805 | 398 | 4.1 |
| | 6.1 | | | | 4.48 | | | 639 | | | |
| | 6.2 | | | | 4.47 | | 22 | 469 | | | |
| PV7 | 9 | 5 | 0.192 | 0.33 | 4.23 | Strand | 30 | 693 | 6720 | 506 | 4.6 |
| PV8 | 7.5 | 5 | 0.192 | 0.33 | 4.09 | Strand | 30 | 626 | 7230 | 443 | 4.8 |
| | 8.1 | | | | | | | 700 | | | |
| PV9 | 9 | 5 | 0.192 | 0.33 | 4.10 | Strand | 30 | 750 | 7140 | 446 | 4.3 |
| PV10 | 7.5 | 5 | 0.192 | 0.33 | 4.12 | Strand | 30 | 750 | 7005 | 394 | 4.0 |
| PV11 | 7.5 | 7.5 | 0.250 | 0.25 | 6.06 | Rod | 30 ^b | 694 | 6830 | 504 | 4.5 |
| | 11.1 | | | | 5.72 | | | 1030 | | | |
| PV12 | 10 | 7.5 | 0.250 | 0.25 | 5.73 | Rod | 30 | 727 | 5860 | 456 | 4.4 |
| PV13 | 12.5 | 7.5 | 0.250 | 0.25 | 5.82 | Rod | 60 | 1356 | 6750 | 490 | 4.2 |
| PV14 | 15 | 7.5 | 0.250 | 0.25 | 5.56 | Rod | 60 | 1370 | 6880 | 465 | 4.3 |
| PV15 | 7.5 | 7.5 | 0.250 | 0.25 | 6.47 | Rod | 60 | 1200 | 7340 | 531 | 4.2 |
| PV16 | 10 | 7.5 | 0.250 | 0.25 | 5.94 | Rod | 60 | 1995 | 7450 | 518 | 4.0 |

^a0.75-in. round Stressteel rods or 0.5-in. round seven-wire strand^bThis vessel was prestressed longitudinally with 28 rods and two lengths of strand.

TABLE B3
MEASURED INTERNAL PRESSURES AT FAILURE

| Mark | Span | Wall | Concrete | Circum. | Long. | Pressure | Mode |
|--------|-----------------------------------|-----------|------------|------------------------------|------------------------------|------------|-------------------------|
| | | Thickness | Strength | Prestress Index ^b | Prestress Index ^c | at Failure | of Failure ^d |
| | Slab Thickness ratio ^a | in. | f'c psi | ksi | ksi | psi | |
| PV1 | 5 | 5 | 5680 | 0.30 | 0.55 | 295 | F |
| PV2 | 5 | 5 | 4955 | 0.30 | 0.55 | 240 | FL |
| PV3 | 4 | 5 | 6250 | 0.31 | 0.55 | 370 | F |
| PV4 | 5 | 5 | 5650 | 0.45 | 0.82 | 390 | F |
| PV5 | 4 | 5 | 6250 | 0.46 | 0.74 | 465 | F |
| PV6 | 3.3 | 5 | 5805 | 0.45 | 0.86 | 570 | L |
| PV6.1 | | | | | 0.90 | 585 | L |
| PV6.2 | | | | | 0.66 | 555 | F |
| PV7 | 3.3 | 5 | 6720 | 0.84 | 0.98 | 870 | F |
| PV8 | 4 | 5 | 7230 | 0.82 | 0.84 | 625 | L |
| 8.1 | | | | | 0.99 | 640 | F |
| PV9 | 3.3 | 5 | 7140 | 0.82 | 1.06 | 887 | F |
| PV10 | 4 | 5 | 7005 | 0.87 | 1.06 | 740 | F |
| PV11 | 3.3 | 7.5 | 6830 | 1.94 | 1.41 | 1600 | L |
| PV11.1 | | | | 1.83 | 2.10 | 2040 | S |
| PV12 | 2.5 | 7.5 | 5860 | 1.83 | 1.48 | 2650 | CL |
| PV13 | 2 | 7.5 | 6750 | 1.86 | 2.76 | 3450 | VL |
| PV14 | 1.67 | 7.5 | 6880 | 1.78 | 2.79 | 3690 | VL |
| PV15 | 3.3 | 7.5 | 7340 | 2.07 | 2.44 | 2300 | S |
| PV16 | 2.5 | 7.5 | 7450 | 1.90 | 4.06 | 3200 | S |

^aRatio of internal diameter to slab thickness

^bRatio of circumferential prestressing force per unit length to the internal diameter

^cRatio of total longitudinal prestressing force to area of cavity at a transverse section

F: Flexural failure of end slab

S: Shear failure of end slab

L: Liner leakage

FL: Test stopped by liner leakage at incipient failure in flexure

CL: Leakage caused by circumferential cracking in the side wall

VL: Leakage caused by longitudinal cracking in the side wall

B1. Test Vessel PV1 ($t = 6.0$ in., $s = 1.0$ in.)PV1

Test vessel PV1 was cast from ready-mix concrete and was nearly two months old at the time of the test. When the form was struck, a circumferential crack in the side wall immediately below the end slab was observed inside the specimen. The cause of this crack was evidently the settlement of the concrete after casting while it was still plastic.

The testing of PV1 was completed without any problems. The test chamber had been lined with 3/4-in. plywood, and the hatch was covered with a single layer of steel netting. Both of these measures proved to be insufficient to restrain the force of the explosion when the vessel failed at 295 psi. A photograph showing the damage is given in Fig. B1.21a.

The entire test lasted about three hours. The pressure was increased in increments of 25 psi up to 100 psi, when the increment of loading was decreased to 20 psi. The final cracking mode is illustrated by a photograph of the pieces of the end slab which were reassembled after the test (Fig. B1.21b).

Vessel PV1 was prestressed longitudinally with 3/4-in. Stressteel rods. Nine of the ten rods in the vessel had been instrumented with strain gages and calibrated. These were monitored during the test.

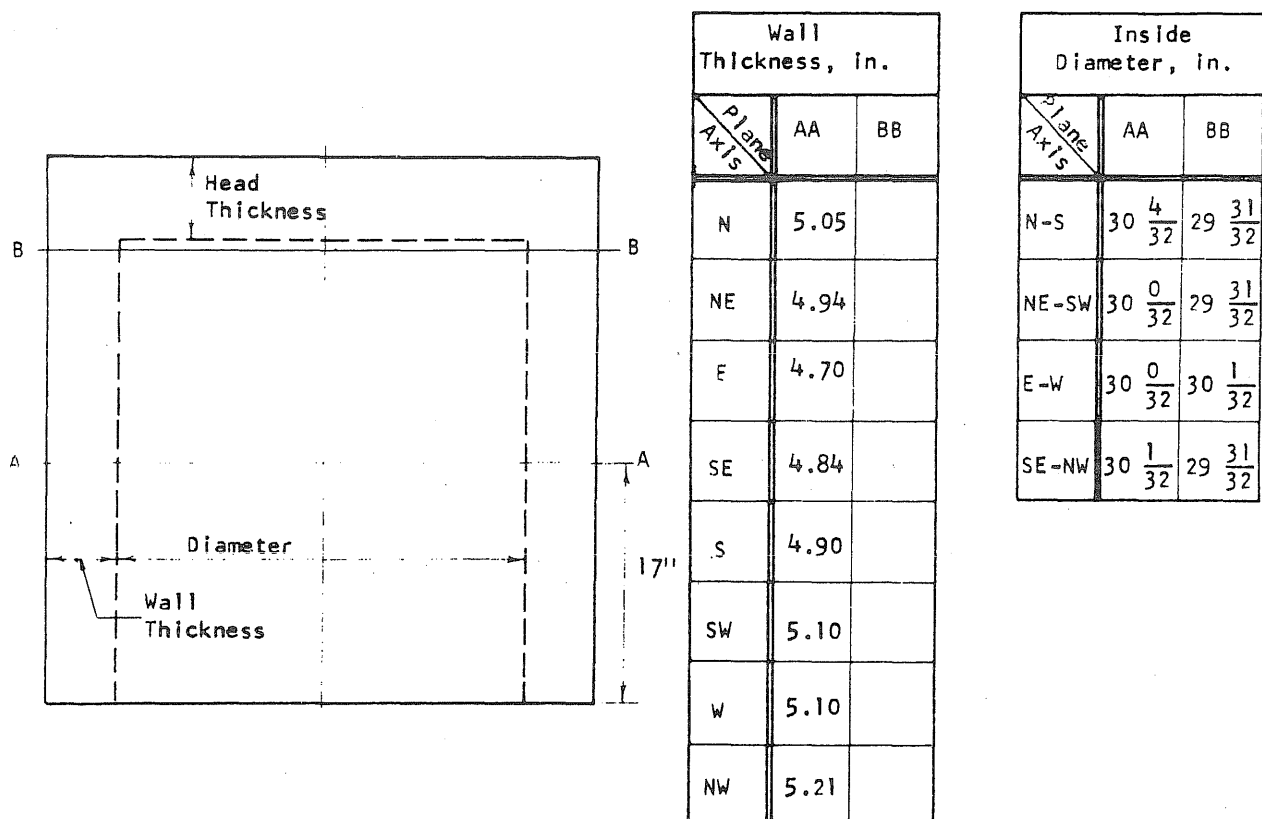


FIG. B1.1 DIMENSIONS OF PVI

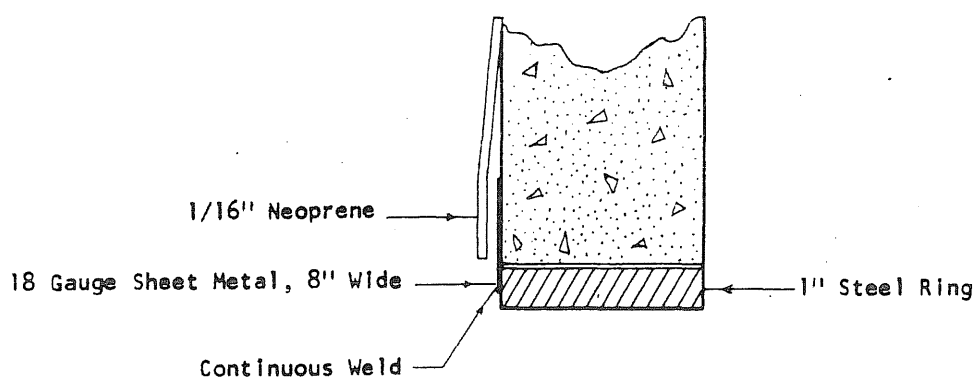
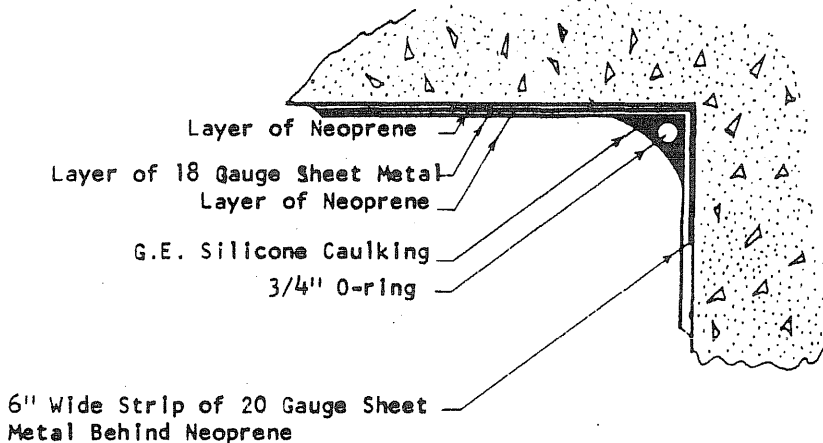
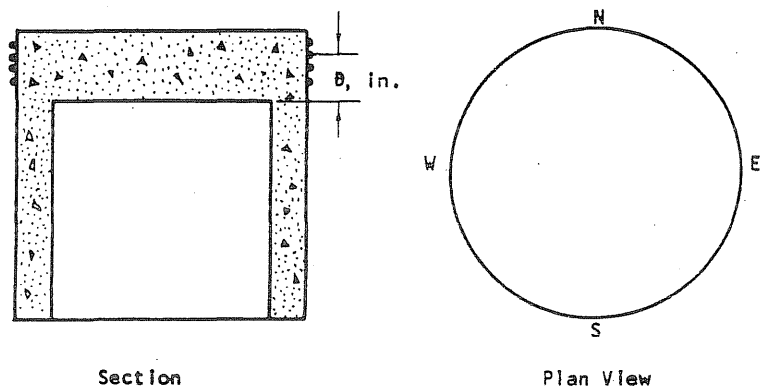


FIG. B1.2 SEALING DETAIL FOR PVI

B8



| Wrap No. | D_N | D_E | D_S | D_W |
|----------|-------|-------|-------|-------|
| 1 | 5 3/8 | 5 | 5 | 5 2/8 |
| 2 | 4 7/8 | 3 7/8 | 4 6/8 | 4 4/8 |
| 3 | 3 5/8 | 2 7/8 | 3 1/8 | 3 3/8 |
| 4 | 2 4/8 | 1 7/8 | 2 1/8 | 2 3/8 |
| 5 | 1 4/8 | 7/8 | 1 | 1 1/4 |
| 6 | 4/8 | -1/8 | 0 | 1/4 |

FIG. B1.3 MEASURED LOCATION OF THE CIRCUMFERENTIAL PRESTRESS WIRE AT THE ENDS OF THE N-S AND E-W DIAMETERS ON PVI

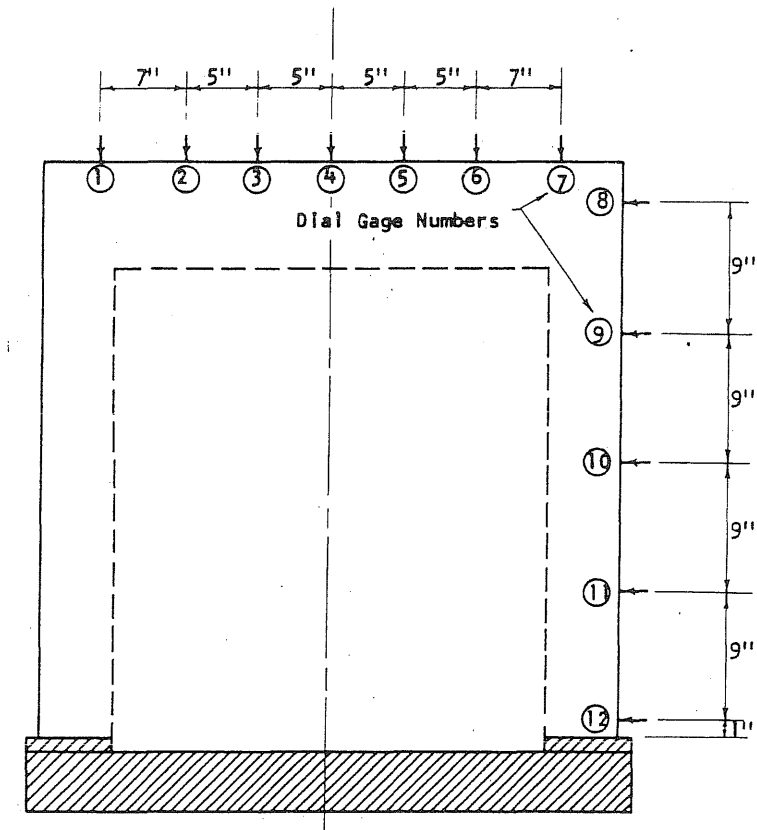


FIG. B1.4 LOCATION OF DEFLECTION GAGES ON PVI

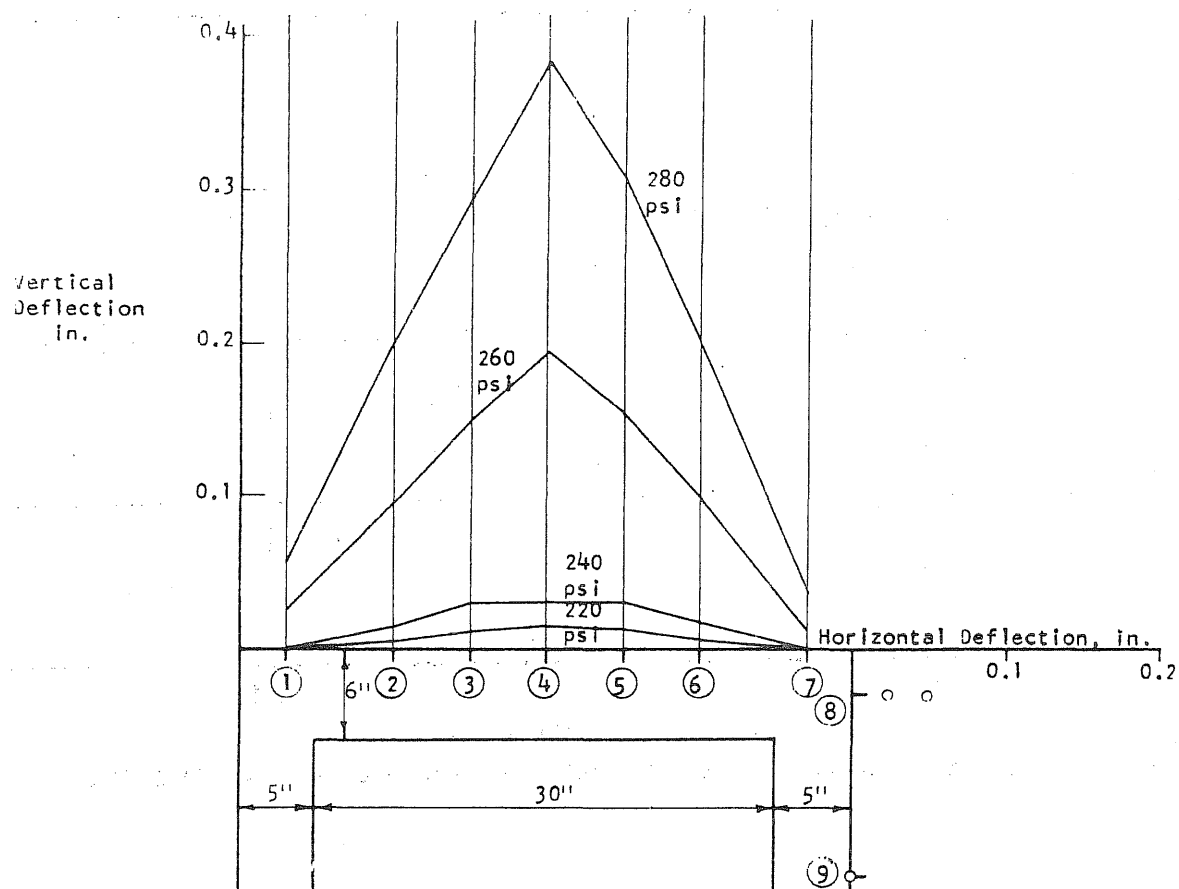


FIG. B1.5 DEFLECTION PROFILES OF THE END SLAB ALONG THE N-S DIAMETER OF PVI

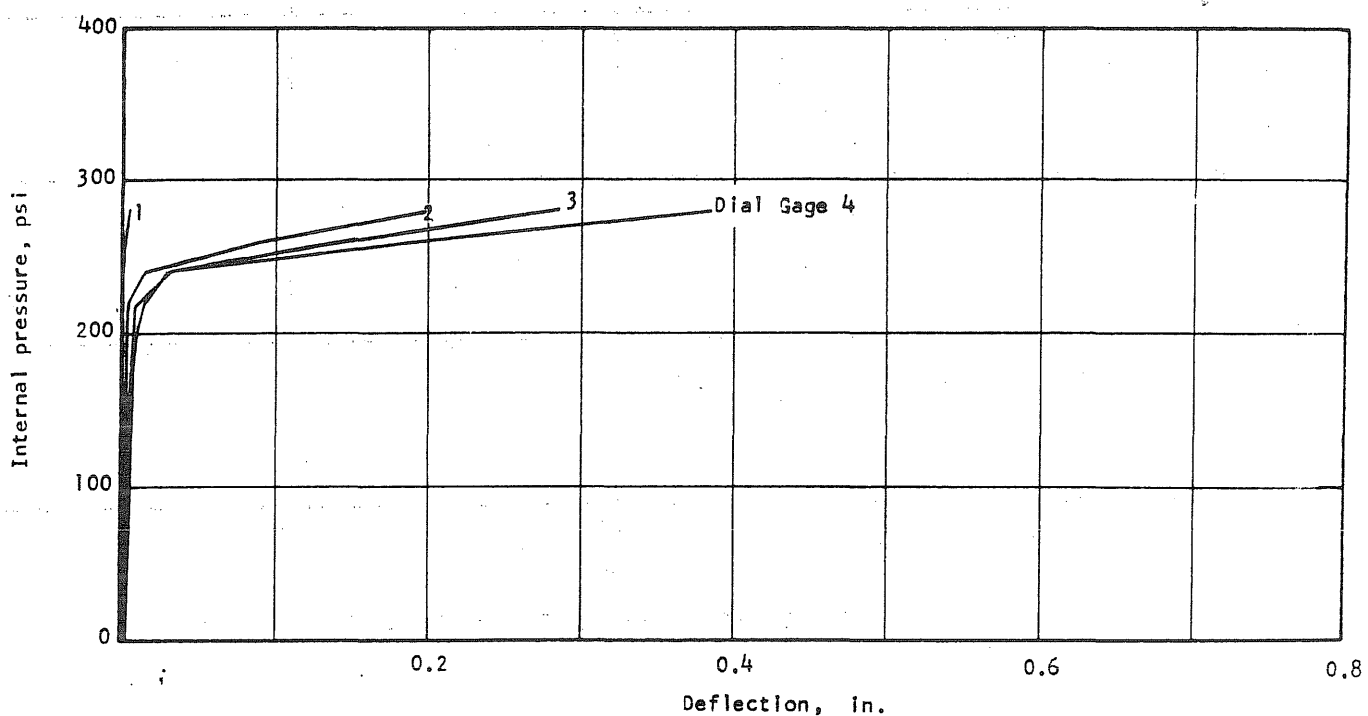


FIG. B1.6 APPLIED PRESSURE VS DEFLECTION ALONG THE N-HALF OF THE N-S DIAMETER OF PVI

Internal pressure, psi

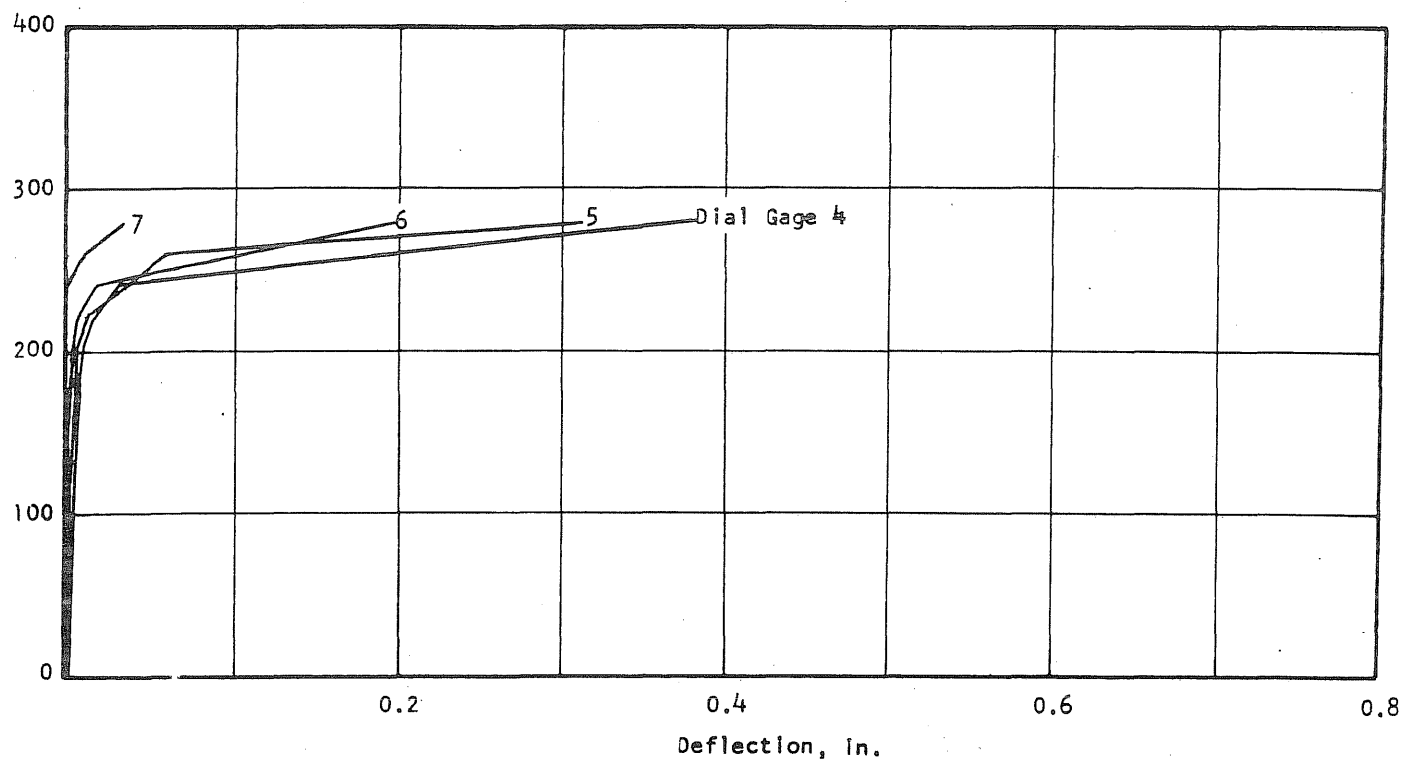


FIG. B1.7 APPLIED PRESSURE VS DEFLECTION ALONG THE S-HALF OF THE N-S DIAMETER OF PVI

Internal pressure, psi

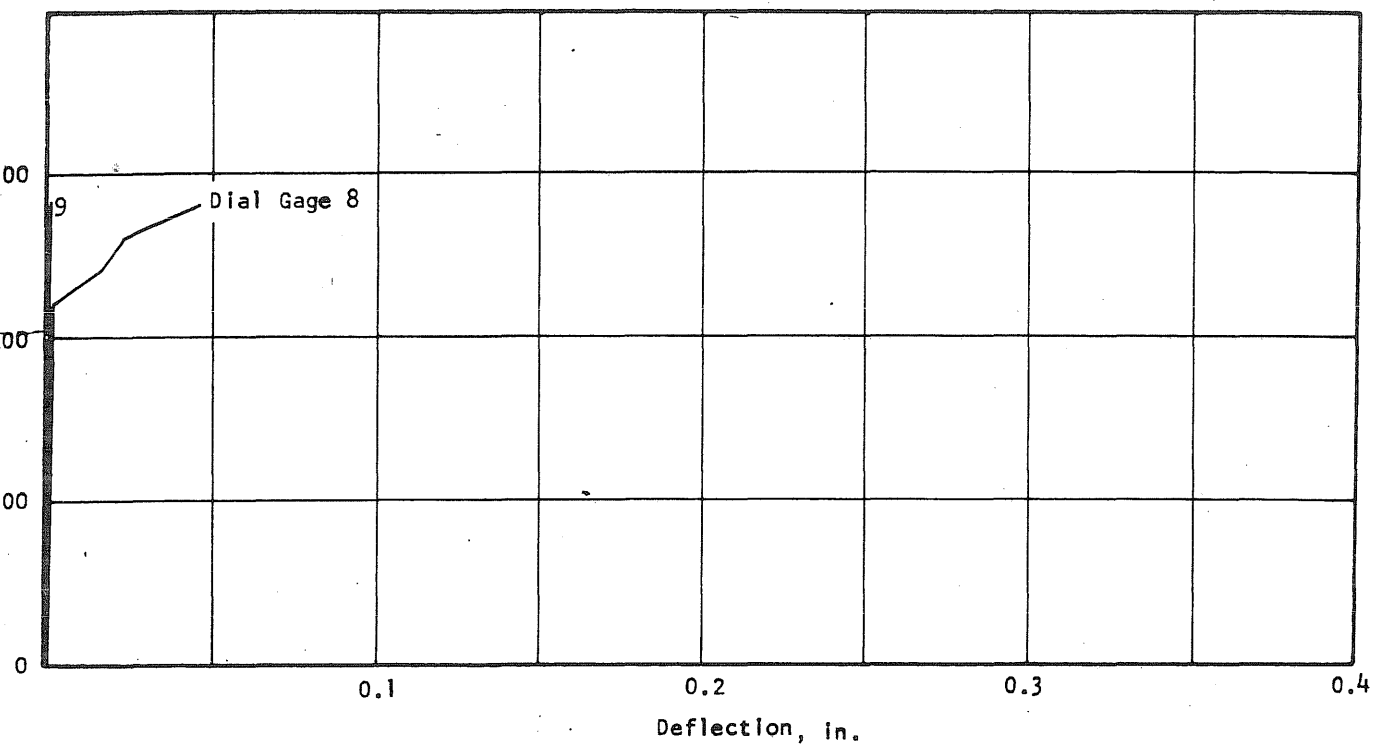
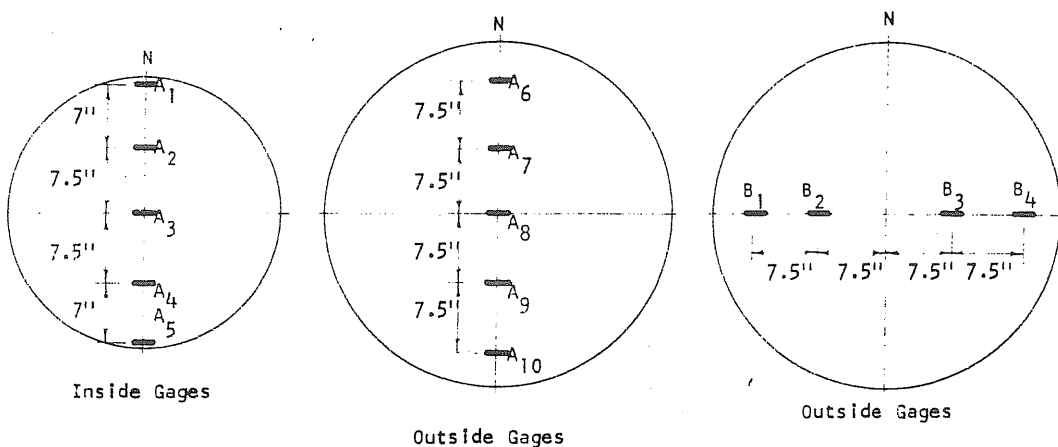
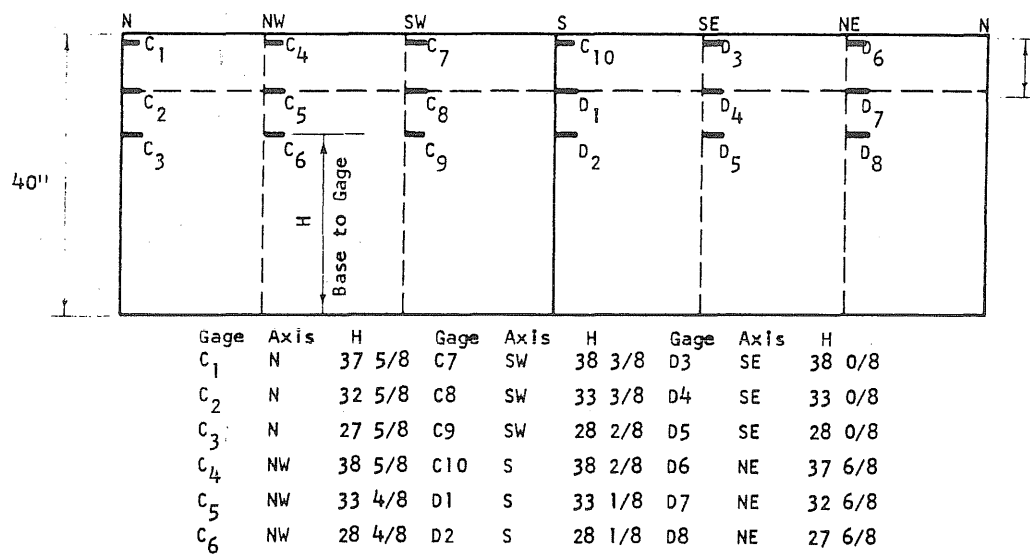


FIG. B1.8 APPLIED PRESSURE VS DEFLECTION OF THE SIDE WALL ON PVI

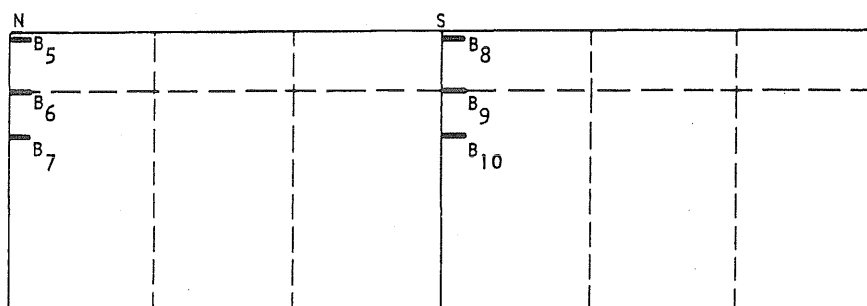
B II
Concrete Gages on The Slab



Steel Gages on Prestressing Wire



Concrete Gages on The Outside of the Vessel



| Gage | Axis | H | Gage | Axis | H |
|----------------|------|--------|-----------------|------|--------|
| B ₅ | N | 37 0/8 | B ₈ | S | 37 6/8 |
| B ₆ | N | 32 1/8 | B ₉ | S | 32 6/8 |
| B ₇ | N | 27 0/8 | B ₁₀ | S | 27 6/8 |

FIG. B1.9 STRAIN GAGE LOCATIONS ON PVI

B12

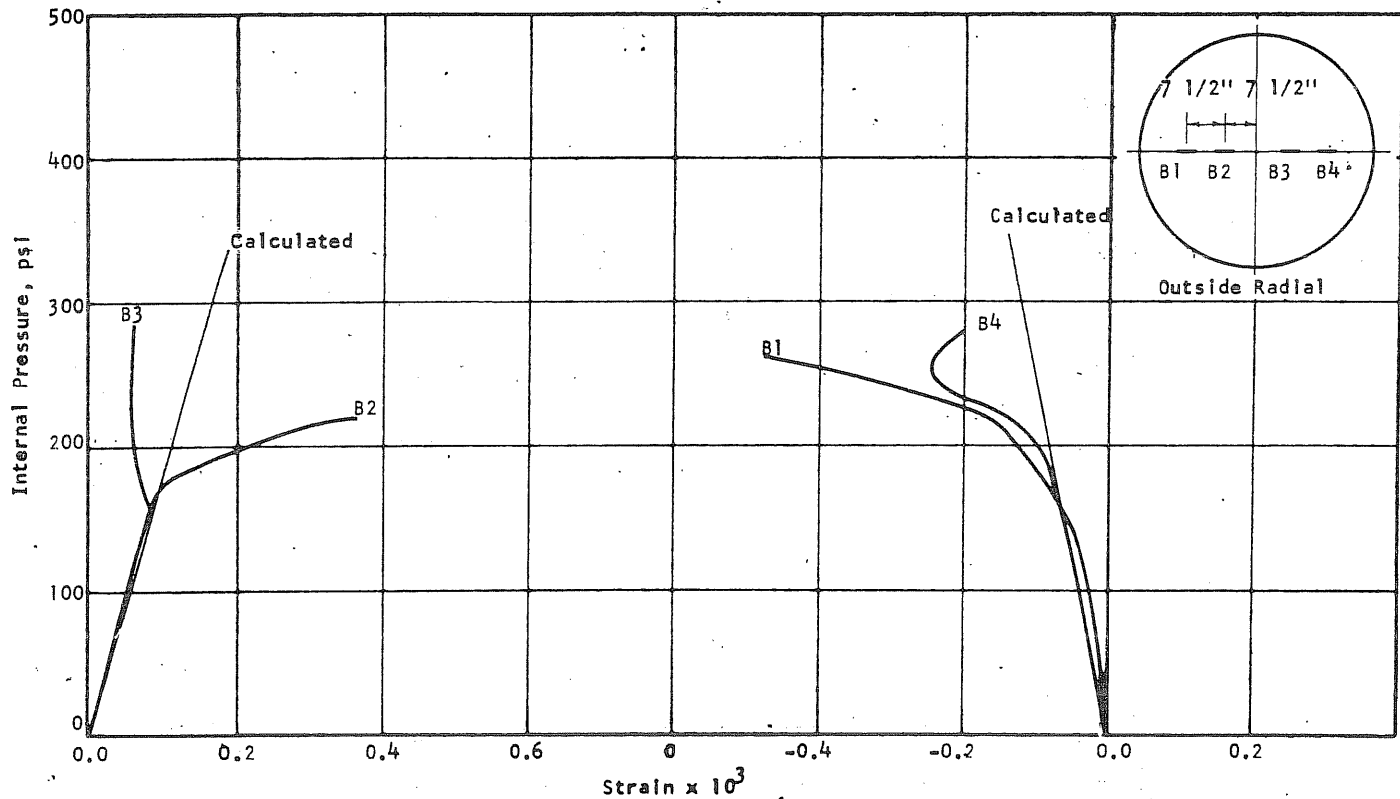


FIG. B1.10 CONCRETE STRAINS, VESSEL PV1

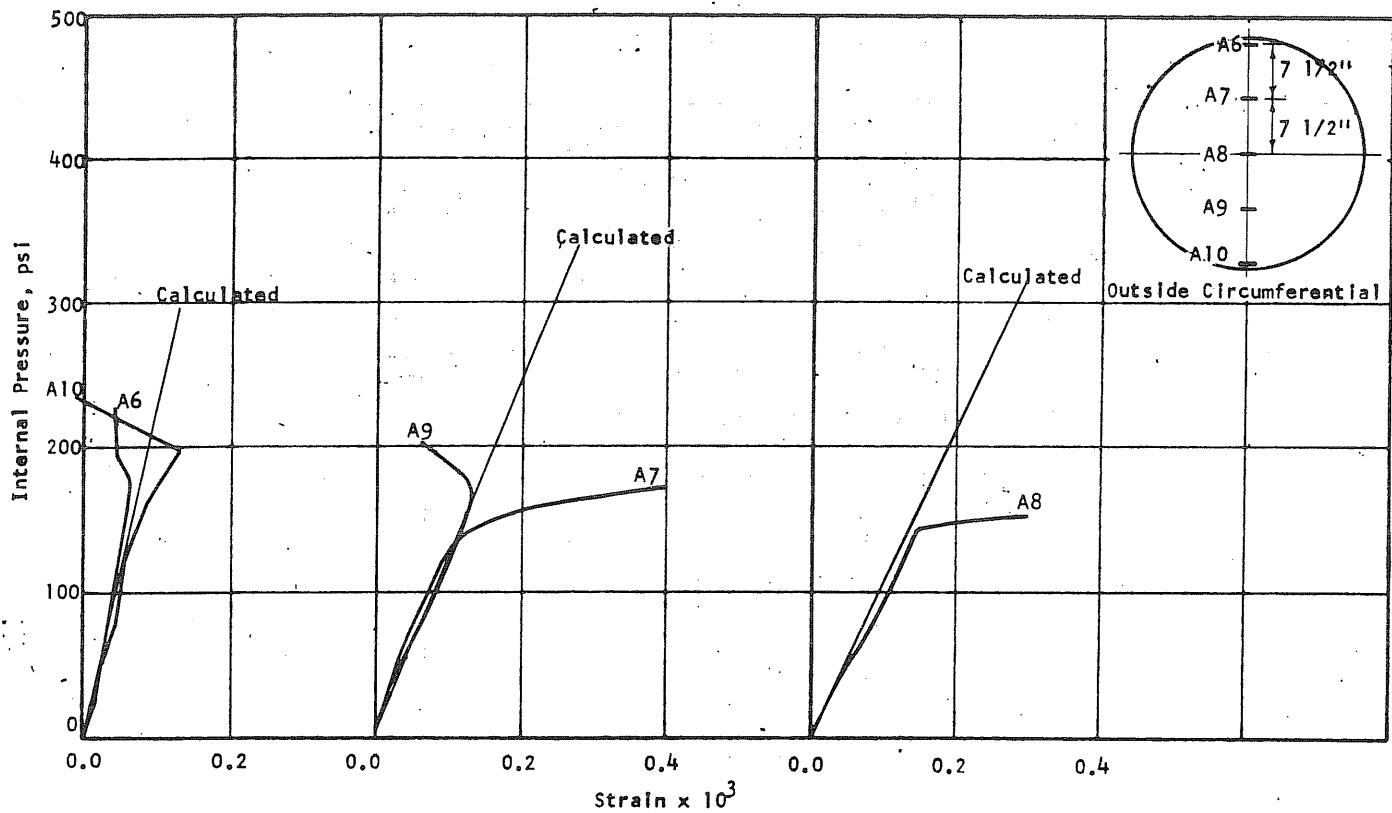


FIG. B1.11 CONCRETE STRAINS, VESSEL PV1

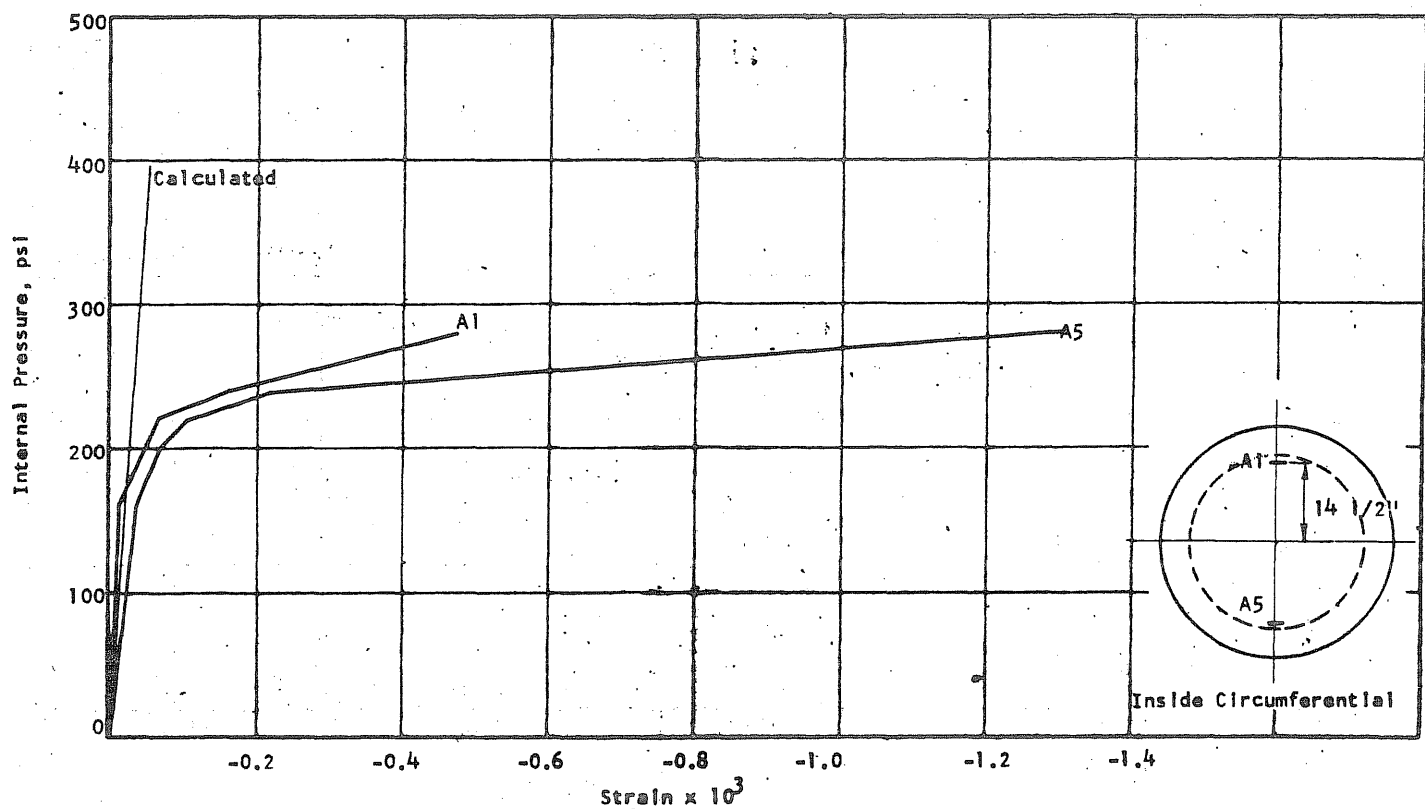


FIG. B1.12 CONCRETE STRAINS, VESSEL PVI

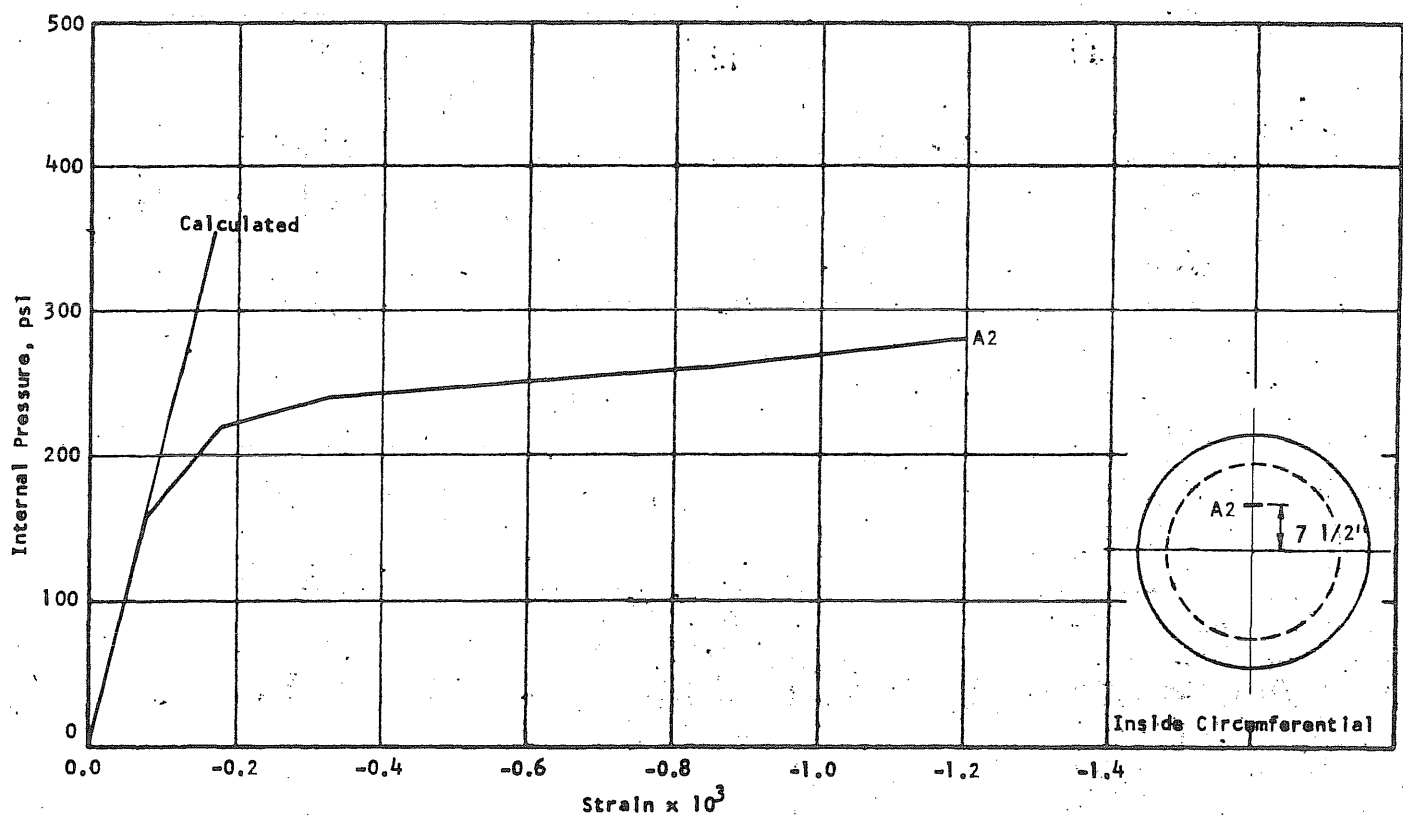


FIG. B1.13 CONCRETE STRAINS, VESSEL PVI

B14

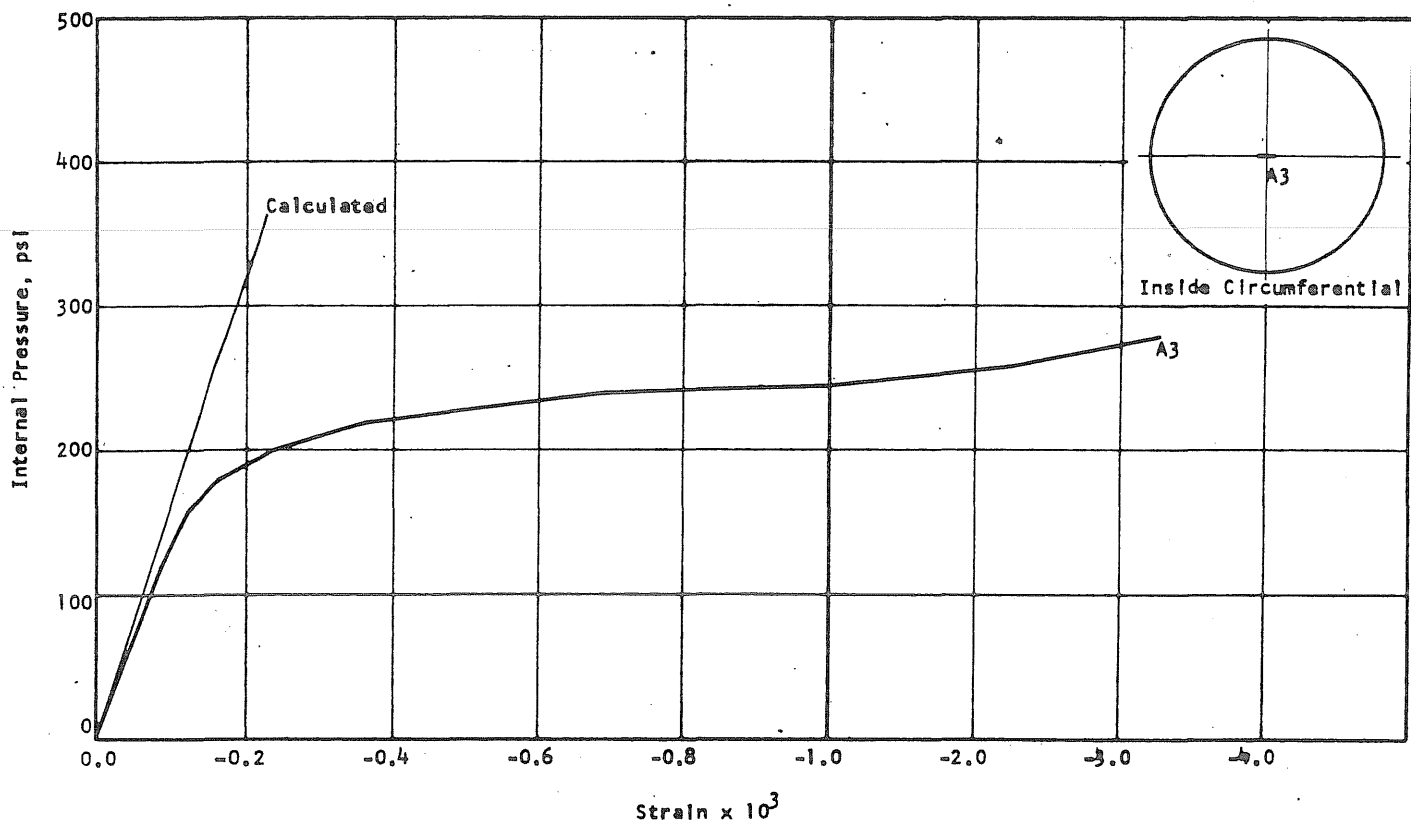


FIG. B1.14 CONCRETE STRAINS, VESSEL PVI

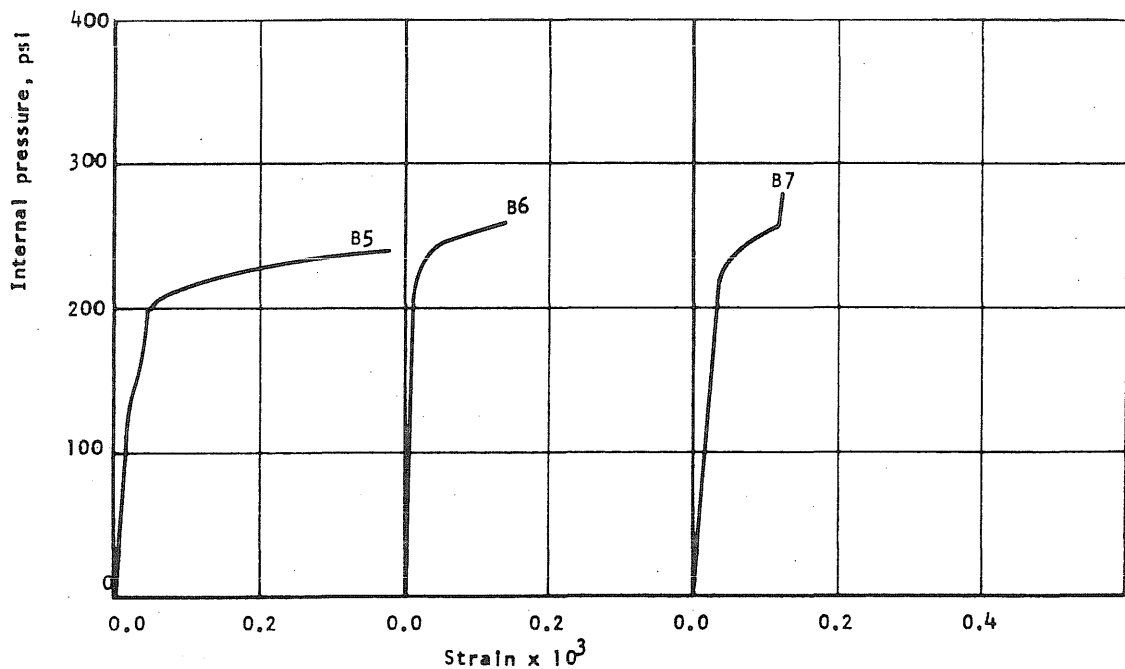


FIG. B1.15 APPLIED PRESSURE vs CIRCUMFERENTIAL STRAIN IN THE WALL OF THE VESSEL AT THE N-END OF THE N-S DIAMETER OF PVI

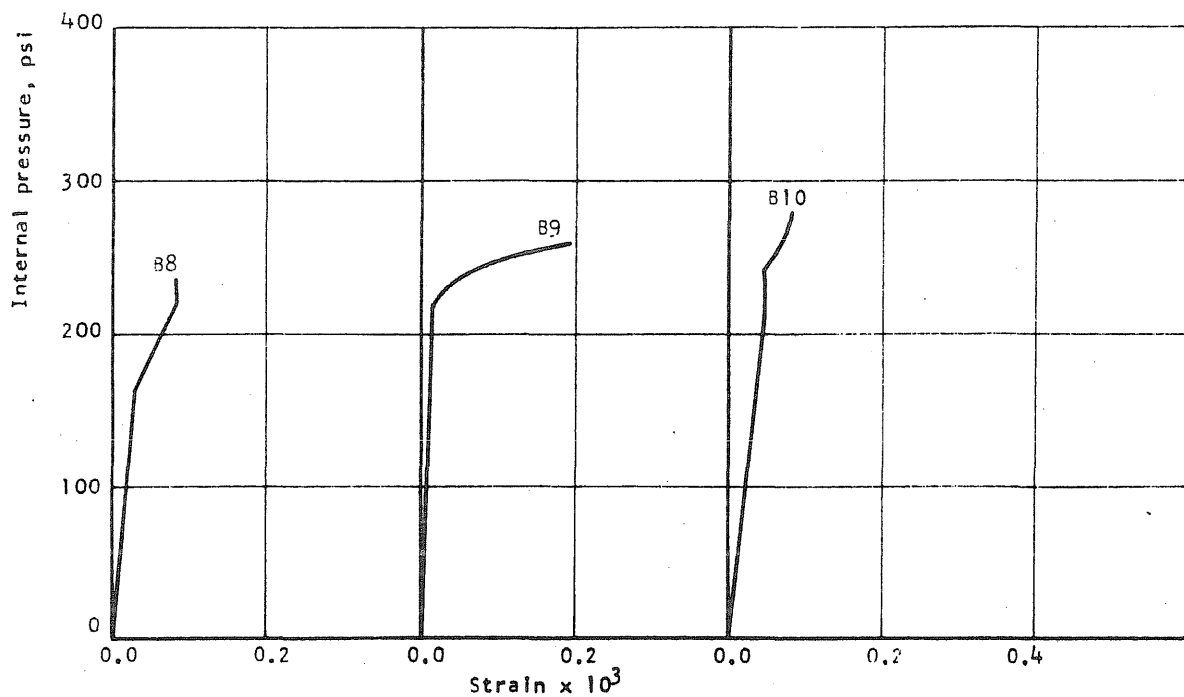


FIG. B1.16 APPLIED PRESSURE vs CIRCUMFERENTIAL STRAIN IN THE WALL OF VESSEL AT THE S-END OF THE N-S DIAMETER OF PVI

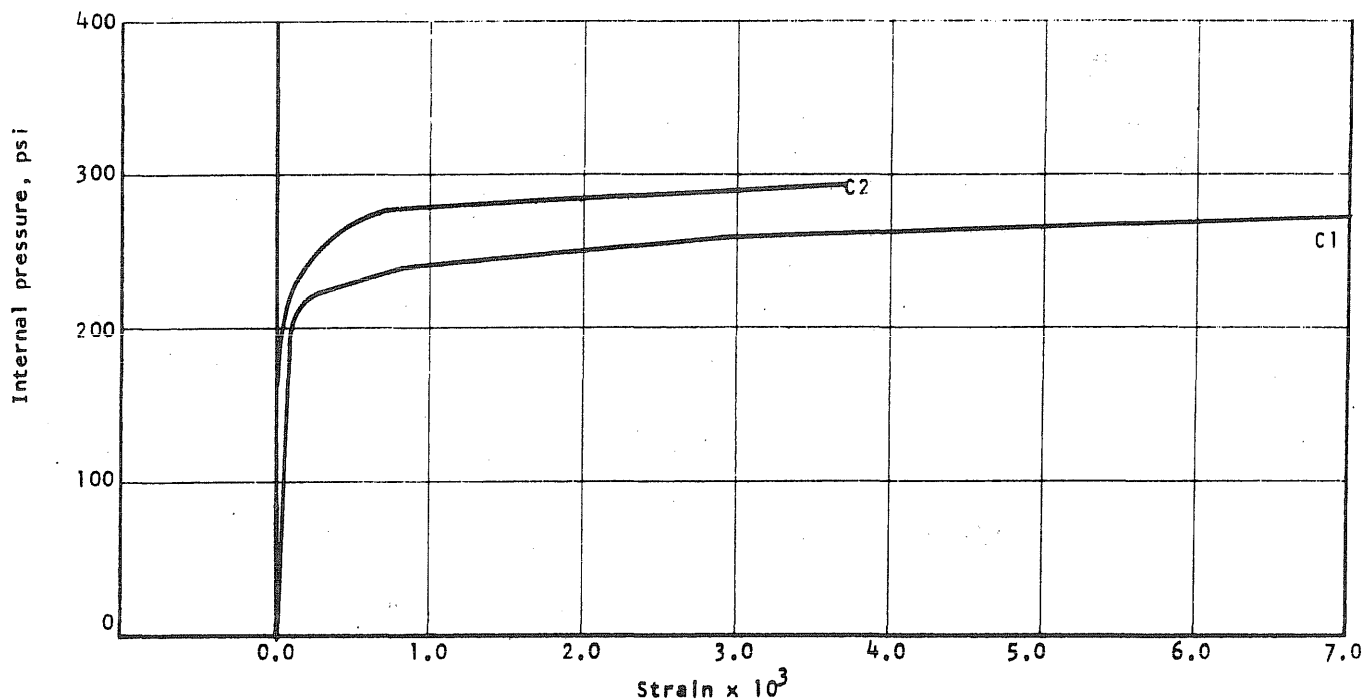


FIG. B1.17 APPLIED PRESSURE vs STRAIN IN THE CIRCUMFERENTIAL PRESTRESS WIRE AT THE N-END OF THE N-S DIAMETER OF PVI

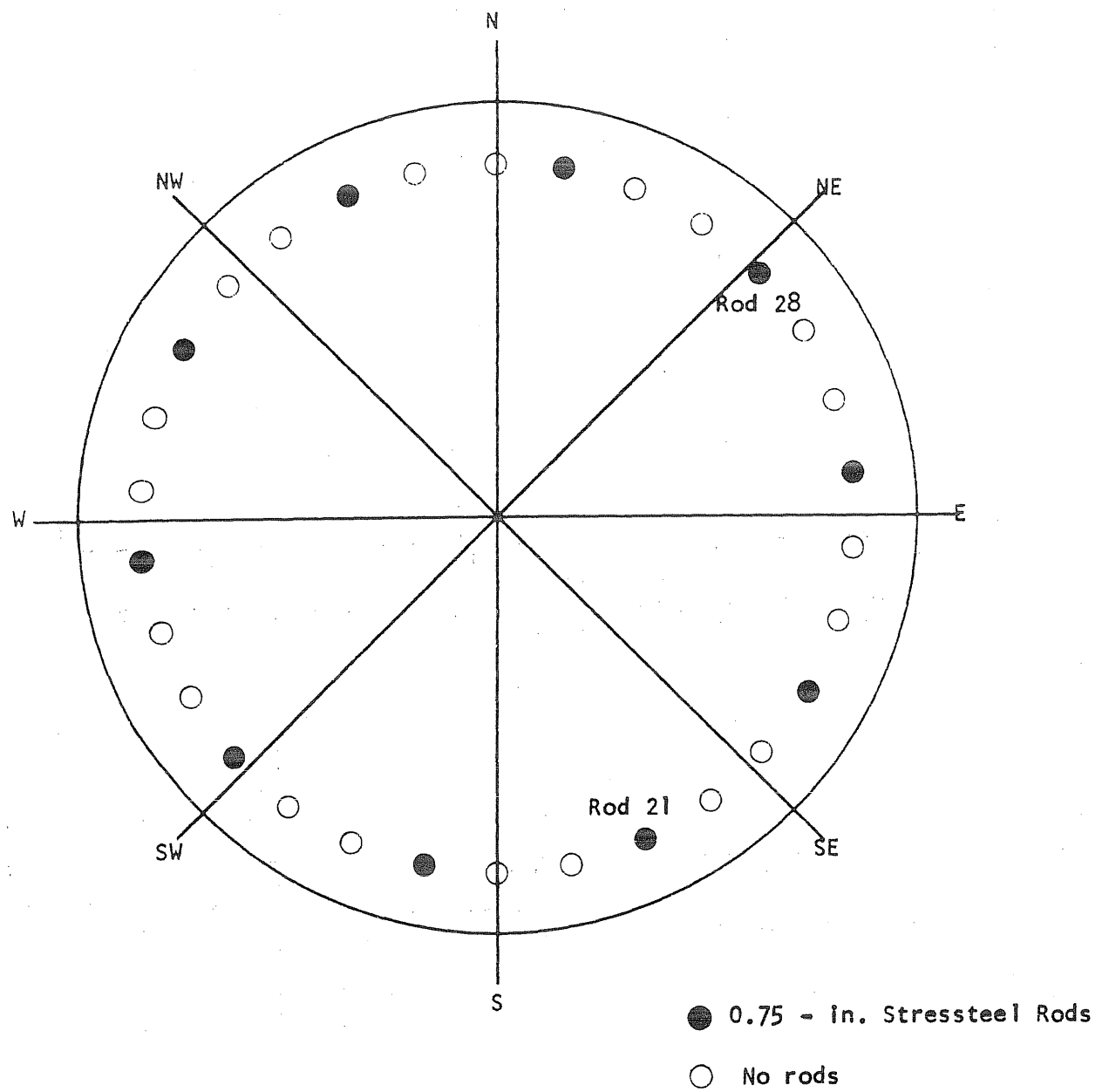


FIG. B1.18 LOCATION OF LONGITUDINAL REINFORCEMENT

B17

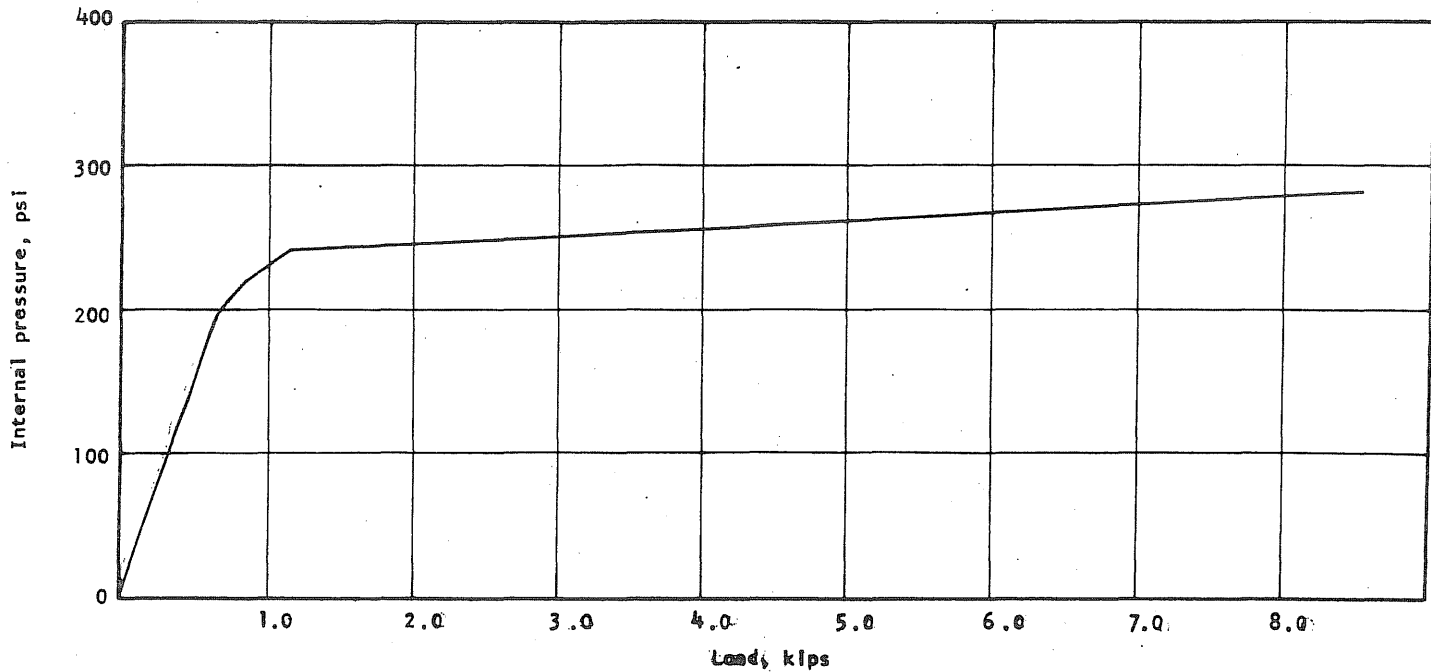


FIG. B1.19 APPLIED PRESSURE VS THE INCREASE IN LOAD IN STRESSTEEL ROD 28 IN PVI

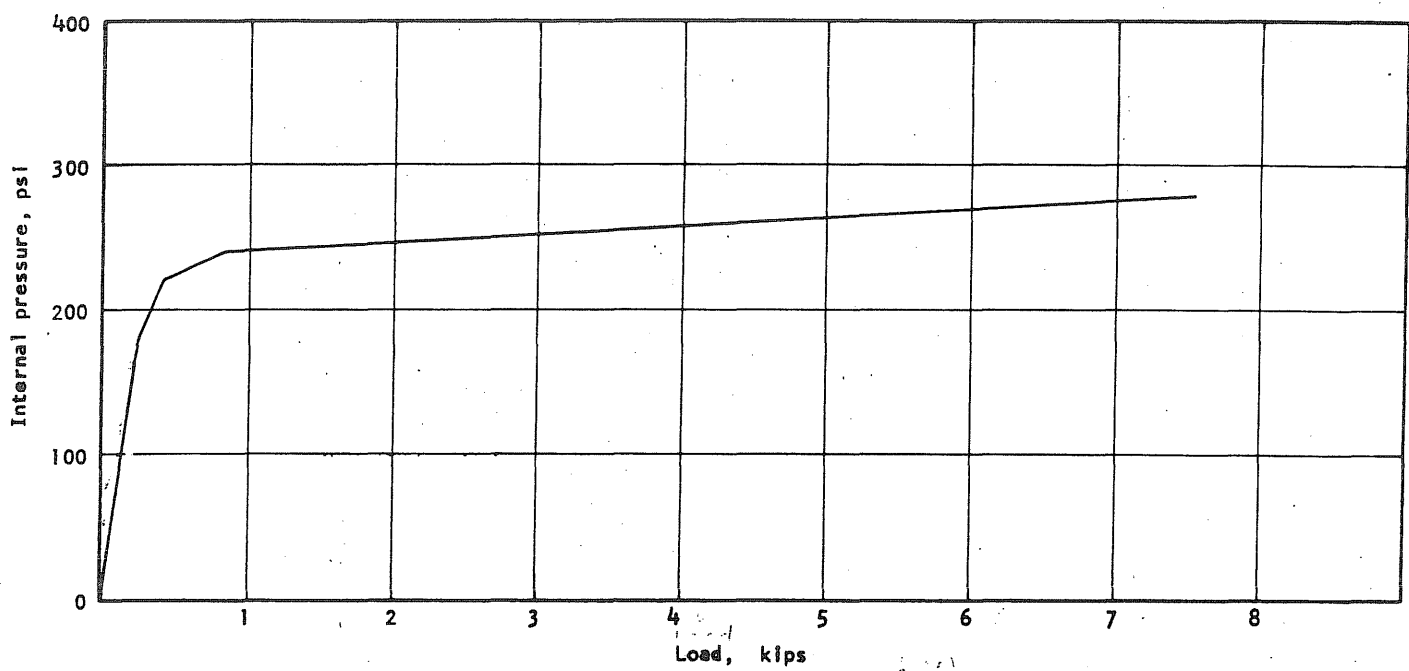


FIG. B1.20 APPLIED PRESSURE VS THE INCREASE IN LOAD IN STRESSTEEL ROD 21 IN PVI

B18

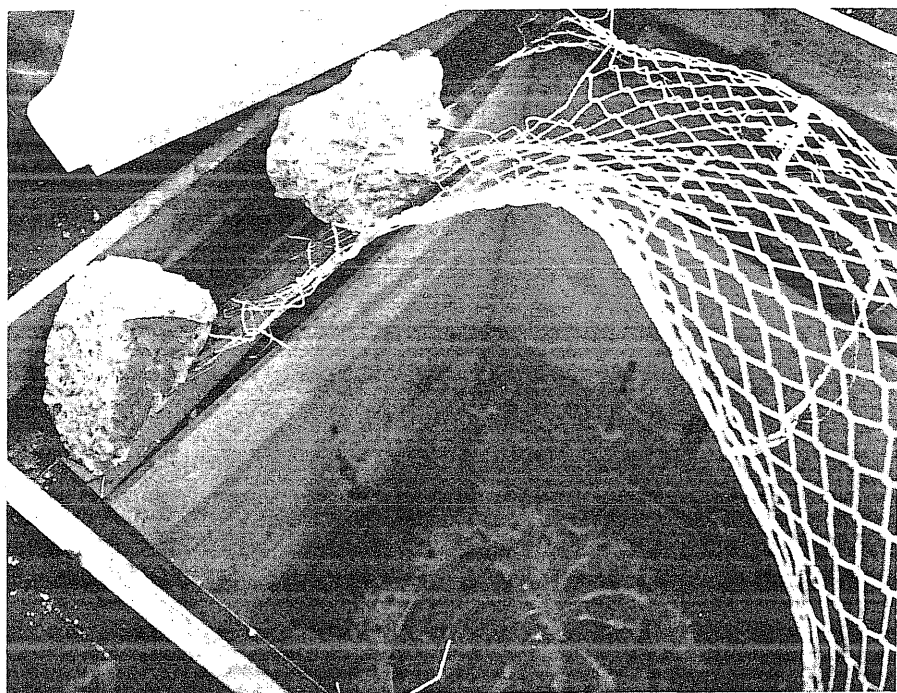


FIG. B1.21a DAMAGE TO NETTING AND PLYWOOD LINER

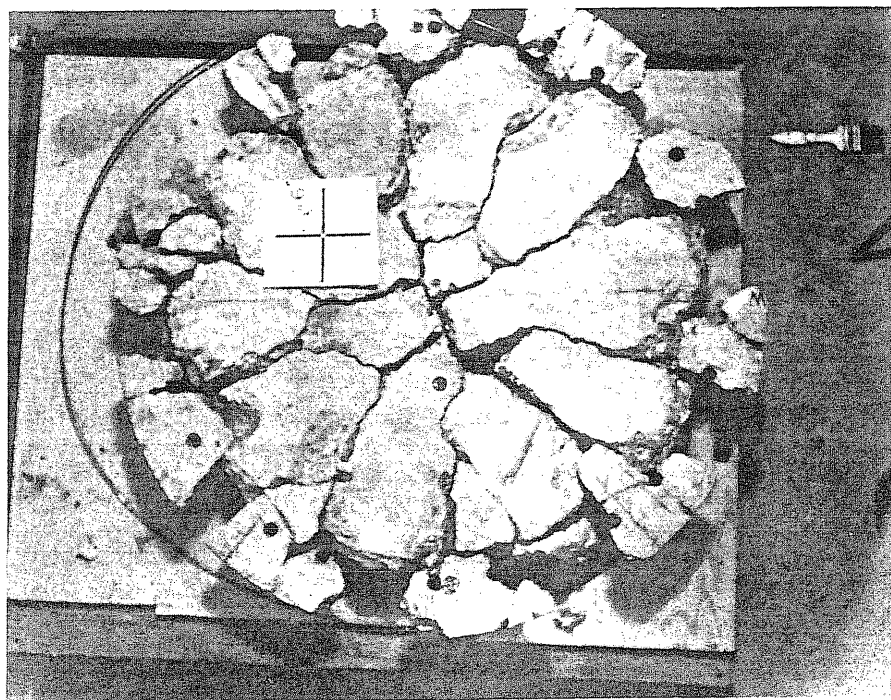


FIG. B1.21b REASSEMBLED PIECES OF THE END SLAB OF PV1

B2 Test Vessel PV2 ($t = 6$ in., $s = 1.0$ in.)

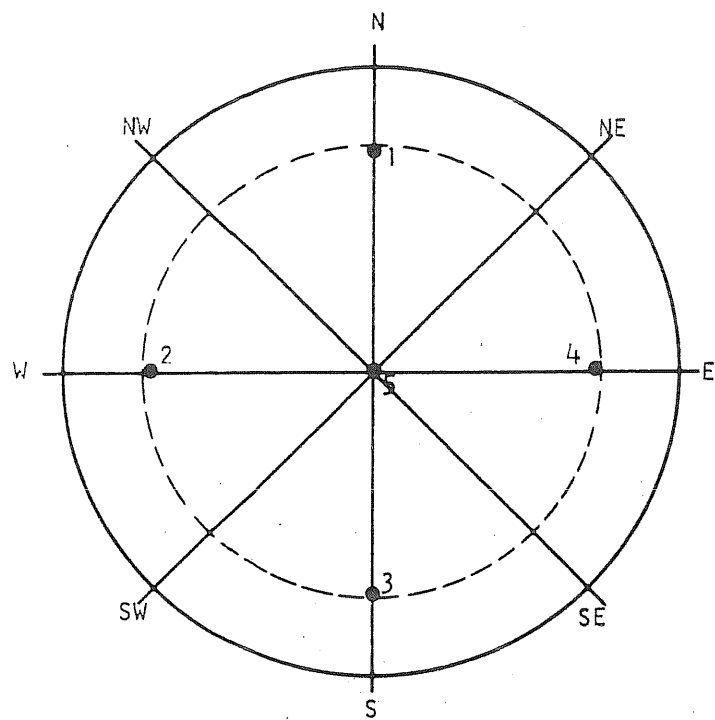
Test vessel PV2 was cast from ready-mix concrete. As in PV1 a circumferential crack at the junction of the slab and skirt was observed inside the specimen when the form was struck.

After the testing of PV1, the test chamber was lined with 0.5-in. thick steel plate rather than plywood. A television camera was installed so that the head of PV2 could be observed during the test. The first crack on the outside of the slab was visible at 170 psi. A second crack became visible at about 220 psi.

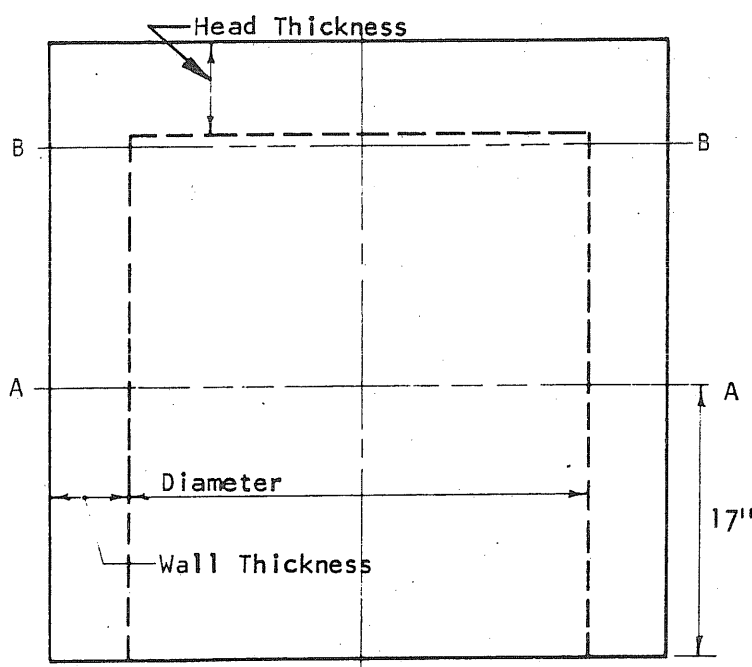
This test also required about 3 hours for completion. The first load increment was 20 psi followed by increments of 10 psi up to the maximum pressure reached which was 240 psi. The vessel had a small leak throughout the test and loading could not be continued to failure. The maximum deflection at the center of the head was 0.8-in. when the test had to be stopped.

Vessel PV2 was longitudinally reinforced with twenty-four 0.5-in. diameter seven-wire strands. None of the strands were equipped with load cells. The vessel was sealed the same way as PV1 except for an extra layer of neoprene on the inside of the end slab which was cut to fit between the gage wires on the end slab in order to make the inside neoprene layer more smooth.

The crack pattern in the end slab is illustrated in Fig. B2.19.



| Head Thickness | |
|----------------|-------------------|
| Point No. | Inches |
| 1 | 6 $\frac{0}{32}$ |
| 2 | 5 $\frac{31}{32}$ |
| 3 | 5 $\frac{30}{32}$ |
| 4 | 6 $\frac{1}{32}$ |
| 5 | 6 $\frac{0}{32}$ |



| Wall Thickness, in. | | |
|---------------------|------|------|
| Plane Axis | AA | BB |
| N | 4.99 | 5.17 |
| NE | 5.13 | 5.17 |
| E | 4.90 | 4.87 |
| SE | 5.00 | 5.00 |
| S | 4.89 | 5.01 |
| SW | 4.93 | 5.01 |
| W | 4.88 | 4.86 |
| NW | 4.99 | 5.02 |

| Inside Diameter, in. | | |
|----------------------|-------------------|-------------------|
| Plane Axis | AA | BB |
| N-S | $30\frac{3}{32}$ | $29\frac{29}{32}$ |
| NE-SW | $30\frac{1}{32}$ | $29\frac{31}{32}$ |
| E-W | $29\frac{31}{32}$ | $30\frac{0}{32}$ |
| SE-NW | $30\frac{0}{32}$ | $29\frac{30}{32}$ |

FIG. B2.1 DIMENSIONS OF PV2

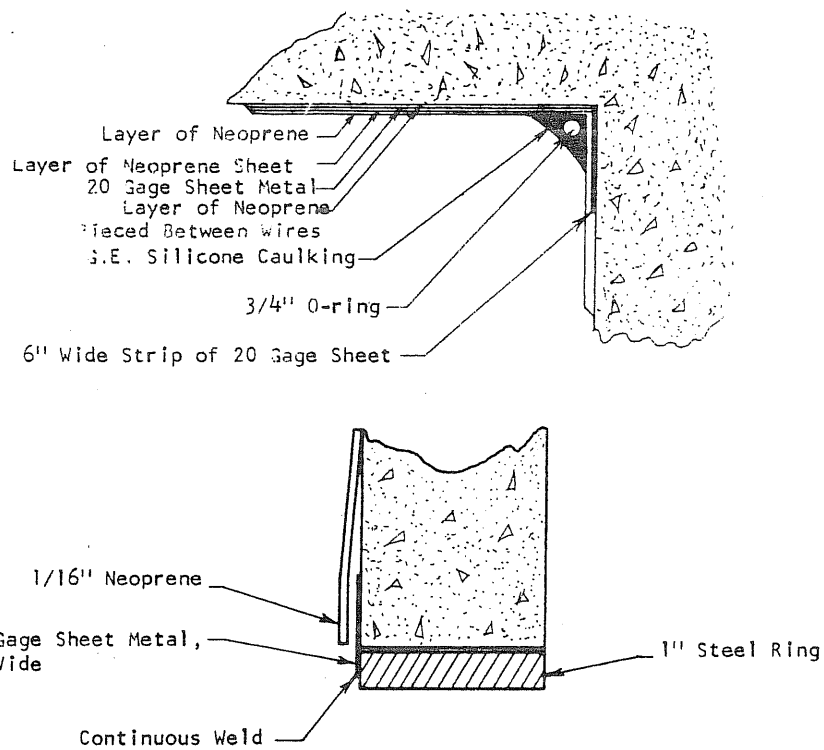
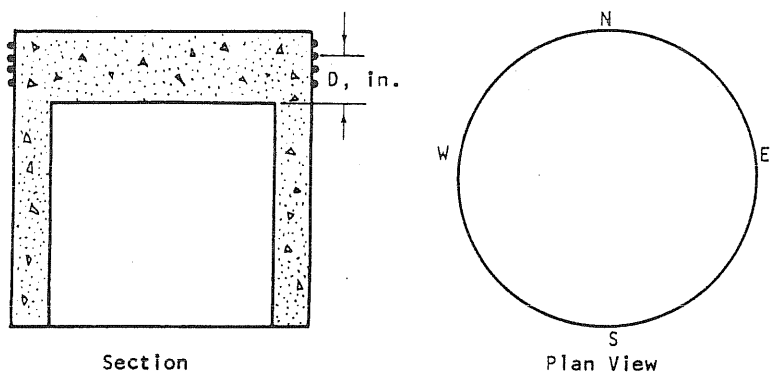


FIG. B2.2 SEALING DETAIL FOR PV2



| Wrap No. | N | W | S | E |
|----------|-------|--------|--------|---------|
| 1 | 5 3/8 | 5 1/4 | 5 | 5 |
| 2 | 4 7/8 | 4 1/2 | 4 3/4 | 3 15/16 |
| 3 | 3 5/8 | 3 3/8 | 3 1/8 | 2 7/8 |
| 4 | 2 1/2 | 2 5/16 | 2 1/16 | 1 13/16 |
| 5 | 1 1/2 | 1 1/4 | 1 | 3/4 |
| 6 | 1/2 | 1/4 | 0 | -1/8 |

FIG. B2.3 MEASURED LOCATION OF THE CIRCUMFERENTIAL PRESTRESS WIRE AT THE ENDS OF THE N-S AND E-W DIAMETERS ON PV2

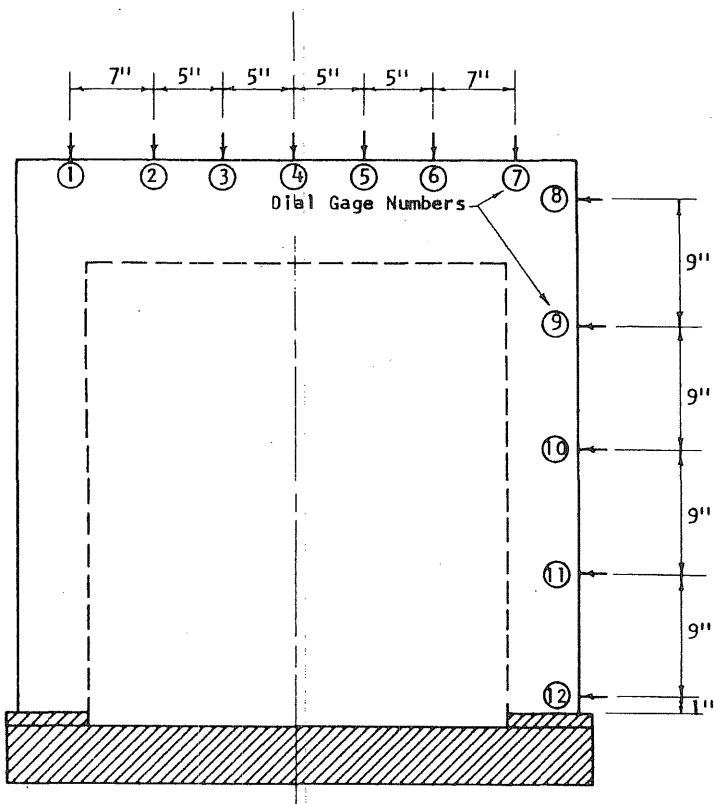


FIG. B2.4. LOCATION OF DEFLECTION GAGES ON PV2

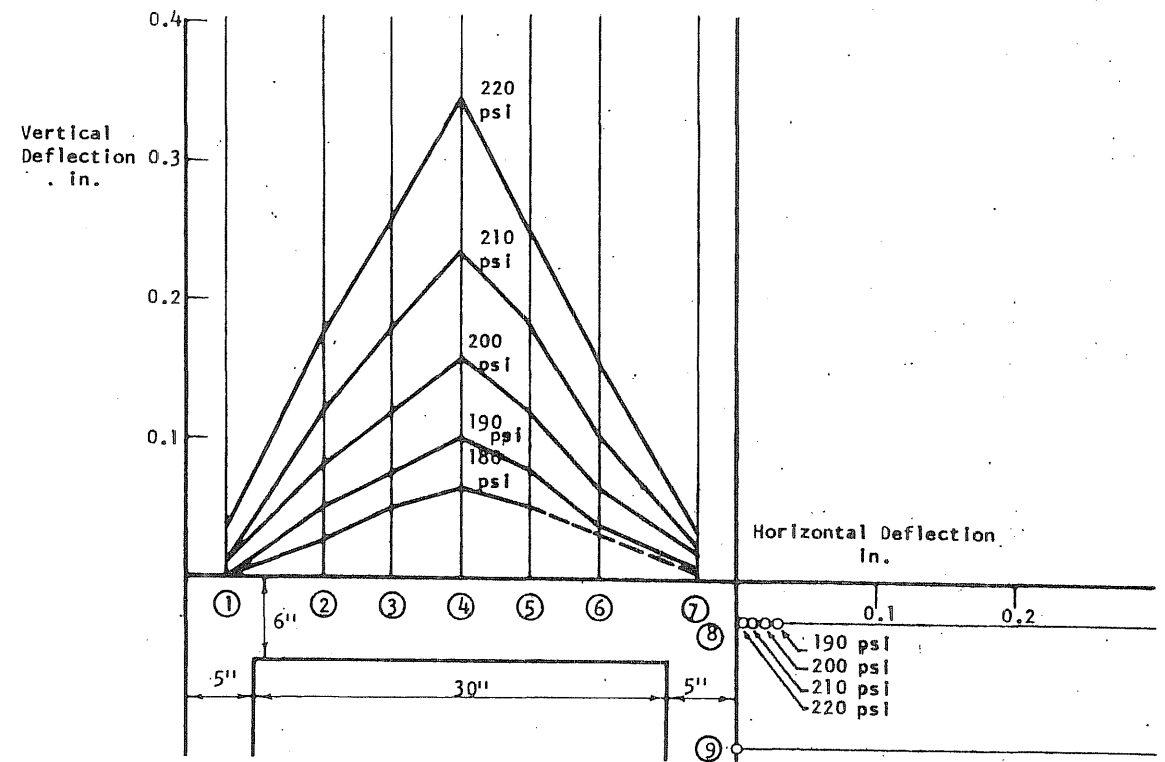


FIG. B2.5 DEFLECTION PROFILES OF THE END SLAB ALONG THE N-S DIAMETER OF PV2

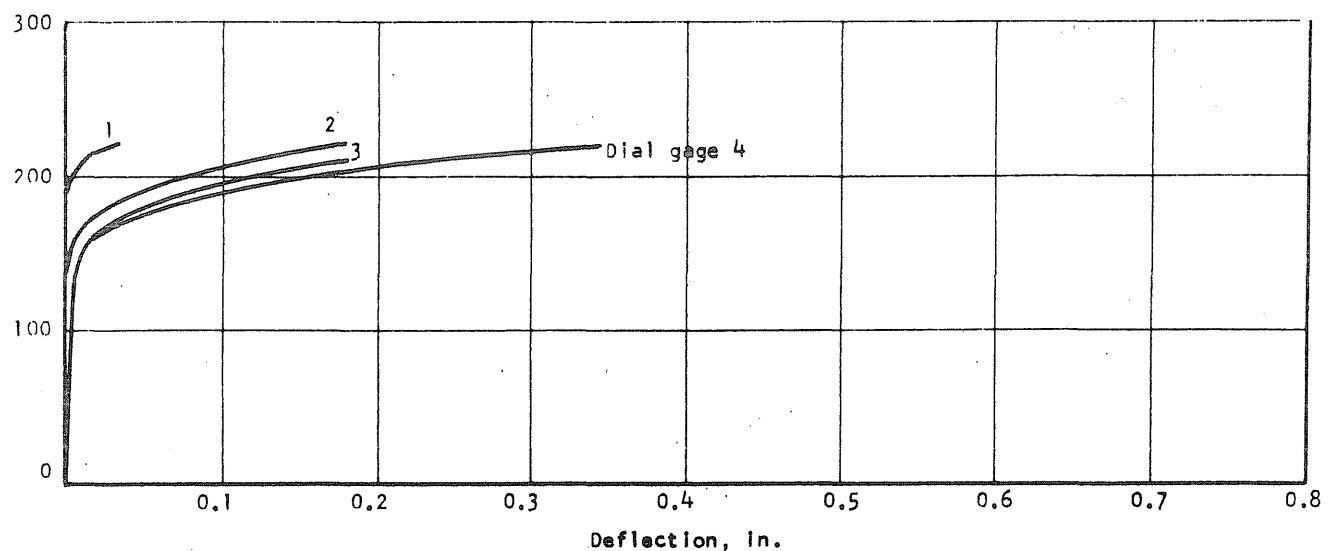


FIG. B2.6 APPLIED PRESSURE vs DEFLECTION ALONG THE N-HALF OF THE N-S DIAMETER OF PV2

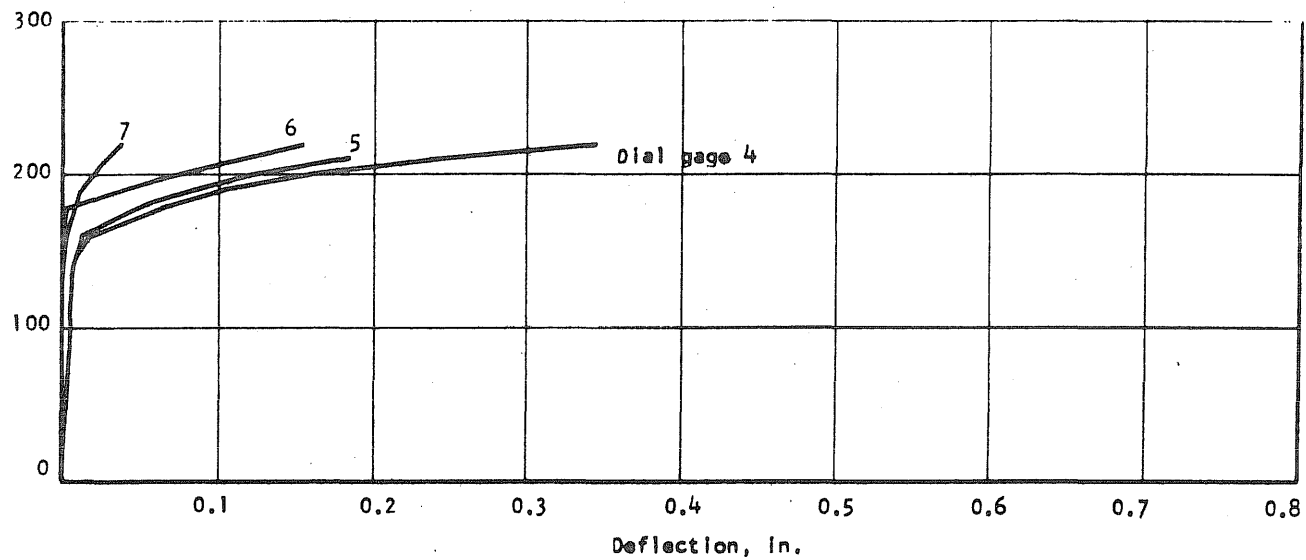


FIG. B2.7 APPLIED PRESSURE vs DEFLECTION ALONG THE S-HALF OF THE N-S DIAMETER OF PV2

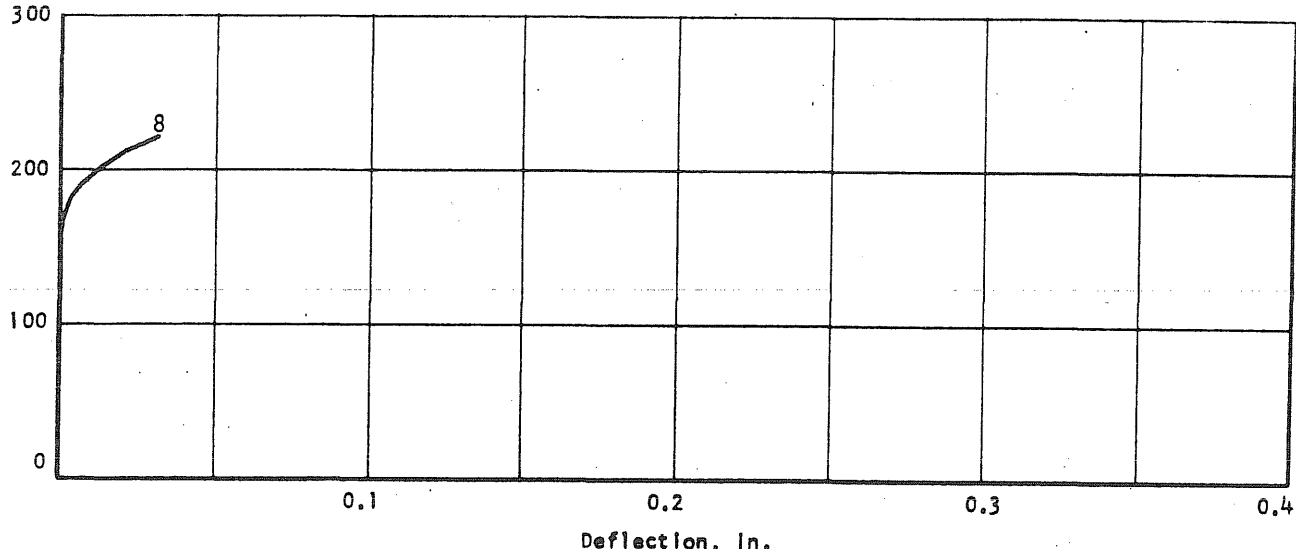
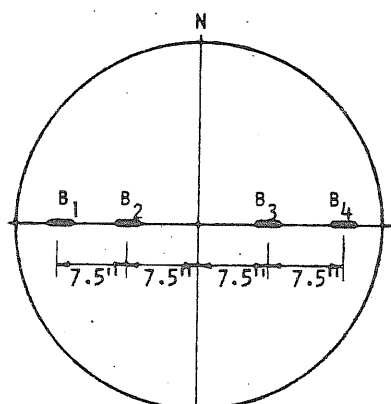
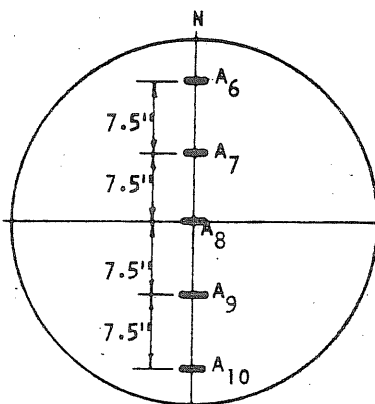
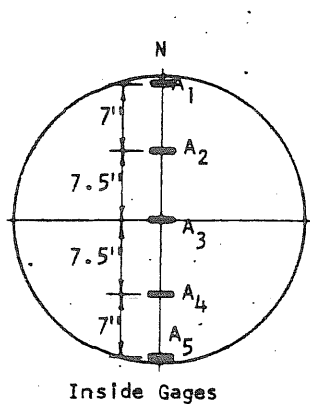


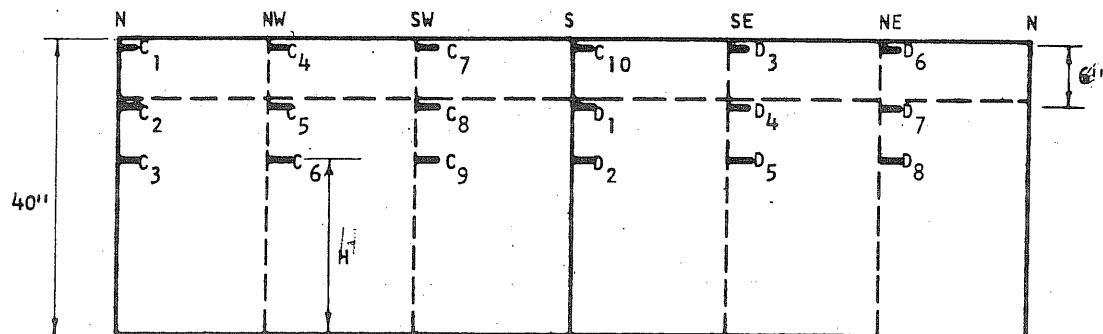
FIG. B2.8 APPLIED PRESSURE vs DEFLECTION OF THE SIDE WALL OF PV2

B 24

Concrete Gages On The End Slab

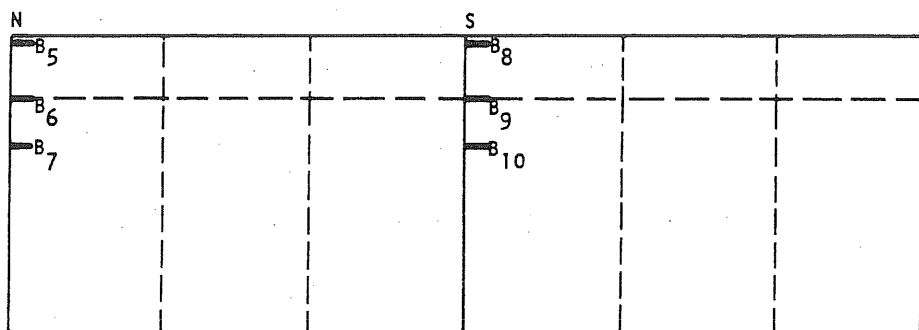


Steel Gages On Prestress Wire



| Gage | Line | H | Gage | Line | H | Gage | Line | H |
|----------------|------|----------|-----------------|------|---------|----------------|------|----------|
| C ₁ | N | 37 10/16 | C ₇ | SW | 38 6/16 | D ₃ | SE | 38 0/16 |
| C ₂ | N | 32 10/16 | C ₈ | SW | 33 5/16 | D ₄ | SE | 33 0/16 |
| C ₃ | N | 27 10/16 | C ₉ | SW | 28 5/16 | D ₅ | SE | 28 0/16 |
| C ₄ | NW | 38 10/16 | C ₁₀ | S | 38 4/16 | D ₆ | NE | 37 13/16 |
| C ₅ | NW | 33 7/16 | D ₁ | S | 33 2/16 | D ₇ | NE | 32 12/16 |
| C ₆ | NW | 28 7/16 | D ₂ | S | 28 2/16 | D ₈ | NE | 27 12/16 |

Concrete Gages On Outside of Vessel



| Gage | Axis | H | Gage | Axis | H |
|----------------|------|---------|-----------------|------|----------|
| B ₅ | N | 37 0/16 | B ₈ | S | 37 12/16 |
| B ₆ | N | 32 2/16 | B ₉ | S | 32 12/16 |
| B ₇ | N | 27 0/16 | B ₁₀ | S | 27 13/16 |

FIG. B2.9 STRAIN GAGE LOCATIONS ON PV2

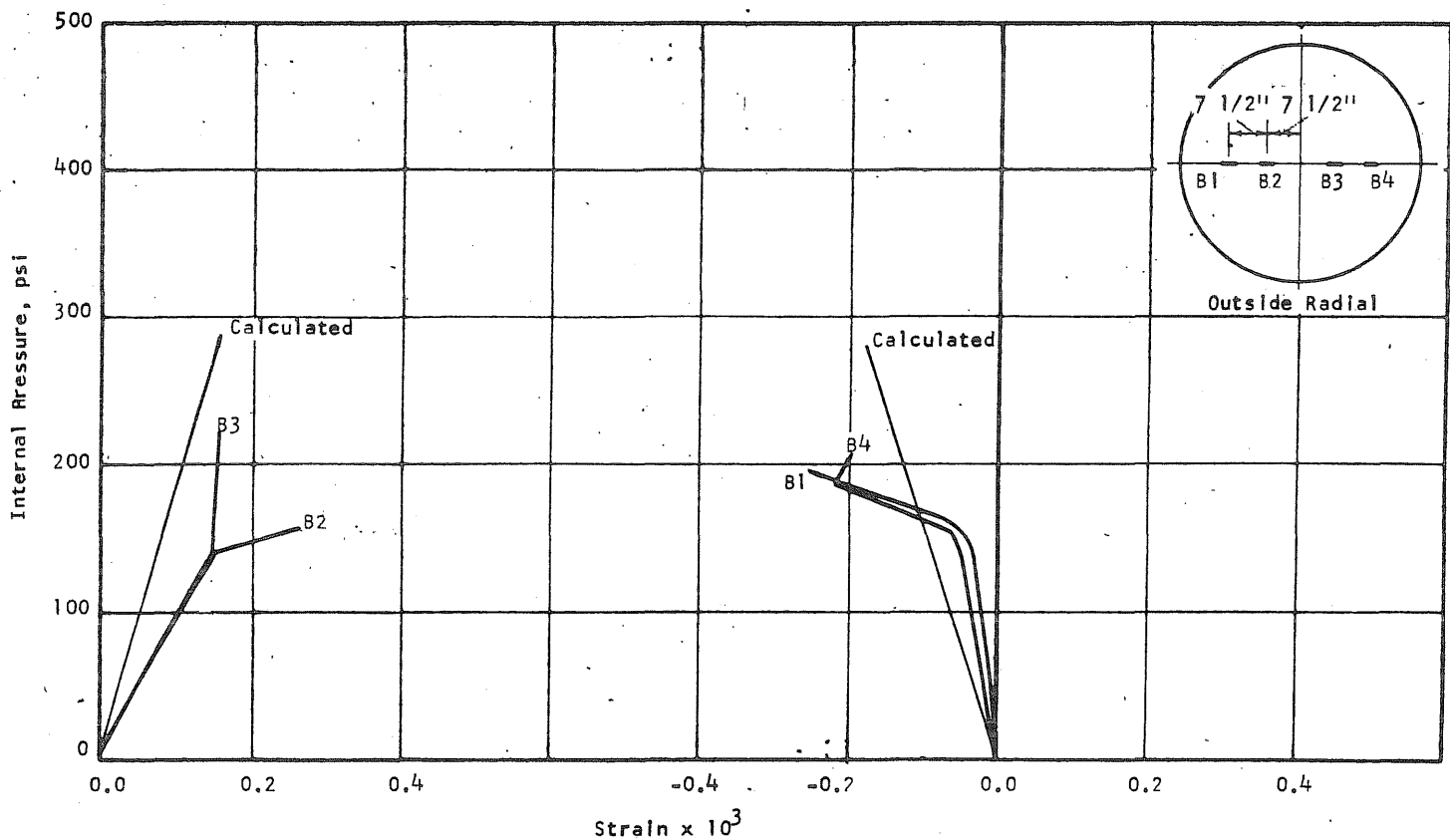


FIG. B2.10 CONCRETE STRAINS, VESSEL PV2

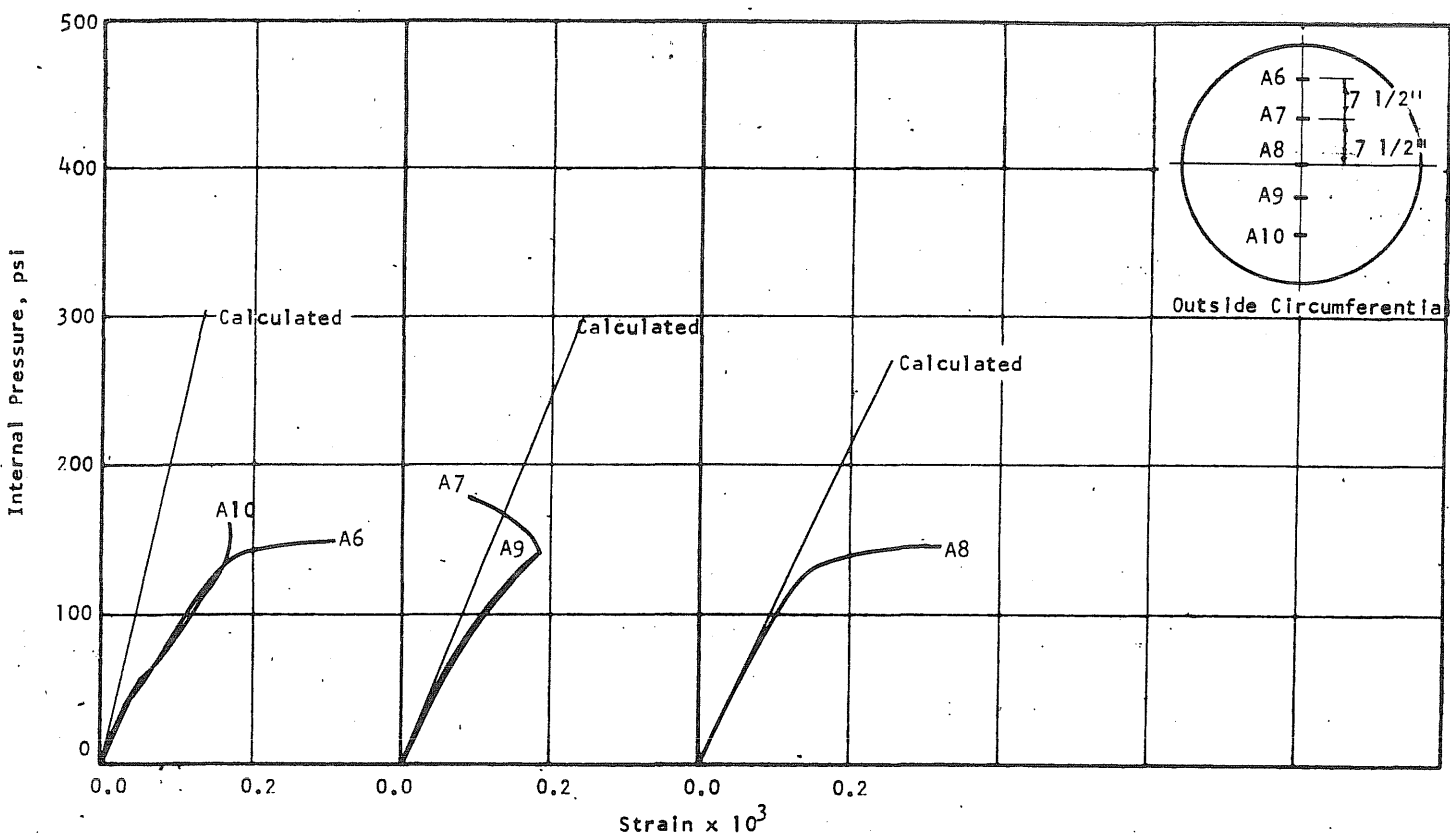


FIG. B2.11 CONCRETE STRAINS, VESSEL PV2

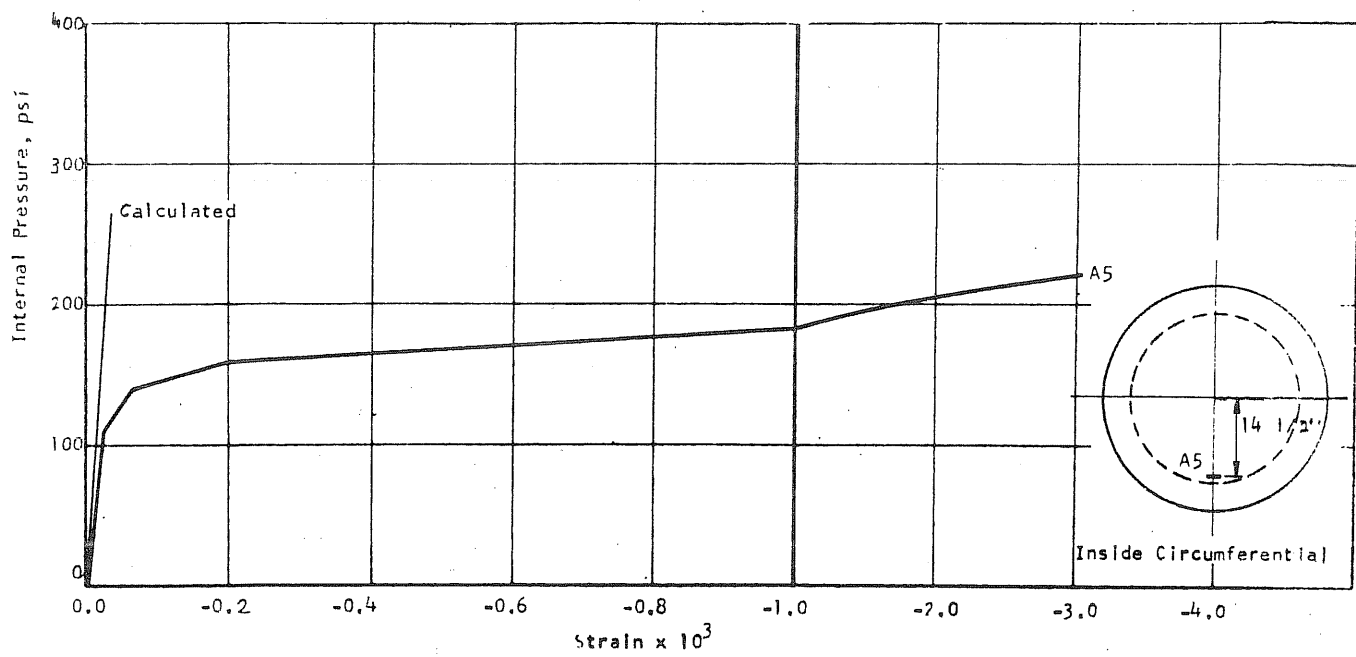


FIG. B2.12 CONCRETE STRAINS, VESSEL PV2

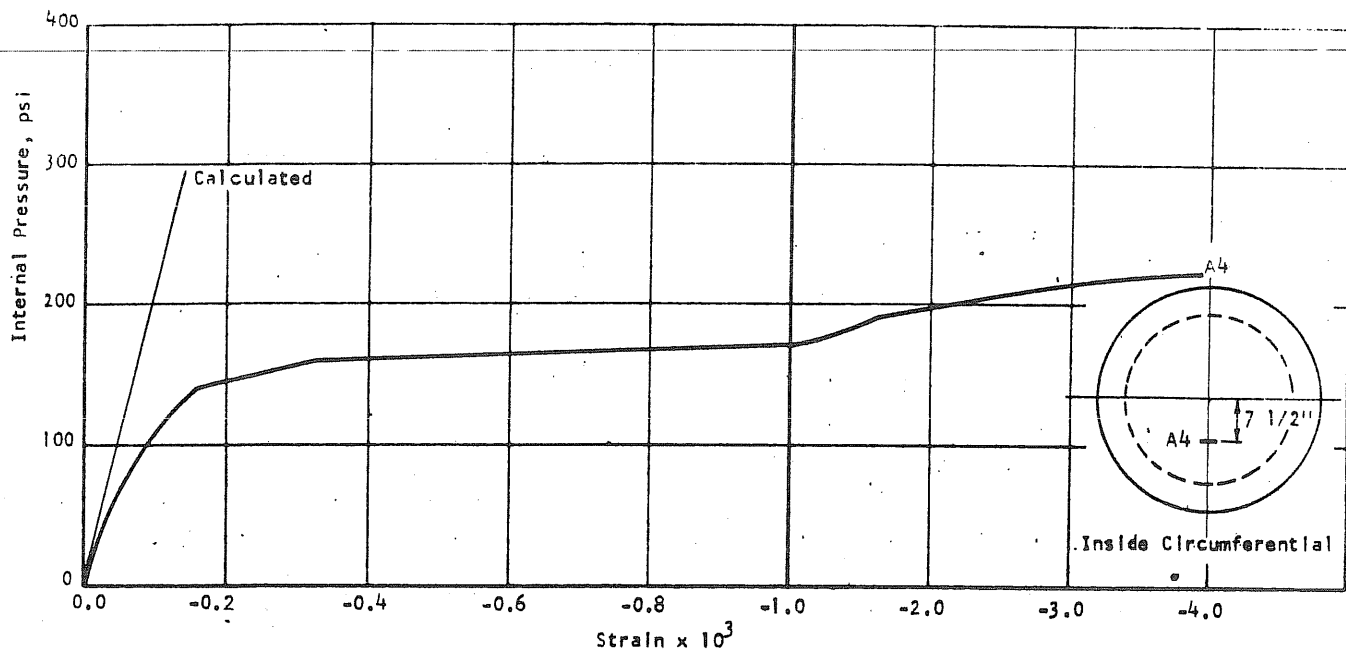


FIG. B2.13 CONCRETE STRAINS, VESSEL PV2

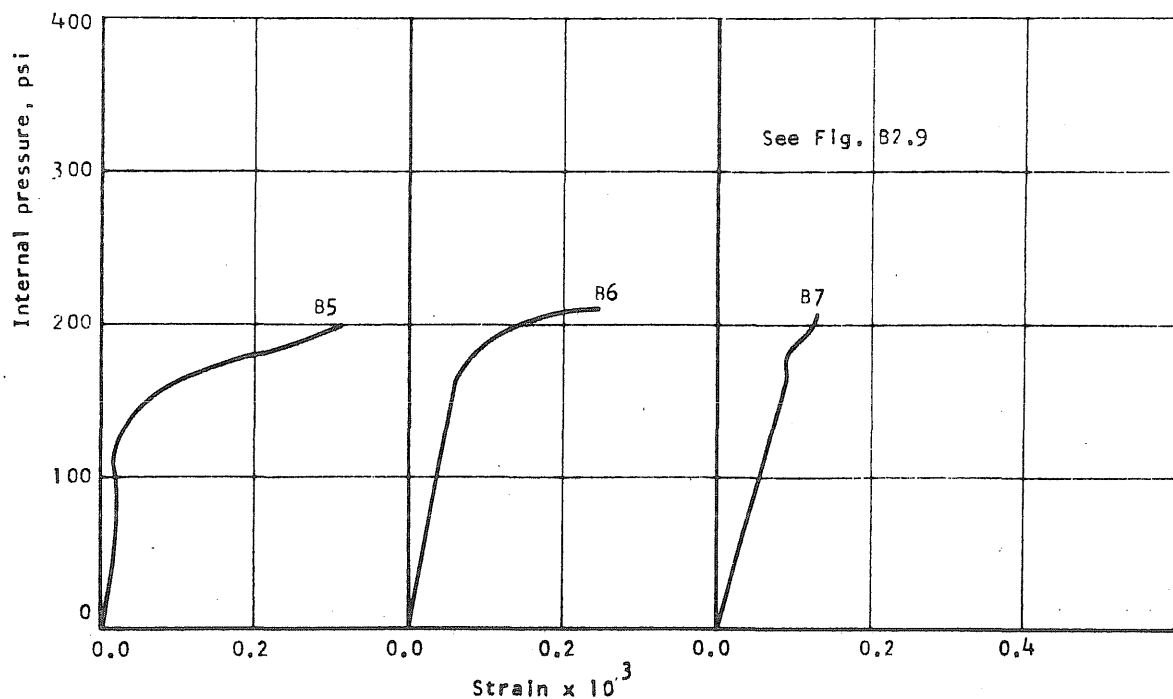


FIG. B2.14 APPLIED PRESSURE vs CIRCUMFERENTIAL STRAIN IN THE WALL OF THE VESSEL AT THE N-END OF THE N-S DIAMETER OF PV2

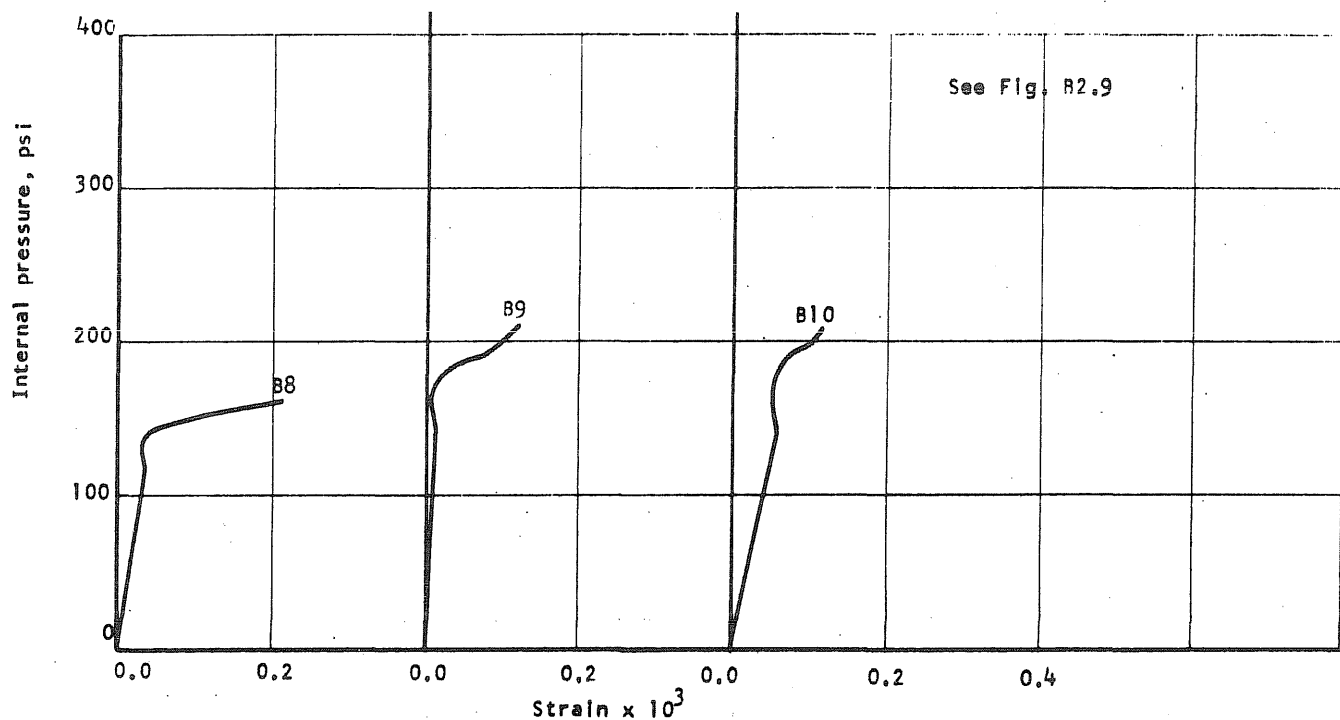


FIG. B2.15 APPLIED PRESSURE vs CIRCUMFERENTIAL STRAIN IN THE WALL OF THE VESSEL AT THE S-END OF THE N-S DIAMETER OF PV2

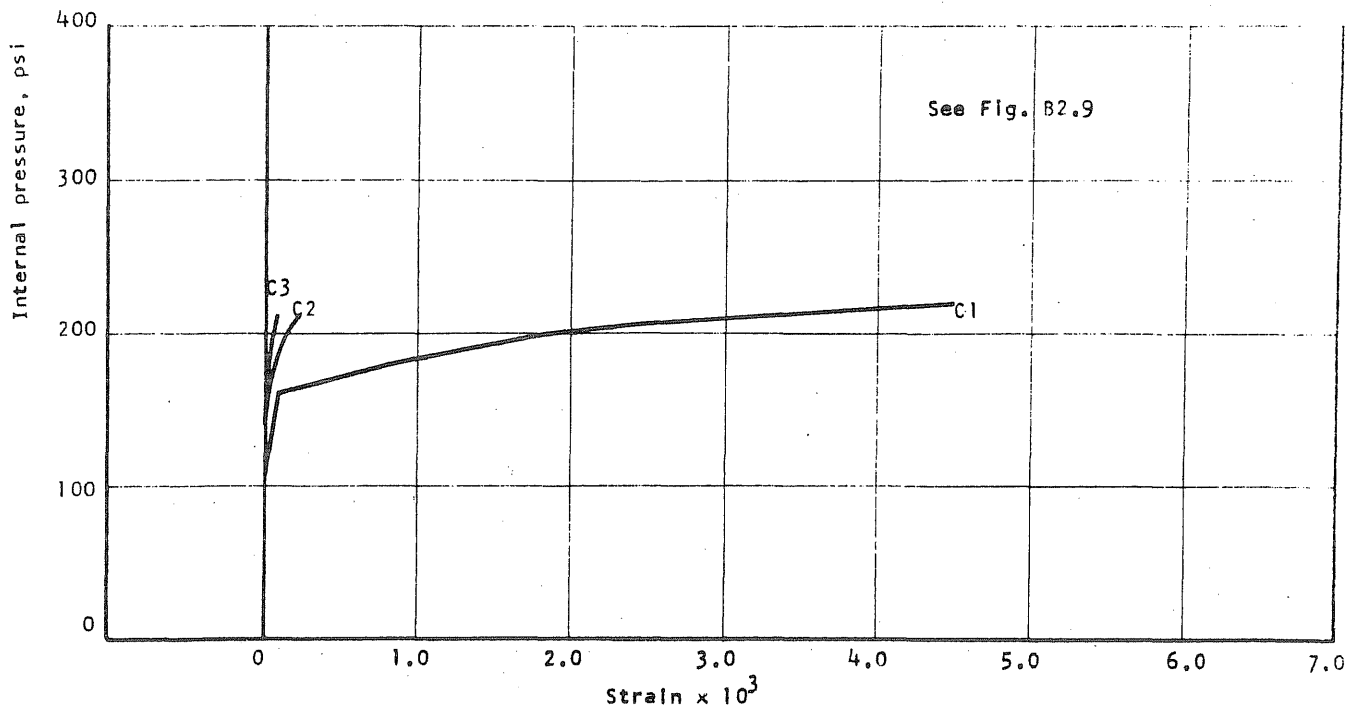


FIG. B2.16 APPLIED PRESSURE VS STRAIN IN THE CIRCUMFERENTIAL PRESTRESS WIRE AT THE N-END OF THE N-S DIAMETER OF PV2

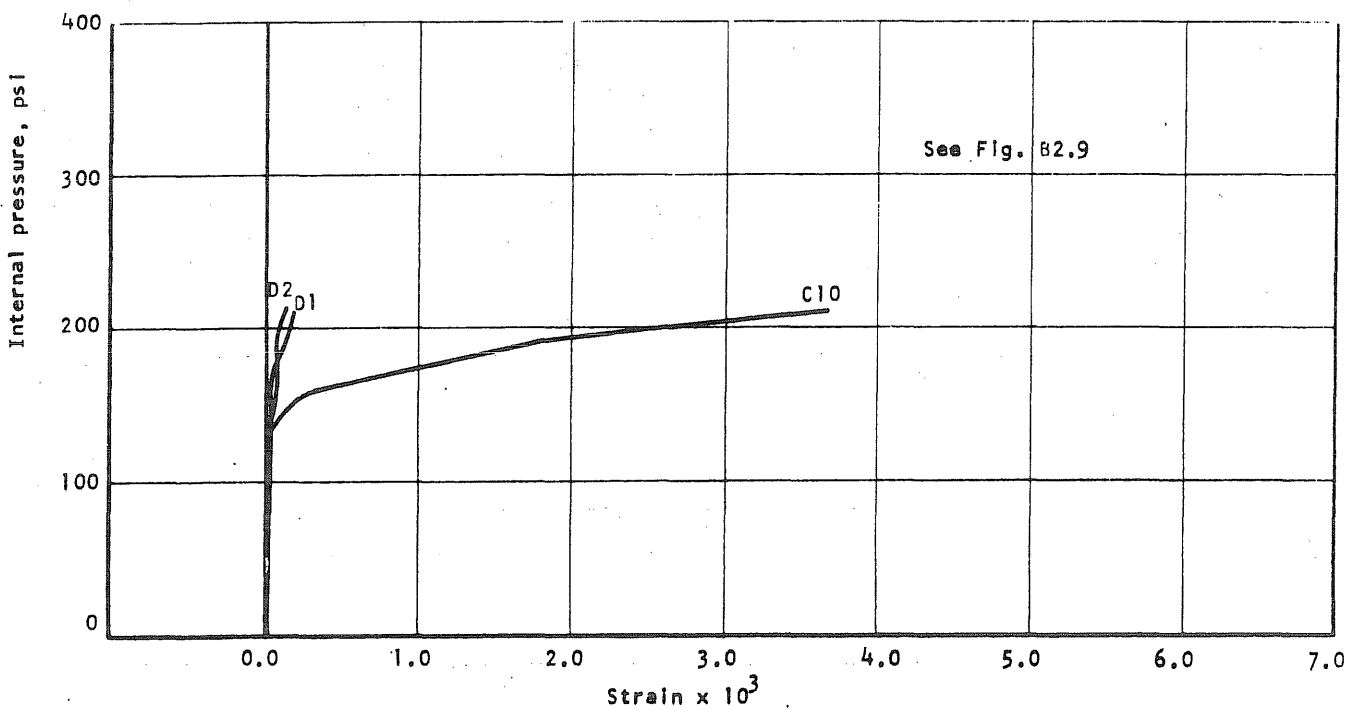


FIG. B2.17 APPLIED PRESSURE VS STRAIN IN THE CIRCUMFERENTIAL PRESTRESS WIRE AT THE S-END OF THE N-S DIAMETER OF PV2

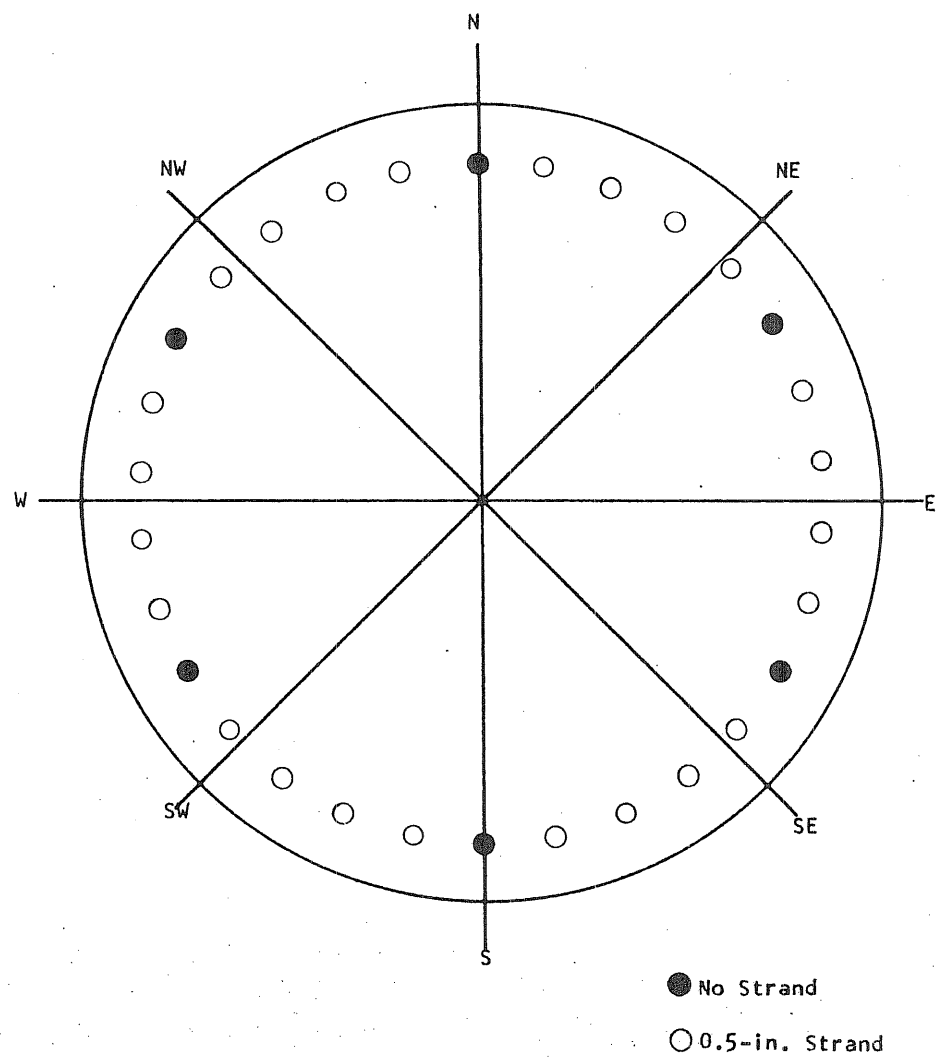


FIG. B2.18 LOCATION OF LONGITUDINAL REINFORCEMENT

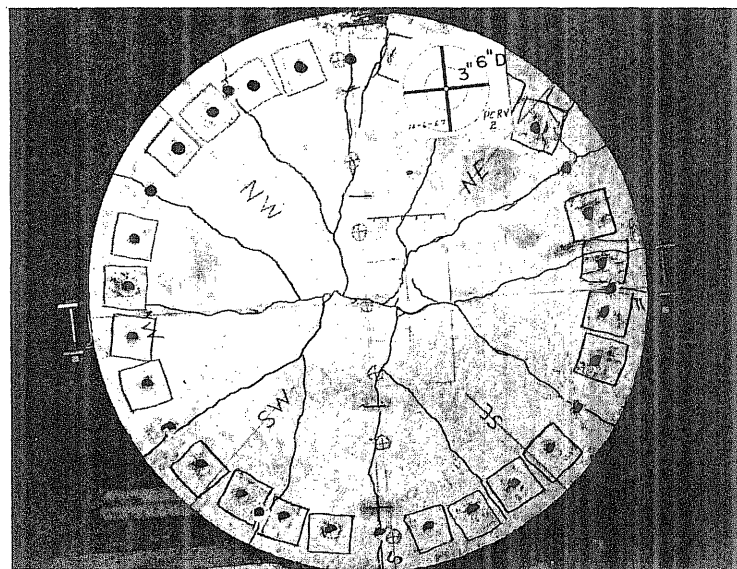


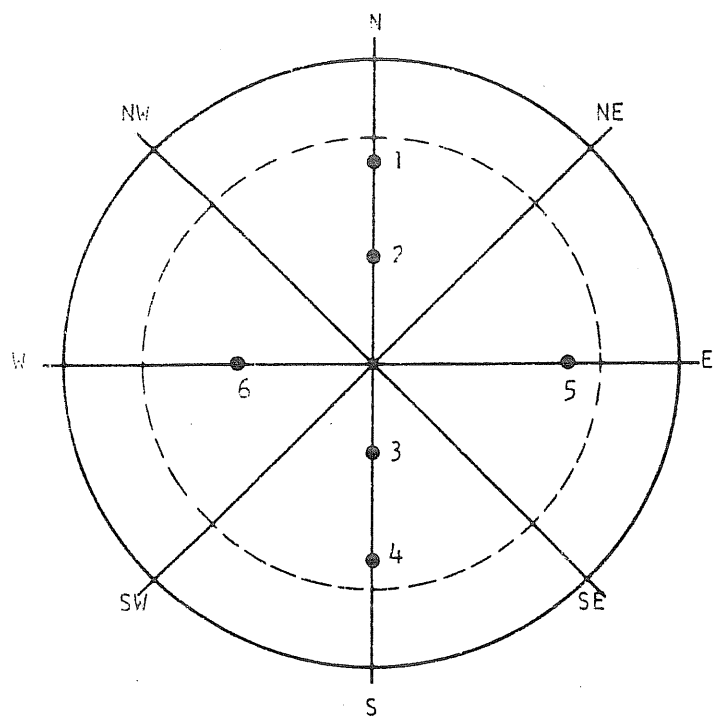
FIG. B2.19 END SLAB OF PV2 AFTER TESTING

B3 Test Vessel PV3 ($t = 7 \frac{1}{2}$ in., $s = 1.0$ in.)

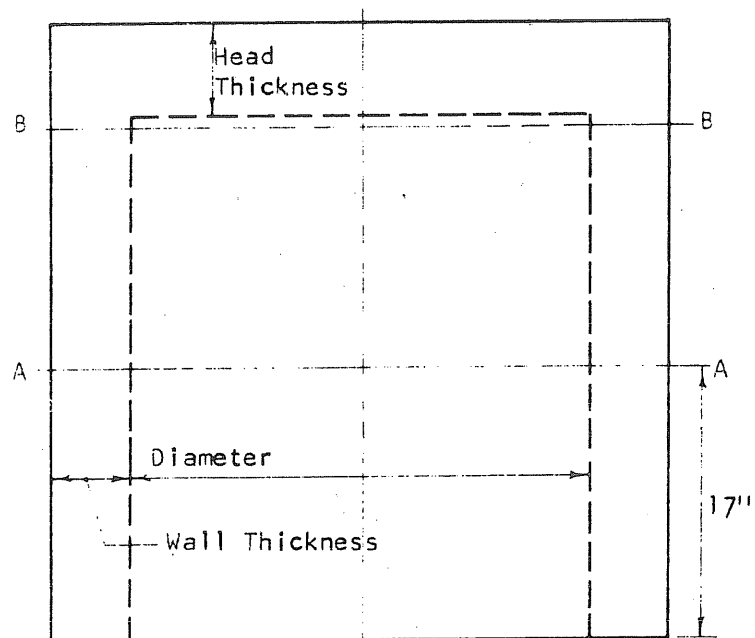
Test vessel PV3 was the first vessel cast from concrete mixed in the laboratory. It was free of cracks at the time of the test.

About three hours were required for the test. Loading was increased in increments of 20 psi until the vessel failed at 370 psi. No problems were encountered with the liner, which was sealed in the same manner as PV2. The block-out inside the vessel also failed when the vessel failed. The blockout, which was a closed steel cylinder filled with vermiculite concrete, developed a leak during the course of the test. When the pressure surrounding the vessel was reduced by failure of the vessel, the gas trapped inside the block-out caused it to burst.

The longitudinal tendons were 0.5-in. strand in PV3. Load cells were placed on nine of the twenty-four strands and were monitored during the test. The crack pattern in the end slab is illustrated by a photograph of the reassembled end slab in Fig. B3.22.



| Head Thickness | |
|----------------|--------|
| Point No. | Inches |
| 1 | 7.8 |
| 2 | 7.8 |
| 3 | 7.75 |
| 4 | 7.8 |
| 5 | 7.7 |
| 6 | 7.75 |



| Wall Thickness, in. | | |
|---------------------|----|-------|
| Plane Axis | AA | BB |
| N | | 5.00 |
| NE | | 4.76 |
| E | | 4.855 |
| SE | | 5.03 |
| S | | 5.11 |
| SW | | 5.12 |
| W | | 4.95 |
| NW | | 5.05 |

| Inside Diameter, in. | | |
|----------------------|------------------|-------------------|
| Plane Axis | AA | BB |
| N-S | $30\frac{5}{32}$ | $29\frac{31}{32}$ |
| NE-SW | $30\frac{1}{32}$ | $2\frac{31}{32}$ |
| E-W | 30 | $30\frac{1}{32}$ |
| SE-NW | $30\frac{1}{32}$ | $29\frac{31}{32}$ |

FIG. B3.1 DIMENSIONS OF PV3

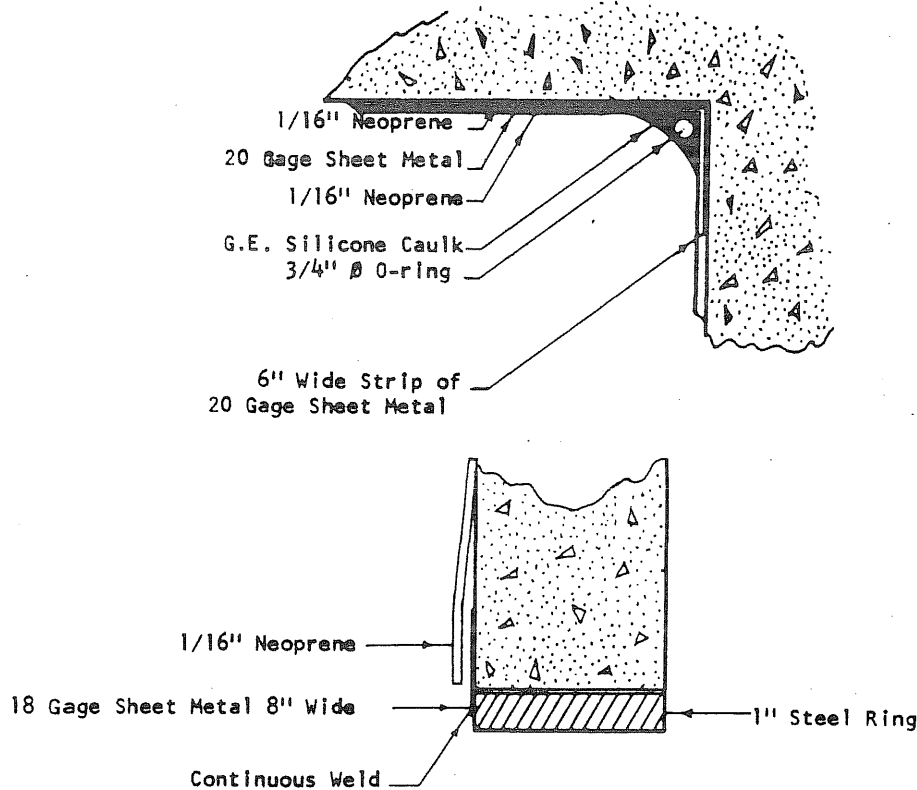
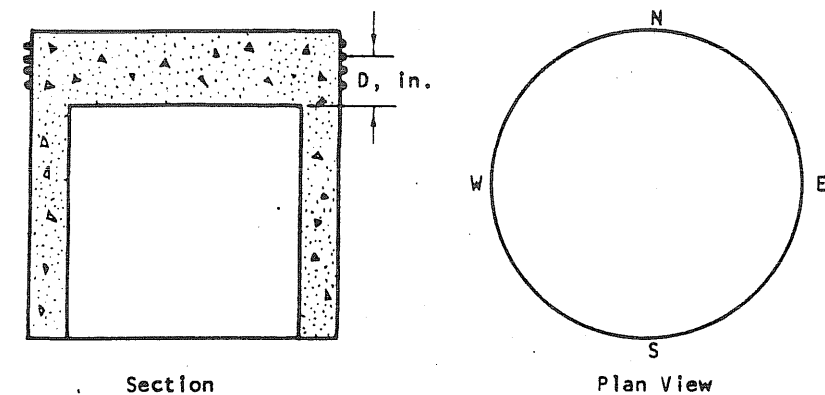


FIG. B3.2 SEALING DETAIL FOR PV3



| Wrap No. | D_N | D_E | D_S | D_W |
|----------|---------|---------|---------|---------|
| 1 | 6 14/16 | 6 15/16 | 6 13/16 | 6 14/16 |
| 2 | 6 5/16 | 6 4/16 | 6 5/16 | 6 7/16 |
| 3 | 5 14/16 | 5 11/16 | 6 2/16 | 6 1/16 |
| 4 | 5 1/16 | 4 13/16 | 5 9/16 | 5 5/16 |
| 5 | 4 1/16 | 3 14/16 | 4 10/16 | 4 7/16 |
| 6 | 3 | 2 12/16 | 3 10/16 | 3 6/16 |
| 7 | 1 15/16 | 1 12/16 | 2 9/16 | 2 6/16 |
| 8 | 15/16 | 11/16 | 1 9/16 | 1 5/16 |
| 9 | -1/16 | -5/16 | 9/16 | 5/16 |

FIG. B3.3 MEASURED LOCATION OF THE CIRCUMFERENTIAL PRESTRESS WIRE AT THE ENDS OF THE N-S AND E-W DIAMETERS ON PV3

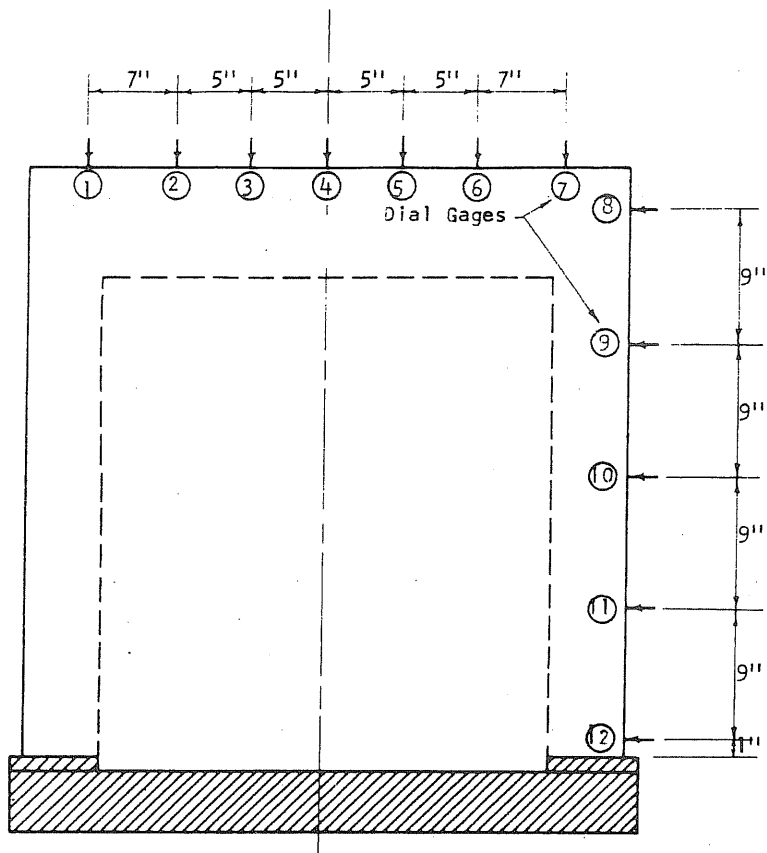


FIG. B3.4 LOCATION OF DEFLECTION GAGES ON PV3

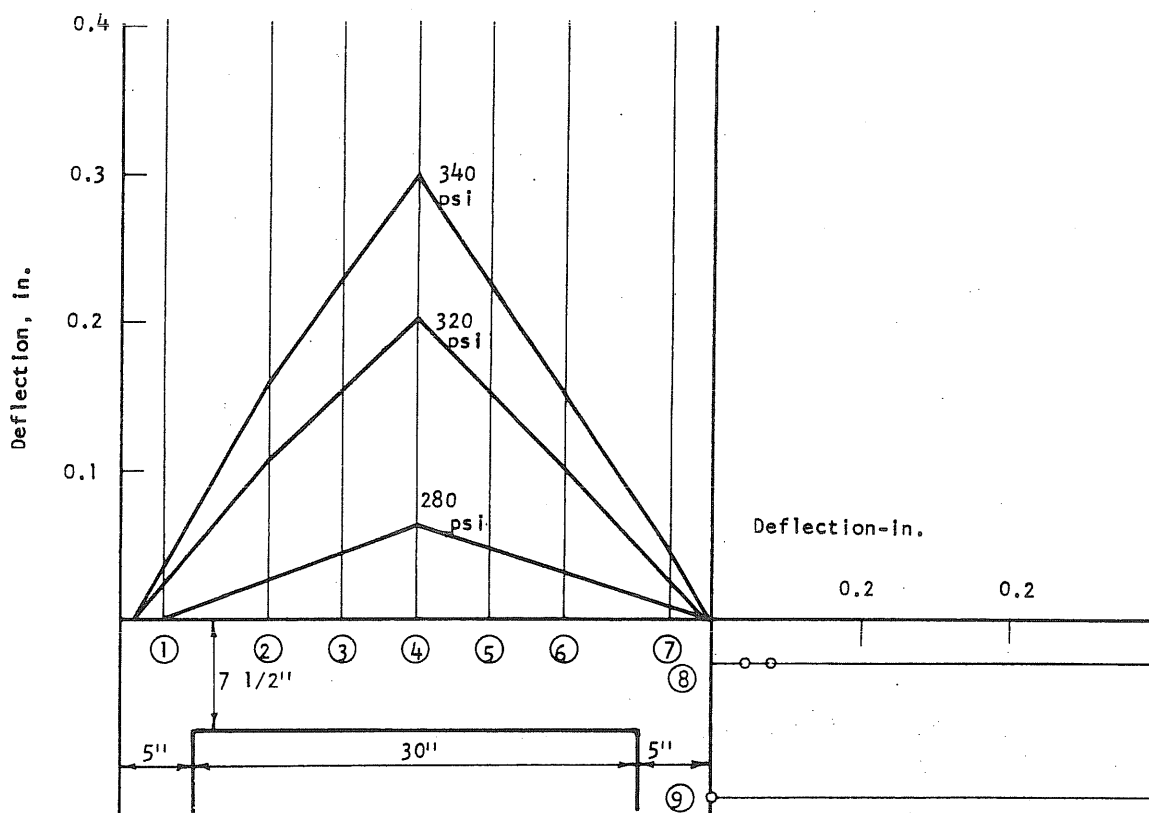


FIG. B3.5 DEFLECTION PROFILES OF THE END SLAB ALONG THE N-S DIAMETER OF PV3

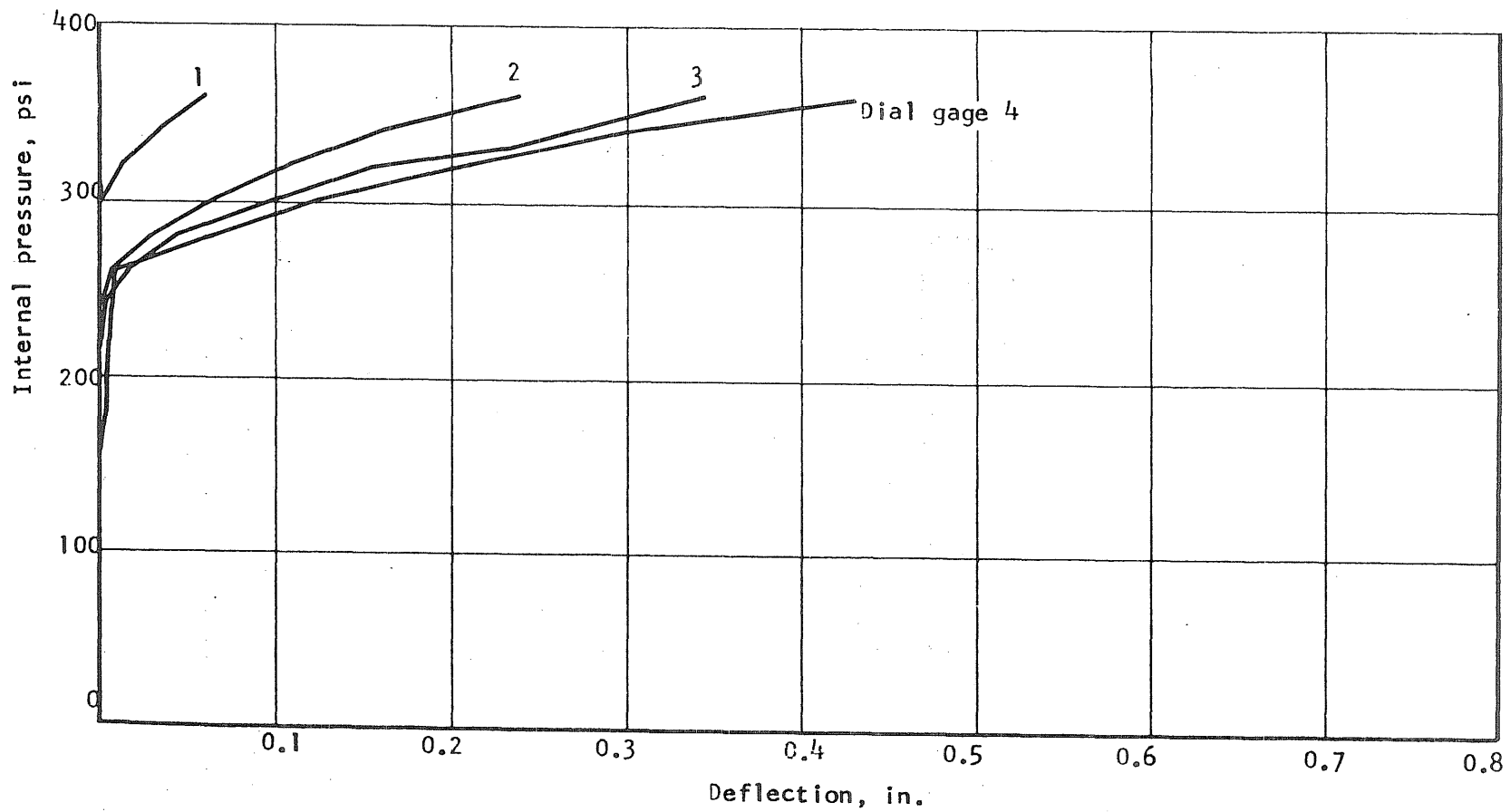


FIG. B3.6 APPLIED PRESSURE vs DEFLECTION ALONG THE N-HALF OF THE N-S DIAMETER OF PV3

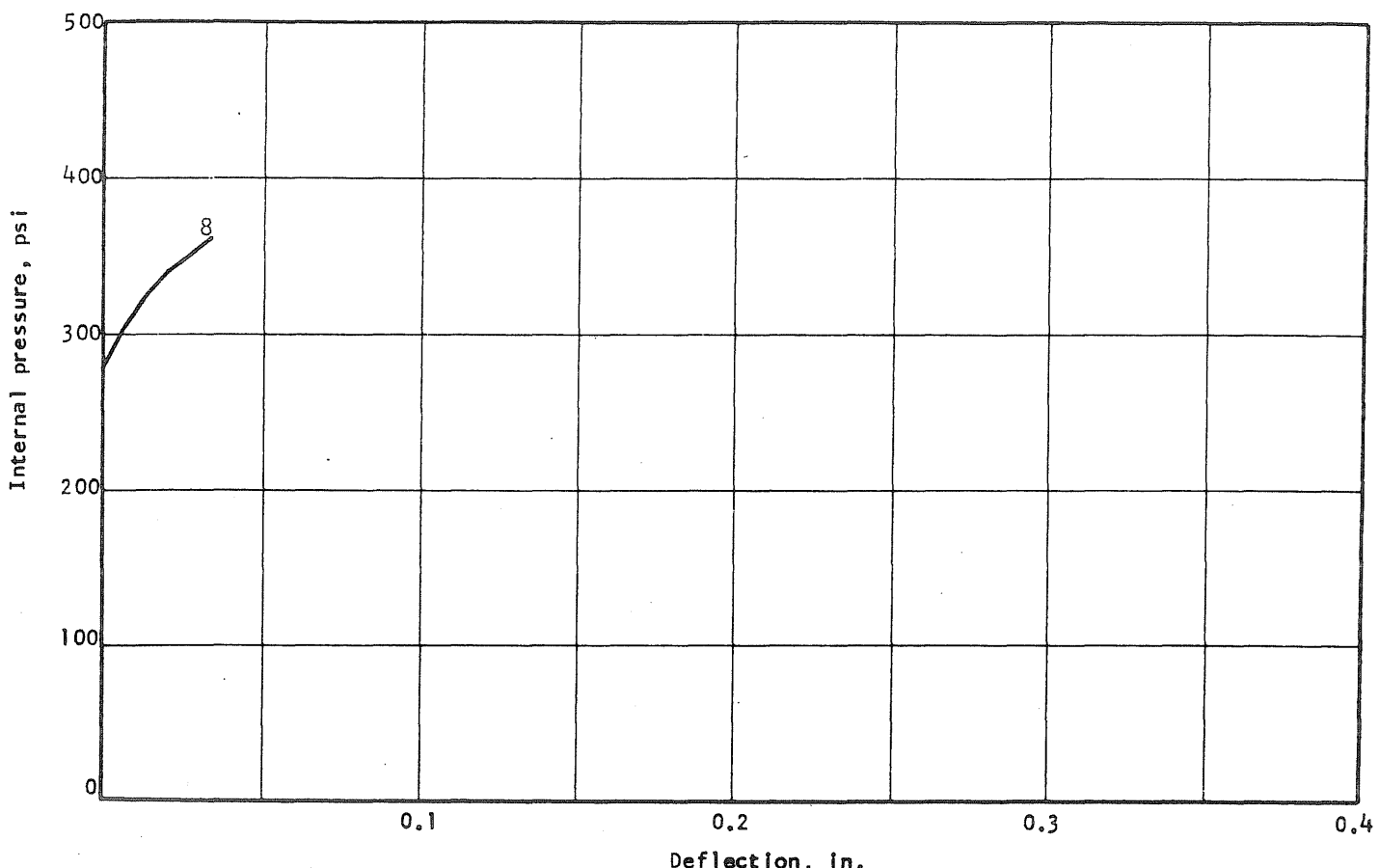


FIG. B3.8 APPLIED PRESSURE vs DEFLECTION OF THE SIDE WALL OF PV3

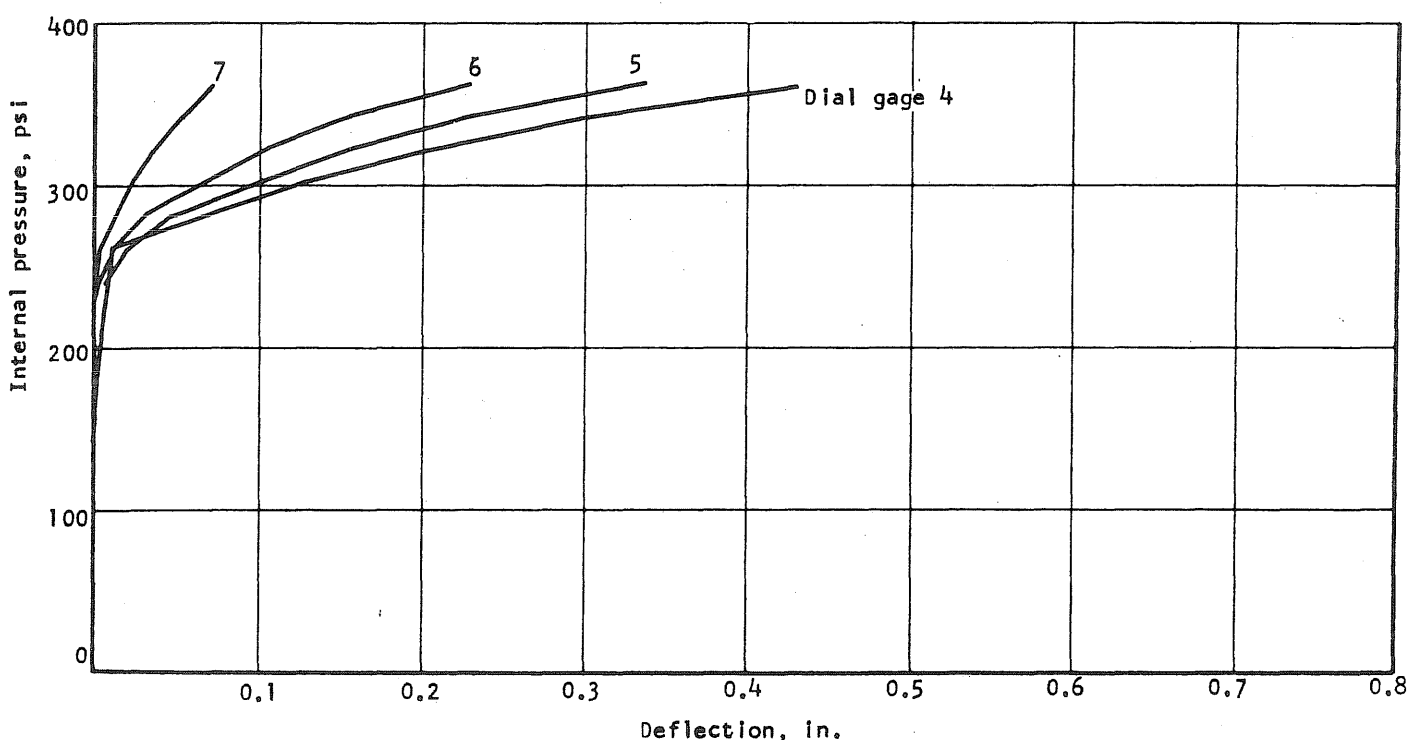
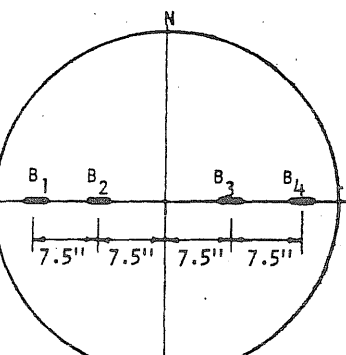
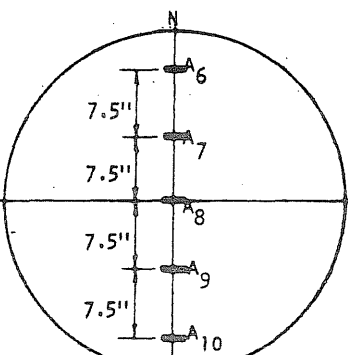
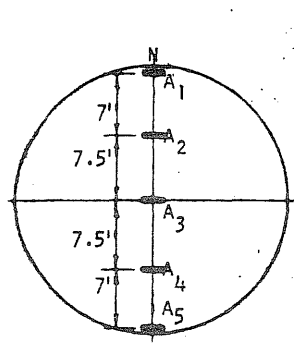


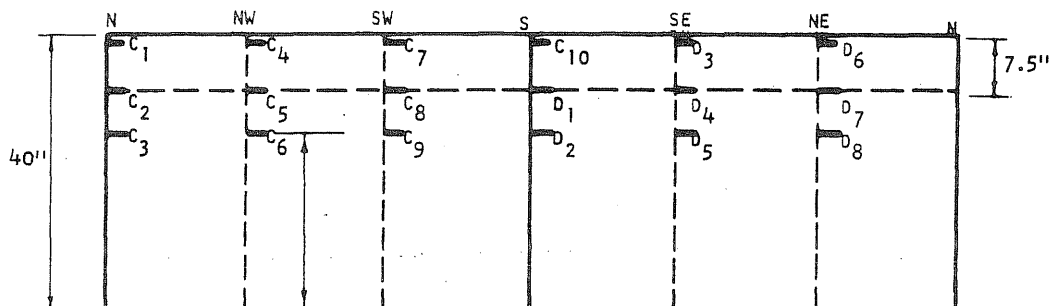
FIG. B3.7 APPLIED PRESSURE vs DEFLECTION ALONG THE S-HALF OF THE N-S DIAMETER OF PV3

B36

Concrete Gages On The Slab

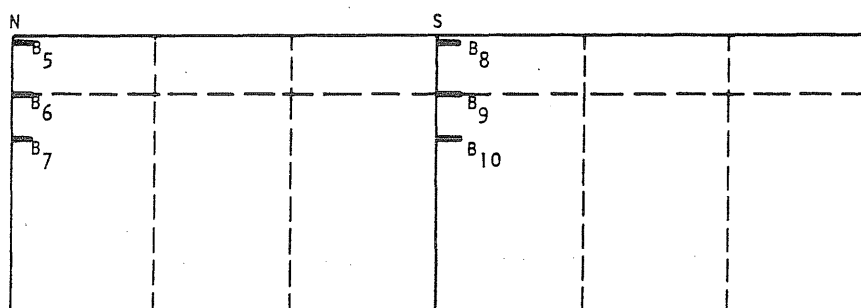


Steel Gages On Prestressing Wire



| Gage | Axis | H | Gage | Axis | H | Gage | Axis | H |
|----------------|------|----------|-----------------|------|----------|----------------|------|----------|
| C ₁ | N | 38 13/16 | C ₇ | SW | 38 14/16 | D ₃ | SE | 38 12/16 |
| C ₂ | N | 32 7/16 | C ₈ | SW | 32 7/16 | D ₄ | SE | 32 10/16 |
| C ₃ | N | 27 8/16 | C ₉ | SW | 27 8/16 | D ₅ | SE | 27 4/16 |
| C ₄ | NW | 38 14/16 | C ₁₀ | S | 38 13/16 | D ₆ | NE | 38 13/16 |
| C ₅ | NW | 32 10/16 | D ₁ | S | 32 1/16 | D ₇ | NE | 32 5/16 |
| C ₆ | NW | 27 10/16 | D ₂ | S | 27 3/16 | D ₈ | NE | 27 6/16 |

Concrete Gages on Outside of Vessel



Concrete gages were placed as close to corresponding steel gages as possible

| Gage | Axis | H | Gage | Axis | H |
|----------------|------|----------|-----------------|------|----------|
| B ₅ | N | 38 10/16 | B ₈ | S | 38 5/16 |
| B ₆ | N | 31 15/16 | B ₉ | S | 32 9/16 |
| B ₇ | N | 27 0/16 | B ₁₀ | S | 26 12/16 |

FIG. B3.9 STRAIN GAGE LOCATIONS ON PV3

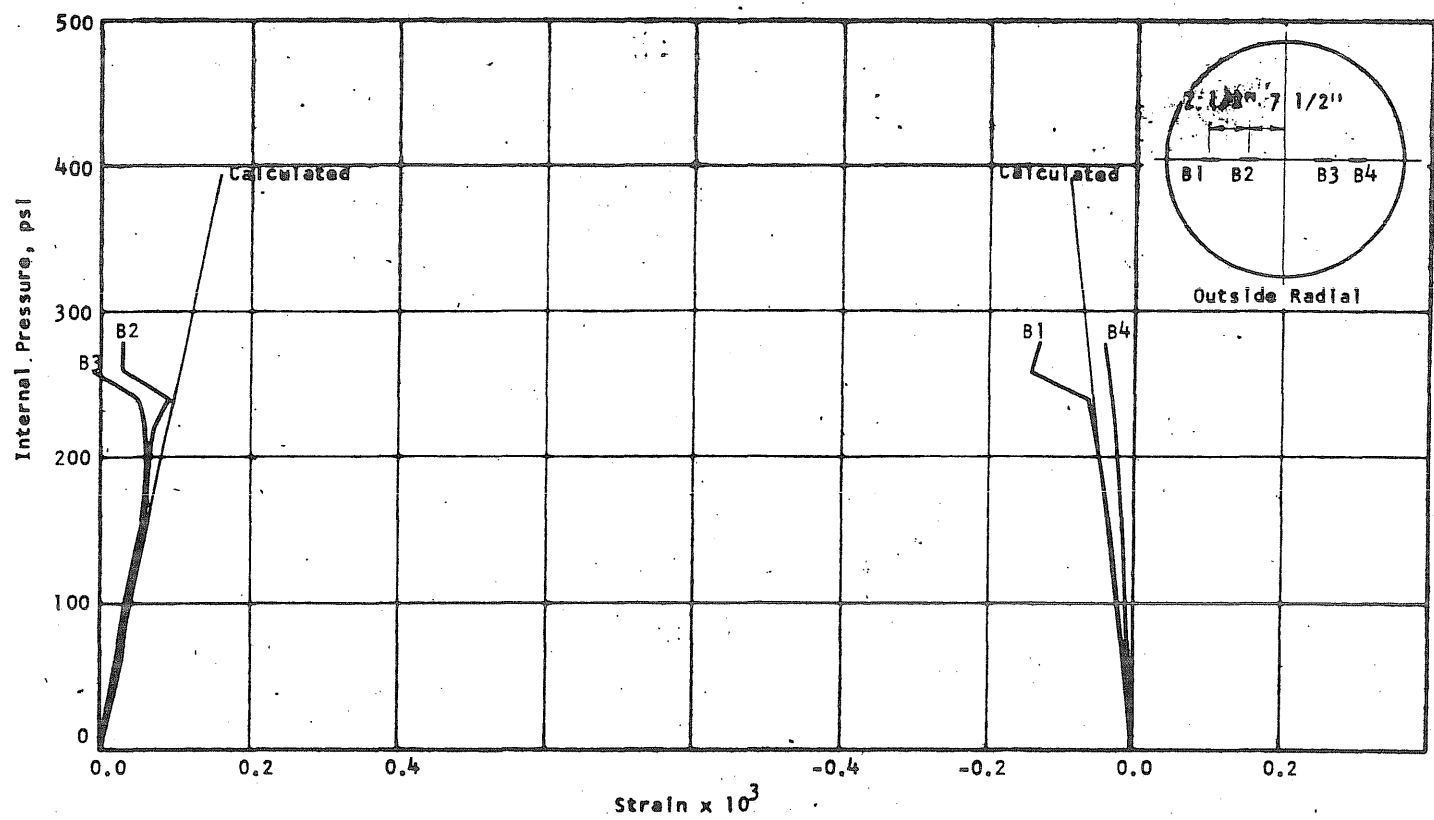


FIG. B3.10 CONCRETE STRAINS, VESSEL PV3

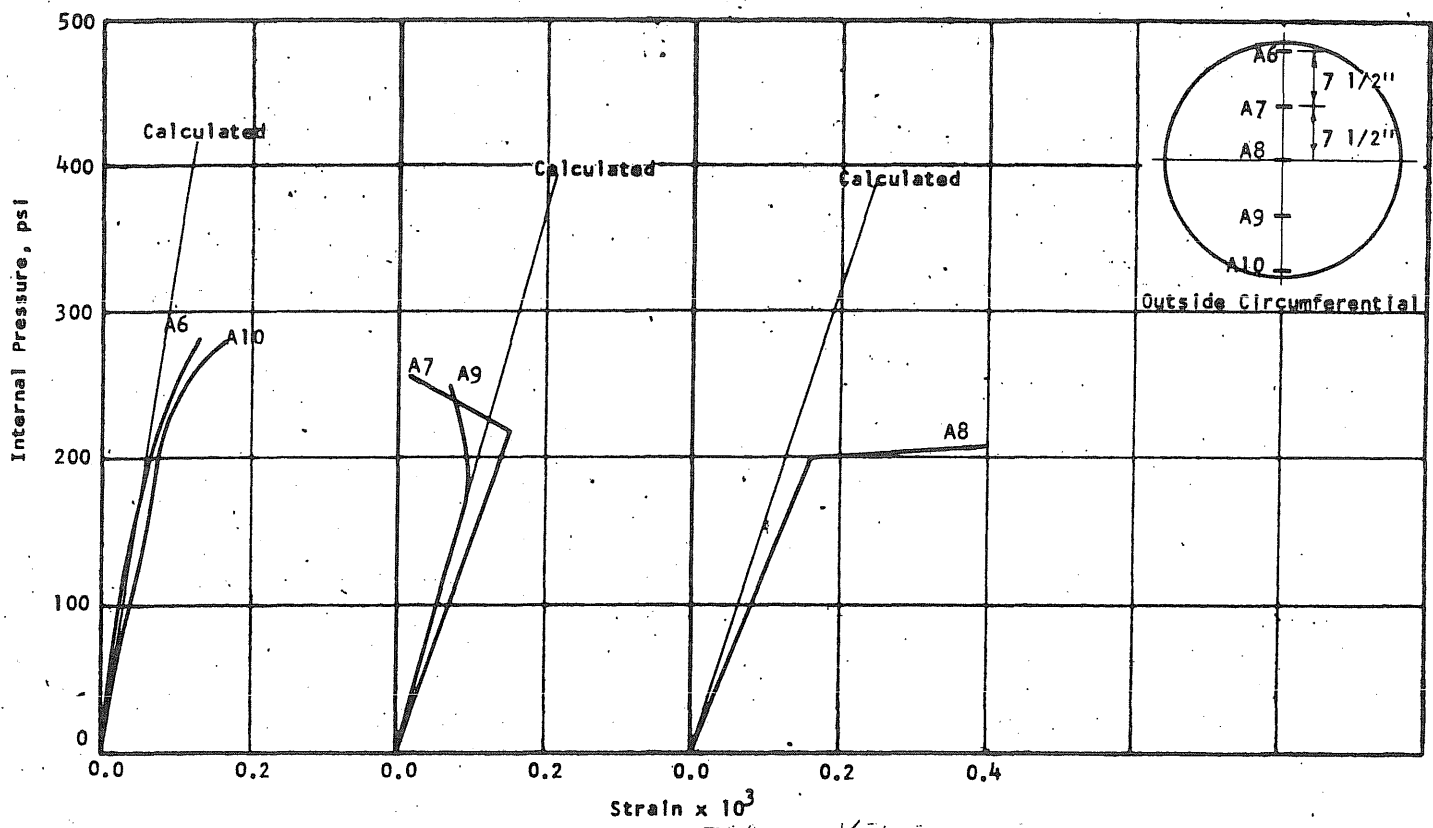


FIG. B3.11 CONCRETE STRAINS, VESSEL PV3

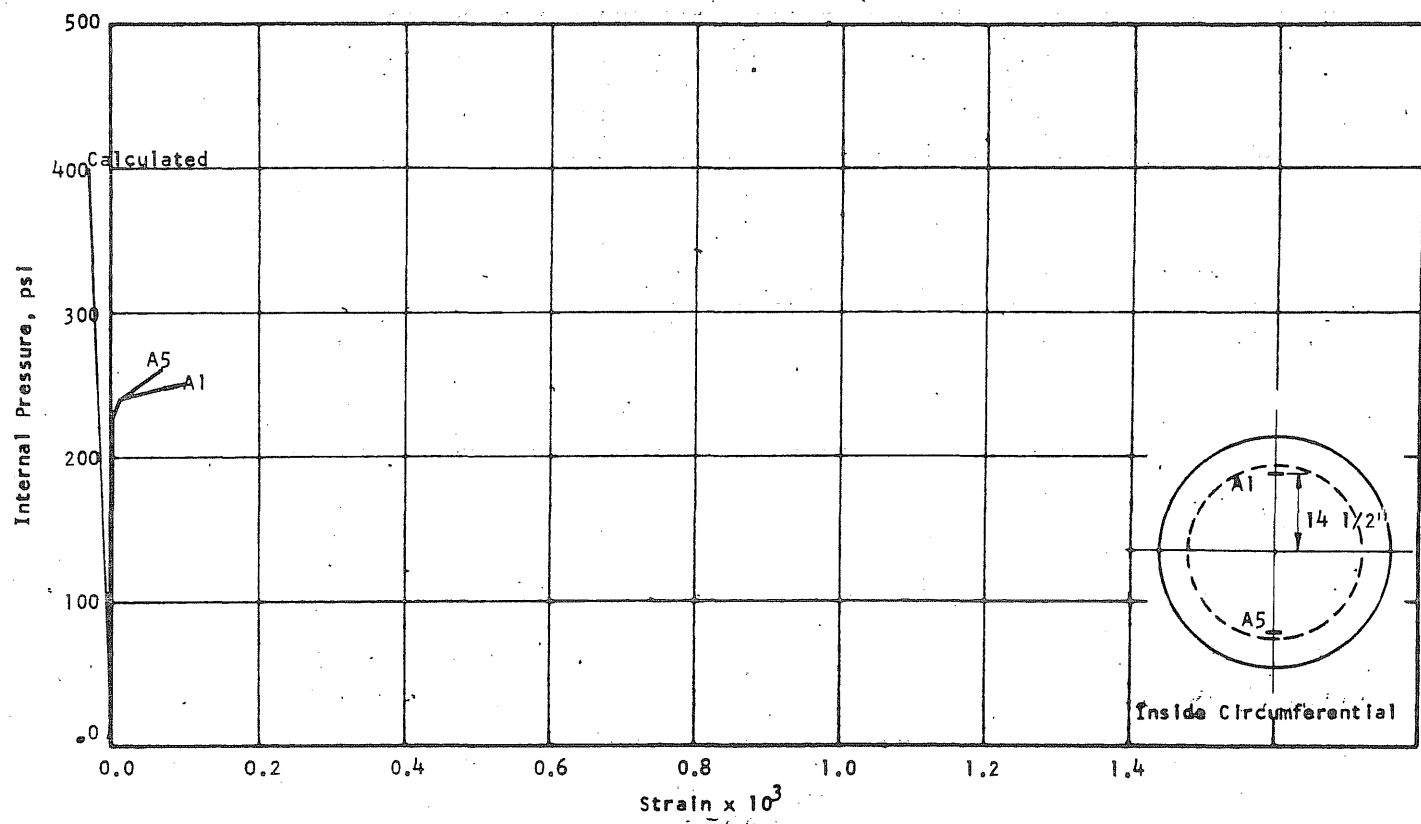


FIG. B3.12 CONCRETE STRAINS, VESSEL PV3

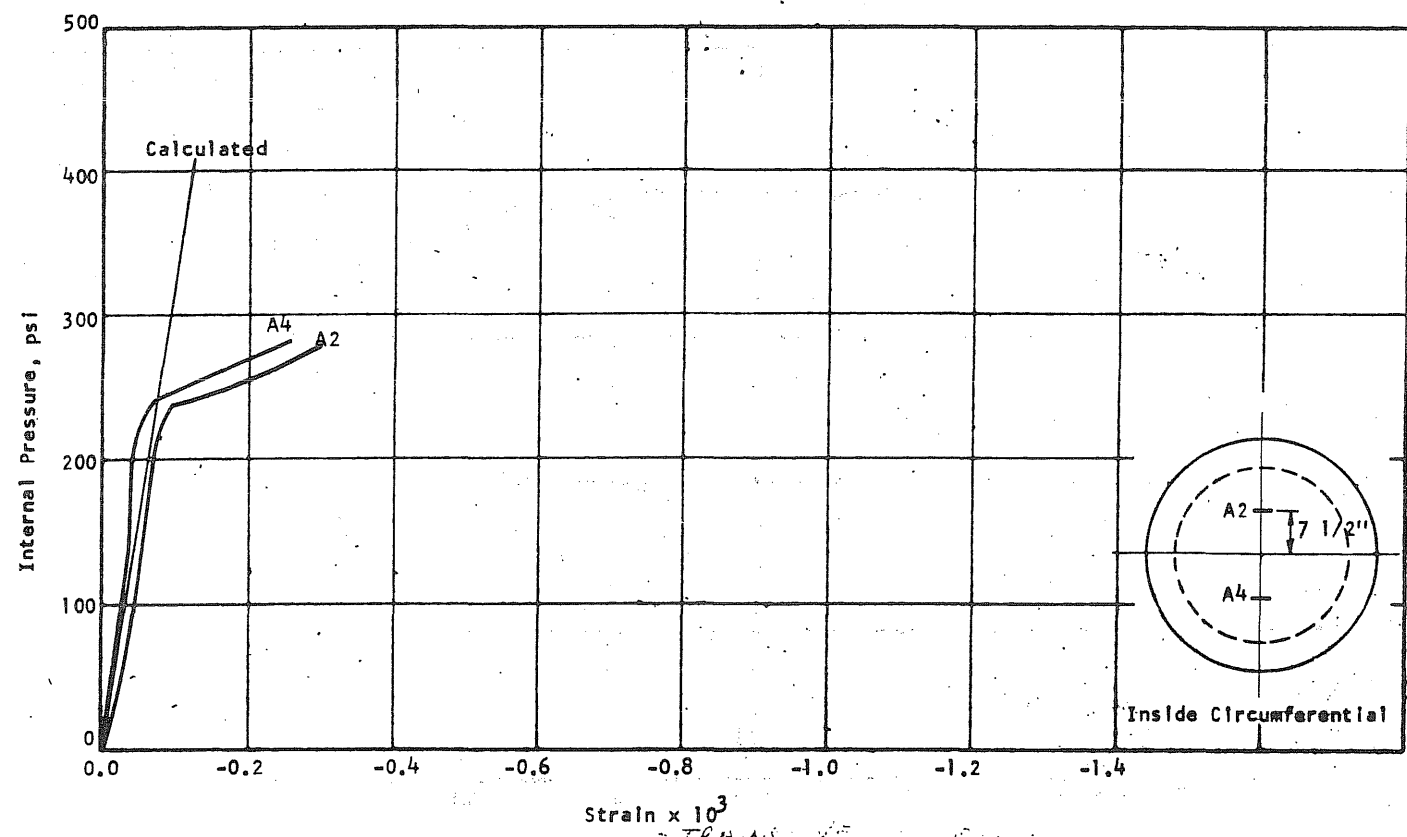


FIG. B3.13 CONCRETE STRAINS, VESSEL PV3

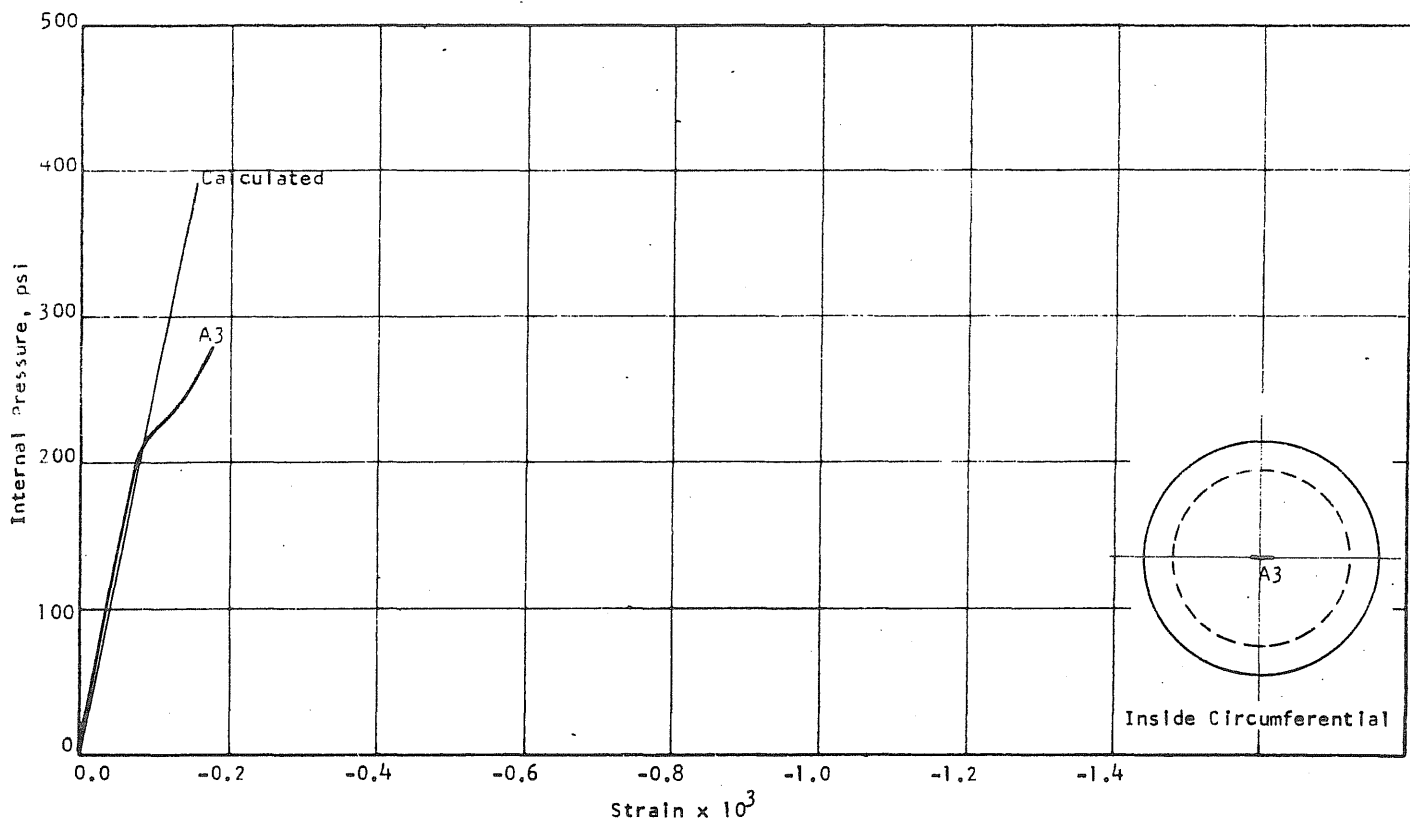


FIG. B3.14 CONCRETE STRAINS, VESSEL PV3

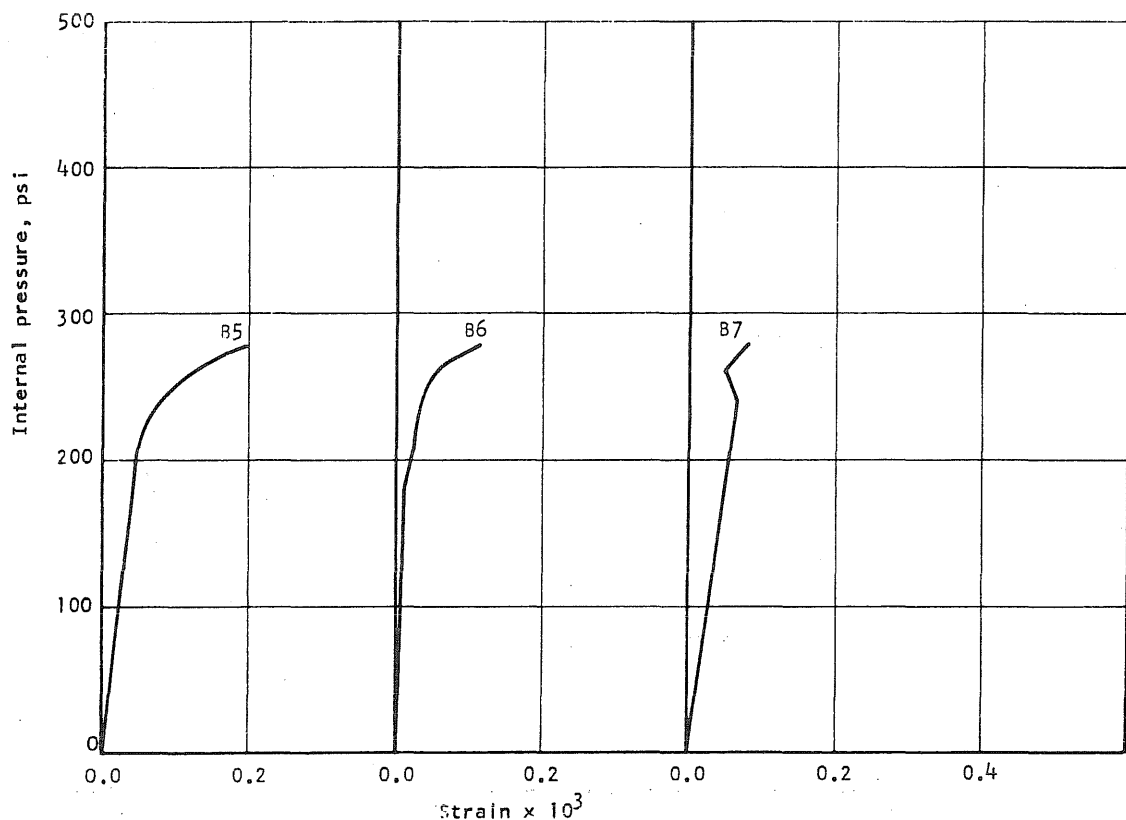


FIG. B3.15 APPLIED PRESSURE vs CIRCUMFERENTIAL STRAIN IN THE WALL OF THE VESSEL AT THE N-END OF THE N-S DIAMETER OF PV3

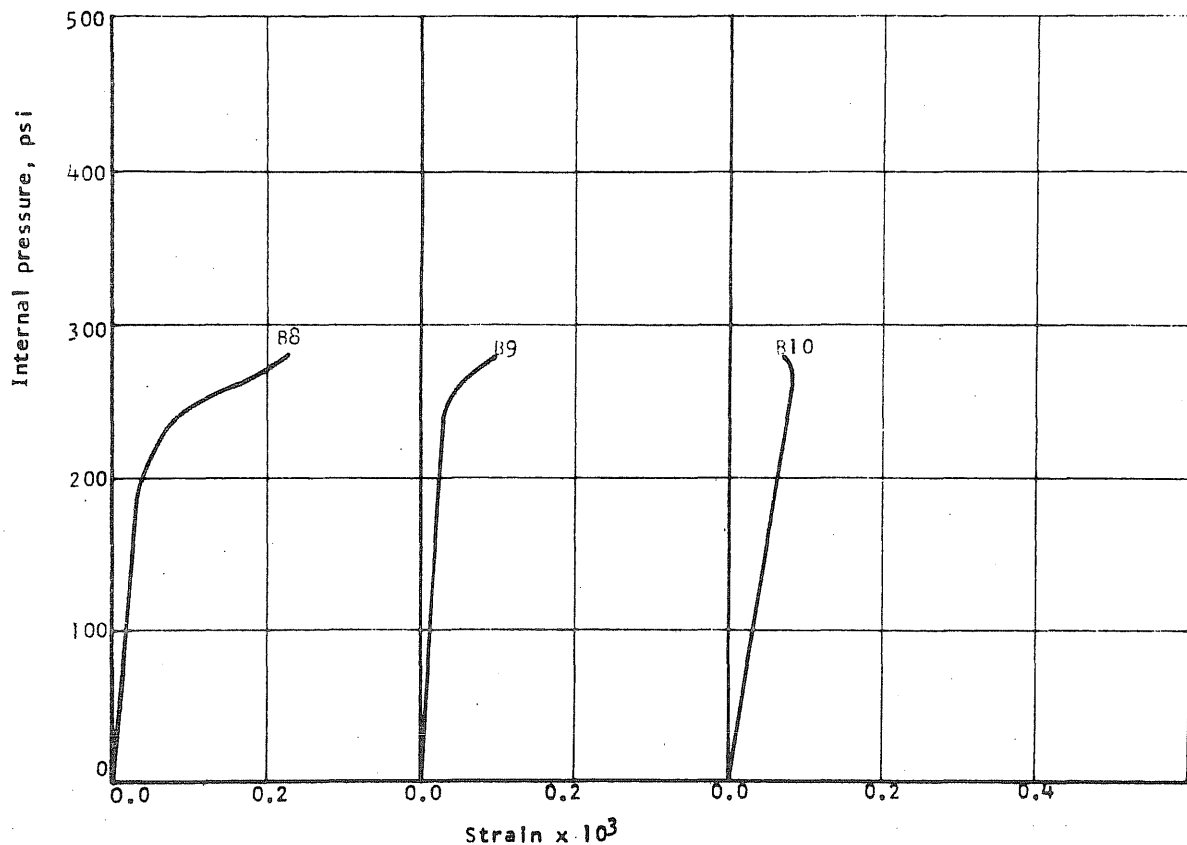


FIG. B3.16 APPLIED PRESSURE vs CIRCUMFERENTIAL STRAIN IN THE WALL OF THE VESSEL
AT THE S-END OF THE N-S DIAMETER OF PV3

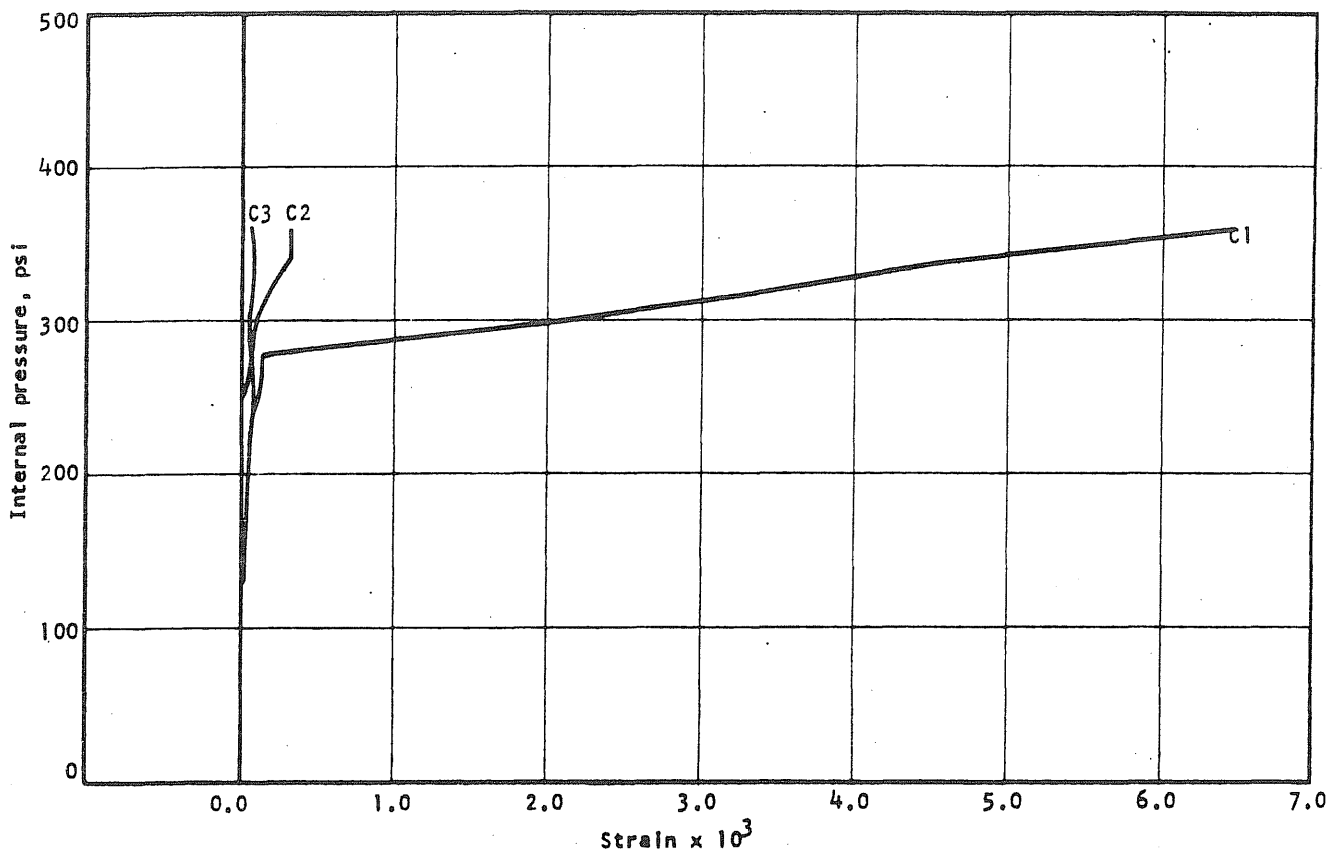


FIG. B3.17 APPLIED PRESSURE vs STRAIN IN THE CIRCUMFERENTIAL PRESTRESS WIRE AT THE N-END
OF THE N-S DIAMETER OF PV3

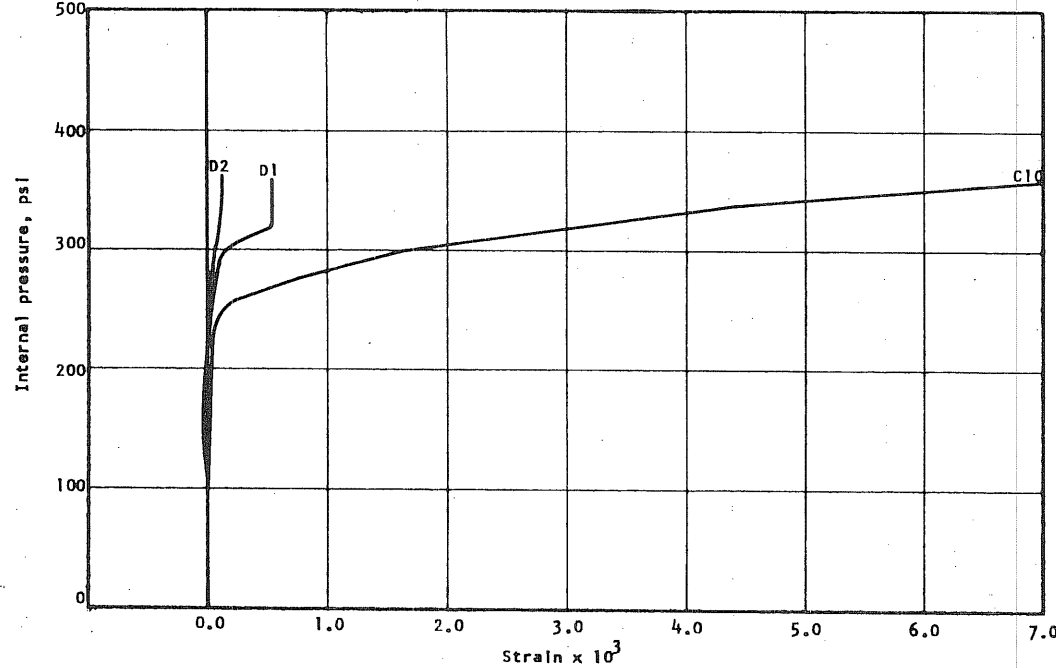


FIG. B3.18 APPLIED PRESSURE vs STRAIN IN THE CIRCUMFERENTIAL PRESTRESS WIRE AT THE S-END OF THE N-S DIAMETER OF PV3

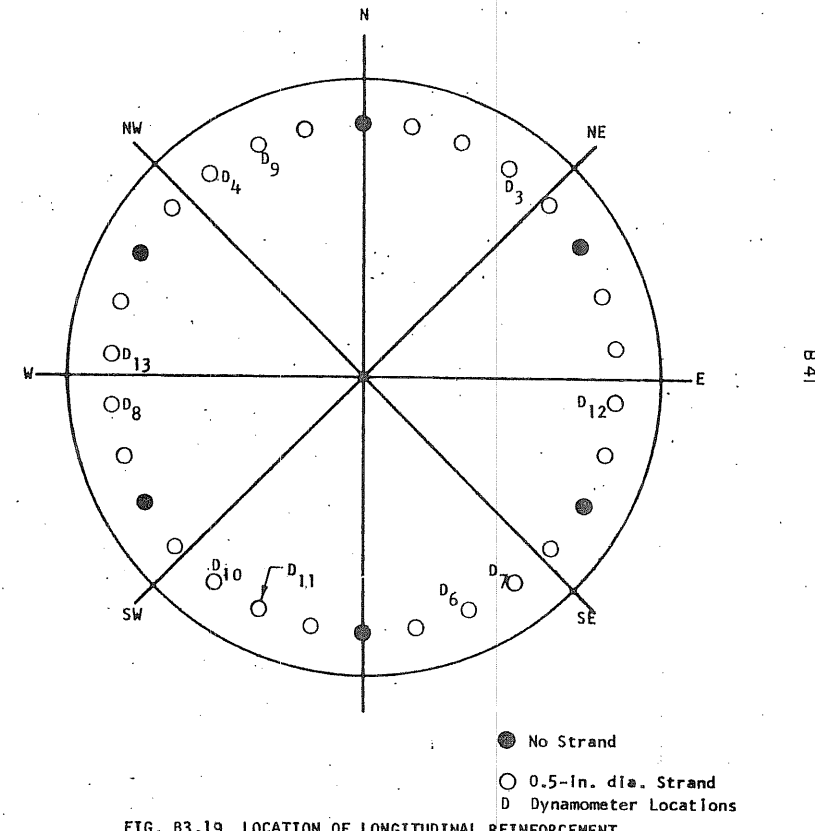


FIG. B3.19 LOCATION OF LONGITUDINAL REINFORCEMENT

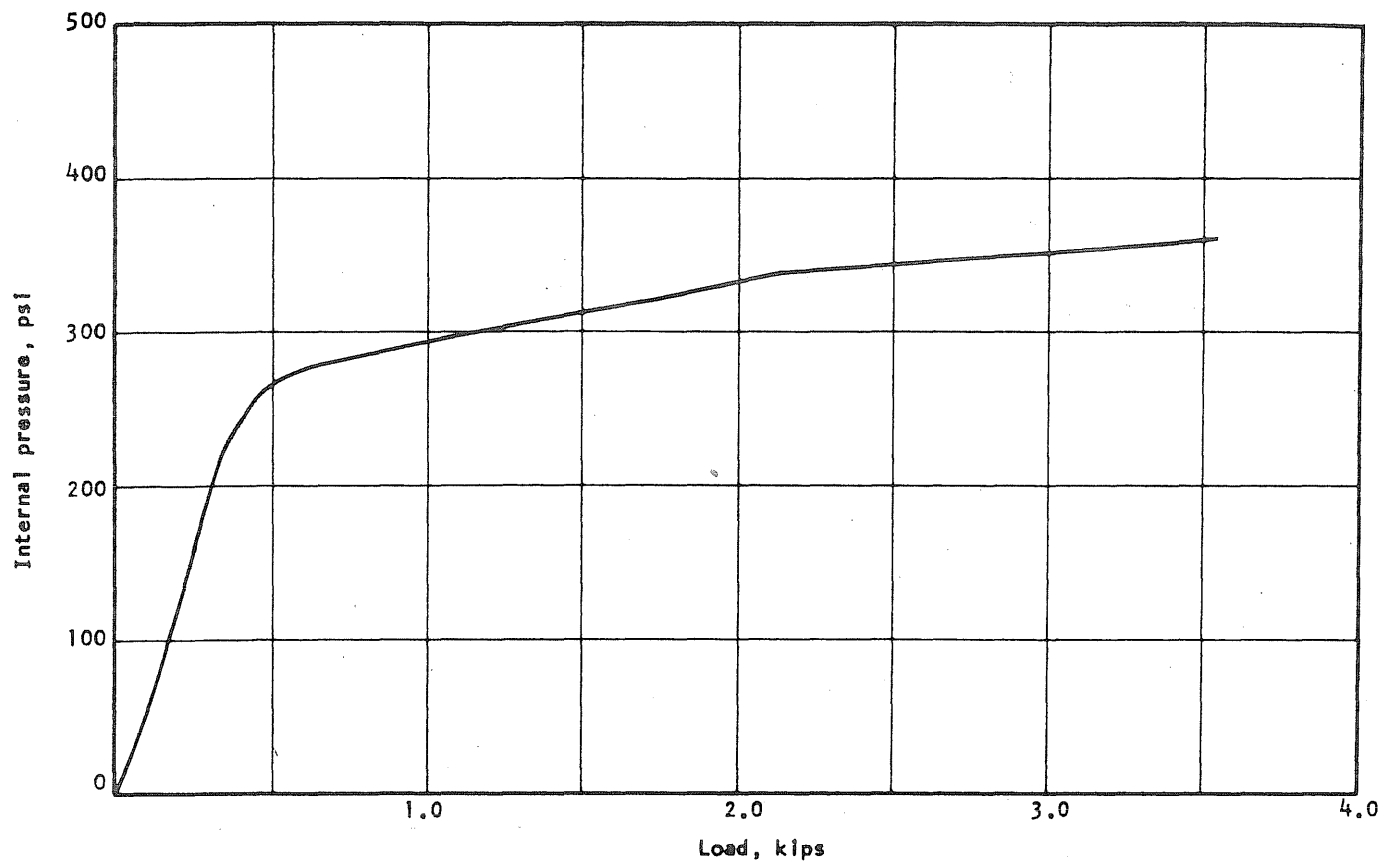


FIG. B3.20 APPLIED PRESSURE vs INCREASE IN LOAD IN DYNAMOMETER NO. 11 IN PV3

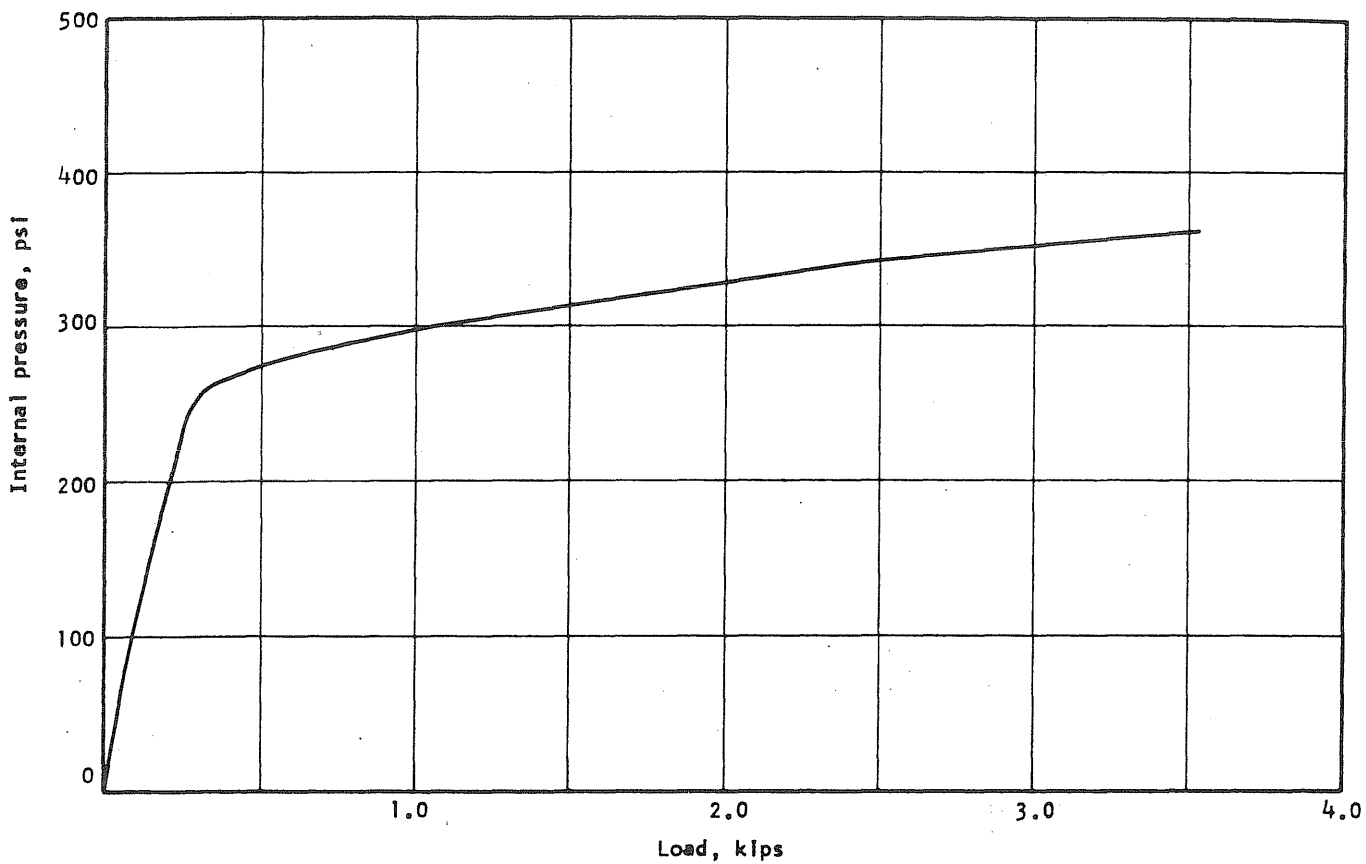


FIG. B3.21 APPLIED PRESSURE vs INCREASE IN LOAD IN DYNAMOMETER NO. 3 IN PV3

B 43

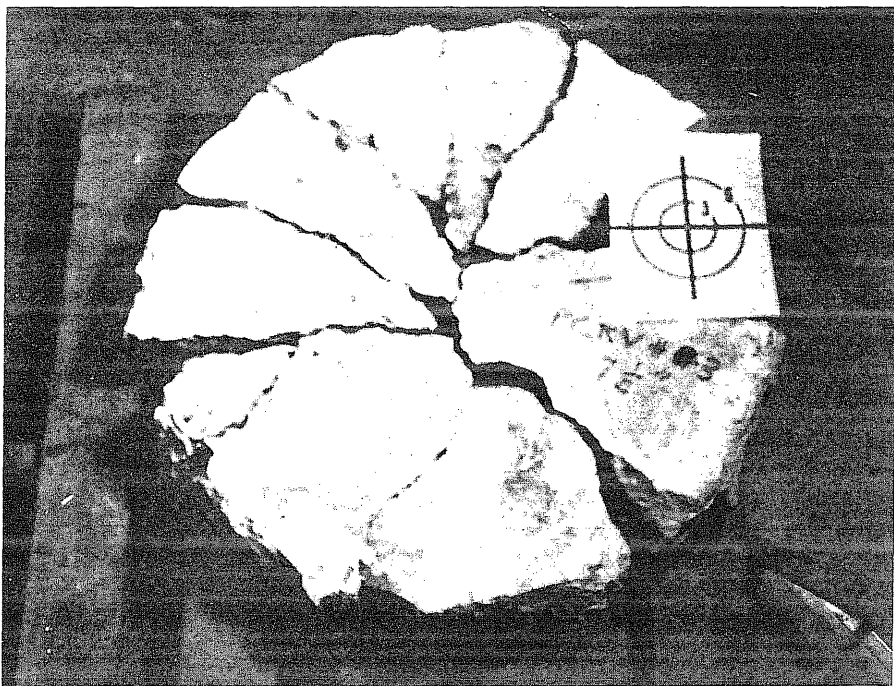


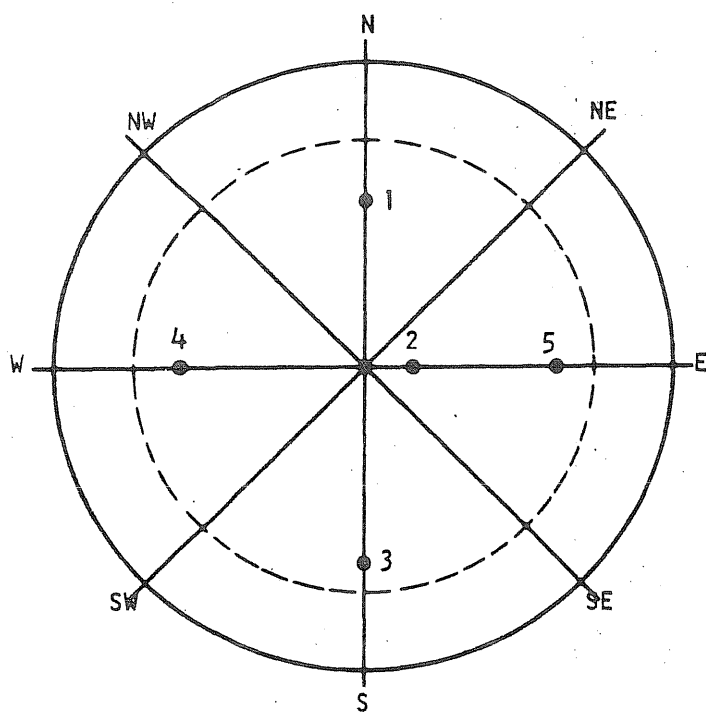
FIG. B3.22 REASSEMBLED END SLAB OF PV3

B4 Test Vessel PV4 ($t = 4$ in., $s = 2/3$ in.)

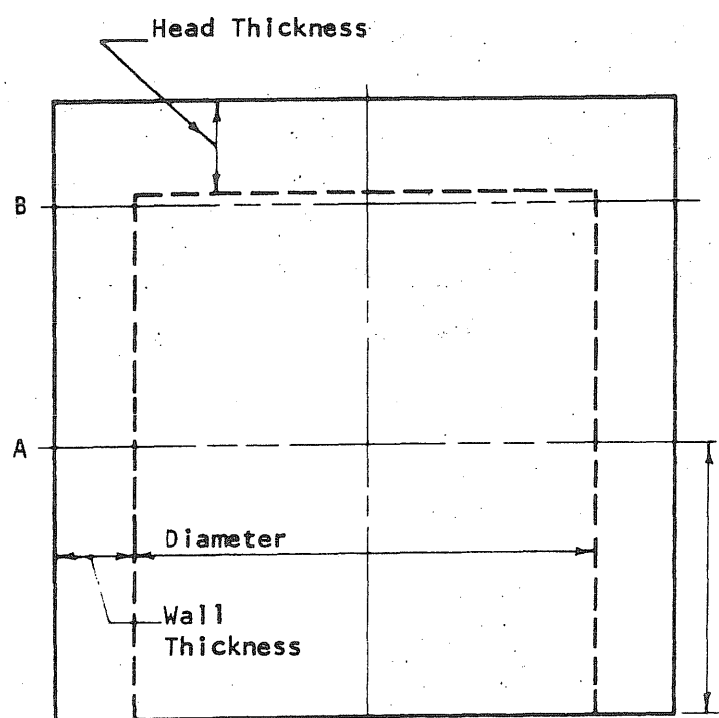
Test vessel PV4 was tested in the manner described for PV1 through PV3 with no unusual occurrences. It was cast of concrete mixed in the laboratory and had no visible cracks at the time of the test.

Nearly four and one-half hours were required to test PV4 as loading proceeded in 20 psi increments to a pressure of 310 psi, when the increment of loading was decreased to 10 psi until the vessel failed at 390 psi. No problems were encountered with the gas seal. The block-out used in PV4 was a steel cylinder filled with water.

Twelve of the twenty-four strands were equipped with load cells and were monitored during the test. The crack pattern in the end slab is illustrated in Fig. B4.21.



| Head Thickness | |
|----------------|--------|
| Point No. | Inches |
| 1 | 6.0 |
| 2 | 6.1 |
| 3 | 6.2 |
| 4 | 6.0 |
| 5 | 6.2 |



| Wall Thickness, in. | | |
|---------------------|----|------|
| Plane Axis | AA | BB |
| N | | 5.07 |
| NE | | 5.10 |
| E | | 4.98 |
| SE | | 5.01 |
| S | | 5.02 |
| SW | | 5.04 |
| W | | 4.97 |
| NW | | 5.02 |

| Inside Diameter, in. | | |
|----------------------|----|--------------------|
| Plane Axis | AA | BB |
| N-S | | 29 $\frac{30}{32}$ |
| NE-SW | | 29 $\frac{30}{32}$ |
| E-W | | 30 $\frac{1}{32}$ |
| SE-NW | | 29 $\frac{30}{32}$ |

FIG. B4.1 DIMENSIONS OF PV4

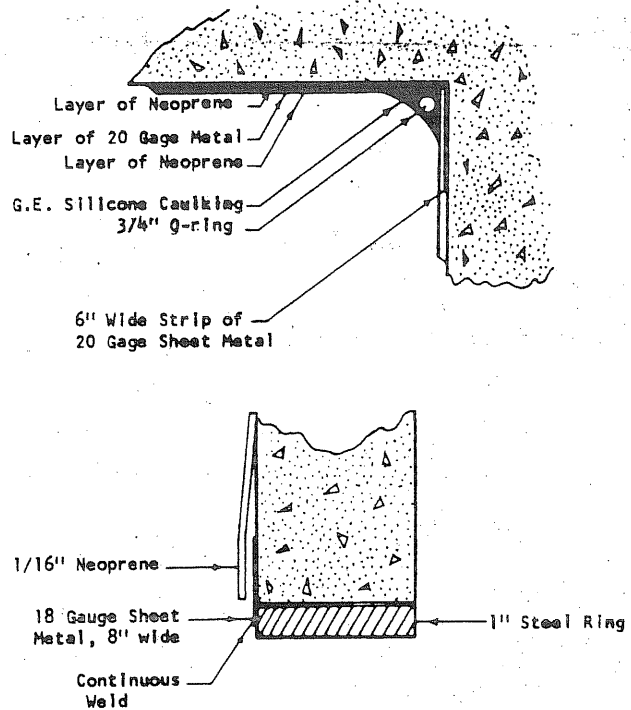
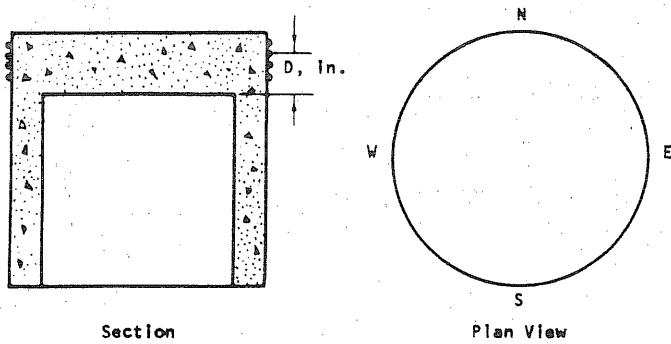


FIG. B4.2 SEALING DETAIL FOR PV4



| Wrap No. | D _N | D _E | D _S | D _W |
|----------|----------------|----------------|----------------|----------------|
| 1 | 5 5/16 | 5 9/16 | 5 10/16 | 5 8/16 |
| 2 | 4 14/16 | 5 1/16 | 5 2/16 | 5 |
| 3 | 4 10/16 | 4 8/16 | 4 10/16 | 4 9/16 |
| 4 | 4 3/16 | 3 15/16 | 4 2/16 | 4 1/16 |
| 5 | 3 9/16 | 3 4/16 | 3 7/16 | 3 7/16 |
| 6 | 2 15/16 | 2 10/16 | 2 13/16 | 2 12/16 |
| 7 | 2 4/16 | 1 15/16 | 2 2/16 | 2 2/16 |
| 8 | 1 10/16 | 1 4/16 | 1 7/16 | 1 7/16 |
| 9 | 14/16 | 10/16 | 12/16 | 12/16 |
| 10 | 4/16 | -1/16 | 2/16 | 1/16 |

FIG. B4.3 MEASURED LOCATION OF THE CIRCUMFERENTIAL PRESTRESS WIRE AT THE ENDS OF THE N-S AND E-W DIAMETERS ON PV4

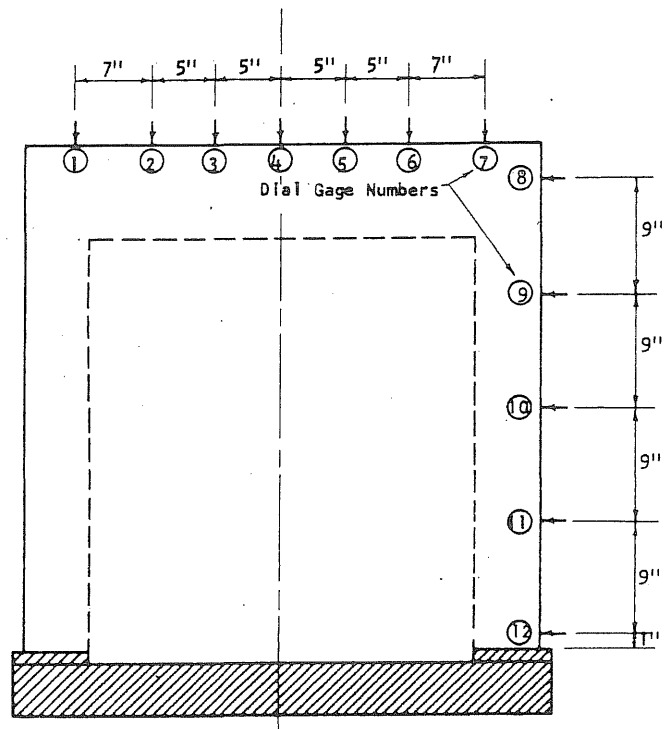


FIG. B4.4 LOCATION OF DEFLECTION GAGES ON PV4

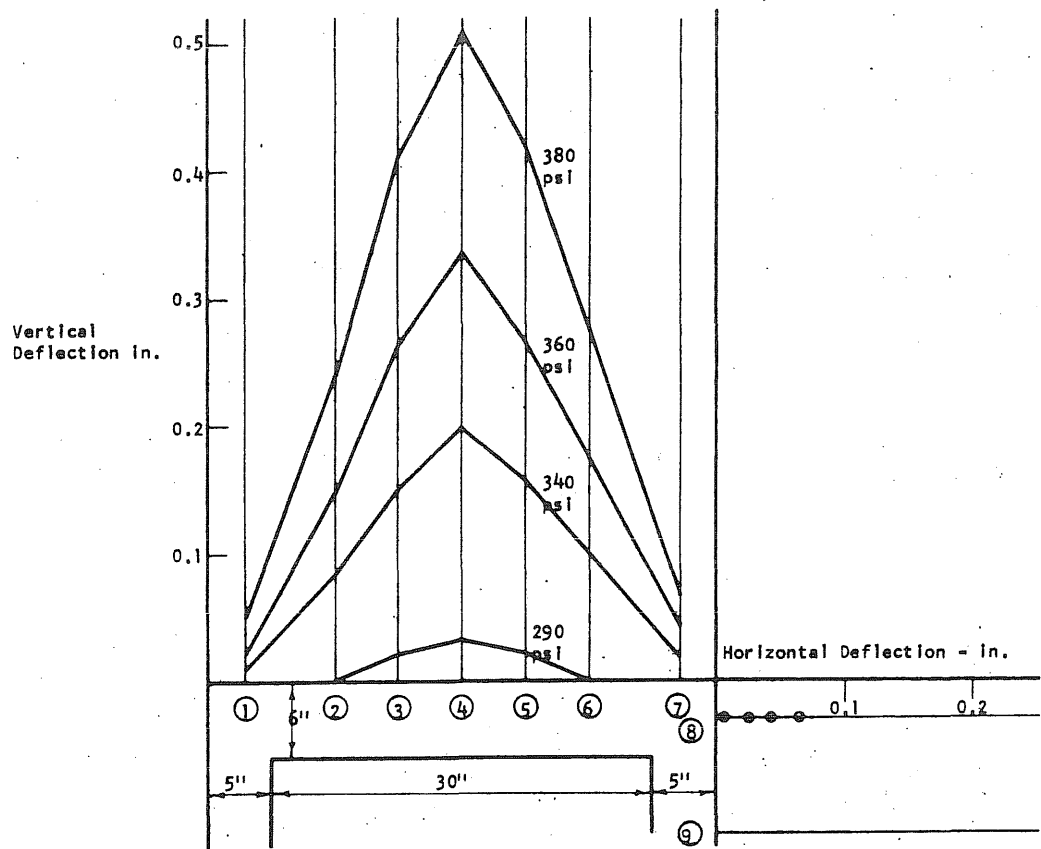


FIG. B4.5 DEFLECTION PROFILES OF THE SLAB ALONG THE N-S DIAMETER

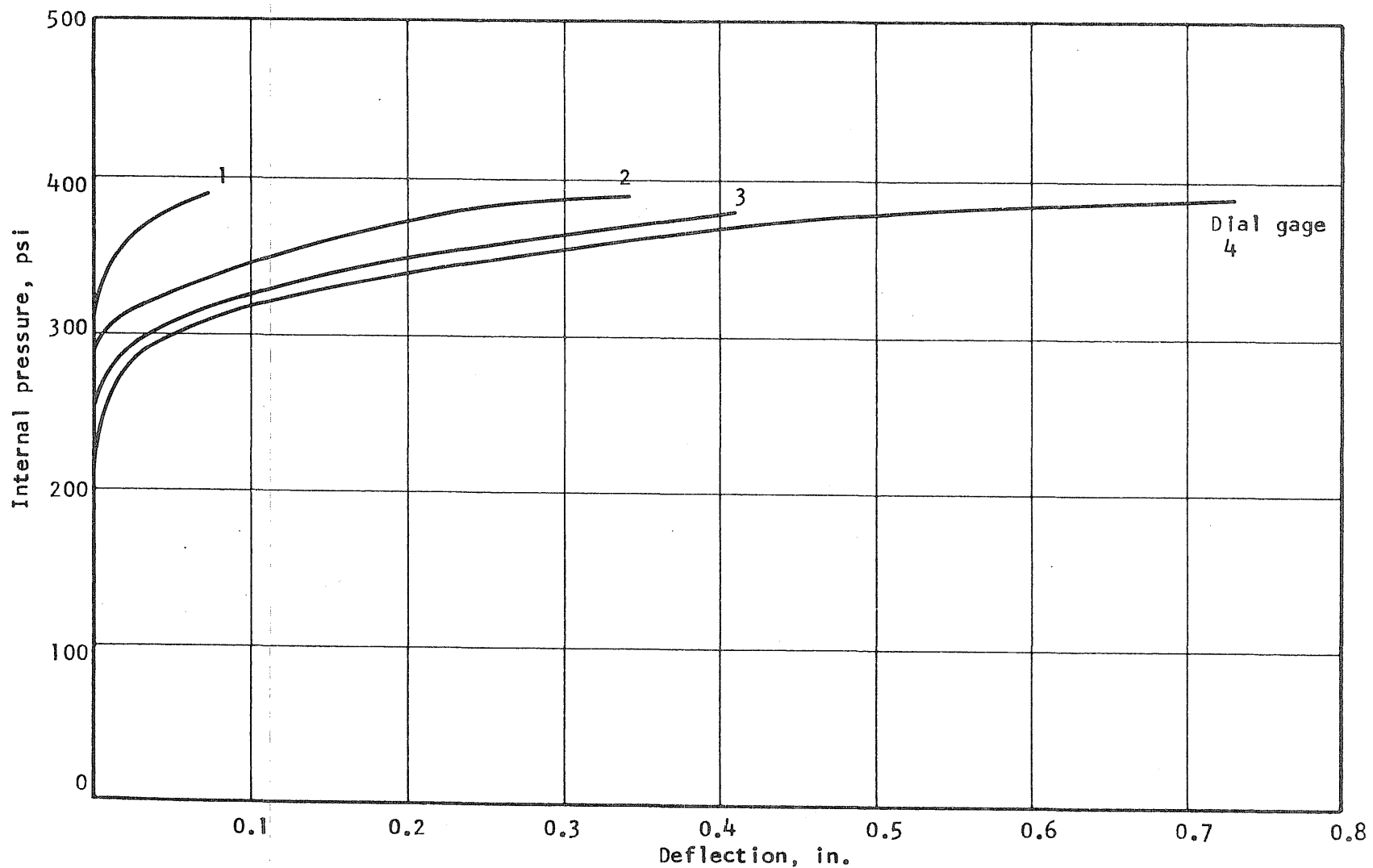


FIG. B4.6 APPLIED PRESSURE vs DEFLECTION ALONG THE N-HALF OF THE N-S DIAMETER OF PV4

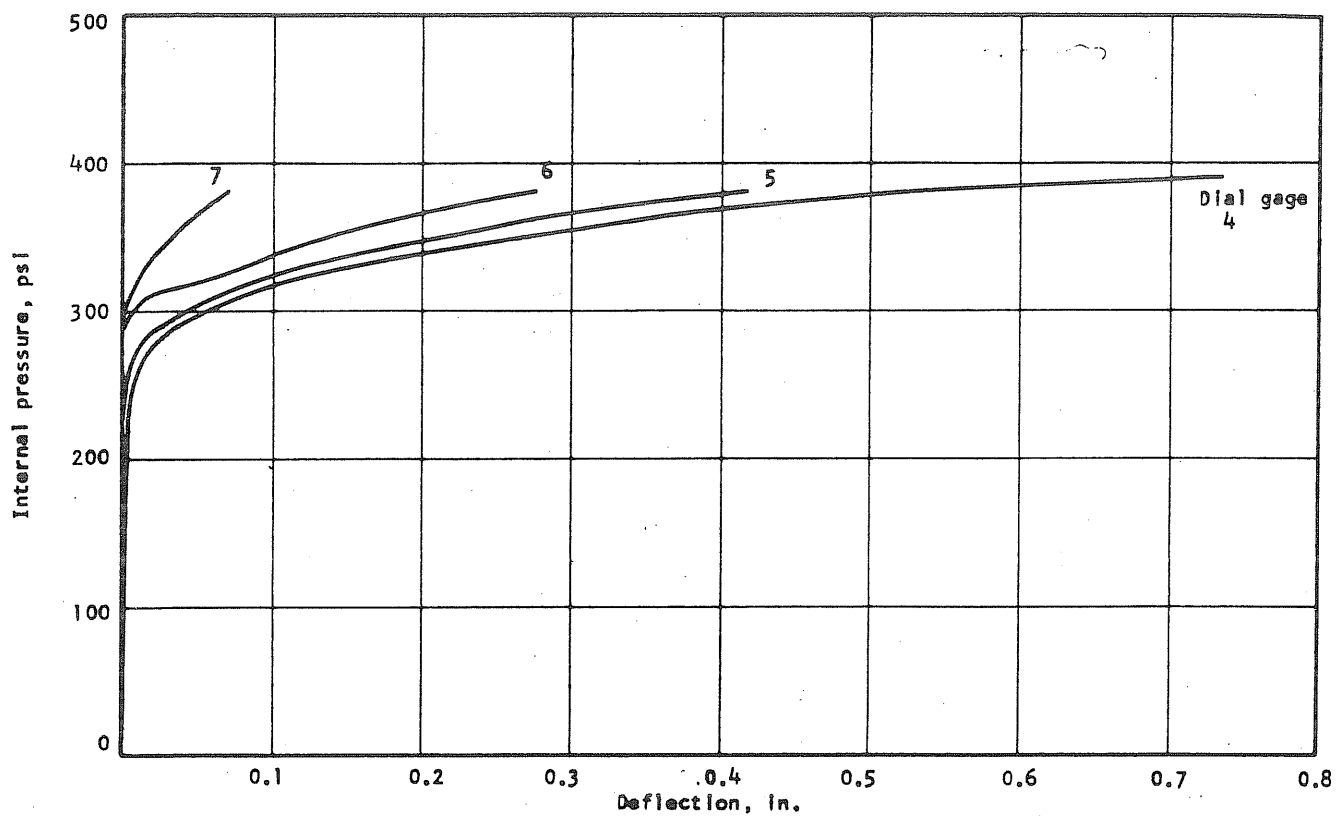


FIG. B4.7 APPLIED PRESSURE VS DEFLECTION ALONG THE S-HALF OF THE N-S DIAMETER OF PV4

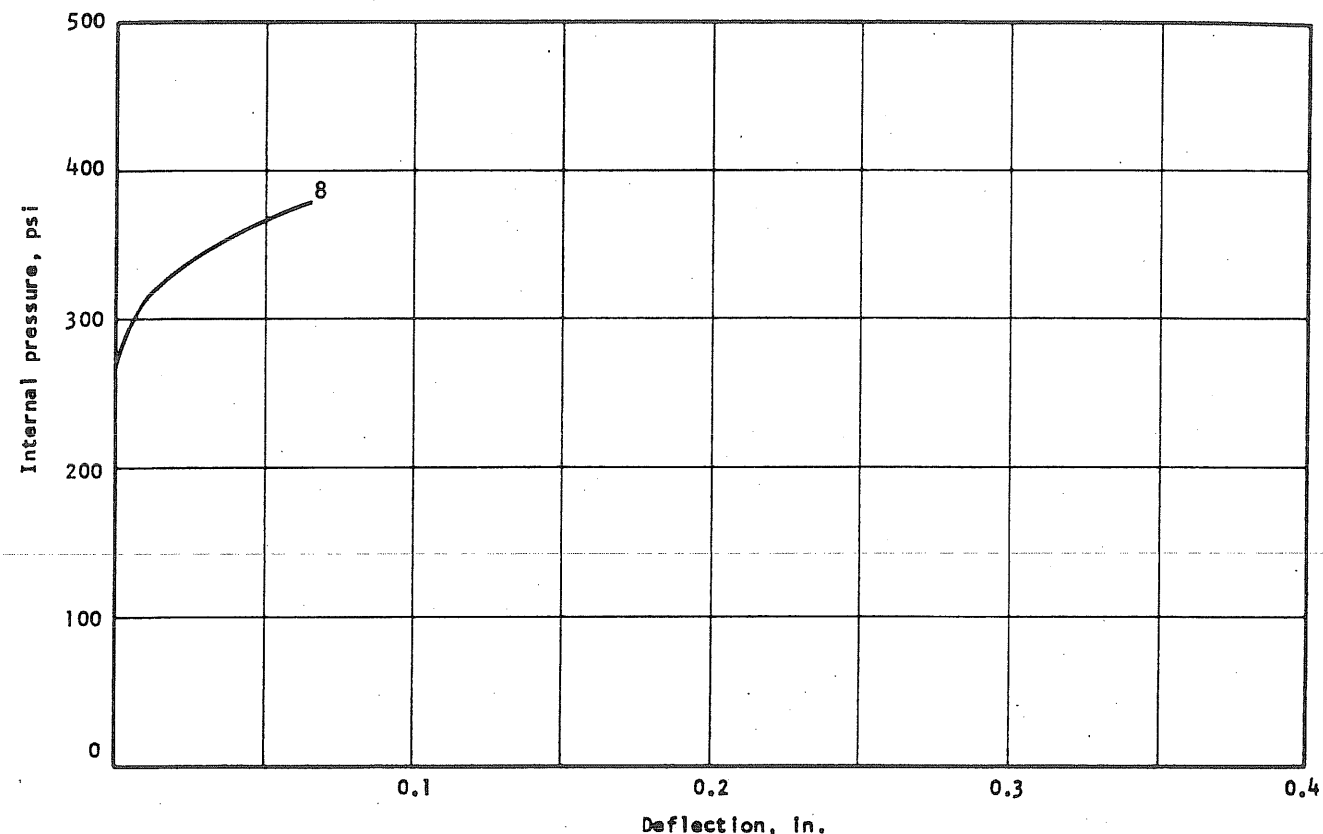
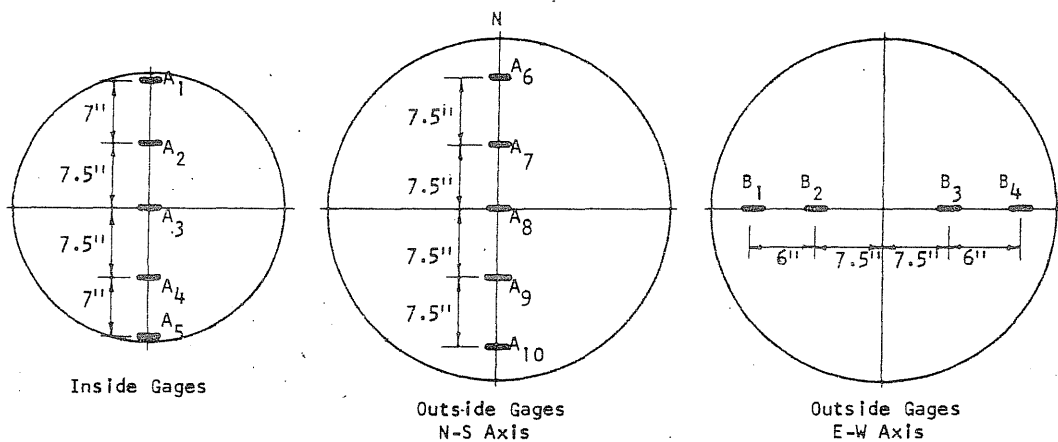


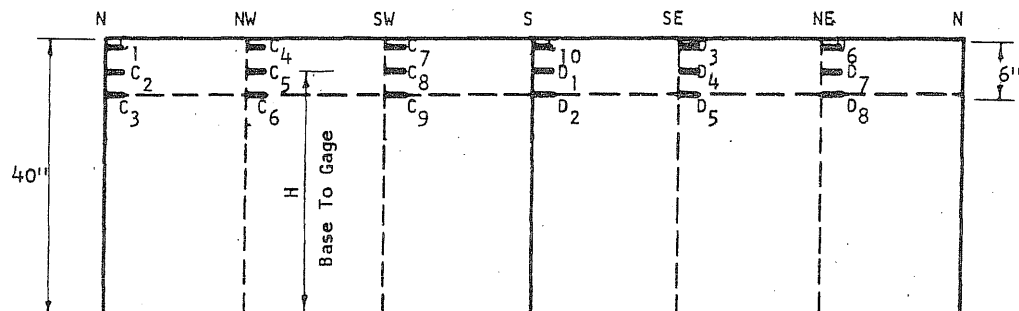
FIG. B4.8 APPLIED PRESSURE VS DEFLECTION OF THE SIDE WALL OF PV4

B 50

Concrete Gages on The Slab

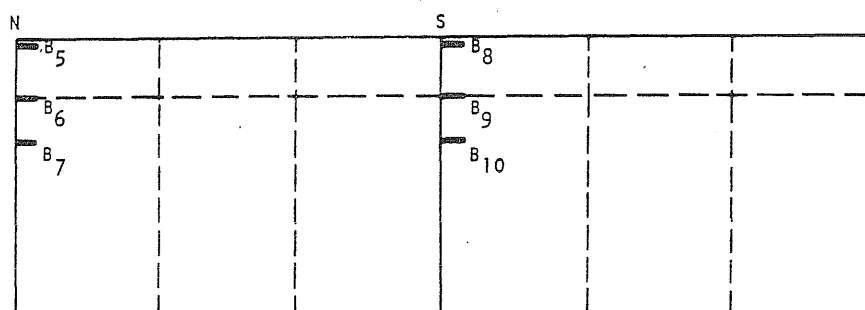


Steel Gages on Prestressing Wire



| Gage | Line | H | Gage | Line | H | Gage | Line | H |
|----------------|------|----------|-----------------|------|----------|----------------|------|----------|
| C ₁ | N | 38 13/16 | C ₇ | SW | 39 1/16 | D ₃ | SE | 39 2/16 |
| C ₂ | N | 36 13/16 | C ₈ | SW | 36 13/16 | D ₄ | SE | 36 11/16 |
| C ₃ | N | 34 4/16 | C ₉ | SW | 34 2/16 | D ₅ | SE | 34 1/16 |
| C ₄ | NW | 38 15/16 | C ₁₀ | S | 39 3/16 | D ₆ | NE | 39 0/16 |
| C ₅ | NW | 36 12/16 | D ₁ | S | 36 13/16 | D ₇ | NE | 36 8/16 |
| C ₆ | NW | 34 2/16 | D ₂ | S | 34 2/16 | D ₈ | NE | 33 14/16 |

Concrete Gages on The Outside of The Vessel



| Gage | Line | H | Gage | Line | H |
|----------------|------|----------|-----------------|------|----------|
| B ₅ | N | 38 6/16 | B ₈ | S | 38 14/16 |
| B ₆ | N | 36 8/16 | B ₉ | S | 36 7/16 |
| B ₇ | N | 33 15/16 | B ₁₀ | S | 33 12/16 |

FIG. B4.9 STRAIN GAGE LOCATIONS ON PV4

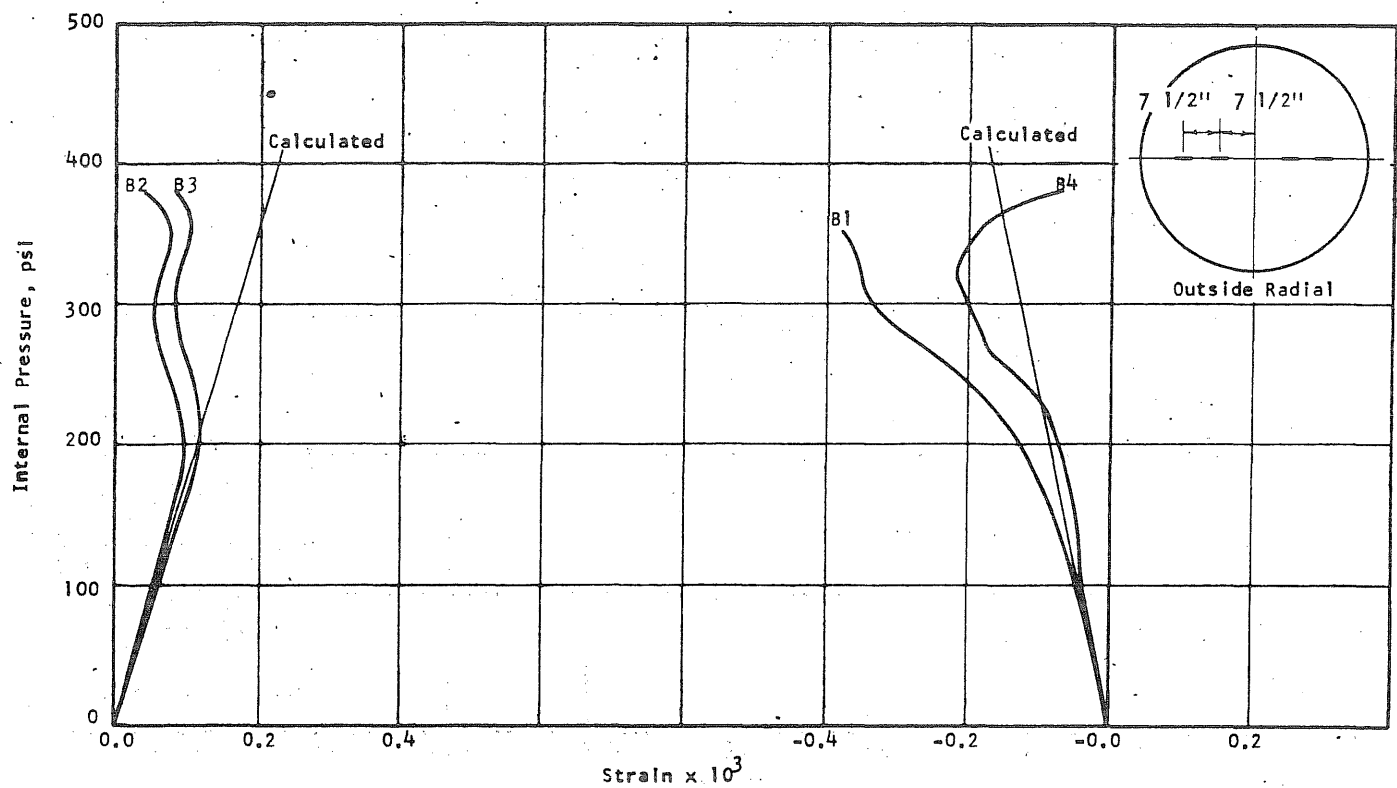


FIG. B4.10 CONCRETE STRAINS, VESSEL PV4

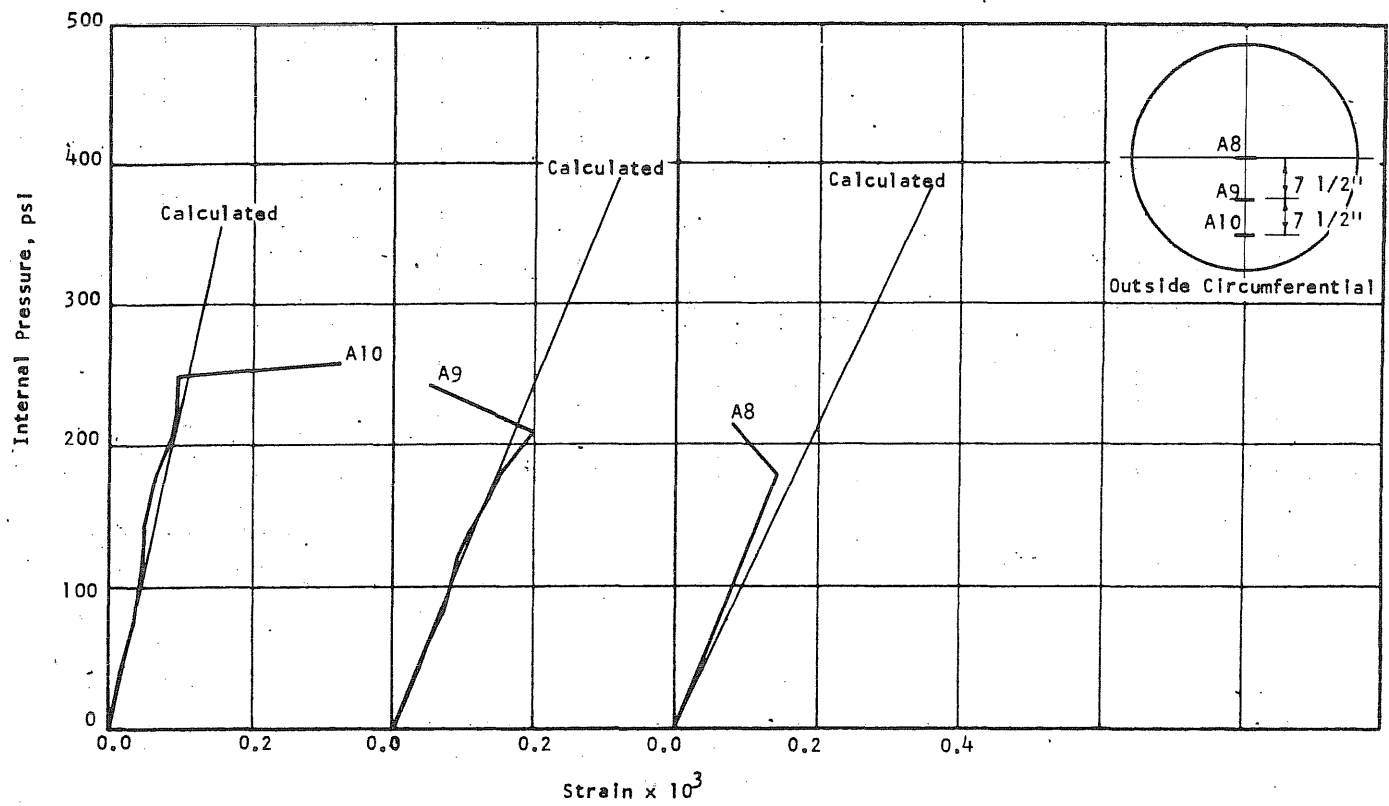


FIG. B4.11 CONCRETE STRAINS, VESSEL PV4

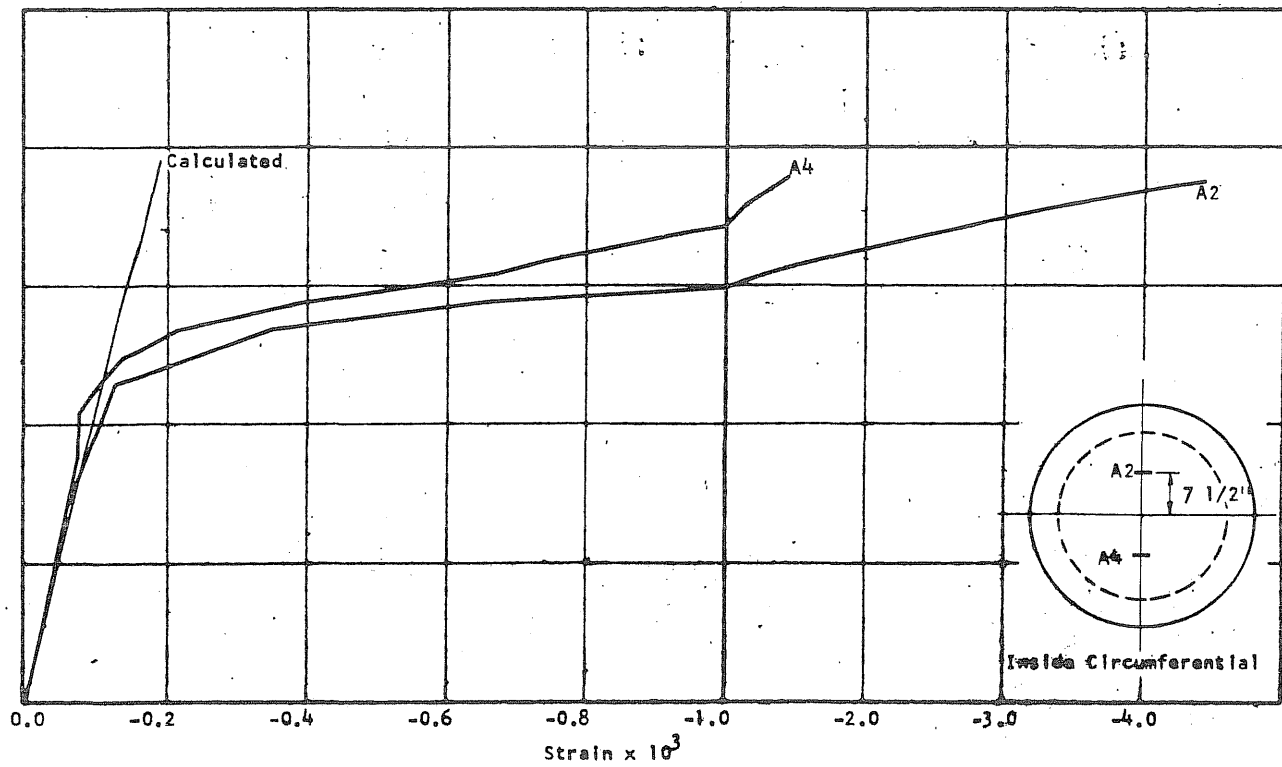


FIG. B4.12 CONCRETE STRAINS, VESSEL PV4

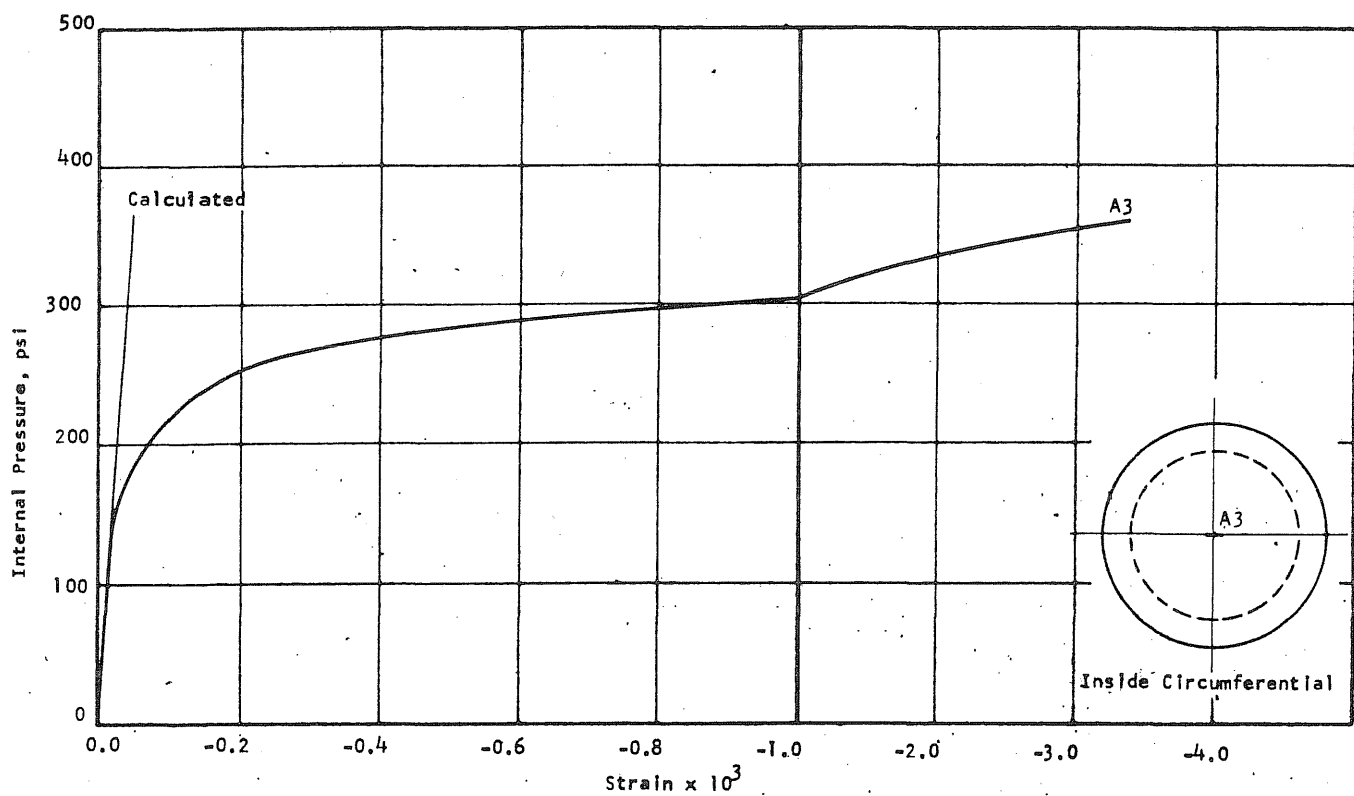
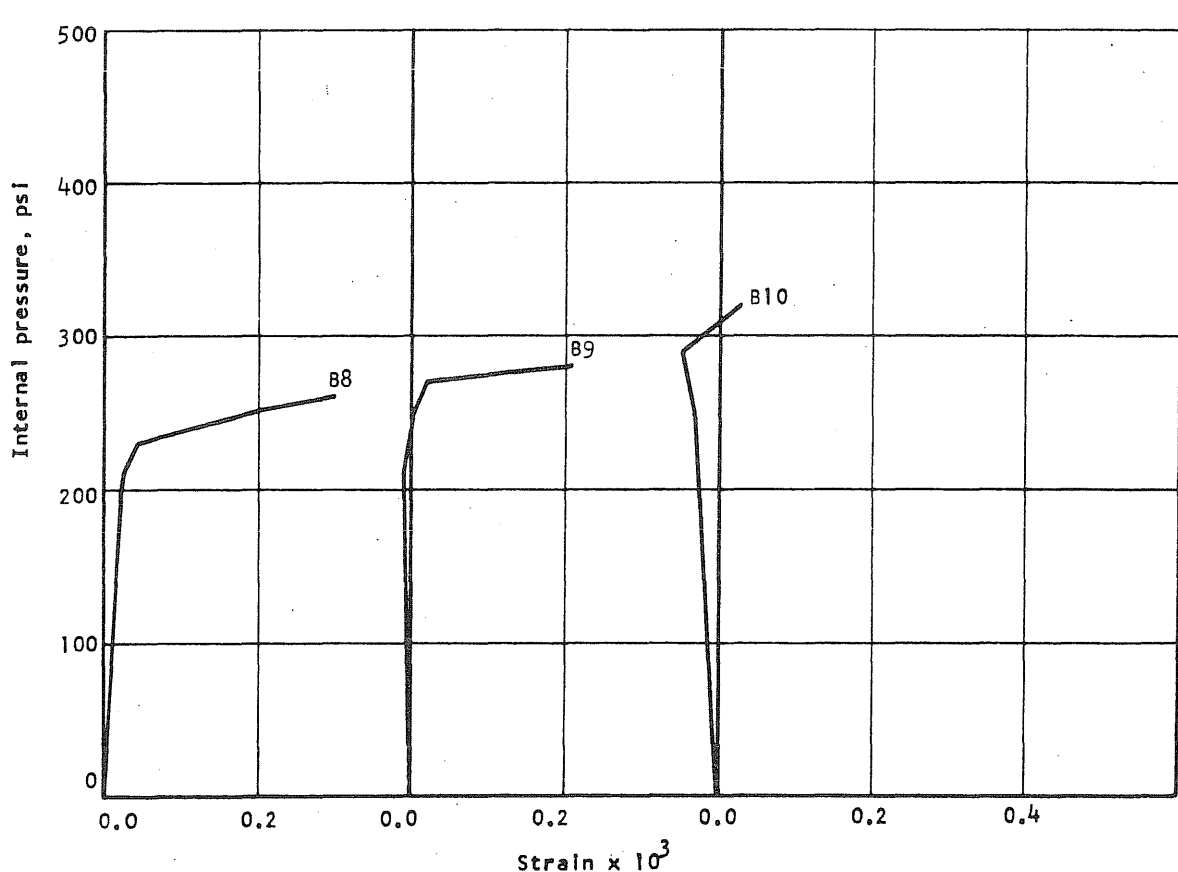
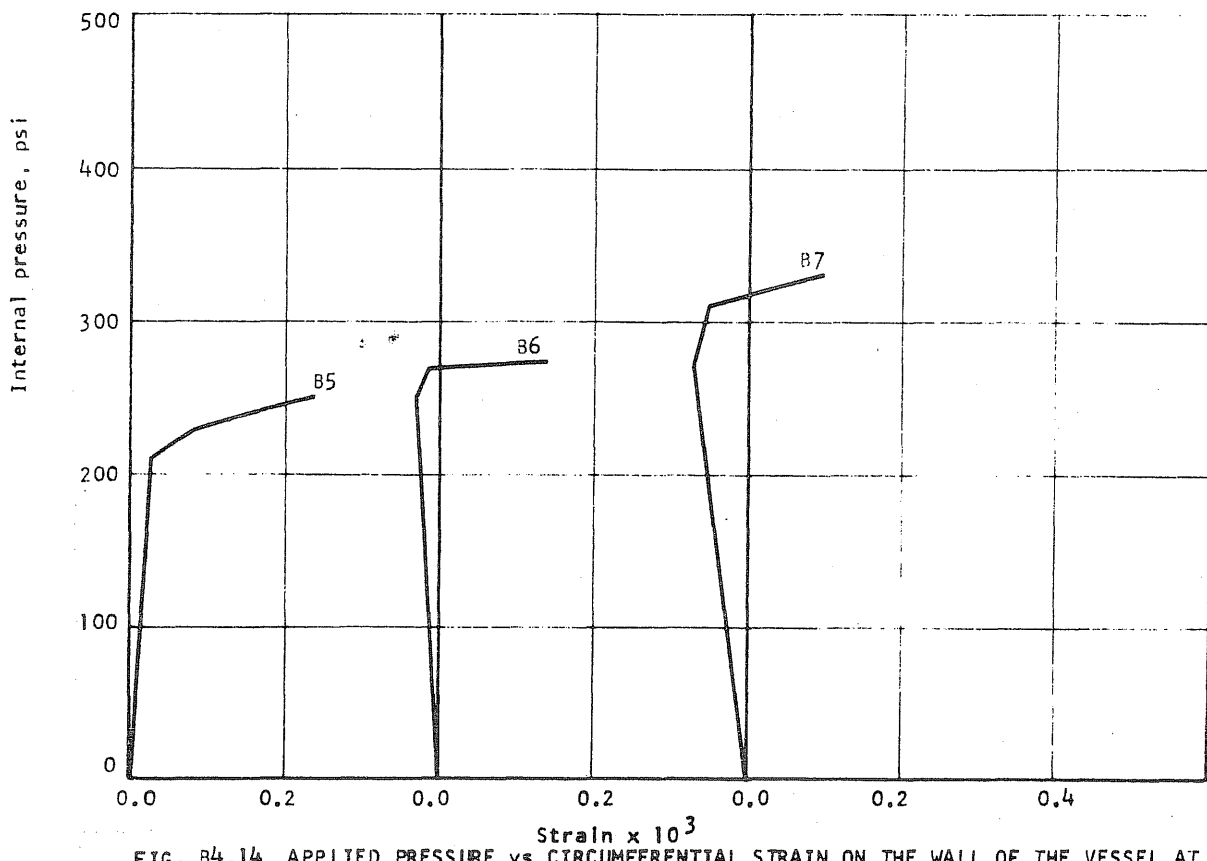


FIG. B4.13 CONCRETE STRAINS, VESSEL PV4



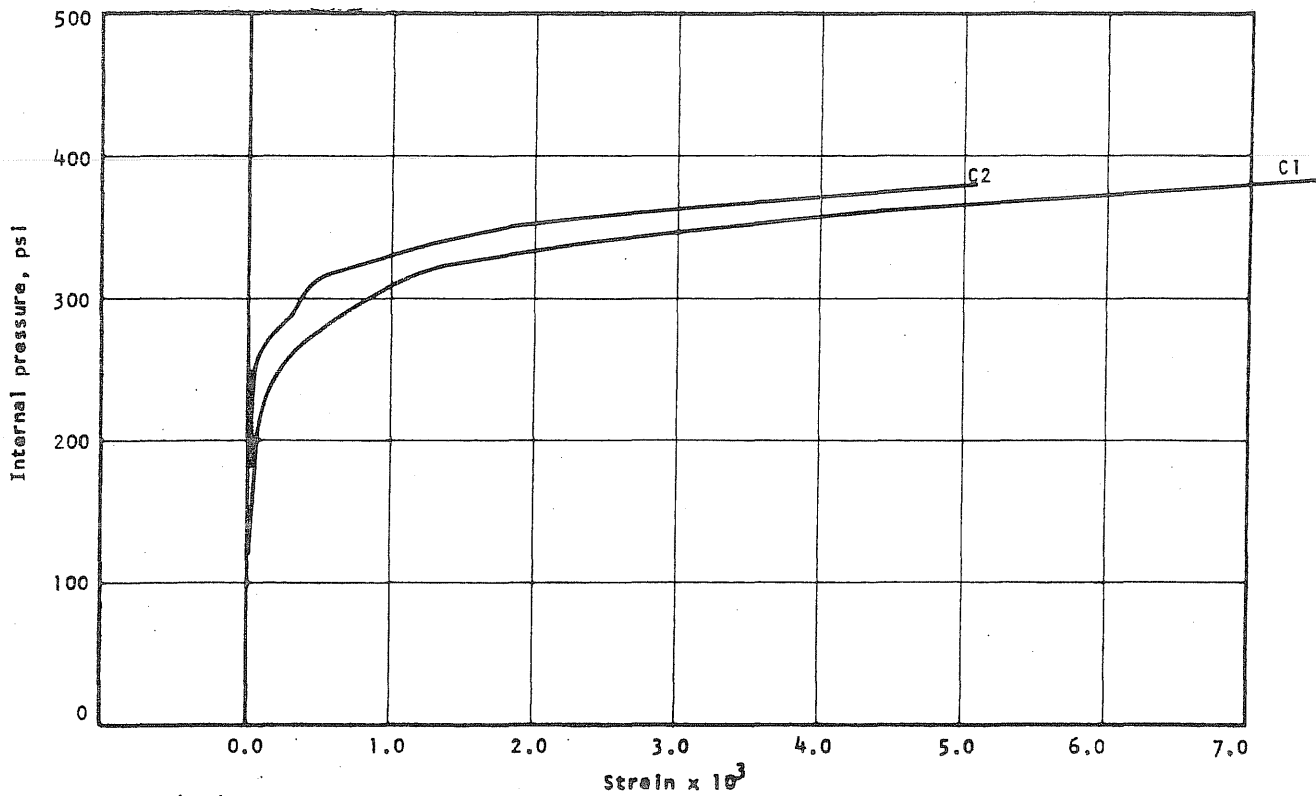


FIG. B4.16 APPLIED PRESSURE VS STRAIN IN THE CIRCUMFERENTIAL PRESTRESS WIRE AT THE N-END OF THE N-S DIAMETER OF PV4

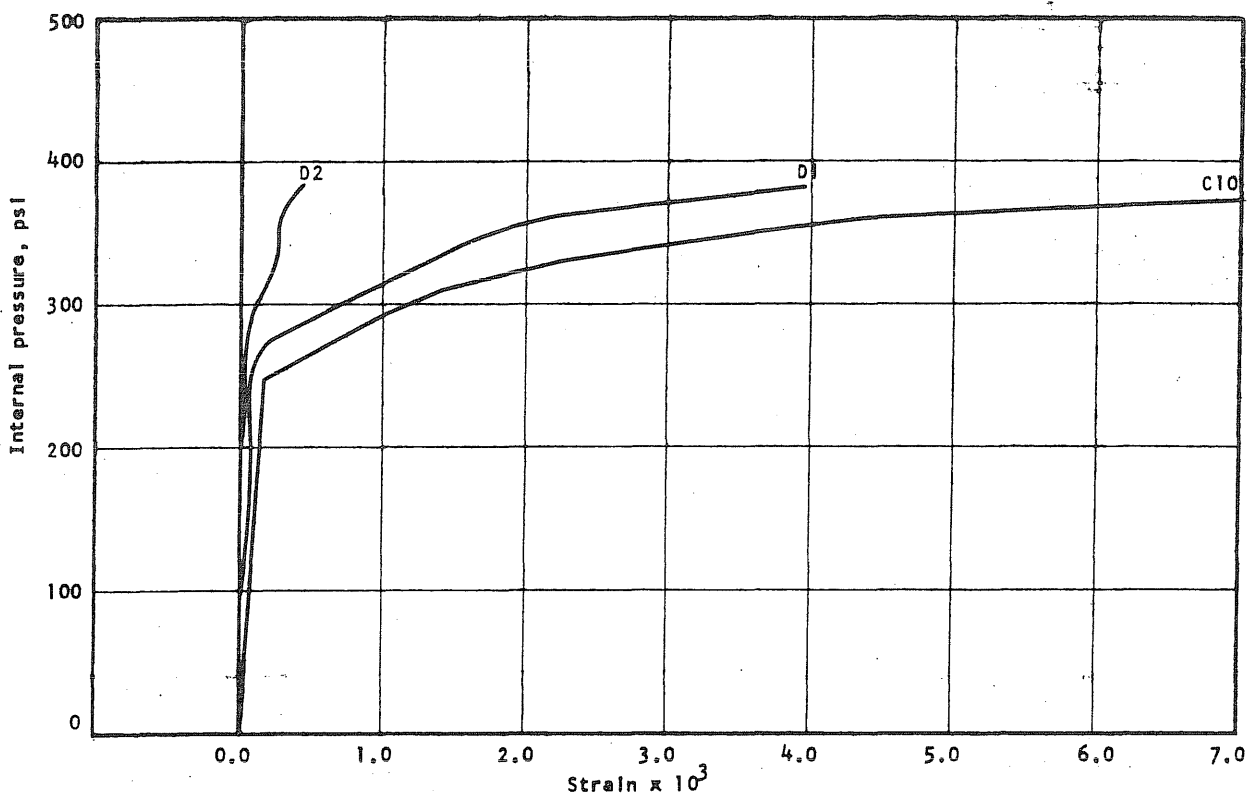


FIG. B4.17 APPLIED PRESSURE VS STRAIN IN THE CIRCUMFERENTIAL PRESTRESS WIRE AT THE S-END OF THE N-S DIAMETER OF PV4

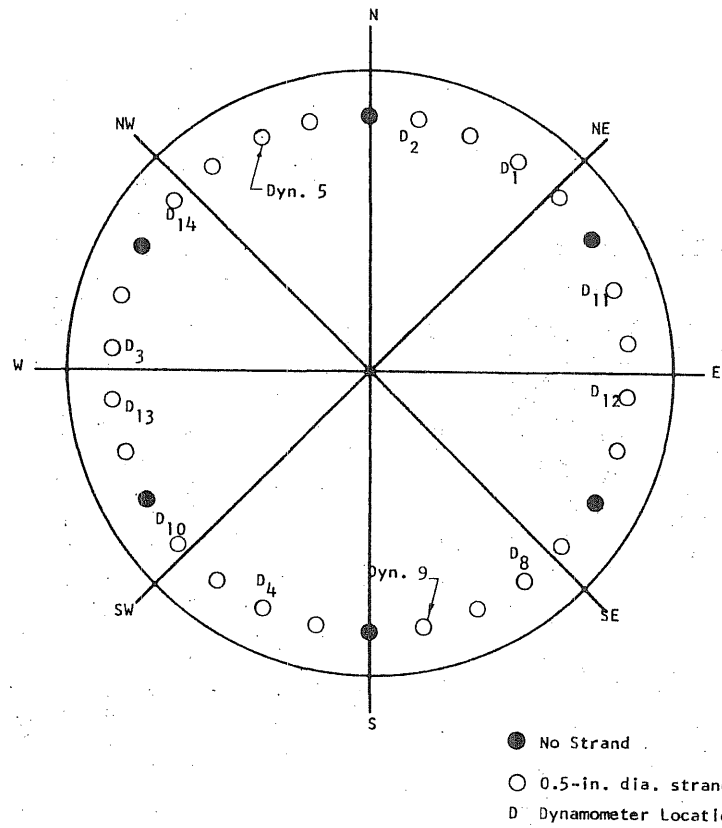


FIG. B4.18 LOCATION OF LONGITUDINAL REINFORCEMENT

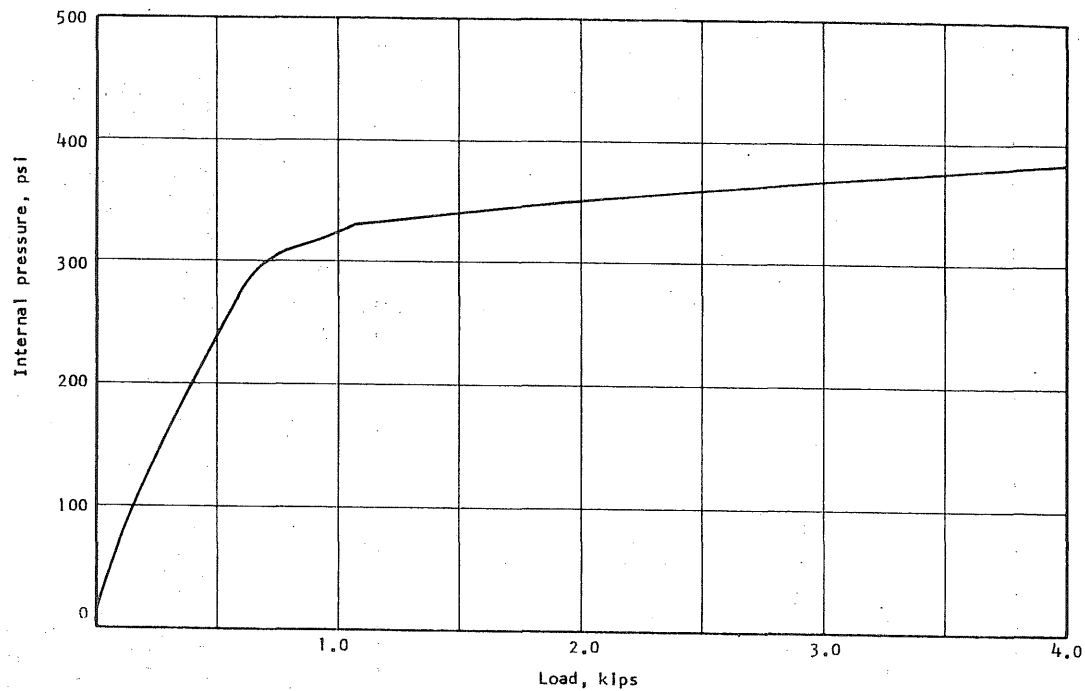


FIG. B4.19 APPLIED PRESSURE vs INCREASE IN LOAD IN DYNAMOMETER NO. 5 IN PV4

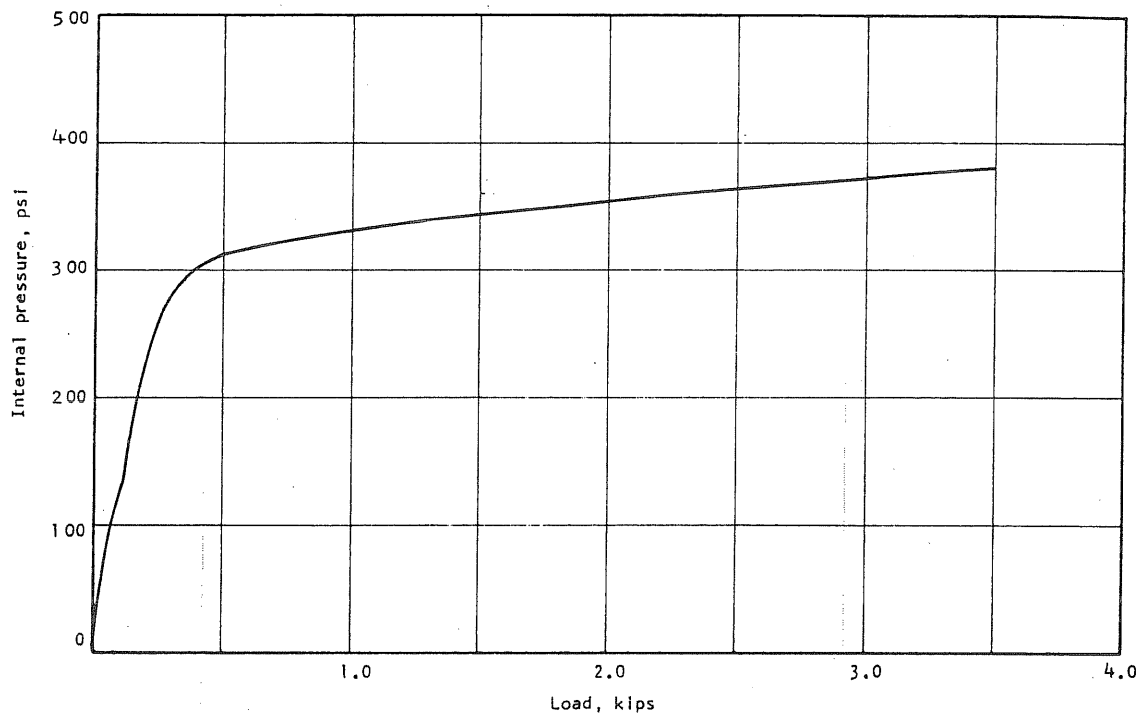


FIG. B4.20 APPLIED PRESSURE vs INCREASE IN LOAD IN DYNAMOMETER NO. 9 IN PV4

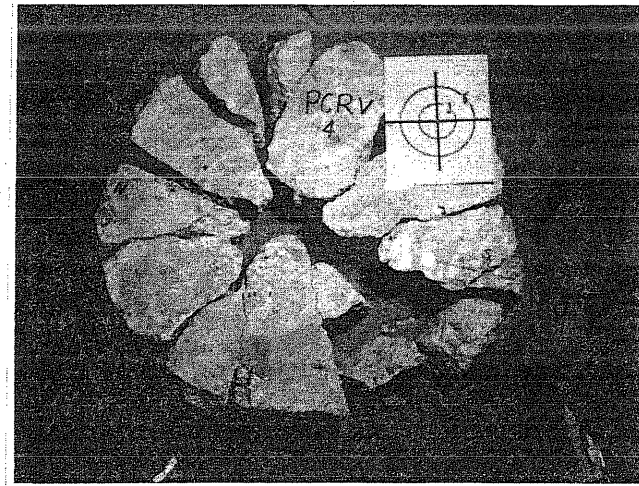


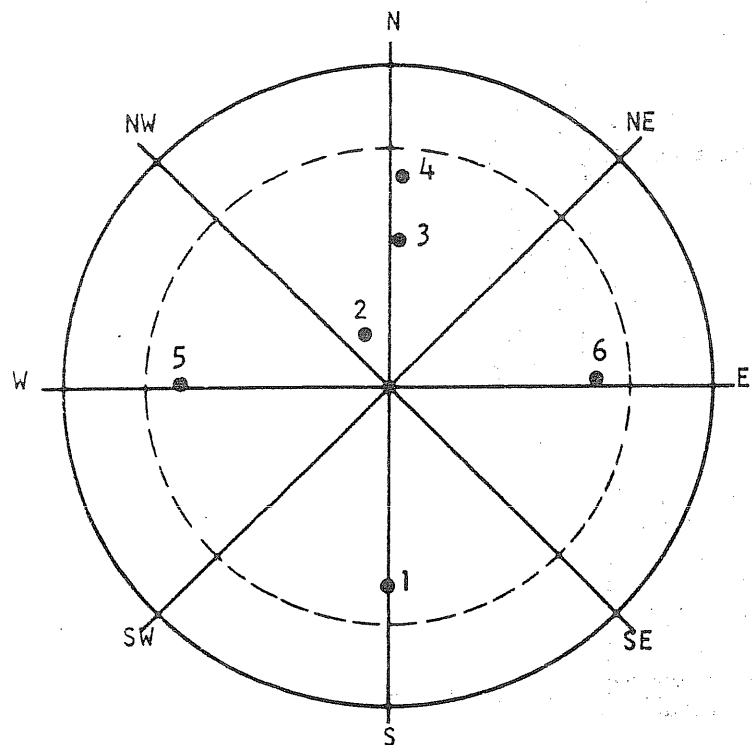
FIG. B4.21 REASSEMBLED END SLAB OF PV4

B5 Test Vessel PV5 ($t = 7 \frac{1}{2}$ in., $s = 2\frac{2}{3}$ in.)

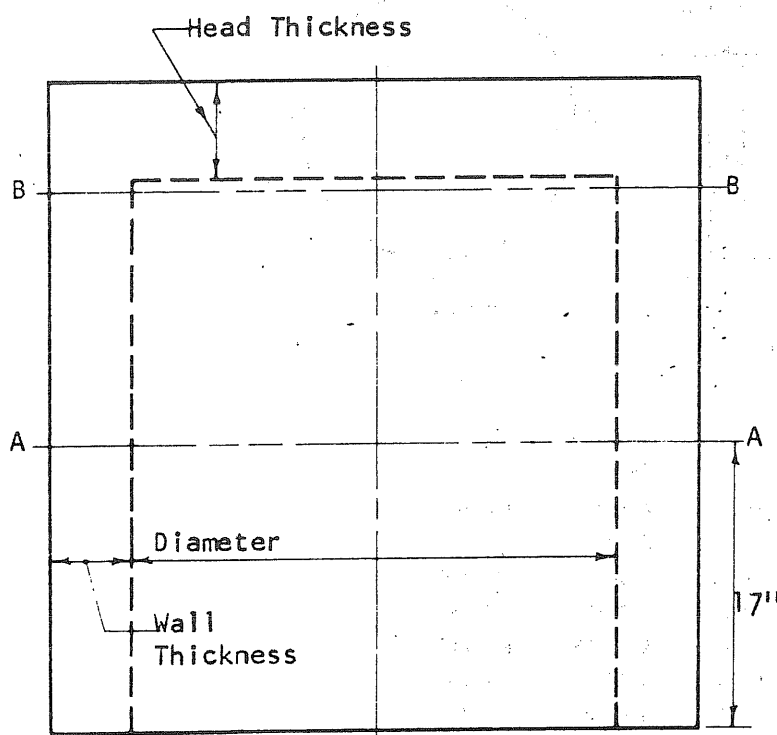
Test vessel PV5 was also tested with no unusual difficulties. It had no visible cracks before the test.

About three hours were required to test PV5. Internal pressure was increased in increments of 50 psi up to a pressure of 200 psi. Loading then proceeded in 25 psi increments until the vessel failed at 465 psi. The crack pattern in the end slab is illustrated in Fig. B5.22.

The longitudinal tendons and the method of sealing were the same as for PV5.



| Head Thickness | |
|----------------|--------|
| Point No. | Inches |
| 1 | 7.7 |
| 2 | 7.75 |
| 3 | 7.75 |
| 4 | 7.65 |
| 5 | 7.75 |
| 6 | 7.60 |



| Wall Thickness, in. | | |
|---------------------|----|------|
| Plane Axis | AA | BB |
| N | | 5.25 |
| NE | | 5.07 |
| E | | 4.86 |
| SE | | 4.90 |
| S | | 5.02 |
| SW | | 5.04 |
| W | | 5.00 |
| NW | | 5.20 |

| Inside Diameter, in. | | |
|----------------------|----|--------------------|
| Plane Axis | AA | BB |
| N-S | | 29 $\frac{12}{16}$ |
| NE-SW | | 29 $\frac{14}{16}$ |
| E-W | | 29 $\frac{15}{16}$ |
| SE-NW | | 29 $\frac{14}{16}$ |

FIG. B5.1 DIMENSIONS OF PV5

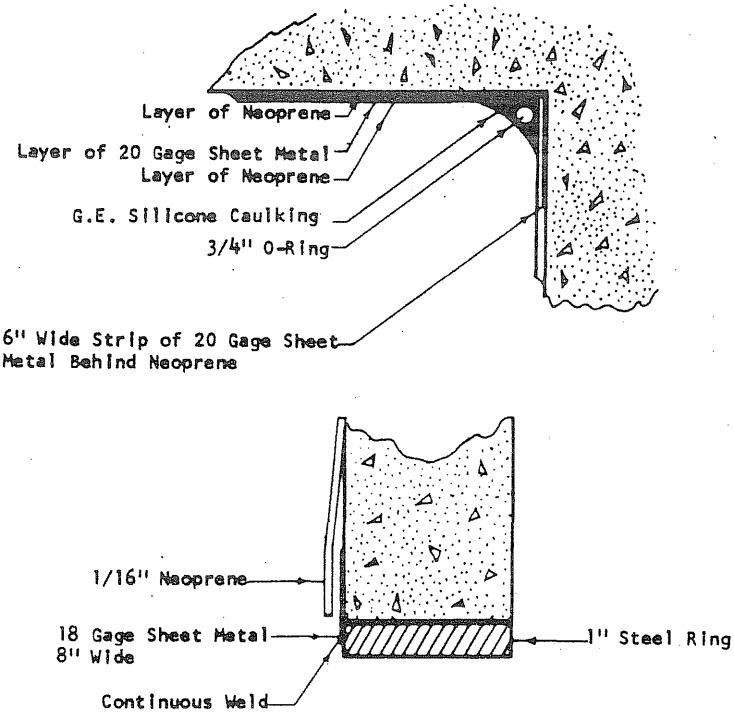
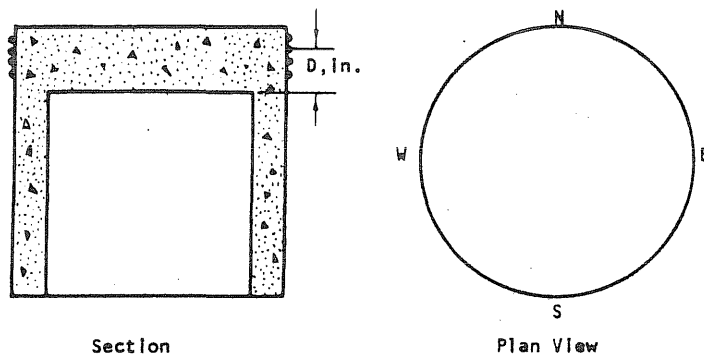


FIG. B5.2 SEALING DETAIL FOR PVS



| Wrap No. | D_N | D_E | D_S | D_W |
|----------|---------|---------|---------|---------|
| 1 | 6 13/16 | 6 14/16 | 6 14/16 | 7 0/16 |
| 2 | 6 6/16 | 6 3/16 | 6 1/16 | 6 1/16 |
| 3 | 6 2/16 | 5 15/16 | 5 12/16 | 5 12/16 |
| 4 | 5 10/16 | 5 7/16 | 5 5/16 | 5 5/16 |
| 5 | 5 4/16 | 5 0/16 | 4 13/16 | 4 12/16 |
| 6 | 4 11/16 | 4 6/16 | 4 2/16 | 4 1/16 |
| 7 | 4 0/16 | 3 12/16 | 3 8/16 | 3 7/16 |
| 8 | 3 6/16 | 3 1/16 | 2 14/16 | 2 13/16 |
| 9 | 2 11/16 | 2 7/16 | 2 3/16 | 2 2/16 |
| 10 | 2 0/16 | 1 12/16 | 1 8/16 | 1 7/16 |
| 11 | 1 6/16 | 1 1/16 | 1 4/16 | 1 2/16 |
| 12 | 11/16 | 7/16 | -8/16 | 2/16 |

FIG. B5.3 MEASURED LOCATION OF THE CIRCUMFERENTIAL PRESTRESS WIRE AT THE ENDS OF THE N-S AND E-W DIAMETERS ON PVS

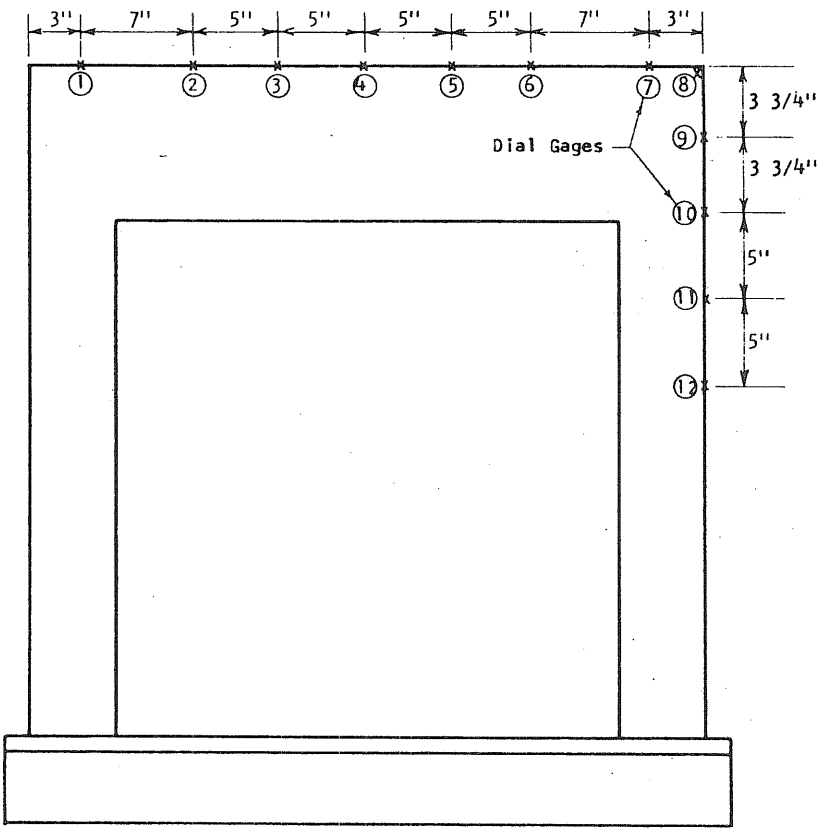


FIG. B5.4 LOCATION OF DEFLECTION GAGES ON PV5

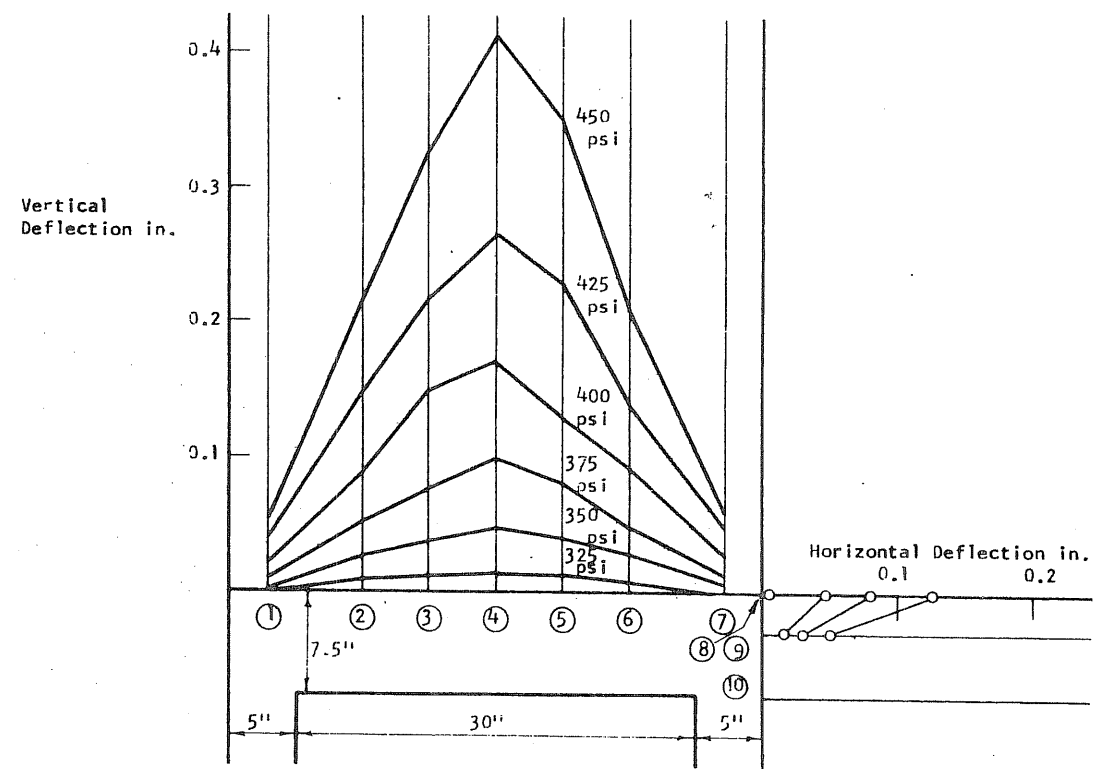


FIG. B5.5 DEFLECTION PROFILES OF THE END SLAB ALONG THE N-S DIAMETER OF PV5

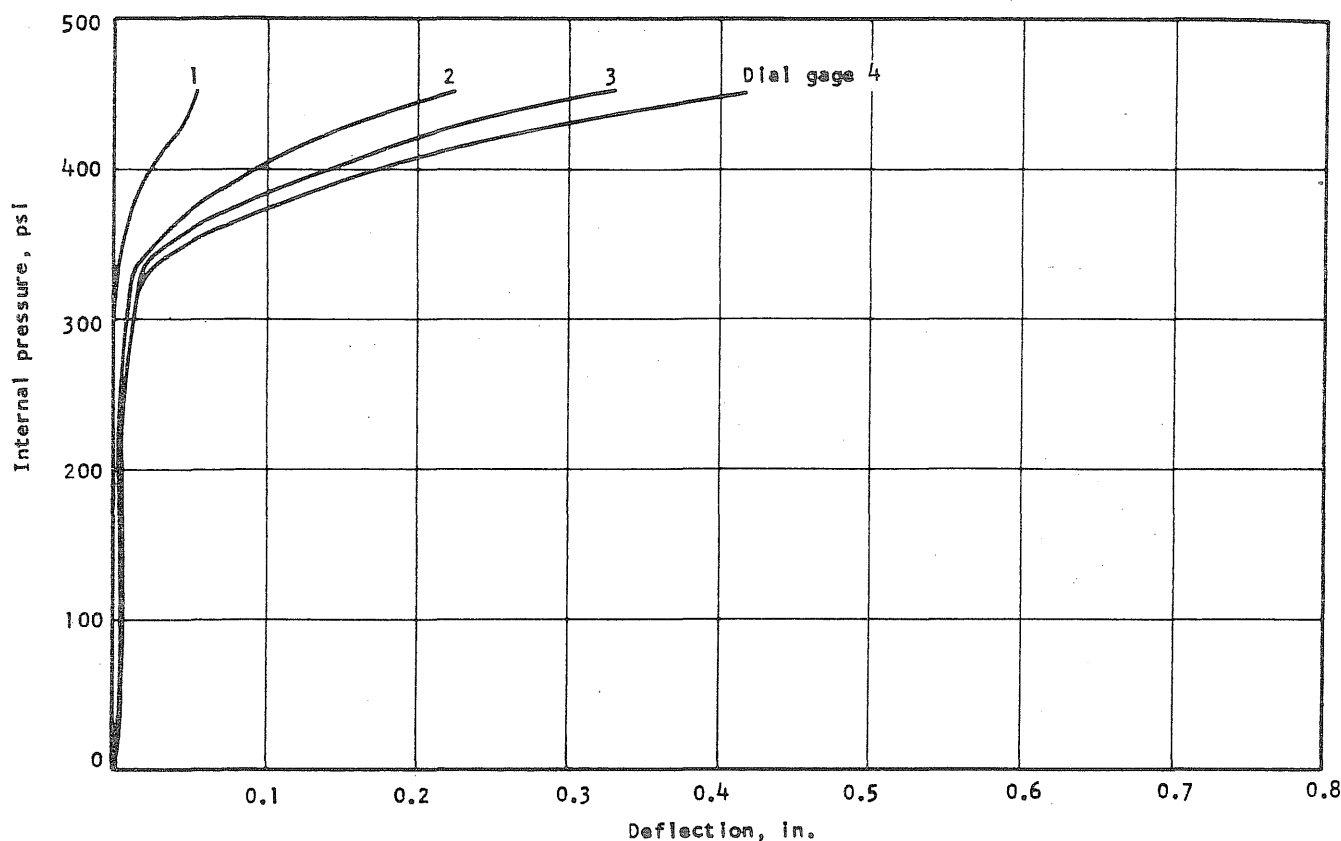


FIG. B5.6 APPLIED PRESSURE vs DEFLECTION ALONG THE N-HALF OF THE N-S DIAMETER OF PV5

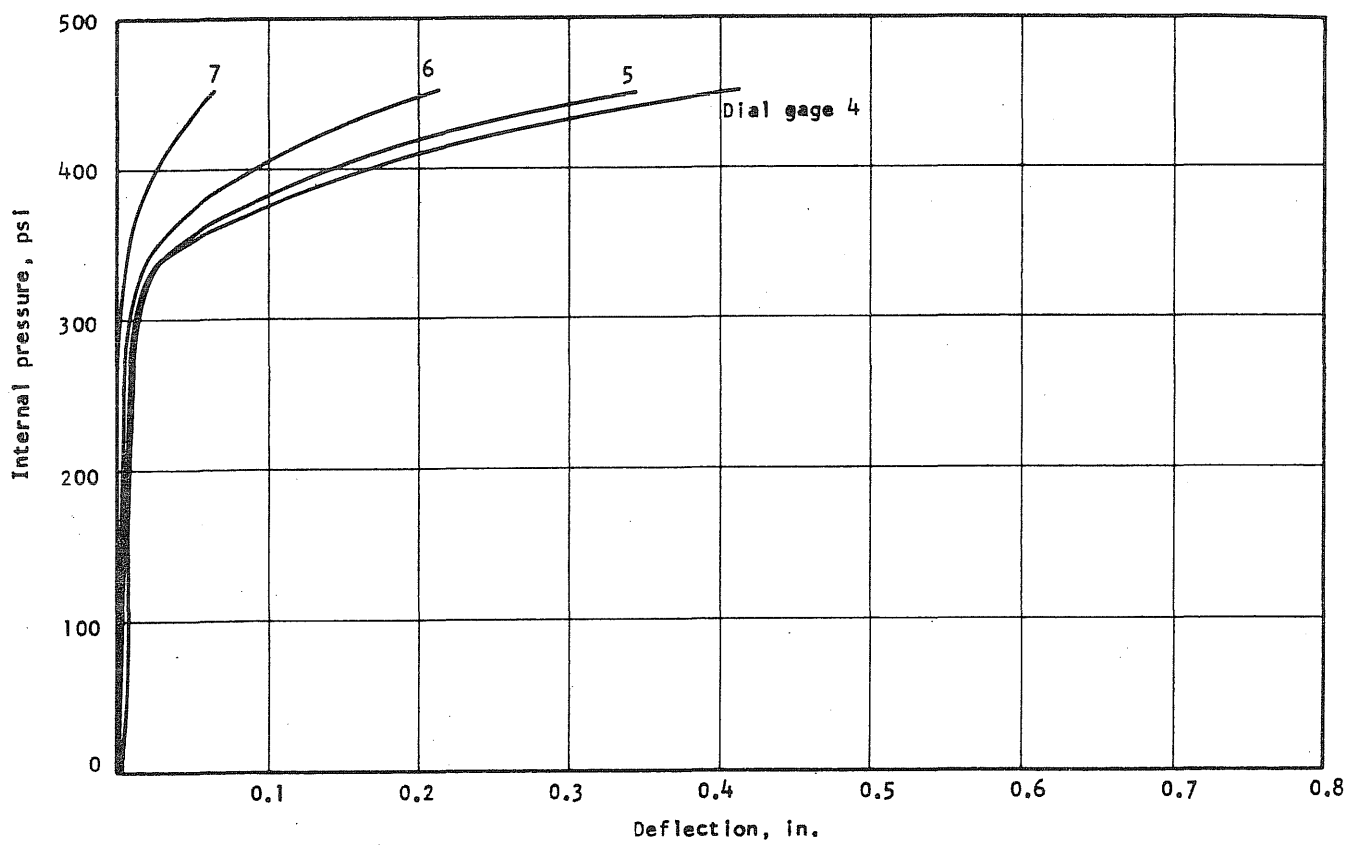


FIG. B5.7 APPLIED PRESSURE vs DEFLECTION ALONG THE S-HALF OF THE N-S DIAMETER OF PV5

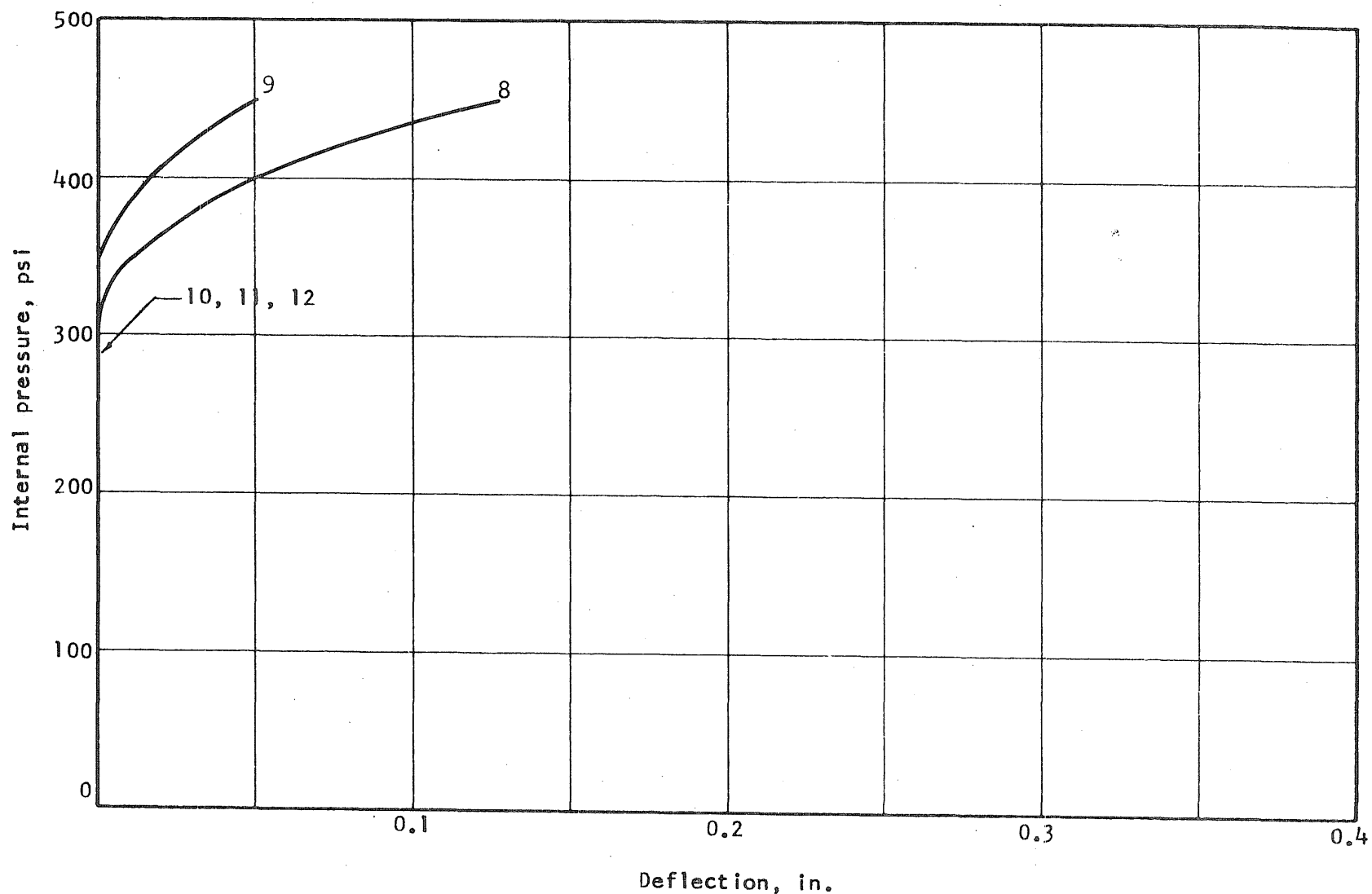
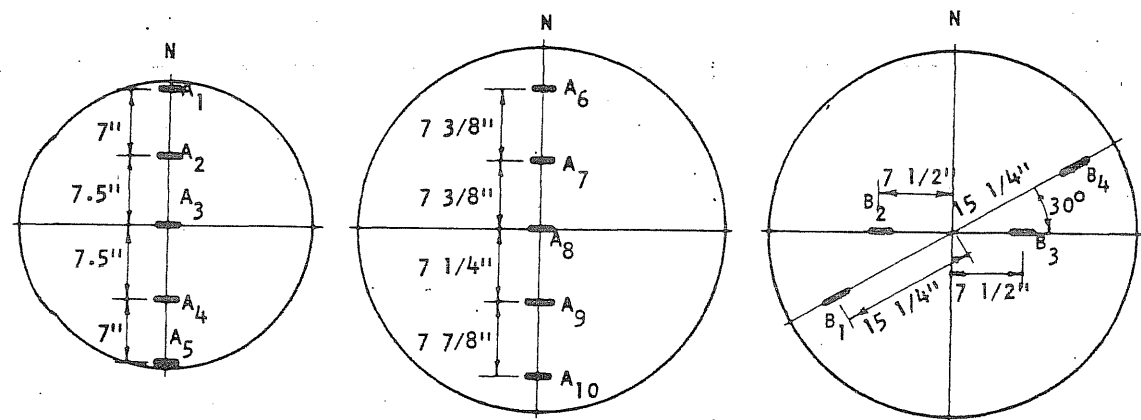


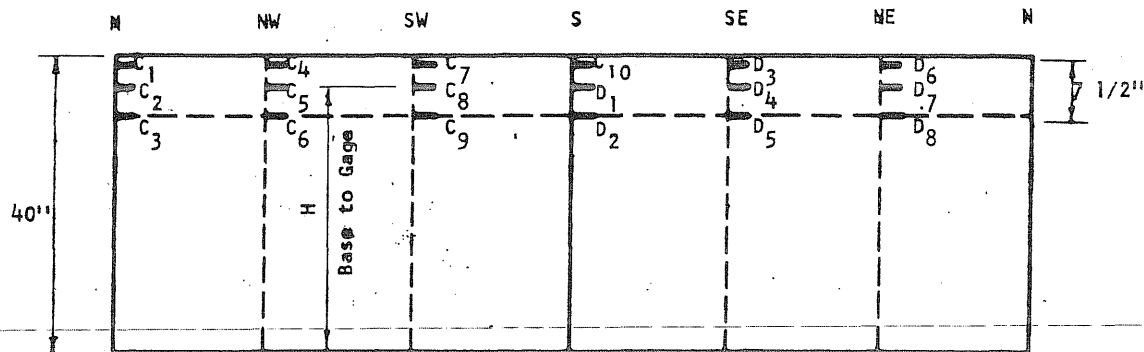
FIG. B5.8 APPLIED PRESSURE vs DEFLECTION OF THE SIDE WALL OF PV5

B 62

Concrete Gages On The Slab

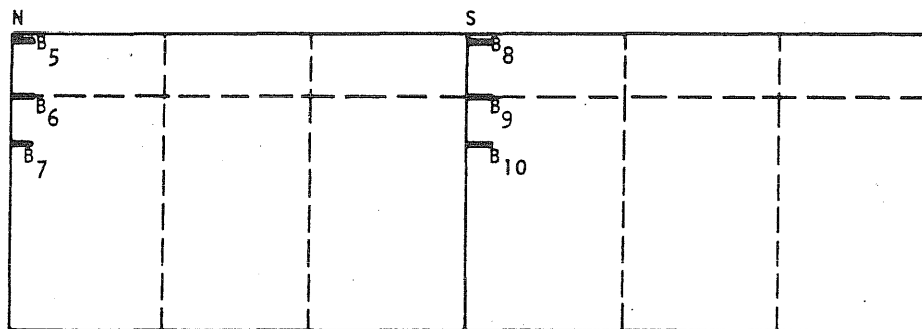


Steel Gages On Prestressing Wire



| Gage | Axis | H | Gage | Axis | H | Gage | Axis | H |
|----------------|------|----------|-----------------|------|----------|----------------|------|----------|
| C ₁ | N | 38 9/16 | C ₇ | SE | 38 10/16 | D ₃ | SW | 38 10/16 |
| C ₂ | N | 35 13/16 | C ₈ | SE | 35 8/16 | D ₄ | SW | 36 0/16 |
| C ₃ | N | 32 8/16 | C ₉ | SE | 32 3/16 | D ₅ | SW | 32 10/16 |
| C ₄ | N | 38 12/16 | C ₁₀ | S | 38 9/16 | D ₆ | NW | 38 10/16 |
| C ₅ | NE | 35 11/16 | D ₁ | S | 35 6/16 | D ₇ | NW | 35 4/16 |
| C ₆ | NE | 32 6/16 | D ₂ | S | 32 1/16 | D ₈ | NW | 32 9/16 |

Concrete Gages On The Outside of The Vessel



| Gage | Axis | H | Gage | Axis | H |
|----------------|------|----------|-----------------|------|----------|
| B ₅ | N | 38 5/16 | B ₈ | S | 39 11/16 |
| B ₆ | N | 36 2/16 | B ₉ | S | 35 10/16 |
| B ₇ | N | 32 14/16 | B ₁₀ | S | 31 12/16 |

FIG. B5.9 STRAIN GAGE LOCATIONS ON PW5

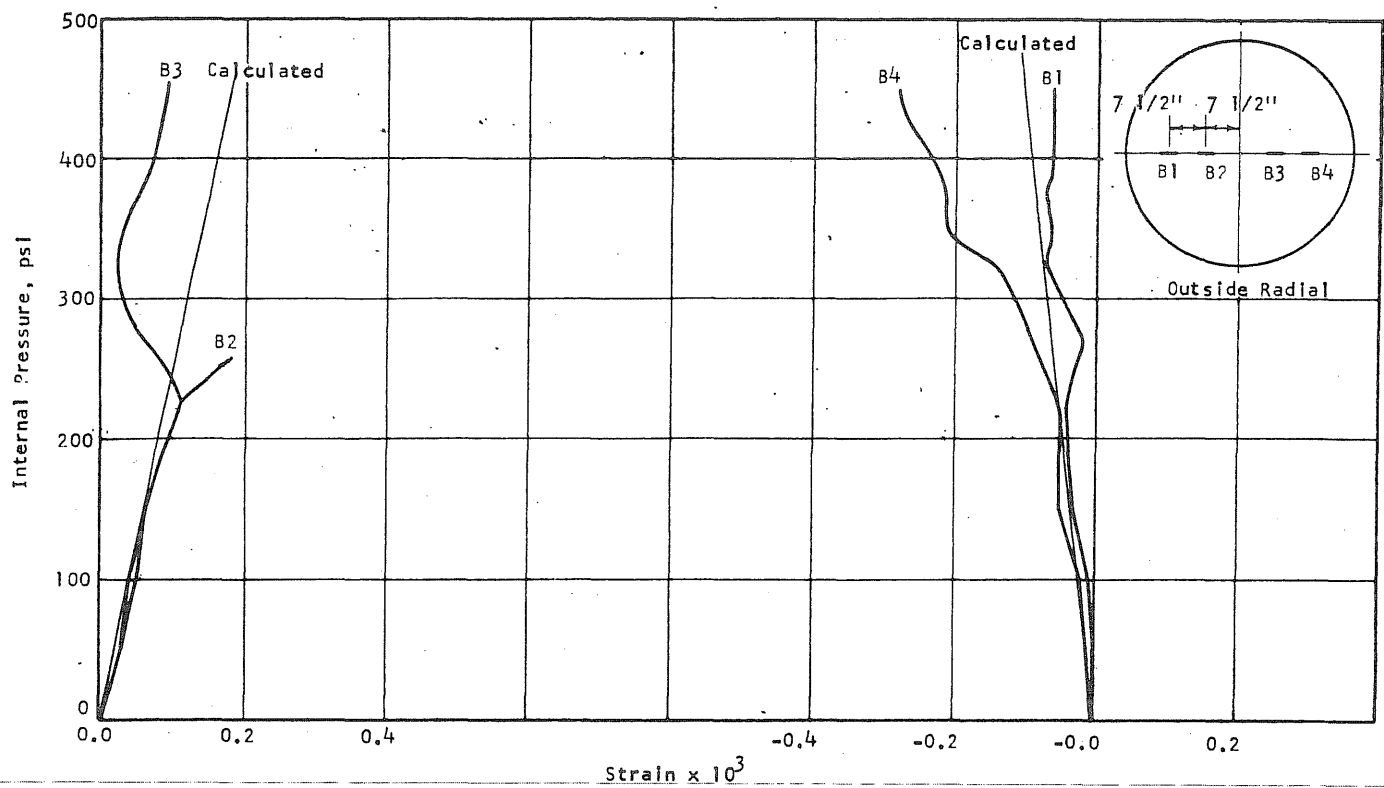


FIG. B5.10 CONCRETE STRAINS, VESSEL PV5

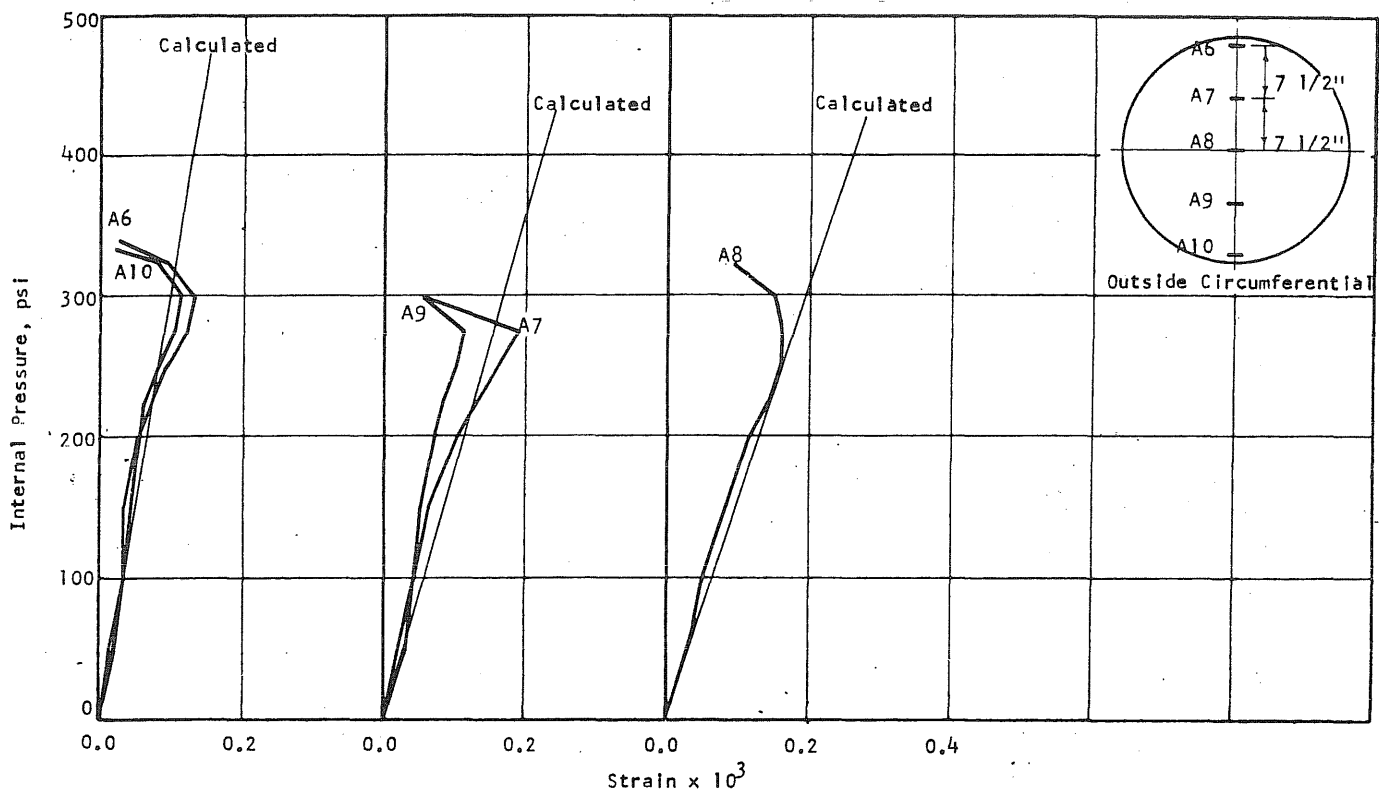


FIG. B5.11 CONCRETE STRAINS, VESSEL PV5

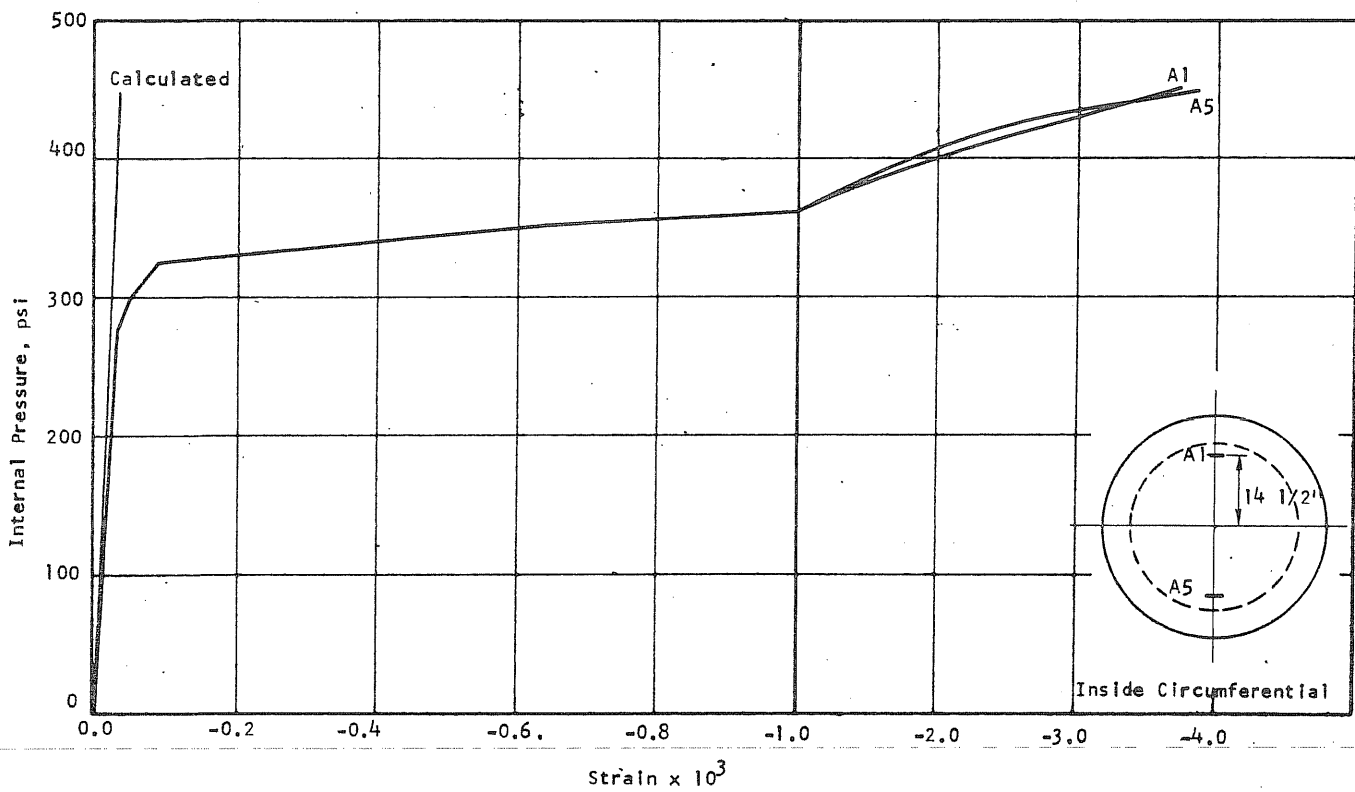


FIG. B5.12 CONCRETE STRAINS, VESSEL PV5

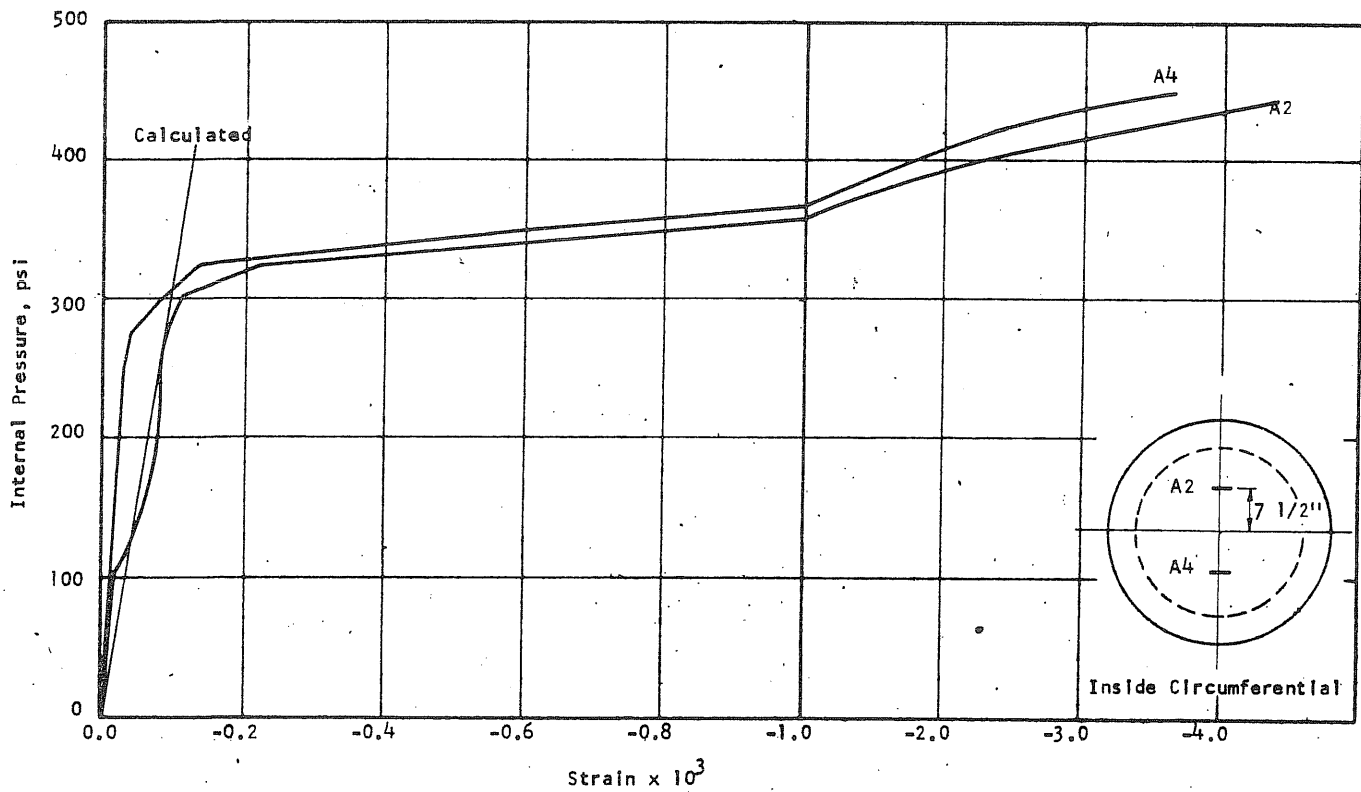


FIG. B5.13 CONCRETE STRAINS, VESSEL PV5

B 65

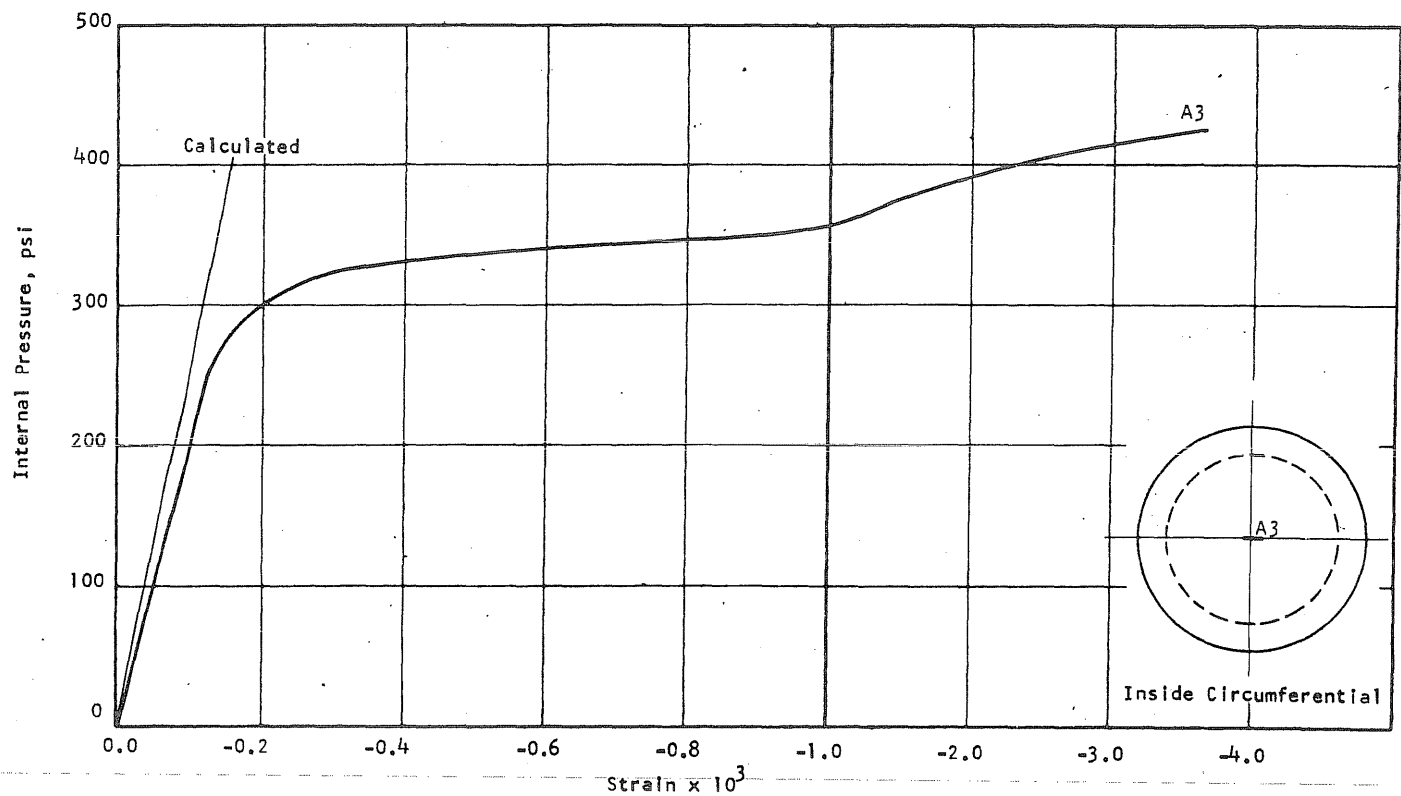


FIG. B5.14 CONCRETE STRAINS, VESSEL PV5

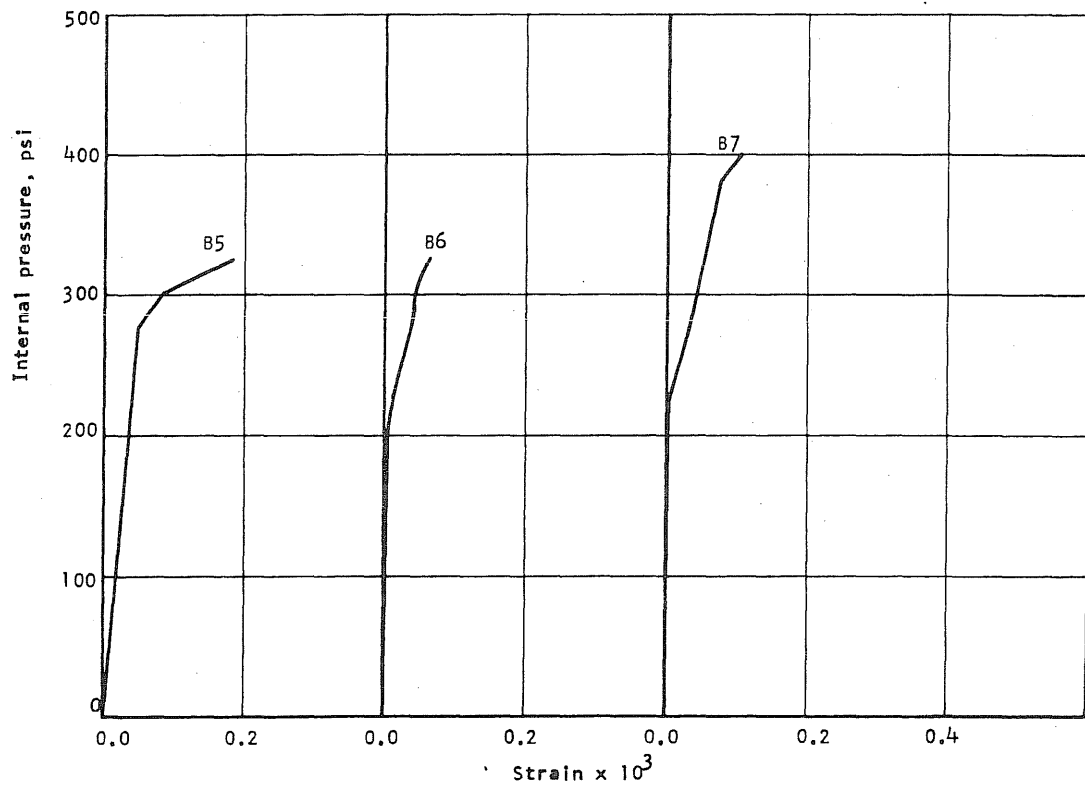


FIG. B5.15 APPLIED PRESSURE vs CIRCUMFERENTIAL STRAIN IN THE WALL OF THE VESSEL AT THE N-END OF THE N-S DIAMETER OF PV5

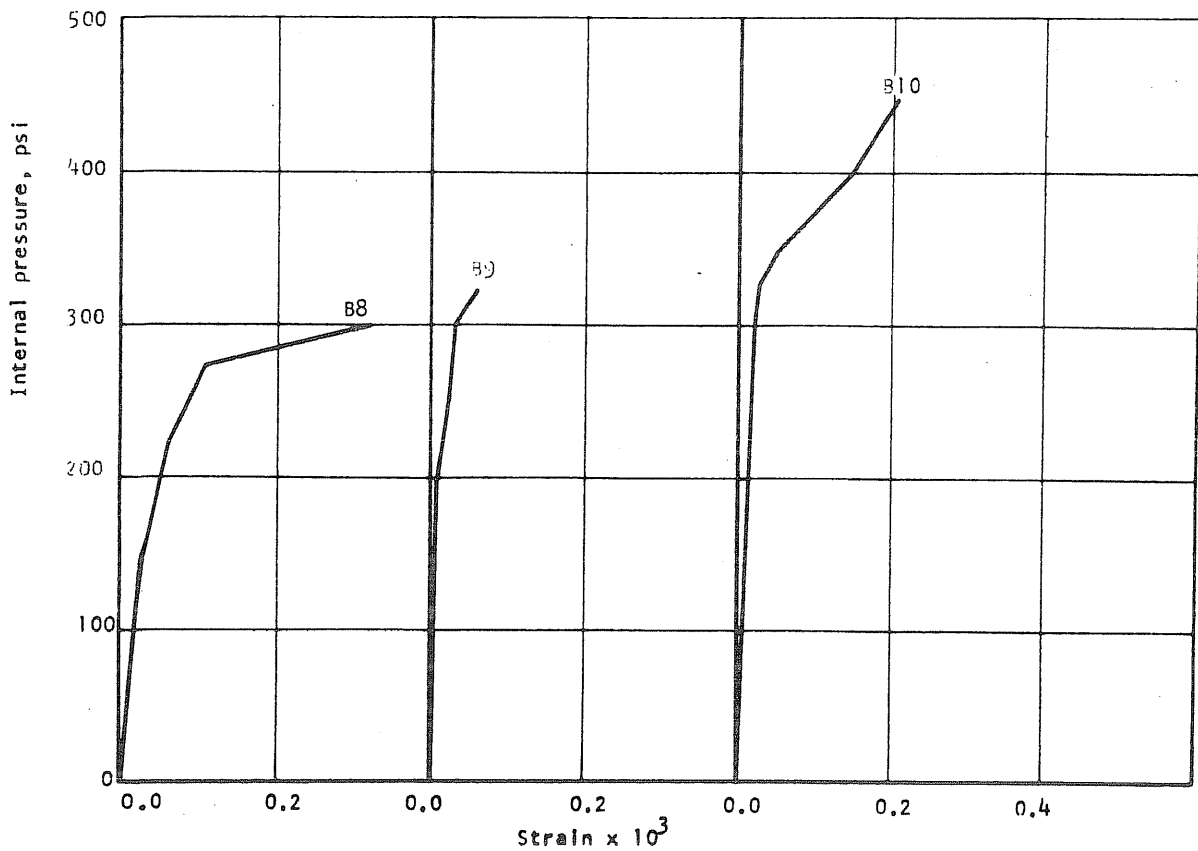


FIG. 85.16 APPLIED PRESSURE VS CIRCUMFERENTIAL STRAIN IN THE WALL OF THE VESSEL AT THE S-END OF THE N-S DIAMETER OF PV5

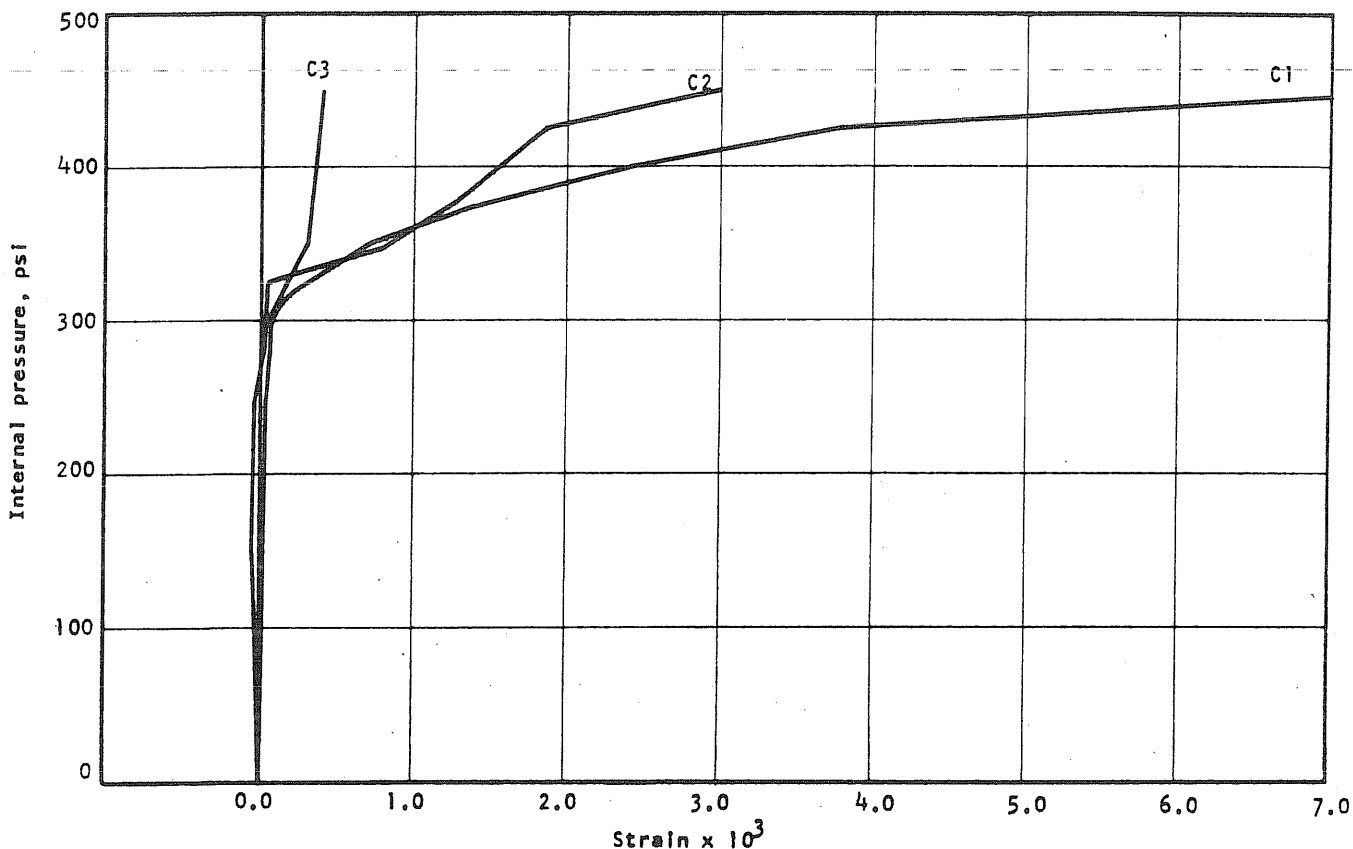


FIG. B5.17 APPLIED PRESSURE VS STRAIN IN THE CIRCUMFERENTIAL PRESTRESS WIRE AT THE N-END OF THE N-S DIAMETER OF PV5

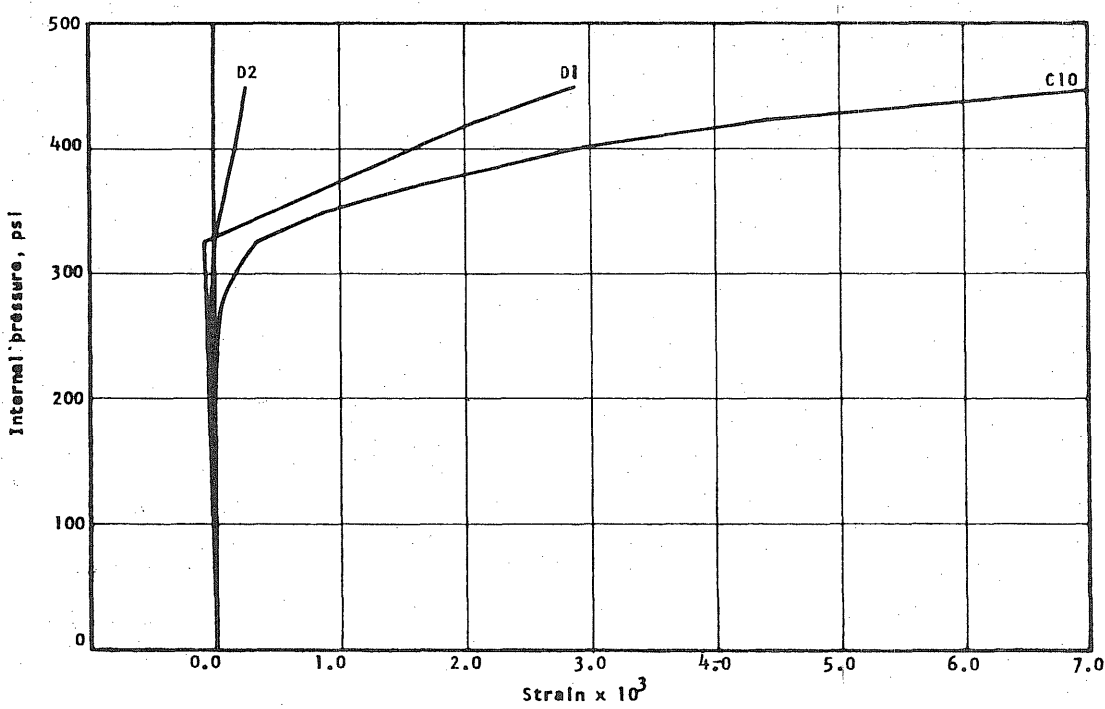


FIG. B5.18 APPLIED PRESSURE VS STRAIN IN THE CIRCUMFERENTIAL PRESTRESS WIRE AT THE S-END OF THE N-S DIAMETER OF PV5

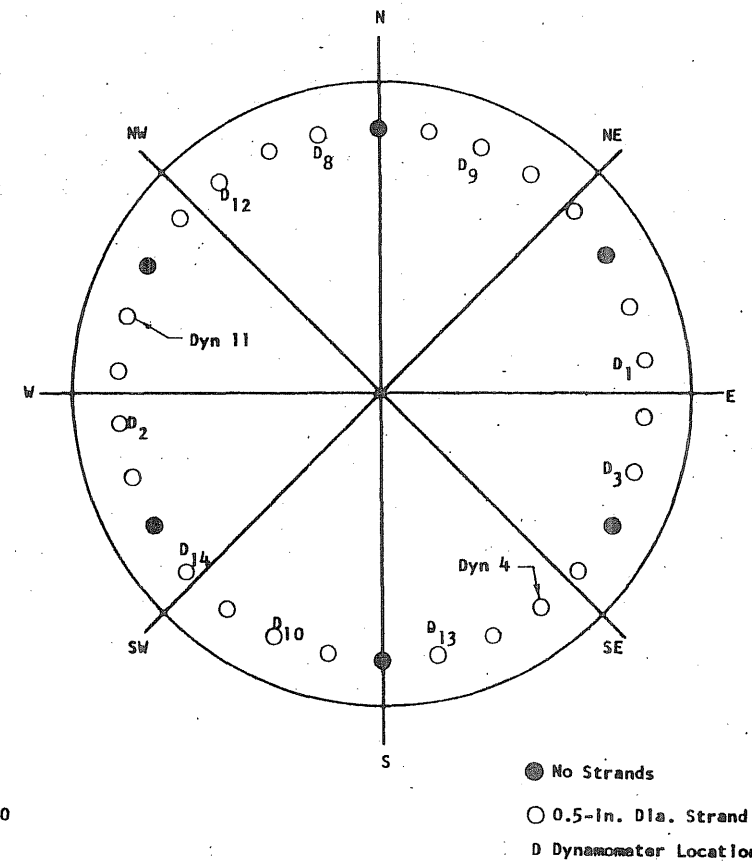


FIG. B5.19 LOCATION OF LONGITUDINAL REINFORCEMENT

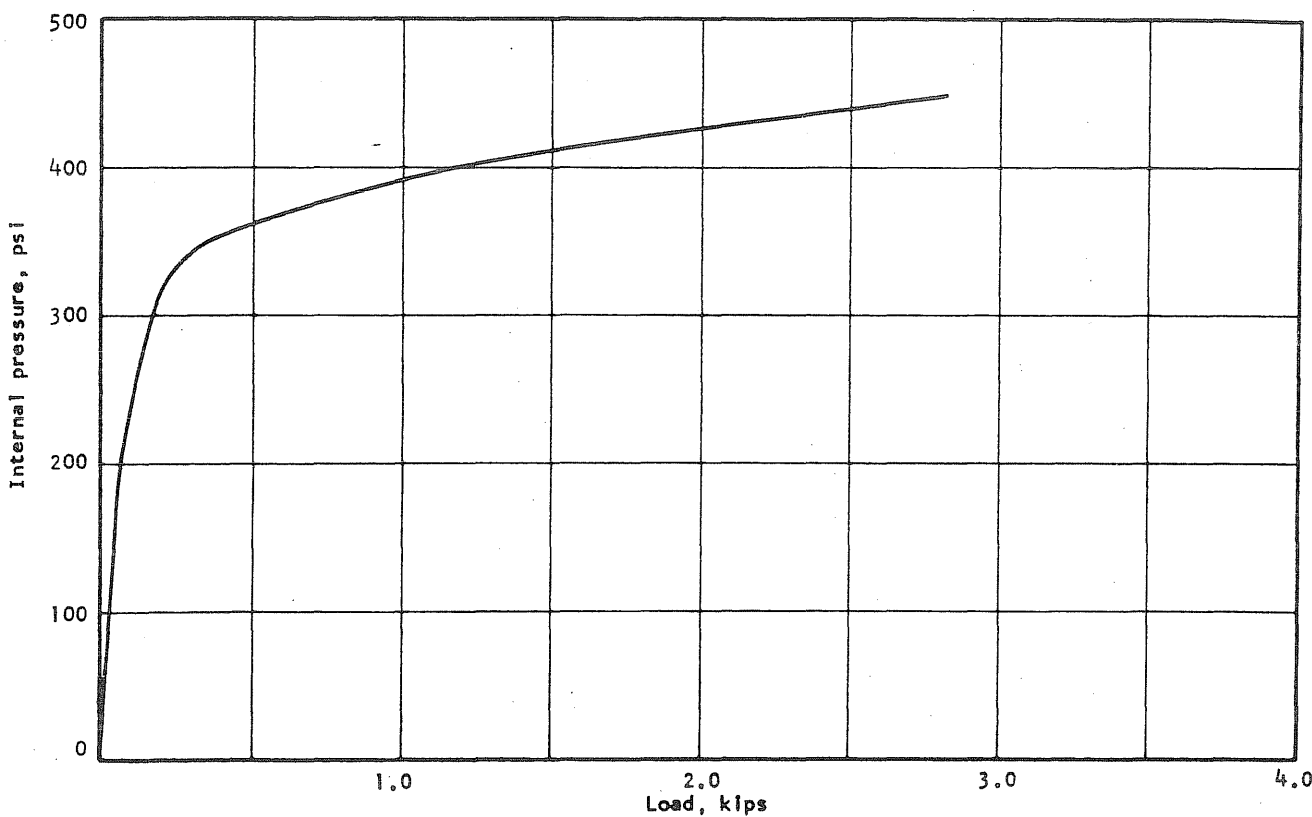


FIG. B5.20 APPLIED PRESSURE vs INCREASE IN LOAD IN DYNAMOMETER NO. 4 IN PV5

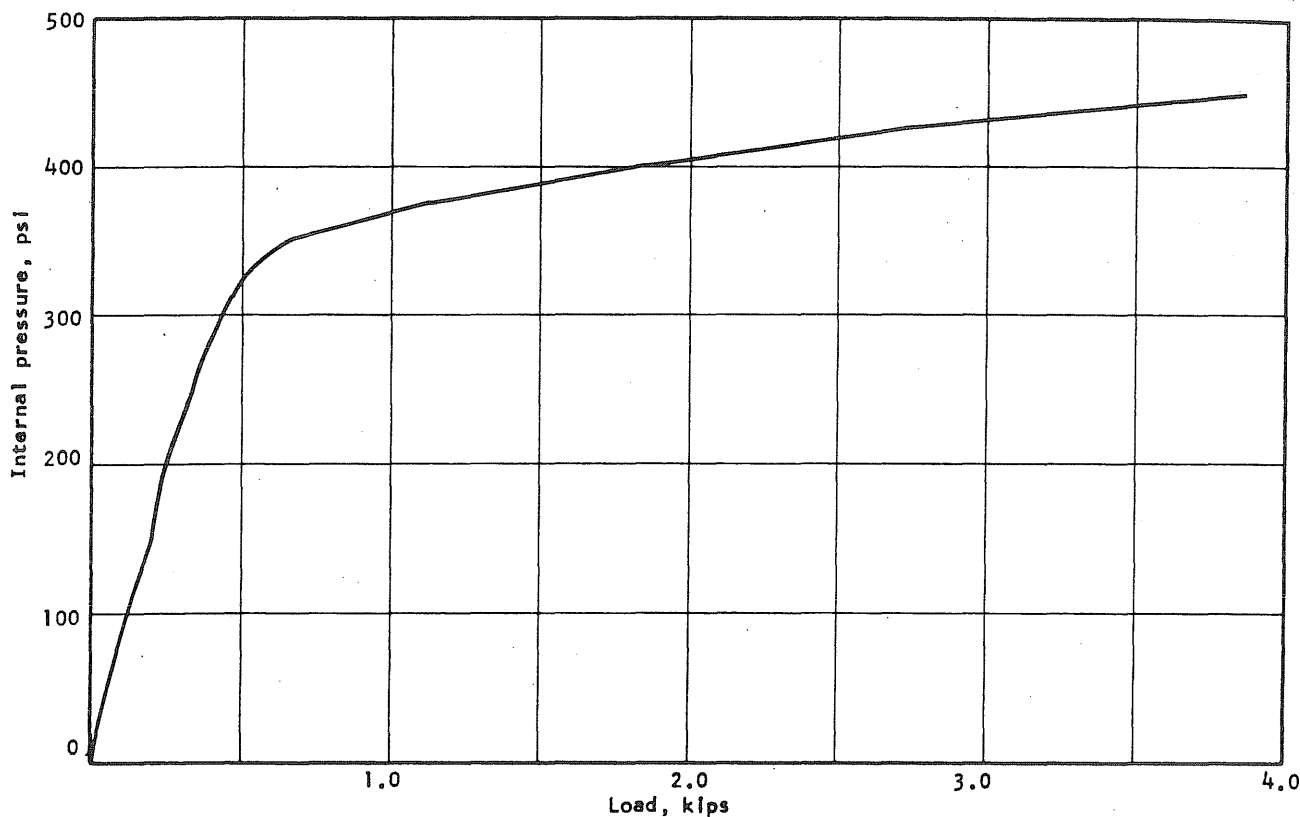


FIG. B5.21 APPLIED PRESSURE vs THE INCREASE IN LOAD IN DYNAMOMETER NO. 11 IN PV5

B 69

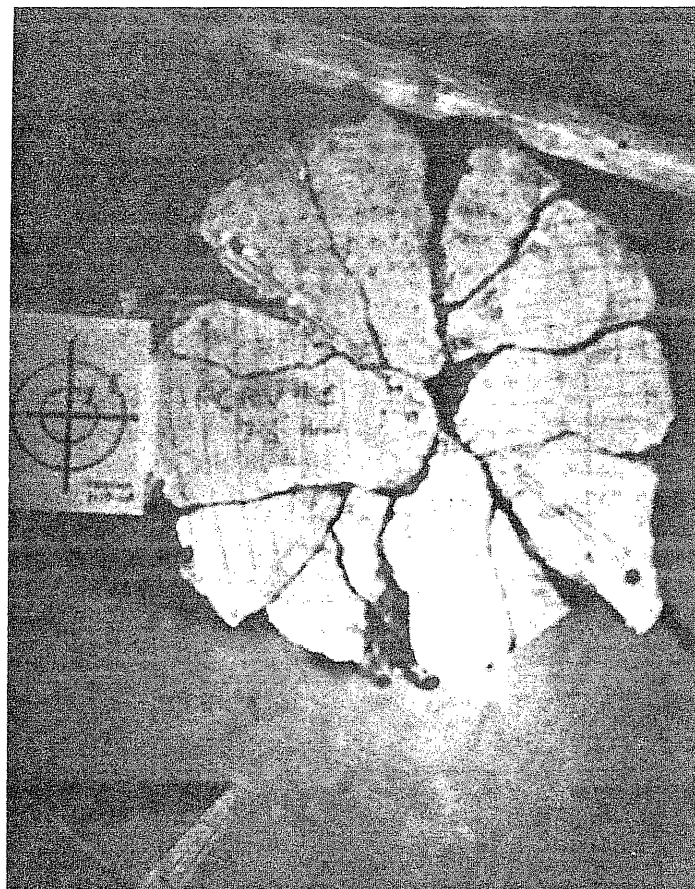


FIG. B5.22 REASSEMBLED END SLAB OF PV5

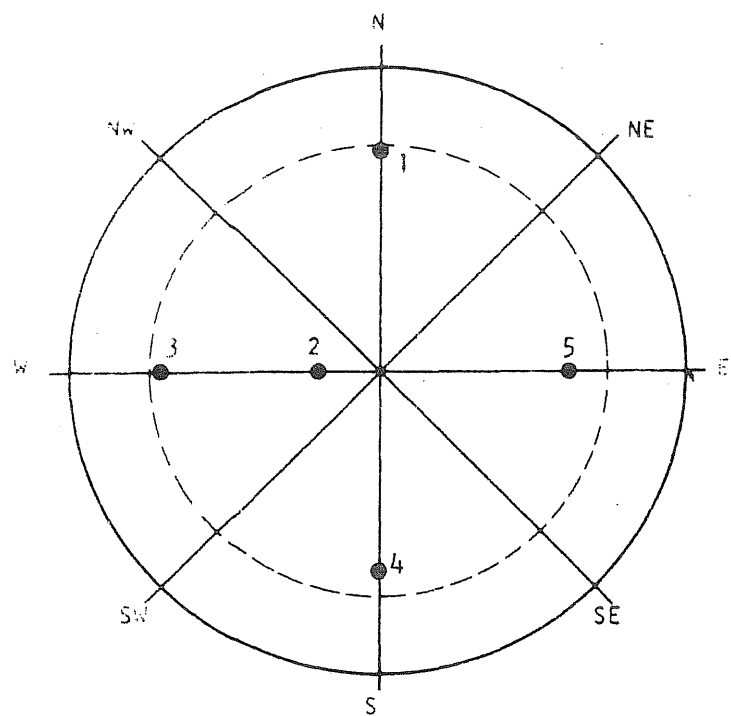
B6 Test Vessel PV6 (t = 9 in. s = 2/3 in.)

Test vessel PV6 was cast using concrete mixed in the laboratory. It was free of visible cracks at the time of the test. The longitudinal prestress was provided by thirty strands. On the first attempt to test PV6, the pressure was increased in 50 psi increments to a pressure of 250 psi. Twenty-five psi increments were added until the pressure reached 450 psi. Pressure was increased in 10 psi increments until a leak in the seal prevented a further increase in pressure at 570 psi. Data for only the first attempt at testing PV6 is presented with the exception of the pressure-deflection curve for the center of the end slab and the change in load in one longitudinal strand on the final test of the vessel. Figure B6.2 shows the sealing detail used for the first attempt. The adhesive used on this vessel was a linoleum cement. Figure B6.19a shows the crack pattern that had developed in the end slab when the test was halted.

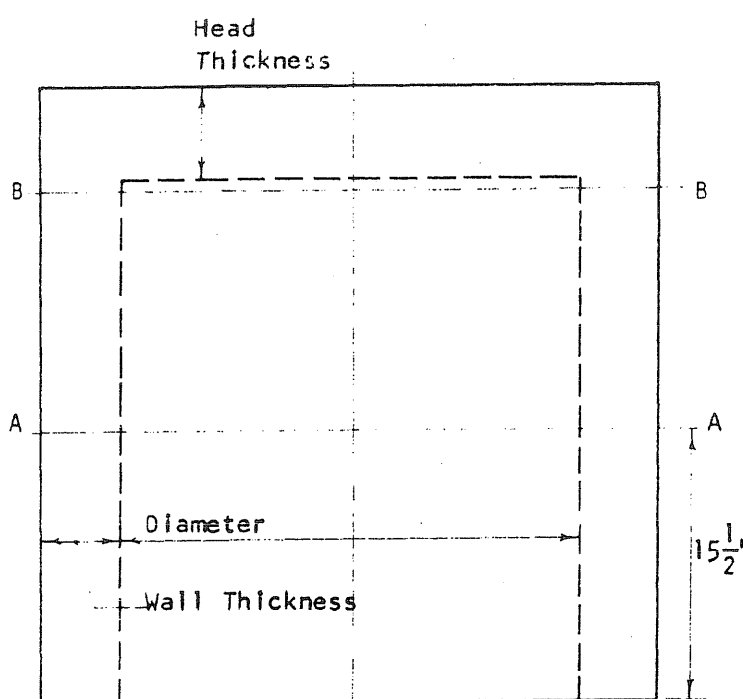
Vessel PV6 was removed from the test chamber and taken off the four-in. steel plate so that the liner could be modified as shown in Fig. B6.3. The modifications included an additional layer of neoprene on the end slab and the replacement of the neoprene on the side wall. Rubber cement was used as the adhesive in this case. The vessel was again secured to the four-in. plate with thirty strands.

The second attempt to reach the ultimate capacity of the vessel was frustrated when severe leaking prevented an increase in pressure beyond 585 psi. Visual examination of the vessel under 300 psi internal pressure disclosed a longitudinal crack about mid-height of the vessel near the SW meridian. The crack was less than 0.005 in. wide.

In order to proceed with the test, eight of the thirty longitudinal strands were removed before it was pressurized for the third time. The layout of longitudinal reinforcement is shown in Fig. B6.18. Pressure was increased in 100 psi increments to failure at a pressure of 400 psi. Fifty psi increments were added from 400 psi until the vessel failed at 555 psi. The reassembled end slab is shown in Fig. B6.19b.



| Head Thickness | |
|----------------|--------------------|
| Point | Inches |
| 1 | 9 $\frac{1}{8}$ " |
| 2 | 9 $\frac{1}{16}$ " |
| 3 | 9 $\frac{1}{8}$ " |
| 4 | 9 $\frac{1}{8}$ " |
| 5 | 9 $\frac{1}{16}$ " |



| Wall Thickness, in. | | |
|---------------------|------|------|
| Piano Axis | AA | BB |
| N | 4.97 | |
| NE | 4.94 | |
| E | 4.93 | 4.98 |
| SE | 4.97 | |
| S | 4.96 | 5.12 |
| SW | 5.09 | |
| W | 5.03 | 5.01 |
| NW | 5.06 | |

| Inside Diameter, in. | | |
|----------------------|-------------------|------------------|
| Piano Axis | AA | BB |
| N-S | $30\frac{4}{32}$ | |
| NE-SW | $30\frac{0}{32}$ | $30\frac{2}{32}$ |
| E-W | $29\frac{31}{32}$ | |
| SE-NW | $30\frac{1}{32}$ | $30\frac{1}{32}$ |

FIG. B6.1 DIMENSIONS OF PV6

B 73

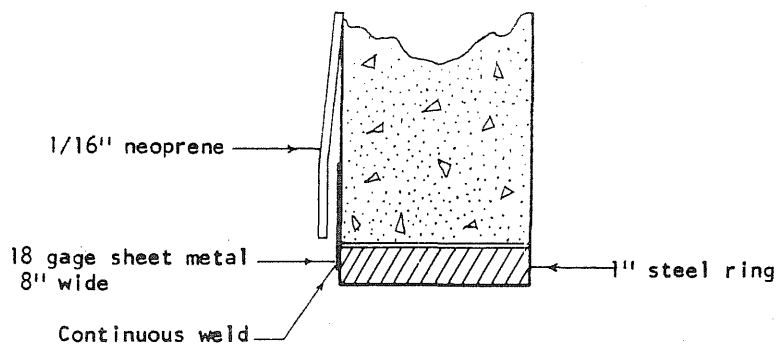
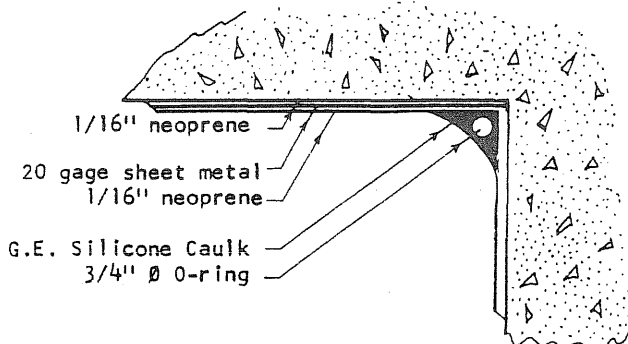
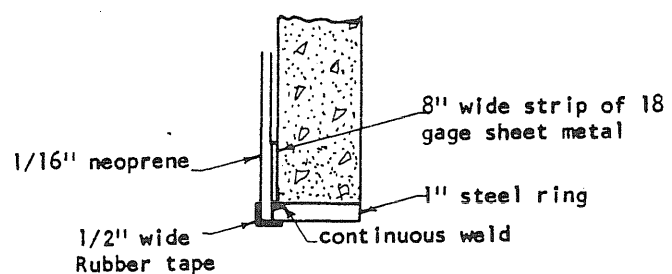
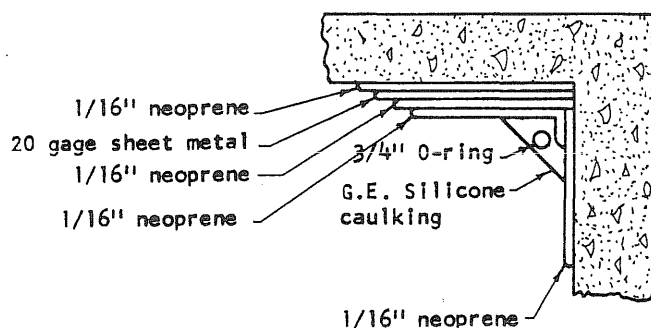
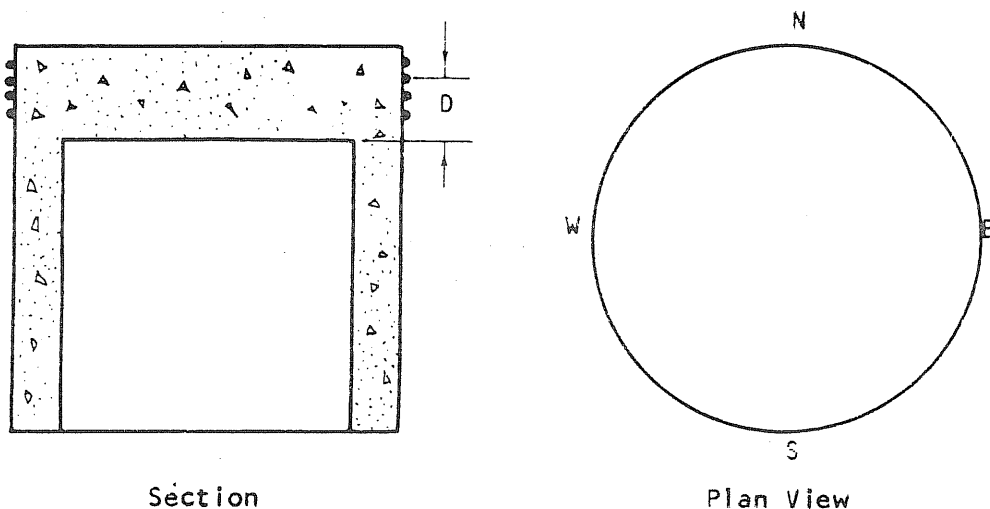


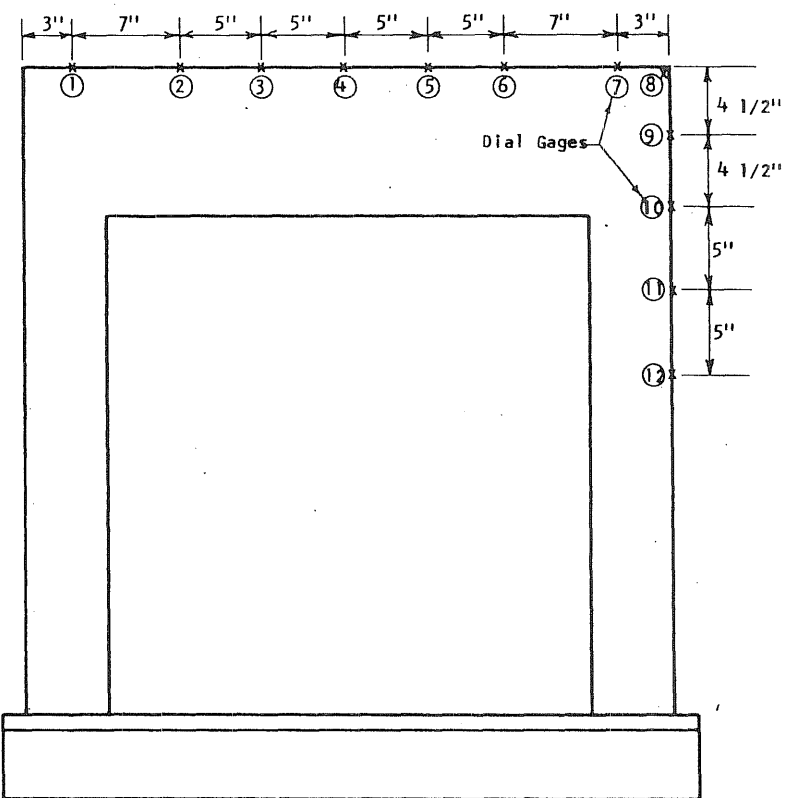
FIG. B6.2 SEALING DETAIL FOR PV6





| Wrap No. | D_N | D_E | D_S | D_W |
|----------|---------|---------|---------|---------|
| 1 | 7 14/16 | 8 2/16 | 8 6/16 | 7 14/16 |
| 2 | 7 11/16 | 7 14/16 | 7 15/16 | 7 11/16 |
| 3 | 7 8/16 | 7 10/16 | 7 12/16 | 7 6/16 |
| 4 | 6 14/16 | 7 1/16 | 7 4/16 | 6 12/16 |
| 5 | 6 4/16 | 6 7/16 | 6 10/16 | 6 1/16 |
| 6 | 5 9/16 | 5 12/16 | 5 15/16 | 5 6/16 |
| 7 | 4 14/16 | 5 1/16 | 5 4/16 | 4 12/16 |
| 8 | 4 4/16 | 4 7/16 | 4 10/16 | 4 1/16 |
| 9 | 3 10/16 | 3 13/16 | 4 0/16 | 3 7/16 |
| 10 | 3 0/16 | 3 2/16 | 3 5/16 | 2 13/16 |
| 11 | 2 2/16 | 2 8/16 | 2 11/16 | 2 2/16 |
| 12 | 1 11/16 | 1 13/16 | 2 0/16 | 1 7/16 |
| 13 | 1 0/16 | 1 3/16 | 1 5/16 | 13/16 |
| 14 | 5/16 | 8/16 | 10/16 | 2/16 |
| 15 | -6/16 | -3/16 | 0 | -9/16 |

FIG. B6.4 MEASURED LOCATION OF THE CIRCUMFERENTIAL PRESTRESS WIRE
AT THE ENDS OF THE N-S AND E-W DIAMETERS ON PV6



Dial Gages
Vertical Deflection In.

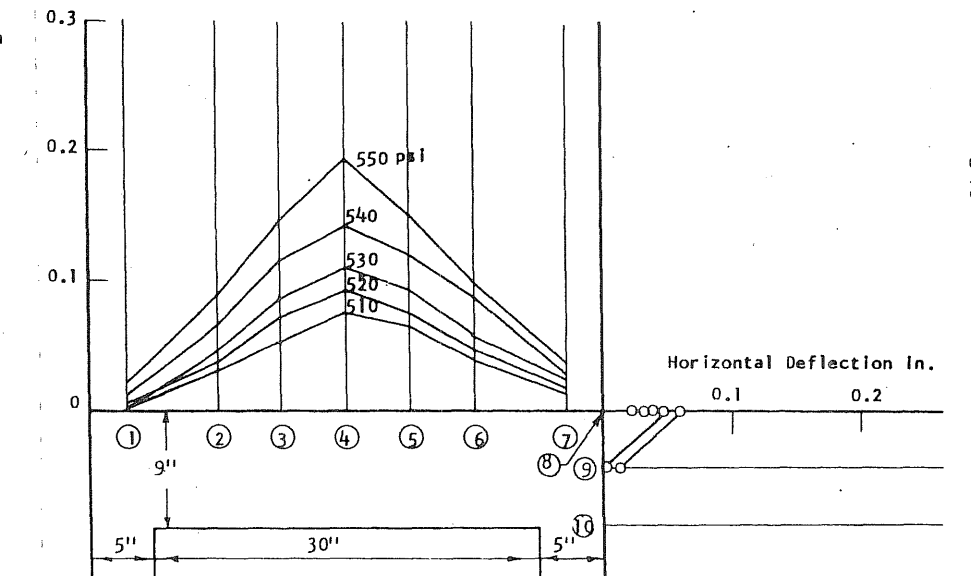


FIG. B6.6 DEFLECTION PROFILES OF THE END SLAB ALONG THE N-S DIAMETER OF PV6

FIG. B6.5 LOCATION OF DEFLECTION GAGES ON PV6

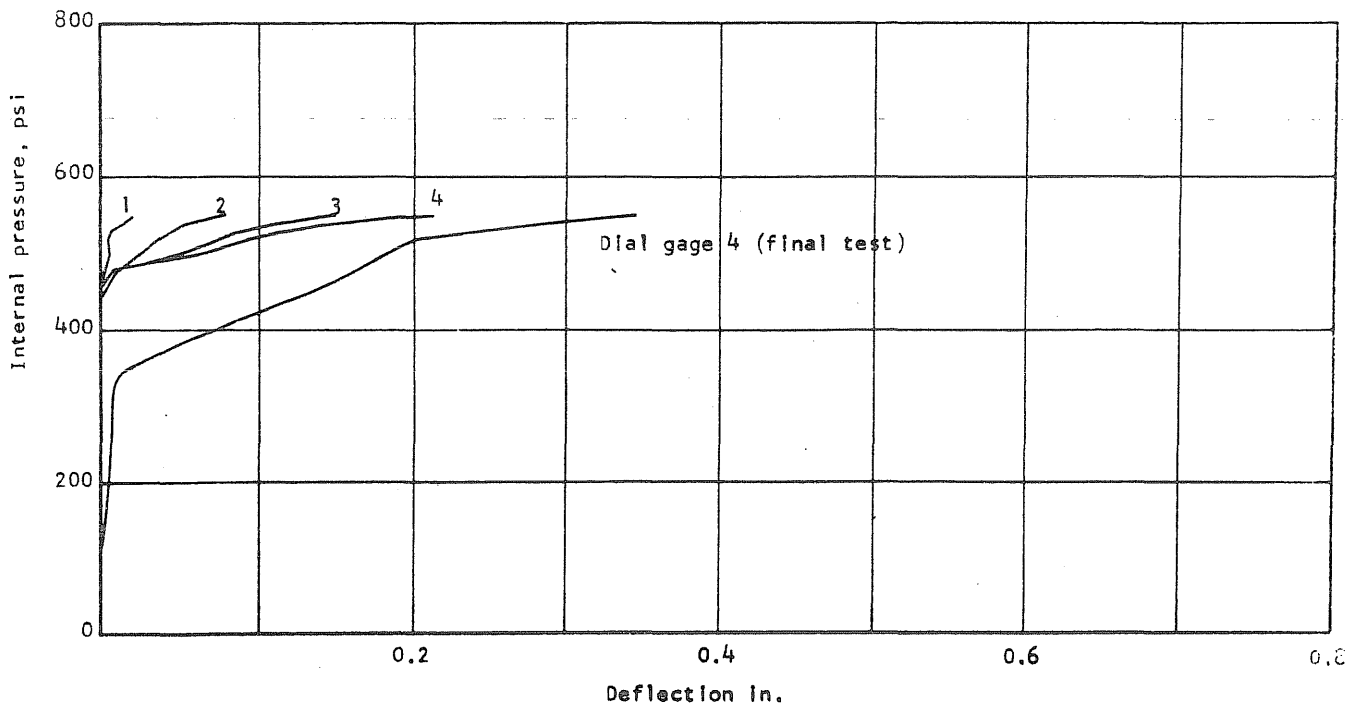


FIG. B6.7 APPLIED PRESSURE vs DEFLECTION ALONG THE N-HALF OF THE N-S DIAMETER OF PV6

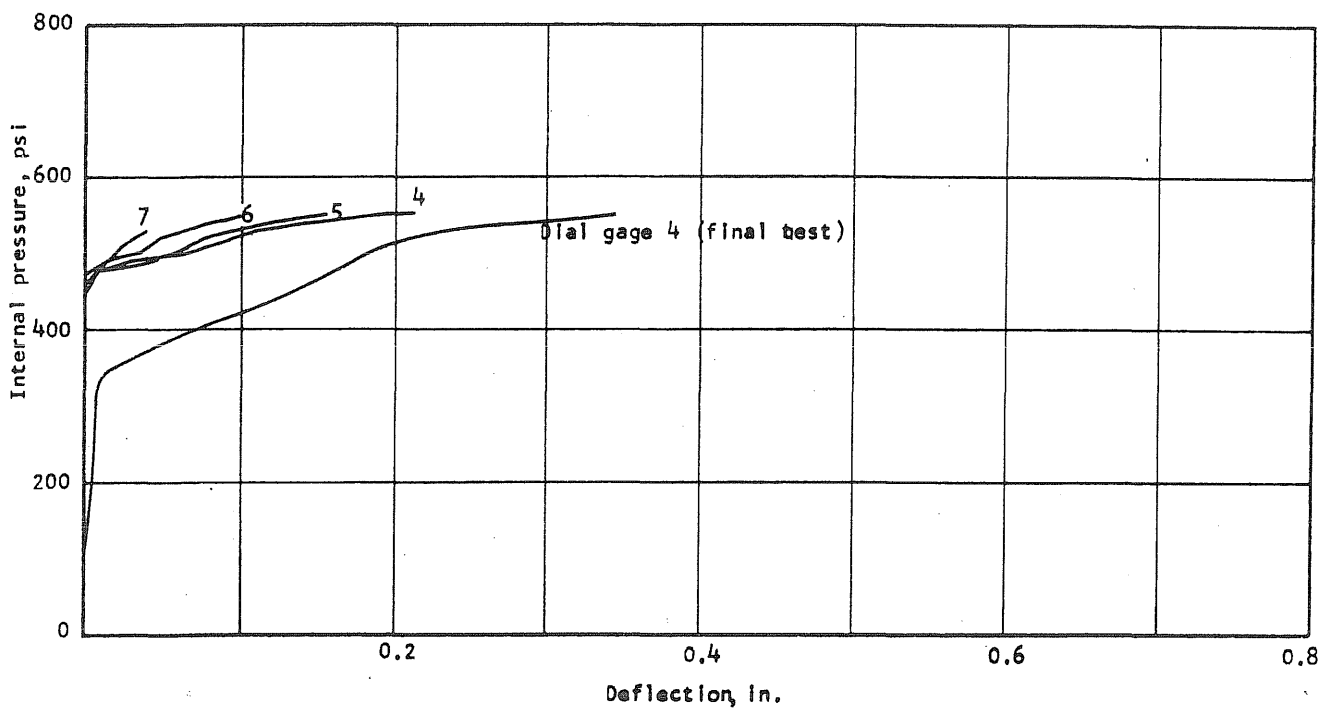


FIG. B6.8 APPLIED PRESSURE vs DEFLECTION ALONG THE S-HALF OF THE N-S DIAMETER OF PV6

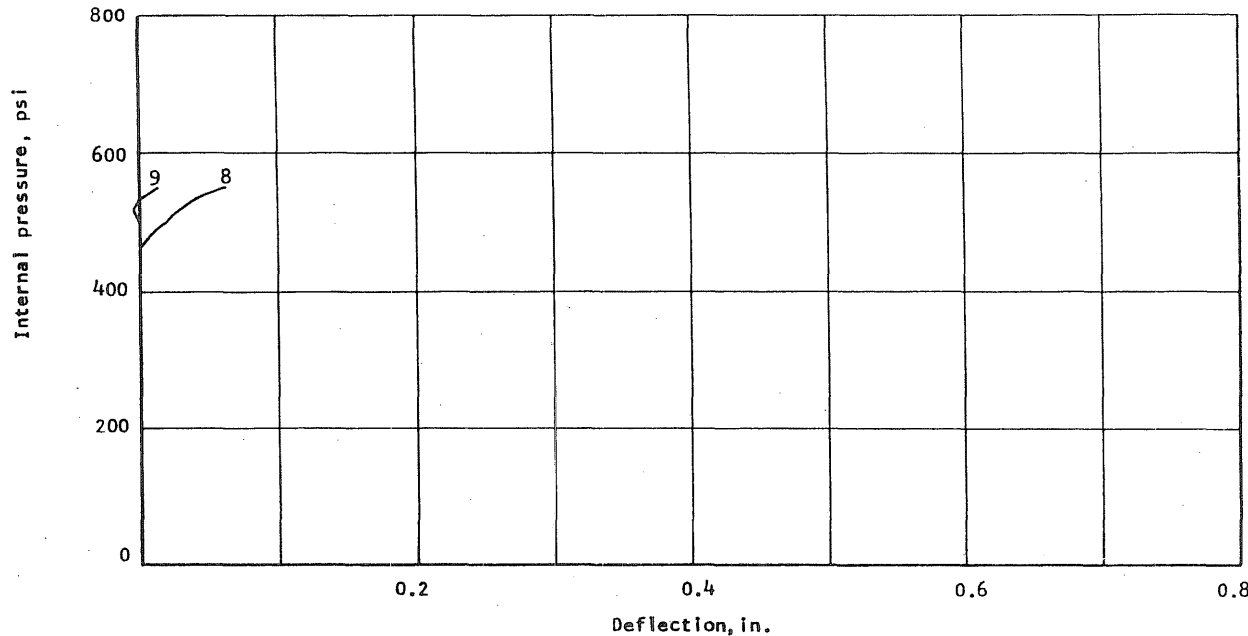


FIG. B6.9 APPLIED PRESSURE vs DEFLECTION OF THE SIDE WALL OF PV6

B
77

Concrete Gages on the Inside of the End Slab

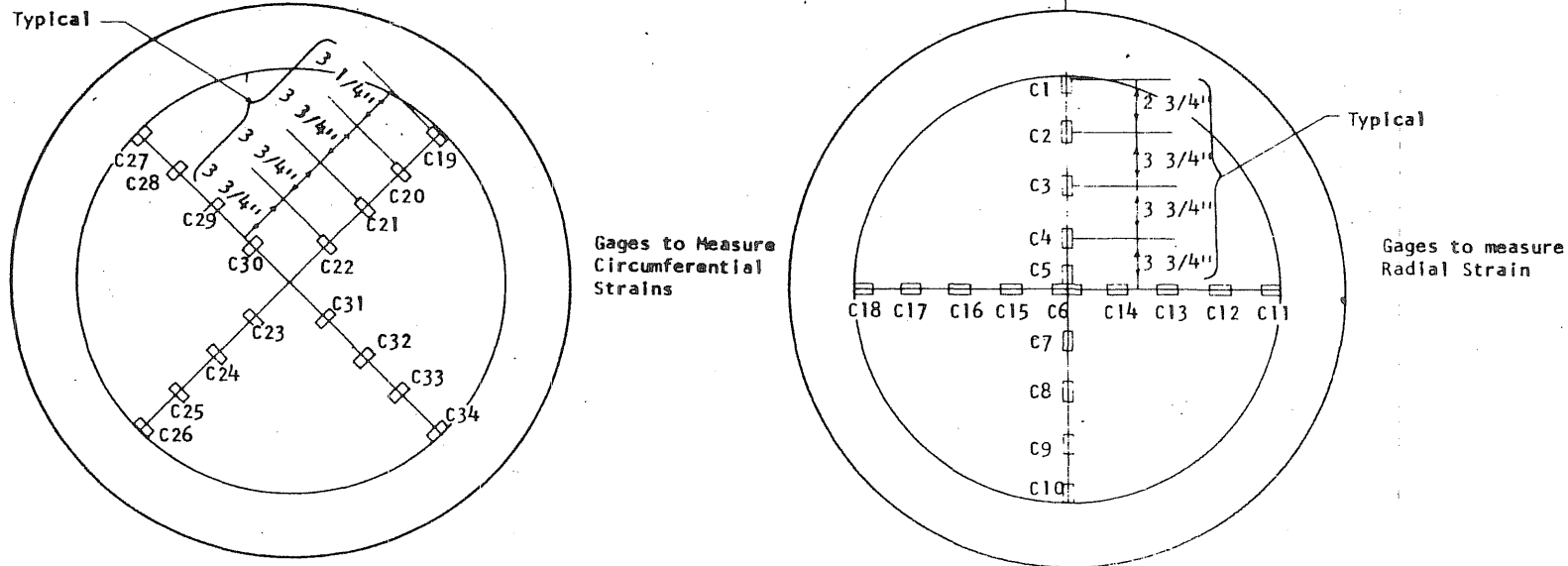
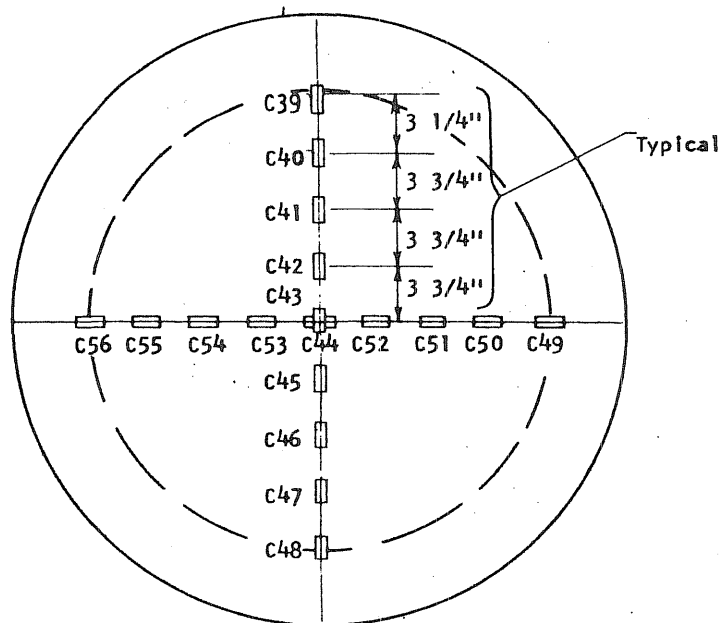
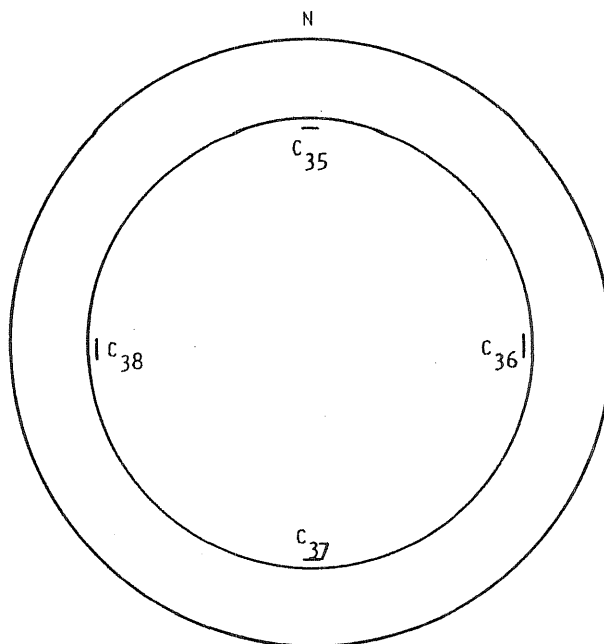


FIG. B6.10 STRAIN GAGE LOCATIONS ON PV6

Concrete Gages on the Outside of the End Slab

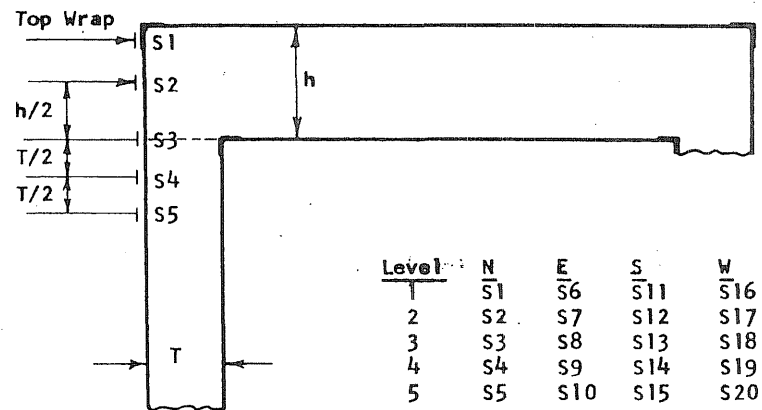


Concrete Gages on The Inside Walls



B
78

Steel Gages on Circumferential Prestress Wire



Gages at the ENDS of the
N-S and E-W Diameters to
measure longitudinal strain

FIG. B6.10 (cont.) STRAIN GAGE LOCATIONS ON PV6

FIG. B6.10 (cont'd) STRAIN GAGE LOCATIONS ON PV6

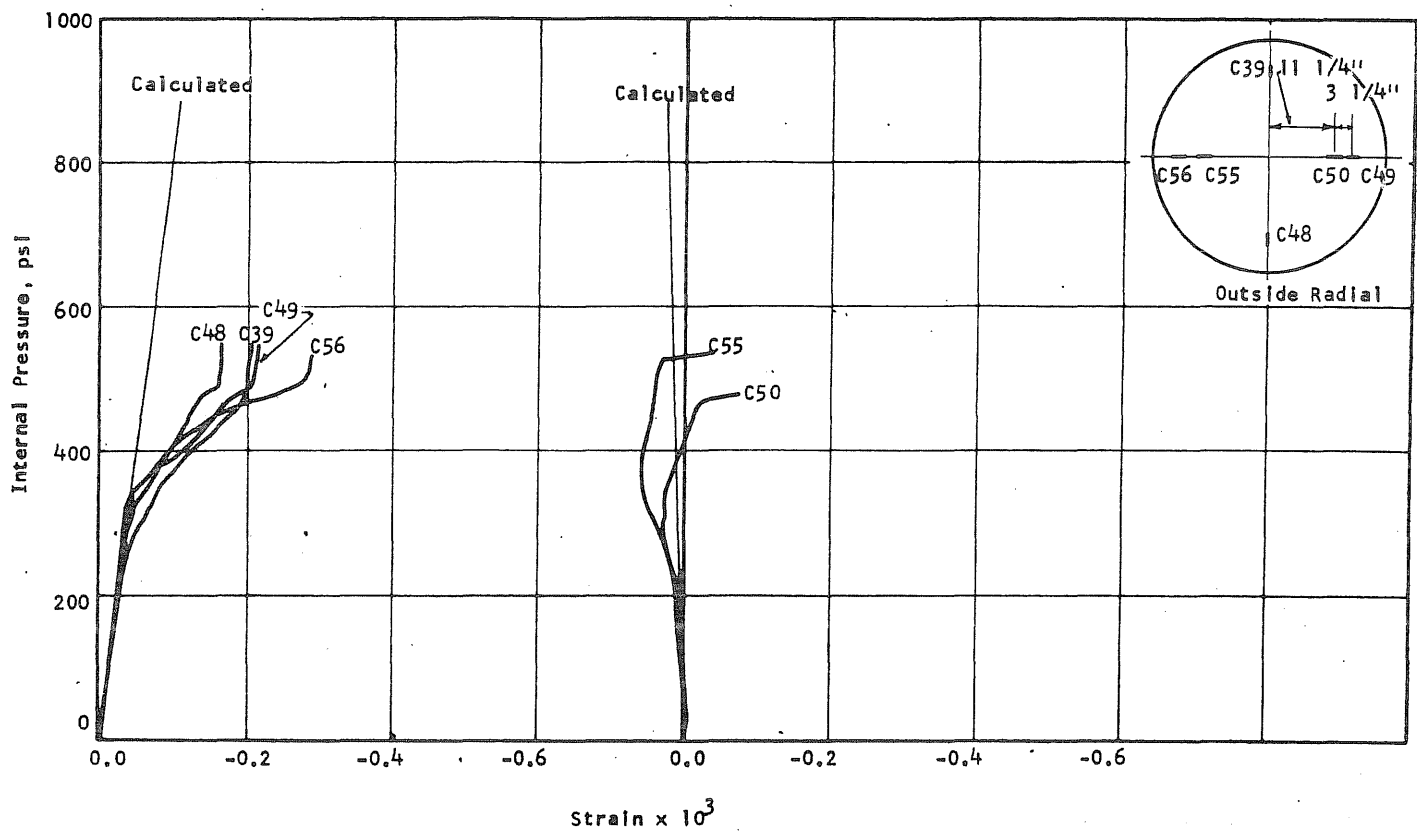


FIG. B6.11 CONCRETE STRAINS, VESSEL PV6

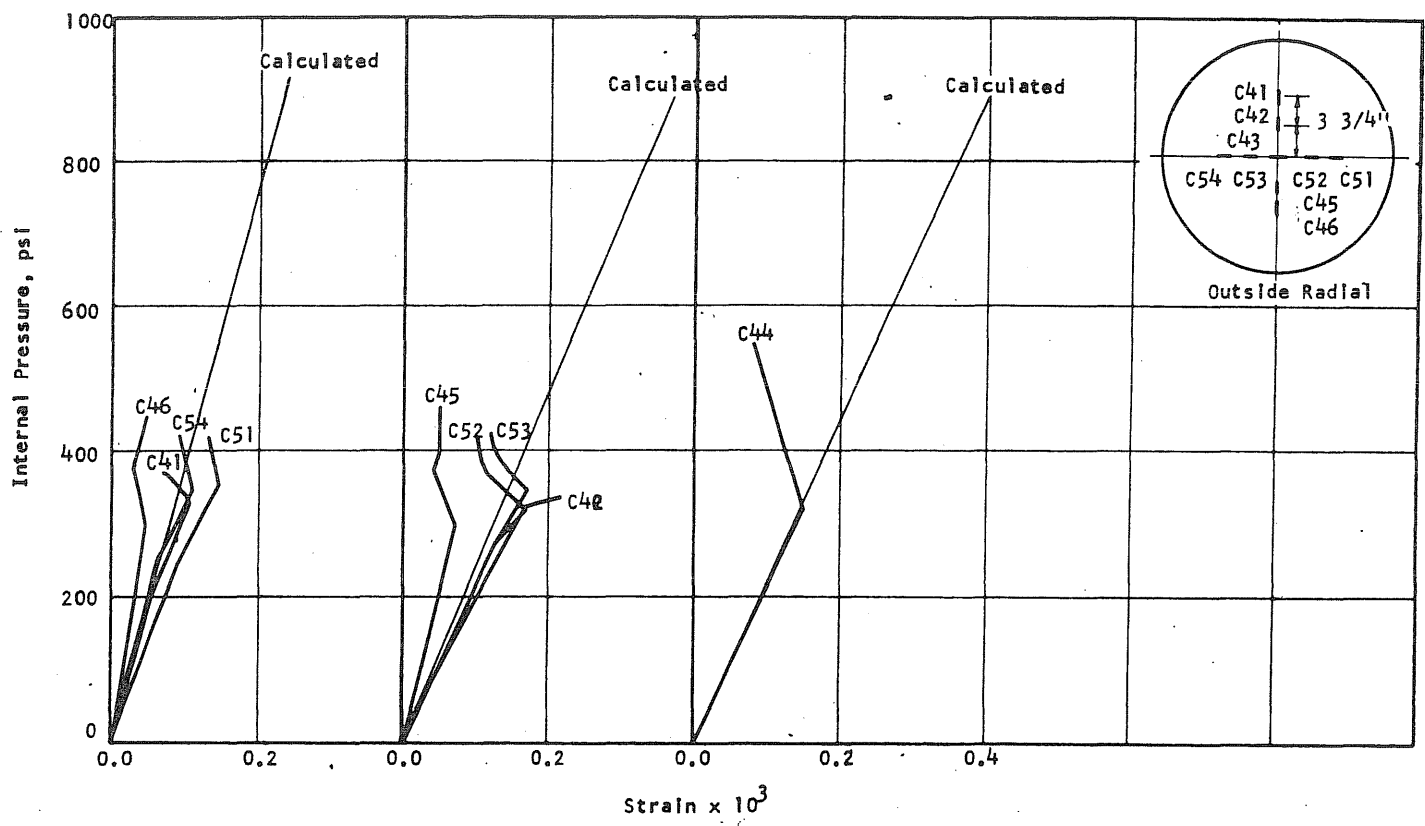


FIG. B6.12 CONCRETE STRAINS, VESSEL PV6

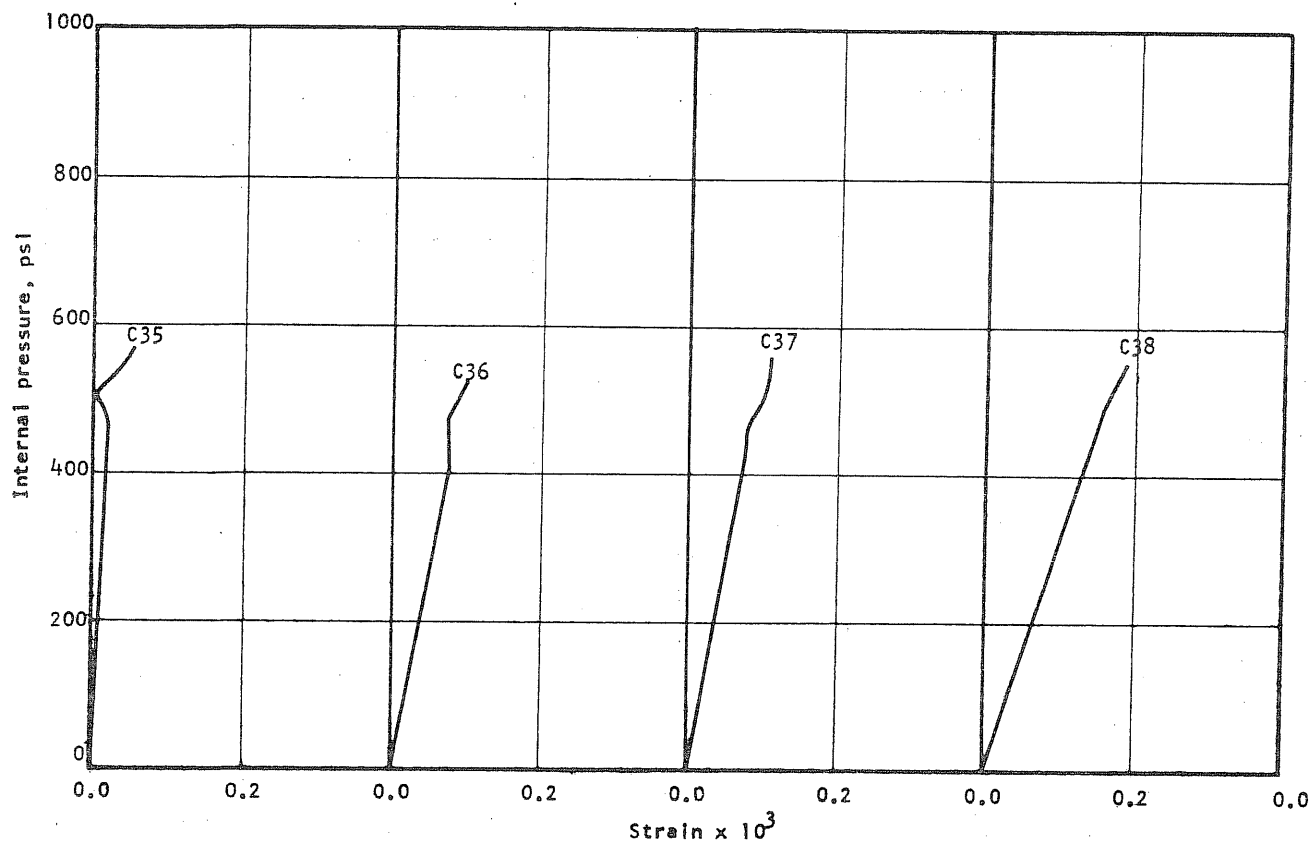


FIG. B6.13 APPLIED PRESSURE vs LONGITUDINAL STRAIN ON THE INSIDE OF THE WALL OF PV6

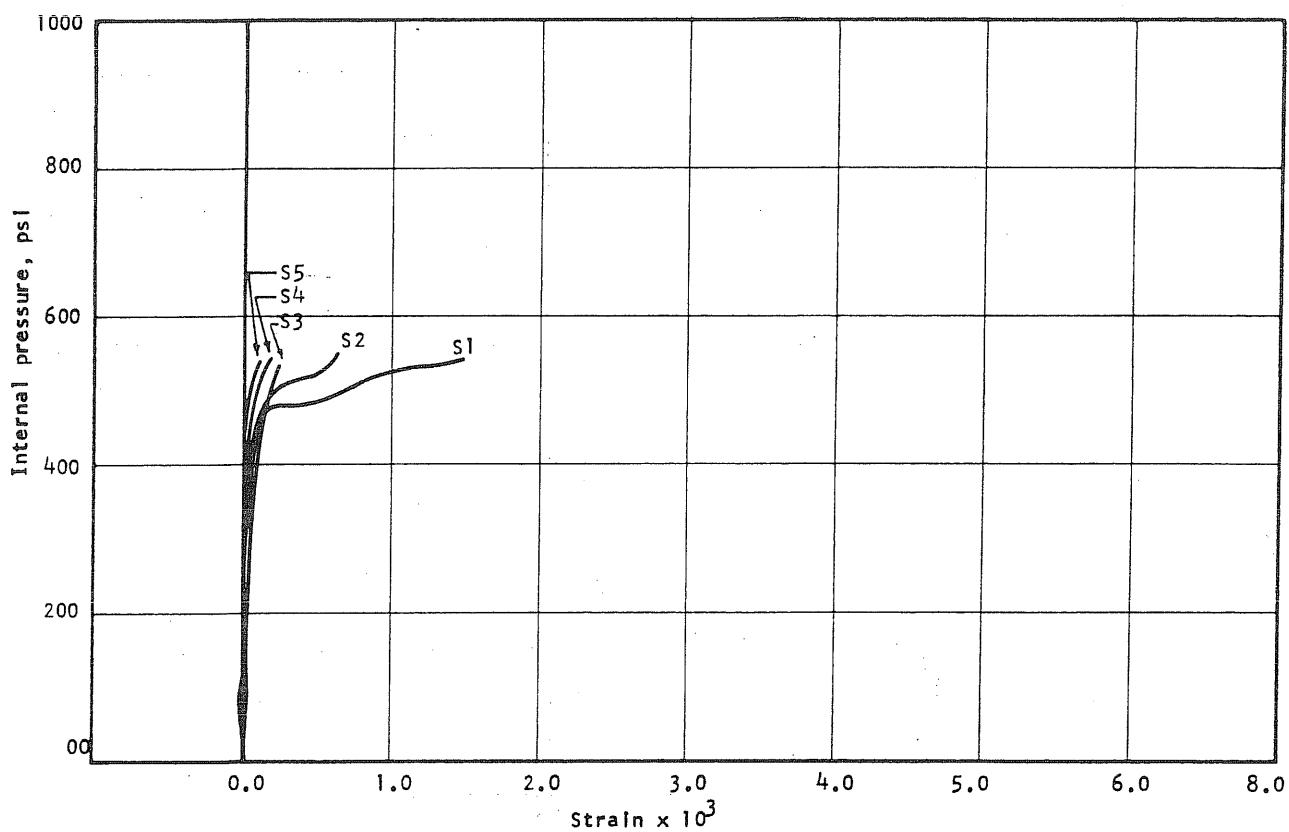


FIG. B6.14 APPLIED PRESSURE vs STRAIN IN THE CIRCUMFERENTIAL PRESTRESS WIRE AT THE N-END OF THE N-S DIAMETER OF PV6

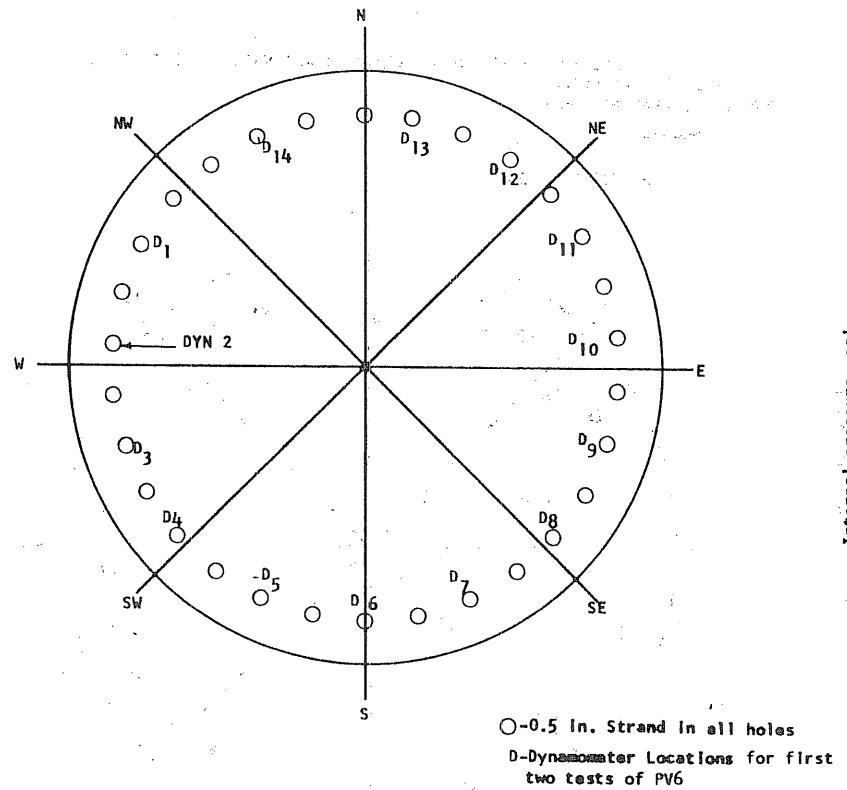


FIG. B6.15 LOCATION OF LONGITUDINAL REINFORCEMENT

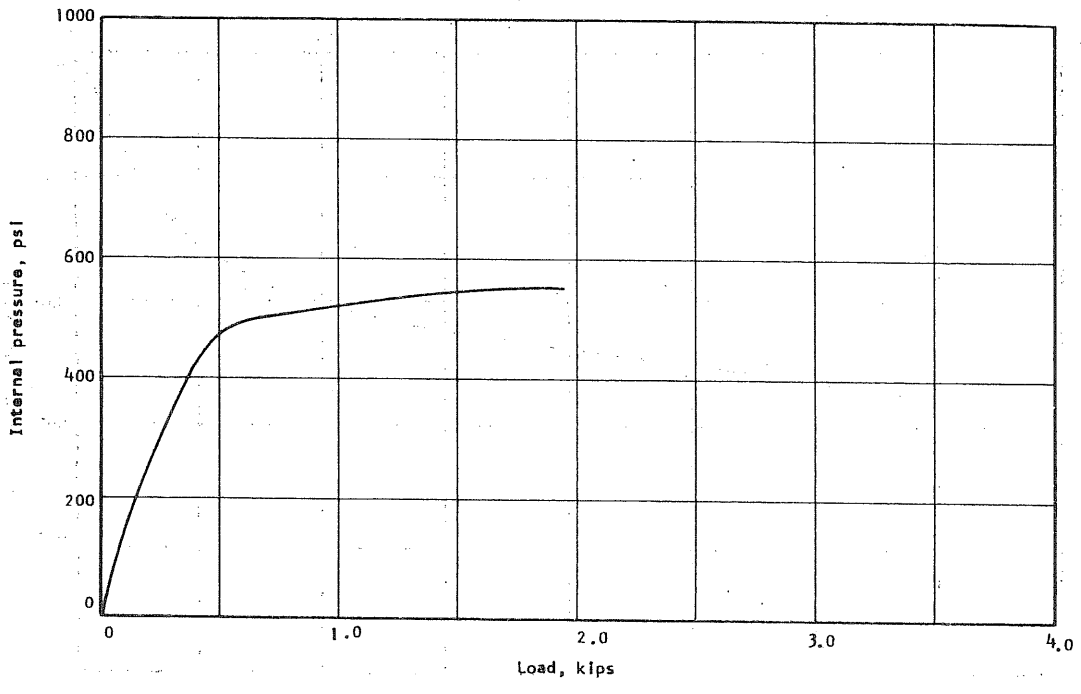


FIG. B6.16 APPLIED PRESSURE vs INCREASE IN LOAD IN DYNAMOMETER NO. 9 ON FIRST TEST OF PV6

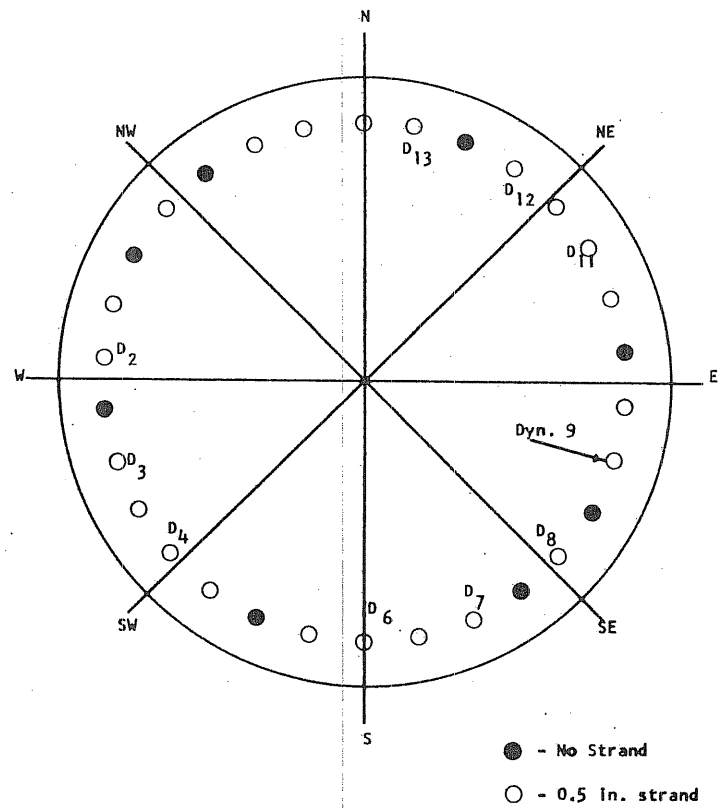


FIG. B6.3.17 LOCATION OF LONGITUDINAL REINFORCEMENT

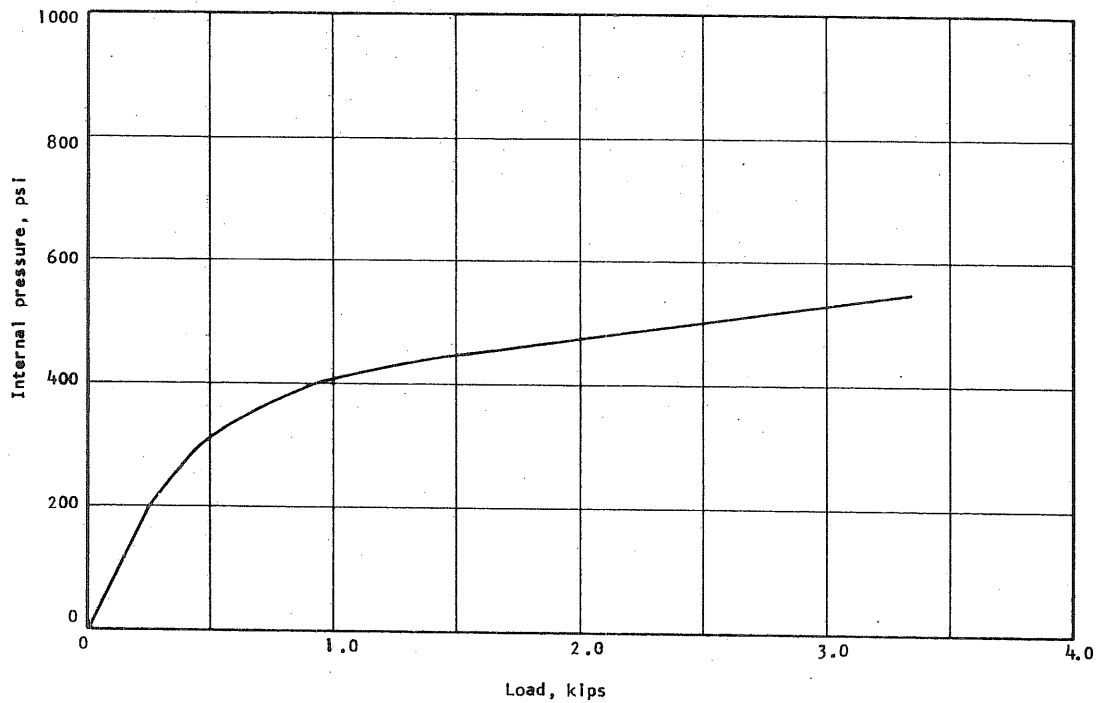


FIG. B6.18 APPLIED PRESSURE vs INCREASE IN LOAD IN DYNAMOMETER NO. 9 ON FINAL TEST OF PV6

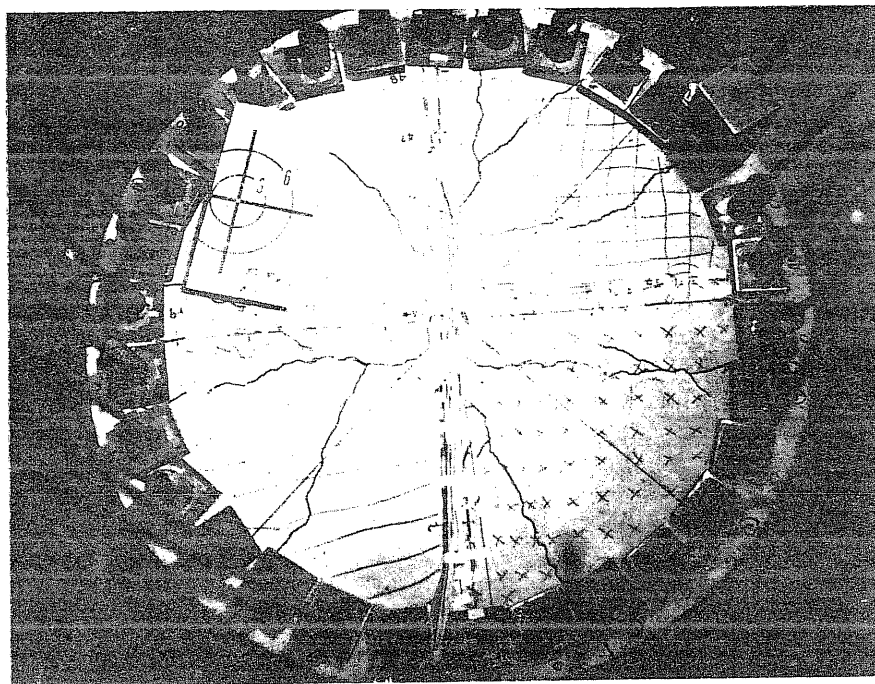


FIG. B6.19a CRACK PATTERN AFTER FIRST TEST ON PV6

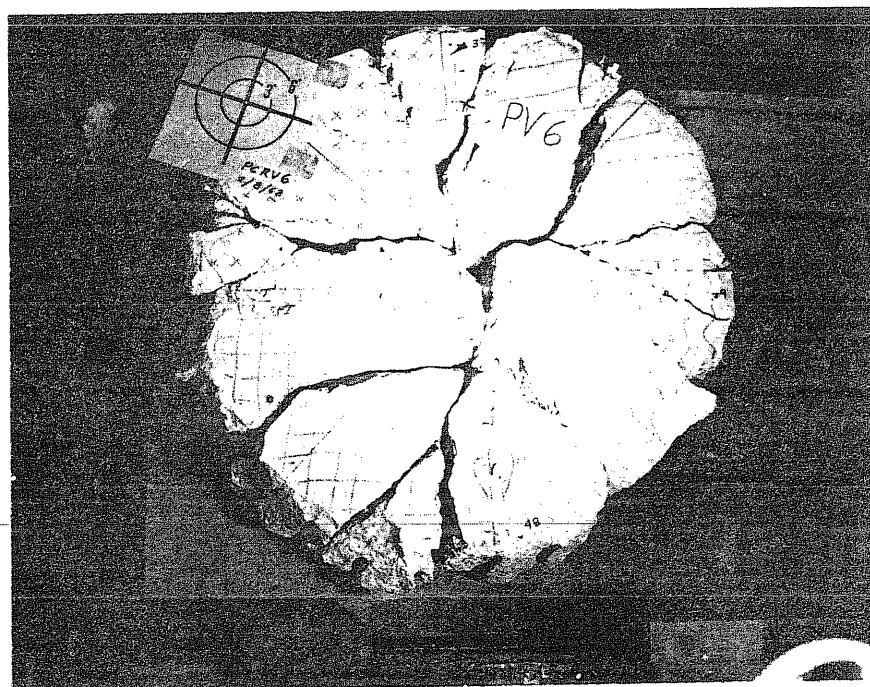


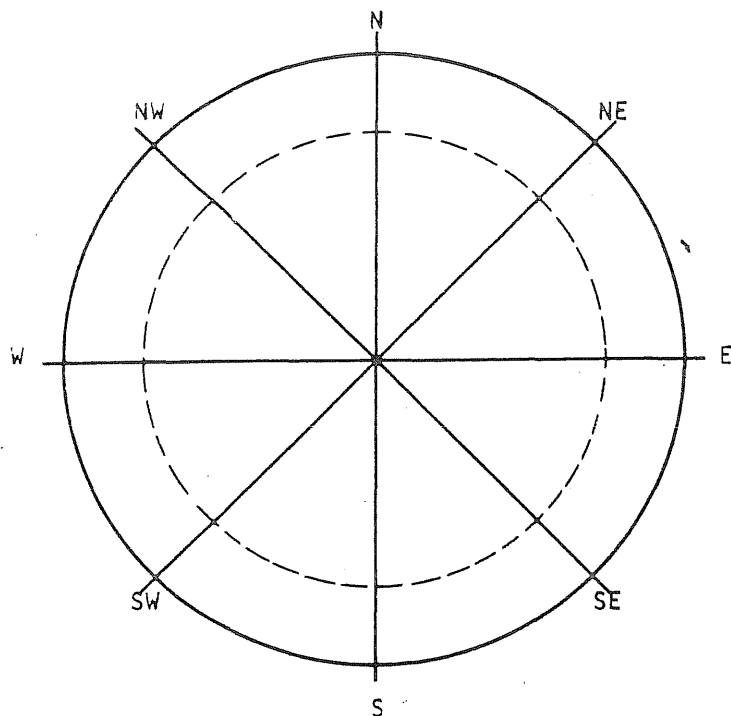
FIG. B6.19b REASSEMBLED END SLAB OF PV6

B7 Test Vessel PV7 ($t = 9.0$ in., $s = 1/3$ in.)

Test vessel PV7 was cast in the laboratory and was uncracked prior to prestressing. The circumferential prestressing applied to the vessel caused a band of circumferential cracks to develop on the outside of the vessel between seven and nine in. from the top. A corresponding band of cracks developed from twelve to nineteen in. below the top on the inside of the vessel. Four longitudinal cables stressed nominally to 24 kips were placed on the vessel to arrest further crack development during the interim between the prestressing operation and assembly of the test setup.

The liner for PV7 was modified considerably from the one that had been used previously. Figure B7.2 is a detail of the liner that was used for PV7. A one-half-in. thick layer of hydrocal was placed on the inside of the end slab to provide a smooth surface over strain gages. A 0.017-in. sheet of aluminum was attached to the side wall in the hope of bridging small pores or cracks more effectively. The round O-ring was replaced by one with a triangular cross section, and the neoprene sheets were lapped about one in. at the junction of the end slab and side wall in an effort to improve the performance of the seal in that vicinity. Rubber cement was used as the adhesive to hold both the aluminum and neoprene in place. Thirty 0.5-in. strands were used for longitudinal reinforcement in the test.

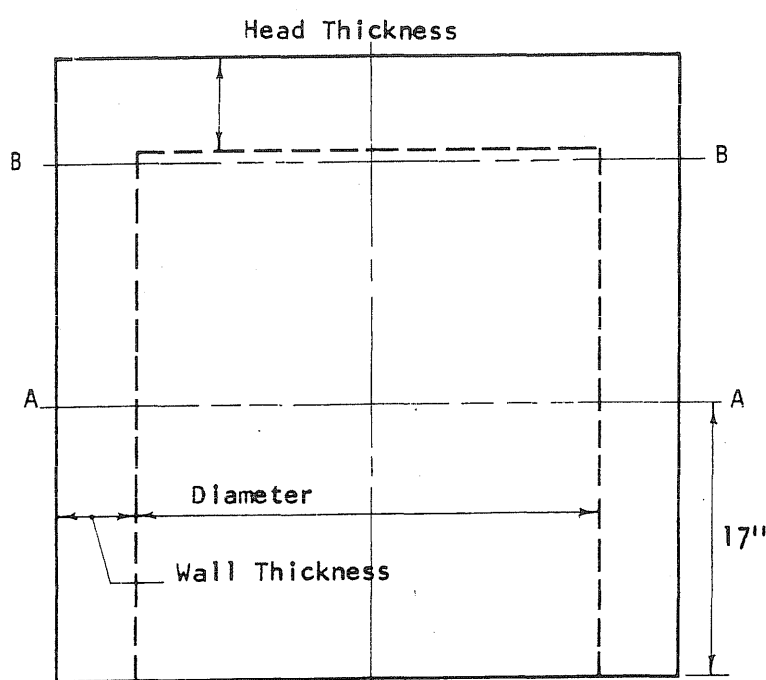
The testing of PV7 was carried out with no difficulty. About two hours were required for the entire test as loading proceeded in 50 psi increments to an internal pressure of 750 psi. Twenty-five psi increments were added up to a pressure of 800 psi. At 800 psi the deflection at midspan was creeping steadily. Therefore, the pressure was increased continuously until the vessel failed at 870 psi. The reassembled end slab is shown in Fig. B7.17.



| Head Thickness | |
|----------------|--------|
| Point No. | Inches |
| * | 7 1/2 |
| | |
| | |
| | |
| | |
| | |
| | |
| | |

Nominal Thickness

| Wall Thickness, in. | | |
|---------------------|------|------|
| Plane Axis | AA | BB |
| N | 5.04 | 5.10 |
| NE | | |
| E | 4.89 | 4.85 |
| SE | | |
| S | 4.90 | 5.00 |
| SW | | |
| W | 4.90 | 4.90 |
| NW | | |



| Inside Diameter, in. | | |
|----------------------|--------------------|--------------------|
| Plane Axis | AA | BB |
| N-S | 30 $\frac{2}{32}$ | 29 $\frac{30}{32}$ |
| NE-SW | 29 $\frac{31}{32}$ | 29 $\frac{30}{32}$ |
| E-W | 29 $\frac{30}{32}$ | 30 |
| SE-NW | 30 | 29 $\frac{31}{32}$ |

FIG. B7.1 DIMENSIONS OF PV7

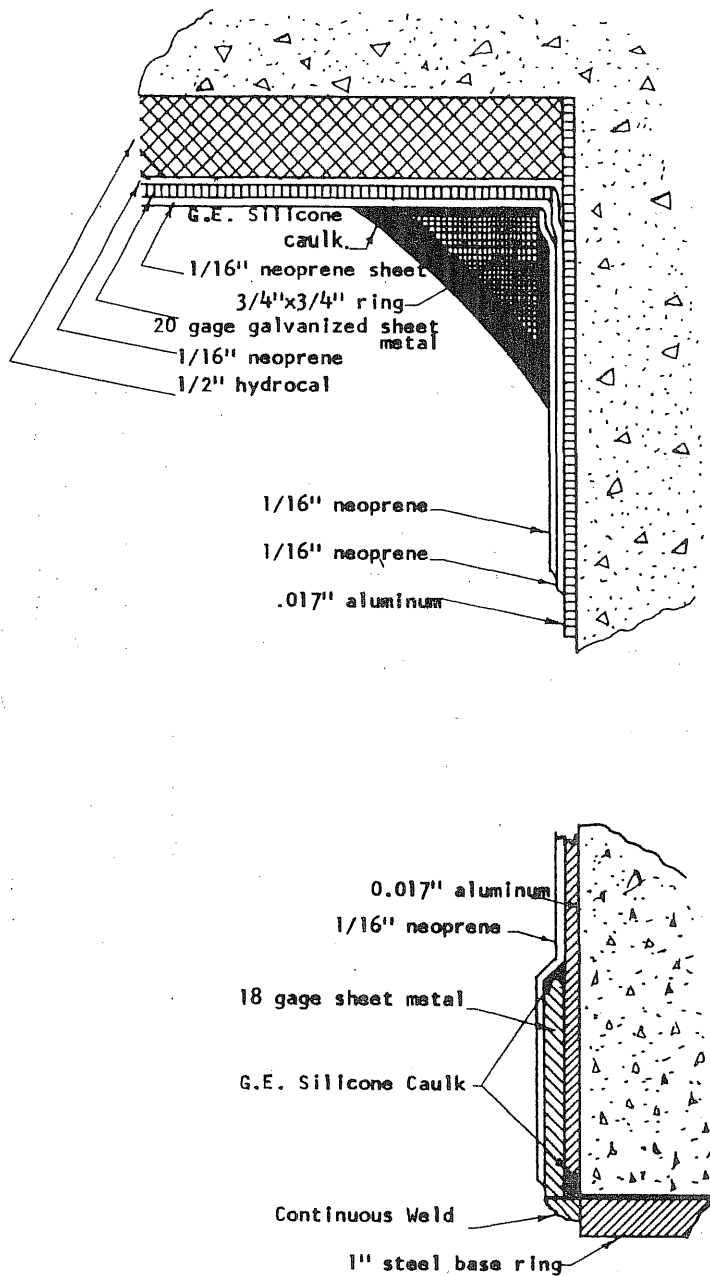
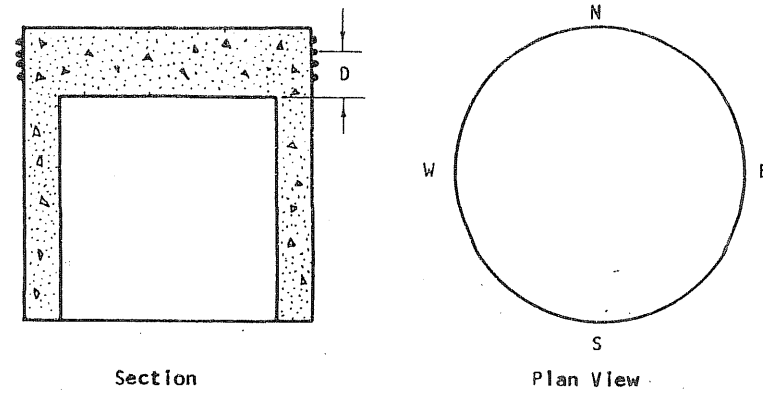


FIG. B7.2 SEALING DETAIL FOR PV7



| Wrap No. | D _N | D _E | D _S | D _W |
|----------|----------------|----------------|----------------|----------------|
| 1 | 8 5/16 | 8 5/16 | 8 3/16 | 8 2/16 |
| 2 | 7 13/16 | 7 14/16 | 7 14/16 | 7 14/16 |
| 3 | 7 10/16 | 7 8/16 | 7 8/16 | 7 8/16 |
| 4 | 7 6/16 | 7 4/16 | 7 4/16 | 7 4/16 |
| 5 | 7 1/16 | 6 15/16 | 6 14/16 | 6 14/16 |
| 6 | 6 11/16 | 6 9/16 | 6 9/16 | 6 8/16 |
| 7 | 6 5/16 | 6 3/16 | 6 3/16 | 6 2/16 |
| 8 | 6 0/16 | 5 14/16 | 5 15/16 | 5 14/16 |
| 9 | 5 12/16 | 5 11/16 | 5 10/16 | 5 10/16 |
| 10 | 5 8/16 | 5 6/16 | 5 6/16 | 5 6/16 |
| 11 | 5 4/16 | 5 2/16 | 5 2/16 | 5 2/16 |
| 12 | 4 15/16 | 4 13/16 | 4 13/16 | 4 12/16 |
| 13 | 4 10/16 | 4 8/16 | 4 7/16 | 4 7/16 |
| 14 | 4 4/16 | 4 1/16 | 4 0/16 | 4 0/16 |
| 15 | 3 14/16 | 3 12/16 | 3 11/16 | 3 11/16 |
| 16 | 3 8/16 | 3 6/16 | 3 6/16 | 3 5/16 |
| 17 | 3 3/16 | 3 1/16 | 3 1/16 | 3 0/16 |
| 18 | 2 14/16 | 2 12/16 | 2 11/16 | 2 11/16 |
| 19 | 2 8/16 | 2 6/16 | 2 6/16 | 2 6/16 |
| 20 | 2 3/16 | 2 0/16 | 2 0/16 | 2 0/16 |
| 21 | 1 14/16 | 1 11/16 | 1 11/16 | 1 10/16 |
| 22 | 1 8/16 | 1 6/16 | 1 6/16 | 1 5/16 |
| 23 | 1 2/16 | 1 0/16 | 1 1/16 | 1 0/16 |
| 24 | 13/16 | 11/16 | 11/16 | 10/16 |
| 25 | 8/16 | 5/16 | 6/16 | 6/16 |
| 26 | 3/16 | 0/16 | 0/16 | -1/16 |

FIG. B7.3 MEASURED LOCATION OF THE CIRCUMFERENTIAL PRESTRESS WIRE AT THE ENDS OF THE N-S AND E-W DIAMETERS ON PV7

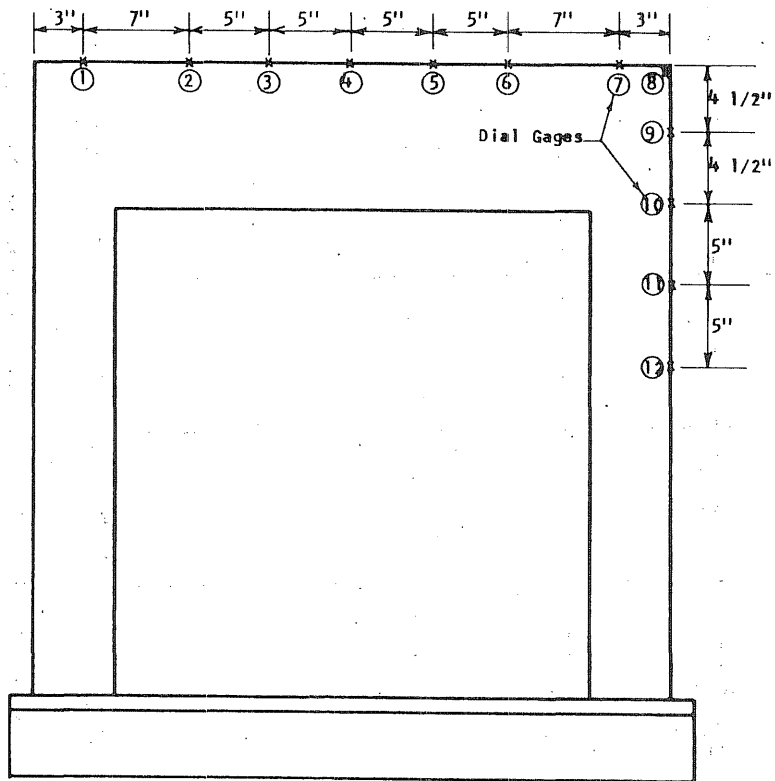


FIG. B7.4 LOCATION OF DEFLECTION GAGES ON PV7

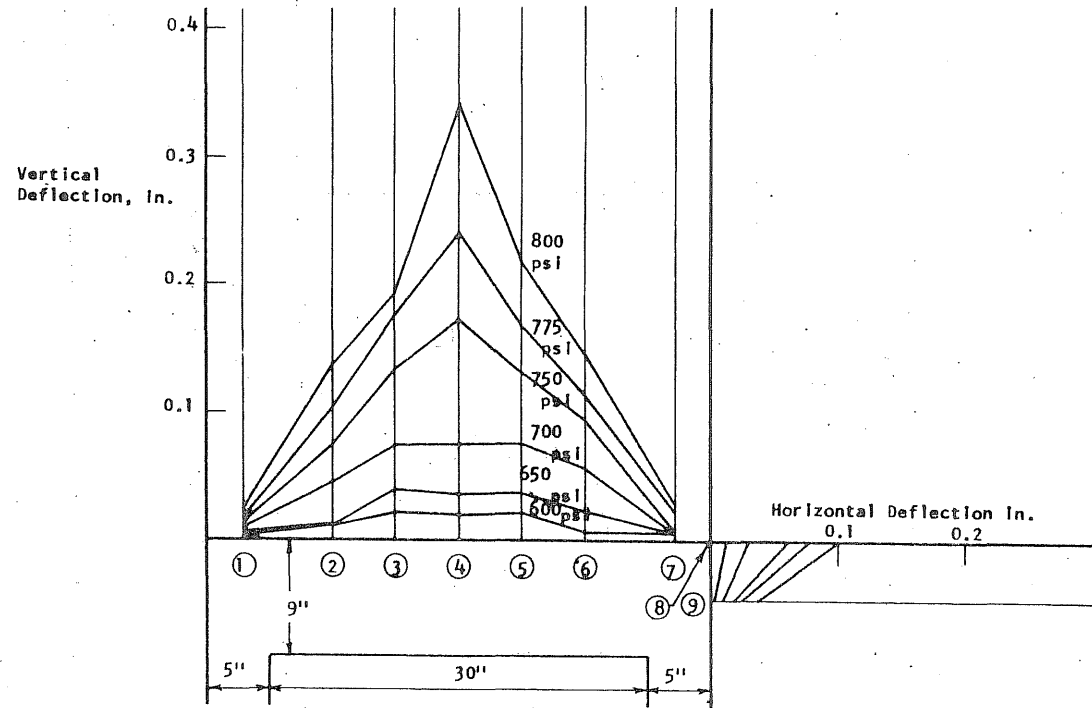


FIG. B7.5 DEFLECTION PROFILES OF THE END SLAB ALONG THE N-S DIAMETER OF PV7

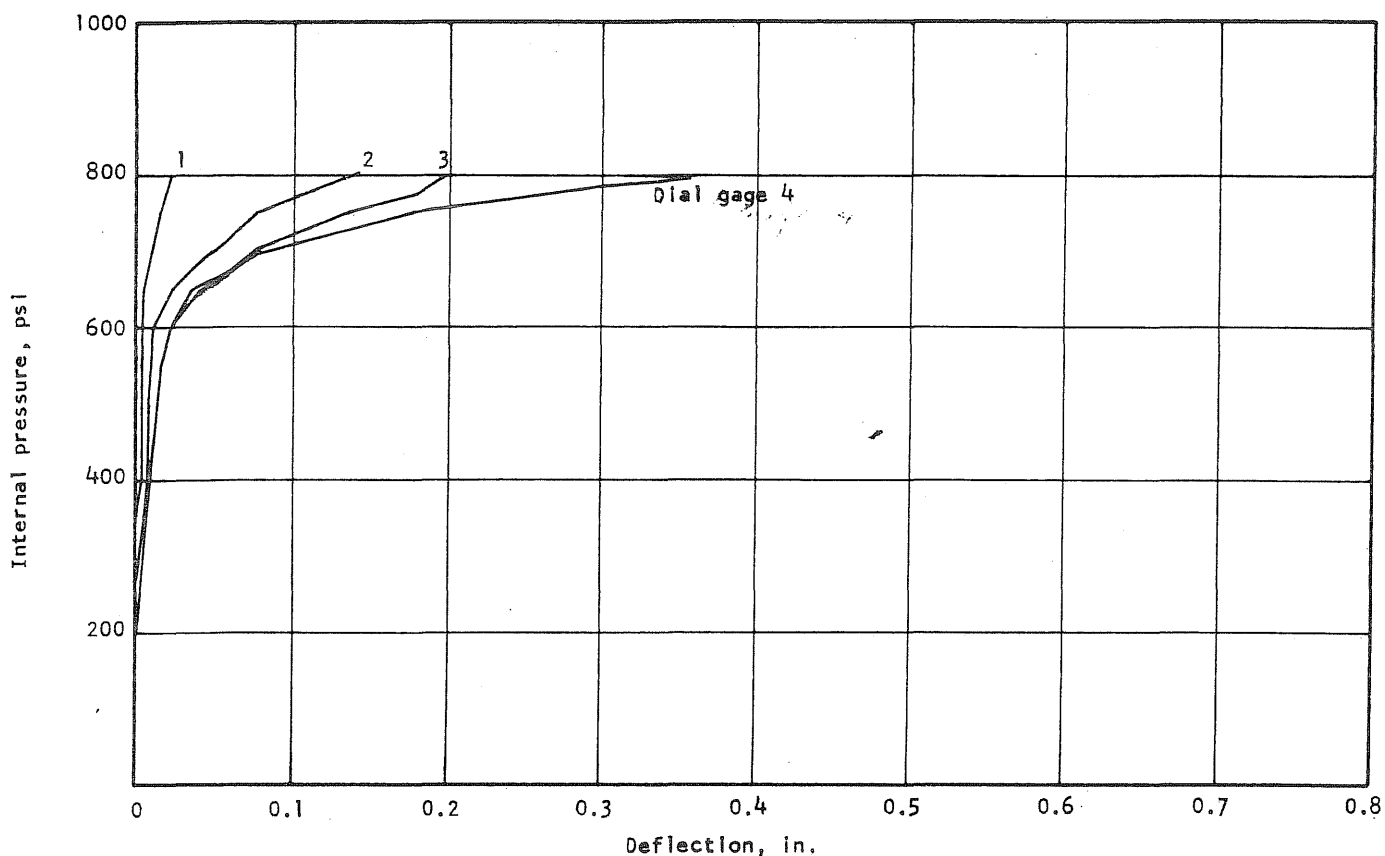


FIG. B7.6 APPLIED PRESSURE vs DEFLECTION ALONG THE N-HALF OF THE N-S DIAMETER OF PV7

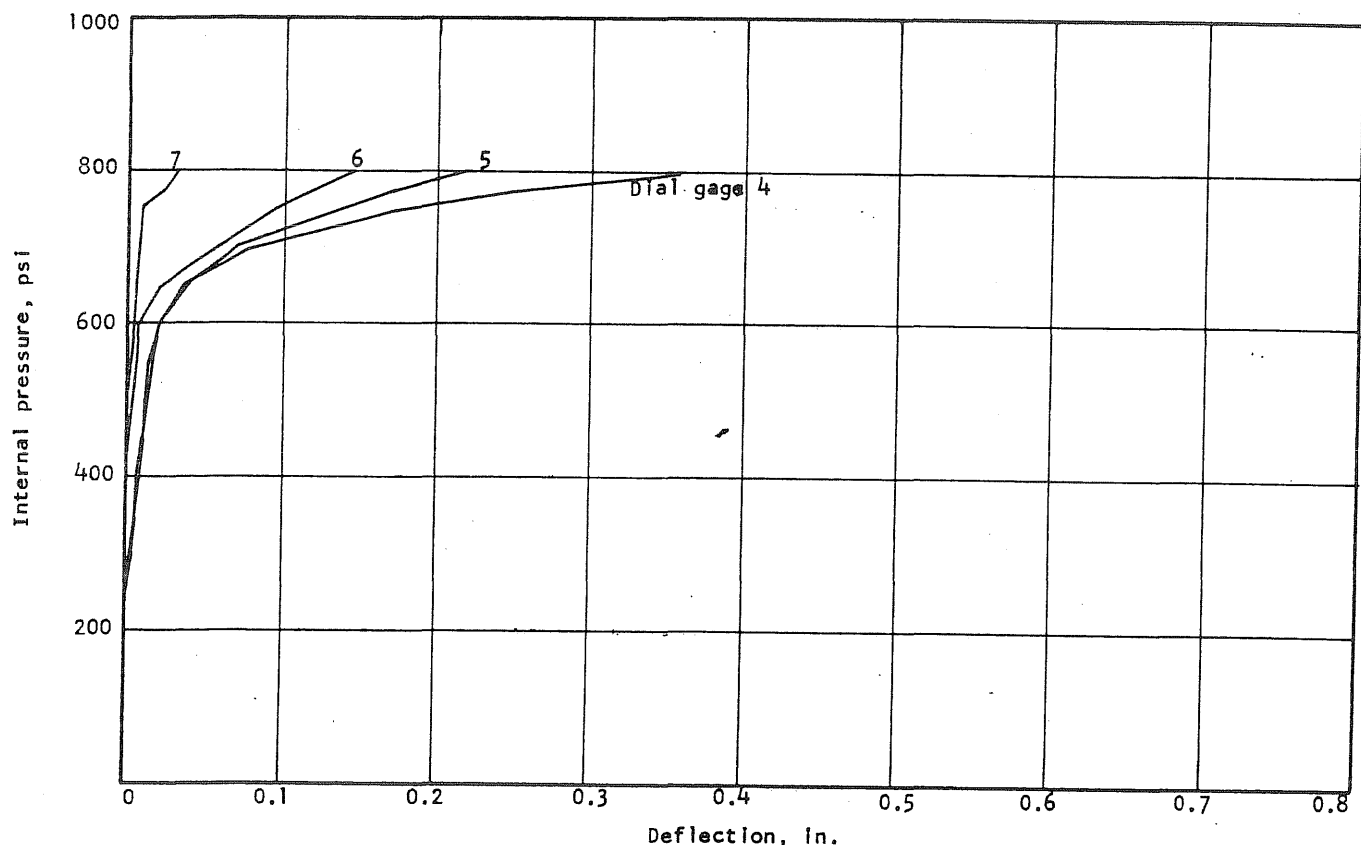


FIG. B7.7 APPLIED PRESSURE vs DEFLECTION ALONG THE S-HALF OF THE N-S DIAMETER OF PV7

B 89

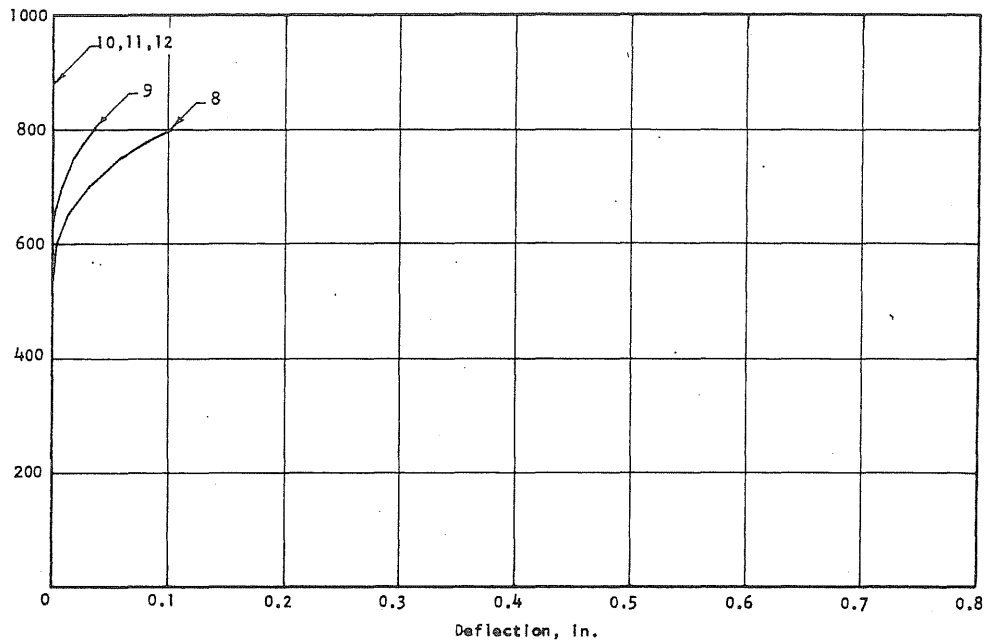


FIG. B7.8 APPLIED PRESSURE vs DEFLECTION OF THE SIDE WALL OF PV7

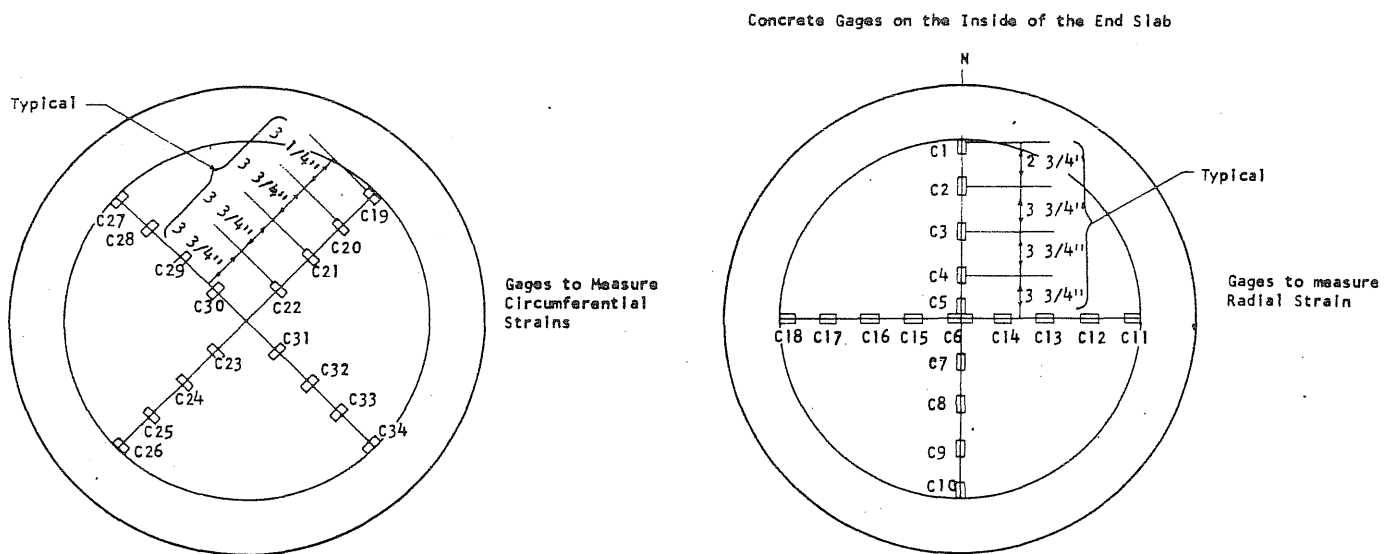
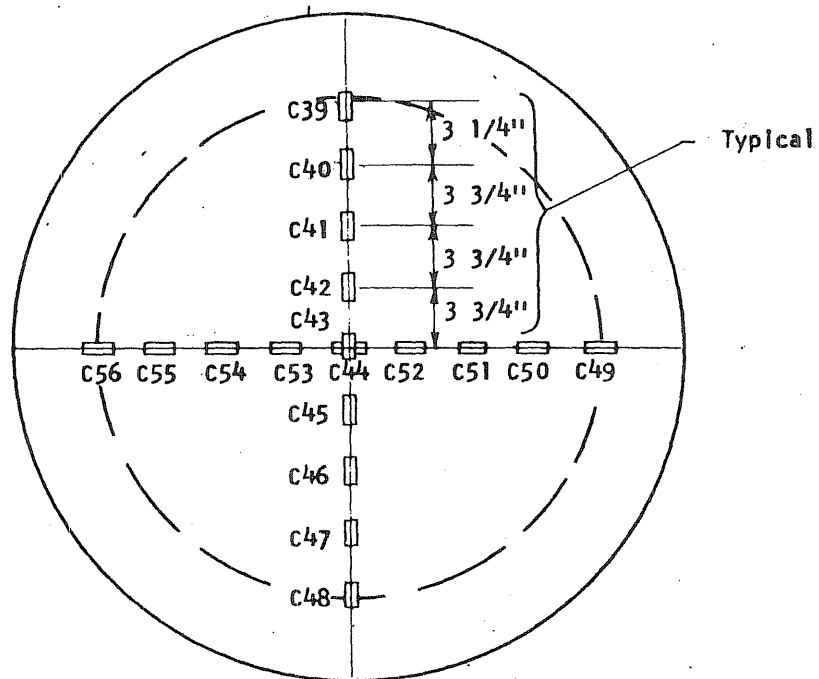
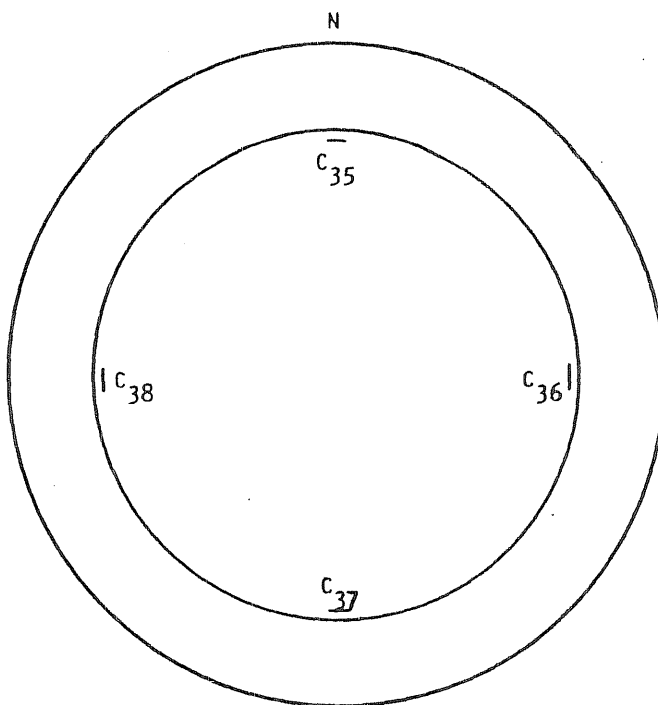


FIG. B7.9 STRAIN GAGE LOCATIONS ON PV7

Concrete Gages on the Outside of the End Slab



Concrete Gages on The Inside Walls



B
69

Steel Gages on Circumferential Prestress Wire

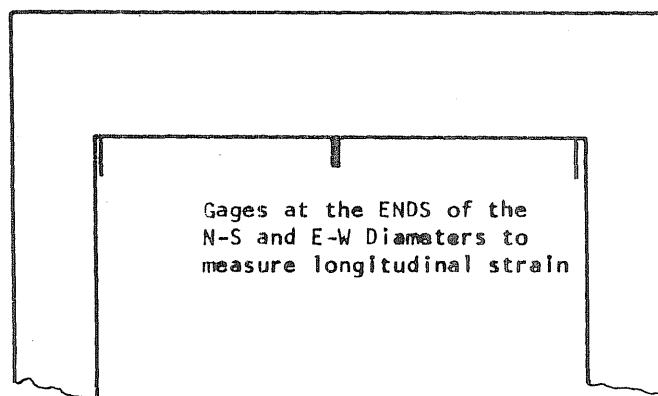
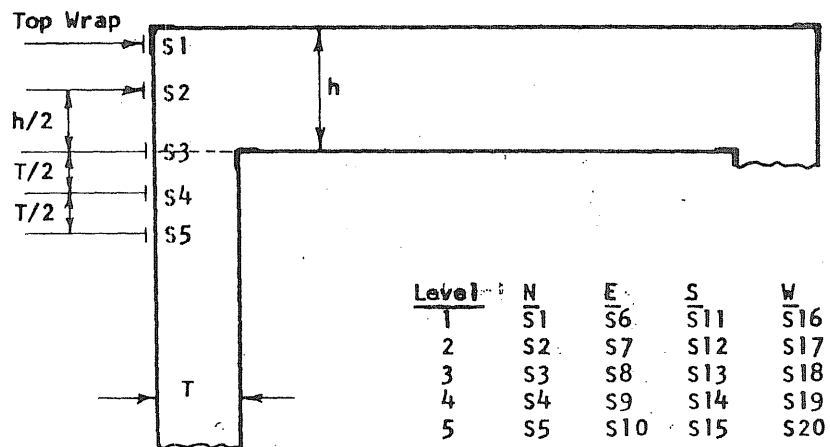


FIG. B7.9 (cont.) STRAIN GAGE LOCATIONS ON PV7

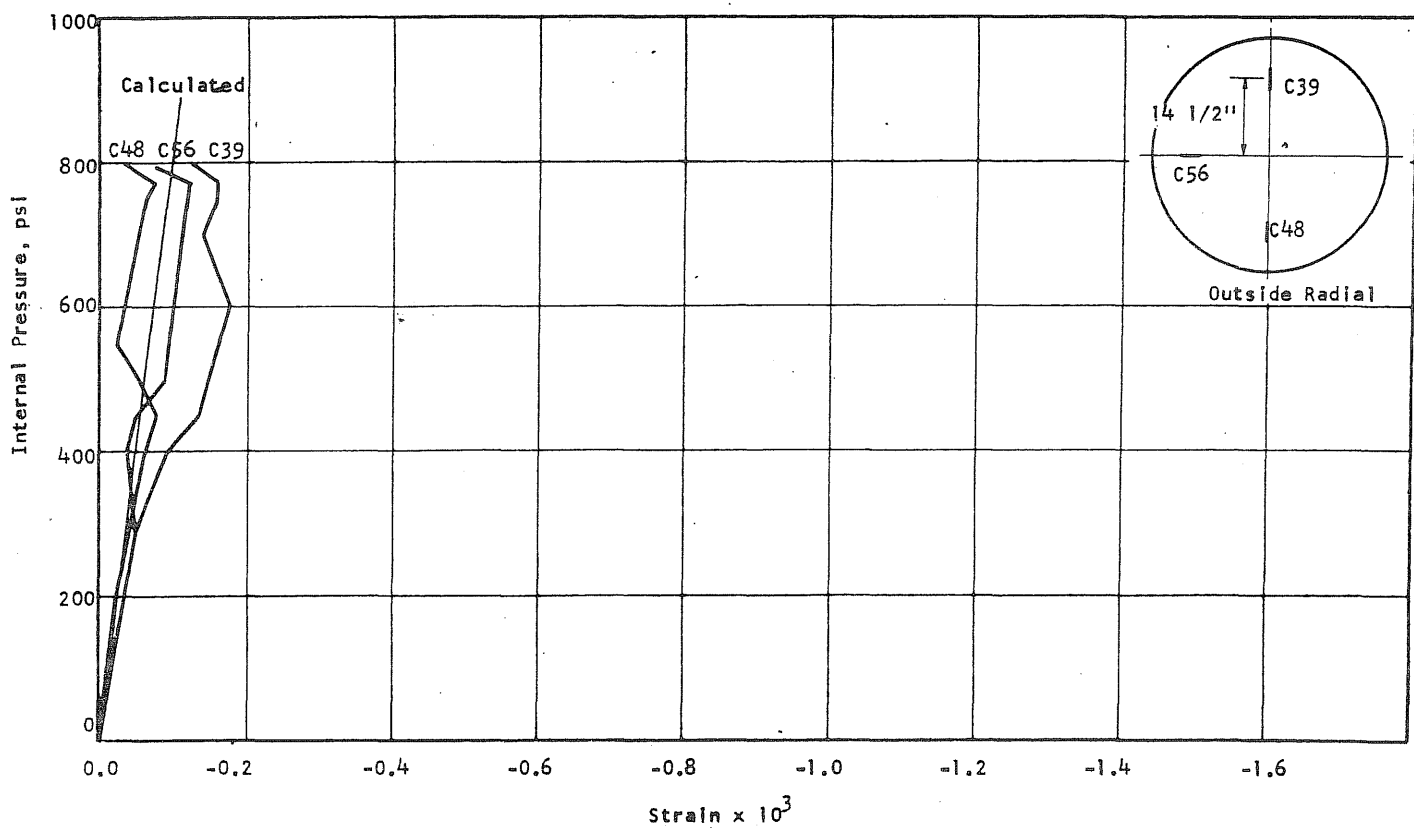


FIG. B7.10 CONCRETE STRAINS, VESSEL PV7

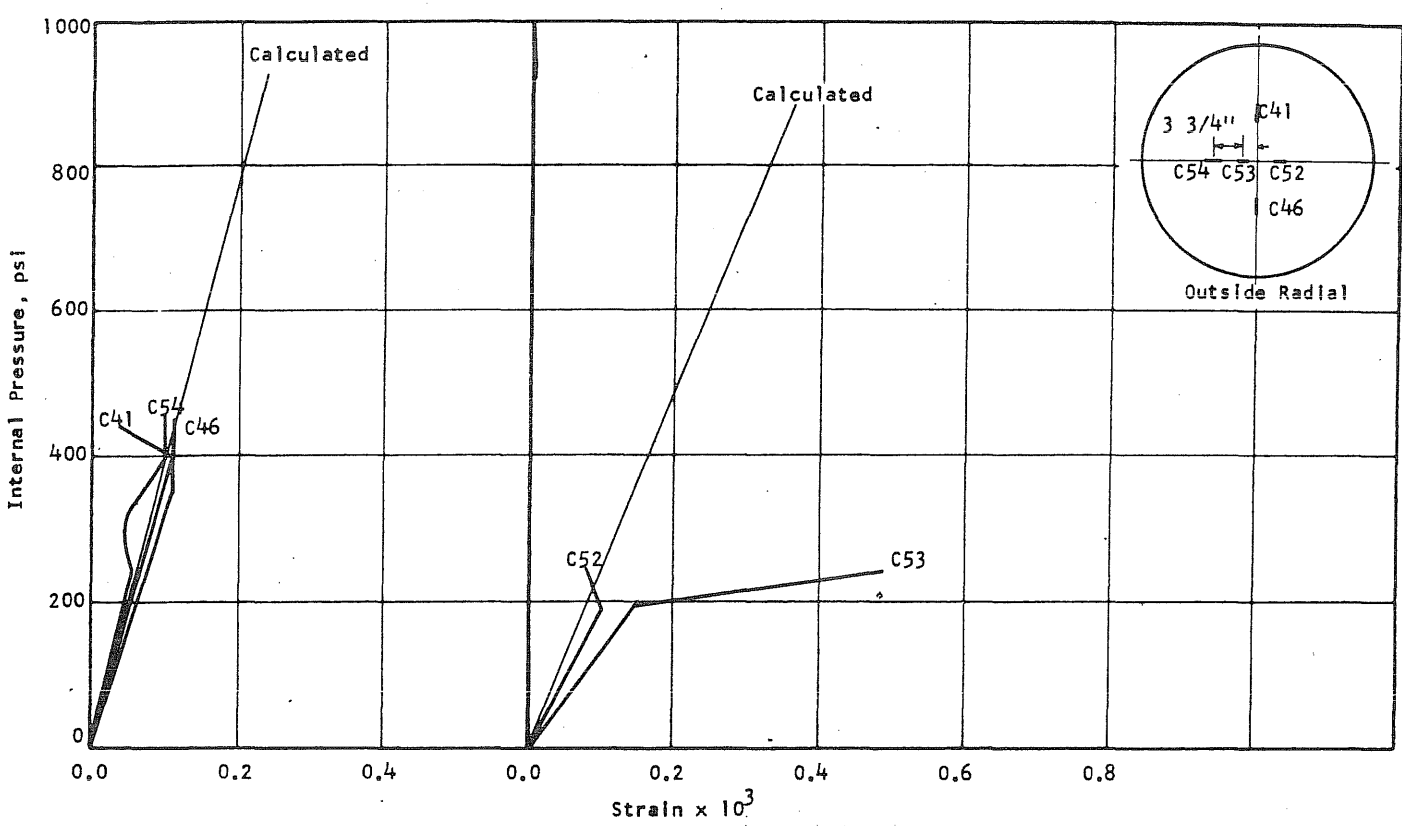


FIG. B7.10 (cont'd) CONCRETE STRAINS, VESSEL PV7

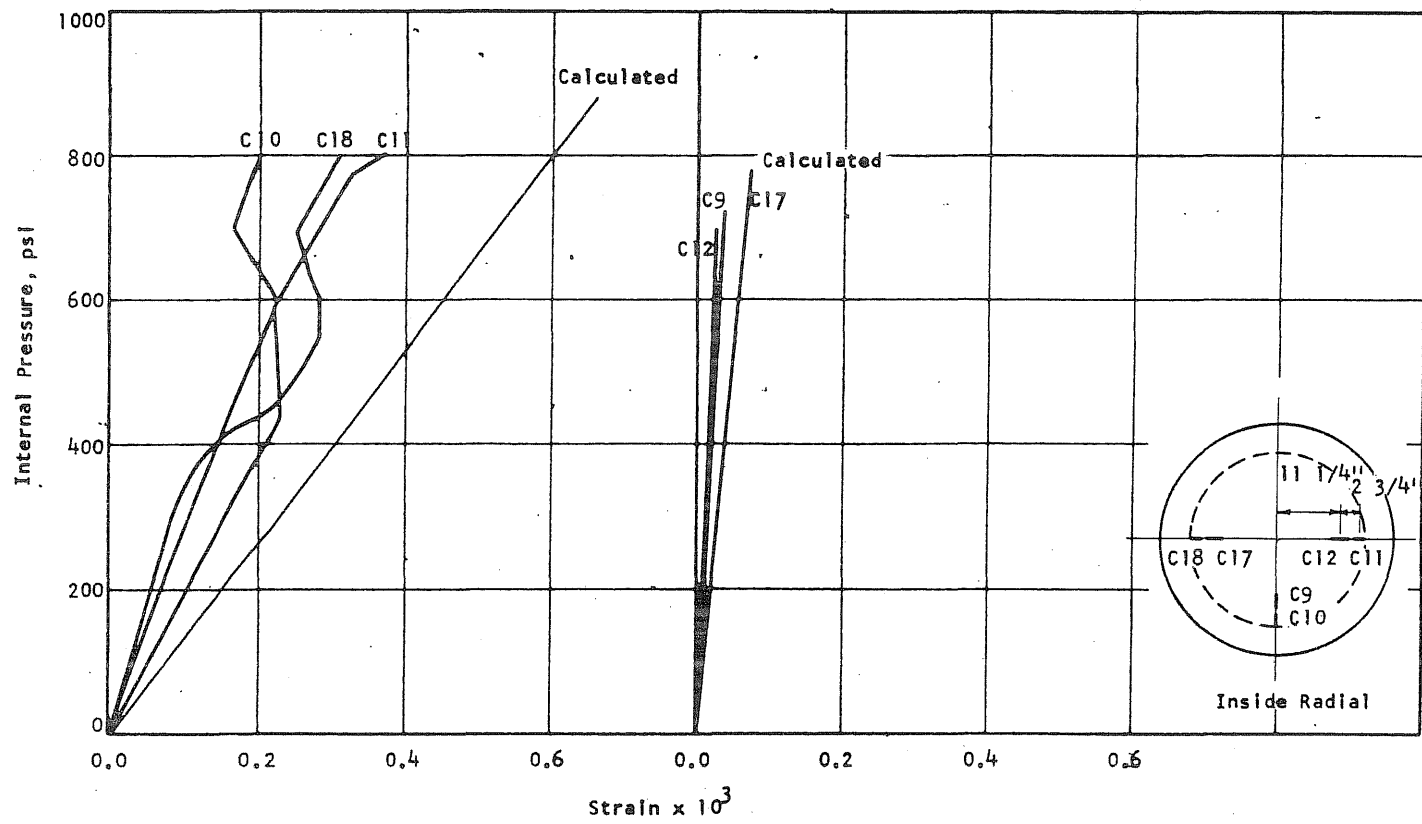


FIG. B7.11 CONCRETE STRAINS, VESSEL PV7

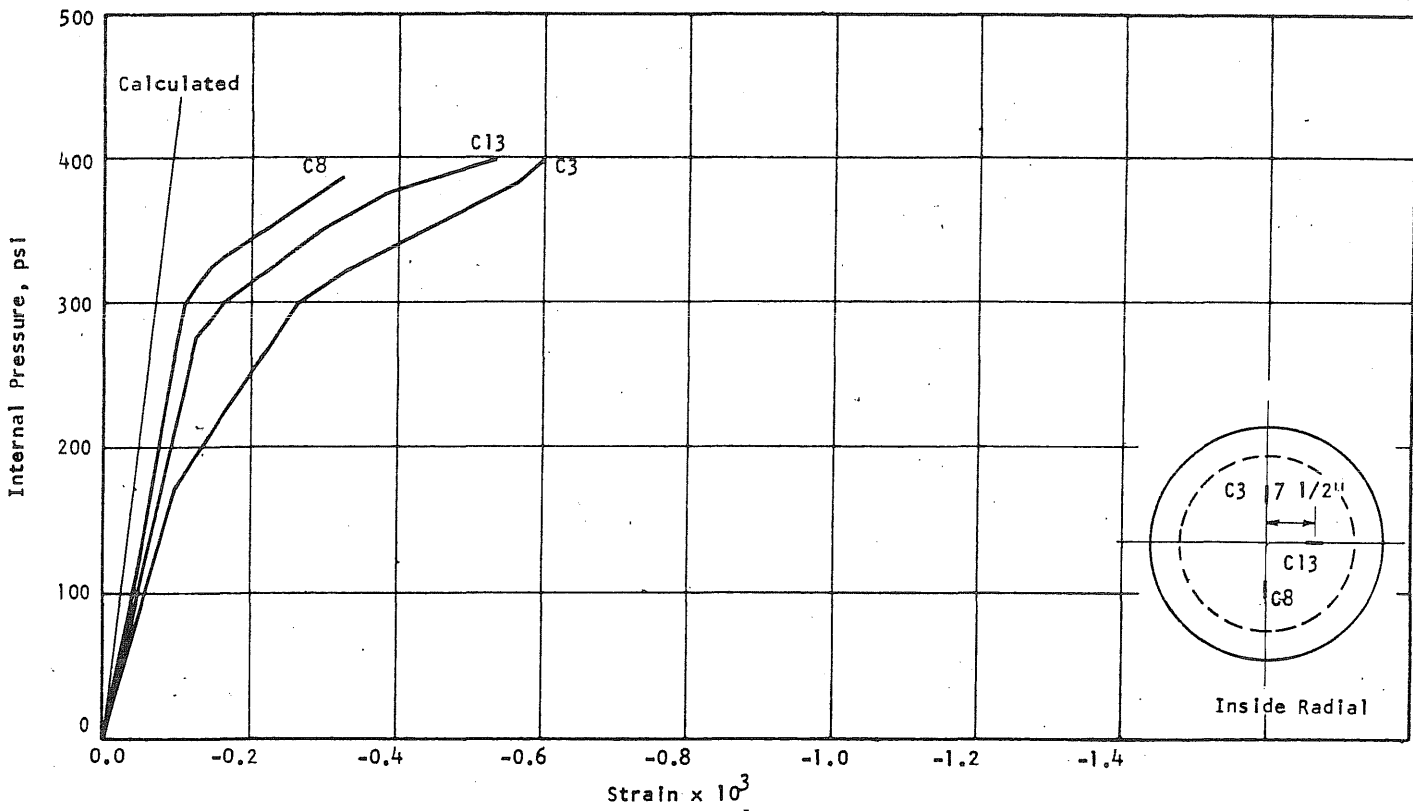


FIG. B7.11 (cont'd) CONCRETE STRAINS, VESSEL PV7

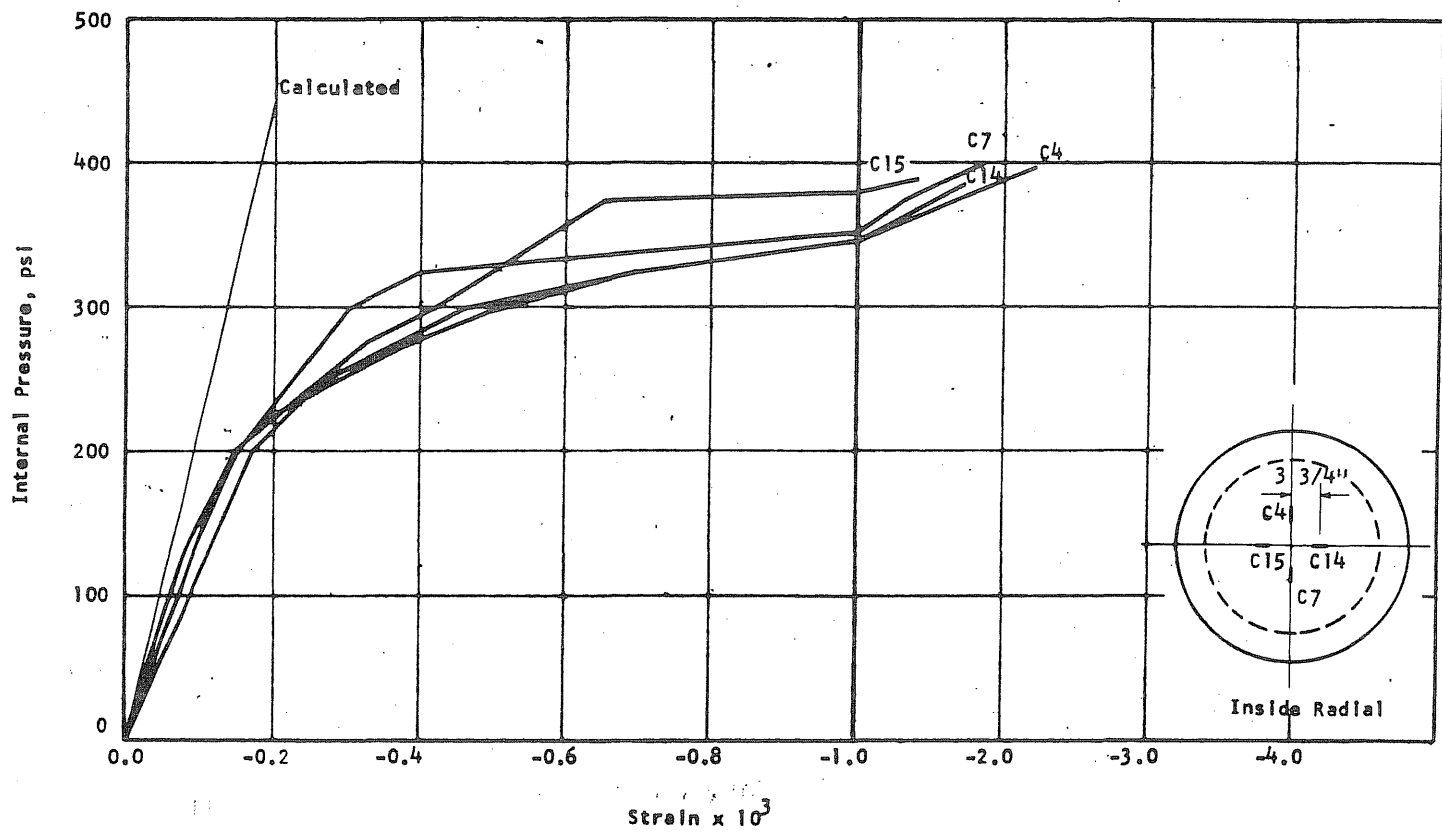


FIG. B7.11 (cont'd) CONCRETE STRAINS, VESSEL PV7

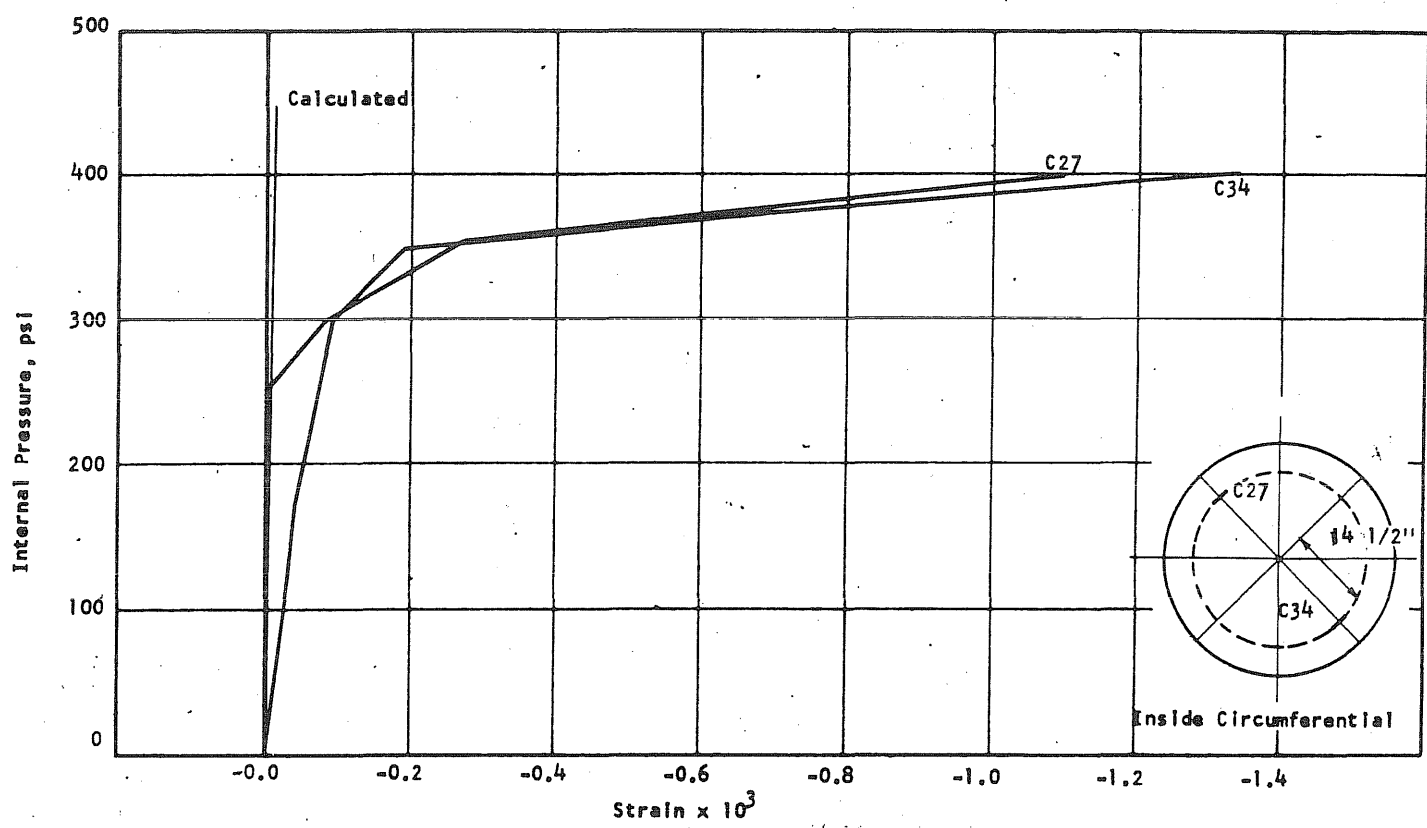


FIG. B7.12 CONCRETE STRAINS, VESSEL PV7

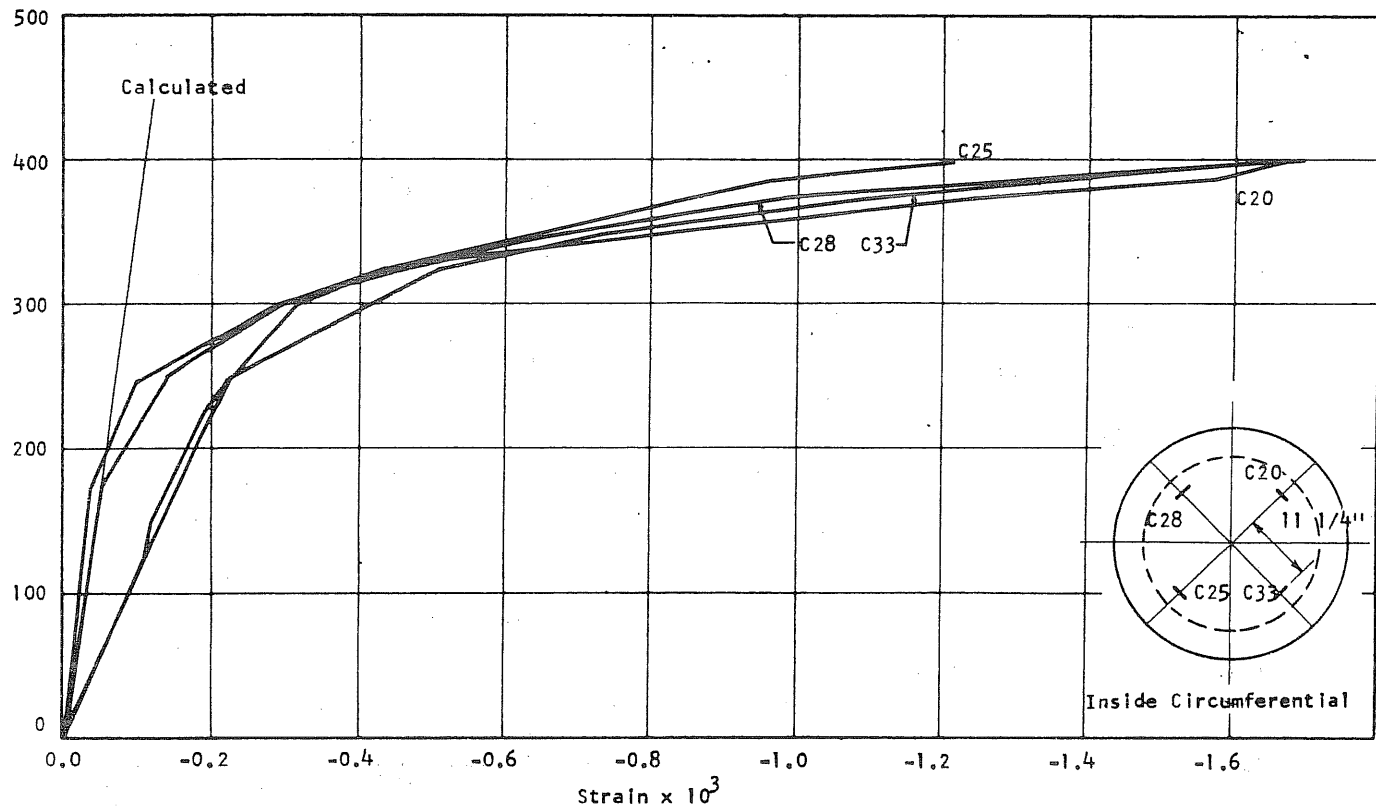


FIG. B7.12 (cont'd) CONCRETE STRAINS, VESSEL PV7

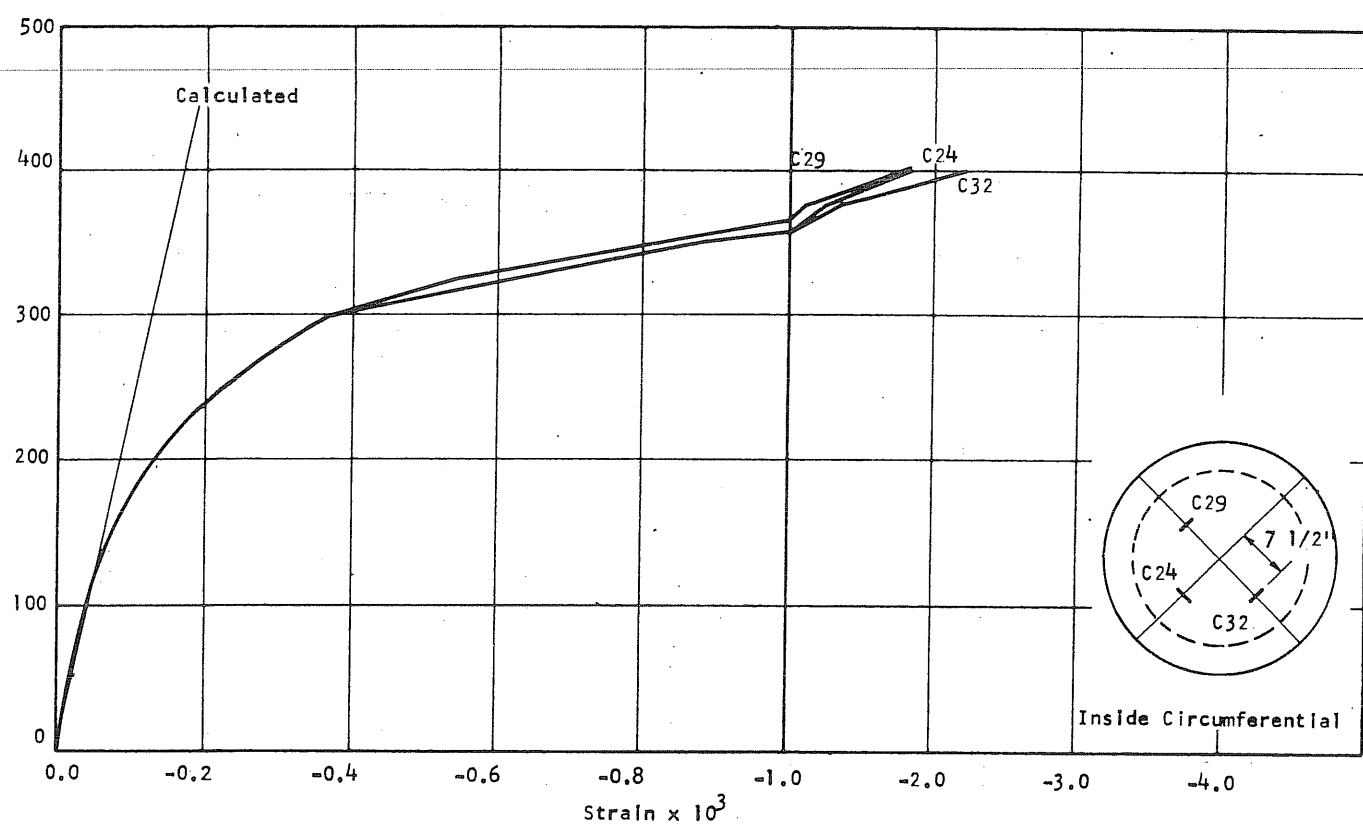


FIG. B7.12 (cont'd) CONCRETE STRAINS, VESSEL PV7

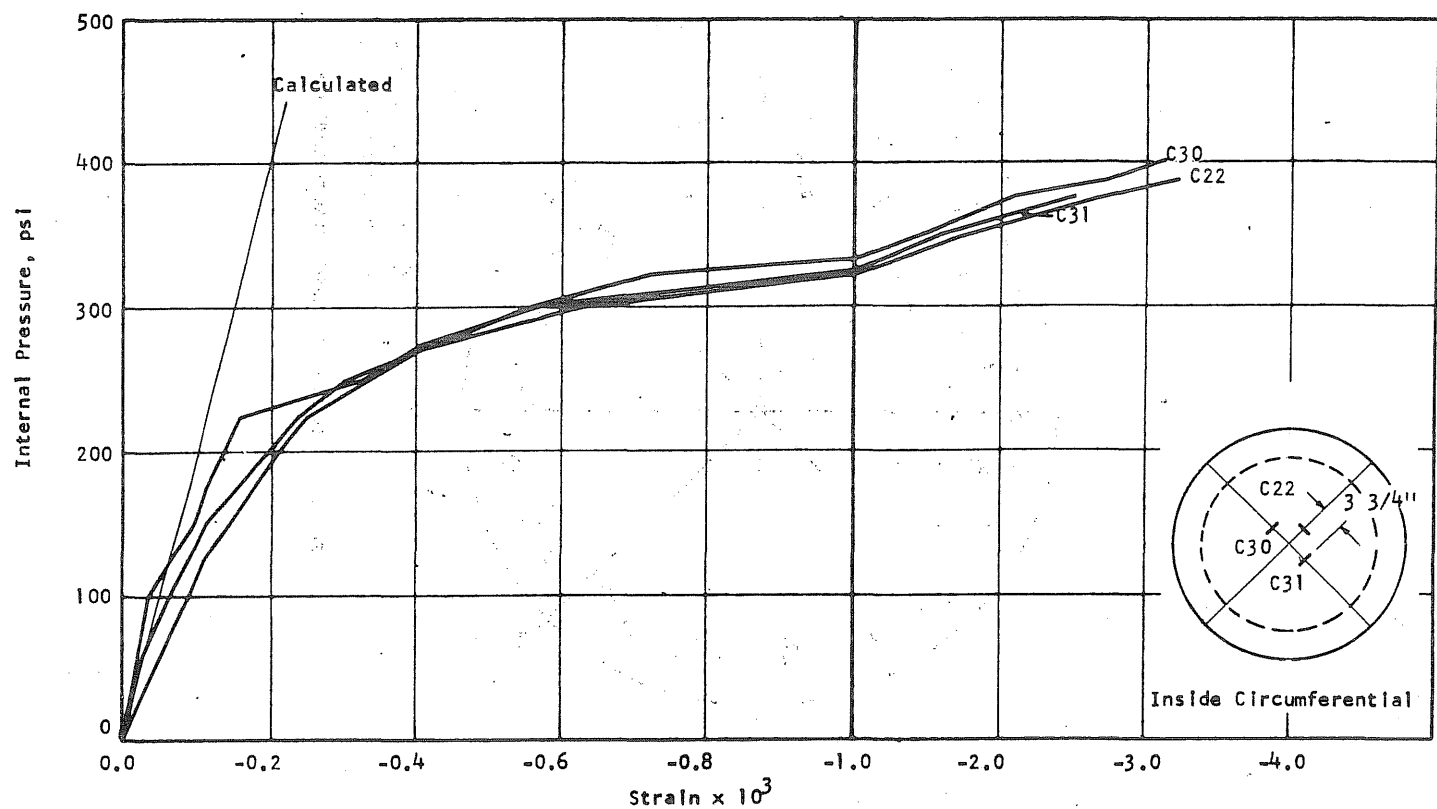


FIG. B7.12 (cont'd) CONCRETE STRAINS, VESSEL PV7

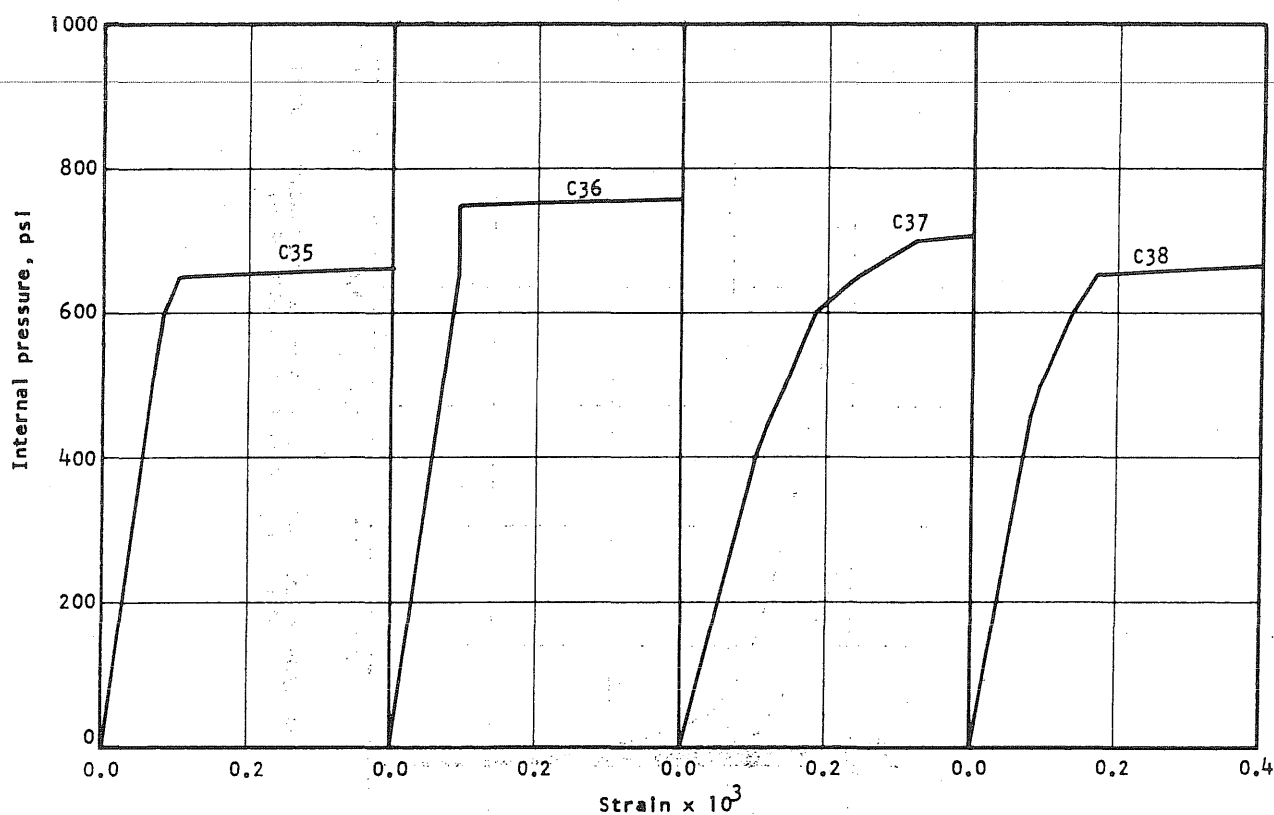


FIG. B7.13 APPLIED PRESSURE vs LONGITUDINAL STRAIN ON THE N-SIDE OF THE WALL OF PV7

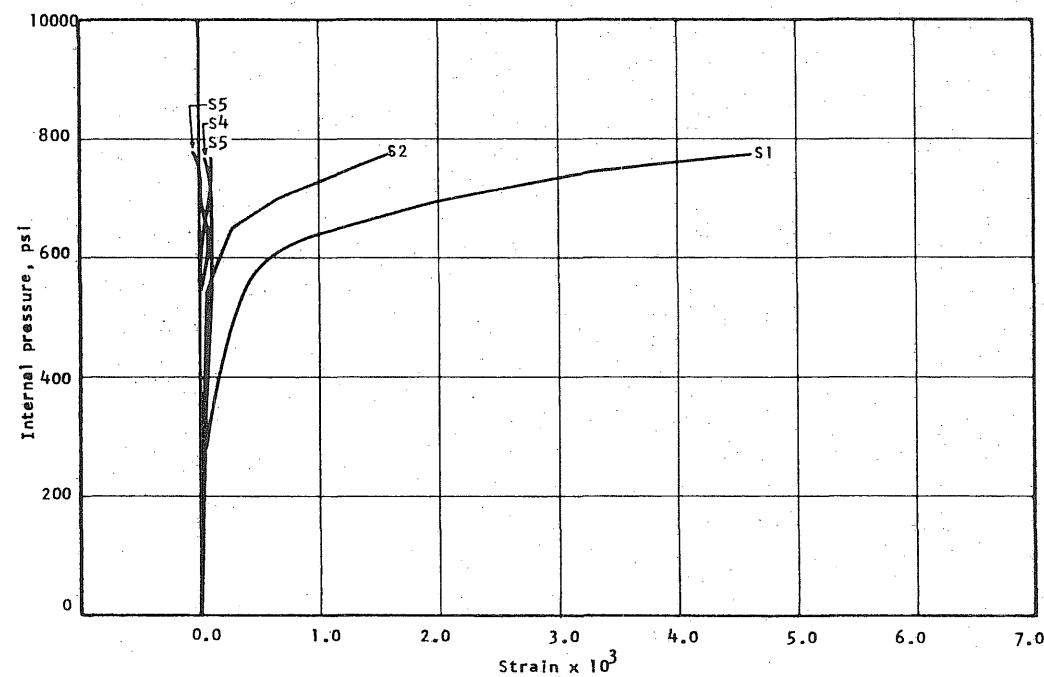


FIG. B7.14 APPLIED PRESSURE VS STRAIN IN THE CIRCUMFERENTIAL PRESTRESS WIRE AT THE N-END OF THE N-S DIAMETER OF PV7

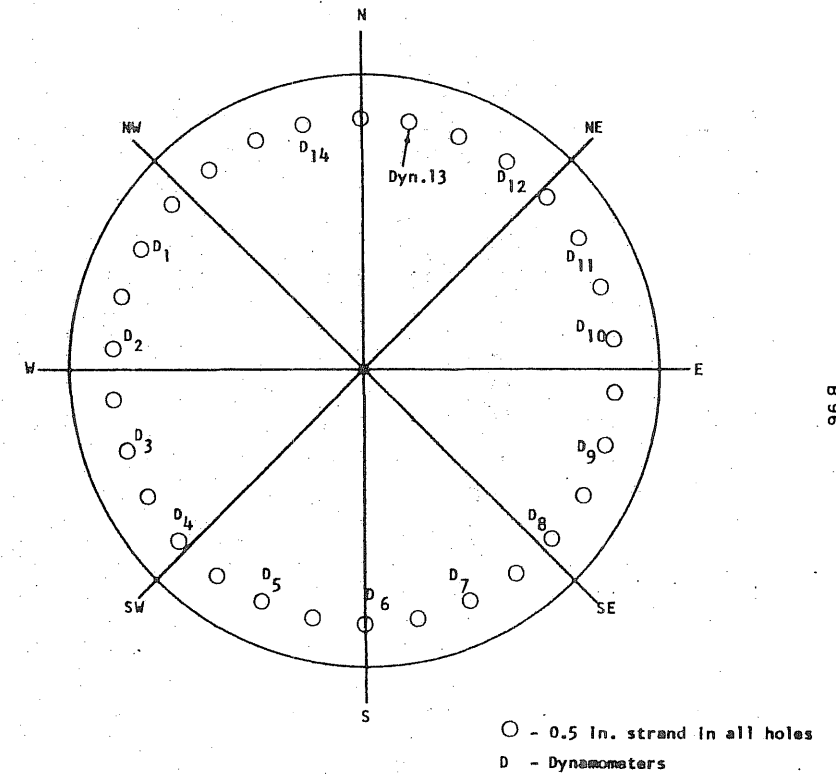


FIG. B7.15 LOCATION OF LONGITUDINAL REINFORCEMENT

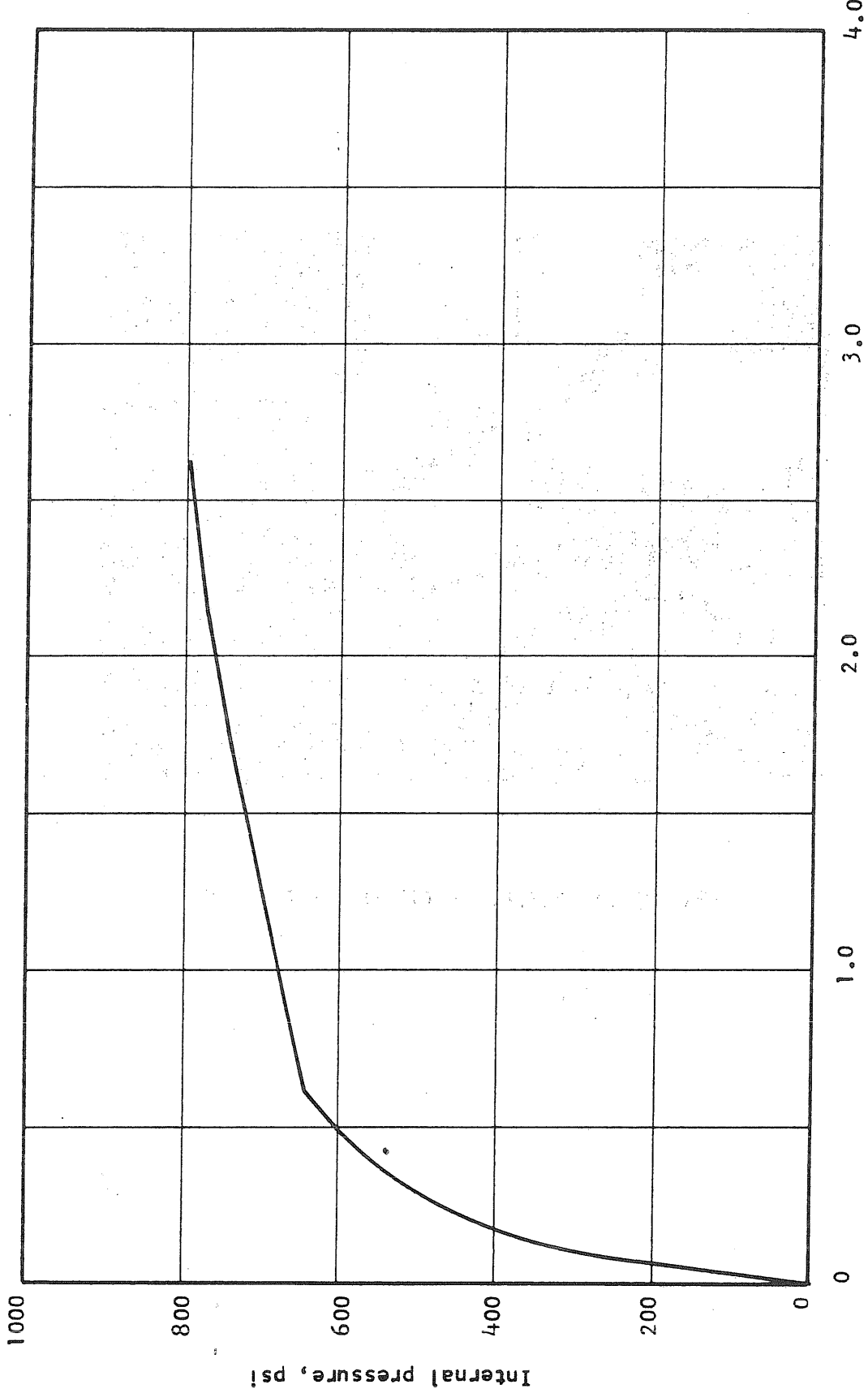


FIG. B7.16 APPLIED PRESSURE VS INCREASE IN LOAD IN DYNAMOMETER NO. 13 ON PV7

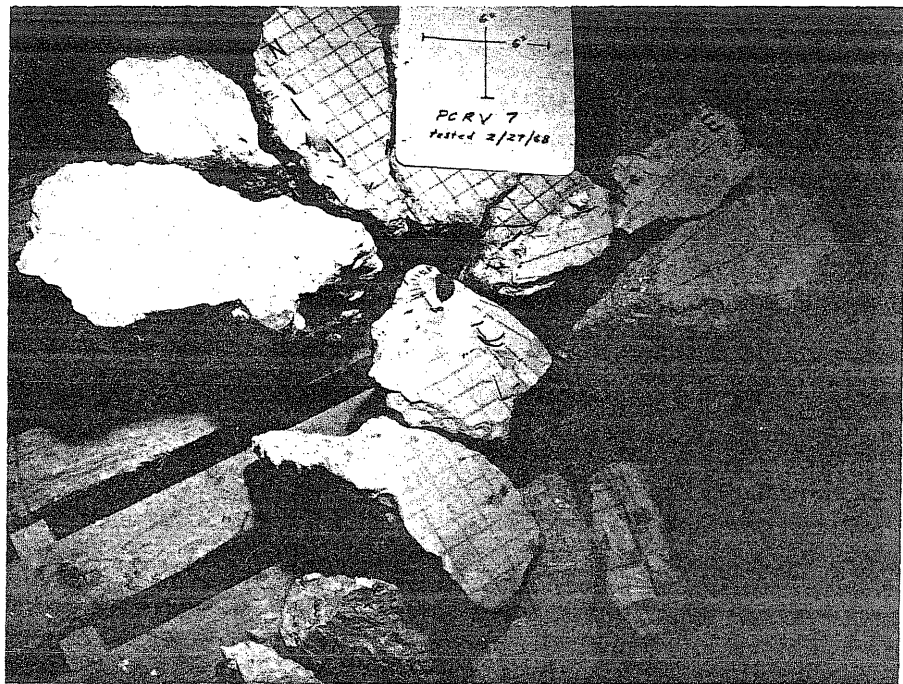


FIG. B7.17 PIECES OF THE END SLAB OF PV7

B8 Test Vessel PV8 ($t = 7 \frac{1}{2}$ in., $s = 1/3$ in.)

The same crack pattern observed in PV7 after circumferential prestressing was evident in PV8. In PV8 the band of circumferential hairline cracks on the outside of the vessel was from six to seven in. below the top of the vessel. The band of hairline cracks on the inside of the vessel was from ten to sixteen in. below the top of the end slab. Four longitudinal tendons with a load of 24 kips in each were placed on the vessel to arrest further cracks development.

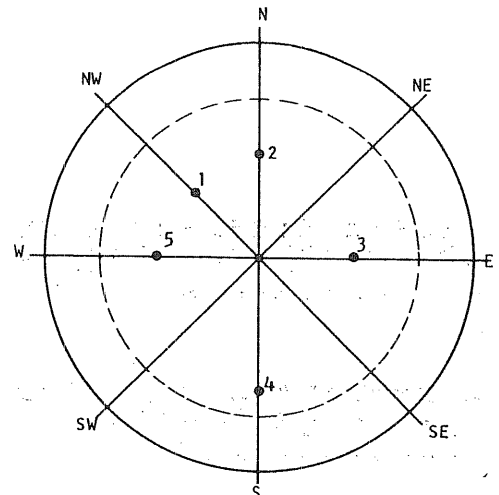
A detail of the liner used on the first attempt to test PV8 is shown in Fig. B8.2. No sheet metal was placed on the end slab. The liner was fabricated by fitting the sheets of neoprene over a form of the same dimensions as the inside of the vessel. The joints at the end slab and the side wall was made by lapping the sheets of neoprene and applying rubber cement to contact surfaces. The neoprene liner was placed in the vessel as a unit and attached to the aluminum and hydrocal with rubber cement. A one-half-in. wide strip of rubber tape was placed around the periphery of the vessel at the joint between the one-in. ring and the neoprene liner. The longitudinal prestressing force was provided by thirty strands. A load cell was placed on each strand.

The first attempt at testing PV8 was not successful. Pressure was increased in 100 psi increments to a pressure of 200 psi and in 50 psi increments until a leak prevented further increase in pressure at 625 psi. Deflection and strain readings suggest that the vessel was close to failure when the test was stopped. The deflection at the center of the end slab

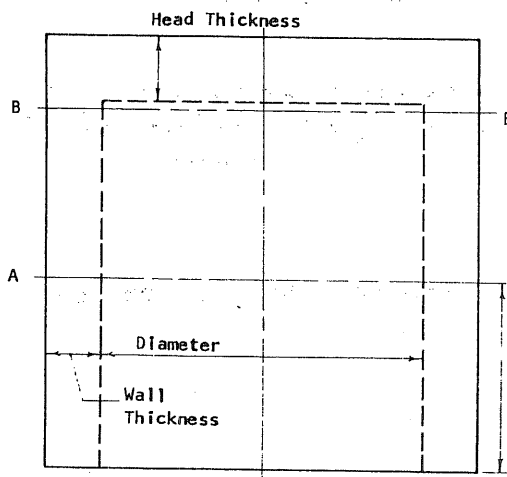
reached 0.79 in., and the strains in the prestressing wire were of a magnitude that the top three layers were loose when the vessel was depressurized.

The method of sealing PV8 for the second attempt is shown in Fig. B8.3. The neoprene on the walls was omitted and the O-ring method of sealing the joint at the end slab was employed. Thirty strands were used for longitudinal prestressing.

One hundred psi load increments were applied until the internal pressure reached 400 psi. The pressure was then increased to 450 psi in 25 psi increments. Readings were taken again at 500 psi. Loading was increased continuously until the vessel failed at 640 psi. A photograph of the pieces of the end slab is shown in Fig. B8.20.



| Head Thickness | |
|----------------|-------------------|
| Point No. | Inches |
| 1 | 7 $\frac{11}{16}$ |
| 2 | 7 $\frac{12}{16}$ |
| 3 | 7 $\frac{10}{16}$ |
| 4 | 7 $\frac{8}{16}$ |
| 5 | 7 $\frac{9}{16}$ |
| | |



| Wall Thickness, in. | | |
|---------------------|--------------------|--------------------|
| Plane Axis | AA | BB |
| N-S | 30 $\frac{2}{32}$ | 29 $\frac{31}{32}$ |
| NE-SW | 29 $\frac{30}{32}$ | 29 $\frac{31}{32}$ |
| E-W | 29 $\frac{30}{32}$ | 30 $\frac{0}{32}$ |
| SE-NW | 30 $\frac{0}{32}$ | 29 $\frac{30}{32}$ |

| Inside Diameter, in. | | |
|----------------------|--------------------|--------------------|
| Plane Axis | AA | BB |
| N-S | 30 $\frac{2}{32}$ | 29 $\frac{31}{32}$ |
| NE-SW | 29 $\frac{30}{32}$ | 29 $\frac{31}{32}$ |
| E-W | 29 $\frac{30}{32}$ | 30 $\frac{0}{32}$ |
| SE-NW | 30 $\frac{0}{32}$ | 29 $\frac{30}{32}$ |

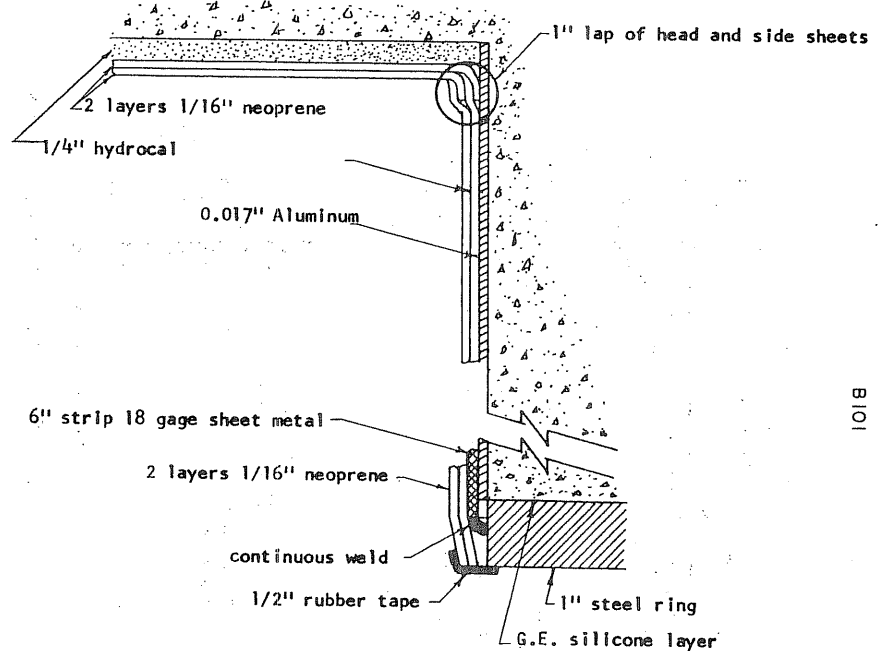


FIG. B8.2 SEALING DETAIL FOR PV8

FIG. B8.1 DIMENSIONS OF PV8

B102

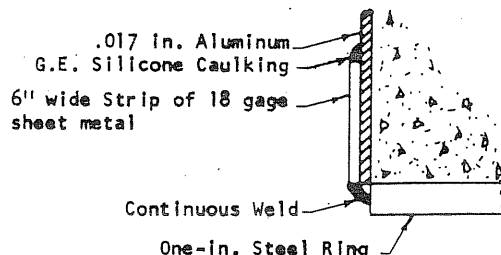
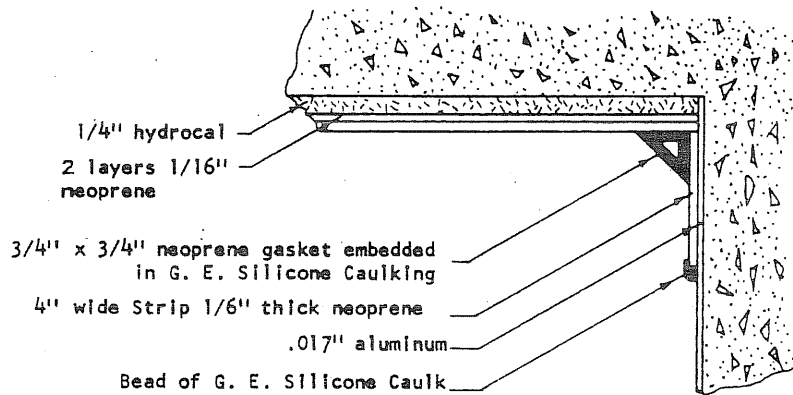
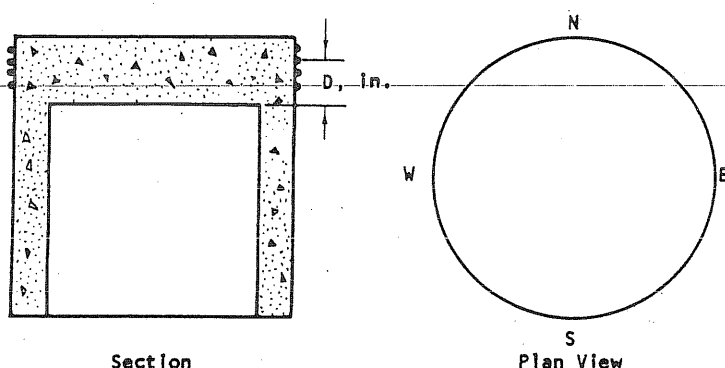


FIG. B8.3 SEALING DETAIL FOR PV8



| Wrap No. | D _N | D _E | D _S | D _W |
|----------|----------------|----------------|----------------|----------------|
| 1 | 6 12/16 | 6 5/16 | 6 8/16 | 6 8/16 |
| 2 | 6 3/16 | 5 15/16 | 5 15/16 | 6 0/16 |
| 3 | 5 14/16 | 5 8/16 | 5 8/16 | 5 9/16 |
| 4 | 5 2/16 | 5 3/16 | 5 3/16 | 5 5/16 |
| 5 | 5 4/16 | 4 15/16 | 4 15/16 | 5 1/16 |
| 6 | 4 15/16 | 4 10/16 | 4 10/16 | 4 12/16 |
| 7 | 4 10/16 | 4 5/16 | 4 5/16 | 4 7/16 |
| 8 | 4 5/16 | 3 15/16 | 3 15/16 | 4 1/16 |
| 9 | 3 14/16 | 3 8/16 | 3 9/16 | 3 10/16 |
| 10 | 3 8/16 | 3 3/16 | 3 4/16 | 3 5/16 |
| 11 | 3 3/16 | 2 15/16 | 2 14/16 | 3 0/16 |
| 12 | 2 12/16 | 2 8/16 | 2 8/16 | 2 9/16 |
| 13 | 2 7/16 | 2 2/16 | 2 2/16 | 2 4/16 |
| 14 | 2 2/16 | 1 13/16 | 1 14/16 | 1 15/16 |
| 15 | 1 13/16 | 1 8/16 | 1 8/16 | 1 9/16 |
| 16 | 1 7/16 | 1 2/16 | 1 3/16 | 1 4/16 |
| 17 | 1 2/16 | 14/16 | 14/16 | 15/16 |
| 18 | 14/16 | 2/16 | 9/16 | 10/16 |
| 19 | 8/16 | 3/16 | 2/16 | 4/16 |
| 20 | 3/16 | -3/16 | -2/16 | -1/16 |

FIG. B8.4 MEASURED LOCATION OF THE CIRCUMFERENTIAL PRESTRESS WIRE AT THE ENDS OF THE N-S AND E-W DIAMETERS ON PV8

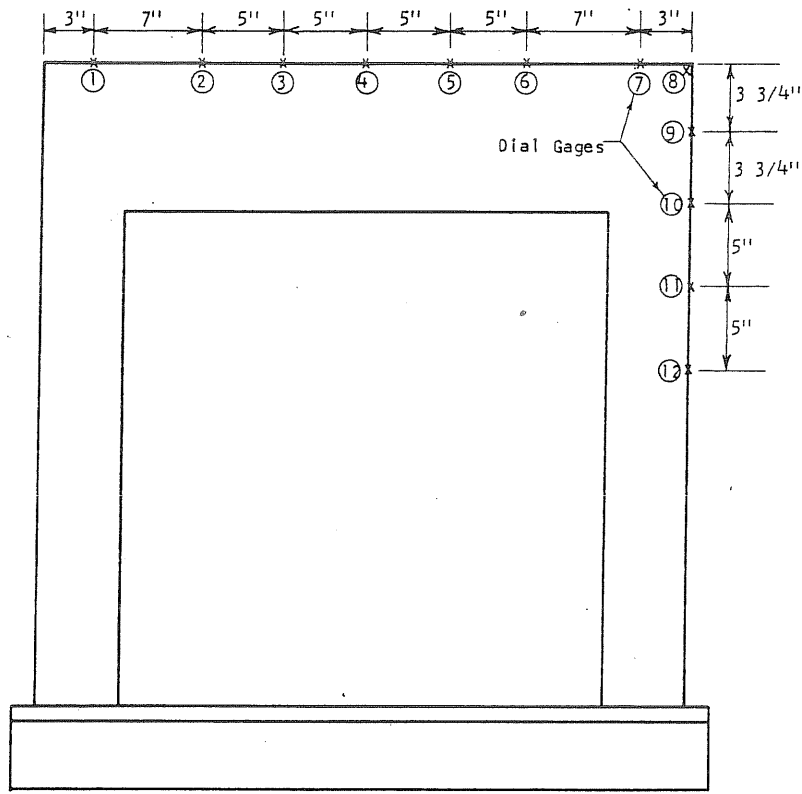


FIG. B8.5 LOCATION OF DEFLECTION GAGES ON PV8

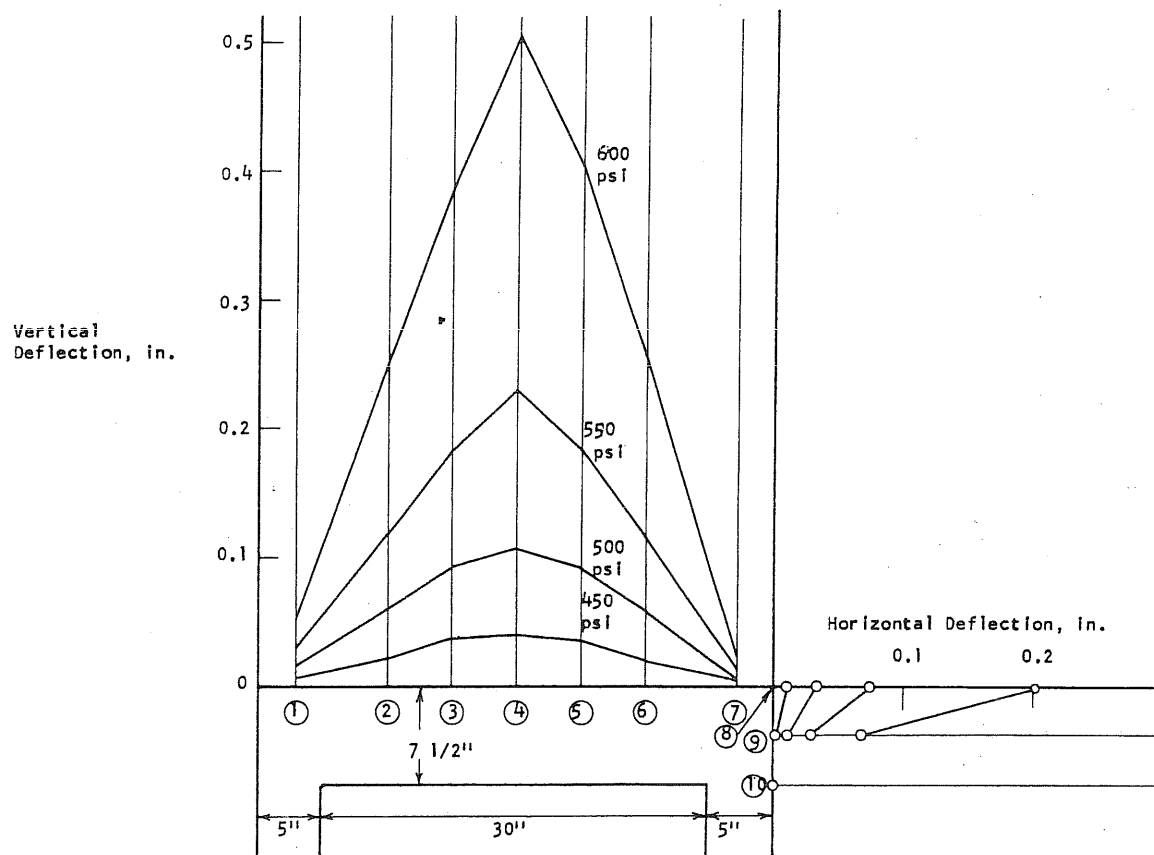


FIG. B8.6 DEFLECTION PROFILES OF THE END SLAB ALONG THE N-S DIAMETER OF PV8

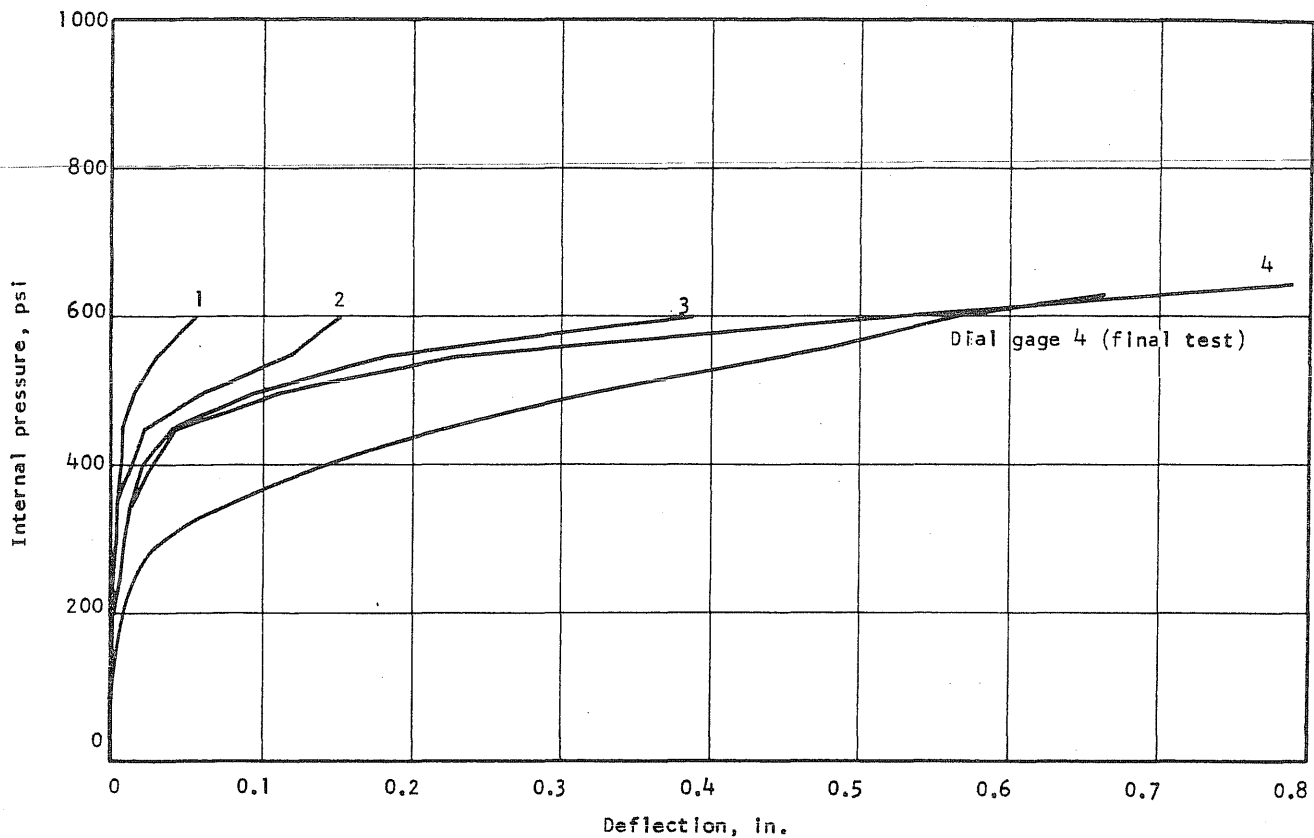


FIG. B8.7 APPLIED PRESSURE VS DEFLECTION ALONG THE N-HALF OF THE N-S DIAMETER OF PV8

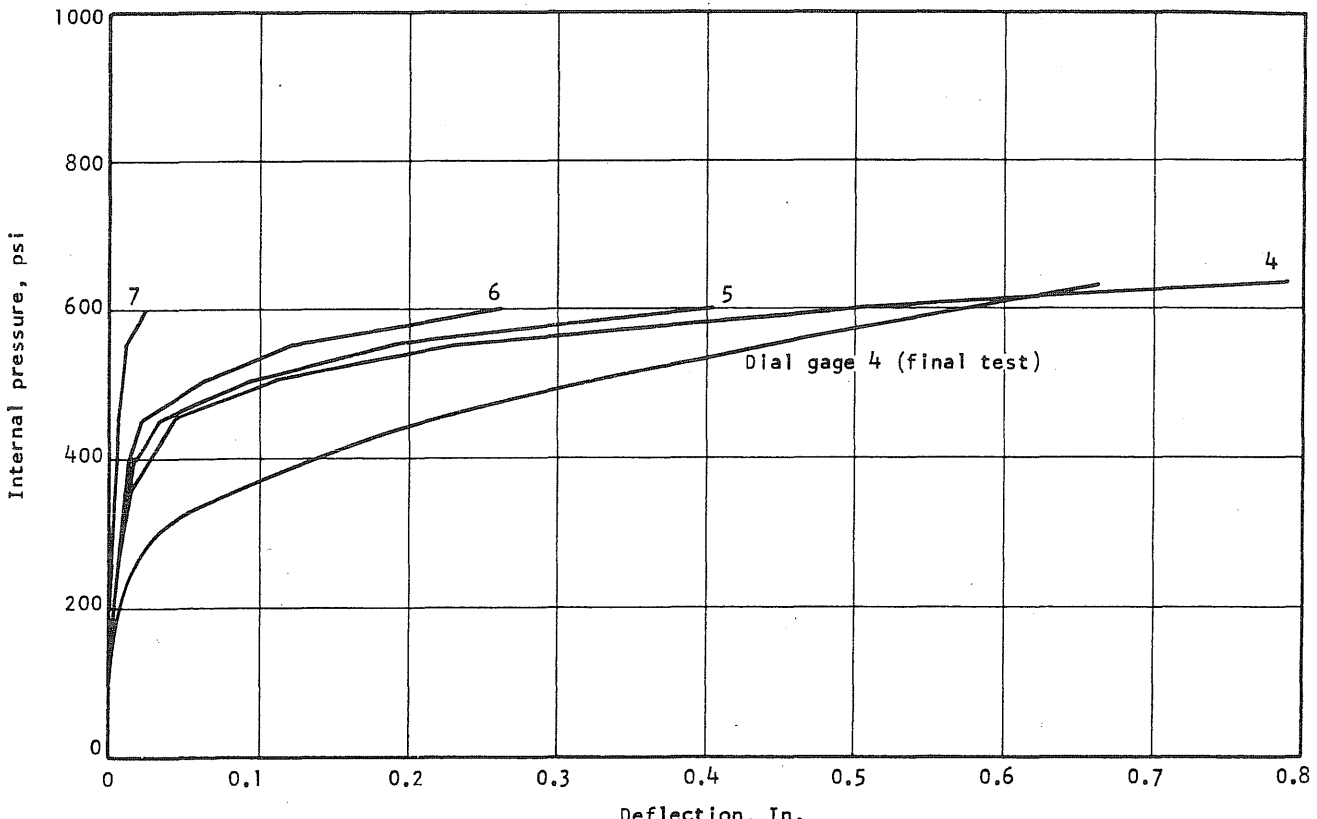


FIG. B8.8 APPLIED PRESSURE VS DEFLECTION ALONG THE S-HALF OF THE N-S DIAMETER OF PV8

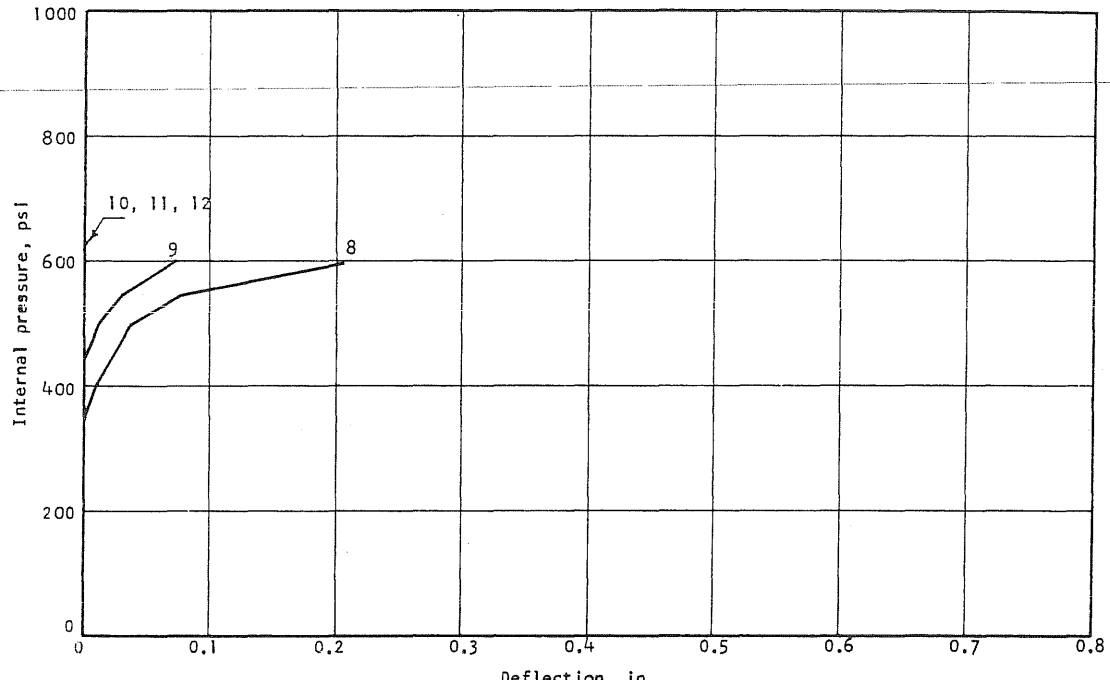


FIG. B8.9 APPLIED PRESSURE vs DEFLECTION OF THE SIDE WALL OF PV8

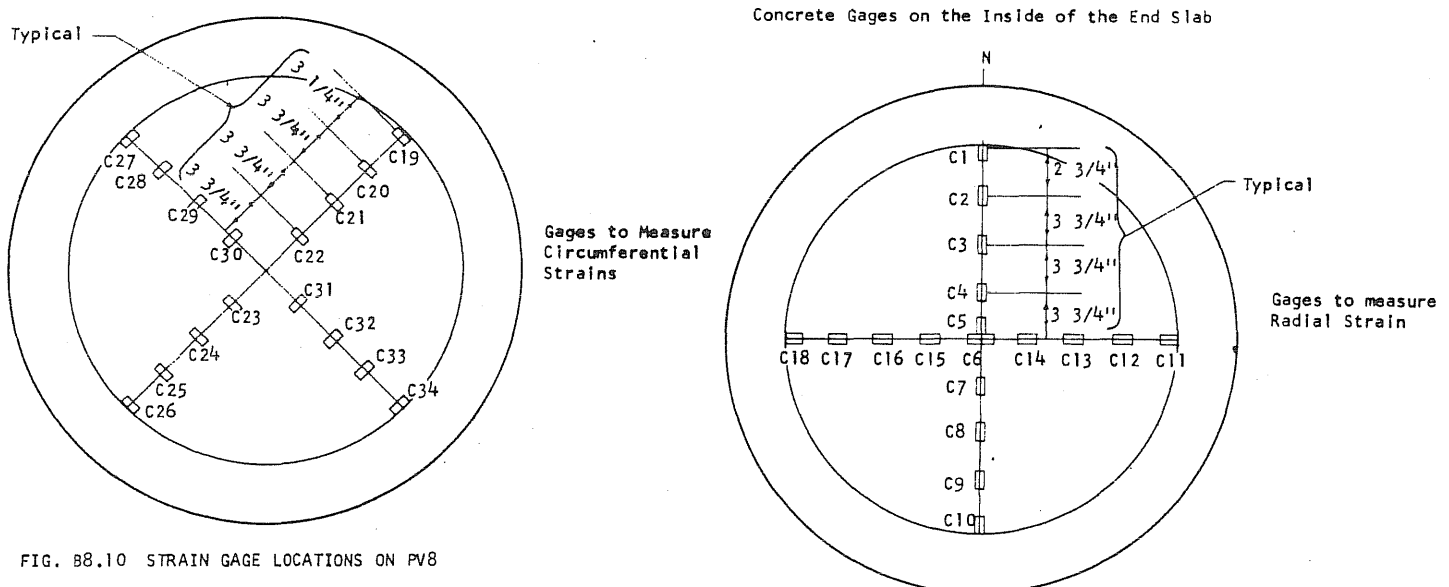
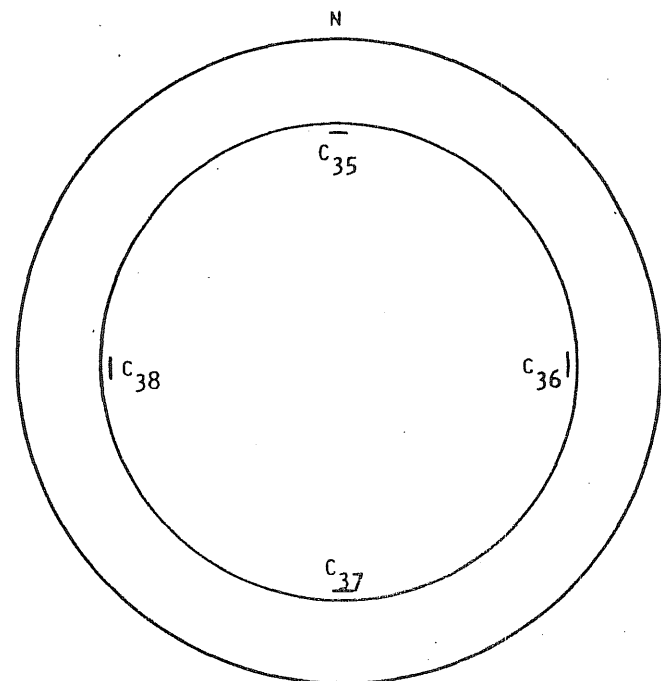
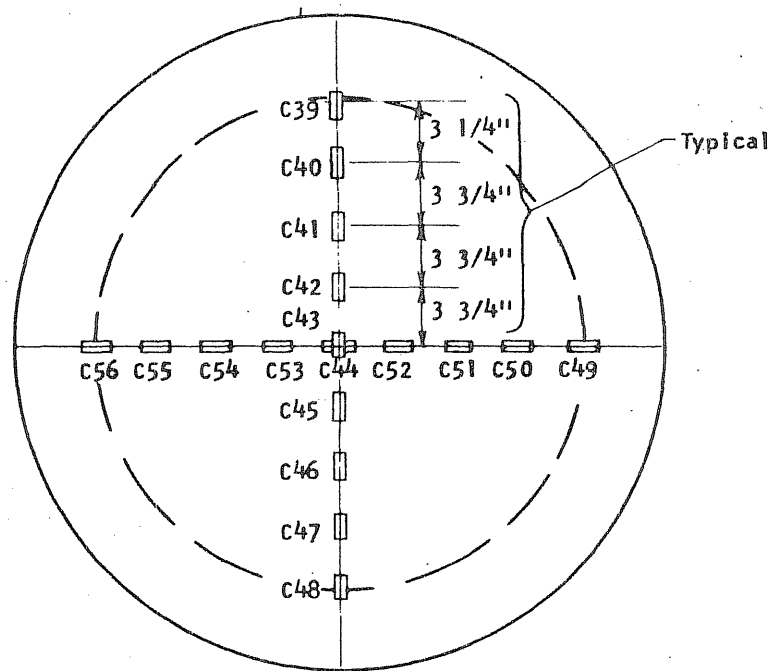


FIG. B8.10 STRAIN GAGE LOCATIONS ON PV8

Concrete Gages on The Inside Walls



Concrete Gages on the Outside of the End Slab



B105

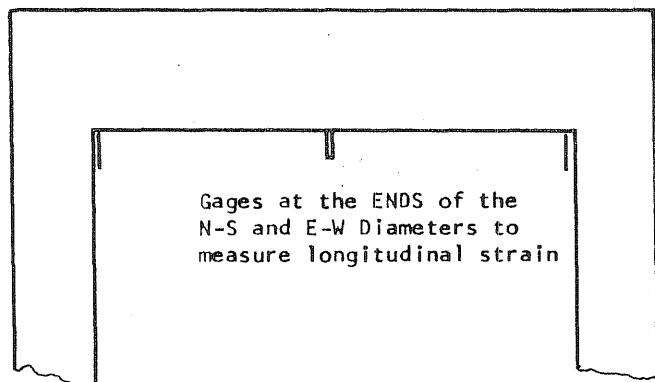


FIG. B8.10 (cont.) STRAIN GAGE LOCATIONS ON PV8

Steel Gages on Circumferential Prestress Wire

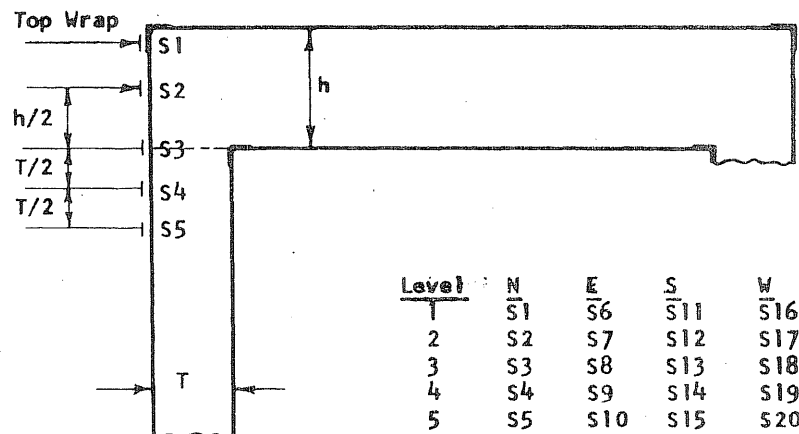


FIG. B8.10 (cont'd) STRAIN GAGE LOCATIONS ON PV8

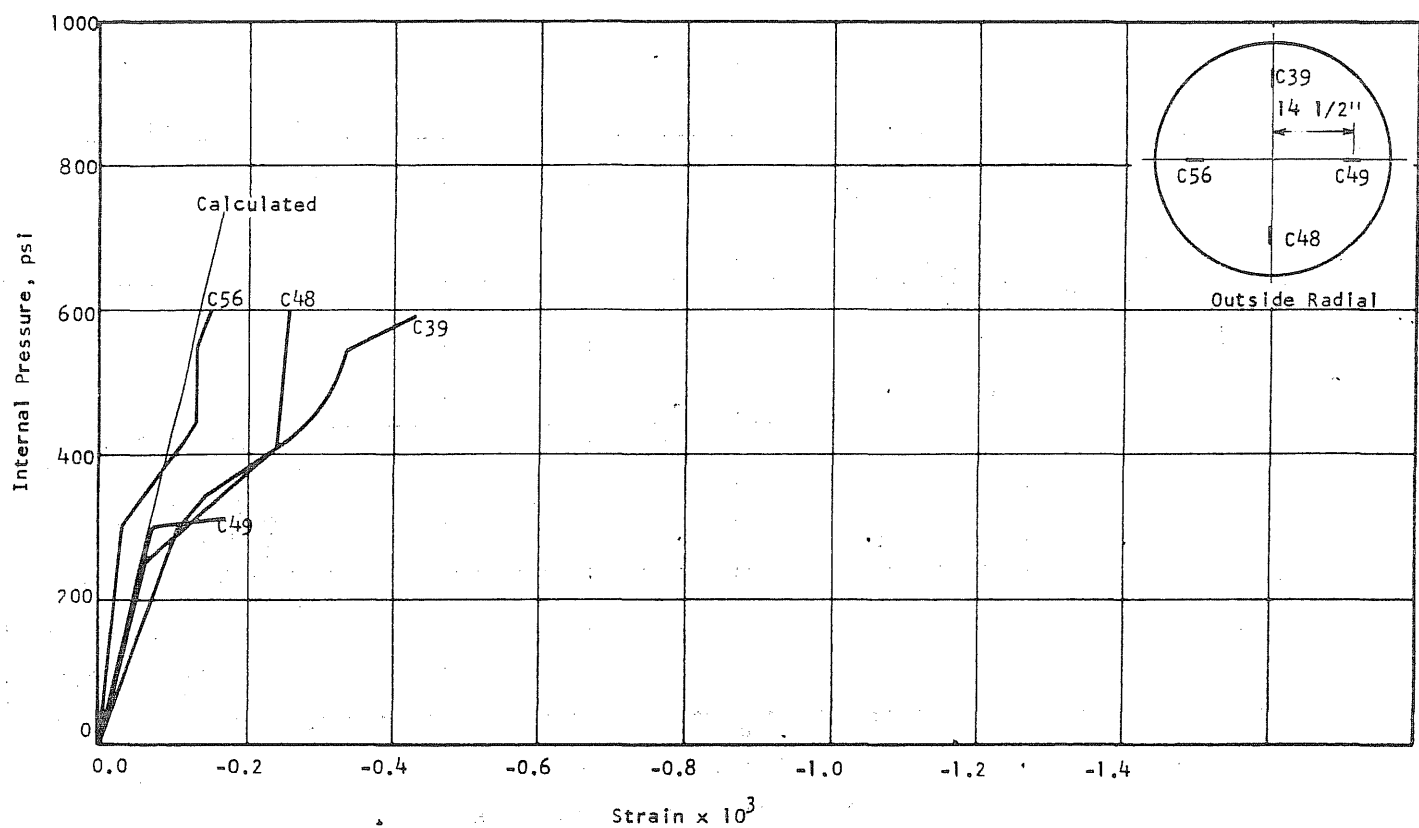


FIG. B8.11 CONCRETE STRAINS, VESSEL PV8

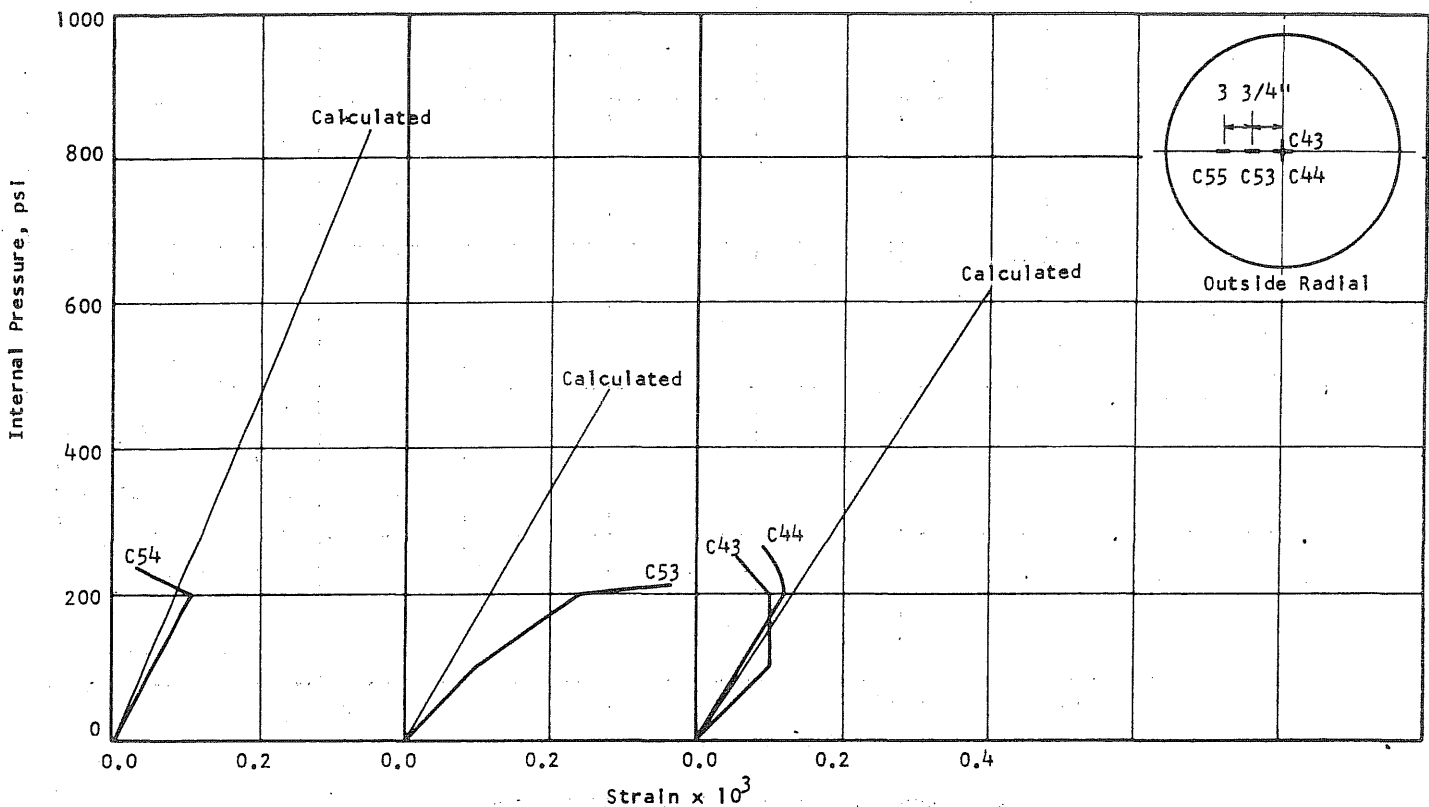


FIG. B8.11 (cont'd) CONCRETE STRAINS, VESSEL PV8

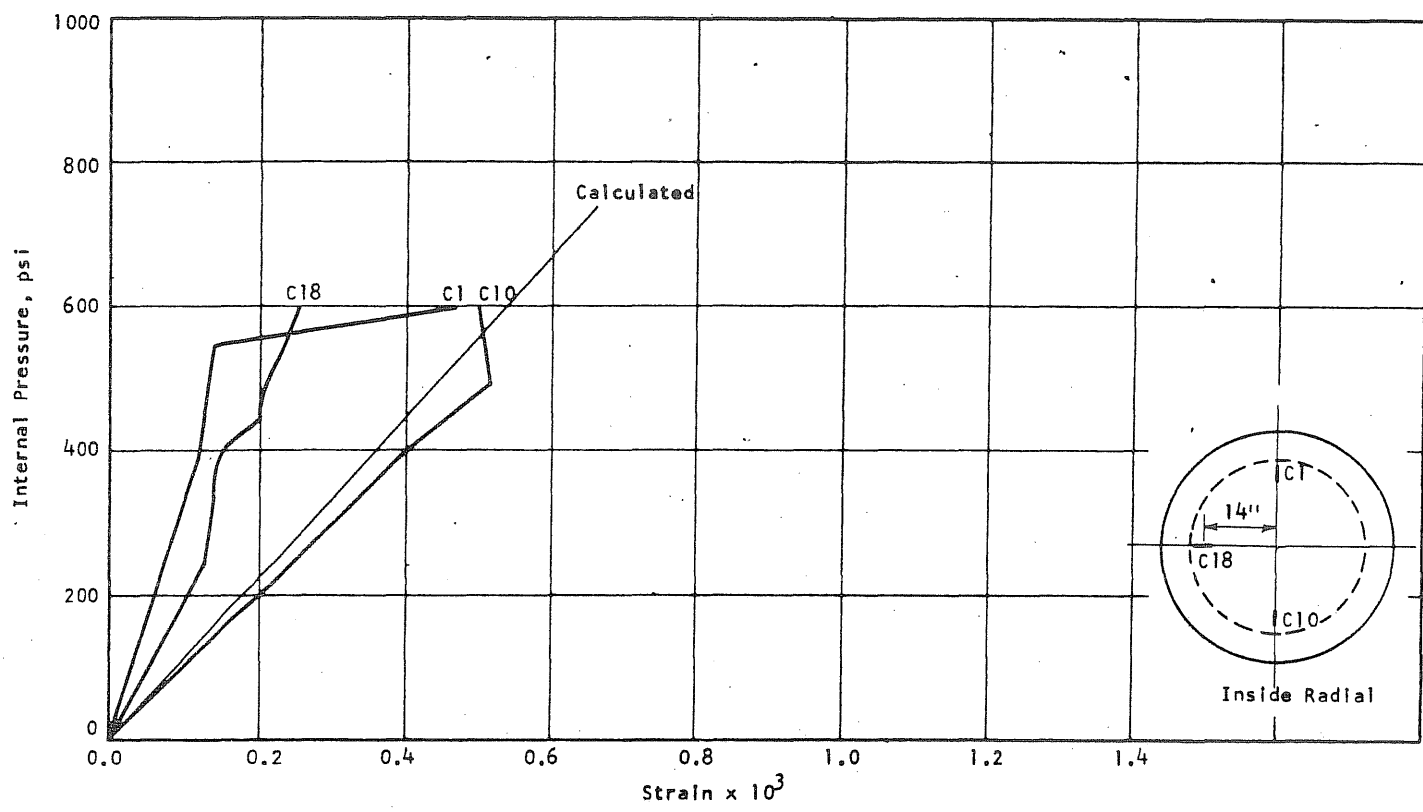


FIG. B8.12 CONCRETE STRAINS, VESSEL PV8

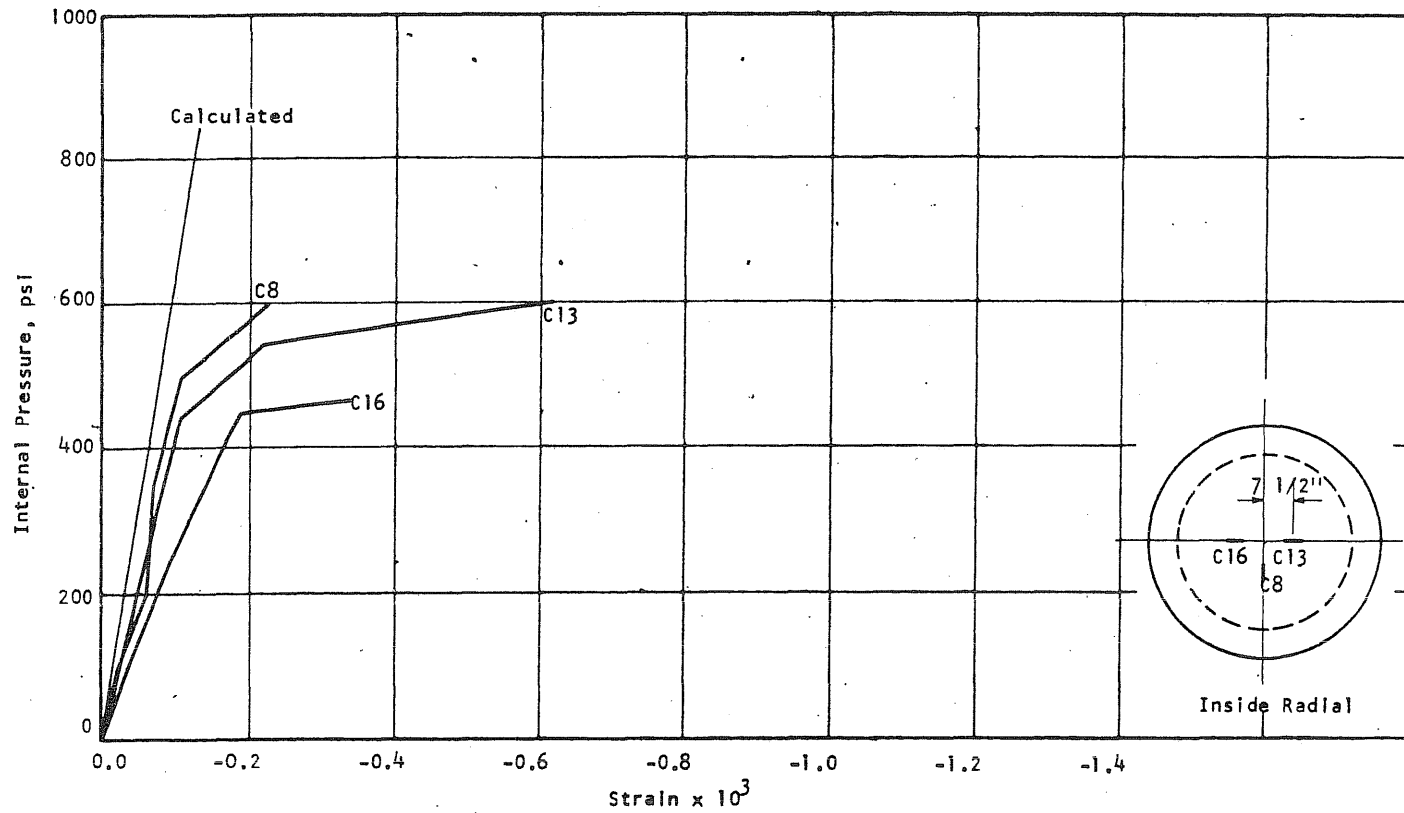


FIG. B8.12 (cont'd) CONCRETE STRAINS, VESSEL PV8

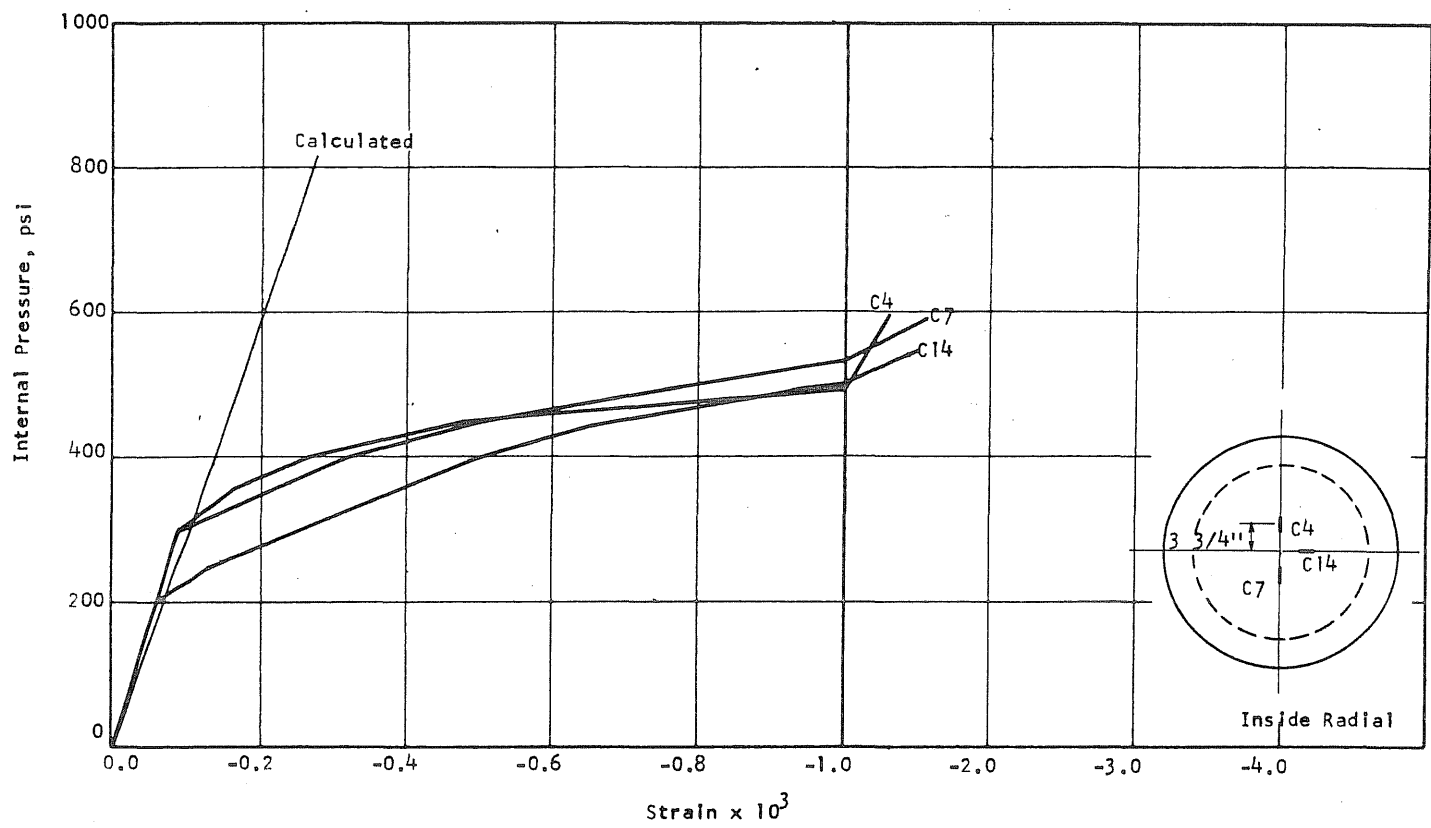


FIG. B8.12 (cont'd) CONCRETE STRAINS, VESSEL PV8

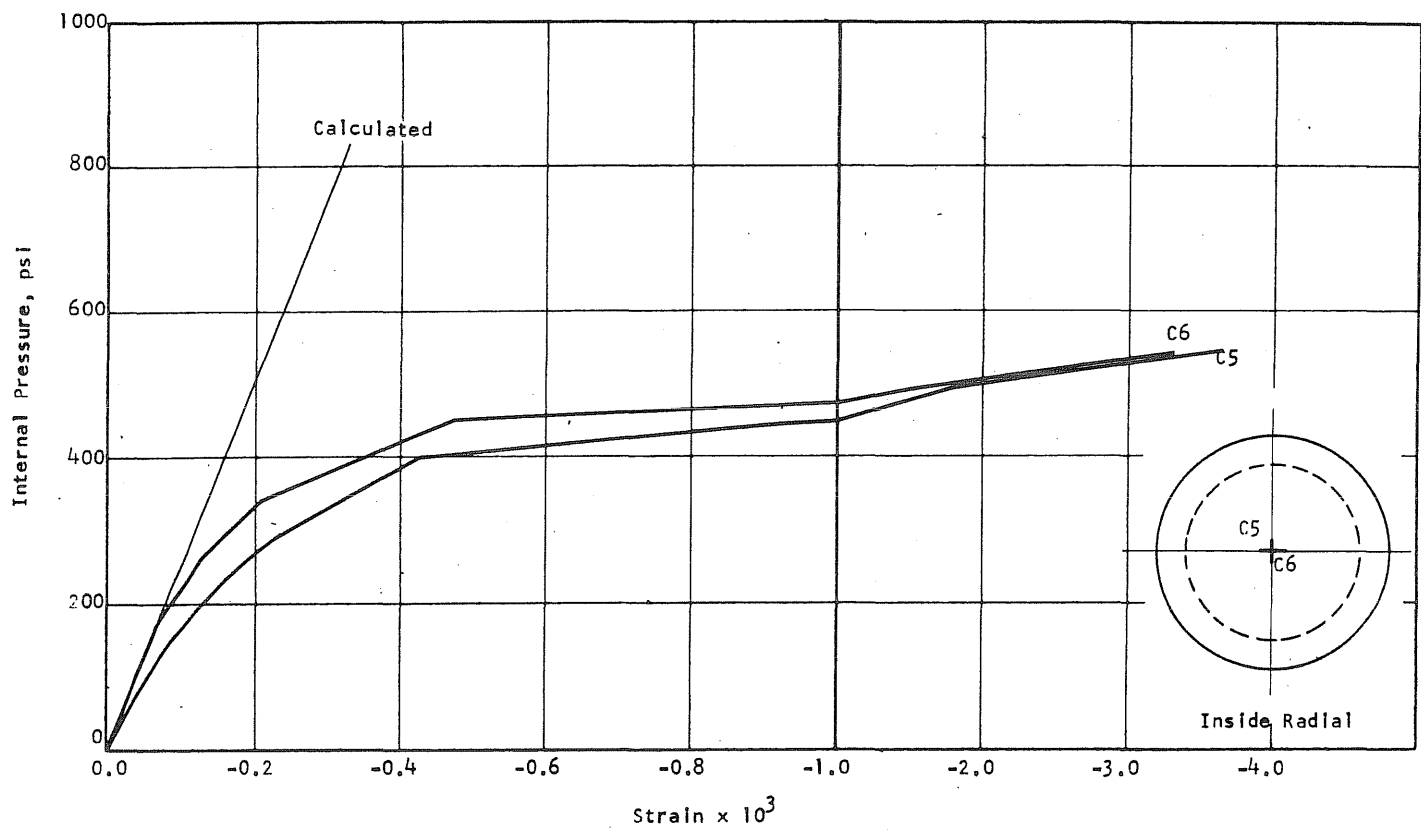


FIG. B8.12 (cont'd) CONCRETE STRAINS, VESSEL PV8

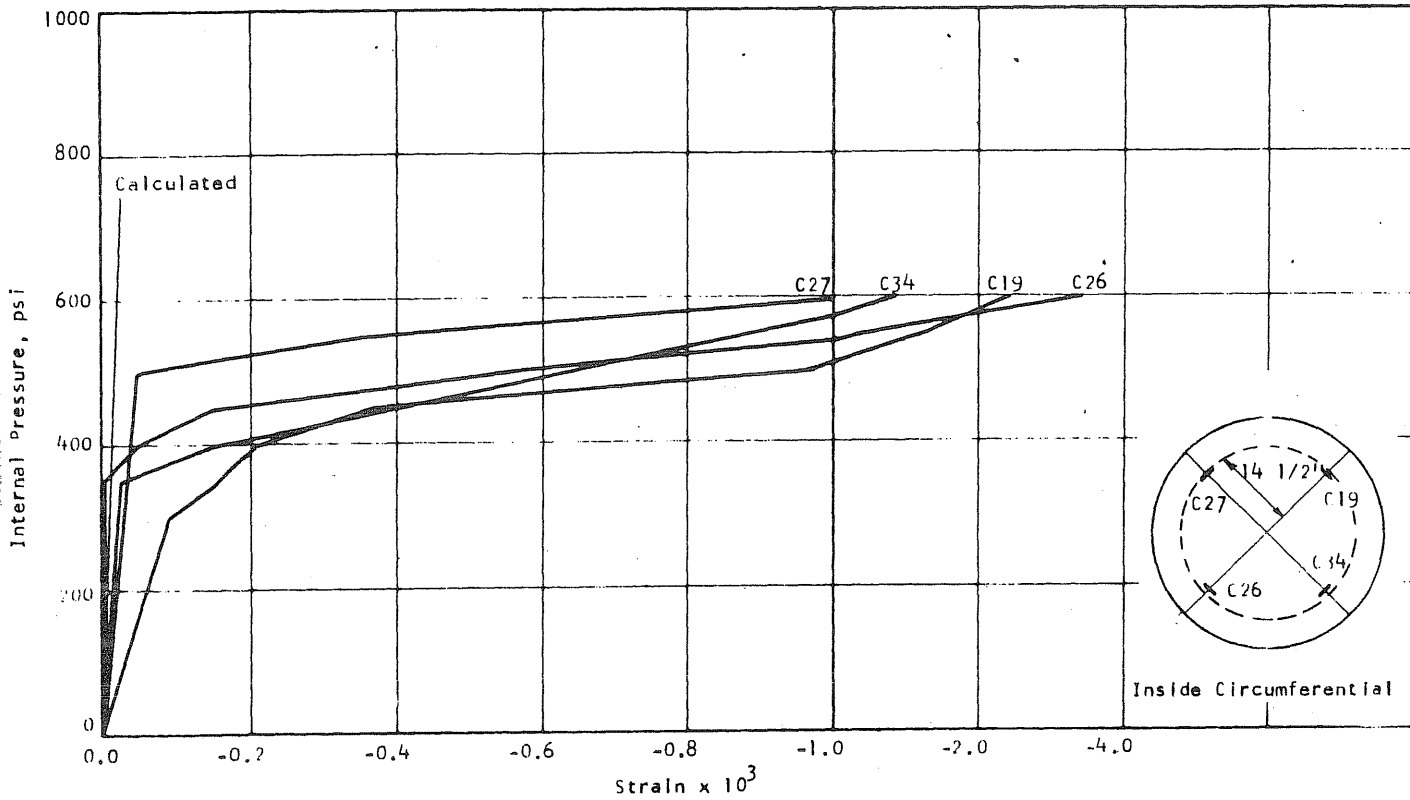


FIG. B8.13 CONCRETE STRAINS, VESSEL PV8

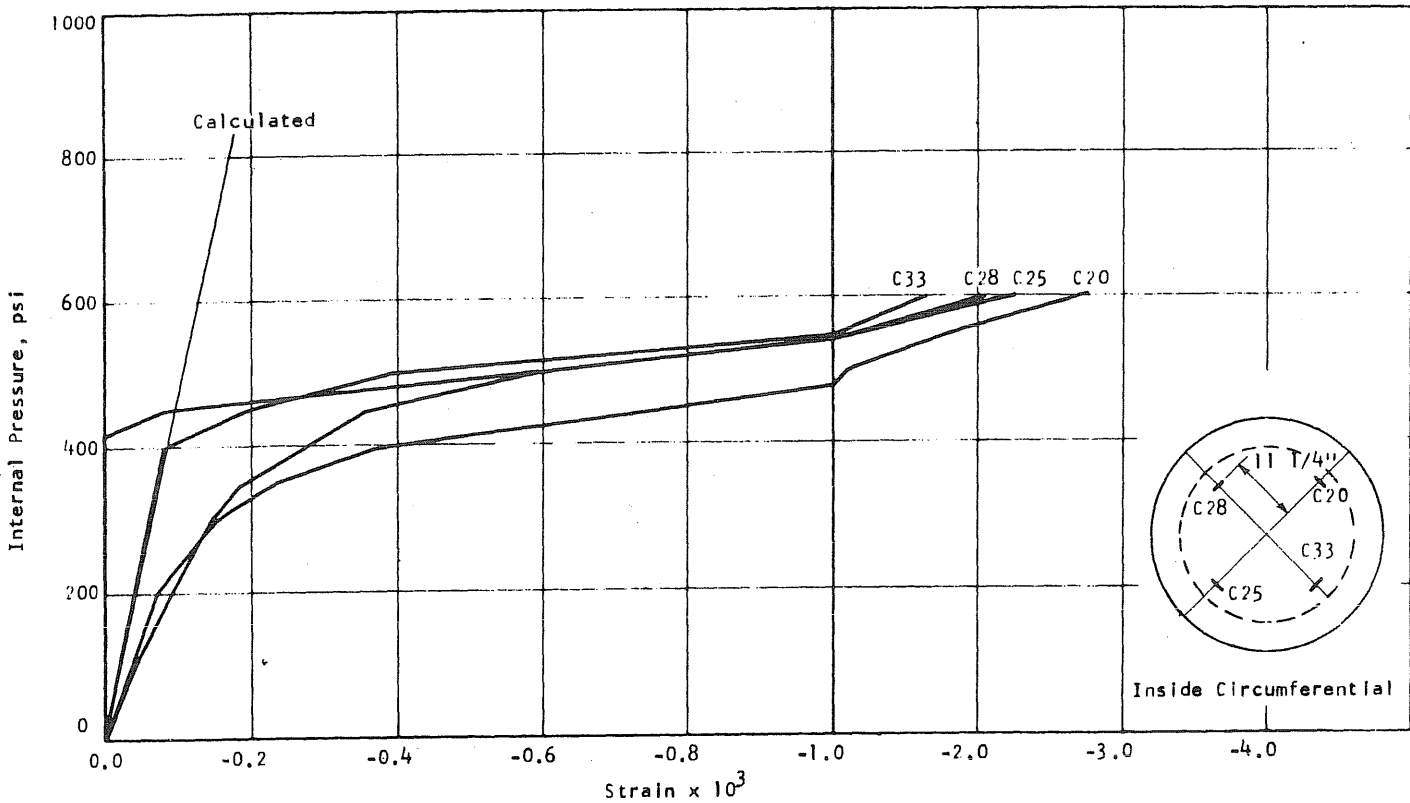


FIG. B8.13 (cont'd) CONCRETE STRAINS, VESSEL PV8

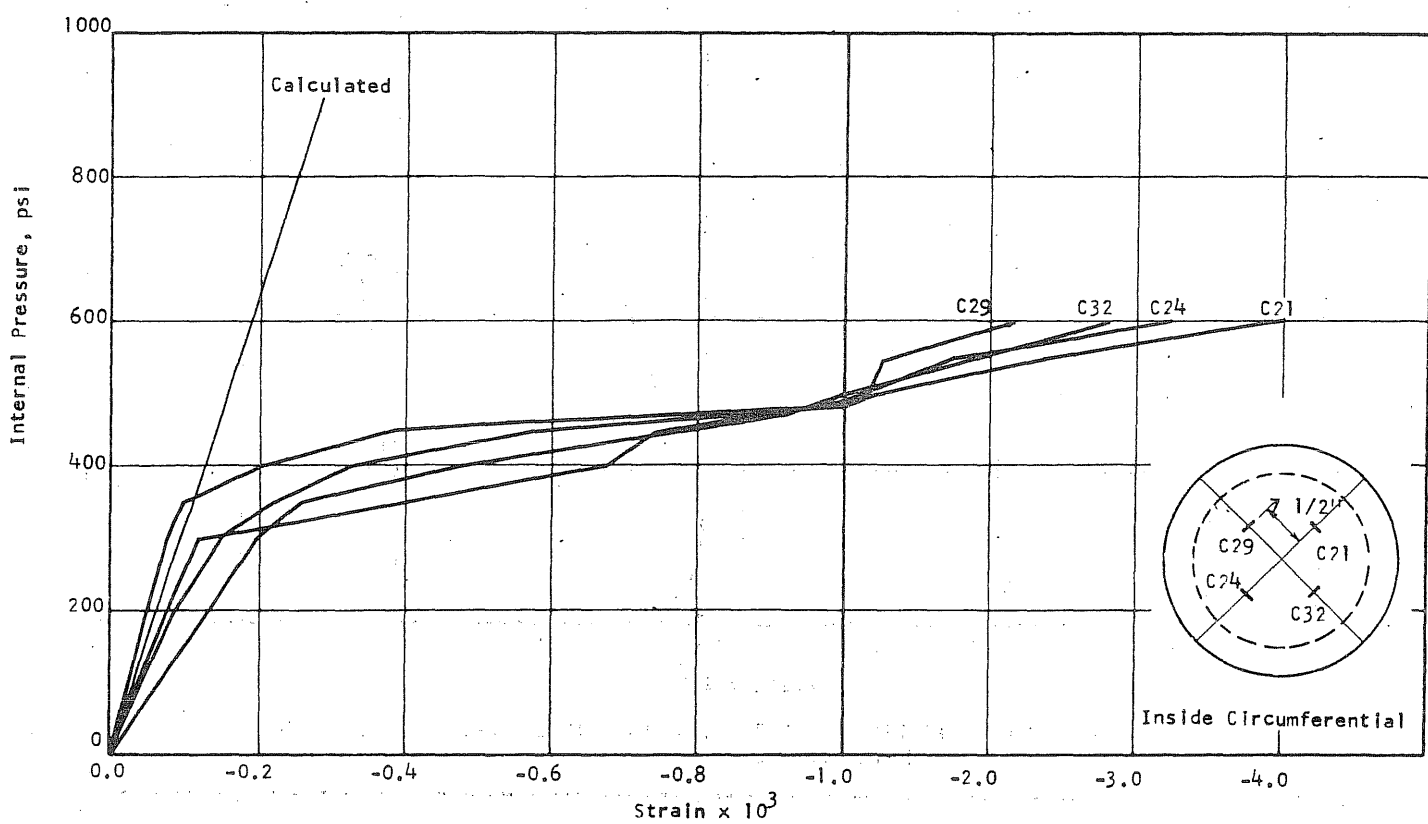


FIG. B8.13 (cont'd) CONCRETE STRAINS, VESSEL PV8

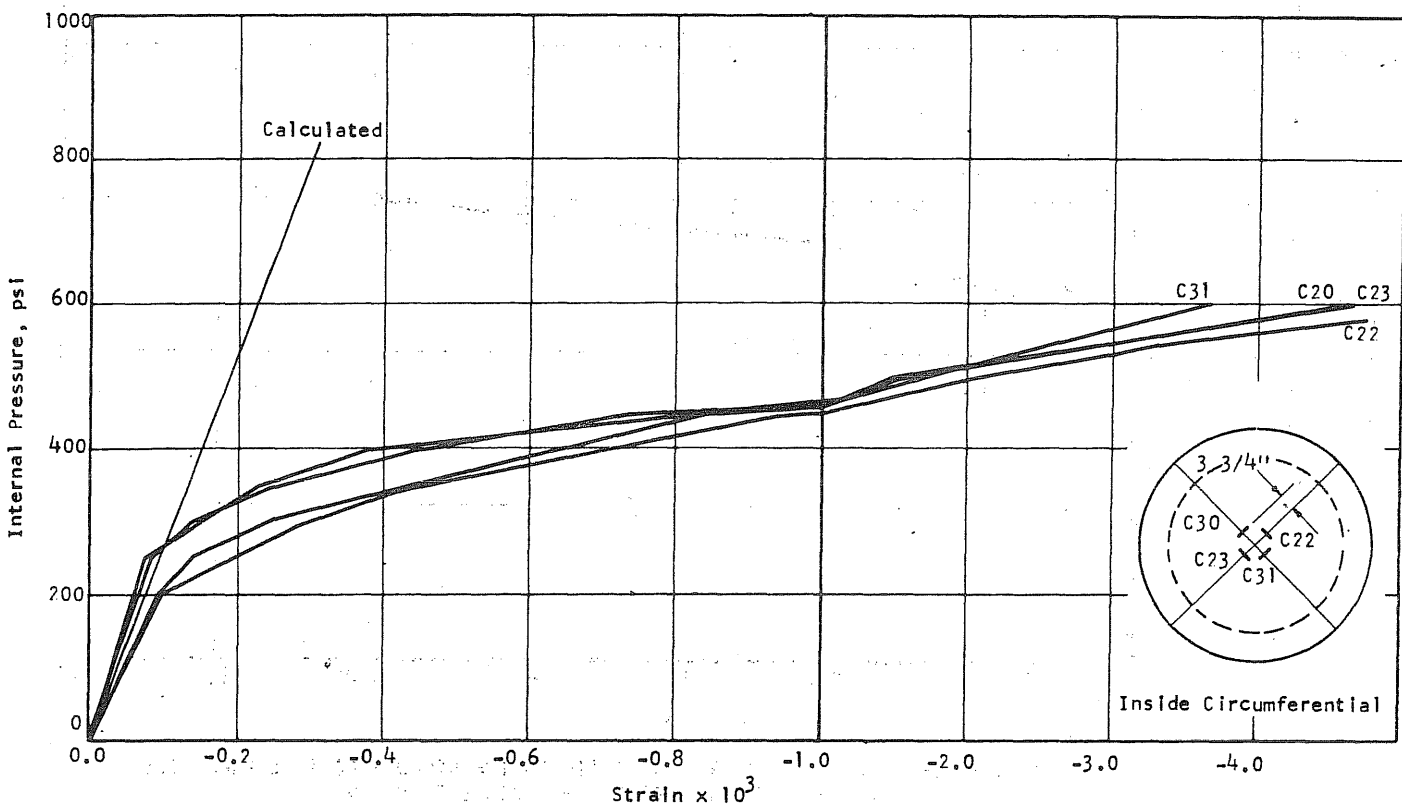


FIG. B8.13 (cont'd) CONCRETE STRAINS, VESSEL PV8

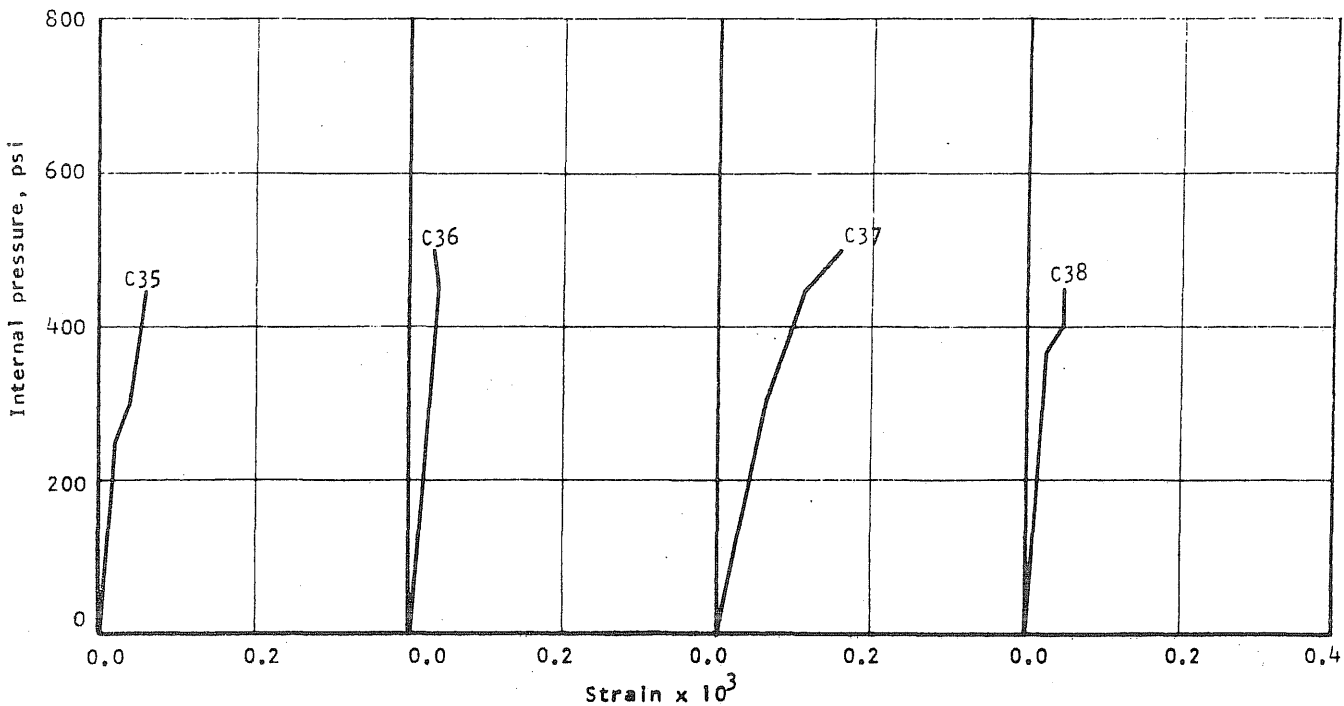


FIG. B8.14 APPLIED PRESSURE vs LONGITUDINAL STRAIN ON THE INSIDE OF THE WALL OF PV8

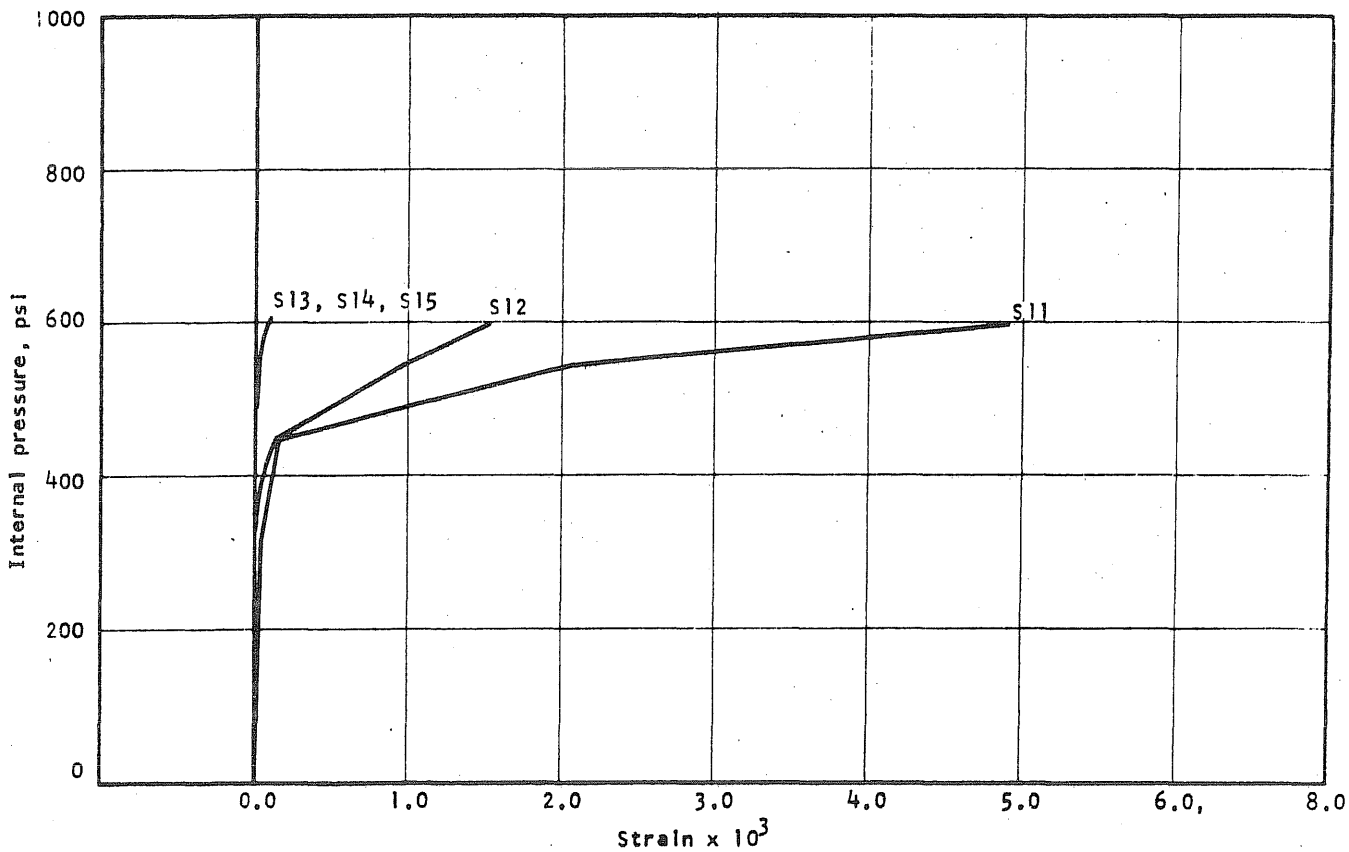


FIG. B8.15 APPLIED PRESSURE vs STRAIN IN THE CIRCUMFERENTIAL PRESTRESS WIRE AT THE S-END OF THE N-S DIAMETER OF PV8

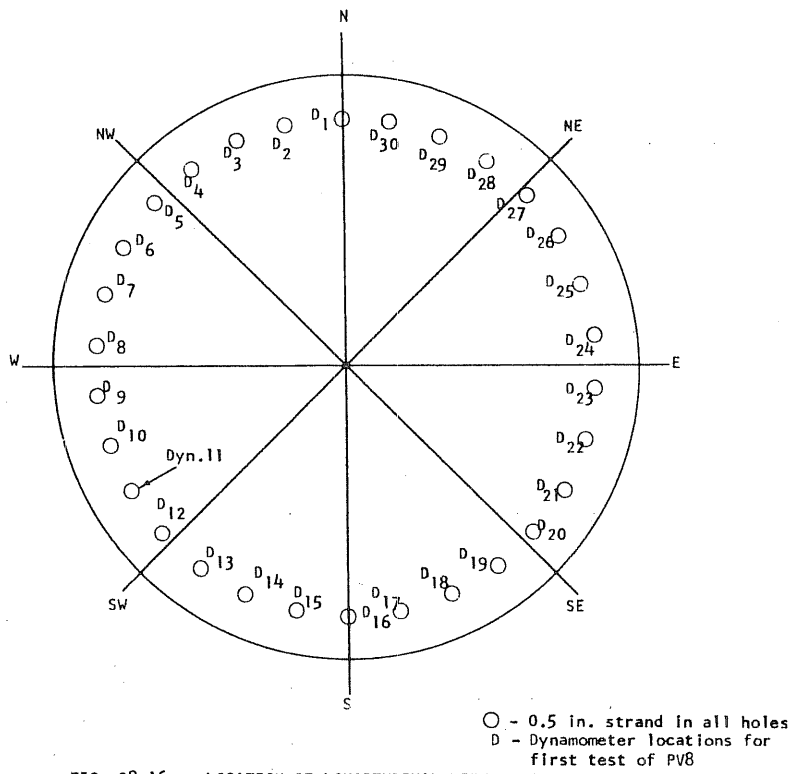


FIG. B8.16 LOCATION OF LONGITUDINAL REINFORCEMENT

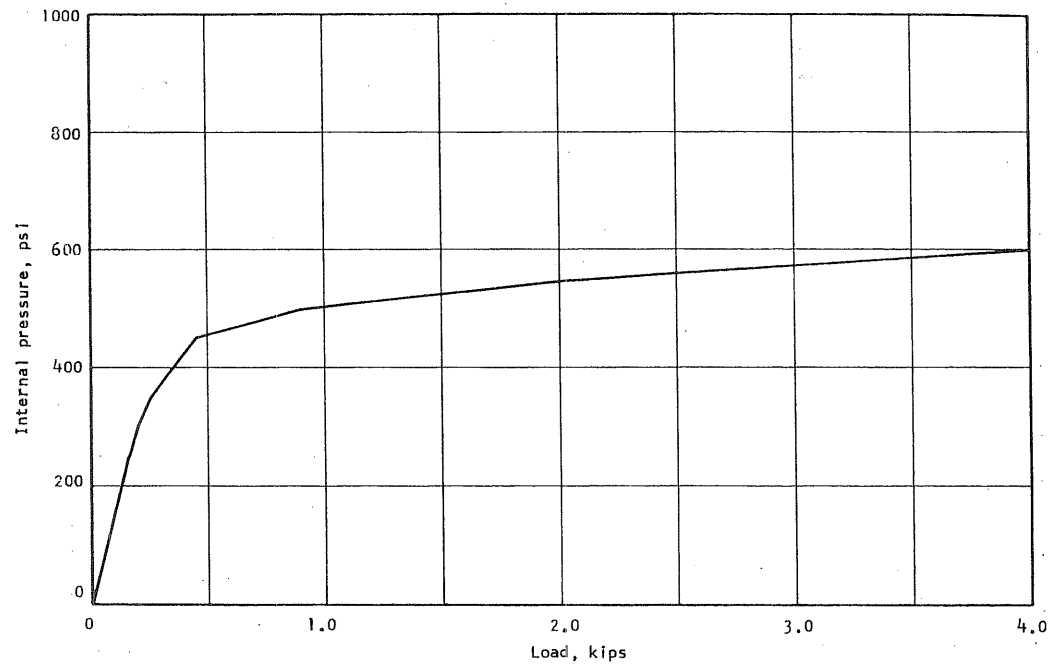


FIG. B8.17 APPLIED PRESSURE vs INCREASE IN LOAD IN DYNAMOMETER NO. 11 FOR FIRST TEST OF PV8

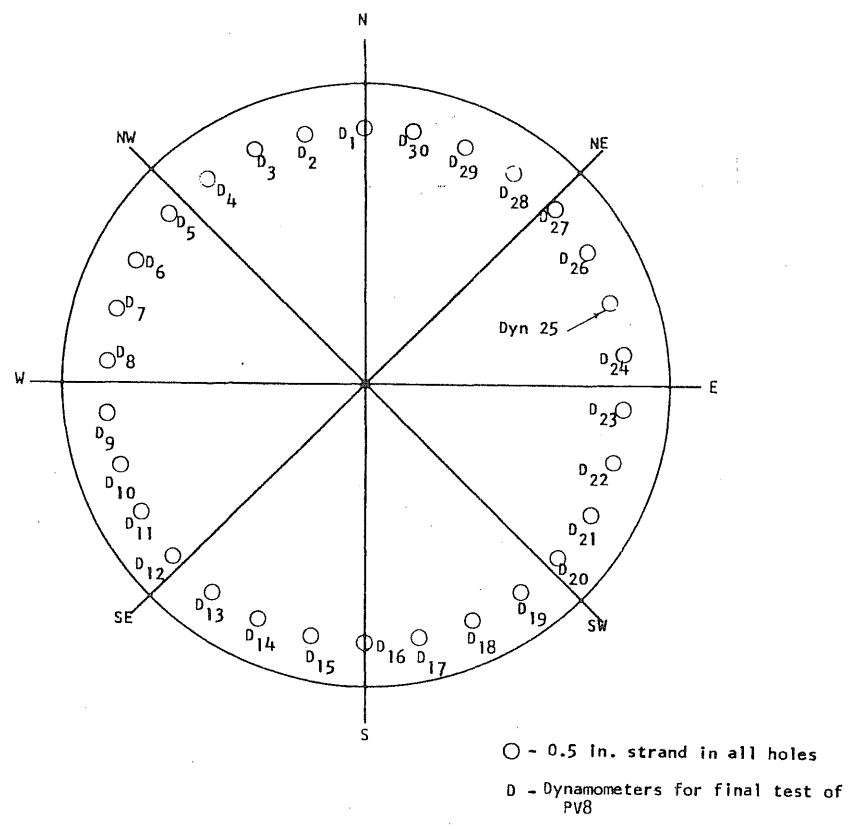


FIG. B8.18 LOCATION OF LONGITUDINAL REINFORCEMENT

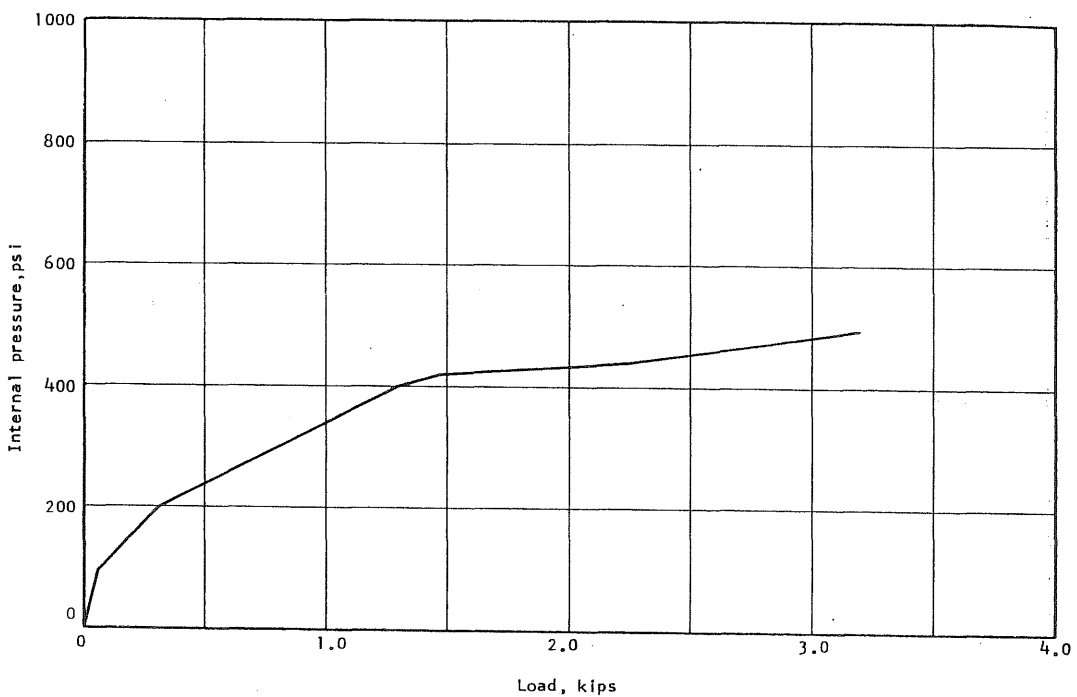


FIG. B8.19 APPLIED PRESSURE vs INCREASE IN LOAD IN DYNAMOMETER NO. 25 ON FINAL TEST OF PV8

B115

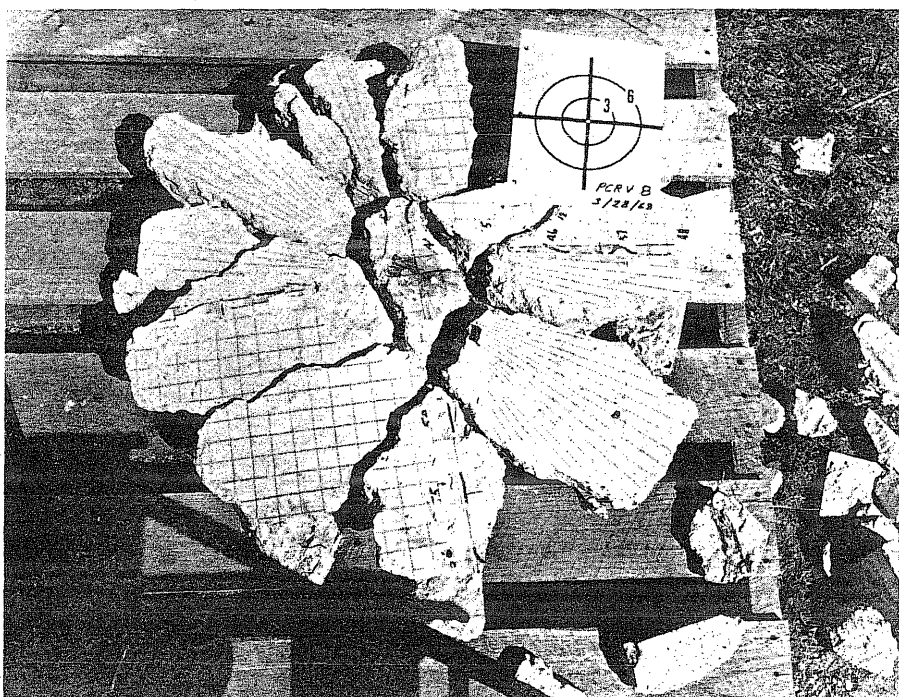


FIG. B8.20 REASSEMBLED END SLAB OF PV8

B9 Test Vessel PV9 ($t = 9$ in., $s = 1/3$ in.)

Test vessel PV9 was cast in the laboratory and was uncracked prior to prestressing. After circumferential prestressing a crack was observed on the inside of the vessel from five to six in. below the end slab and seven to nine in. below the top on the outside.

A detail of the liner is shown in Fig. B9.2 and is similar to the sealing detail successfully employed in vessel PV10, which was tested before PV9. The longitudinal prestressing force was provided by thirty strands.

This vessel was filled completely with water. The water pressure was increased by pumping oil into a buffer tank which was connected to the cavity of the vessel.

Pressure was increased in 50-psi increments to 850 psi and then in smaller increments until failure at 887 psi. Failure occurred when the circumferential wire broke. Advanced necking was observed in several wraps on opposite sides of the vessel. After failure the end slab was observed to be heavily cracked with vertical cracks on the side. The cracks at the center of the end slab were about one-half in. wide at the time of failure. The deflection at the center of the end slab reached 0.61 in. A photograph showing the crack pattern of the end slab after failure is shown in Fig. B9.14.

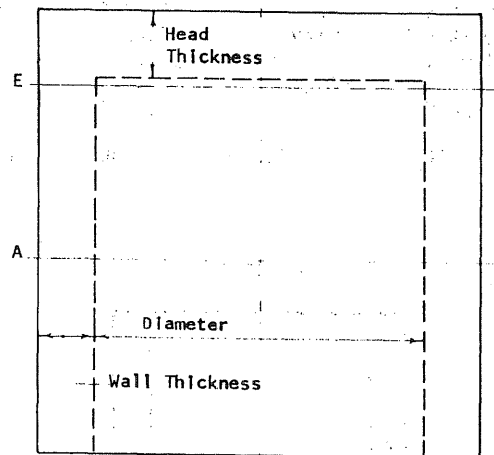
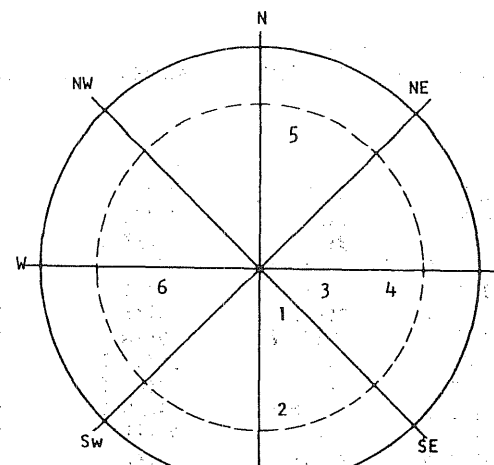


FIG. B9.1 DIMENSIONS OF PV9

| Head Thickness | |
|----------------|-------|
| 1 | 9 1/8 |
| 2 | 9 1/8 |
| 3 | 9 1/8 |
| 4 | 9 1/8 |
| 5 | 9 1/8 |
| 6 | 9 1/8 |
| 7 | 9" |

| Wall Thickness, In. | | |
|---------------------|-------|-------|
| Plane Axis | AA | BB |
| N | 5.210 | 5.320 |
| NE | 5.240 | 5.270 |
| E | 5.044 | 5.014 |
| SE | 5.117 | 5.149 |
| S | 5.084 | 5.237 |
| SW | 5.139 | 5.216 |
| W | 5.049 | 5.061 |
| NW | 5.327 | 5.211 |

| Inside Diameter, In. | | |
|----------------------|--------------------|--------------------|
| Plane Axis | AA | BB |
| N-S | 30 $\frac{2}{32}$ | 30 $\frac{2}{32}$ |
| NE-SW | 30 | 30 |
| E-W | 29 $\frac{30}{32}$ | 29 $\frac{31}{32}$ |
| SE-NW | 30 | 30 $\frac{30}{32}$ |

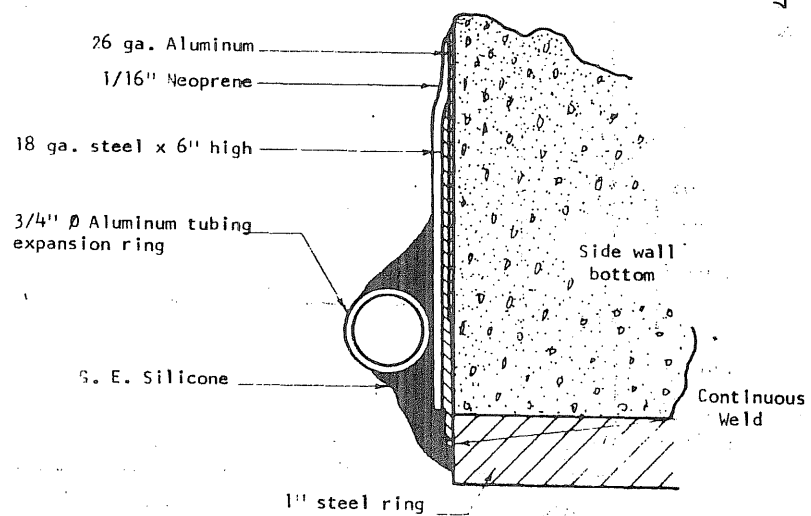
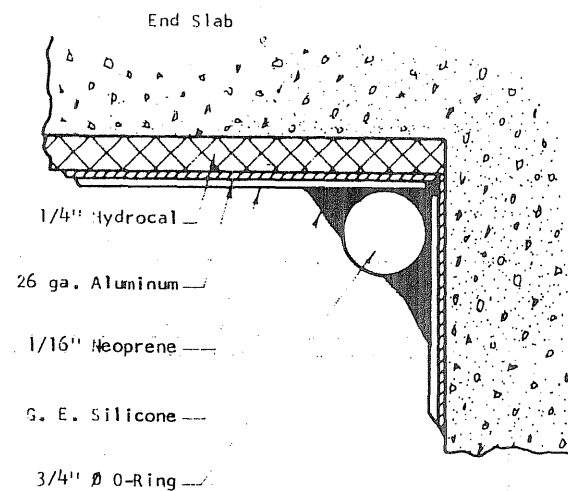
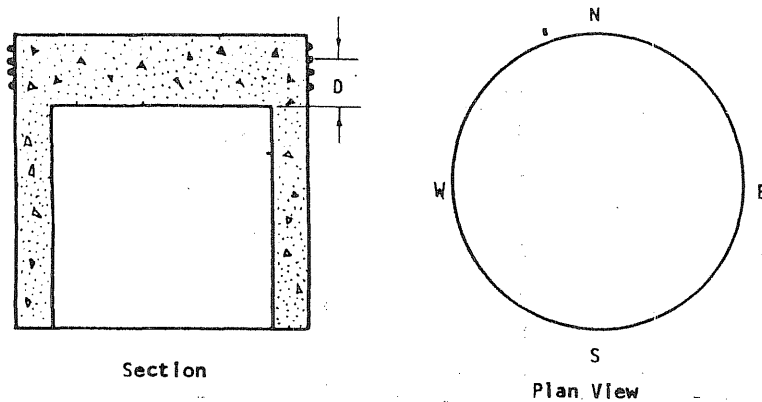


FIG. B9.2 SEALING DETAIL FOR PV9



| Wrap No. | DN | DE | DS | DW |
|----------|---------|---------|---------|---------|
| 1 | 8 5/6 | 8 2/16 | 8 2/16 | 8 5/16 |
| 2 | 7 13/16 | 7 14/16 | 7 14/16 | 7 15/16 |
| 3 | 7 10/16 | 7 9/16 | 7 10/16 | 7 11/16 |
| 4 | 7 6/16 | 7 4/16 | 7 4/16 | 7 5/16 |
| 5 | 7 2/16 | 7 15/16 | 7 6/16 | 7 6/16 |
| 6 | 6 13/16 | 6 11/16 | 6 12/16 | 6 12/16 |
| 7 | 6 9/16 | 6 6/16 | 6 6/16 | 6 7/16 |
| 8 | 6 4/16 | 6 0/16 | 6 1/16 | 6 2/16 |
| 9 | 5 15/16 | 5 11/16 | 5 12/16 | 5 13/16 |
| 10 | 5/11/16 | 5 5/16 | 5 6/16 | 5 7/16 |
| 11 | 5 3/16 | 4 15/16 | 5 0/16 | 5 1/16 |
| 12 | 4 13/16 | 4 10/16 | 4 11/16 | 4 11/16 |
| 13 | 4 8/16 | 4 4/16 | 4 5/16 | 4 6/16 |
| 14 | 4 3/16 | 3 15/16 | 4 0/16 | 4 0/16 |
| 15 | 3 13/16 | 3 9/16 | 3 10/16 | 3 11/16 |
| 16 | 3 8/16 | 3 4/16 | 3 5/16 | 3 6/16 |
| 17 | 3 3/16 | 2 15/16 | 3 0/16 | 3 0/16 |
| 18 | 2 13/16 | 2 9/16 | 2 10/16 | 2 11/16 |
| 19 | 2 8/16 | 2 3/16 | 2 5/16 | 2 5/16 |
| 20 | 2 3/16 | 1 14/16 | 1 15/16 | 2 0/16 |
| 21 | 1 13/16 | 1 9/16 | 1 9/16 | 1 10/16 |
| 22 | 1 7/16 | 1 3/16 | 4 1/10 | 1 5/16 |
| 23 | 1 2/16 | 14/16 | 14/16 | 1 0/16 |
| 24 | 12/16 | 9/16 | 9/16 | 10/16 |
| 25 | 7/16 | 3/16 | 4/16 | 5/16 |
| 26 | 2/16 | - | - | 0/16 |

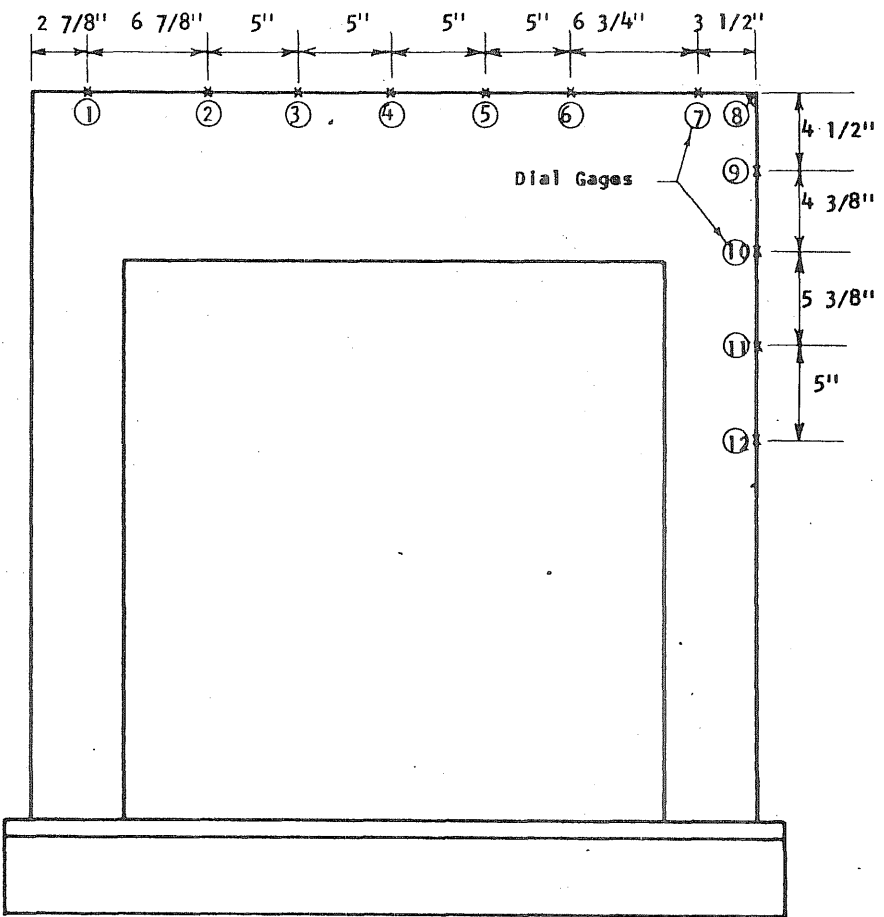


FIG. B9.4 LOCATION OF DEFLECTION GAGES ON PV9

FIG. B9.3 MEASURED LOCATION OF THE CIRCUMFERENTIAL PRESTRESS WIRE AT THE ENDS OF THE N-S AND E-W DIAMETERS ON PV9

B 119

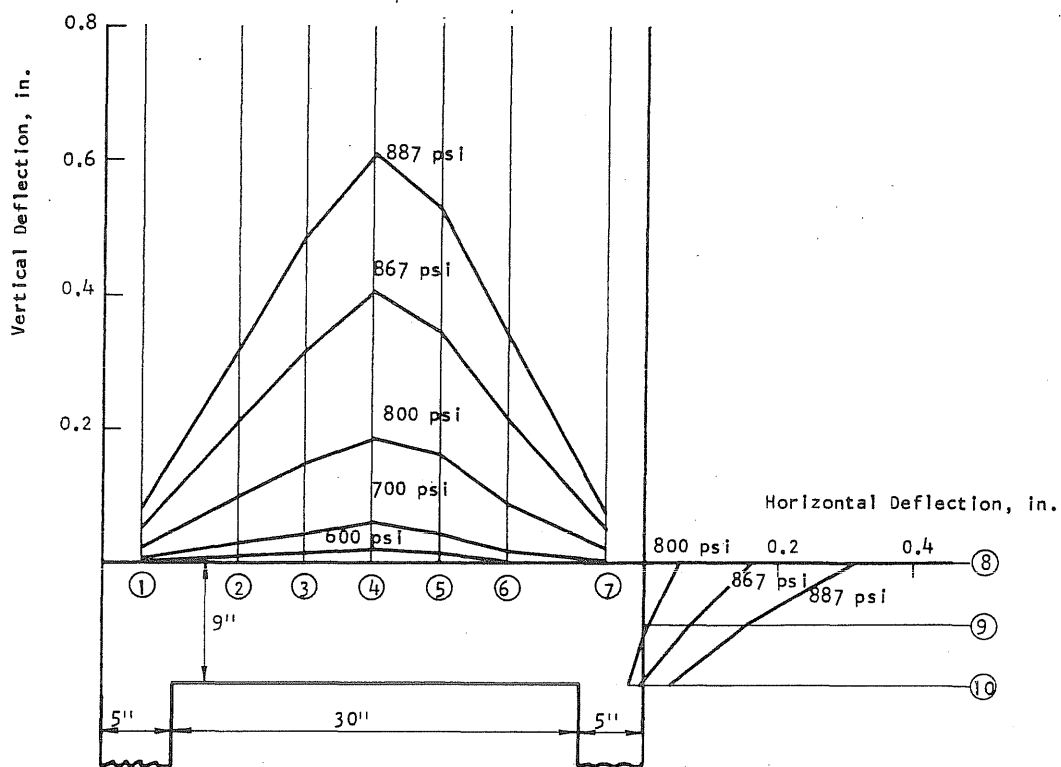


FIG. B9.5 DEFLECTION PROFILES OF THE END SLAB ALONG THE
N-S DIAMETER OF VESSEL PV9

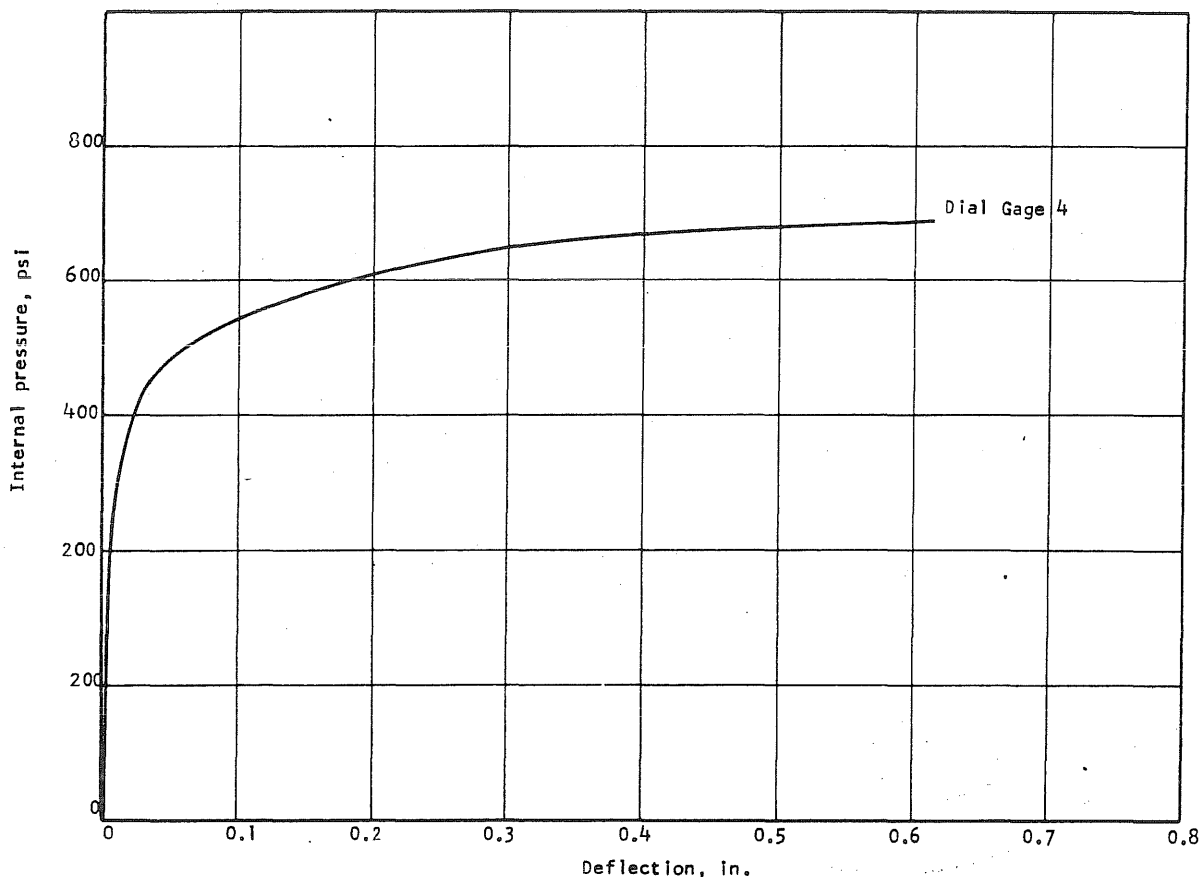
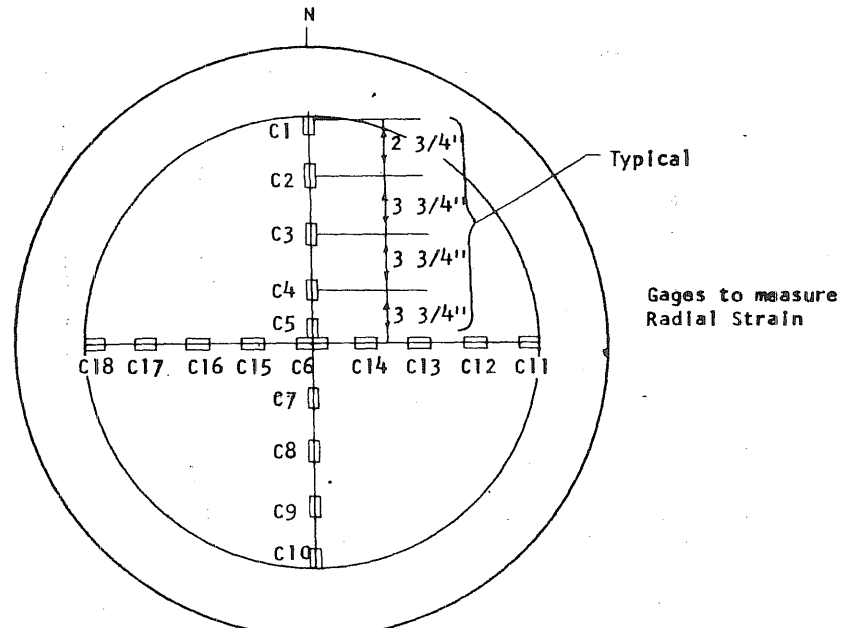


FIG. 9.6 APPLIED PRESSURE VS DEFLECTION AT MIDSPAN OF PV9

Concrete Gages on the Inside of the End Slab



Concrete Gages on the Outside of the End Slab

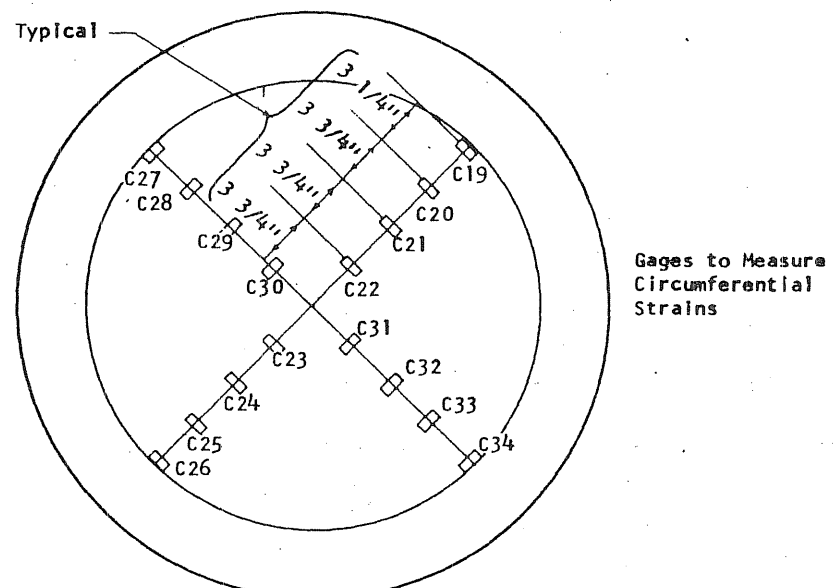
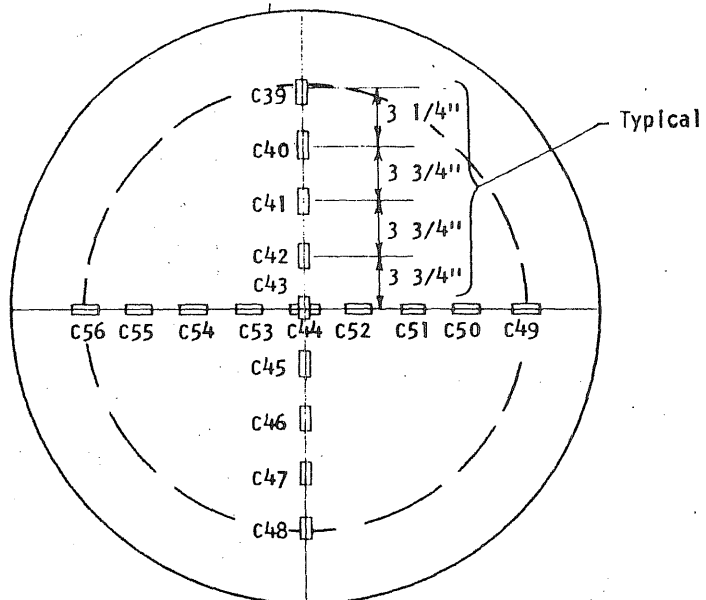


FIG. B9.7 STRAIN GAGE LOCATIONS ON PV9

Steel Gages on Circumferential Prestress Wire

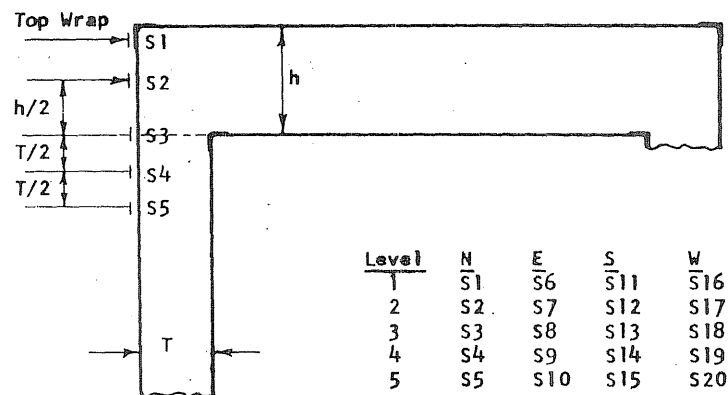


FIG. B9.7 (cont'd) STRAIN GAGE LOCATIONS ON PV9

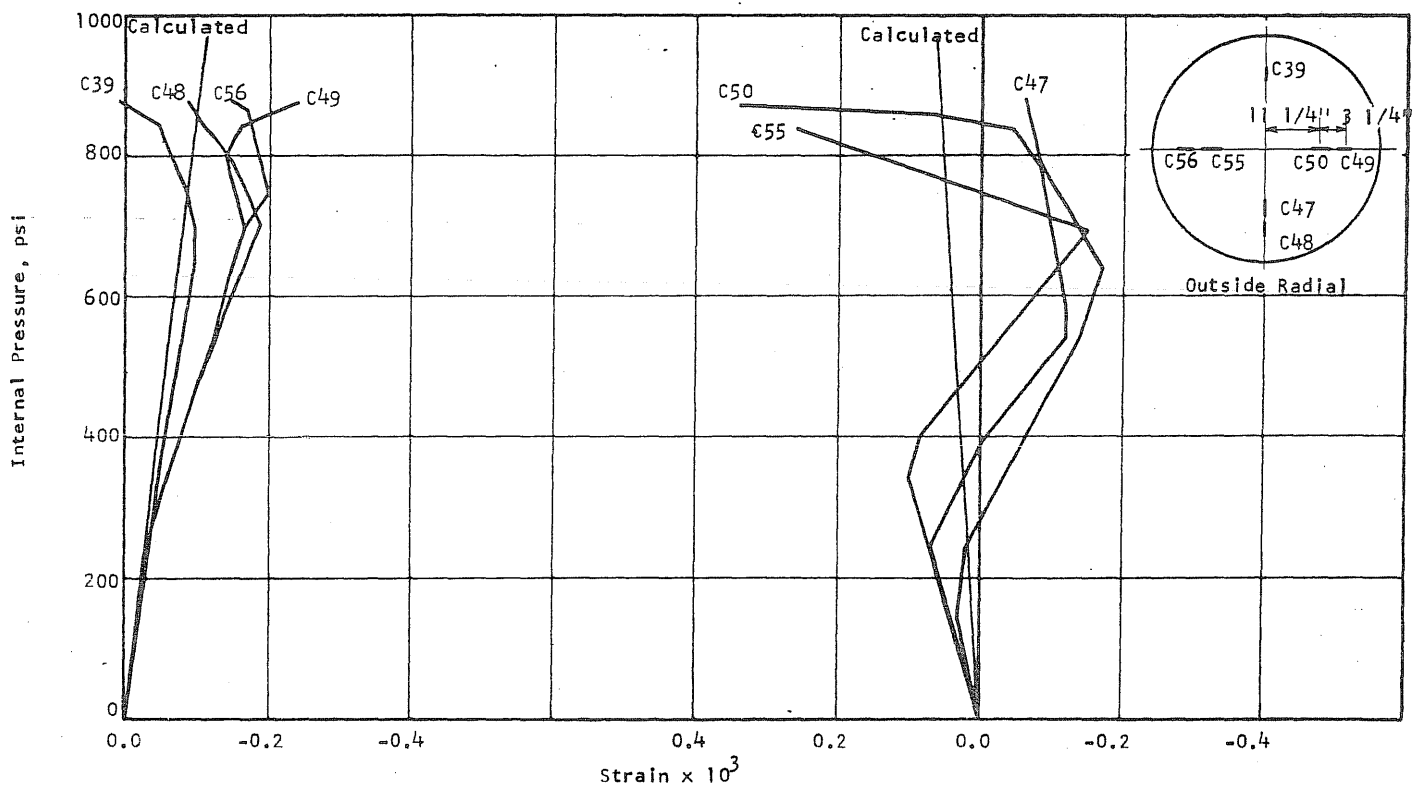


FIG. B9.8 CONCRETE STRAINS, VESSEL PV9

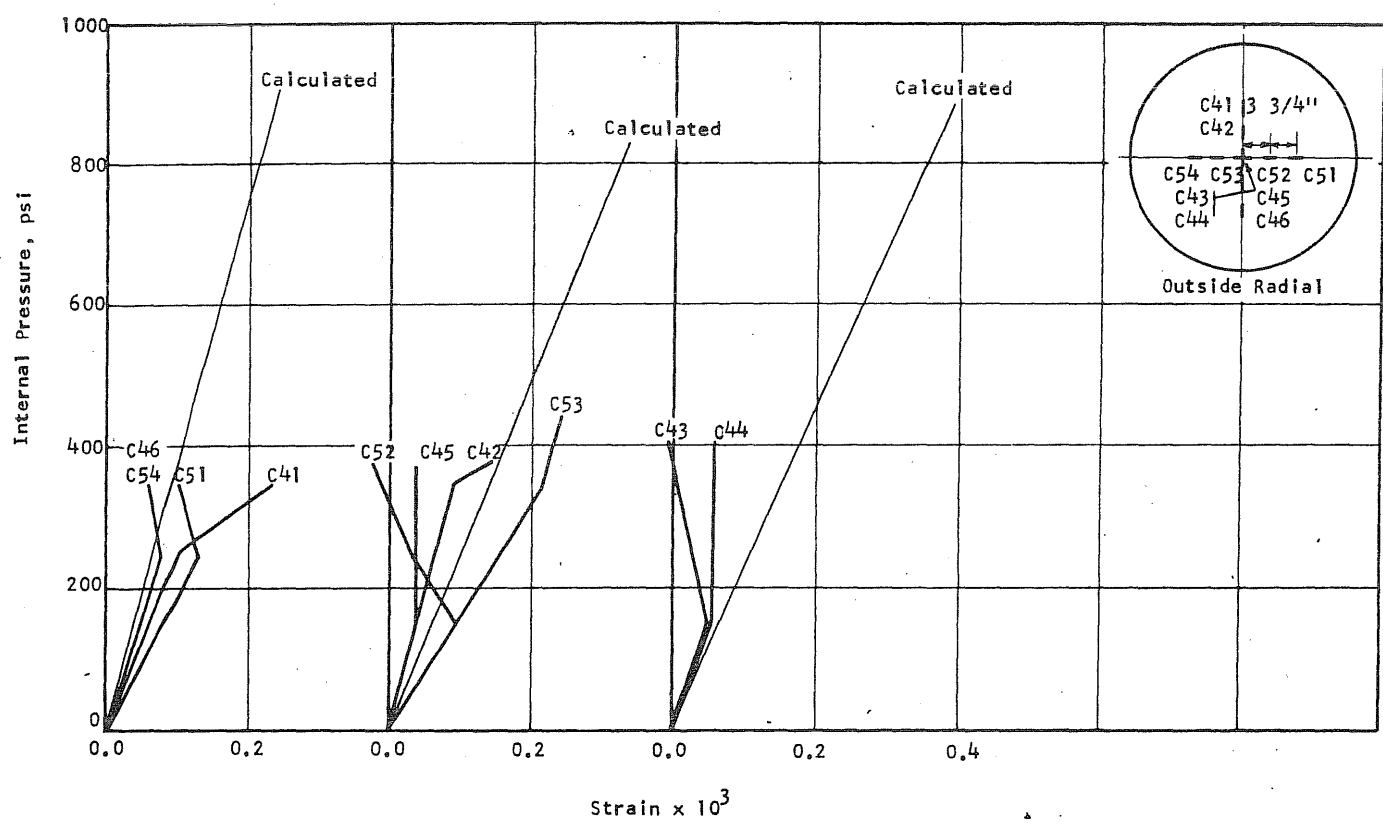


FIG. B9.8 (cont'd) CONCRETE STRAINS, VESSEL PV9

B122

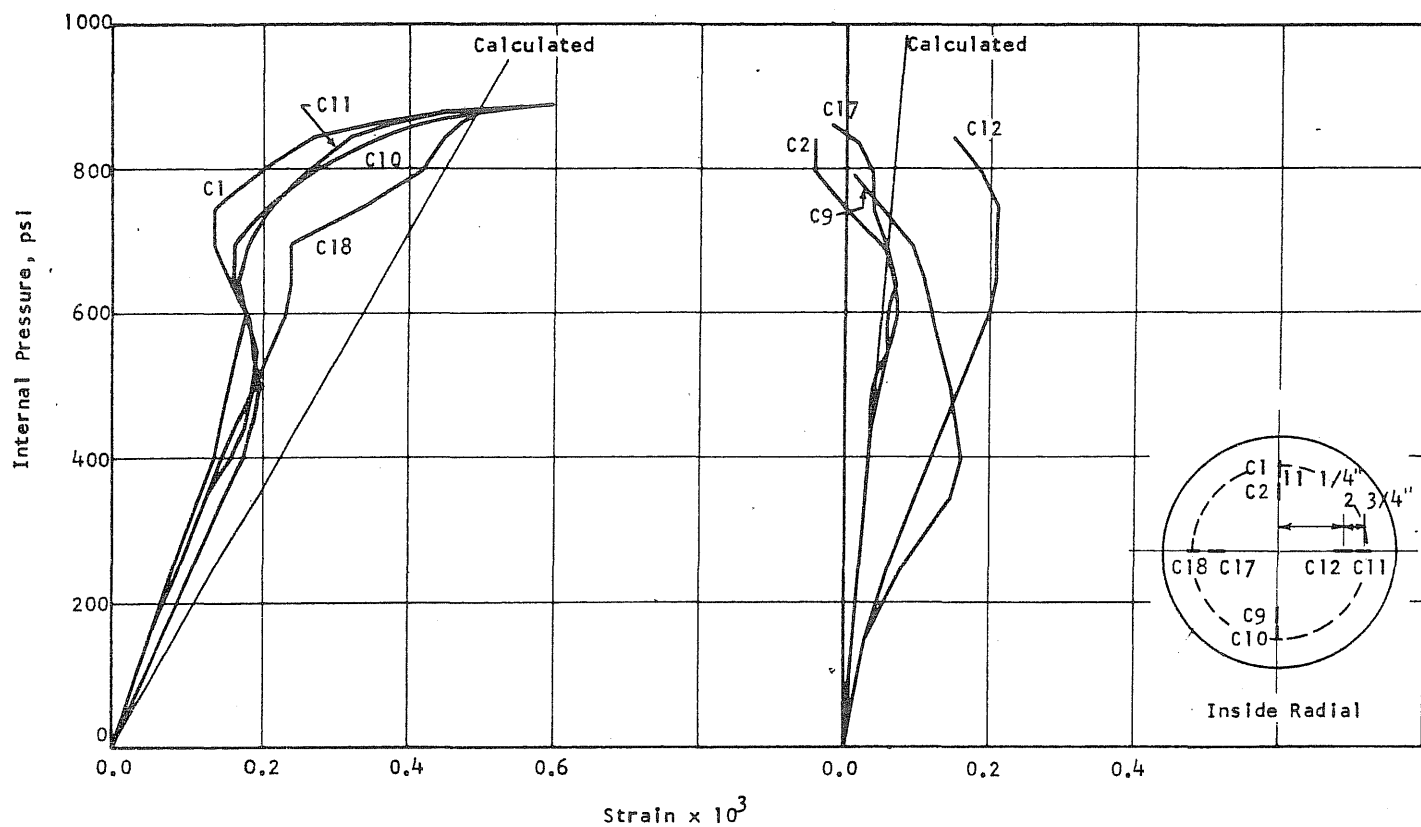


FIG. B9.9 CONCRETE STRAINS, VESSEL PV9

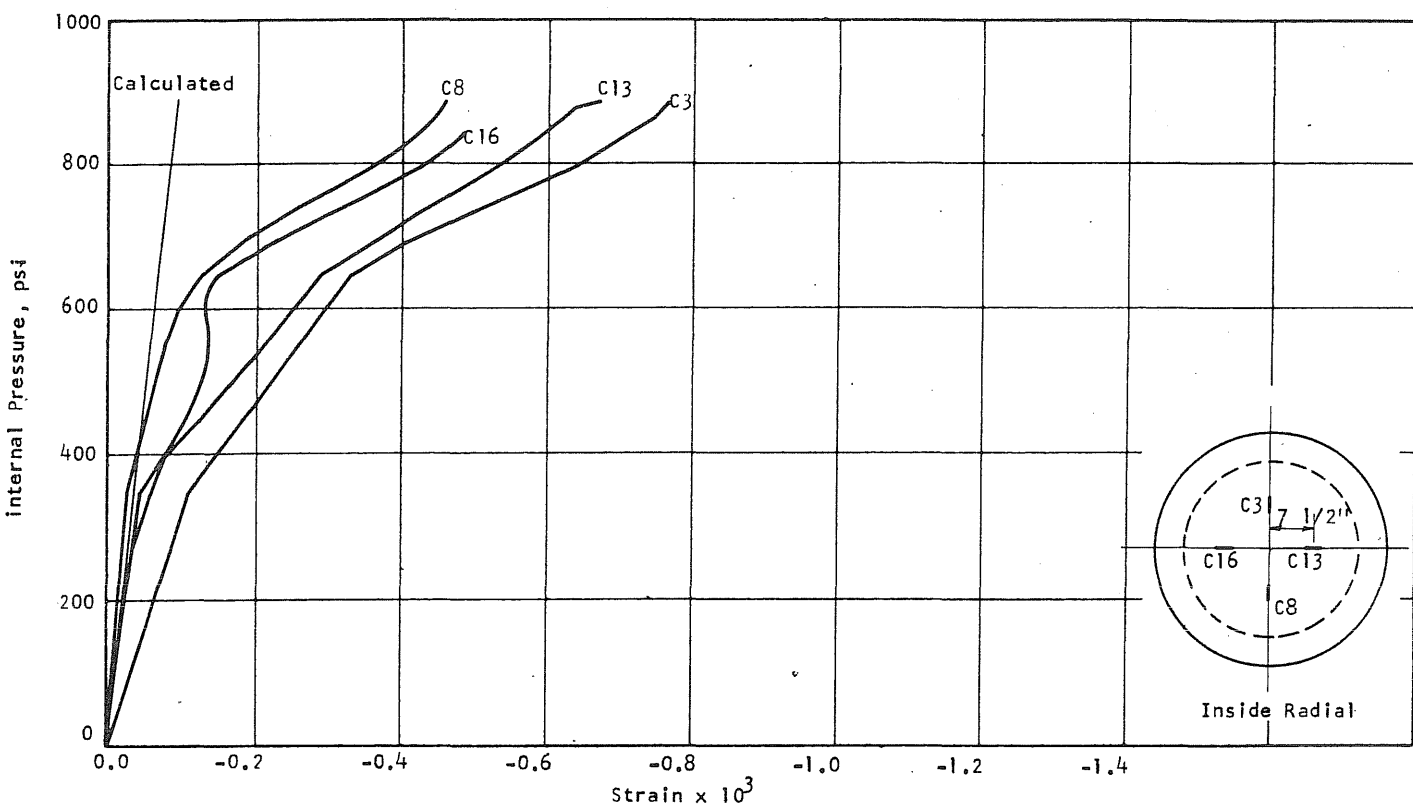


FIG. B9.9 (cont'd) CONCRETE STRAINS, VESSEL PV9

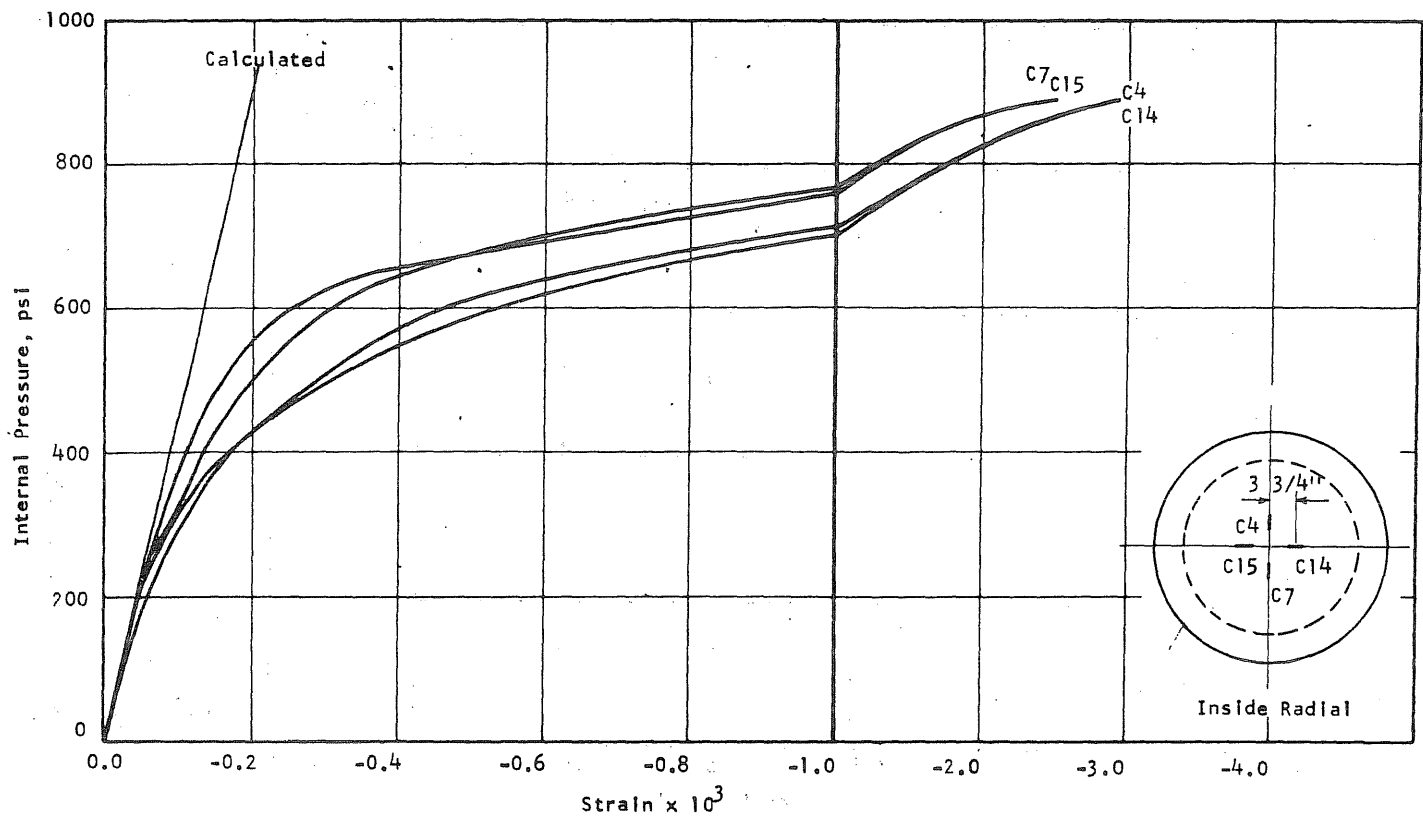


FIG. B9.9 (cont'd) CONCRETE STRAINS, VESSEL PV9

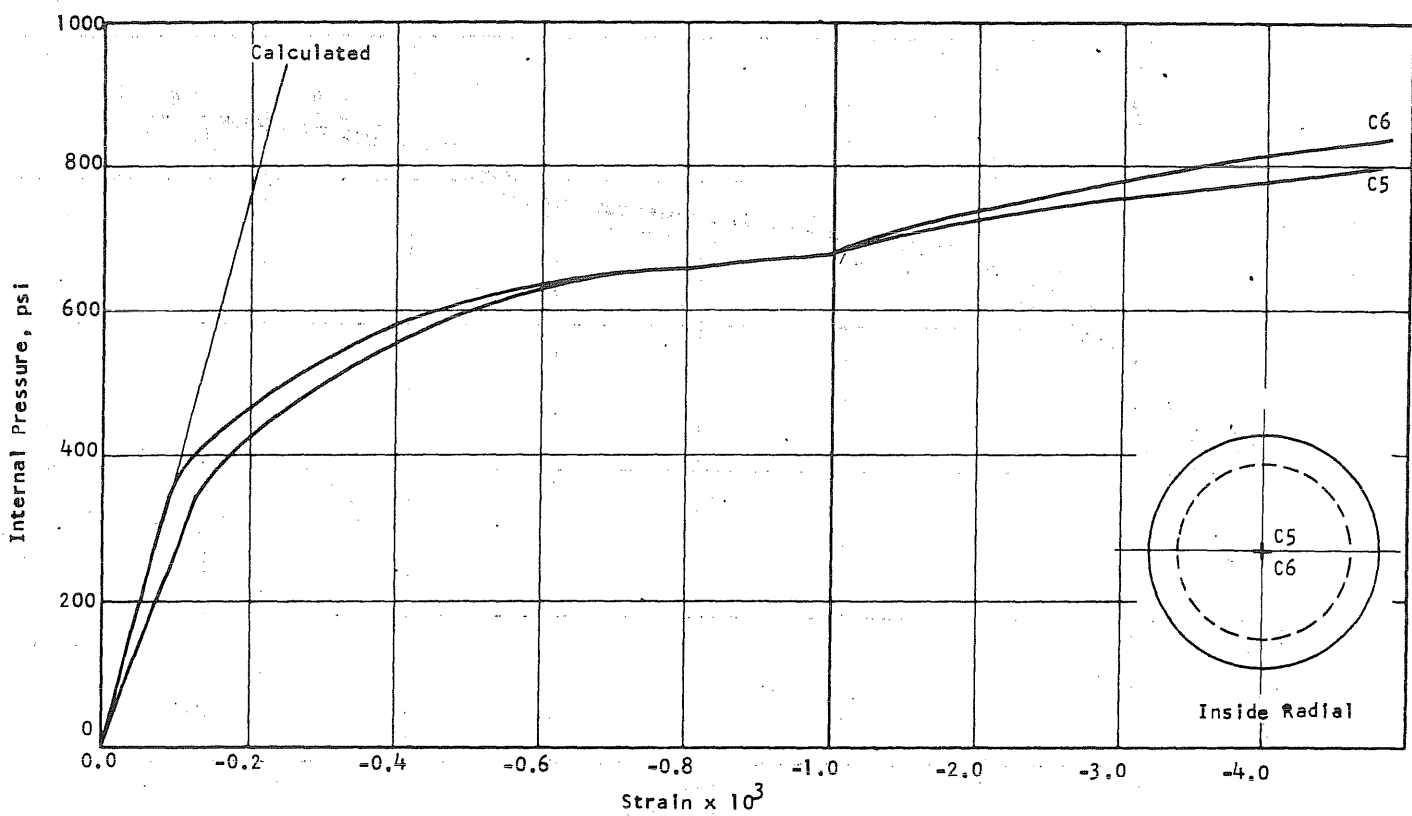


FIG. B9.9 (cont'd) CONCRETE STRAINS, VESSEL PV9

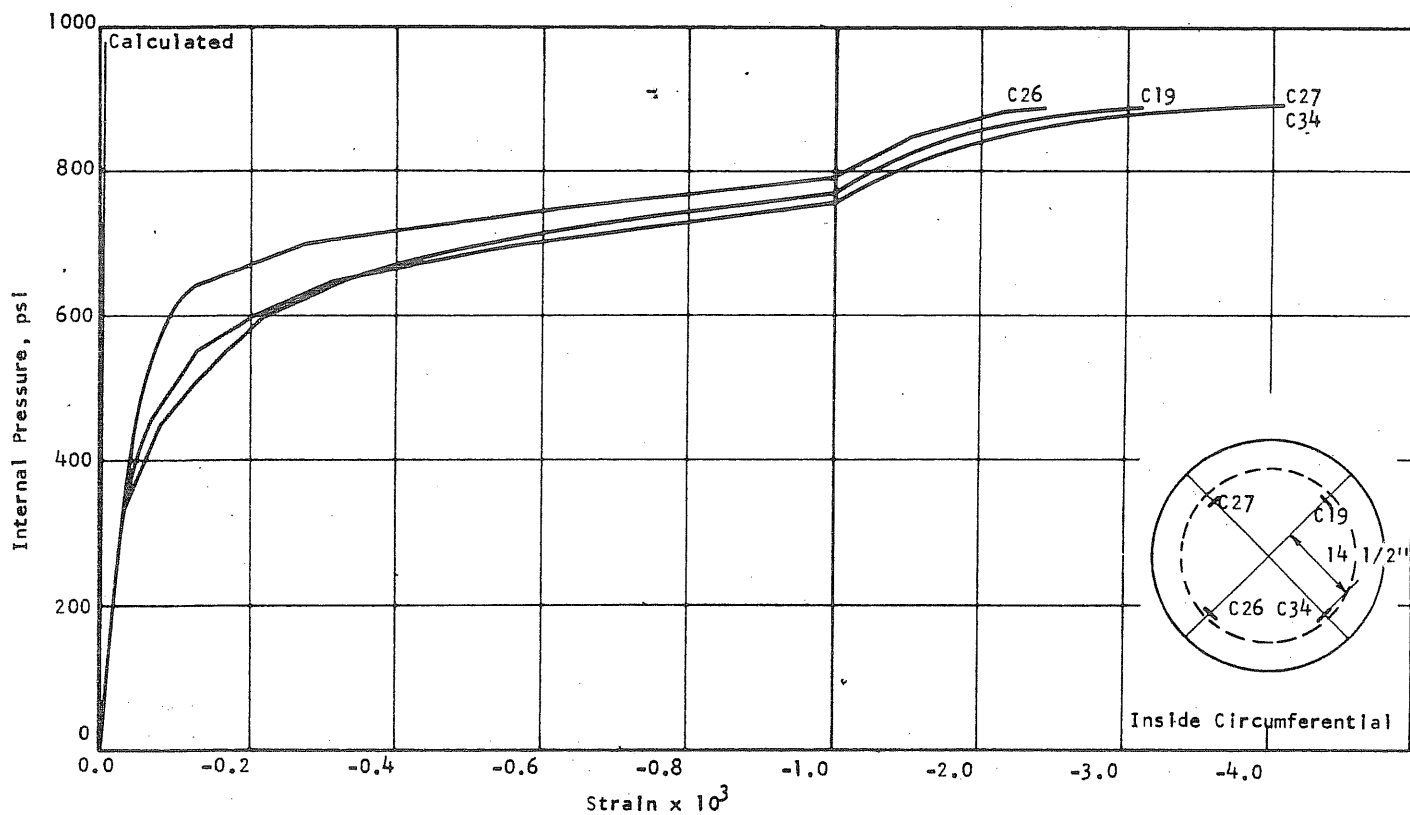


FIG. B9.10 CONCRETE STRAINS, VESSEL PV9

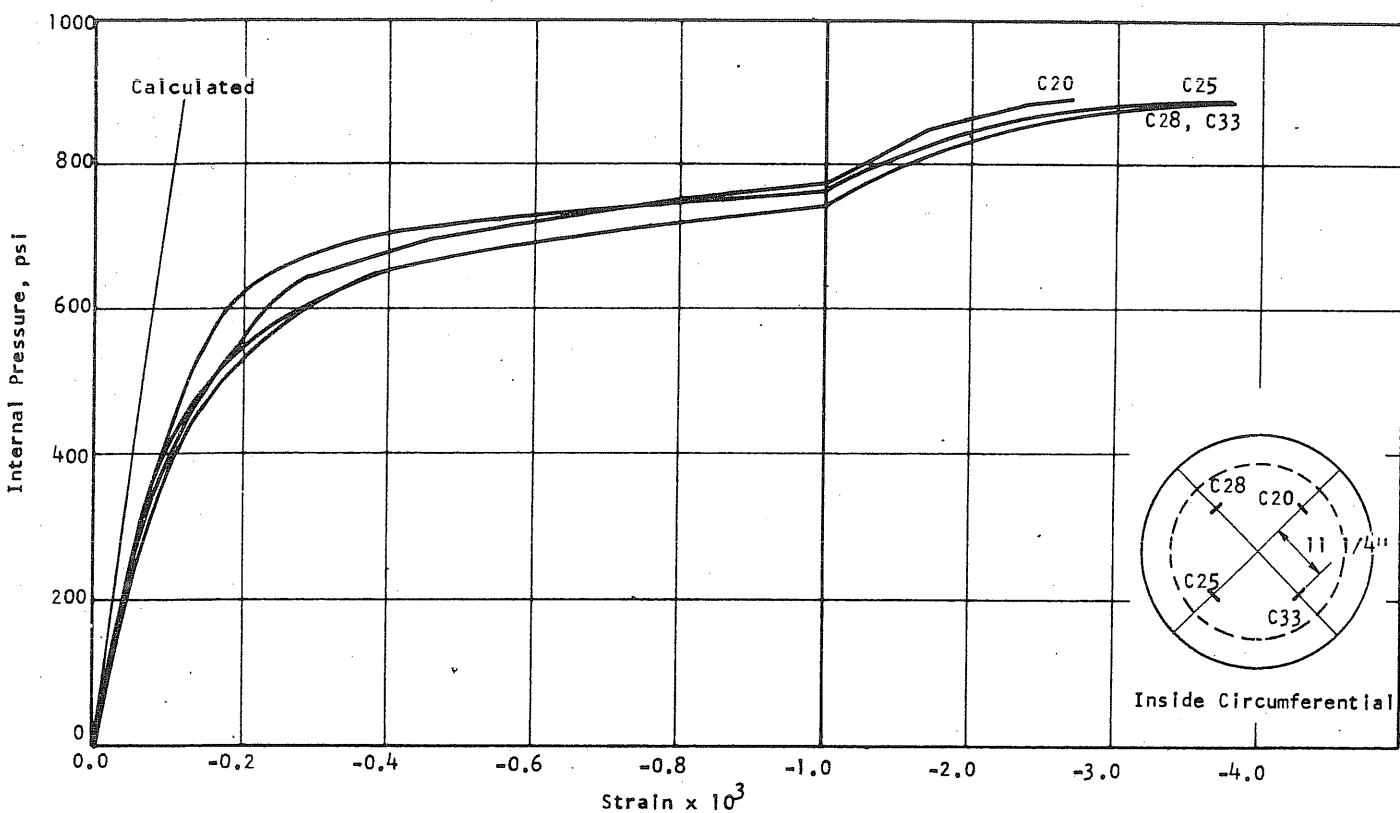


FIG. B9.10 (cont'd) CONCRETE STRAINS, VESSEL PV9

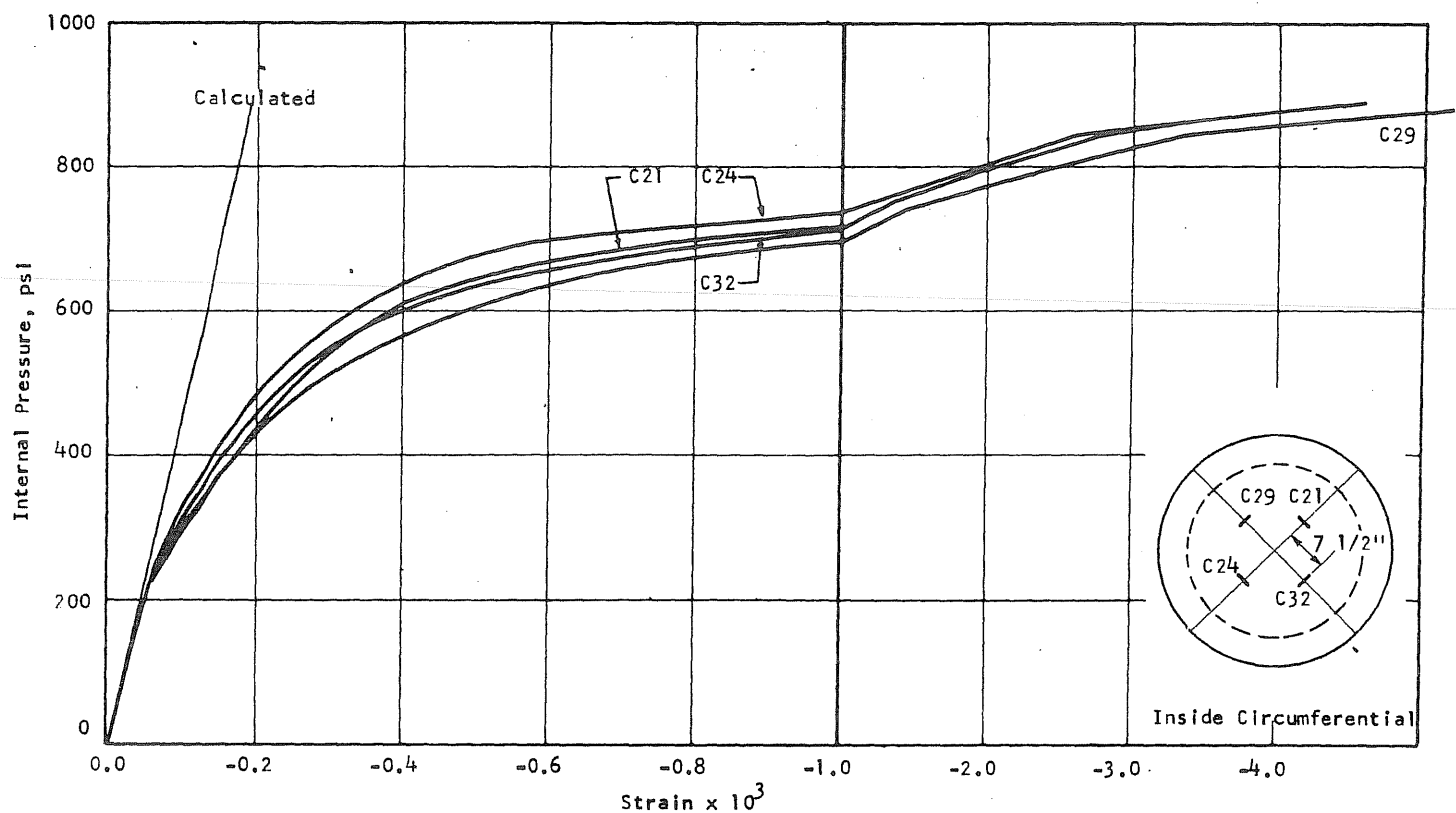


FIG. B9.10 (cont'd) CONCRETE STRAINS, VESSEL PV9

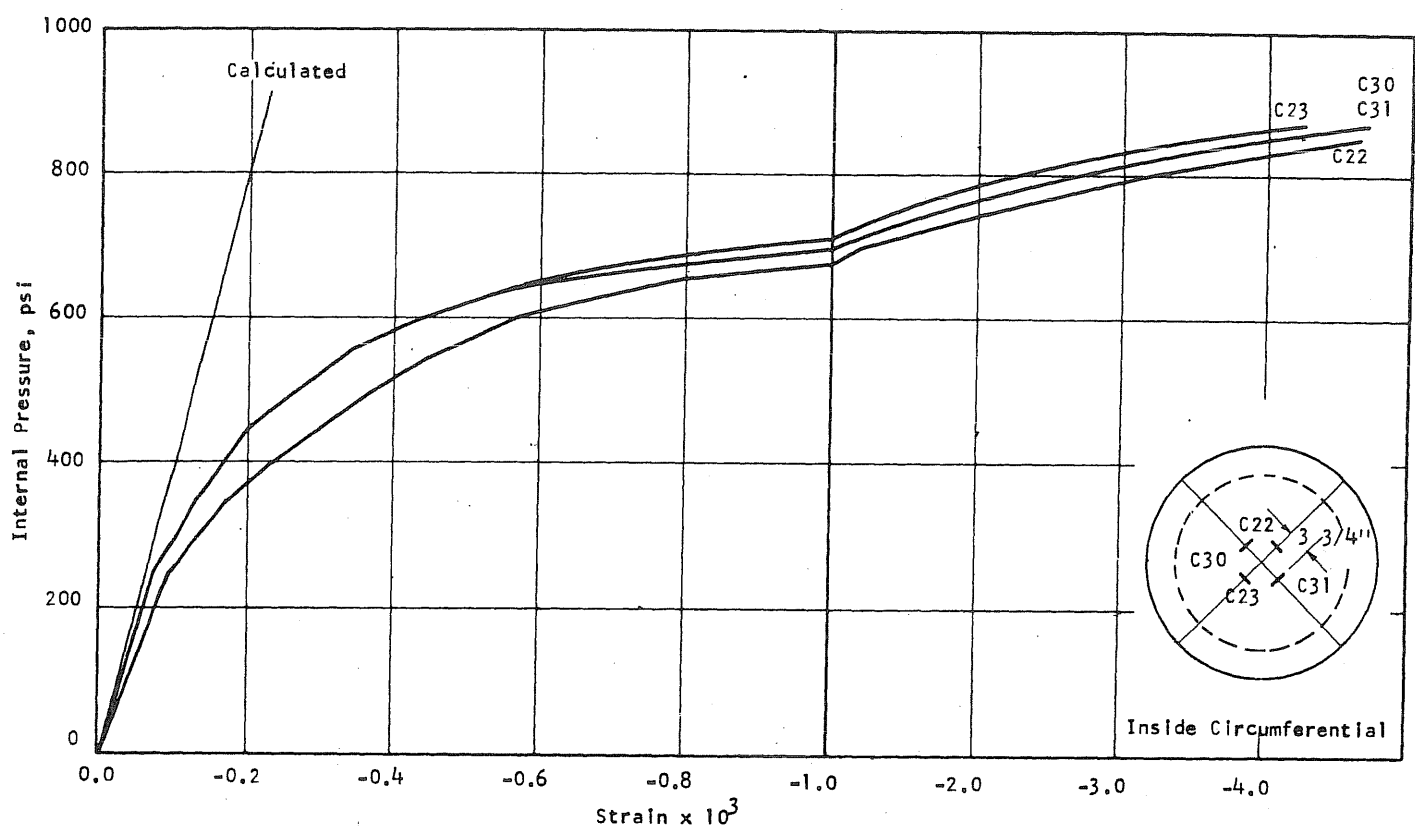


FIG. B9.10 (cont'd) CONCRETE STRAINS, VESSEL PV9

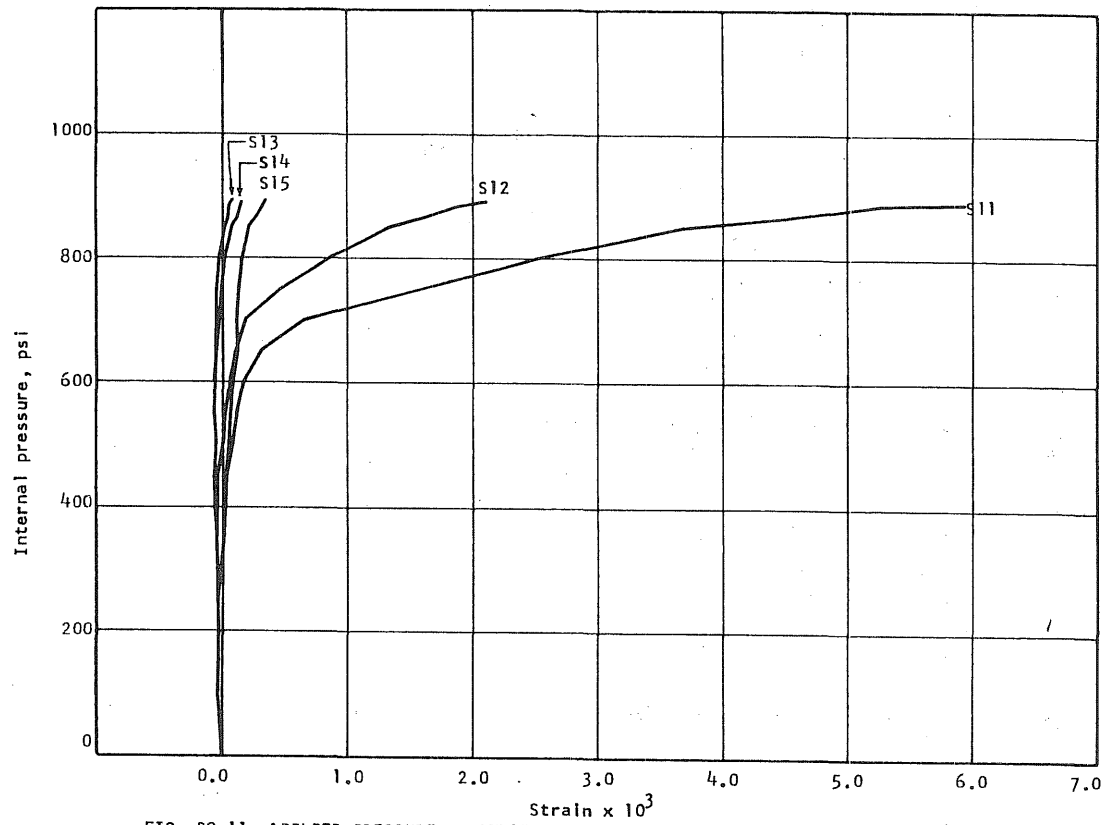


FIG. B9.11 APPLIED PRESSURE vs STRAIN IN CIRCUMFERENTIAL PRESTRESS WIRE AT THE S-END OF THE N-S DIAMETER OF PV9

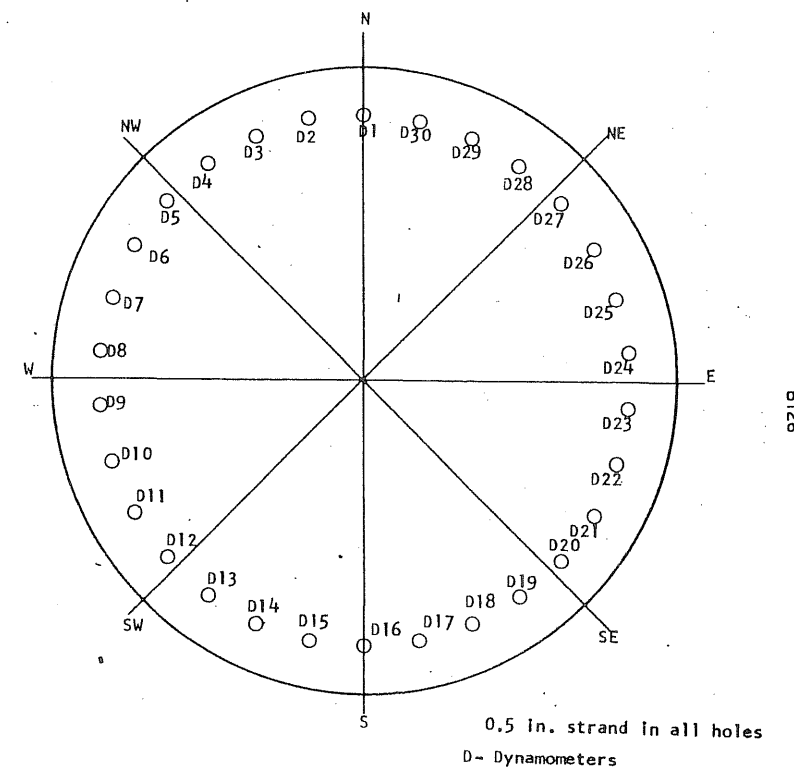


FIG. B9.12 LOCATION OF LONGITUDINAL REINFORCEMENT FOR PV9

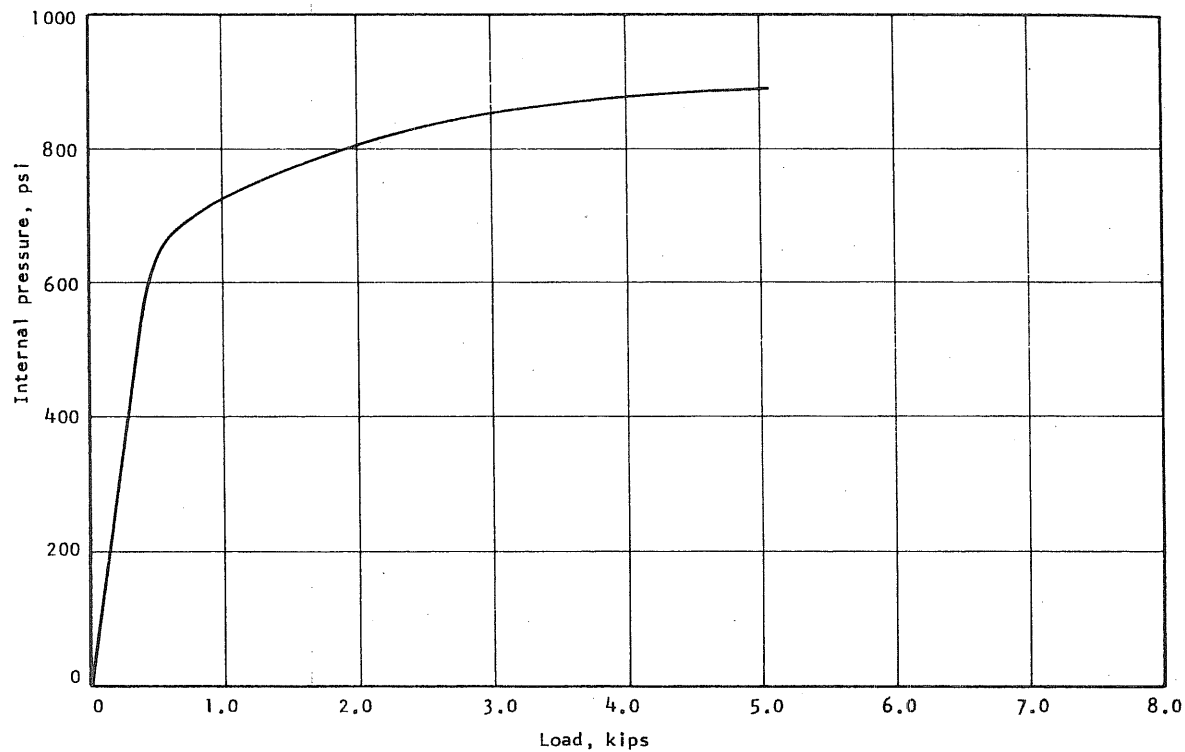


FIG. B9.13 APPLIED PRESSURE vs INCREASE IN LOAD IN DYNAMOMETER NO. 10

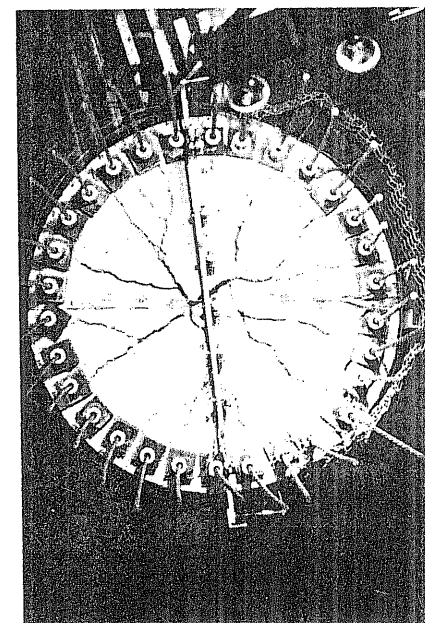


FIG. B9.14 END SLAB AFTER FAILURE

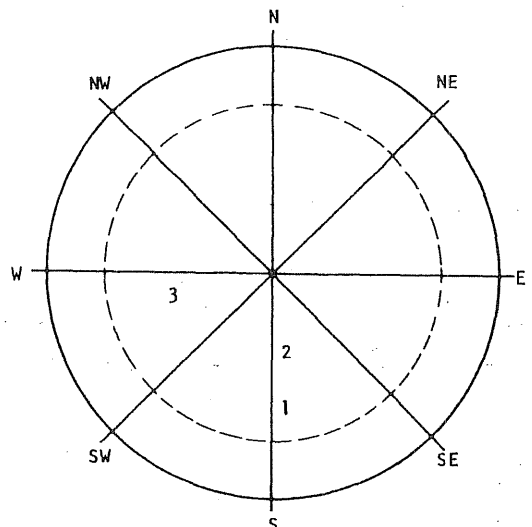
B10 Test Vessel PV10 ($t = 7.5$ in., $s = 1/3$ in.)

Test vessel PV10 was cast without any visible flaws. After circumferential prestressing, it developed two circumferential cracks. One was on the outside approximately seven in. from the top. The other was on the inside approximately ten in. from the top.

Vessel PV10 was the first specimen tested hydraulically. The vessel was pressurized with a hydraulic pump connected to the vessel through a buffer tank. The vessel cavity was filled with water before the test.

The liner detail was changed significantly from PV8 and is shown in Fig. B10.2. The aluminum liner was assembled outside the vessel and then dropped in place. A mechanical interlock was made at the end slab joint and at the lap in the wall. Both joints were tinned flat. A neoprene liner and a 0.75-in. neoprene O-ring was added as in previous vessels. The neoprene wall and end slab pieces butted at the end slab joint but did not lap. Thirty strands were used for longitudinal reinforcement.

Pressure was increased in 50-psi increments to 600 psi. The vessel began to leak slightly at 600 psi but it was still possible to pressurize the vessel using the vertical deflection of the end slab as a loading criterion. The load decreased during the reading of the gages but the deflections did not change significantly. Failure occurred at 737 psi when the prestressing wire failed. A photograph showing the crack pattern of the end slab after failure is given in Fig. B10.14.



| Head Thickness | |
|----------------|-------------------|
| Point No. | inches |
| 1 | 7 $\frac{11}{16}$ |
| 2 | 7 $\frac{6}{8}$ |
| 3 | 7 $\frac{10}{16}$ |
| - | 7 $\frac{8}{16}$ |
| - | 7 $\frac{11}{16}$ |
| - | 7 $\frac{8}{16}$ |

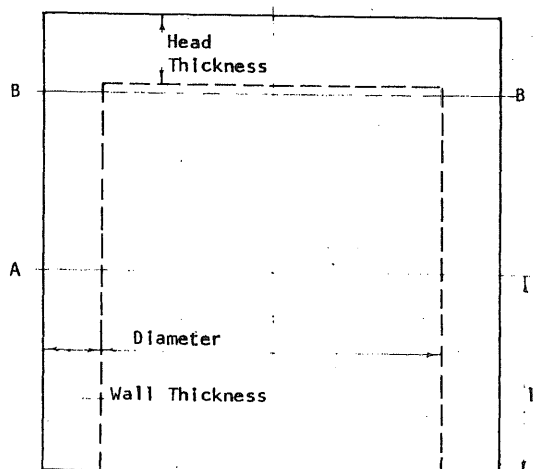
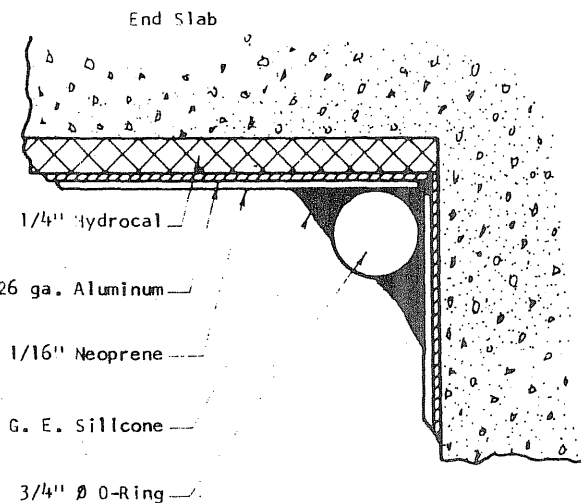


FIG. B10.1 DIMENSIONS OF PV10

| Wall Thickness | | |
|----------------|-------|-------|
| Plane Axis | AA | BB |
| N | 4.950 | 5.118 |
| NE | 5.100 | 5.170 |
| E | 5.232 | 5.178 |
| SE | 5.307 | 5.323 |
| S | 5.209 | 5.277 |
| SW | 5.127 | 5.147 |
| W | 4.982 | |
| NW | 4.915 | 4.890 |

| Inside Diameter, in. | | |
|----------------------|--------------------|--------------------|
| Plane Axis | AA | BB |
| N-S | 30 $\frac{1}{32}$ | 29 $\frac{27}{32}$ |
| NE-SW | 29 $\frac{31}{32}$ | 29 $\frac{30}{32}$ |
| E-W | 29 $\frac{31}{32}$ | 30 |
| SE-NW | 29 $\frac{31}{32}$ | 29 $\frac{30}{32}$ |



B10.2

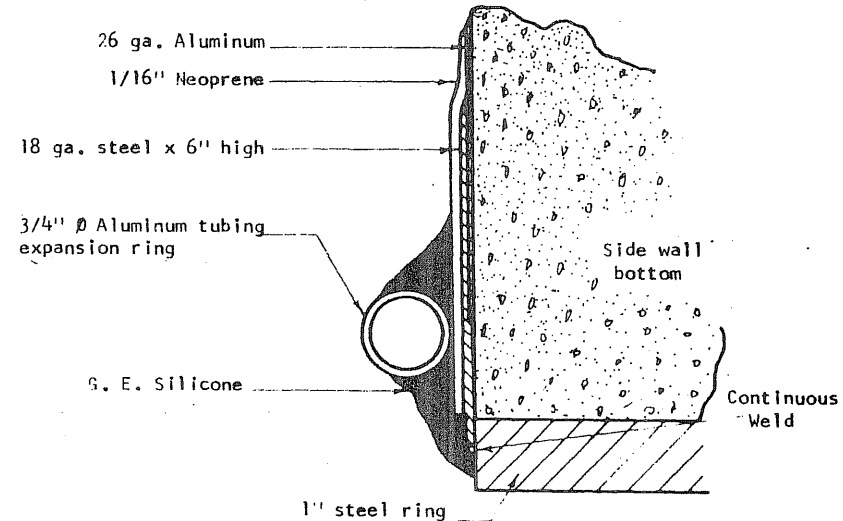
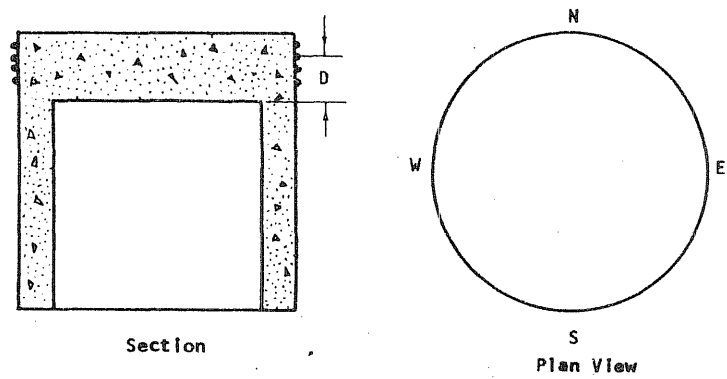


FIG. B10.2 SEALING DETAIL FOR PV10



| Wrap No. | DN | DE | DS | DW |
|----------|---------|---------|---------|---------|
| 1 | 6 13/16 | 7 0/16 | 7 0/16 | 6 14/16 |
| 2 | 6 8/16 | 6 11/16 | 6 11/16 | 6 8/16 |
| 3 | 6 5/16 | 6 7/16 | 6 7/16 | 6 4/16 |
| 4 | 5 13/16 | 6 3/16 | 6 2/16 | 5 15/16 |
| 5 | 5 9/16 | 5 14/16 | 5 14/16 | 5 11/16 |
| 6 | 5 3/16 | 5 9/16 | 5 9/16 | 5 4/16 |
| 7 | 4 13/16 | 5 3/16 | 5 2/16 | 4 14/16 |
| 8 | 4 9/16 | 4 14/16 | 4 14/16 | 4 11/16 |
| 9 | 4 6/16 | 4 10/16 | 4 10/16 | 4 7/16 |
| 10 | 4 0/16 | 4 6/16 | 4 5/16 | 4 2/16 |
| 11 | 3 10/16 | 4 1/16 | 4 0/16 | 3 13/16 |
| 12 | 3 5/16 | 3 11/16 | 3 5/16 | 3 7/16 |
| 13 | 3 0/16 | 3 6/16 | 3 1/16 | 3 3/16 |
| 14 | 2 11/16 | 3 1/16 | 2 11/16 | 2 14/16 |
| 15 | 2 6/16 | 2 11/16 | 2 6/16 | 2 8/16 |
| 16 | 2 1/16 | 2 6/16 | 2 1/16 | 2 3/16 |
| 17 | 1 11/16 | 2 1/16 | 1 12/16 | 1 13/16 |
| 18 | 1 6/16 | 1 12/16 | 1 6/16 | 1 2/16 |
| 19 | 1 1/16 | 1 7/16 | 1 1/16 | 1 2/16 |
| 20 | 12/16 | 1 1/16 | 12/16 | 13/16 |
| 21 | 7/16 | 12/16 | 6/16 | 9/16 |
| 22 | 1/16 | 7/16 | 1/16 | 4/16 |

FIG. B10.3. MEASURED LOCATION OF THE CIRCUMFERENTIAL PRESTRESS WIRE AT THE ENDS OF THE N-S and E-W DIAMETERS ON PV10

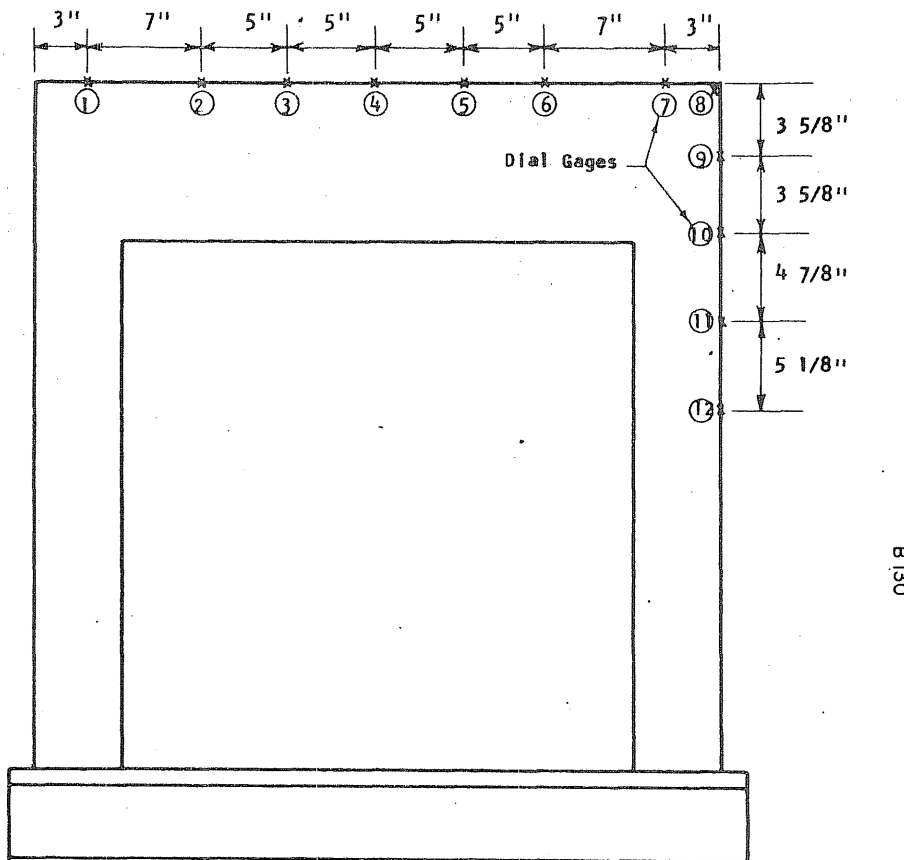


FIG. B10.4 LOCATION OF DEFLECTION GAGES ON PV10

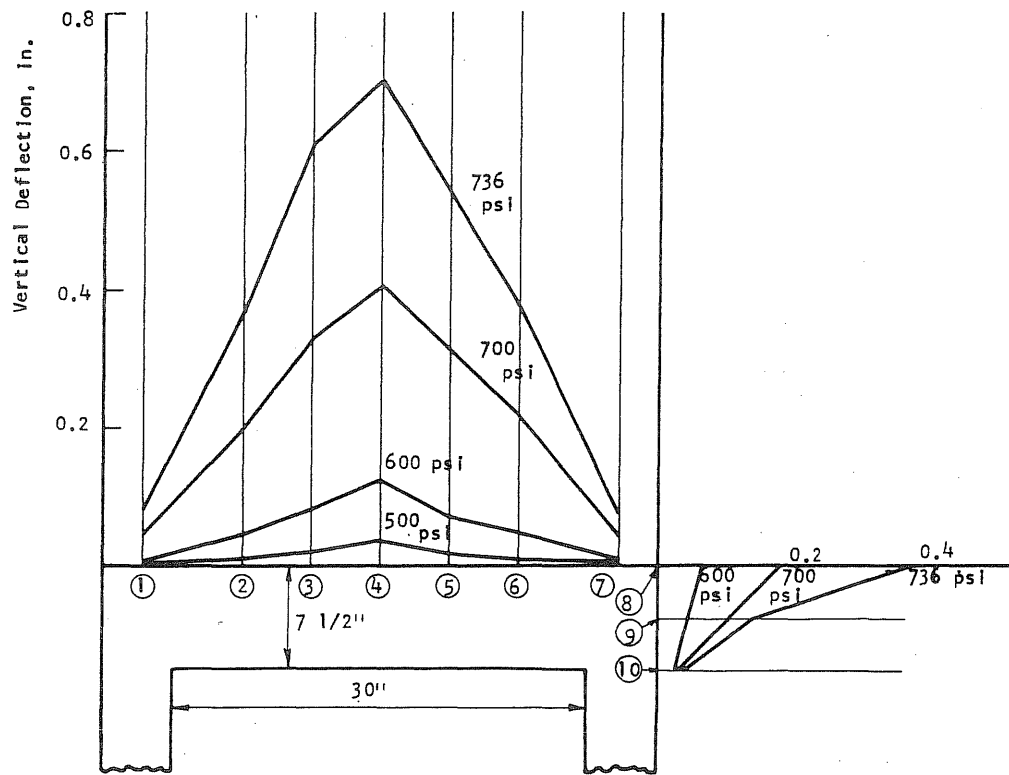


FIG. B10.5 DEFLECTION PROFILES OF THE END SLAB ALONG THE N-S DIAMETER OF PV10

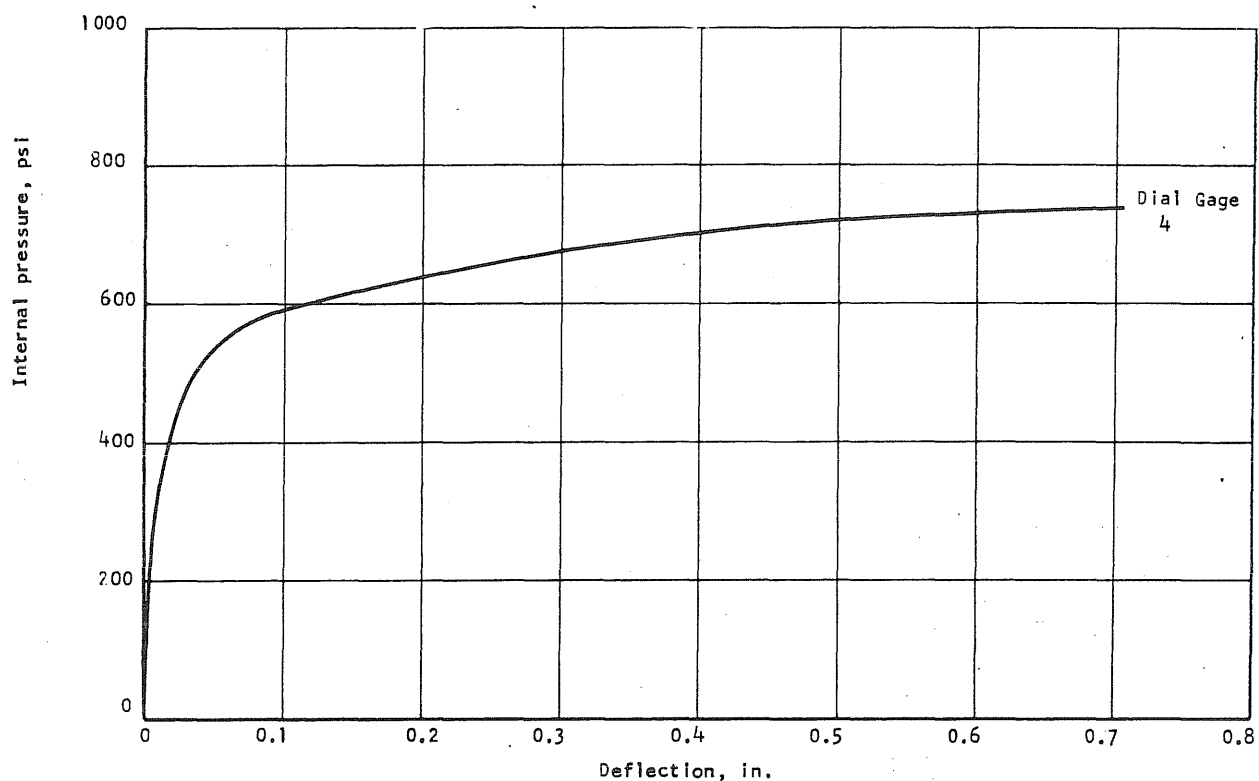
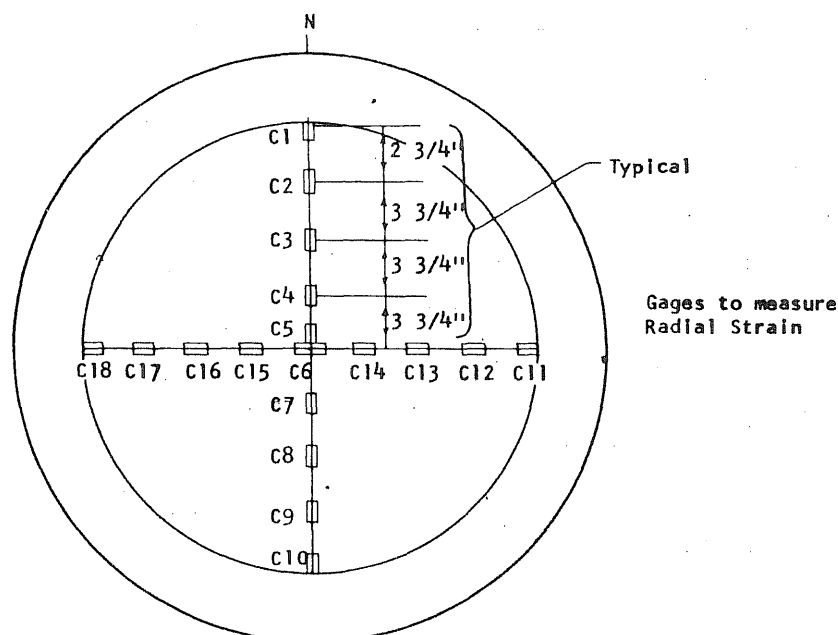
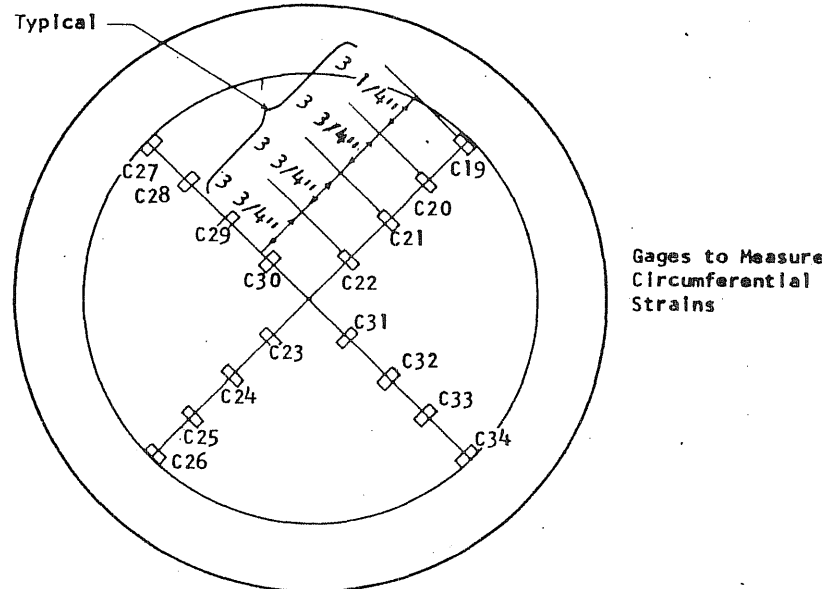
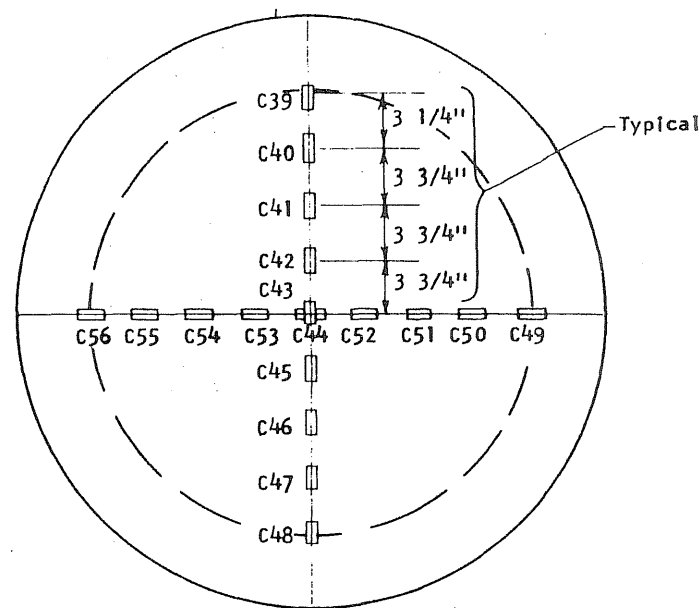


FIG. B10.6 APPLIED PRESSURE VS DEFLECTION AT MIDSPAN OF PV10

Concrete Gages on the Inside of the End Slab



Concrete Gages on the Outside of the End Slab



Steel Gages on Circumferential Prestress Wire

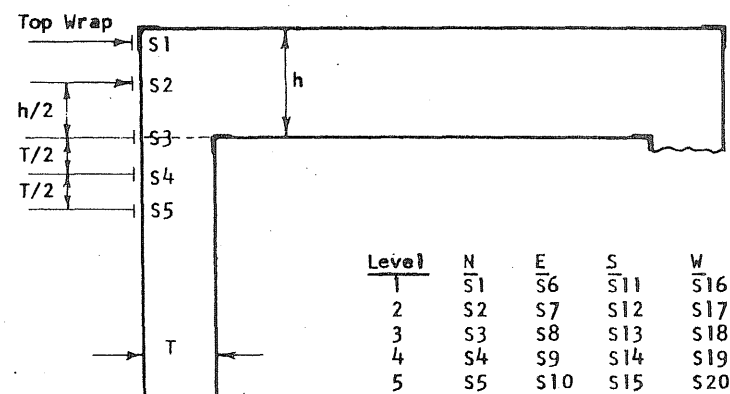


FIG. B10.7 (cont'd) STRAIN GAGE LOCATIONS ON PV10

FIG. B10.7 STRAIN GAGE LOCATION ON PV10

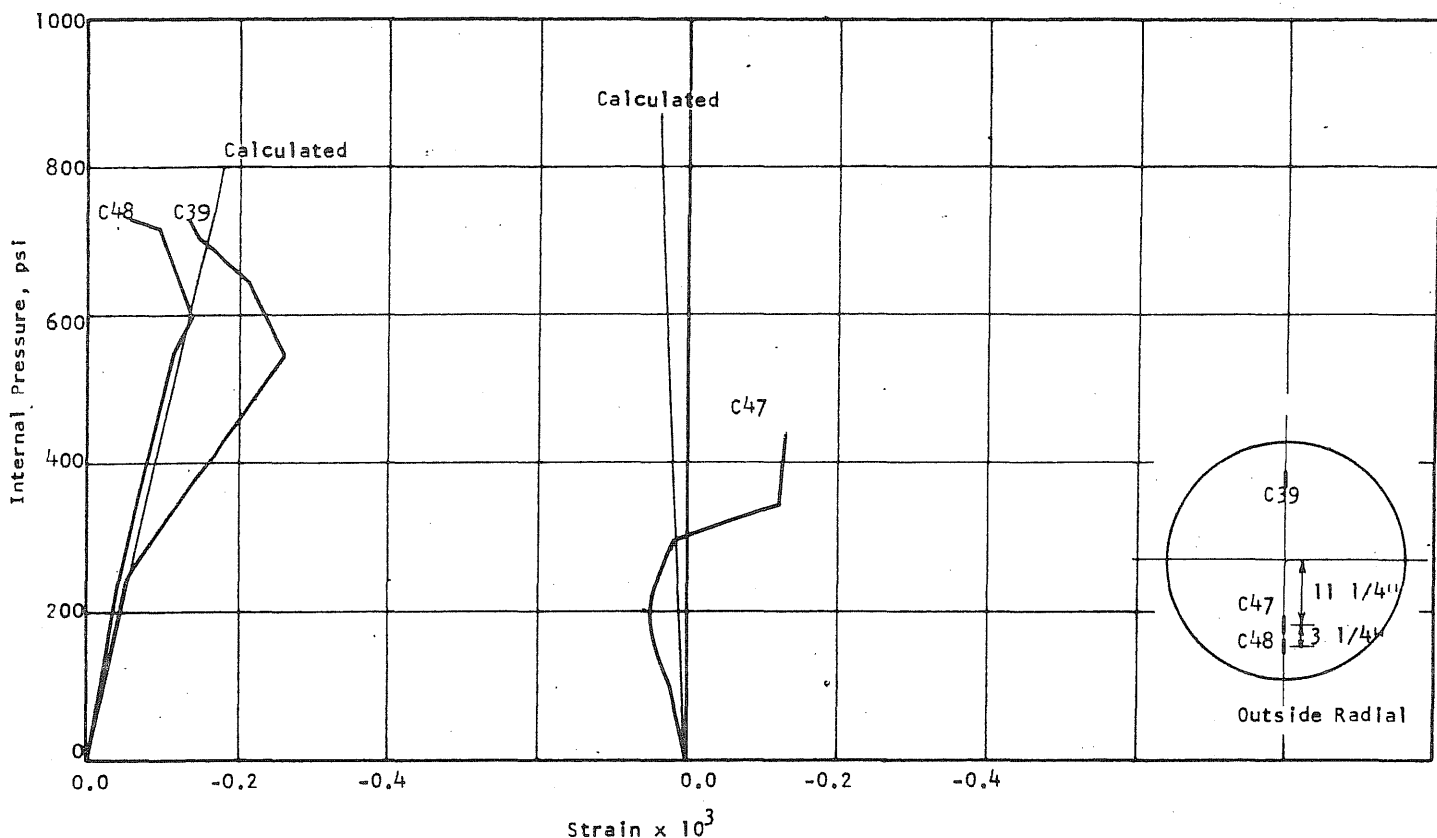


FIG. B10.8 CONCRETE STRAINS, VESSEL PV10

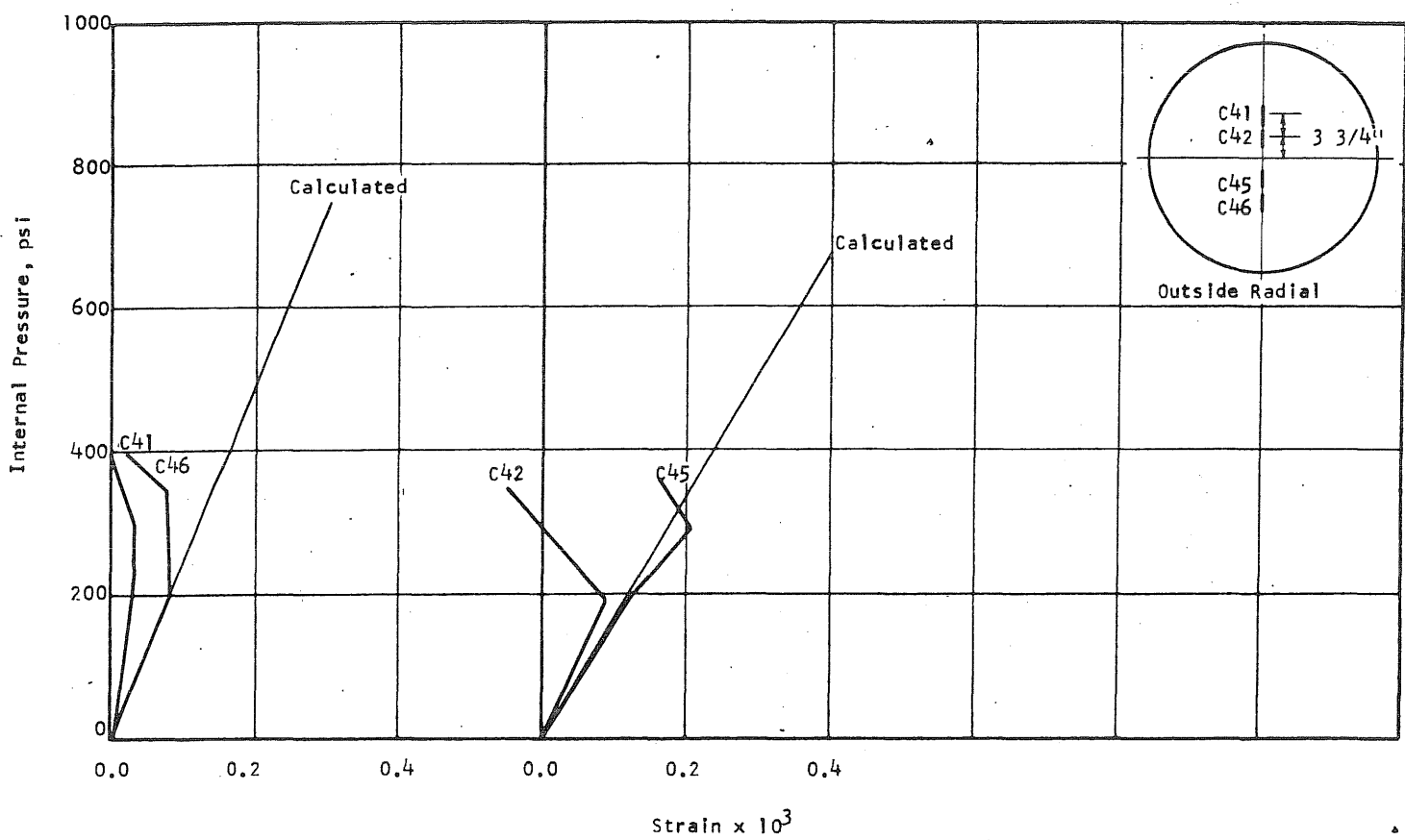


FIG. B10.8 (cont'd) CONCRETE STRAINS, VESSEL PV10

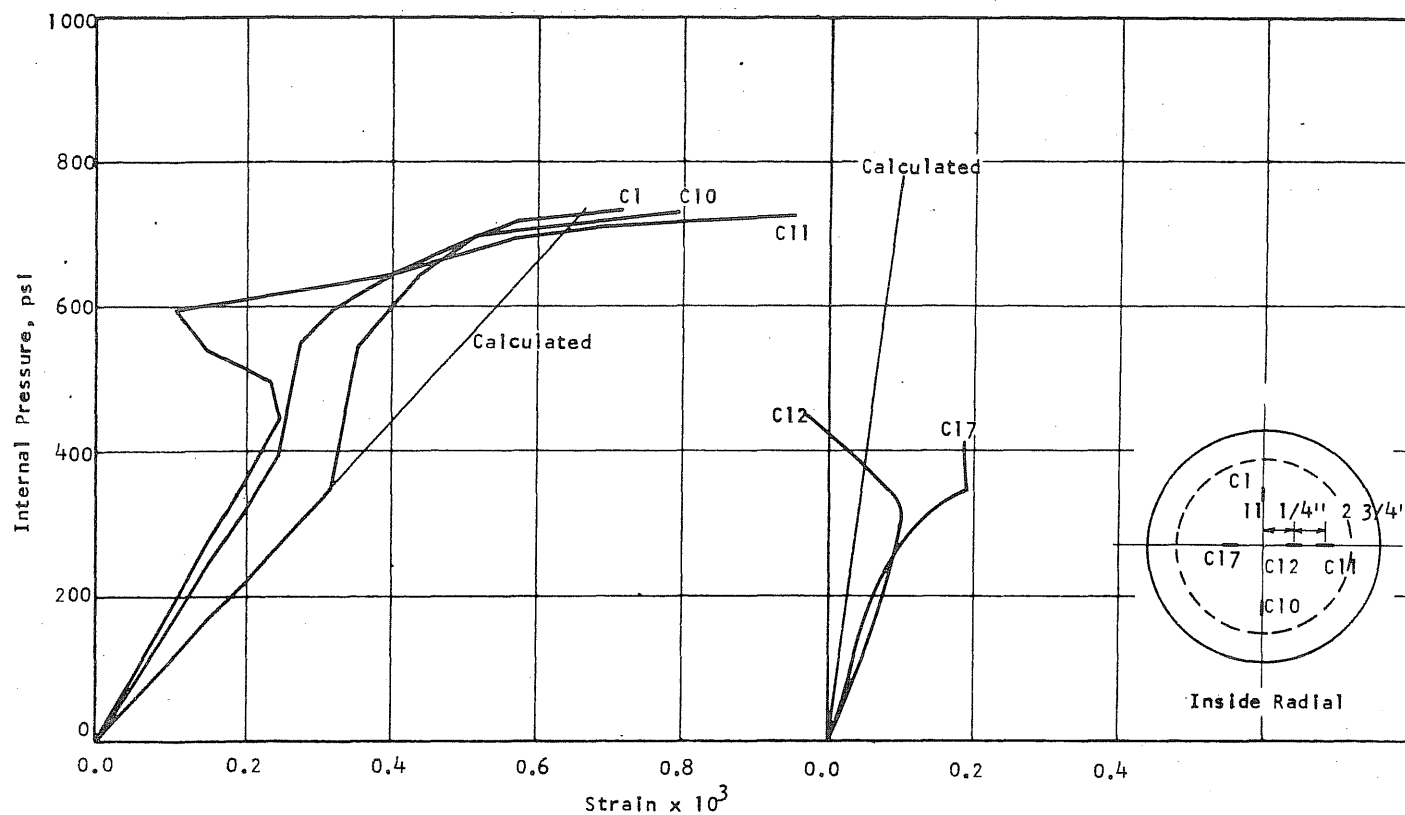


FIG. 810.9 CONCRETE STRAINS, VESSEL PV10

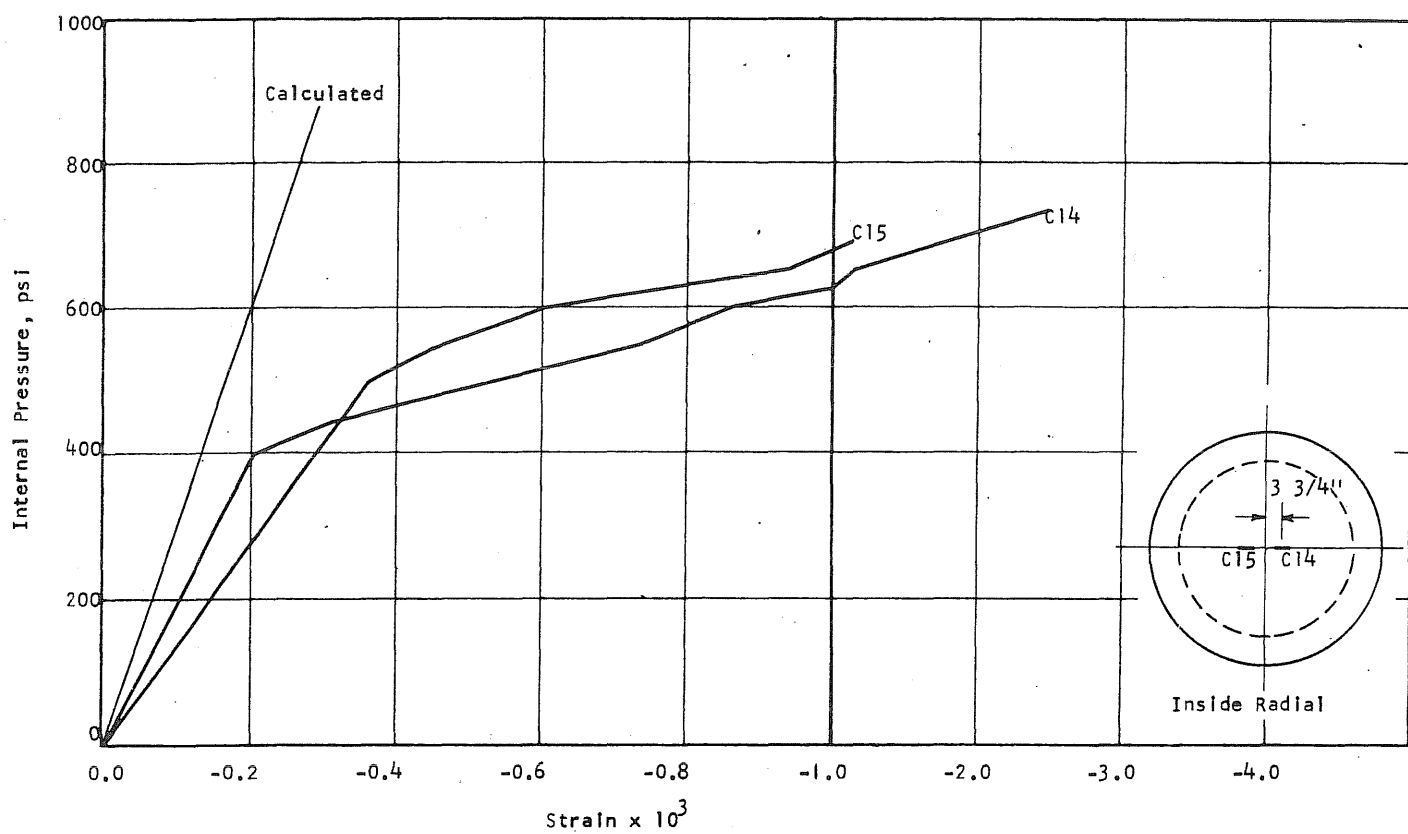


FIG. 810.9 (cont'd) CONCRETE STRAINS, VESSEL PV10

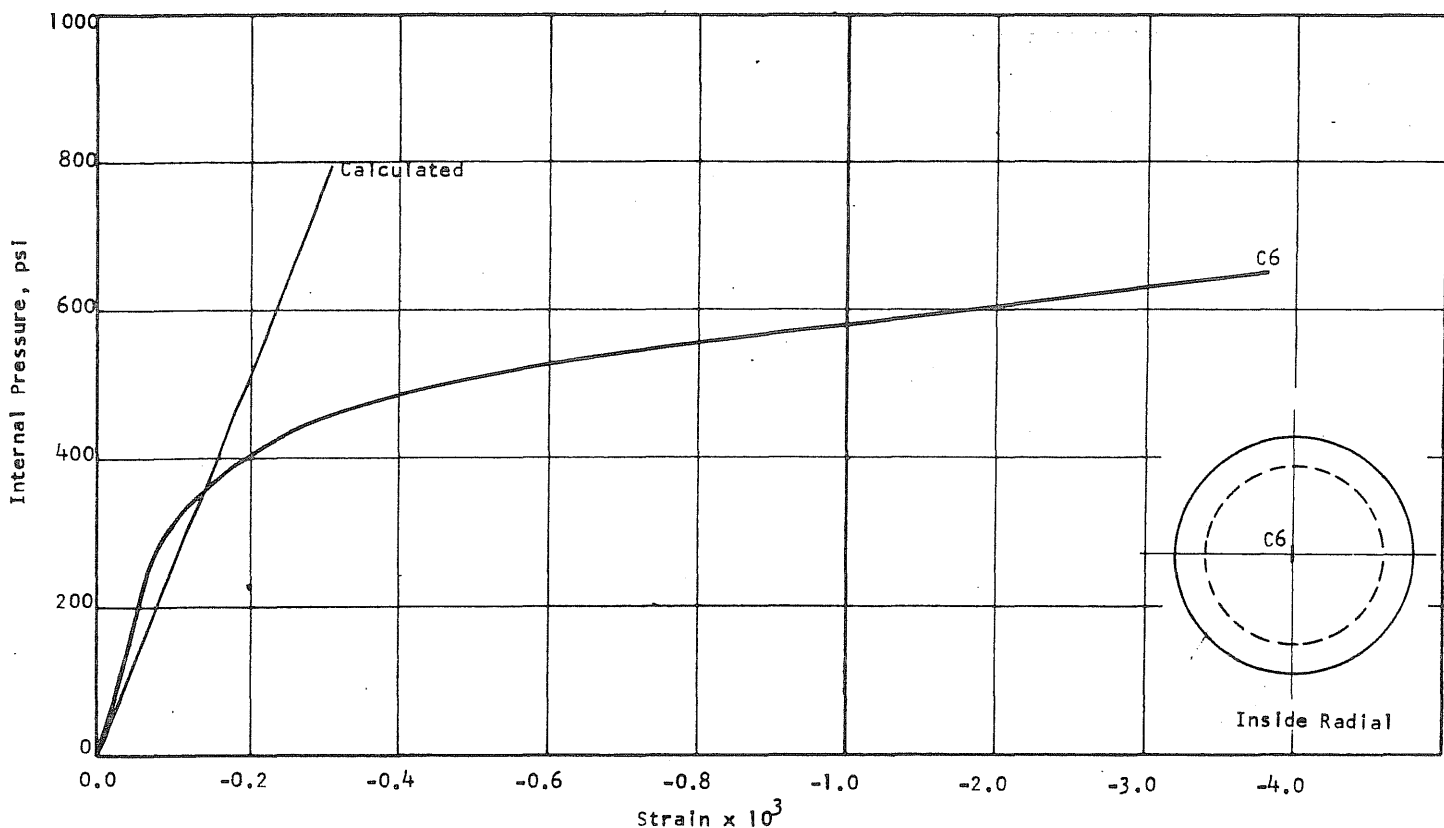


FIG. B10.9 (cont'd) CONCRETE STRAINS, VESSEL PV10

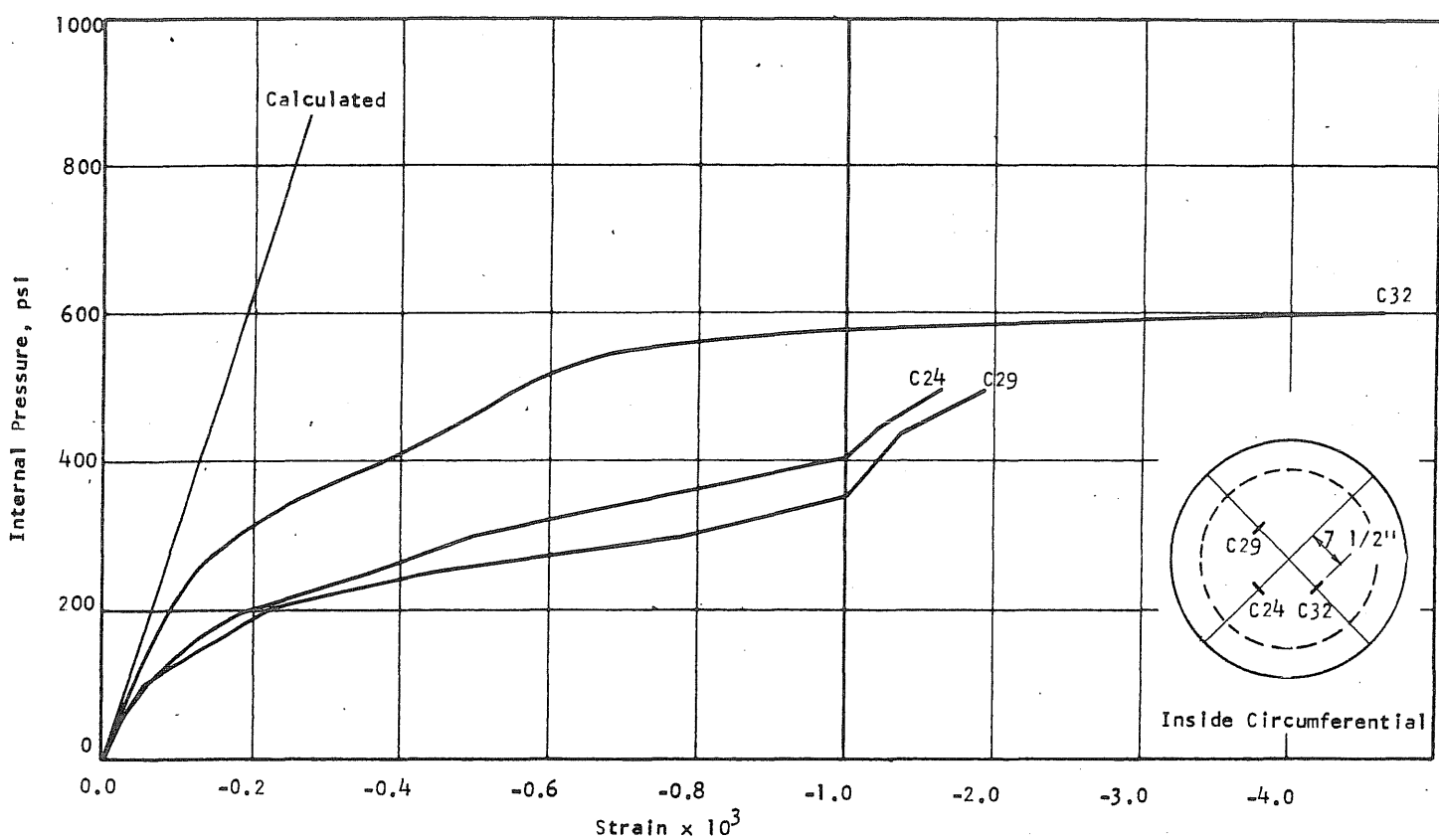


FIG. B10.10 CONCRETE STRAINS, VESSEL PV10

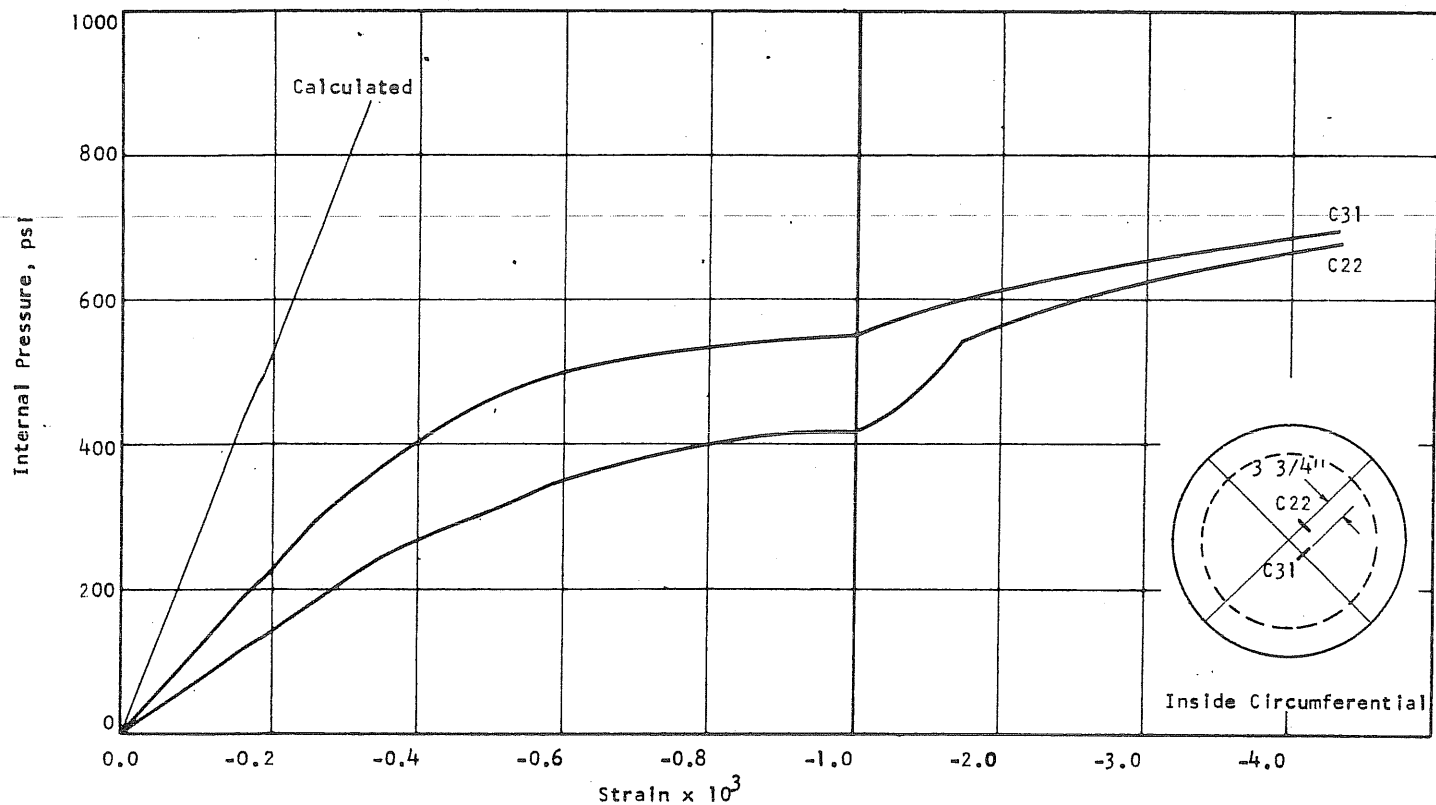


FIG. B10.10 (cont'd) CONCRETE STRAINS, VESSEL PV10

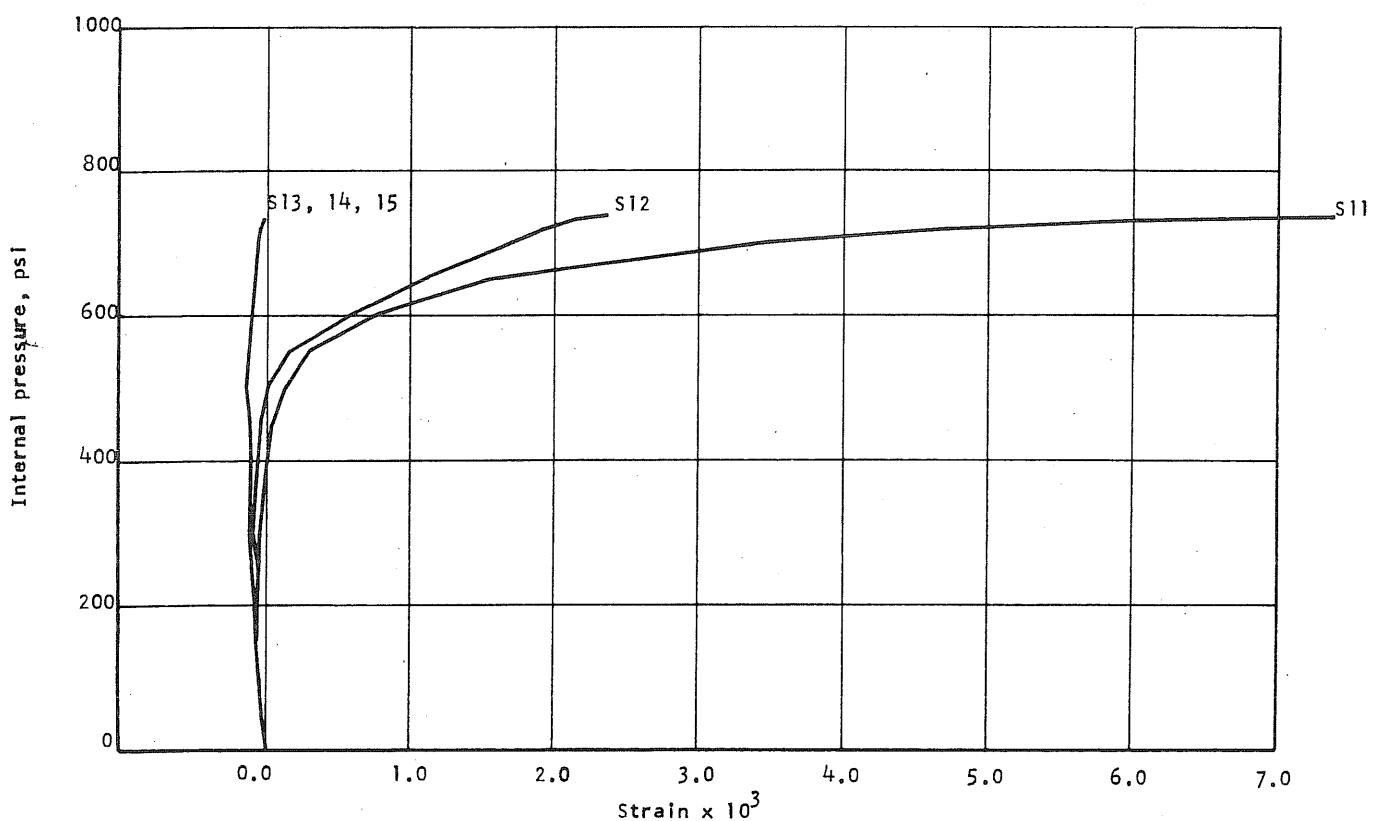


FIG. B10.11 APPLIED PRESSURE vs STRAIN IN CIRCUMFERENTIAL PRESTRESS WIRE AT THE S-END OF THE N-S DIAMETER OF PV10

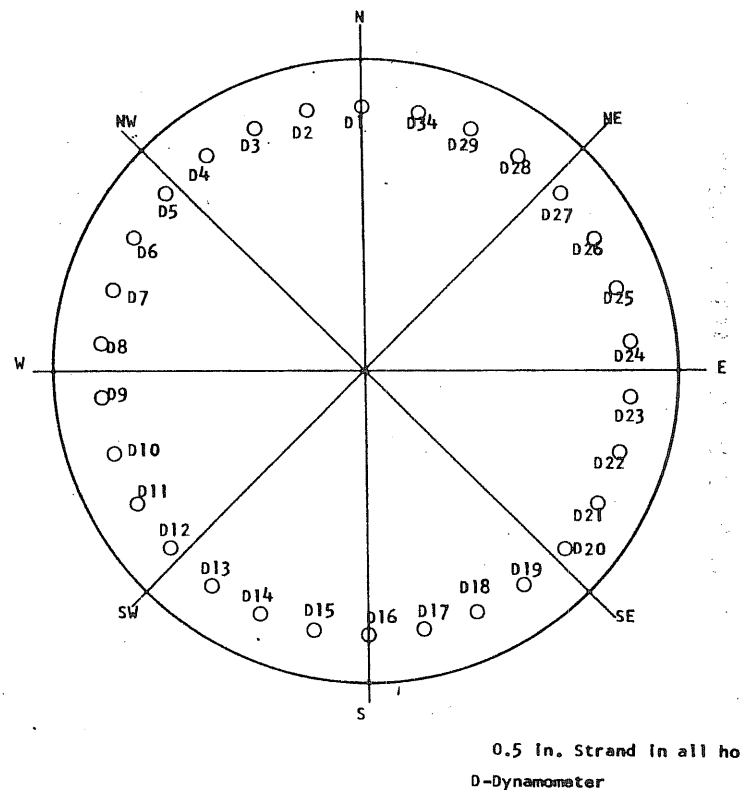


FIG. B10.12 LOCATION OF LONGITUDINAL REINFORCEMENT

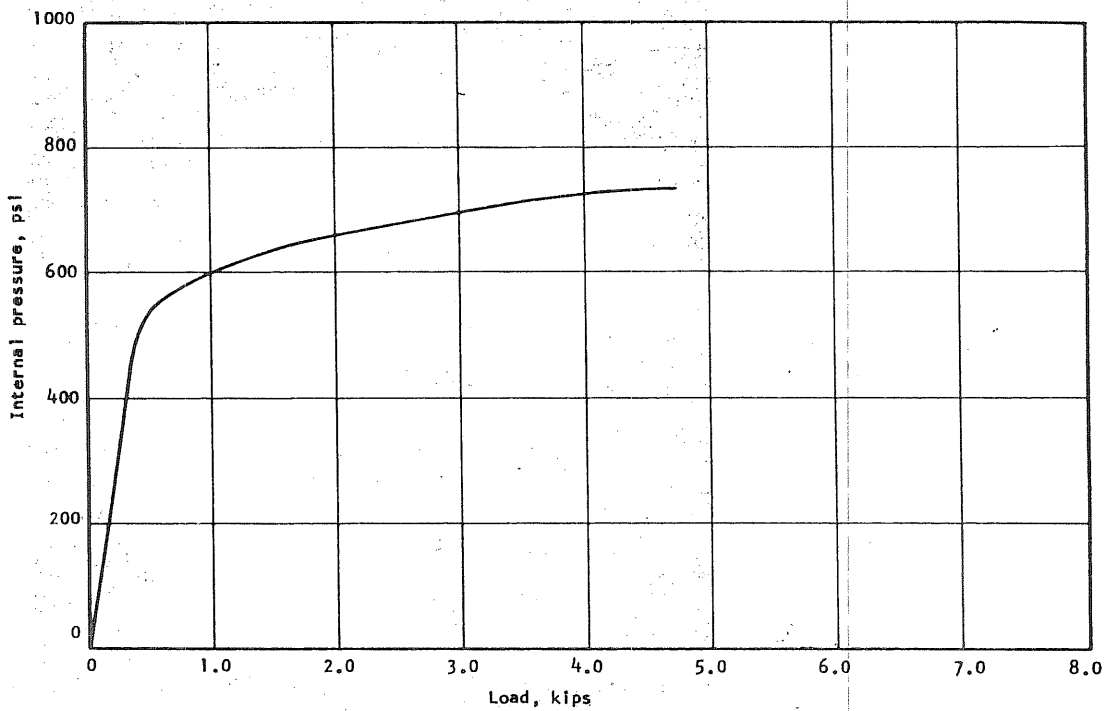


FIG. B10.13 APPLIED PRESSURE vs INCREASE IN LOAD IN DYNAMOMETER NO. 26

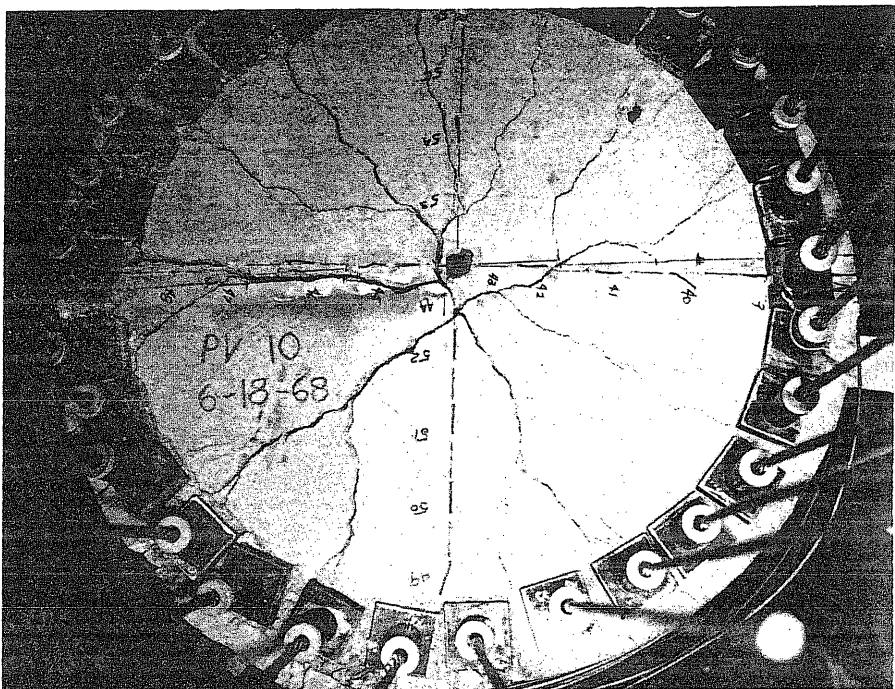


FIG. B10.14 END SLAB AFTER FAILURE

B11 Test Vessel PV11 ($t = 7.5$ in., $s = 1/4$ in.)

Test vessel PV11 was cast in the laboratory and was uncracked prior to prestressing. After circumferential prestressing a crack was observed on the inside of the vessel at 13.5 in. from the top. The 1/4-in. circumferential prestressing wire was wrapped continuously so that cracking on the outside could not be observed.

The liner detail was similar to the one used for PV9 and PV10. The aluminum liner was temporarily sealed and pressed into place with 70 psi air pressure before the neoprene was put on. A combination of 28 stressteel rods and two strands were used for the longitudinal prestressing.

Pressure was increased in 100-psi increments up to 1600 psi, when a seal blew in the gas regulator causing a leak. The pressure decreased to 250 psi while a higher capacity regulator was being installed. When repressurizing was attempted, it was found that the sealing in the vessel had failed. The vessel had a well developed system of radial cracks. A new 3/4-in. O-ring was installed after the old O-ring and caulking were removed. A second test was attempted and a pressure of 1830 psi was reached over a period of about 2 hours. At that pressure a leak in the liner became so severe that further increase in pressure was impossible. Center deflection was about 0.15 in.

The vessel was resealed which involved removing the O-ring and neoprene from the end slab surface and pouring a one-in. thick layer of hydrocal over the exposed aluminum. This hydrocal was covered with aluminum and neoprene and a new 3/4-in. O-ring was installed. It was hoped that the additional hydrocal would move the corner seal away from the actual corner

of the vessel and minimize deformations in the seal. This time 30 stresssteel rods were used for prestressing.

The vessel was again tested and reached 1980 psi in 45 minutes with only deflection readings being taken. The vessel leaked again. The leak was determined to be in the end slab since no water was being expelled. It was a small leak. The regulator was bypassed and the gas supply flowed directly from a 2600 psi nitrogen bottle into the specimen. The vessel failed at 2040 psi in about five minutes while reading the center deflection. A photograph showing the type of failure is shown in Fig. B11.13. Data from only the first test is presented with the exception of the load deflection curve for the center of the end slab for the final test.

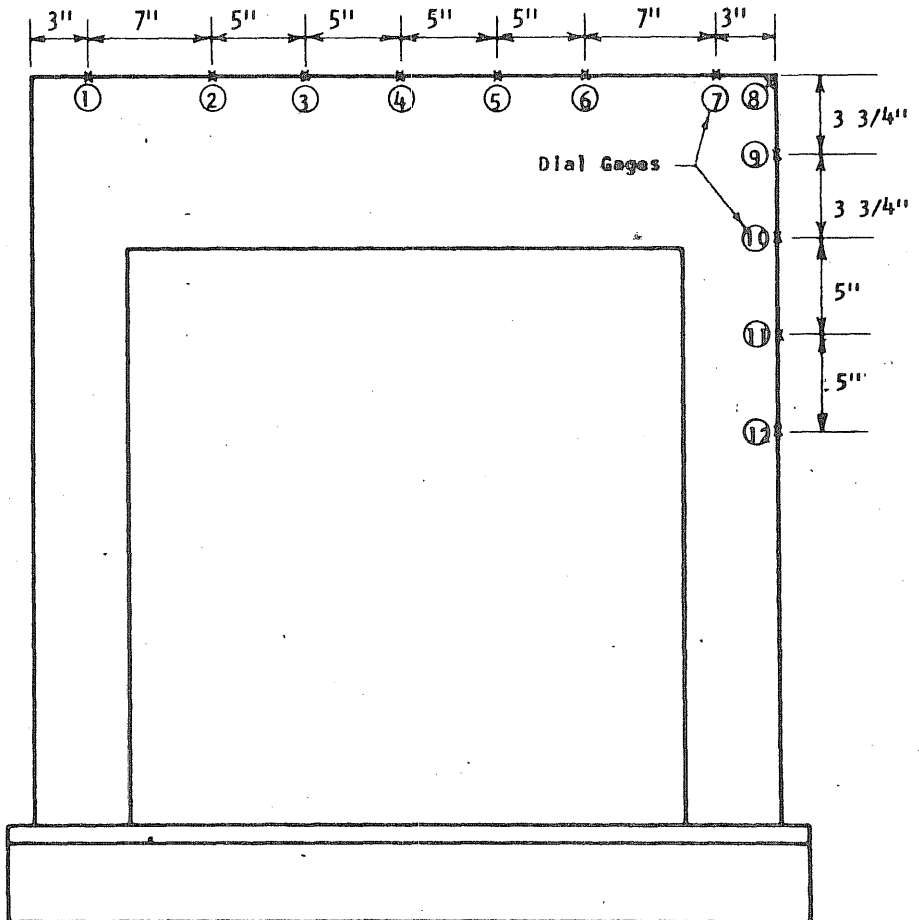
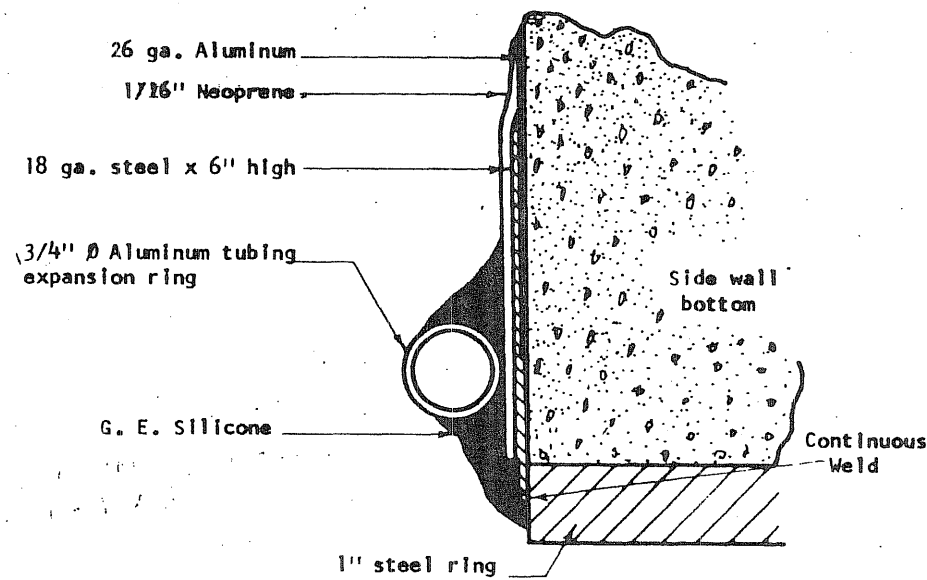
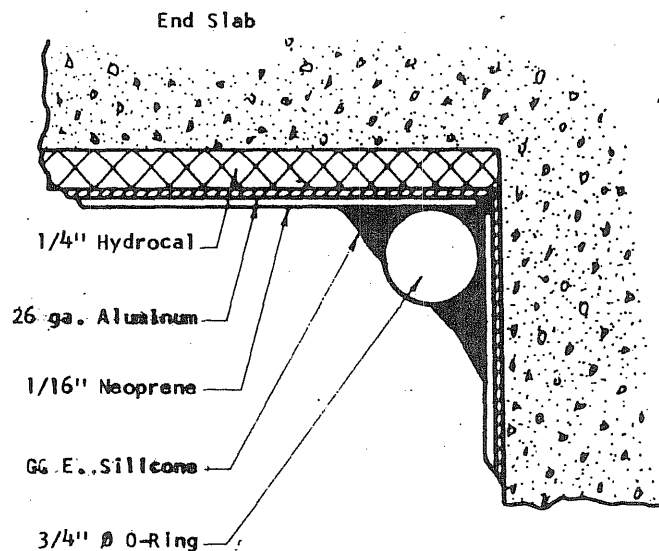


FIG. B11.2 LOCATION OF DEFLECTION GAGES ON PVII

FIG. B11.1 SEALING DETAIL FOR PVII

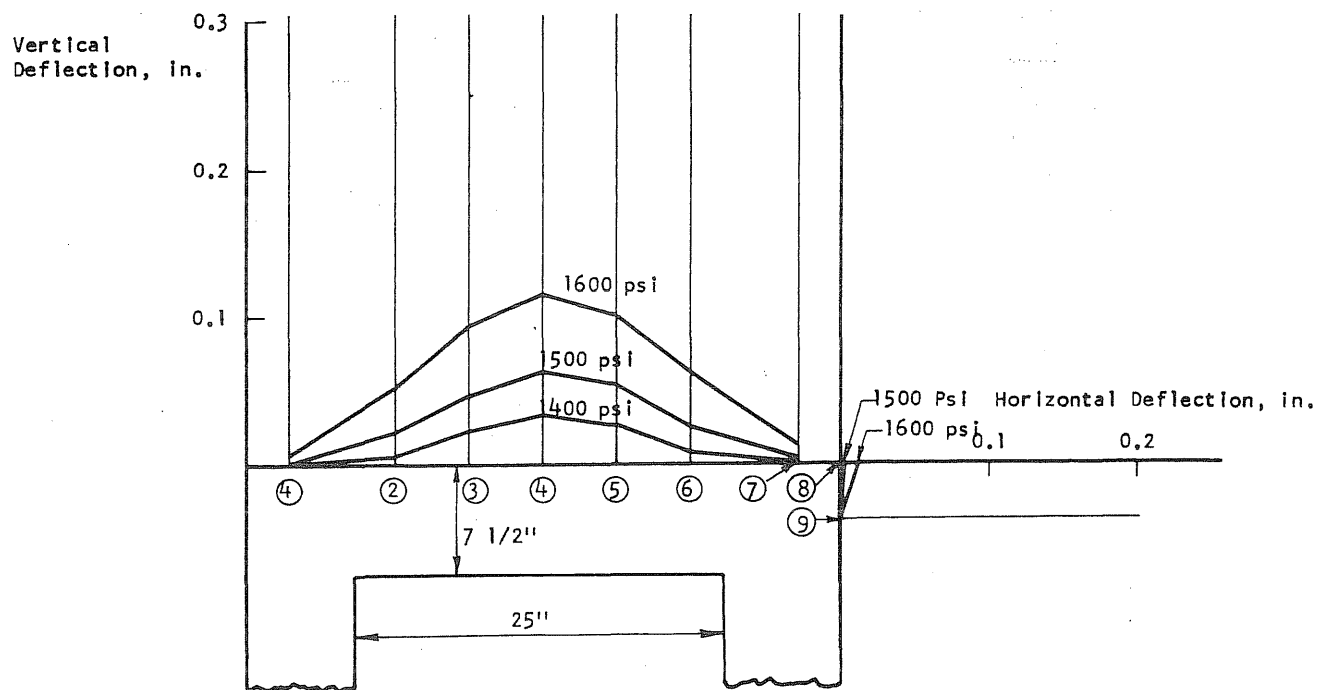


FIG. B11.3 DEFLECTION PROFILES OF THE END SLAB ALONG THE N-S DIAMETER OF PV11

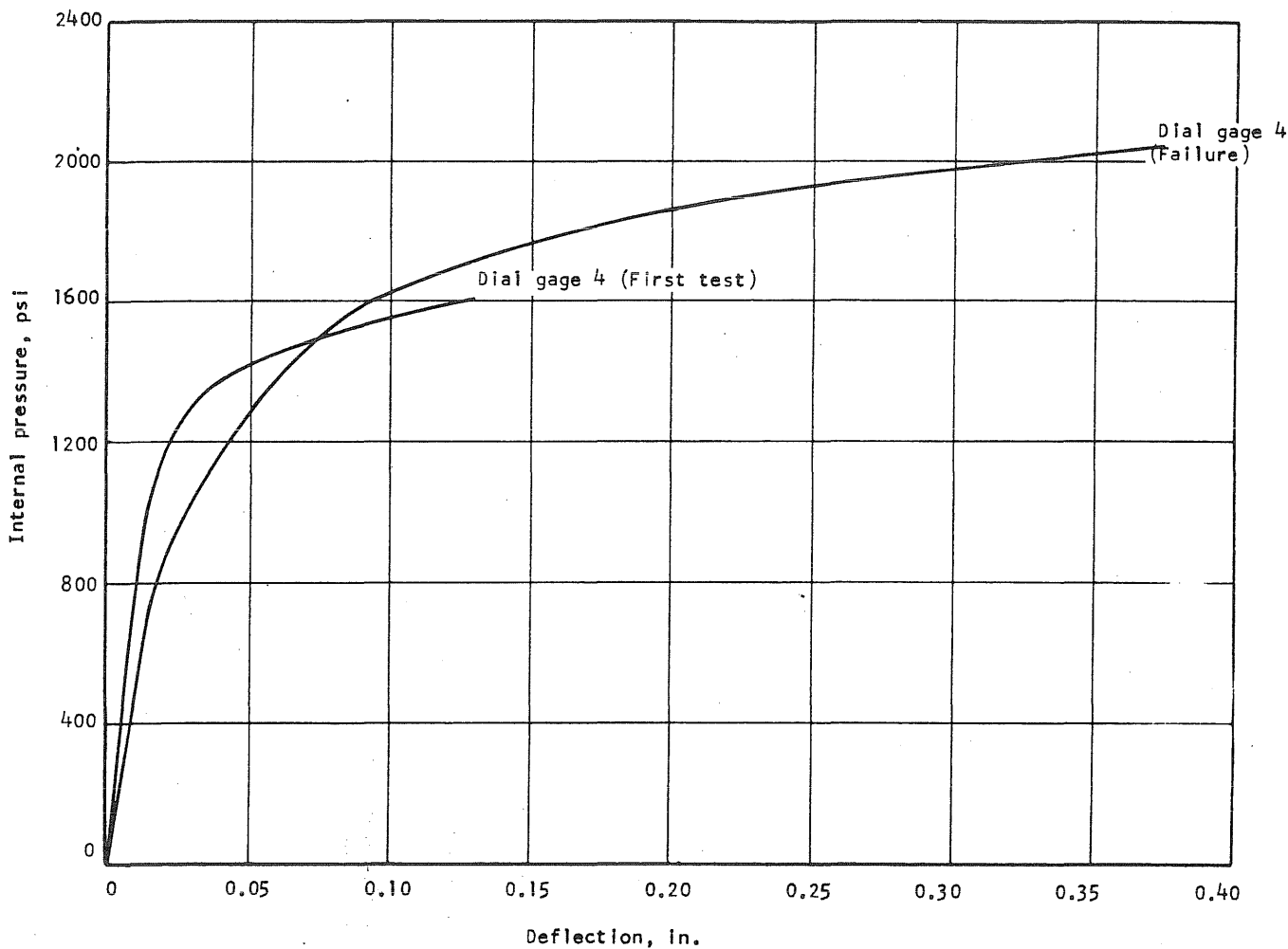
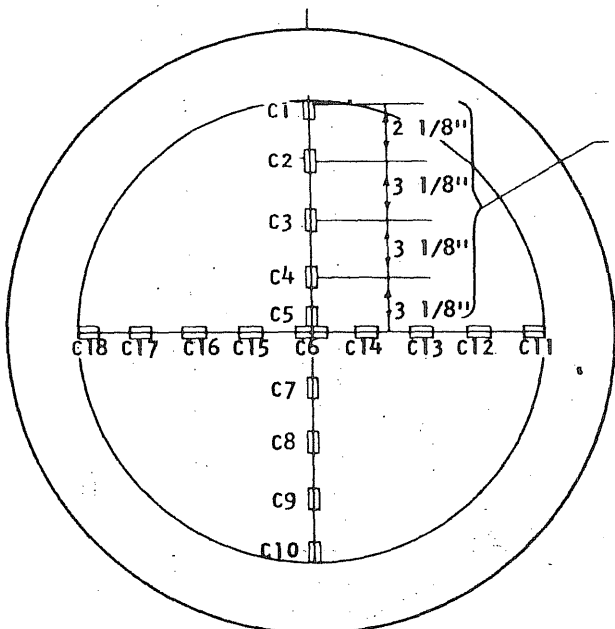


FIG. B11.4 APPLIED PRESSURE VS DEFLECTION AT MIDSPAN OF PV11

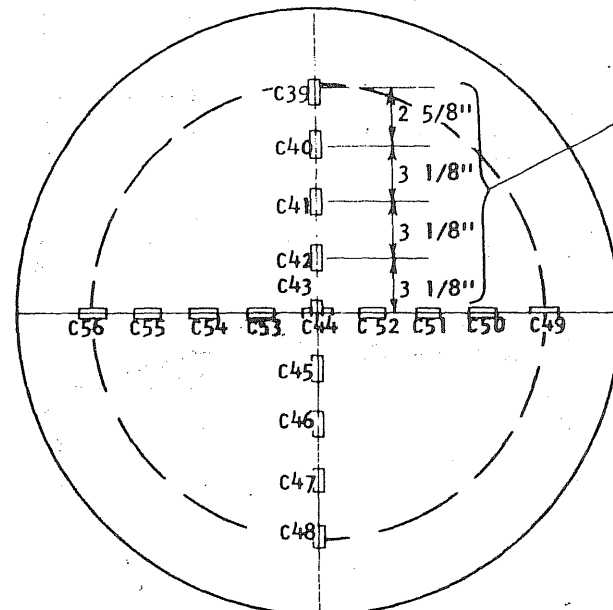
Concrete Gages on the Inside of the End Slab



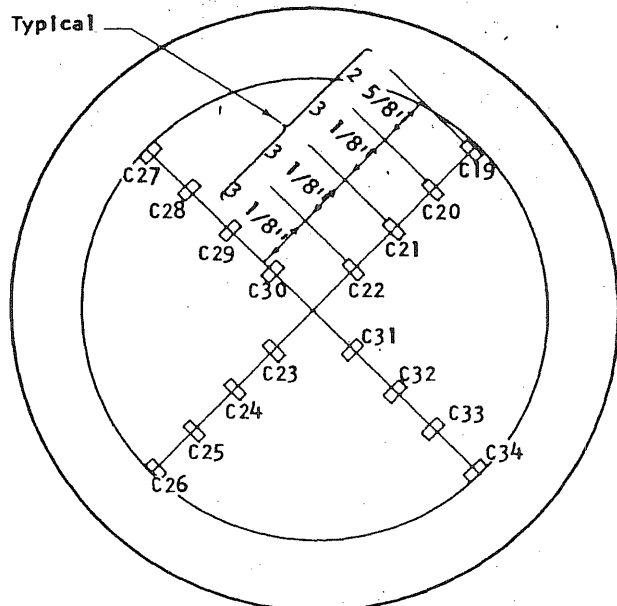
Typical

Gages to Measure
Radial Strain

Concrete gages on the Outside of the End Slab



Typical



Gages to Measure
Circumferential
Strains

B-143

Steel Gages on Circumferential Prestress Wire

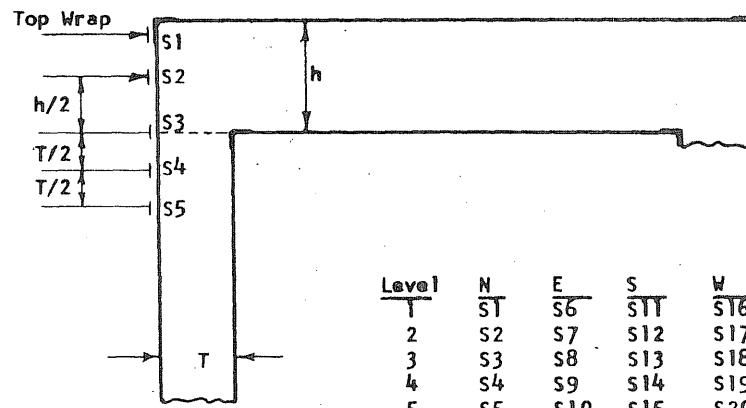


FIG. B11.5 (cont'd) STRAIN GAGE LOCATIONS ON PVII

FIG. B11.5 STRAIN GAGE LOCATIONS ON PVII

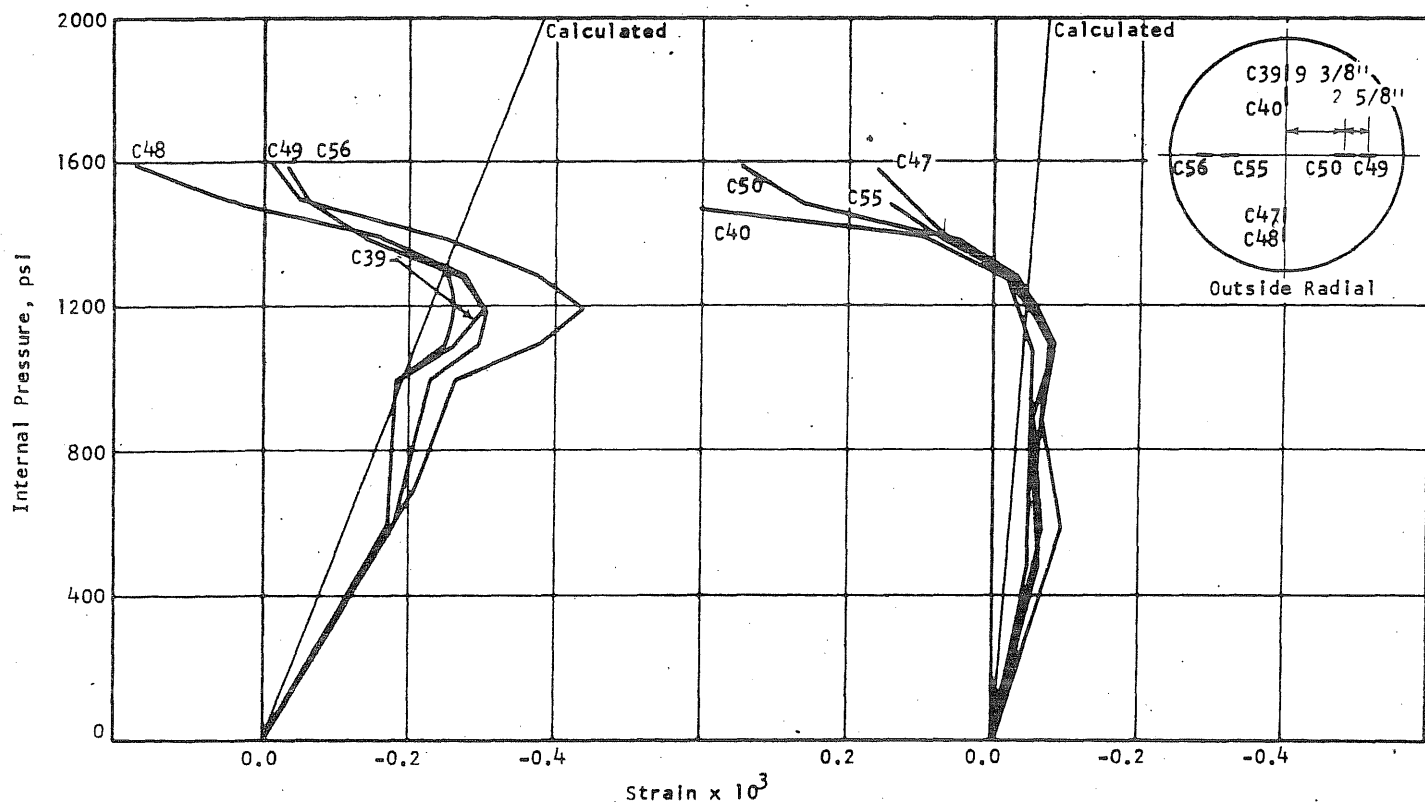


FIG. B11.6 CONCRETE STRAINS, VESSEL PVII

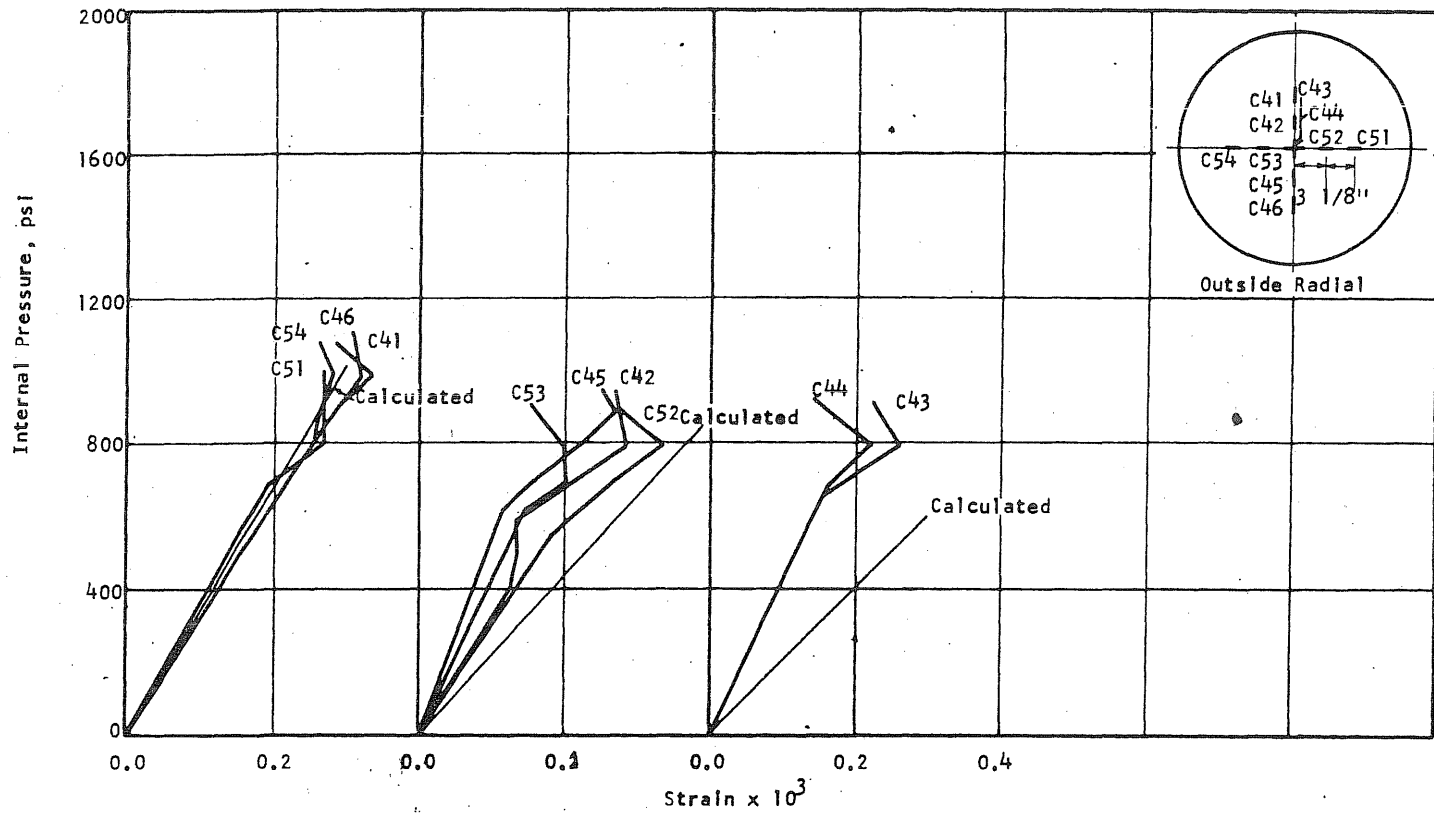


FIG. B11.6 (cont'd) CONCRETE STRAINS, VESSEL PVII

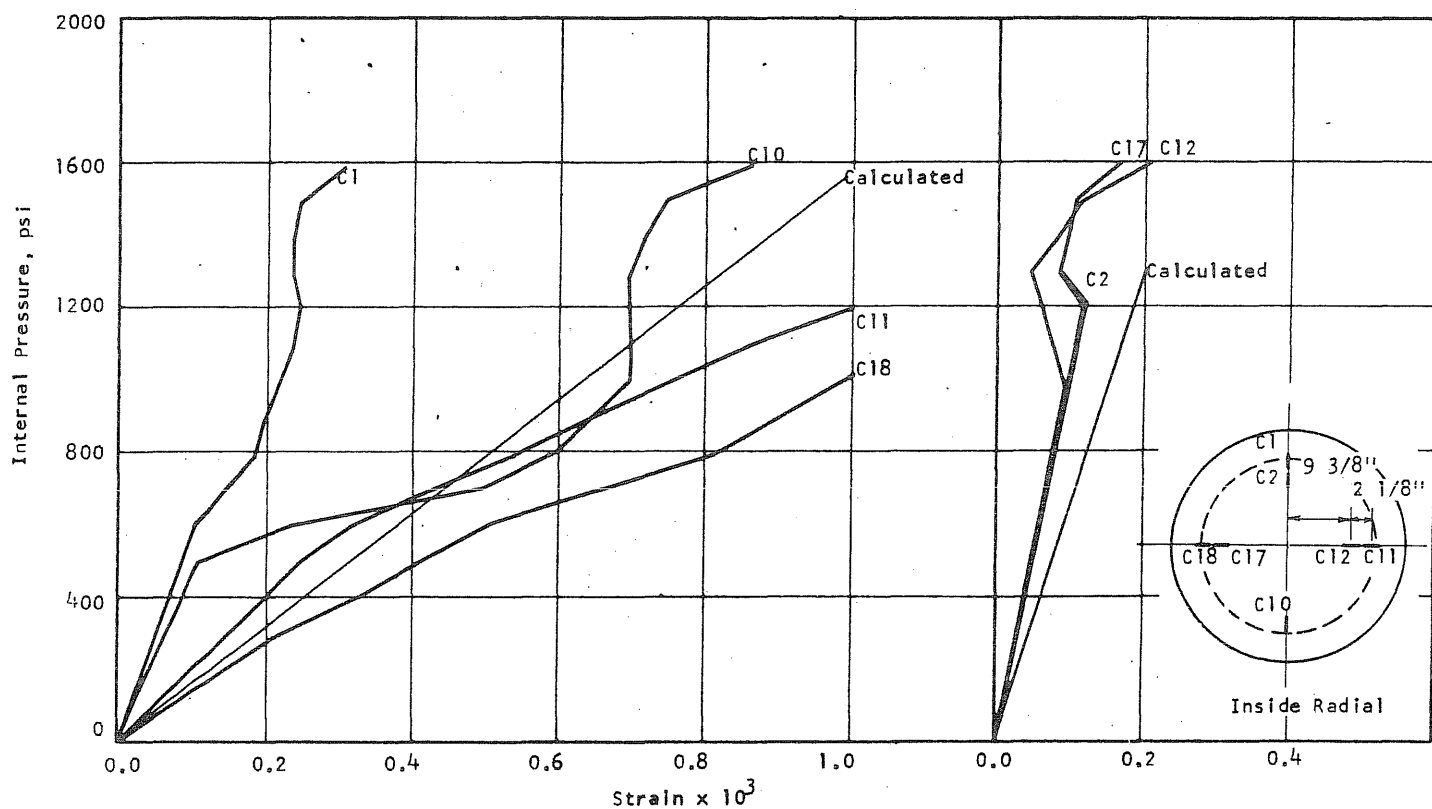


FIG. B11.7 CONCRETE STRAINS, VESSELS PV11

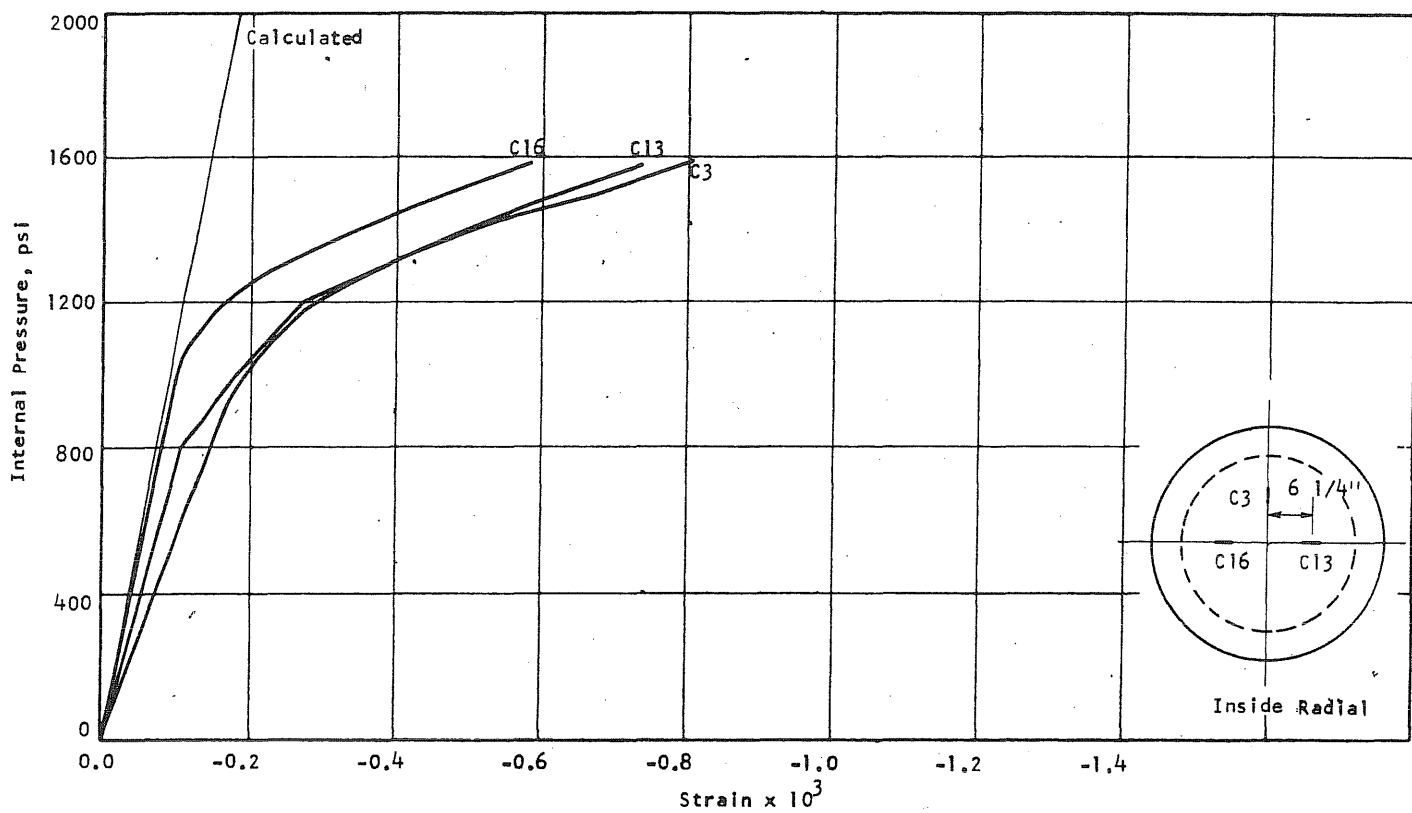


FIG. B11.7 (cont'd) CONCRETE STRAINS, VESSELS PV11

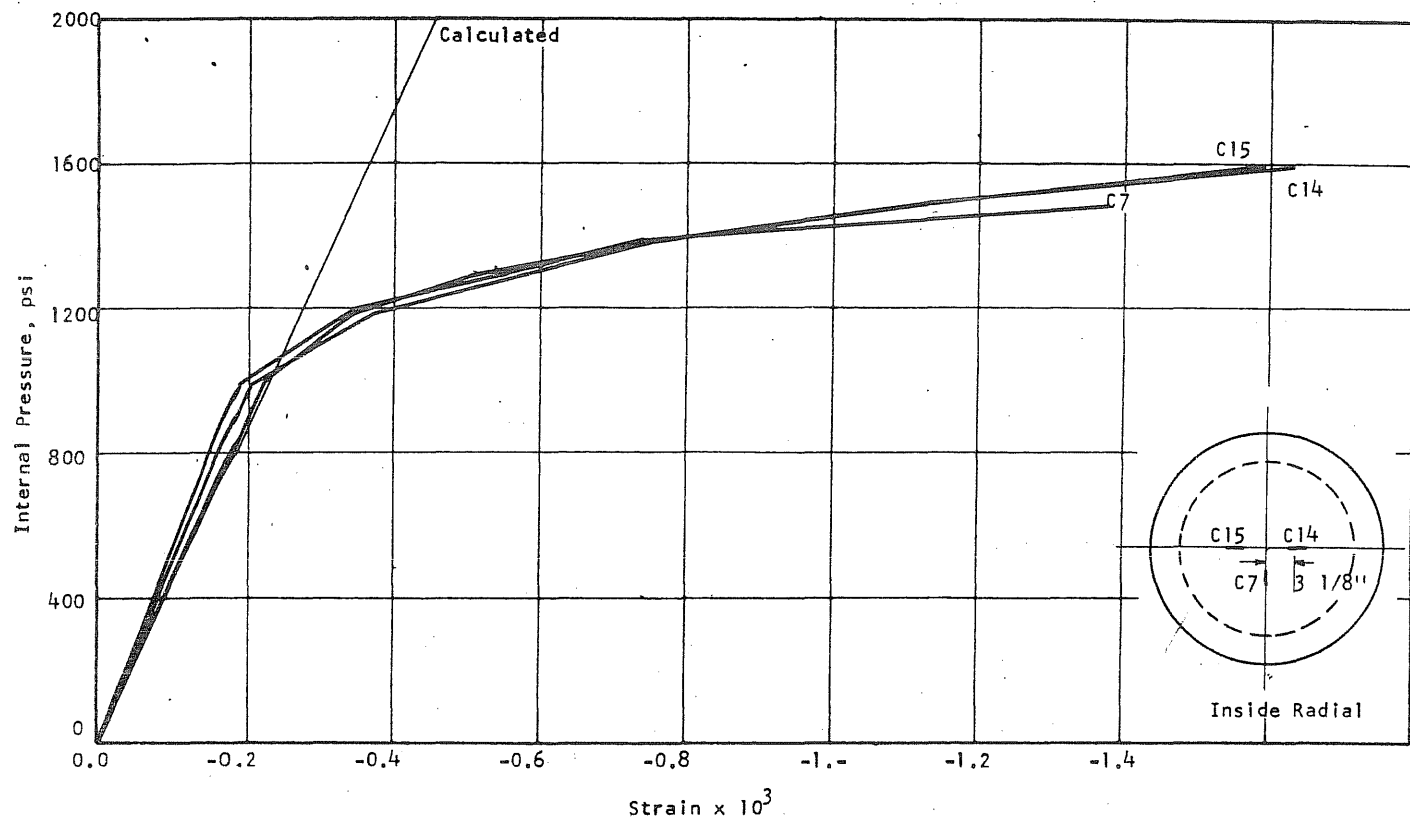


FIG. B11.7 (cont'd) CONCRETE STRAINS, VESSELS PVII

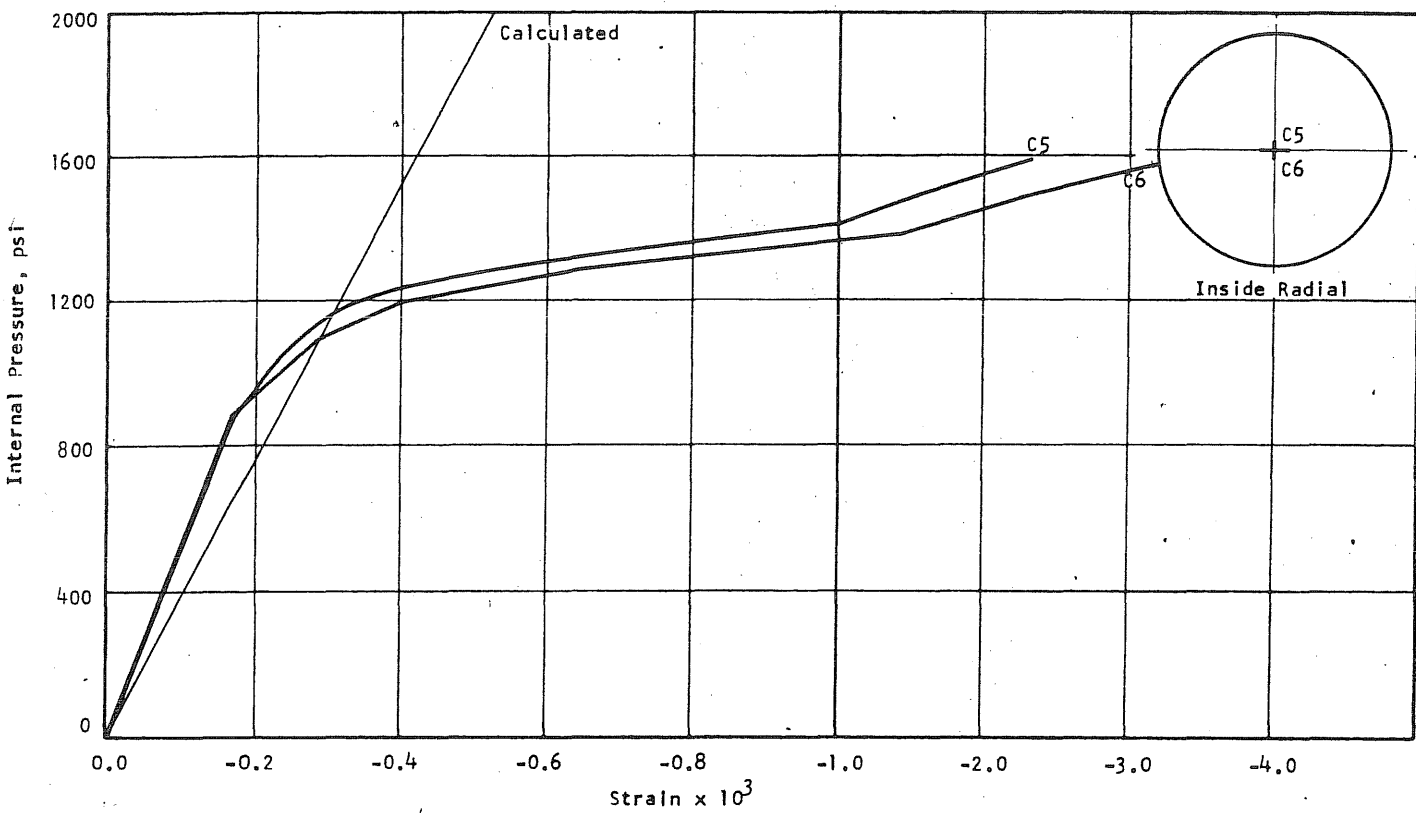


FIG. B11.7 (cont'd) CONCRETE STRAINS, VESSELS PVII

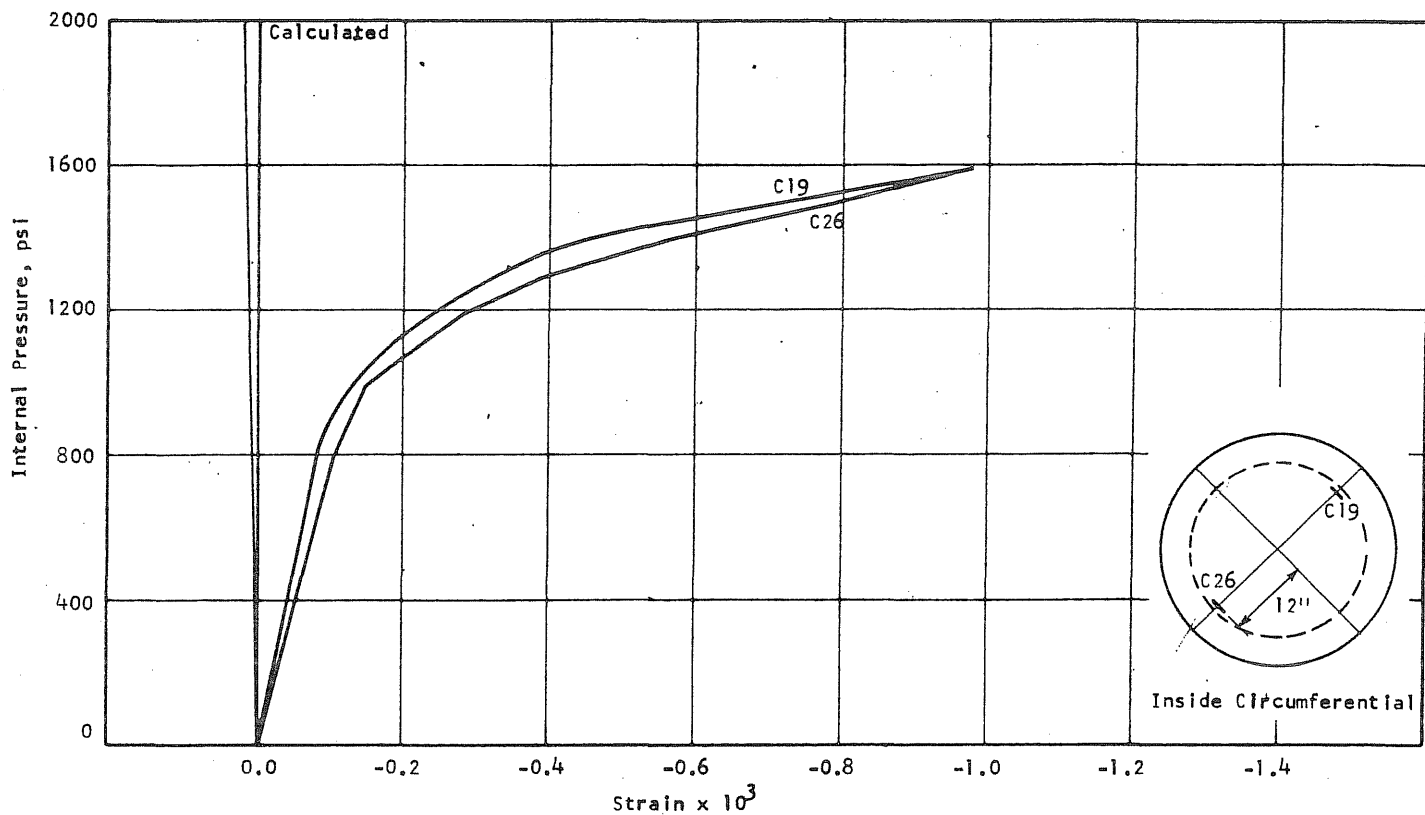


FIG. B11.8 CONCRETE STRAINS, VESSEL PV11

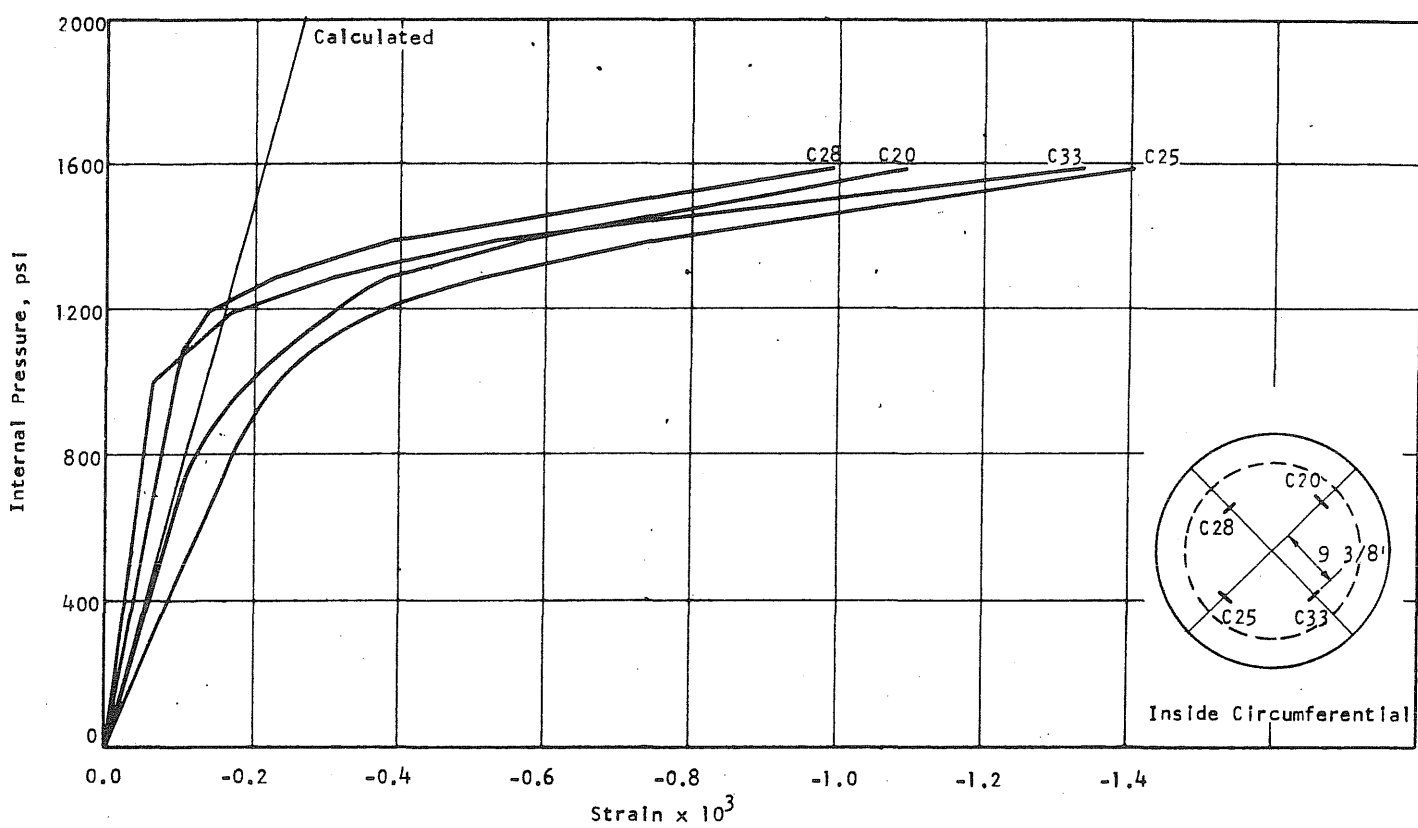


FIG. B11.8 (Cont'd) CONCRETE STRAINS, VESSEL PV11

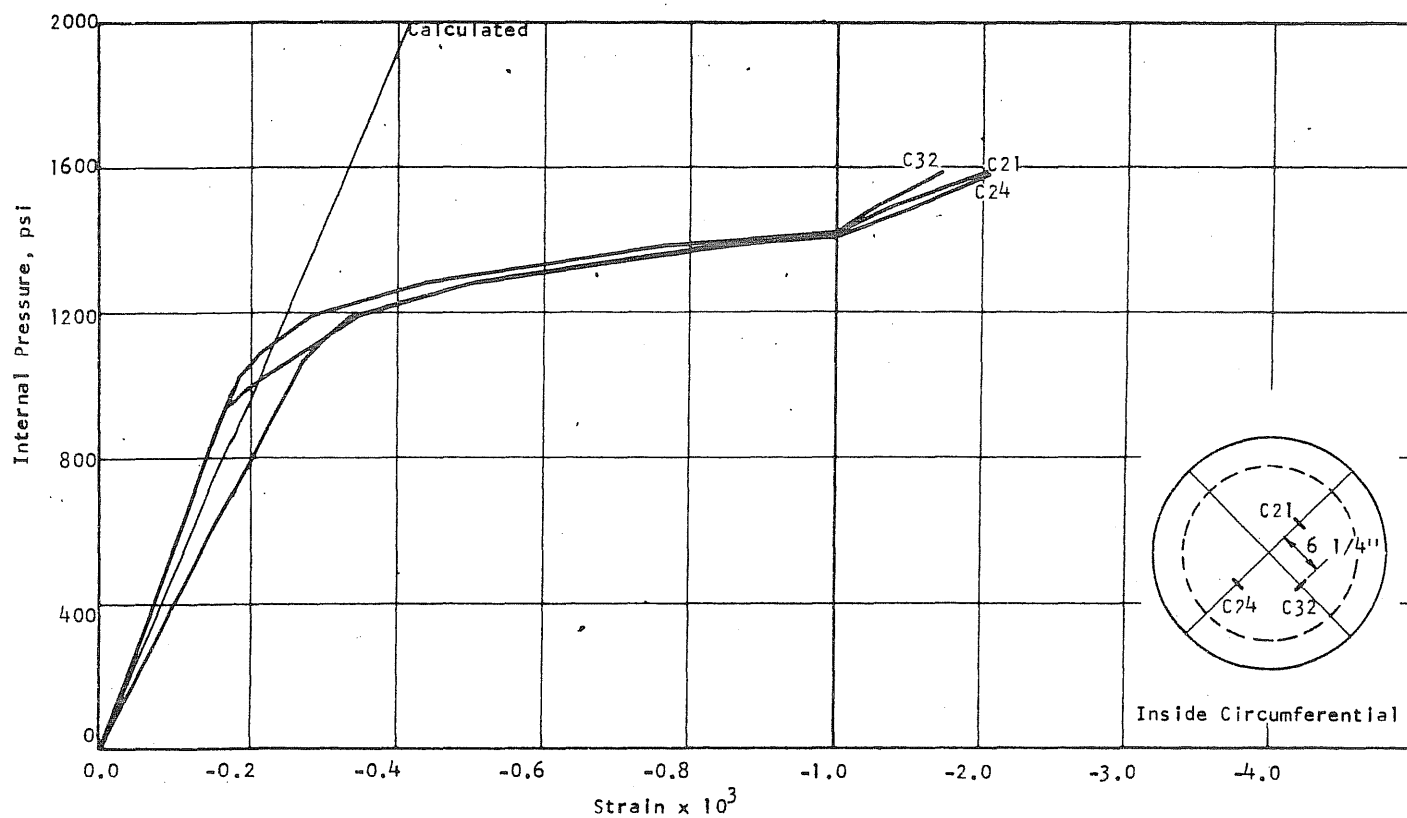


FIG. B11.8 (cont'd) CONCRETE STRAINS, VESSEL PV11

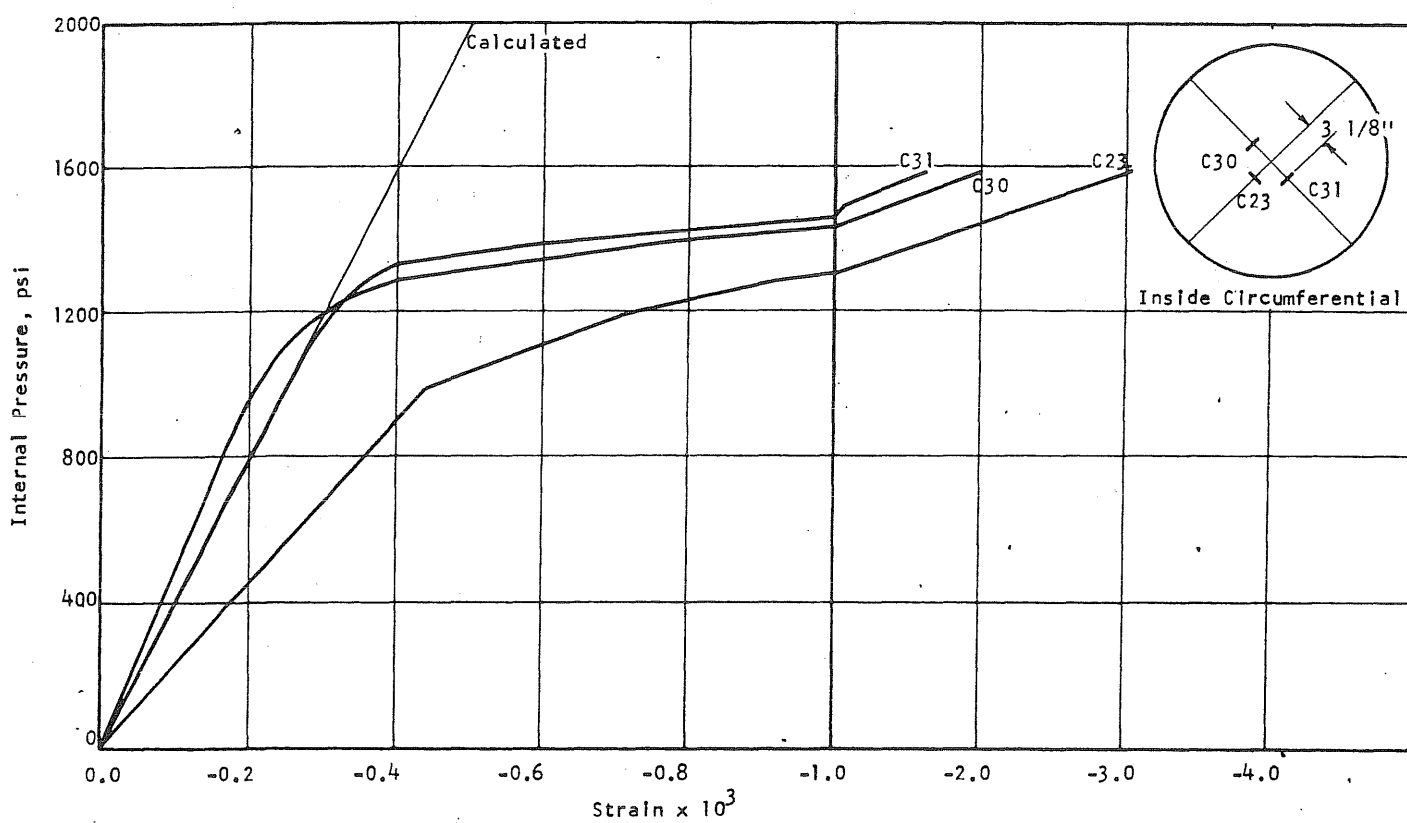


FIG. B11.8 (cont'd) CONCRETE STRAINS, VESSEL PV11

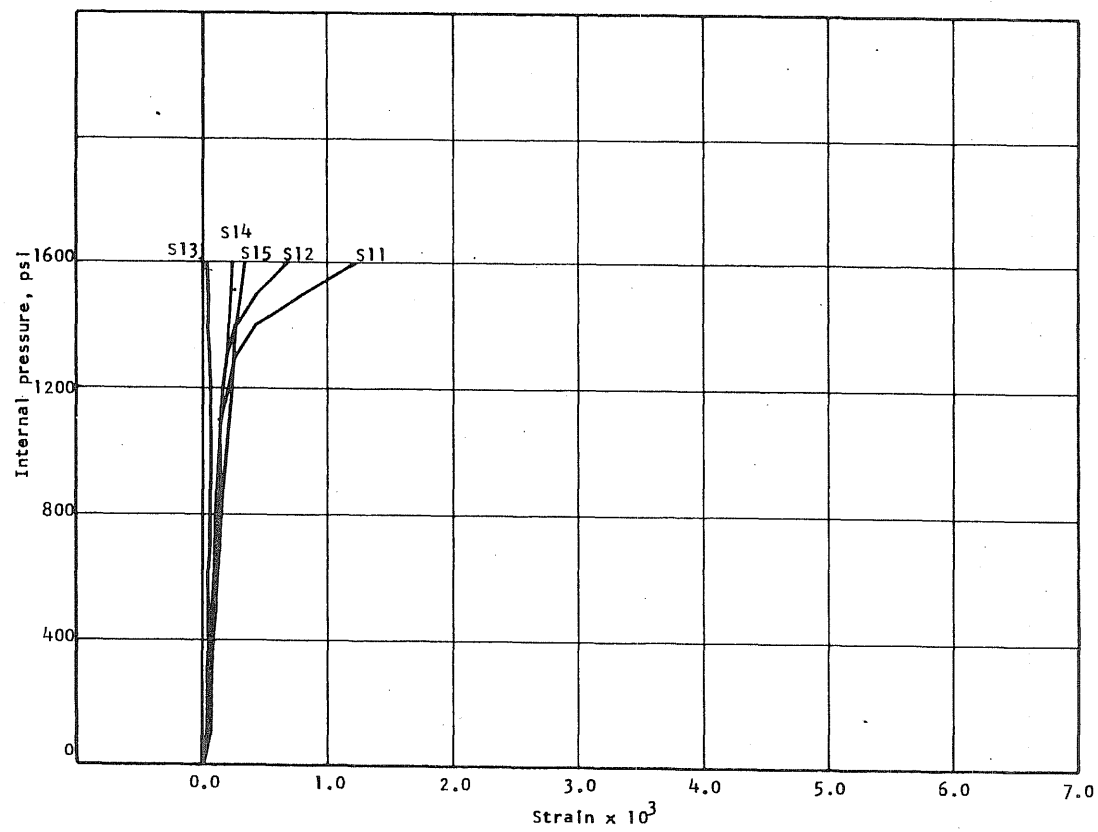


FIG. B11.9 APPLIED PRESSURE vs STRAIN IN CIRCUMFERENTIAL PRESTRESS WIRE AT THE S-END OF THE N-S DIAMETER OF PVII

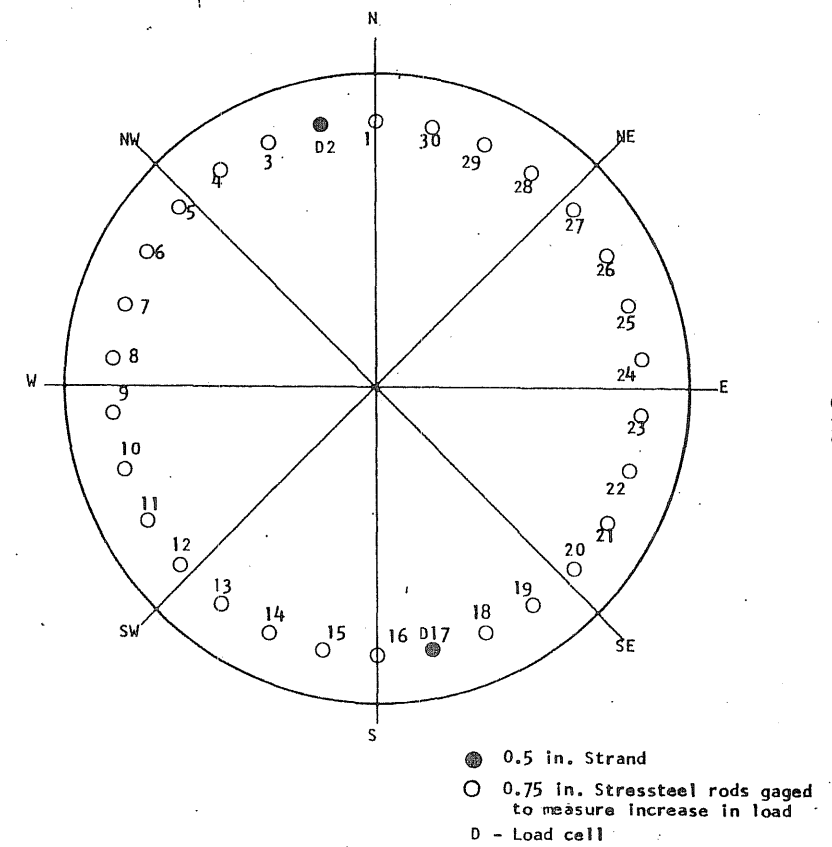


FIG. B11.10 LOCATION OF LONGITUDINAL REINFORCEMENT

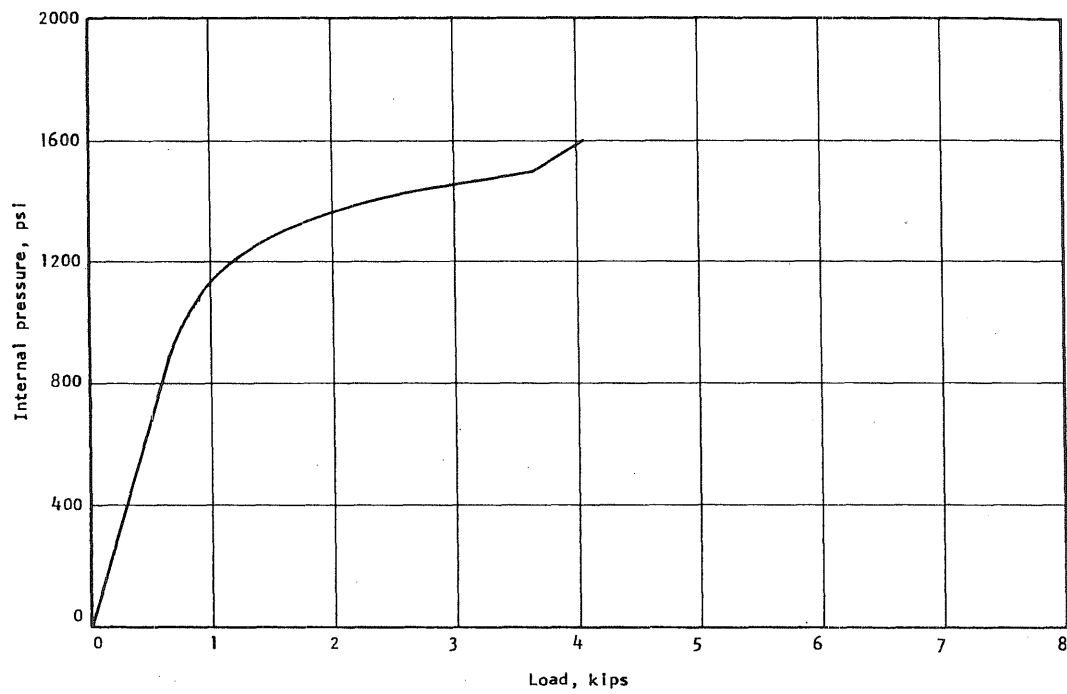


FIG. B11.11 APPLIED PRESSURE vs INCREASE IN LOAD IN STRESSTEEL ROD NO. 4

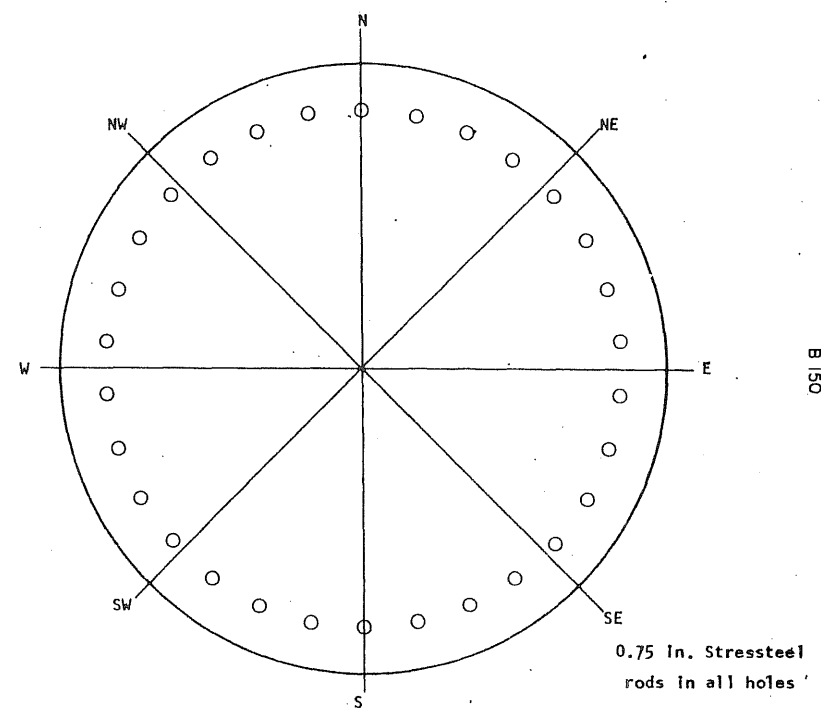


FIG. B11.12 LOCATION OF LONGITUDINAL REINFORCEMENT

B 151

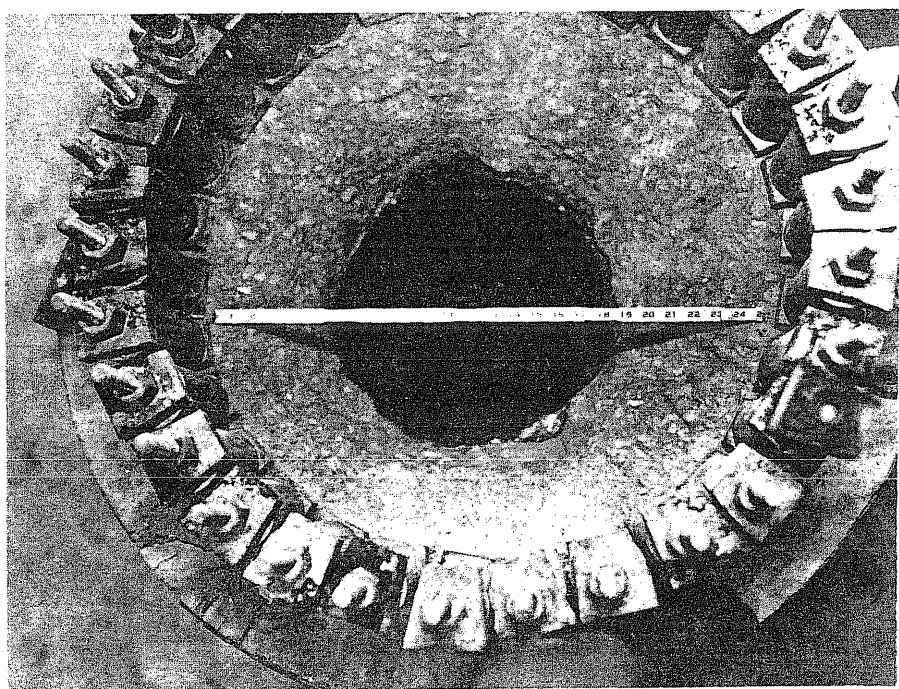


FIG. B11.13 END SLAB AFTER FAILURE

B12 Test Vessel PV12 ($t = 10$ in., $s = 1/4$ in.)

Test vessel PV12 was cast in the laboratory and was uncracked prior to prestressing. After circumferential prestressing a crack was observed on the inside of the vessel at 19 in. below the top.

The liner detail was changed significantly for this vessel and the resulting sealing detail was used on all the following tests. The sealing detail is shown in Fig. B12.1. The longitudinal prestressing was provided by 30 stressteel rods.

Nitrogen gas was used to pressurize the vessel in 250-psi increments up to 2250 psi. Since the nitrogen gas bottles used had a maximum pressure of 2600 psi, they had a limited capacity above 2000 psi. Therefore, oil pressure was used above 2250 psi with the help of a fully charged gas bottle. The pressure was increased to 2650 psi at which time the seal in the base was broken. It was found that a one-in. long piece of the small O-ring in the base had been extruded and the remainder had been partially extruded as shown in Fig. B12.12a. Figure B12.12b shows the crack pattern of the end slab after the test.

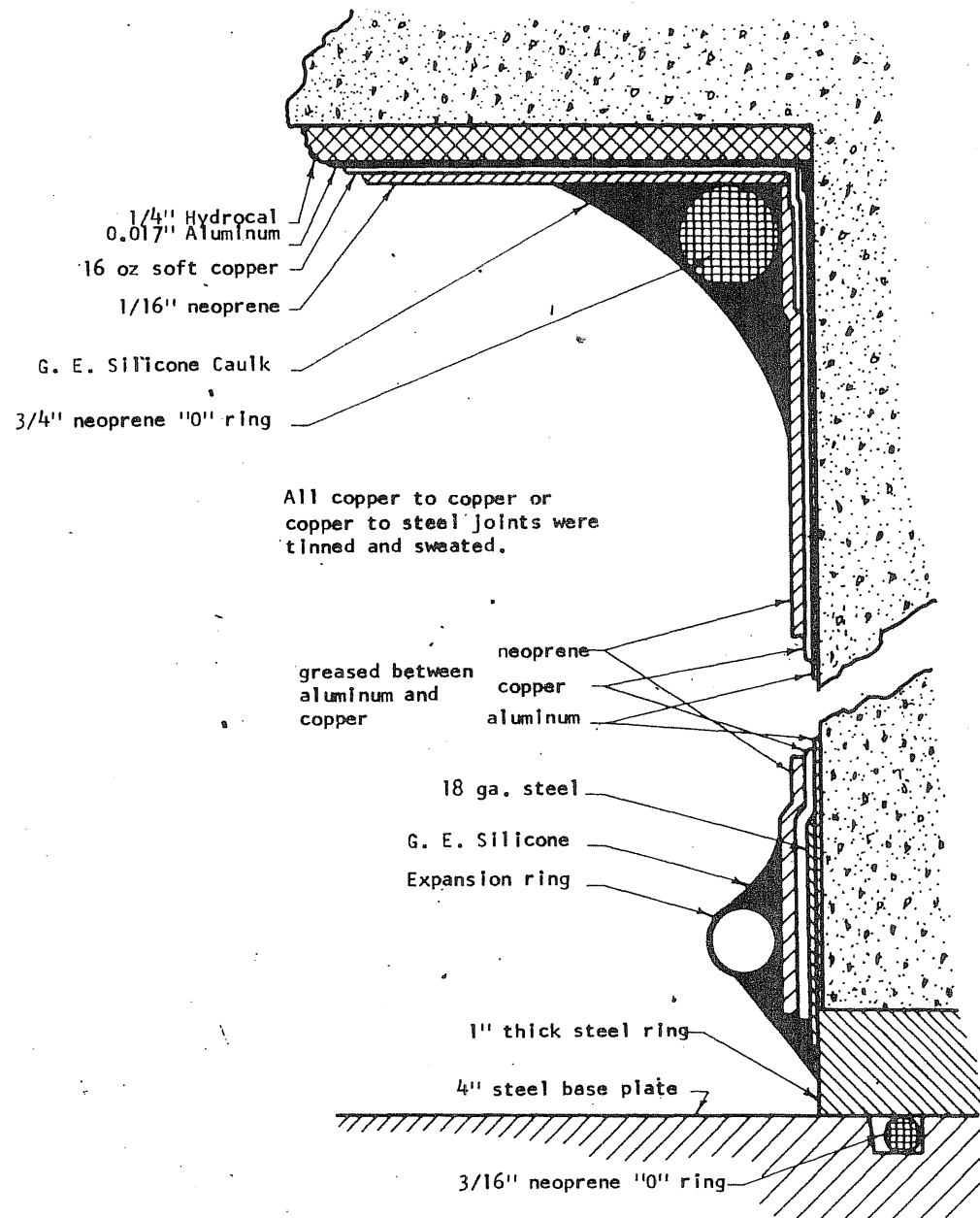


FIG. B12.1 SEALING DETAIL FOR PV12

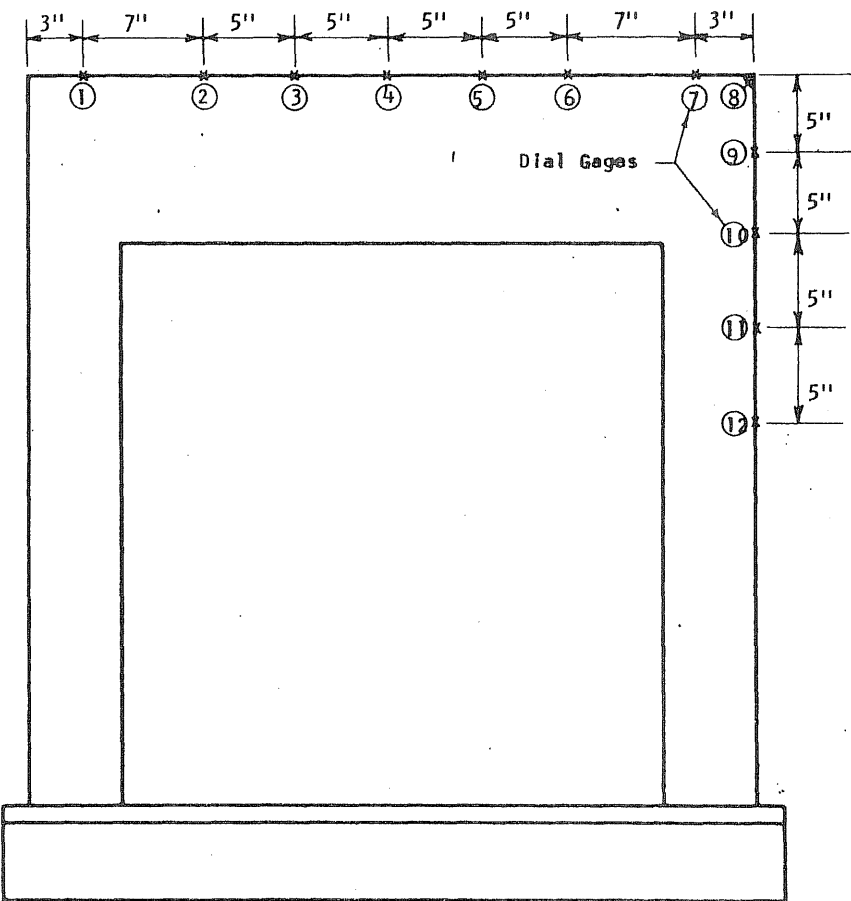


FIG. B12.2 LOCATION OF DEFLECTION GAGES ON PV12

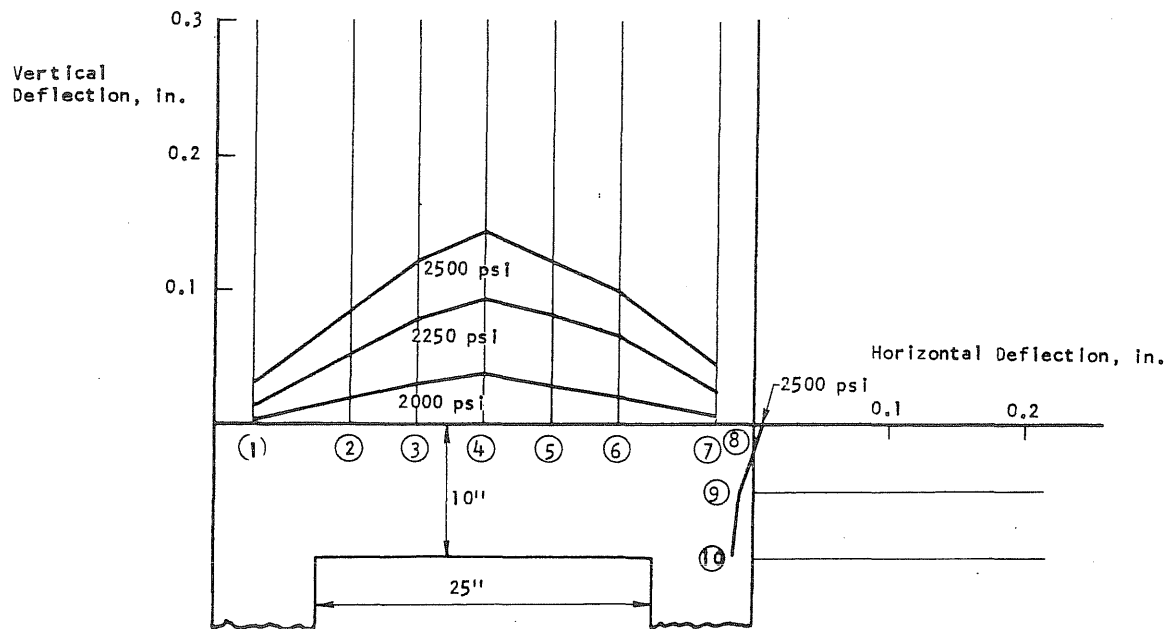


FIG. B12.3 DEFLECTION PROFILES OF THE END SLAB ALONG THE N-S DIAMETER OF PV12

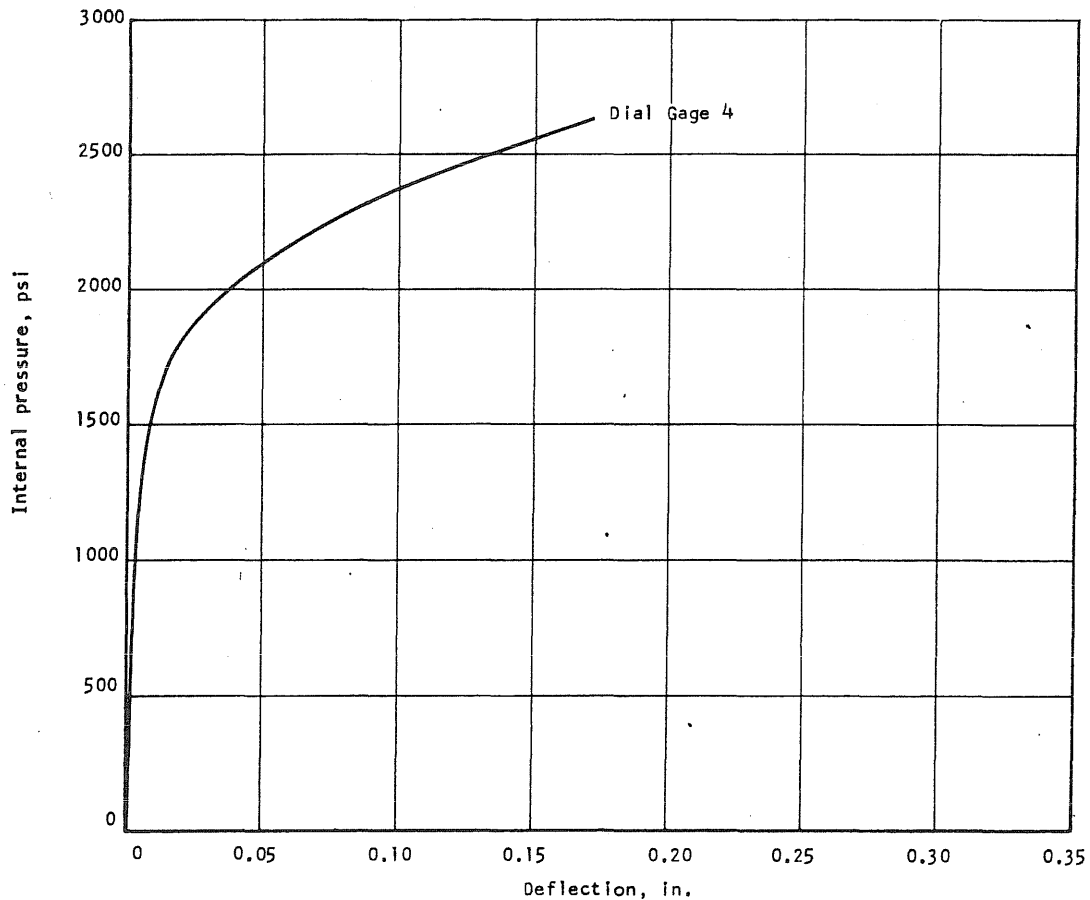
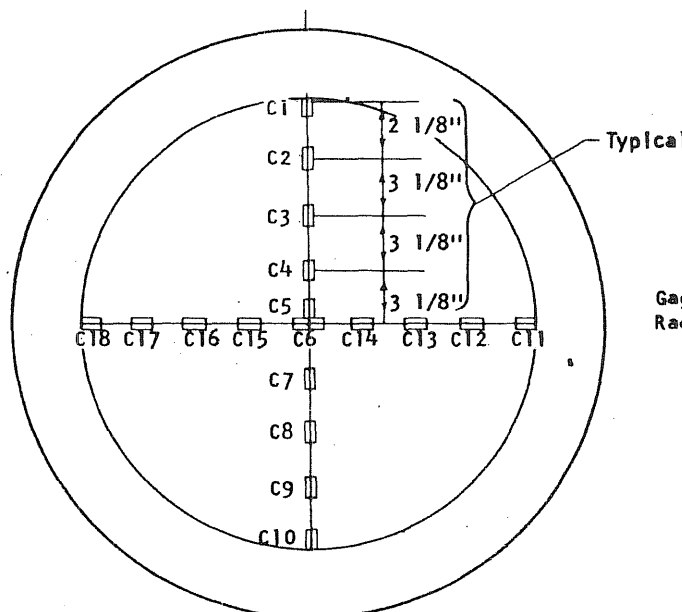


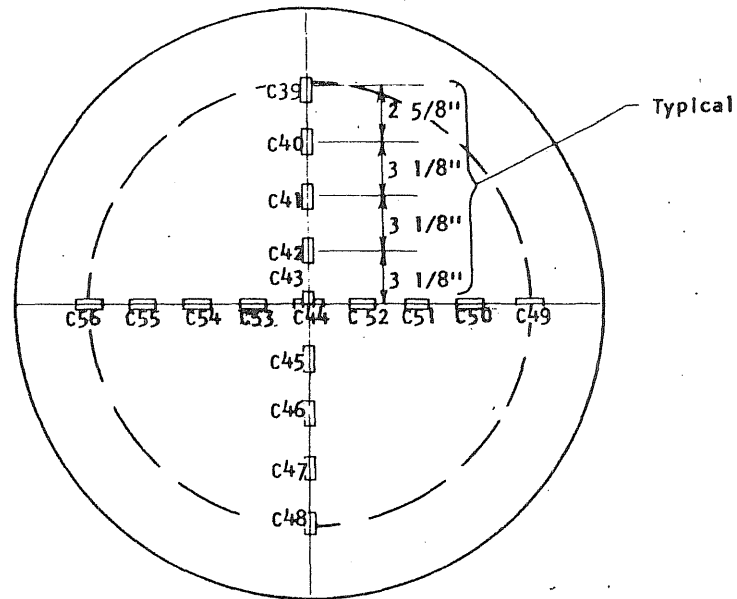
FIG. B12.4 APPLIED PRESSURE VS DEFLECTION AT MIDSPAN OF PV12

Concrete Gages on the Inside of the End Slab

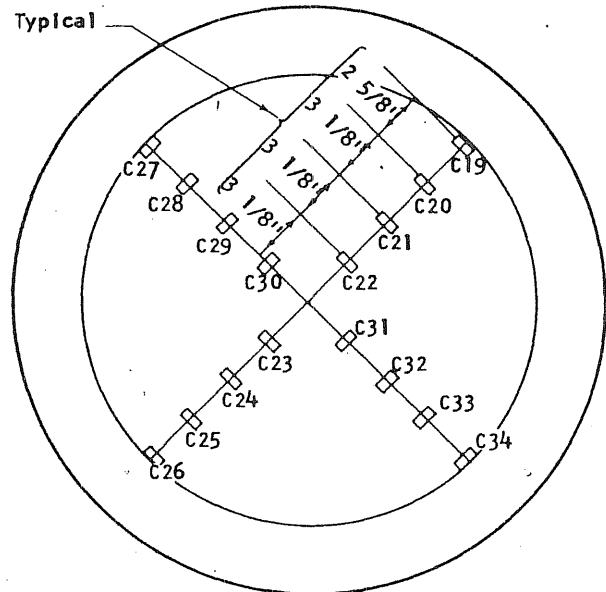


Gages to Measure
Radial Strain

Concrete gages on the Outside of the End Slab



B12.5



Gages to Measure
Circumferential
Strains

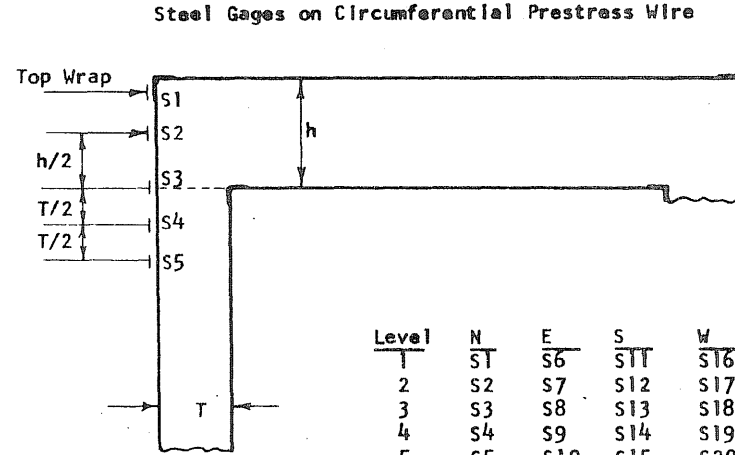


FIG. B12.5 (cont'd) STRAIN GAGE LOCATIONS ON PV12

FIG. B12.5 STRAIN GAGE LOCATIONS ON PV12

B156

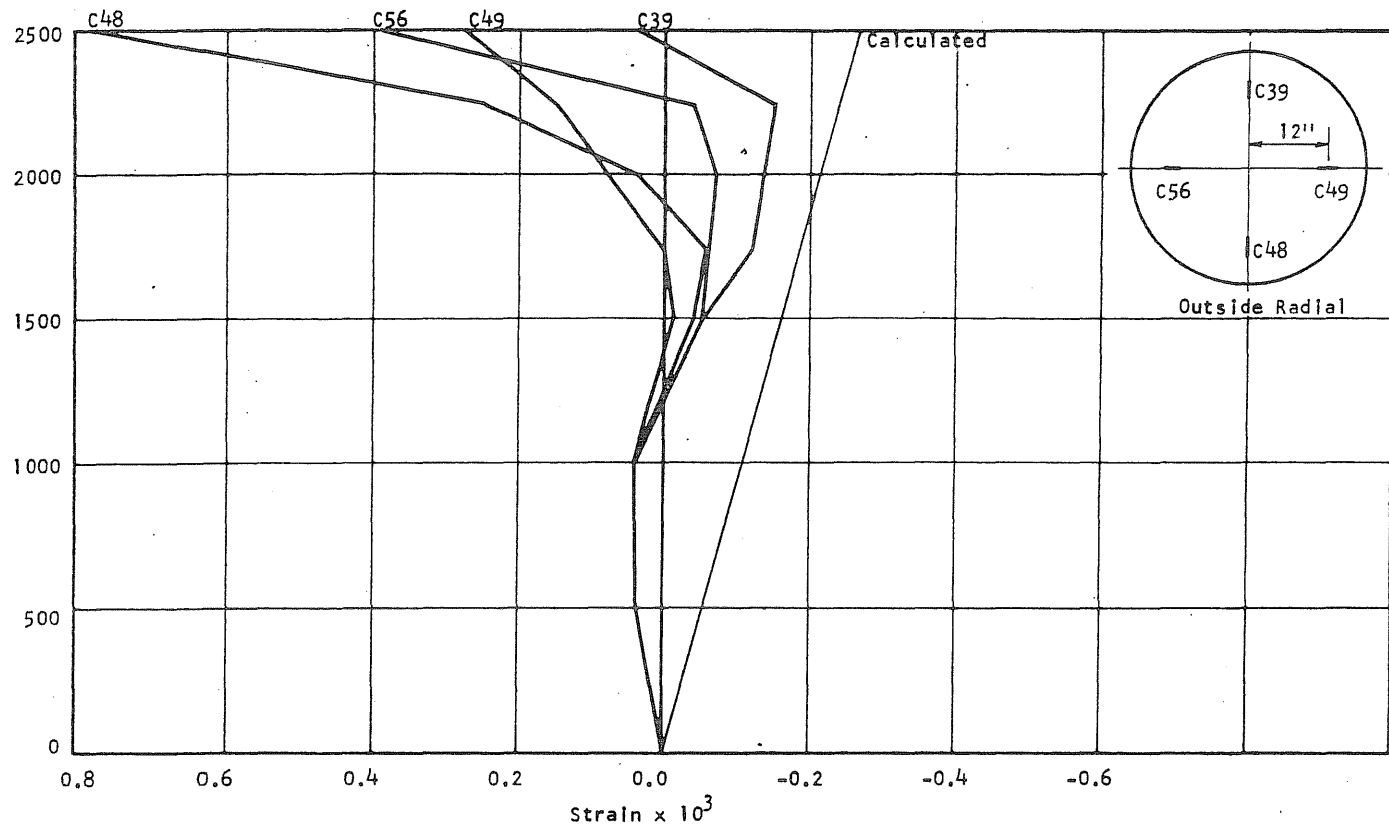


FIG. B12.6 CONCRETE STRAINS, VESSEL PV12

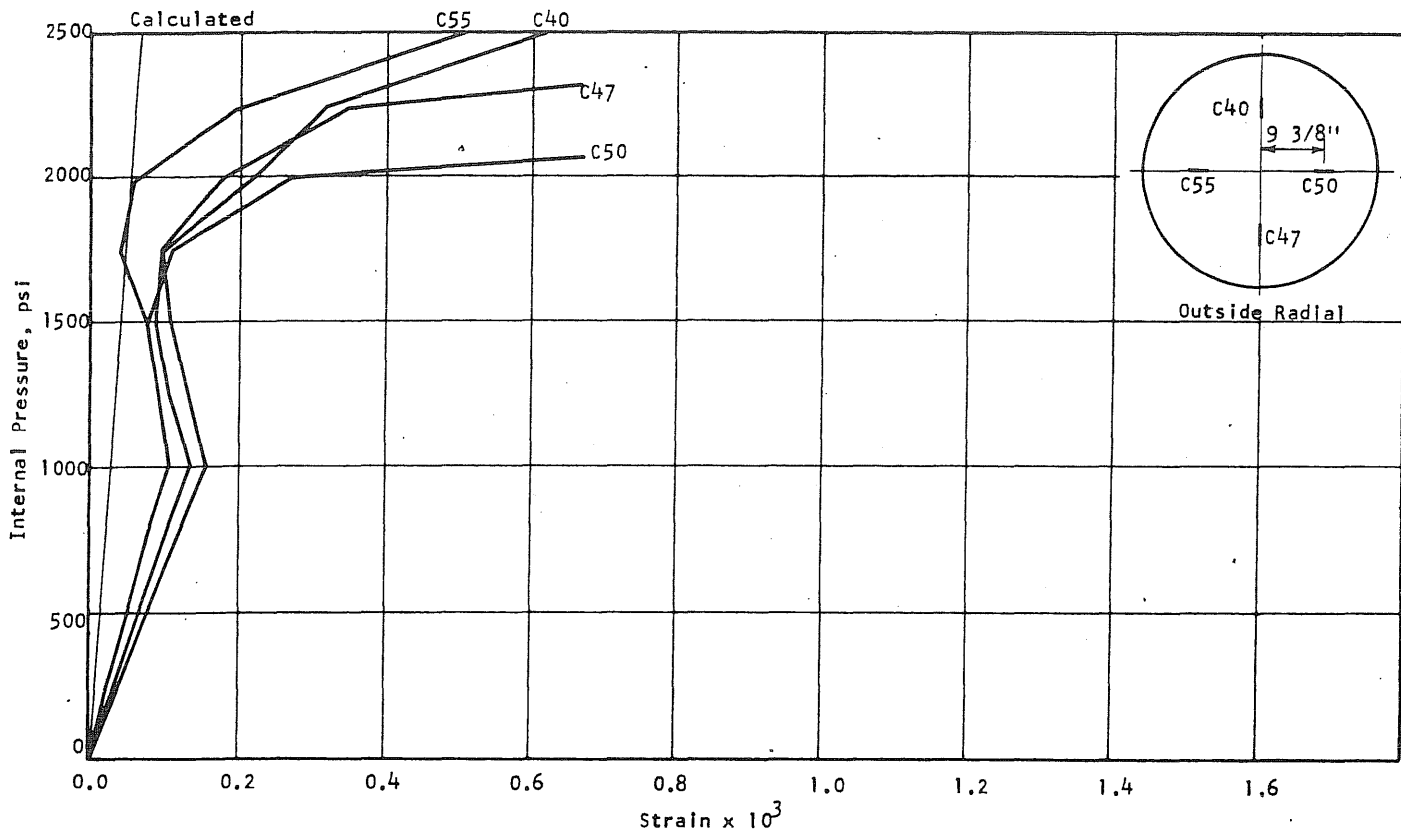


FIG. B12.6 (cont'd) CONCRETE STRAINS, VESSEL PV12

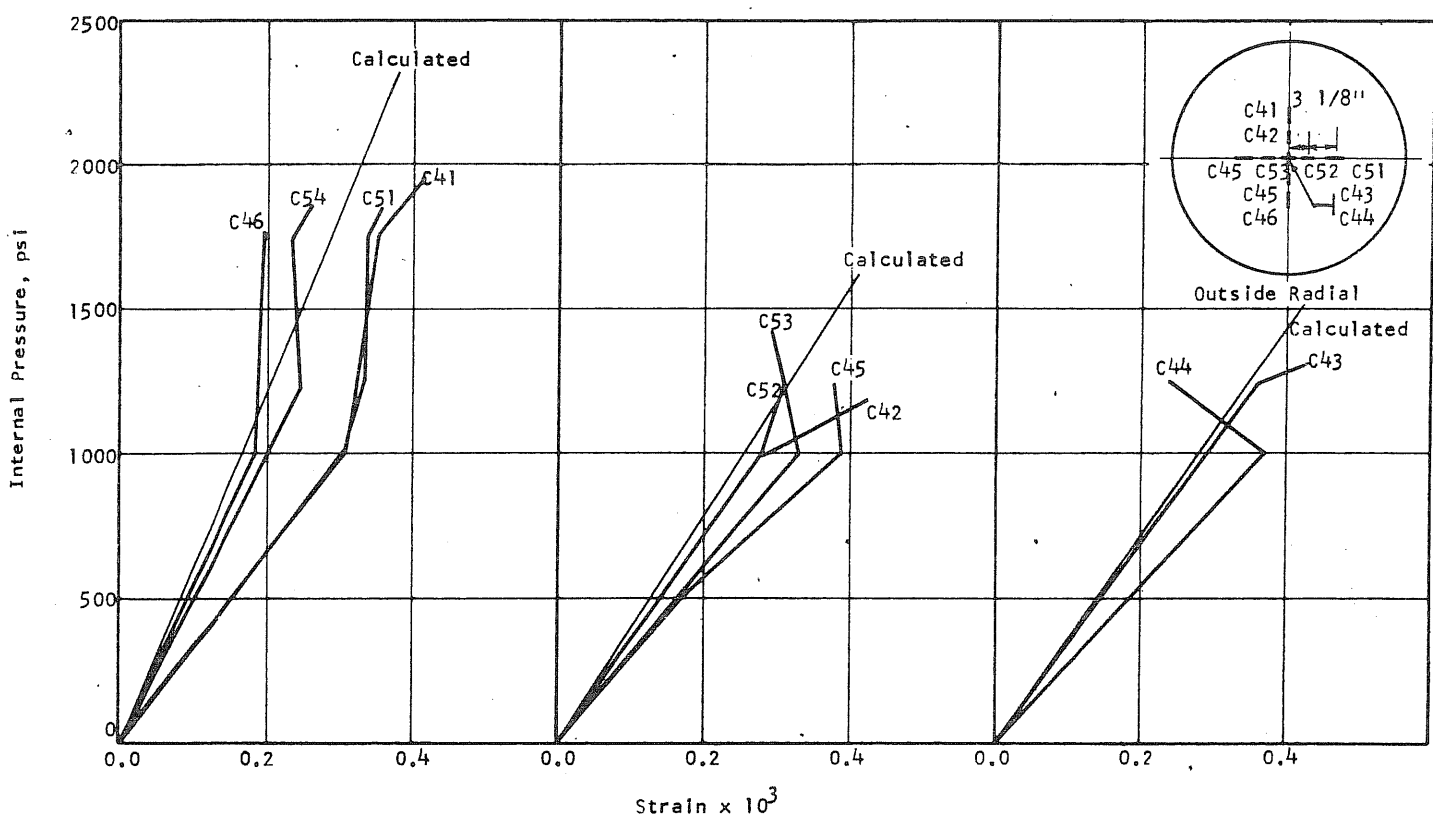


FIG. B12.6 (cont'd) CONCRETE STRAINS, VESSEL PV12

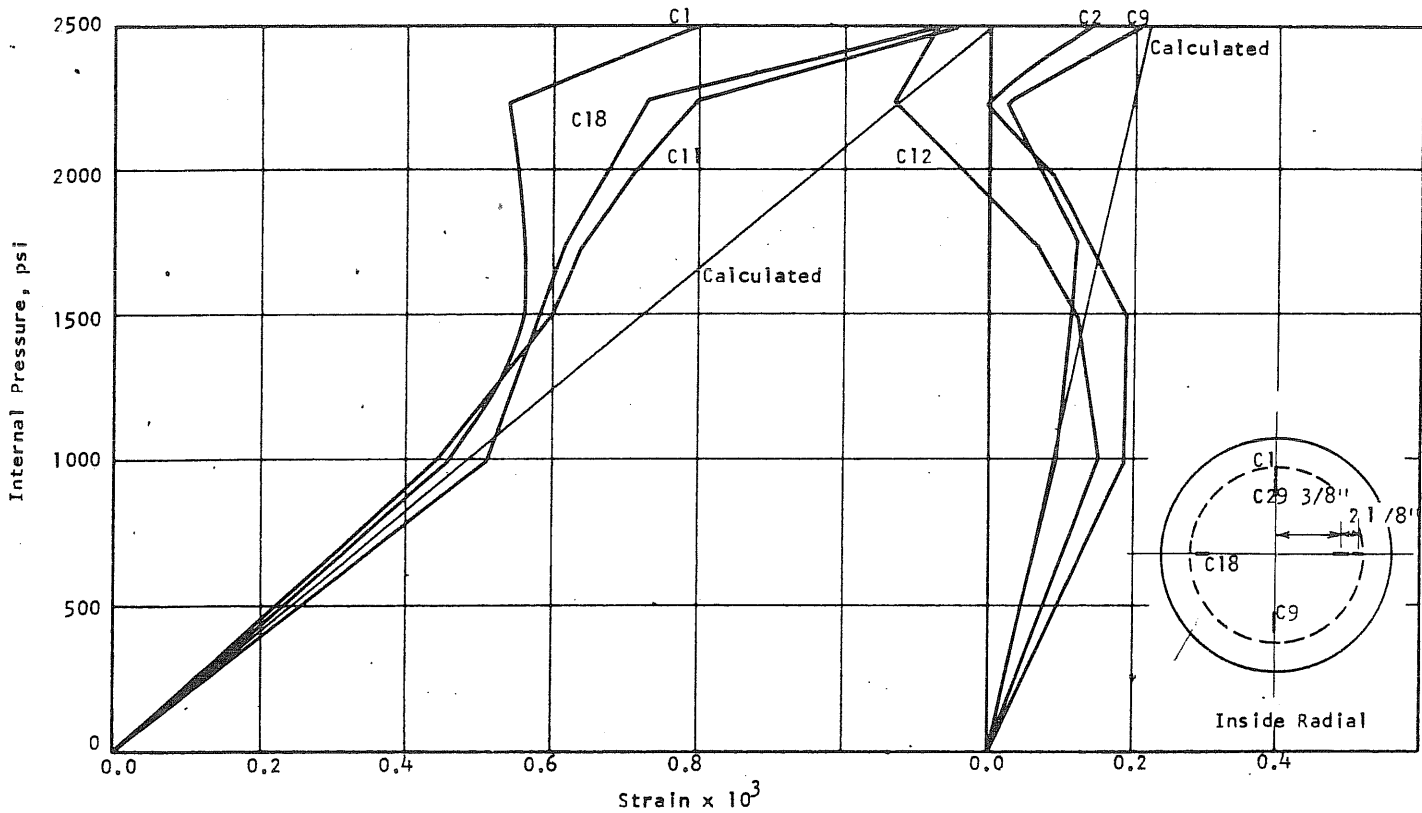


FIG. B12.7 CONCRETE STRAINS, VESSEL PV12

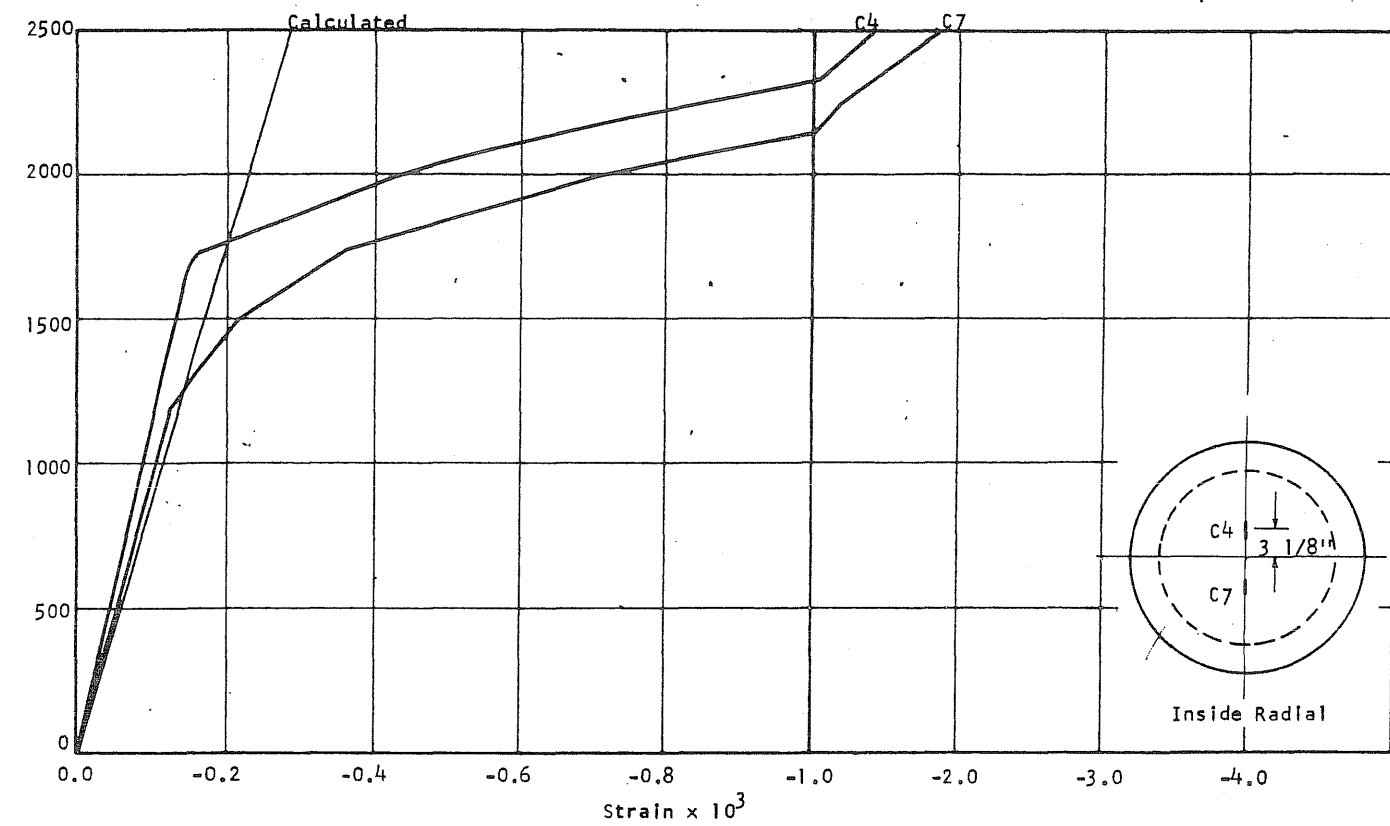


FIG. B12.7 (cont'd) CONCRETE STRAINS, VESSEL PV12

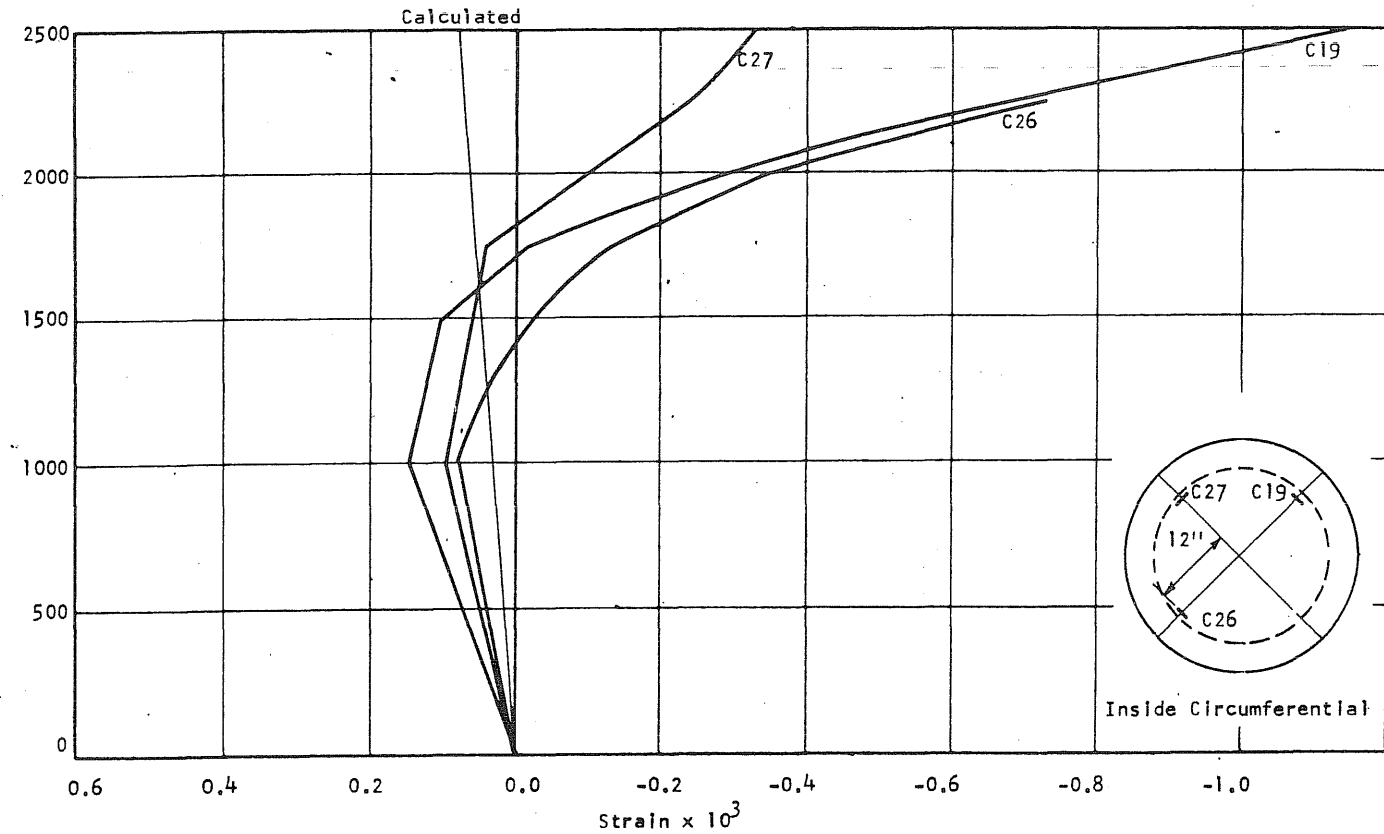


FIG. B12.8 CONCRETE STRAINS, VESSEL PV12

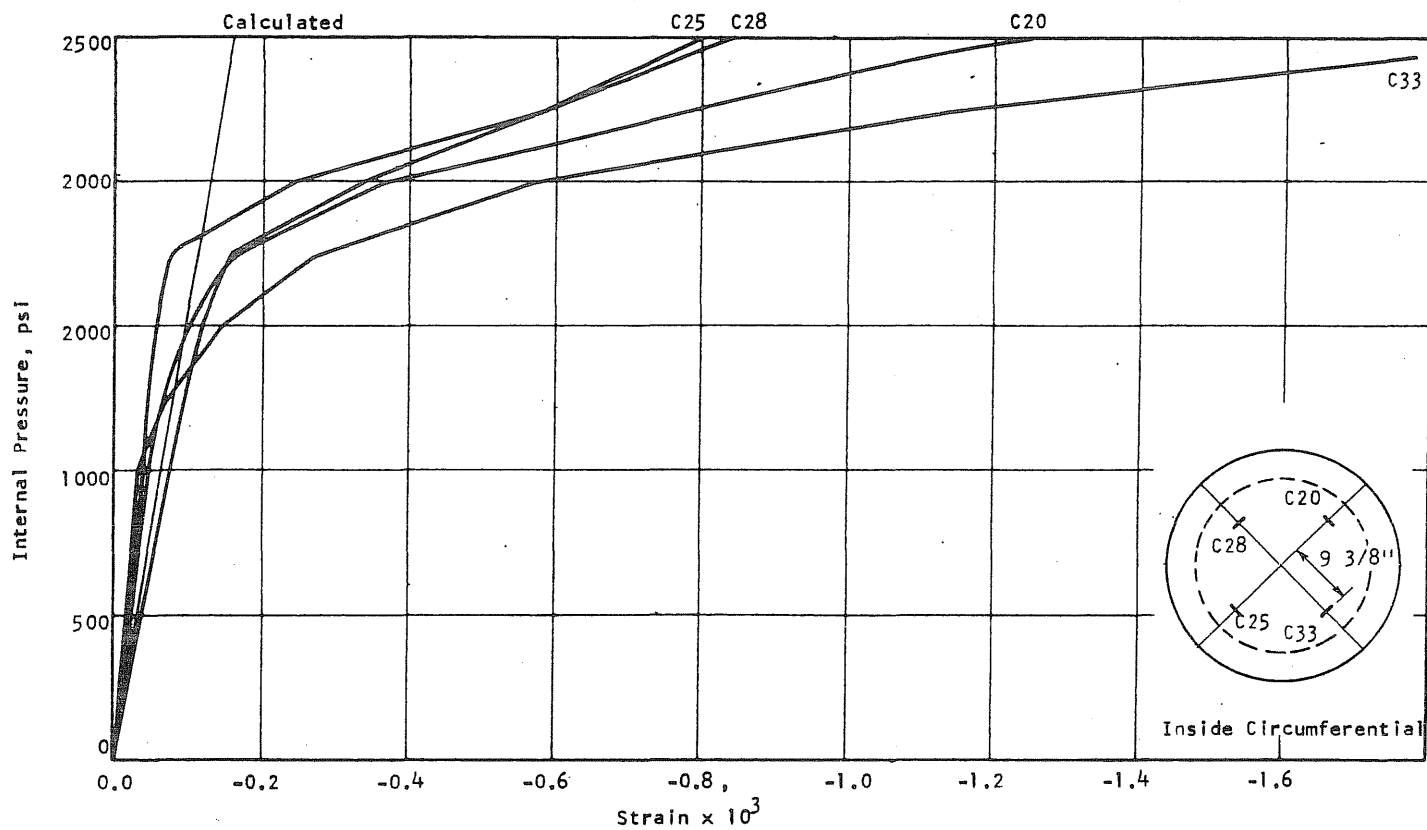


FIG. B12.8 (cont'd) CONCRETE STRAINS, VESSEL PV12

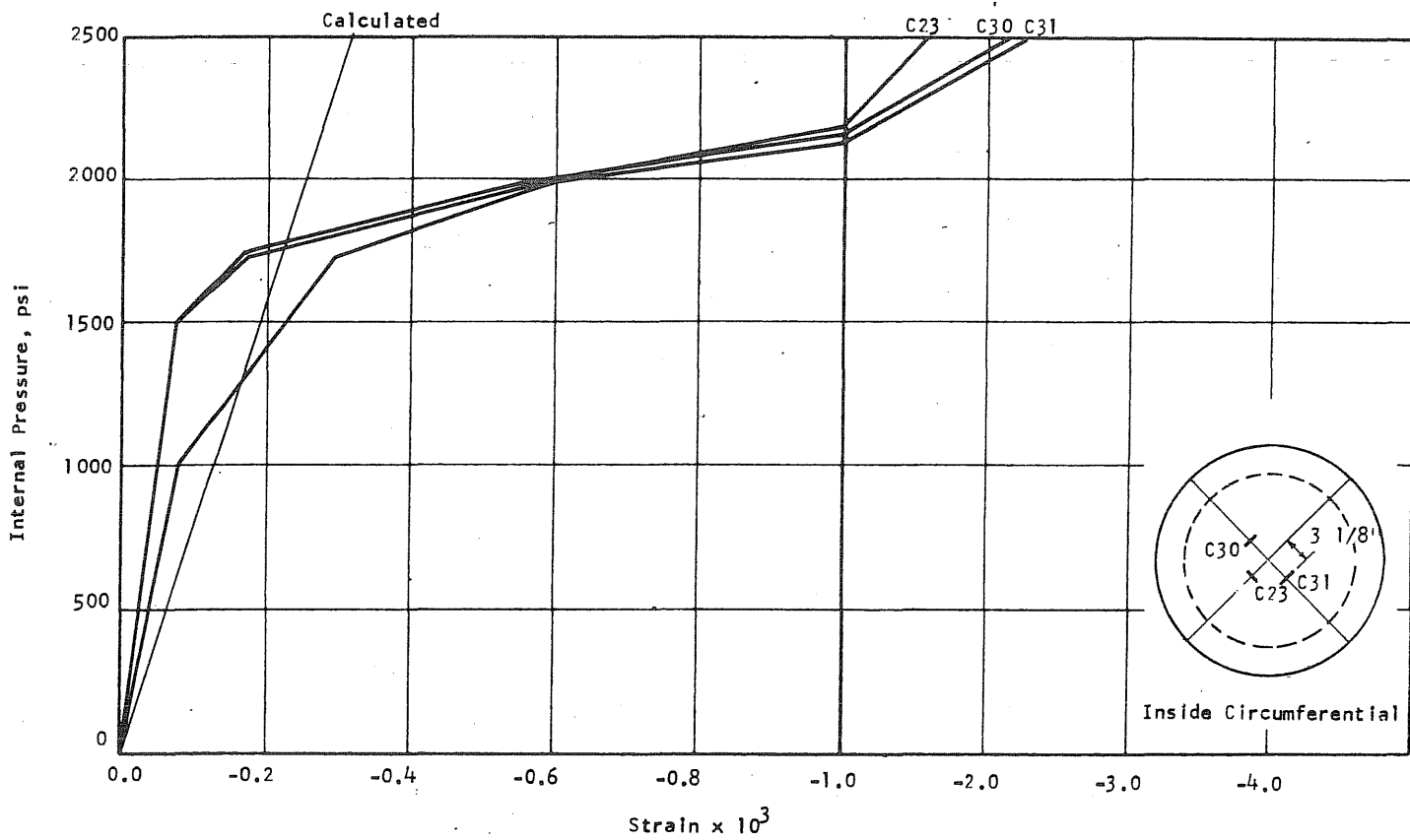


FIG. B12.8 (cont'd) CONCRETE STRAINS, VESSEL PV12

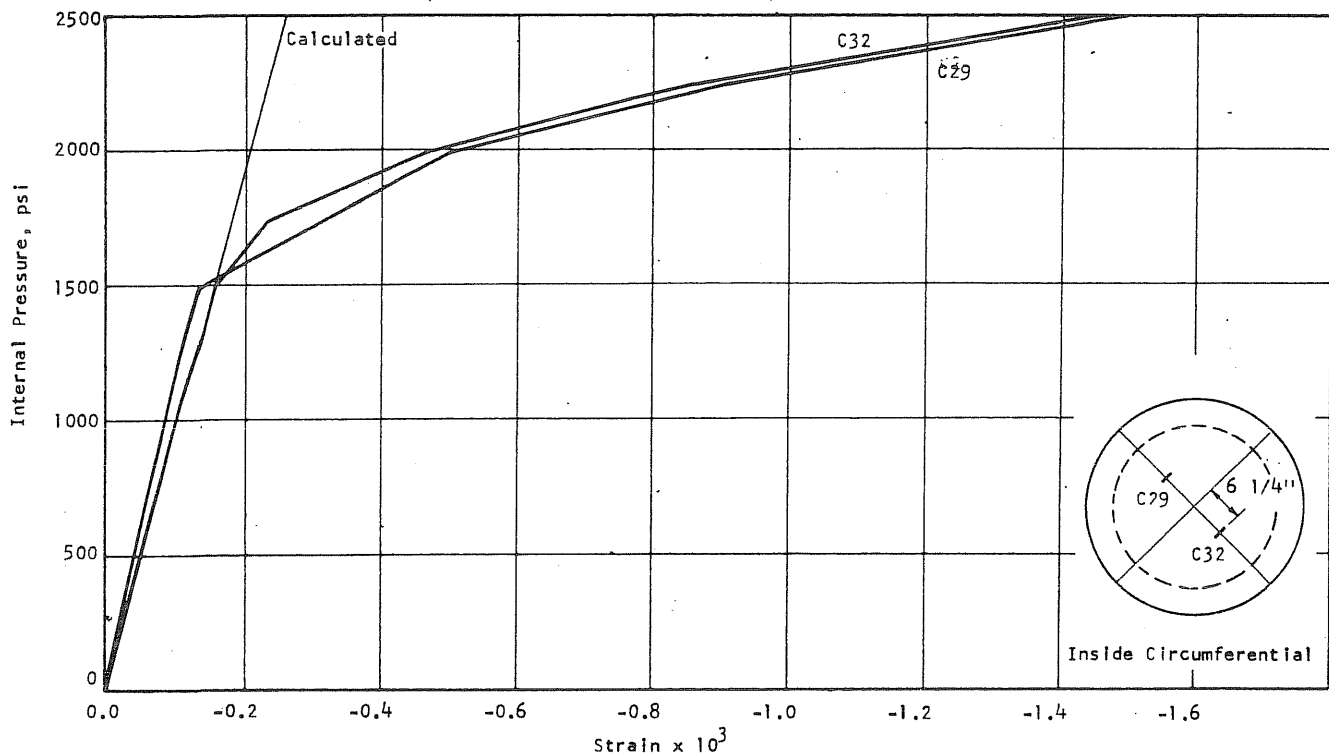


FIG. B12.8 (cont'd) CONCRETE STRAINS, VESSEL PV12

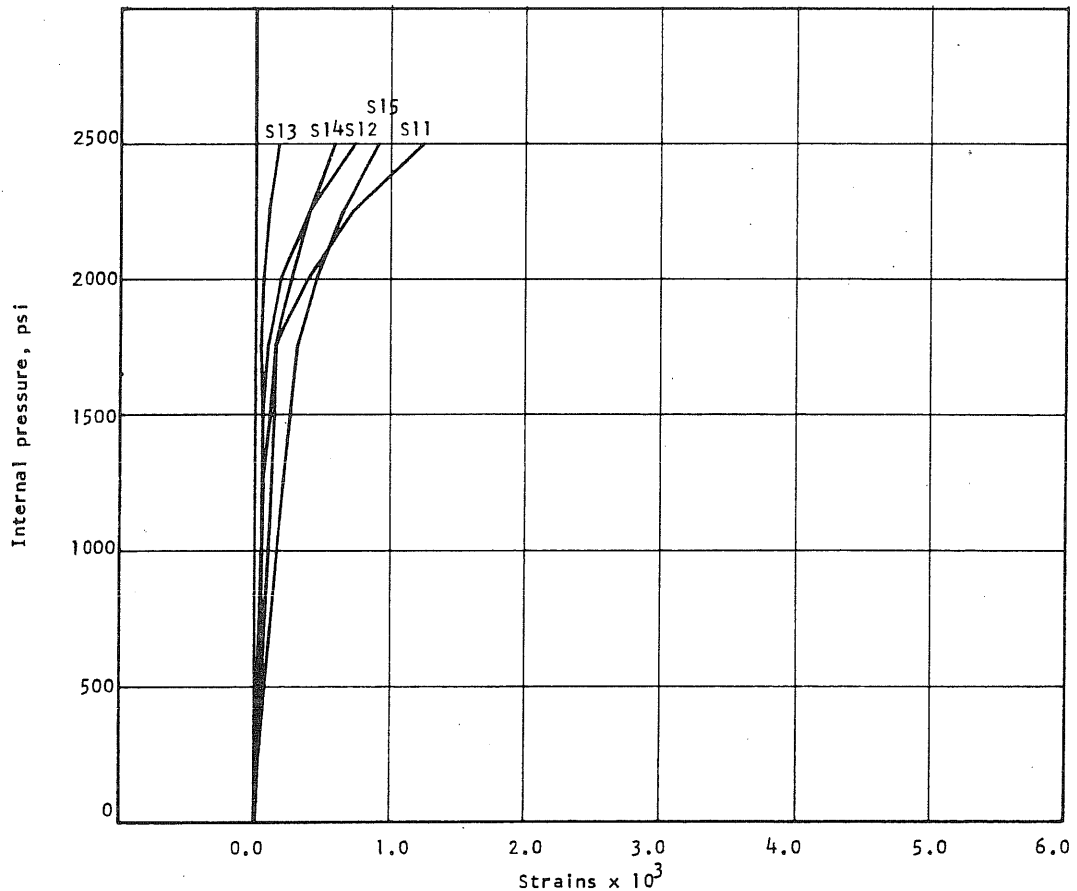


FIG. B12.9 APPLIED PRESSURE vs STRAINS IN CIRCUMFERENTIAL PRESTRESS WIRE AT THE S-END OF THE N-S DIAMETER OF PV12

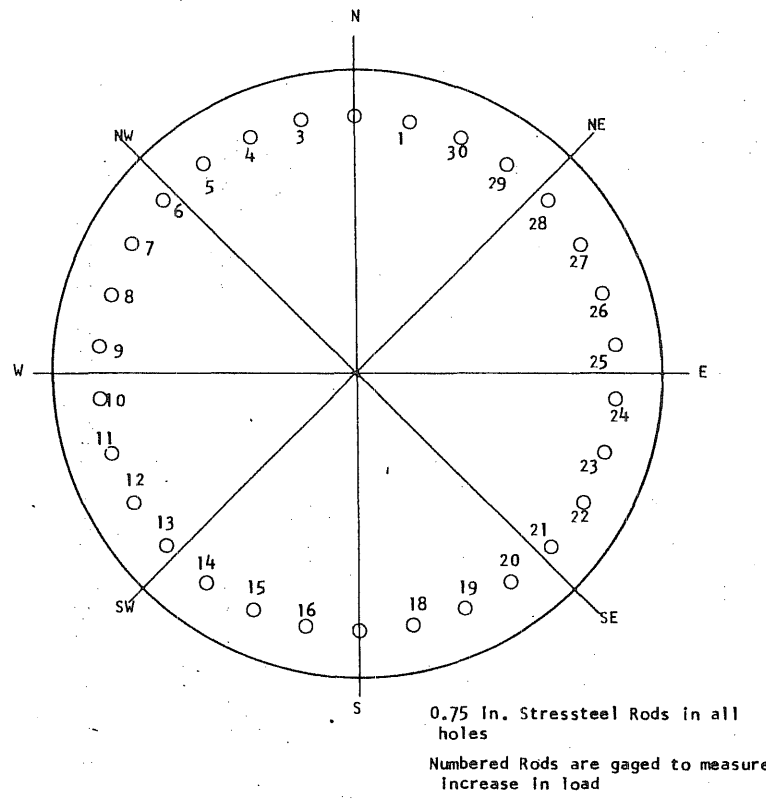


FIG. 12.10 LOCATION OF LONGITUDINAL REINFORCEMENT

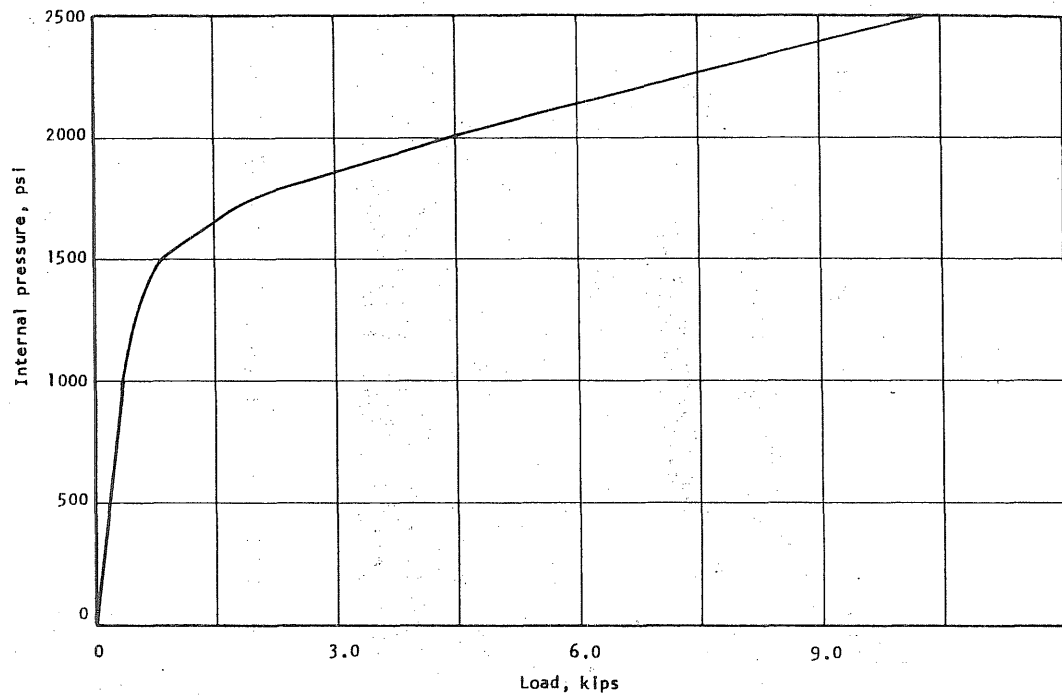


FIG. B12.11 APPLIED PRESSURE vs INCREASE IN LOAD IN STRESSTEEL ROD NO. 22

B 162



FIG. B12.12a EXTRUDED O-RING AFTER TEST

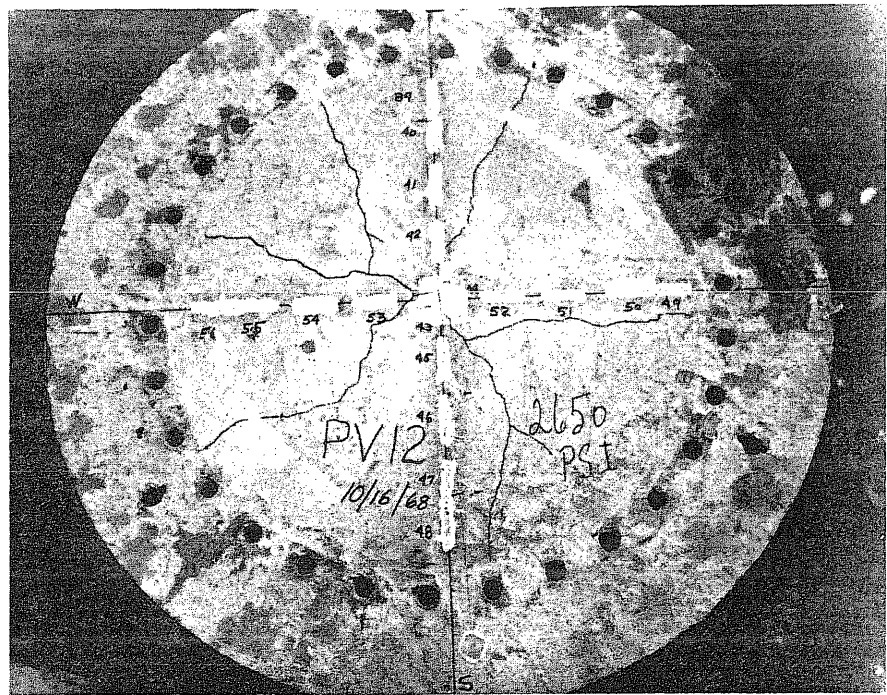


FIG. B12.12b END SLAB AFTER TEST OF PV12

B13 Test Vessel PV13 ($t = 12.5$ in., $s = 1/4$ in.)

This vessel was provided with an additional row of longitudinal reinforcement (Fig. 1.2). To accommodate the second row of reinforcement, two donut shaped plates of 1 1/4-in. thick steel were cut and drilled for two circles of rods. Centerlines of the rod circles were at diameters of 29 in. and 43-3/8 in. The inner diameter of the plate was 26 in. and the outer diameter was 45 in. One plate was placed on top of the specimen and one below the four-in. steel closure plate. The plate on the top was bedded in Hydrocal to provide a smooth bearing surface. Longitudinal prestressing was provided with 60 stressteel rods. Figure B13.10 shows PV13 in the test shed before the test.

A detail of the liner is shown in Fig. B13.1 and is basically the same as for PV12 except that two expansion ridges were formed into the copper liner near the joint with the end slab piece.

The vessel was tested with nitrogen gas and reached a pressure of 3450 psi before the seal between the base plate and one-in. seal ring was lost. (After testing PV12, 6000-psi gas bottles were used.) After the vessel was taken apart, the O-ring in the closure plate was found to be feathered as in PV12. Radial cracks were visible in the end of the side wall. Twenty-three of the rod holes had cracks running through them. These cracks were visible for about 10 to 15 in. up the side wall. There were 3 rings of circumferential cracks at about 12 in., 18 in., and 23 in. from the base of the side wall on the inside. The dial gages on the top of the vessel did not record any significant deflections. Gage 12, located 17.5 in. from the base, indicated a deflection of 0.158 in. at failure. Deflection-pressure curves and deflection profiles are therefore not shown for this test.

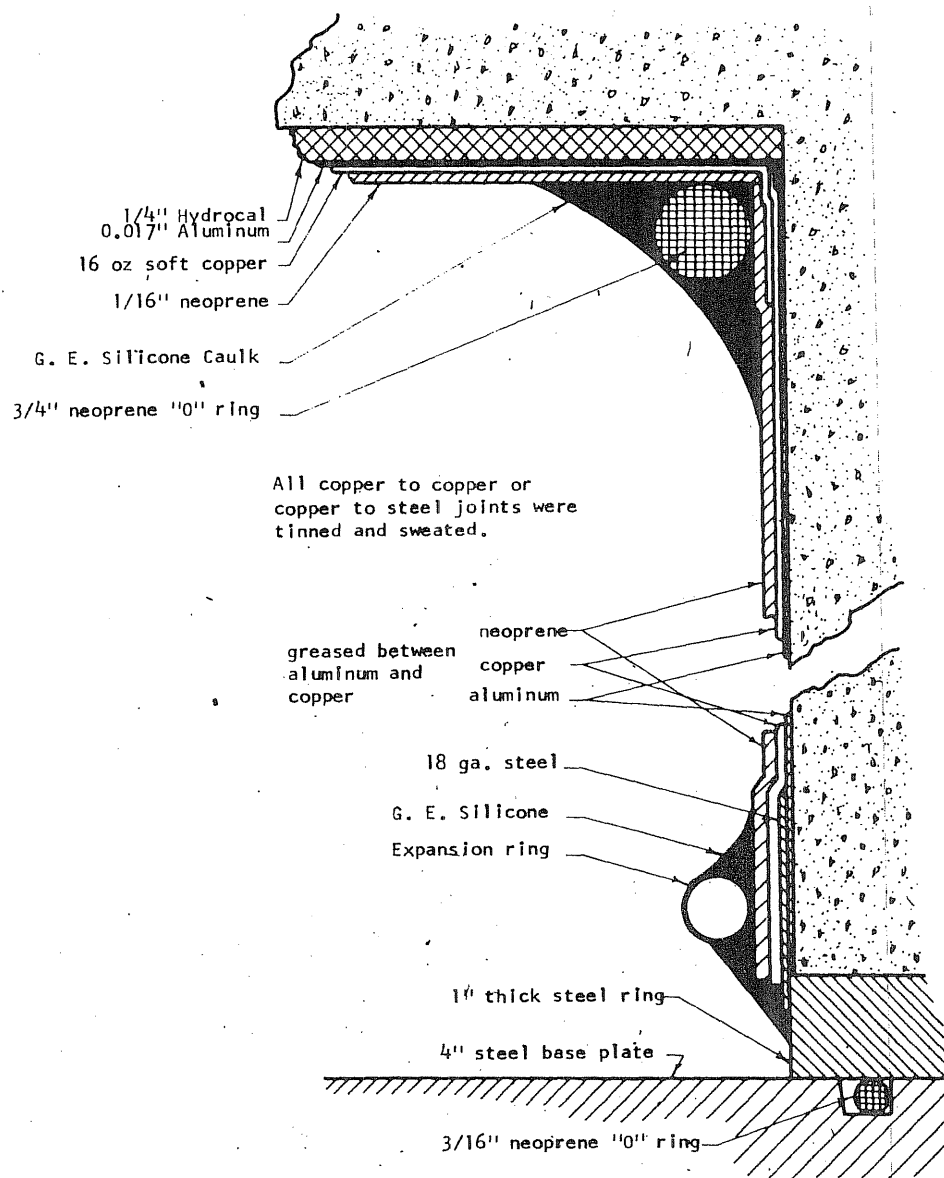


FIG. B13.1 SEALING DETAIL FOR PV13

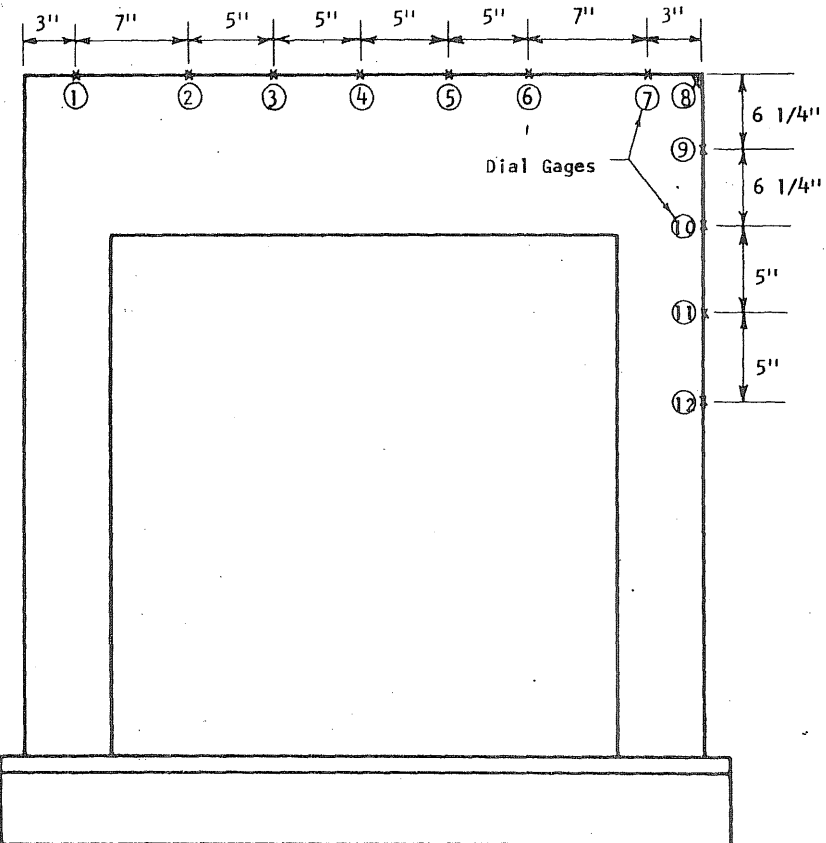
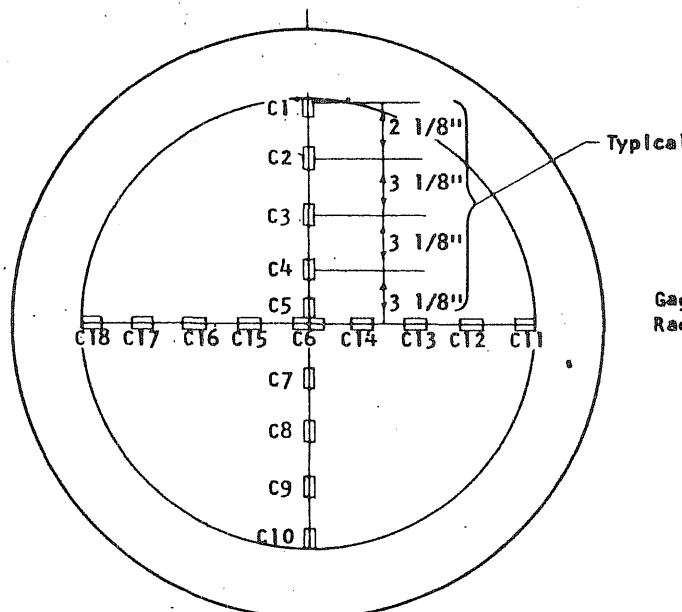


FIG. B13.2 LOCATION OF DEFLECTION GAGES ON PV13

Concrete Gages on the Inside of the End Slab



Concrete gages on the Outside of the End Slab

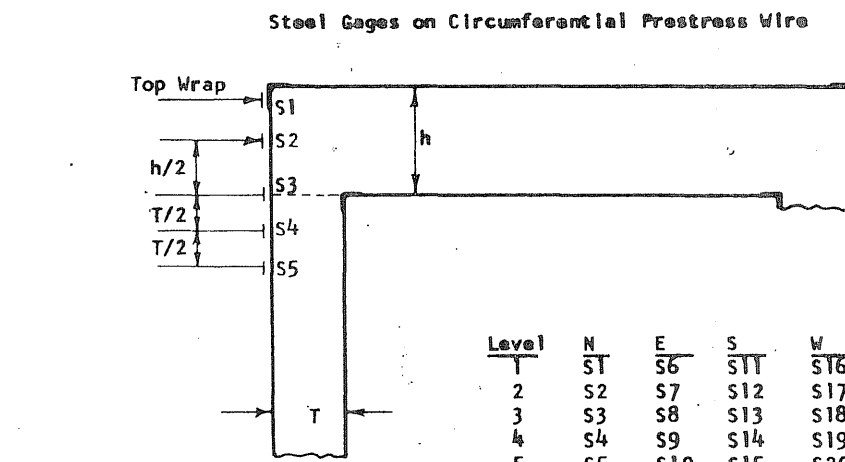
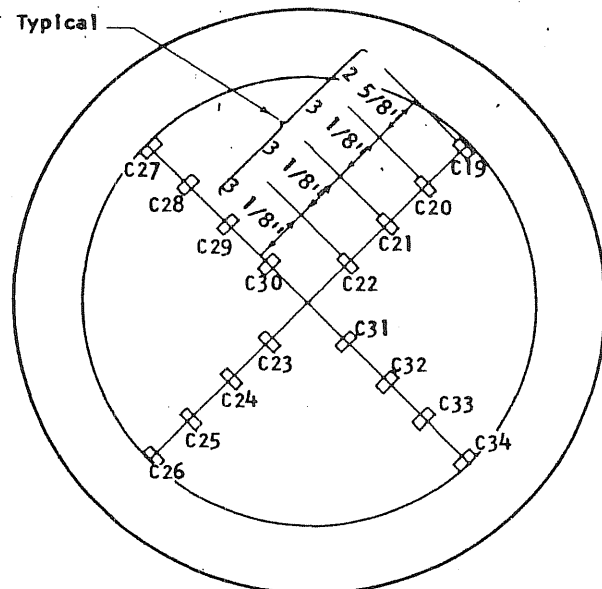
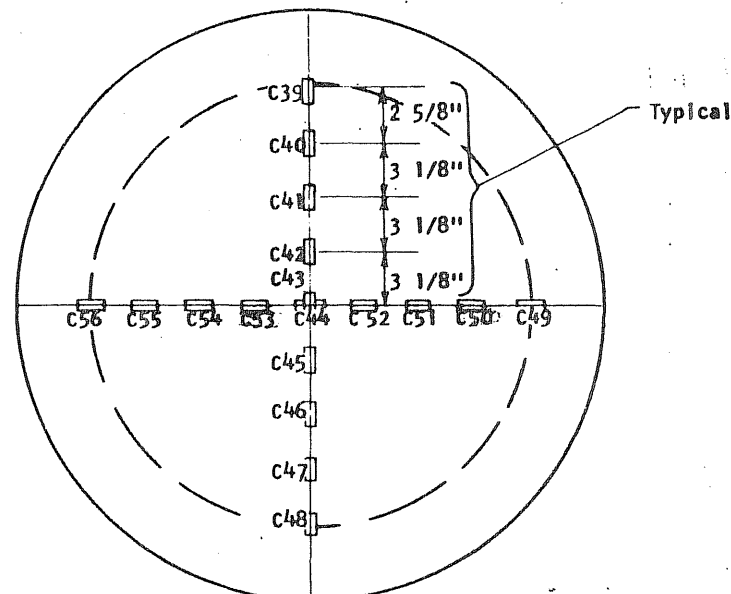


FIG. B13.3 (cont'd) STRAIN GAGE LOCATIONS ON PV13

FIG. B13.3 STRAIN GAGE LOCATIONS ON PV13

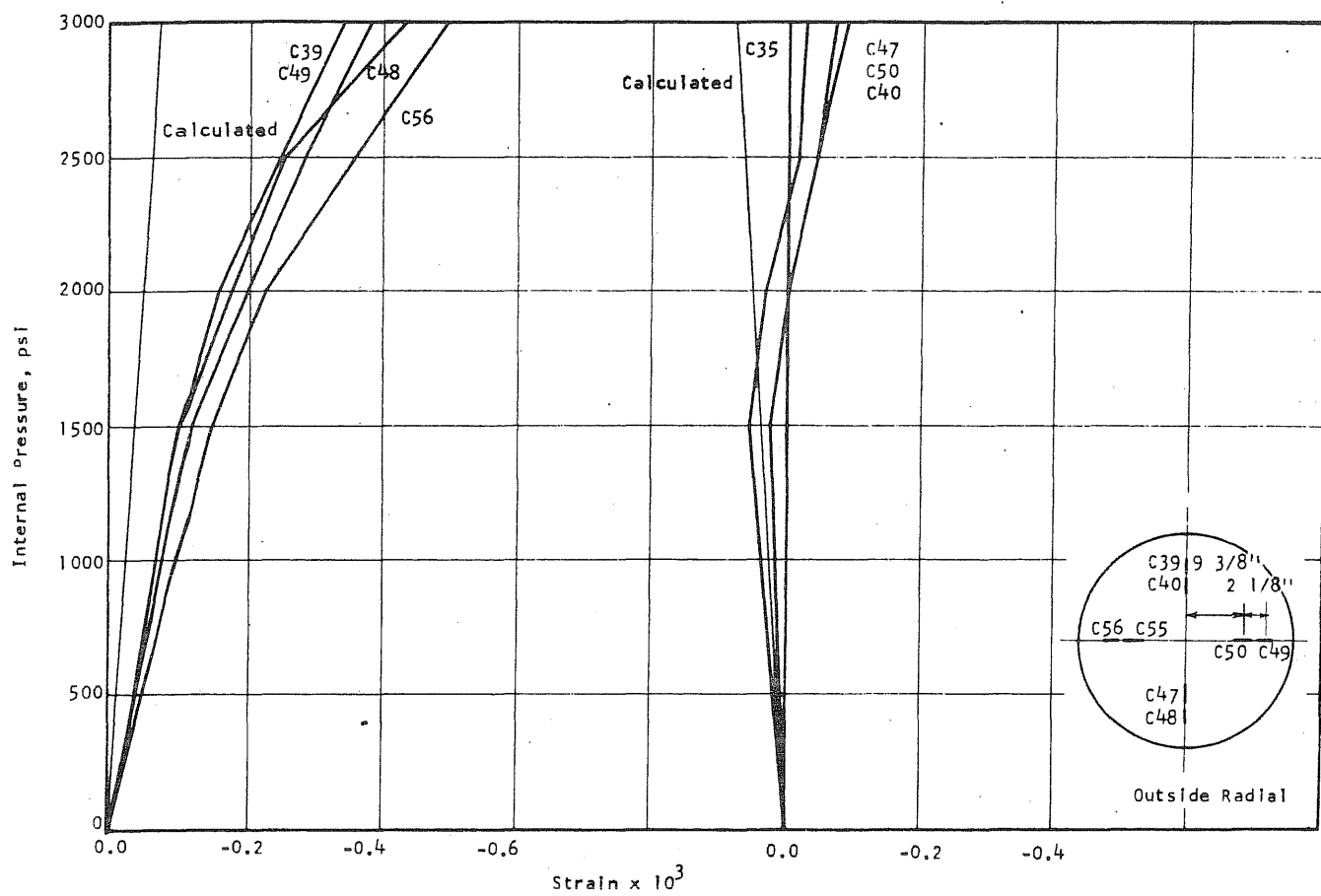


FIG. B13.4 CONCRETE STRAINS, VESSEL PV13

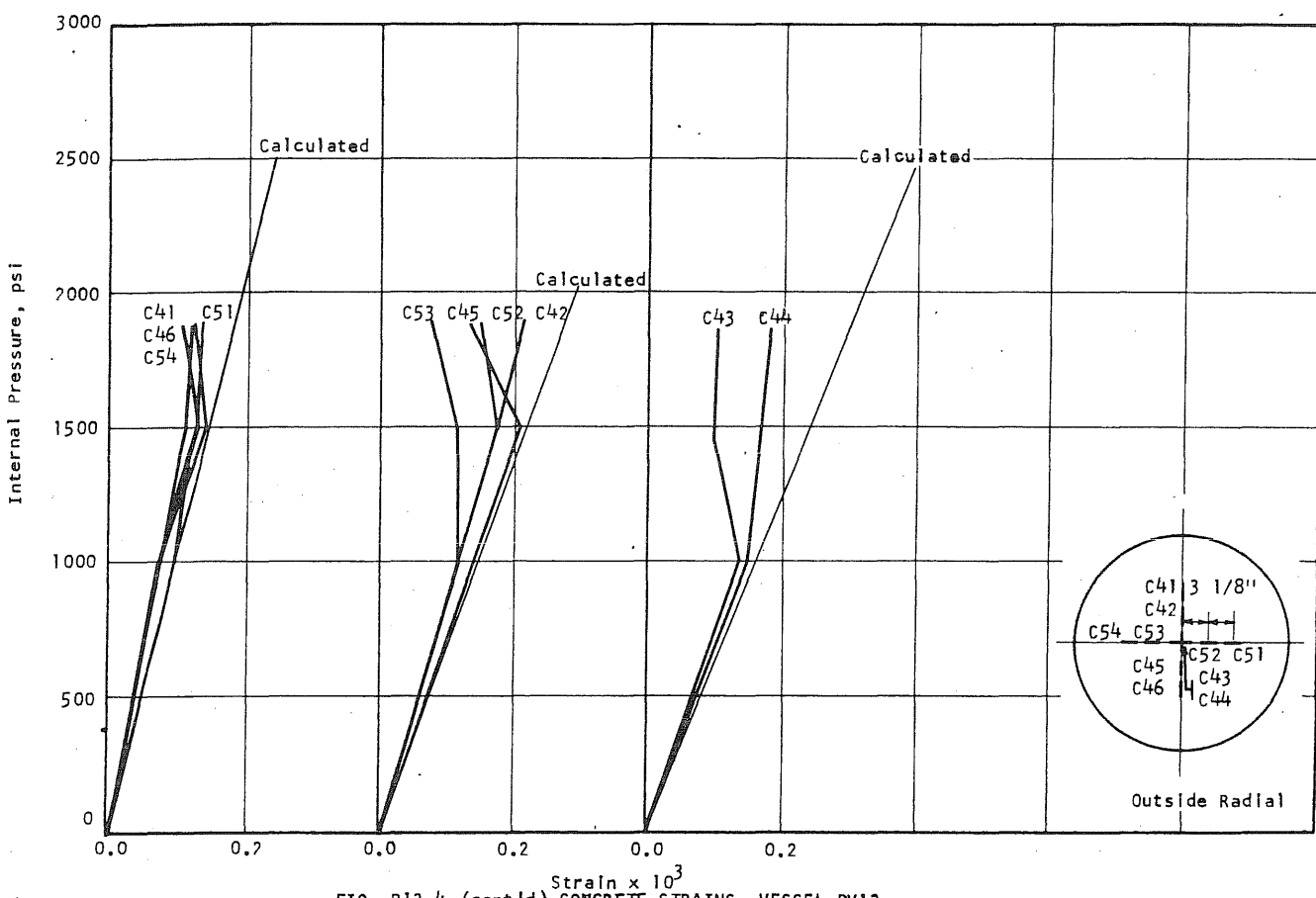
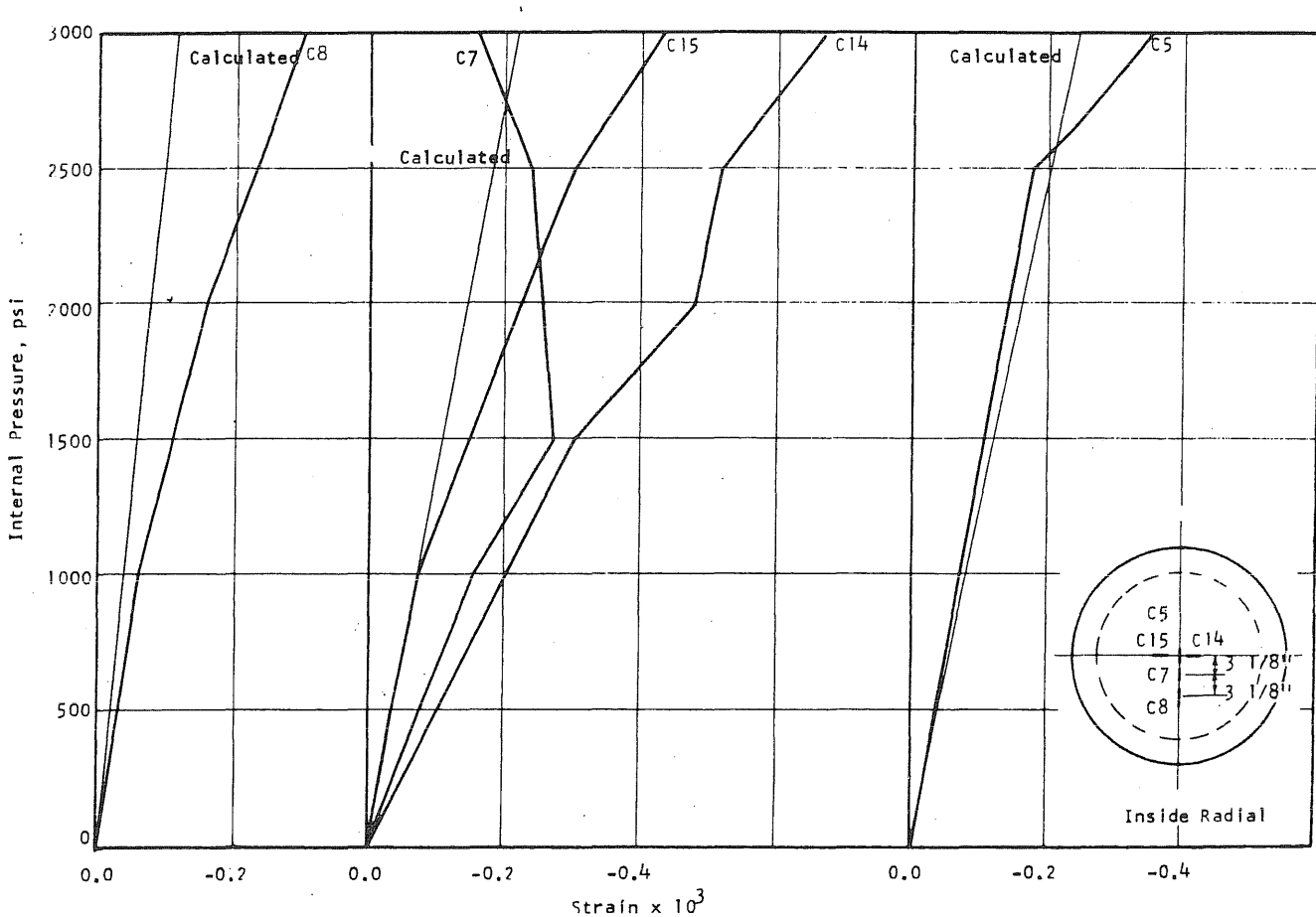
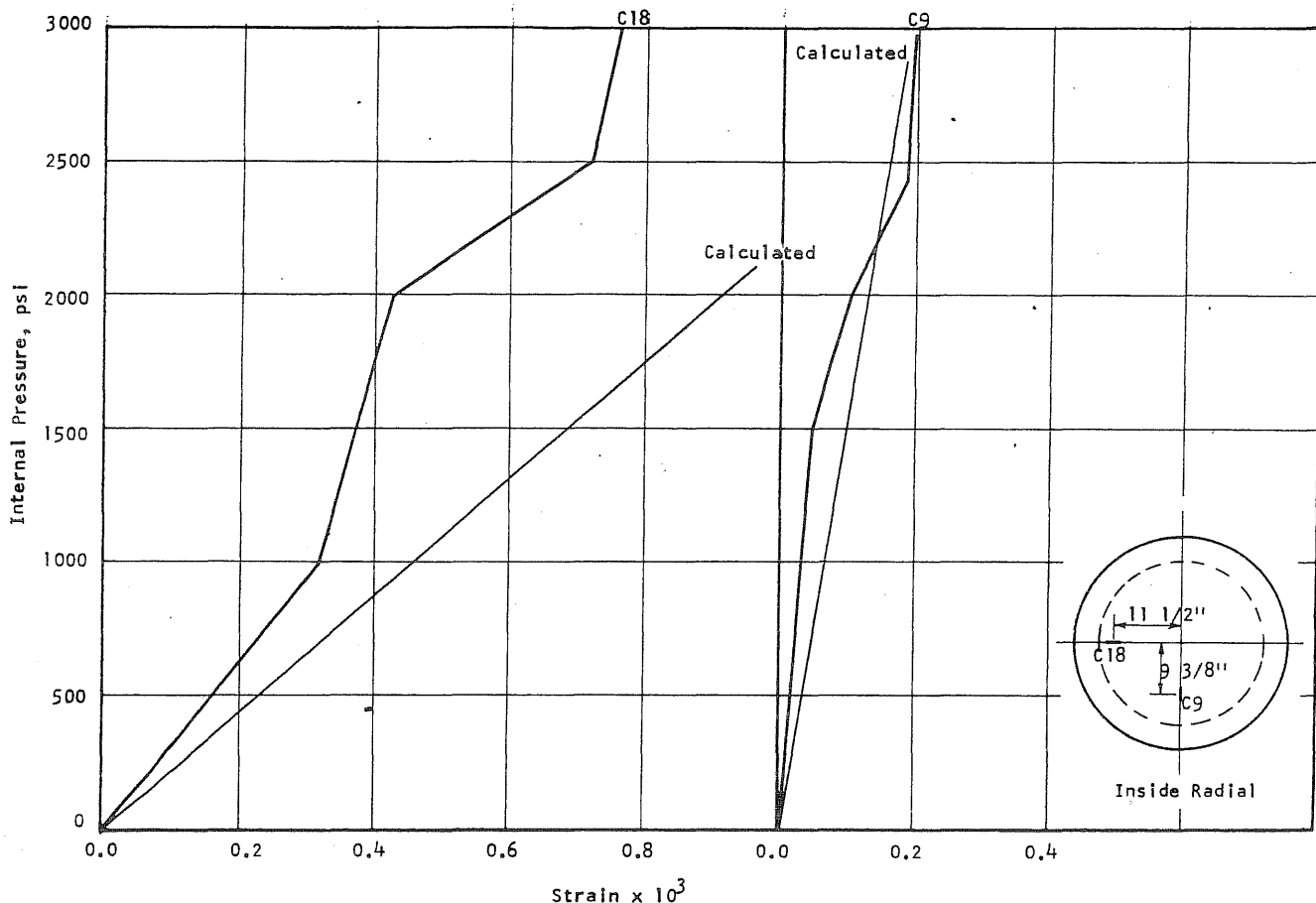


FIG. B13.4 (cont'd) CONCRETE STRAINS, VESSEL PV13



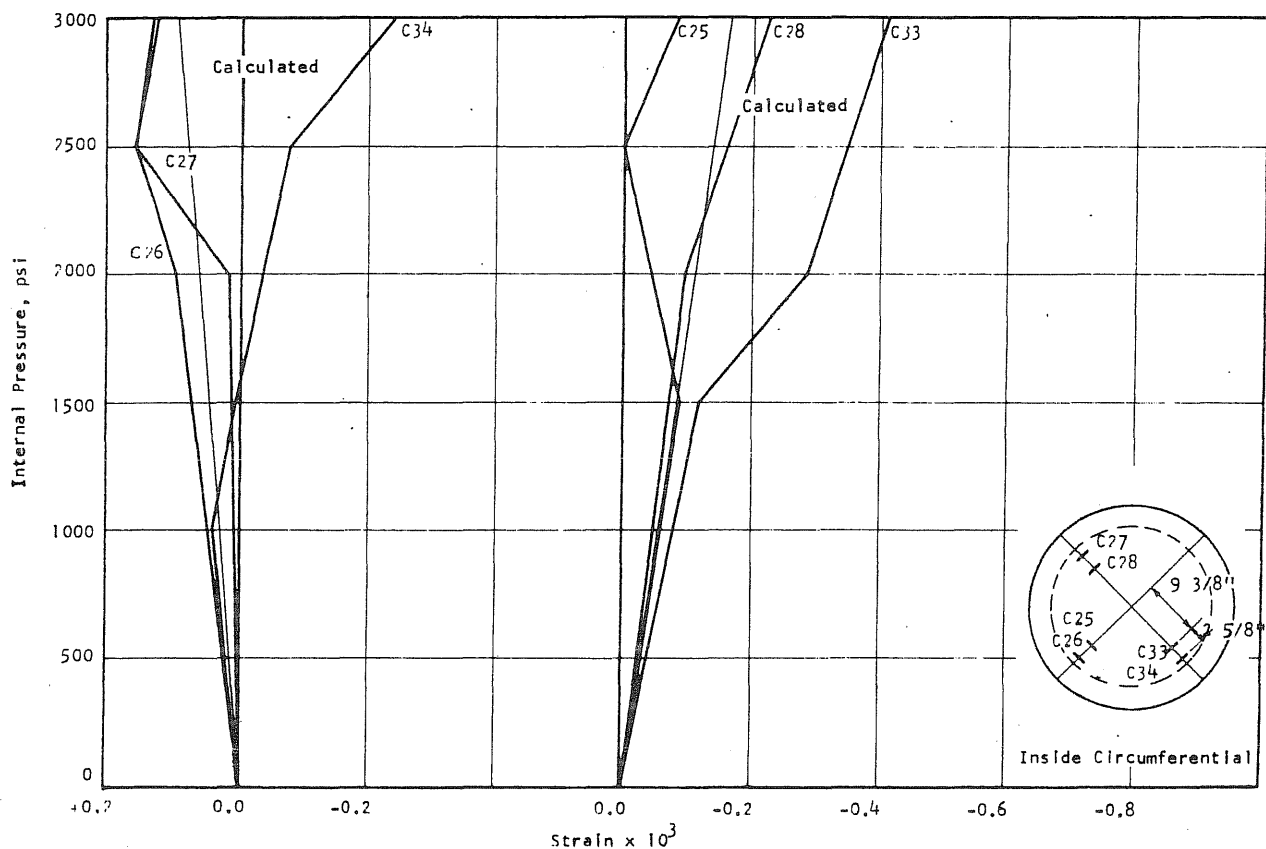


FIG. B13.6 CONCRETE STRAINS, VESSEL PV13

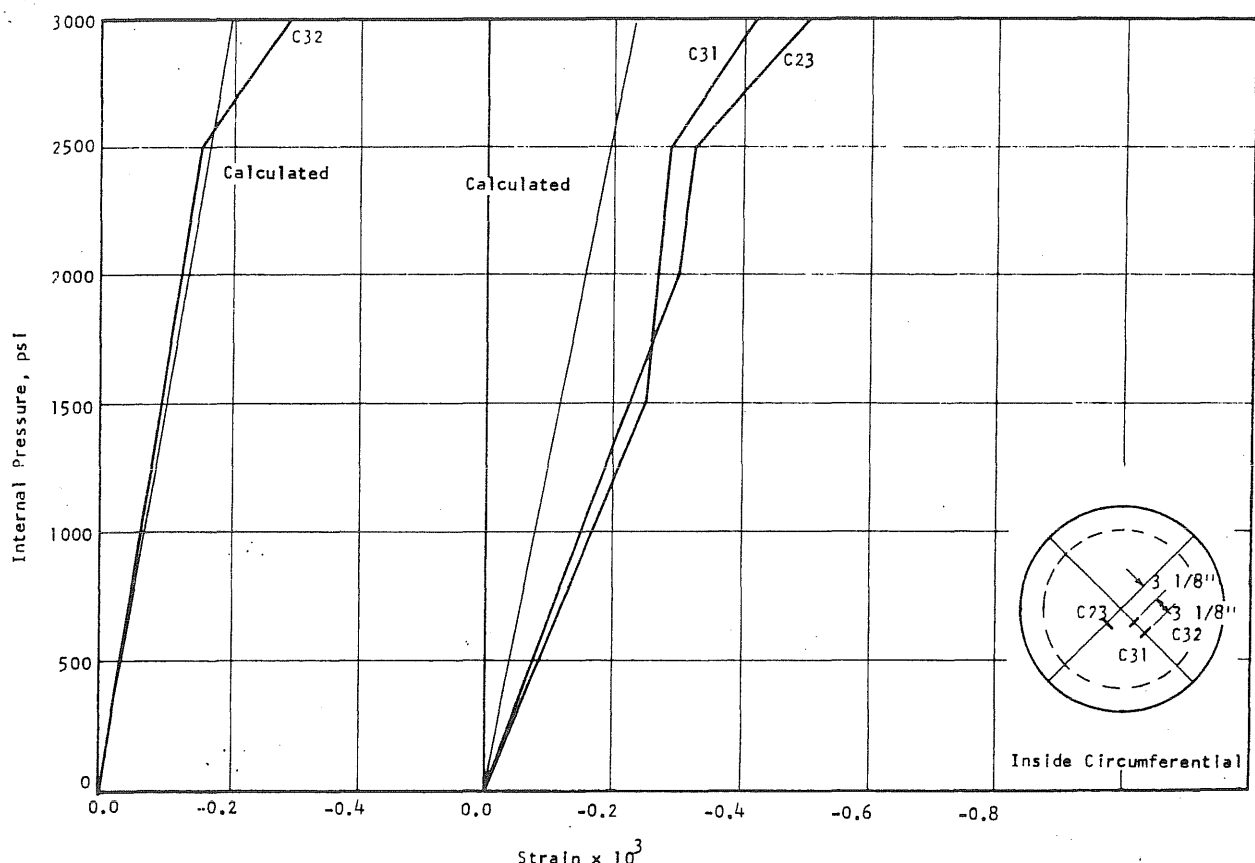


FIG. B13.6 (cont'd) CONCRETE STRAINS, VESSEL PV13

Internal pressure, psi

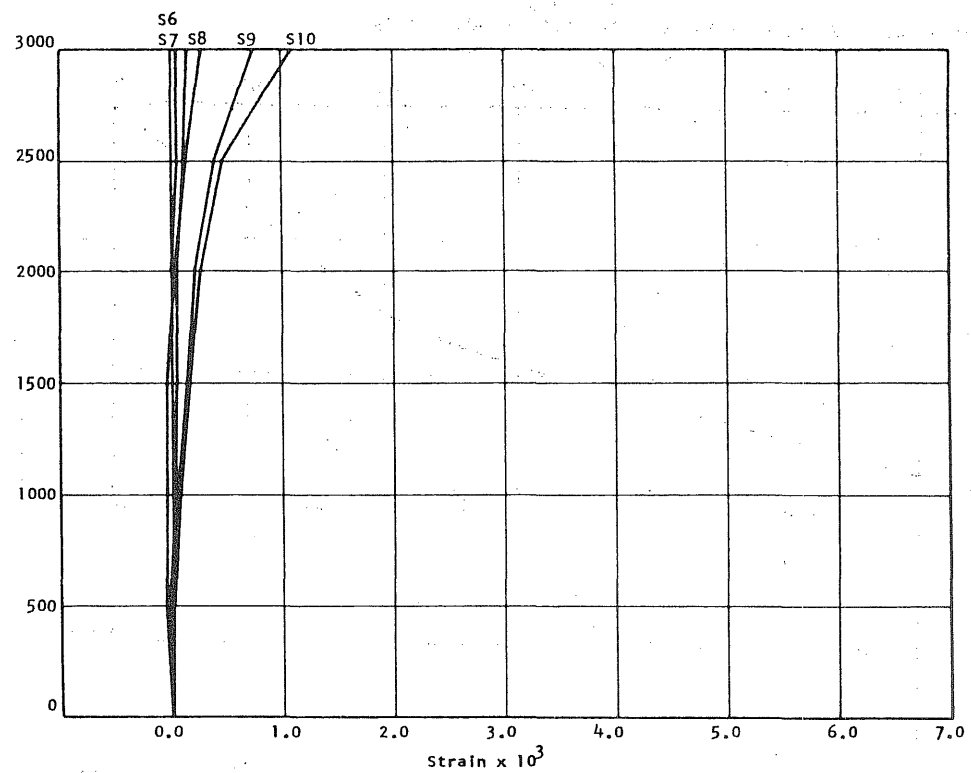


FIG. B13.7 APPLIED PRESSURE VS STRAIN IN CIRCUMFERENTIAL PRESTRESS WIRE AT THE E-END OF THE E-W DIAMETER OF PV13

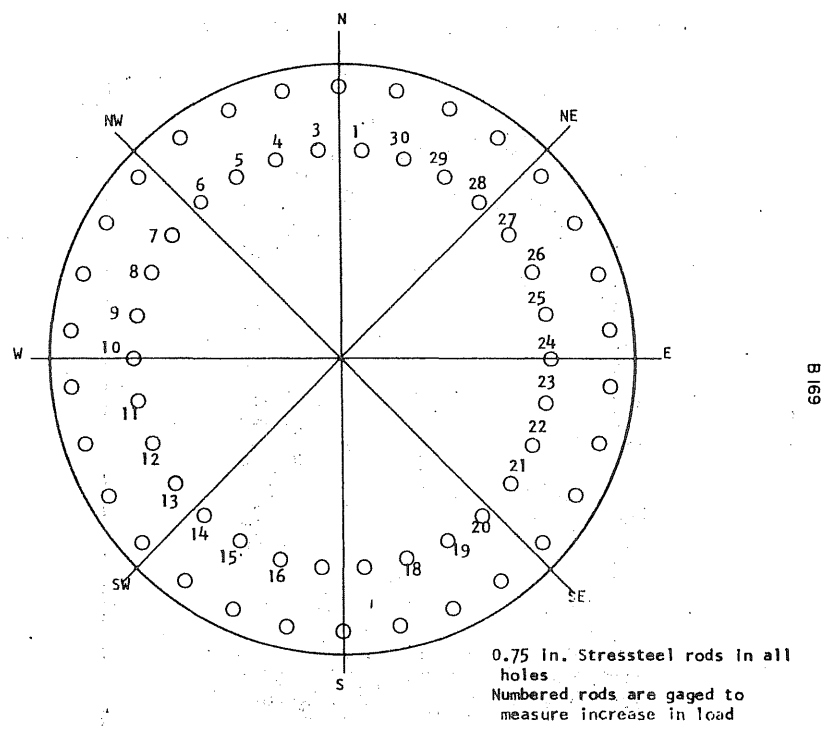


FIG. B13.8 LOCATION OF LONGITUDINAL REINFORCEMENT

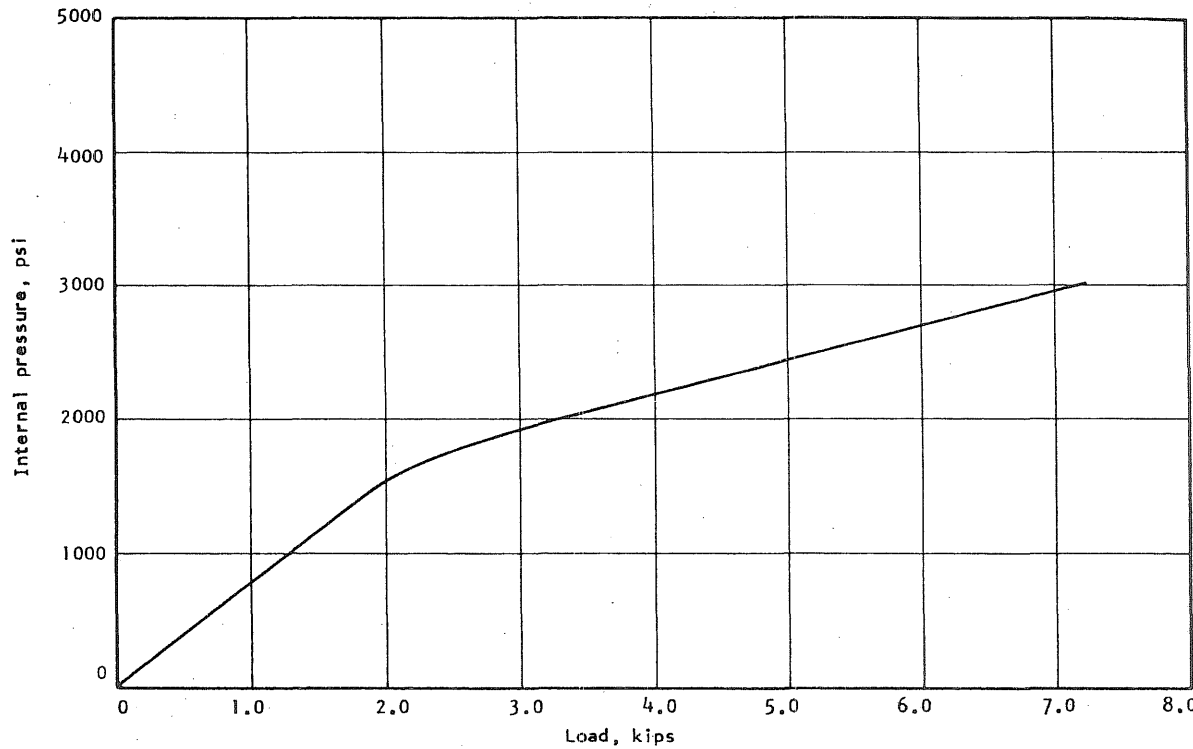


FIG. B13.9 APPLIED PRESSURE VS INCREASE IN LOAD IN STRESSTEEL
ROD NO. 11

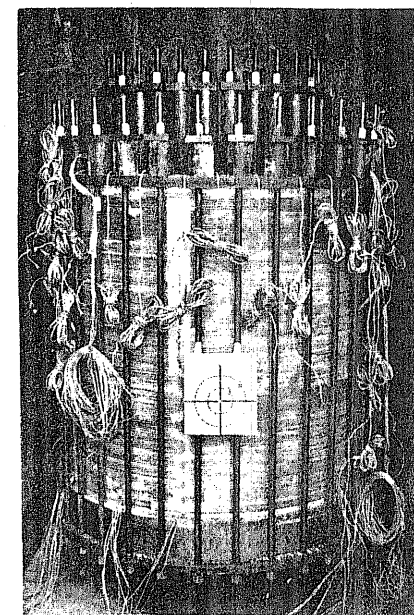


FIG. B13.10 VESSEL PV13 READY TO BE TESTED

B170

B14 Test Vessel PV14 ($t = 15$ in., $s = 1/4$ in.)

Since PV13 had not developed an end slab failure, PV14 was used to test the circumferential prestress wire and the side wall capacity.

Two vertical grooves (3/4 in. x 3/8 in.) were cut in the inside of the side wall at 180° apart and were intended to be crack initiators. Small grooves were made across the main grooves at 2 in., 9 in., 17 in., and 24 in. from the base of the side wall. A-12 concrete gages were located in these grooves perpendicular to the main crack. The locations of gages on the circumferential reinforcement are shown in Fig. B14.3 and Fig. B14.4. The gages on the west half of the vessel were at the same level as the concrete gages. Deflection measurements were taken on the side of the vessel at nine locations as shown in Fig. B14.2. None were taken on the top. The longitudinal prestressing was similar to that of vessel PV13.

The vessel was pressurized in increments of 250 psi up to 2000 psi, increased to 500-psi increments up to 3000 psi, and reduced increments up to failure. A small leak occurred at the beginning of the test up to 3000 psi but then suddenly stopped and there was no more leakage until failure occurred at 3690 psi.

After the test, the vessel was observed to be heavily cracked and five of the rod holes had collapsed onto the rods. Small radial cracks were visible through all of the rod holes after the vessel was broken up, but many of these were not visible on the side of the vessel. A circumferential crack with a diameter of 35 in. was visible in the end of the side wall. No cracks were visible in the top of the end slab.

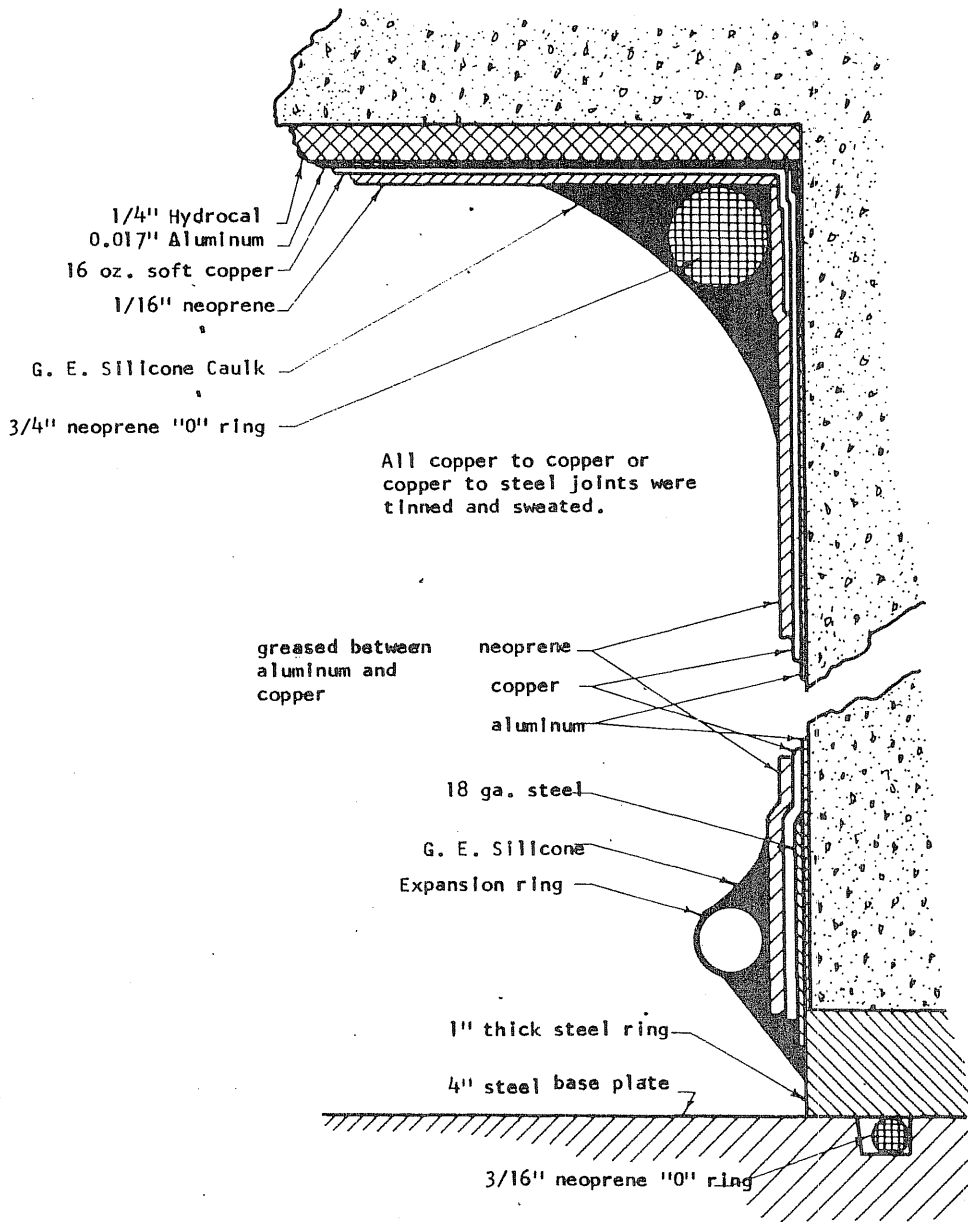


FIG. B14.1 SEALING DETAIL FOR PV14

All Dial Gages Are On West Axis

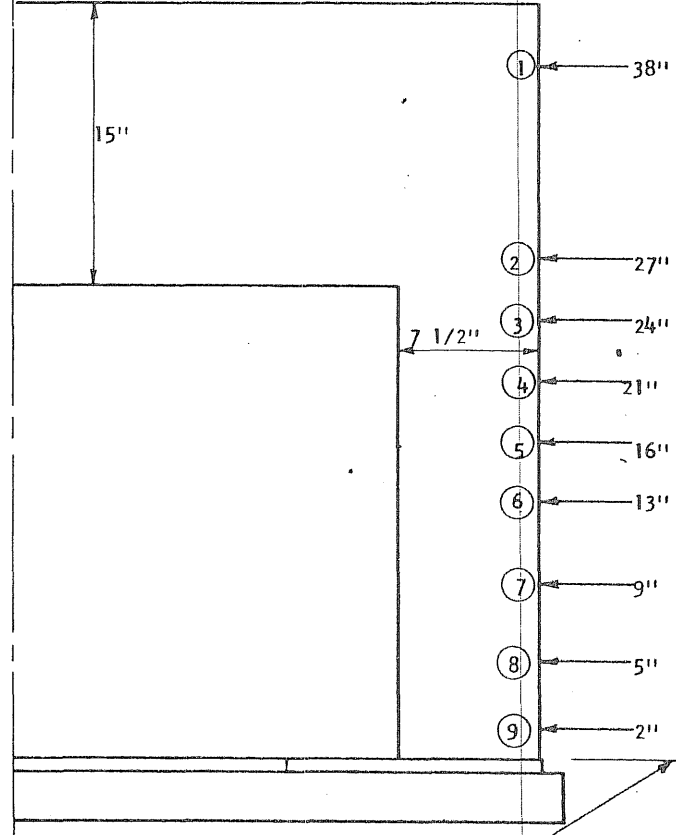


FIG. B14.2 LOCATION OF DEFLECTION GAGES ON PV14

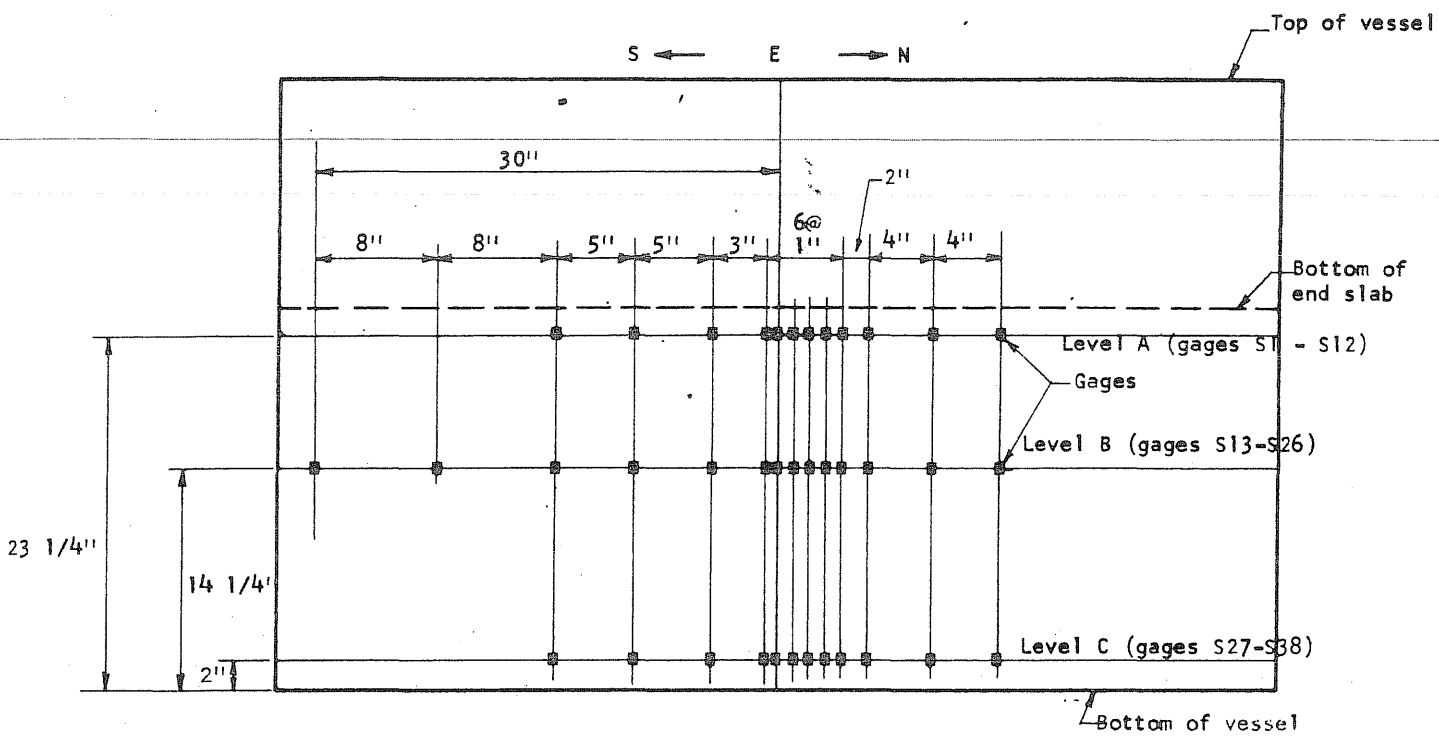


FIG. B14.3 LOCATION OF CIRCUMFERENTIAL REINFORCEMENT GAGES FOR EAST HALF OF PV14

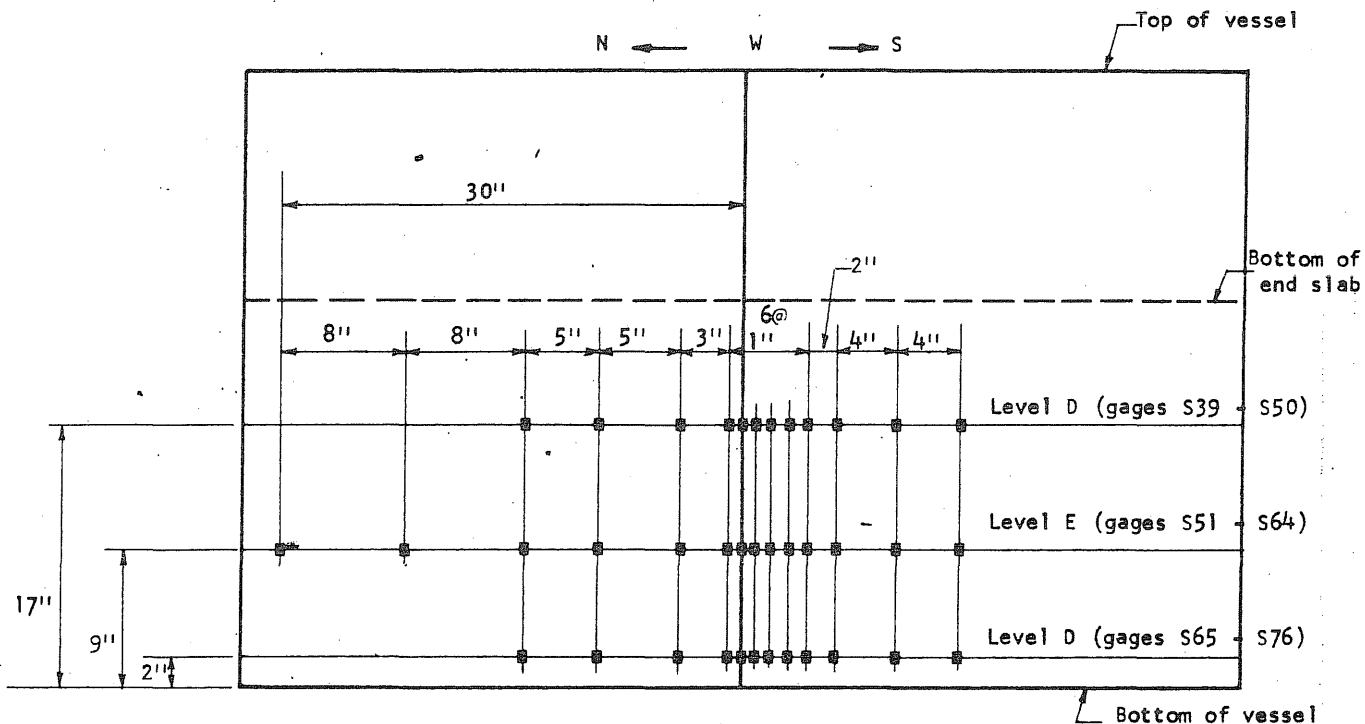


FIG. B14.3 (cont'd) LOCATION OF CIRCUMFERENTIAL REINFORCEMENT GAGES FOR WEST HALF OF PV14

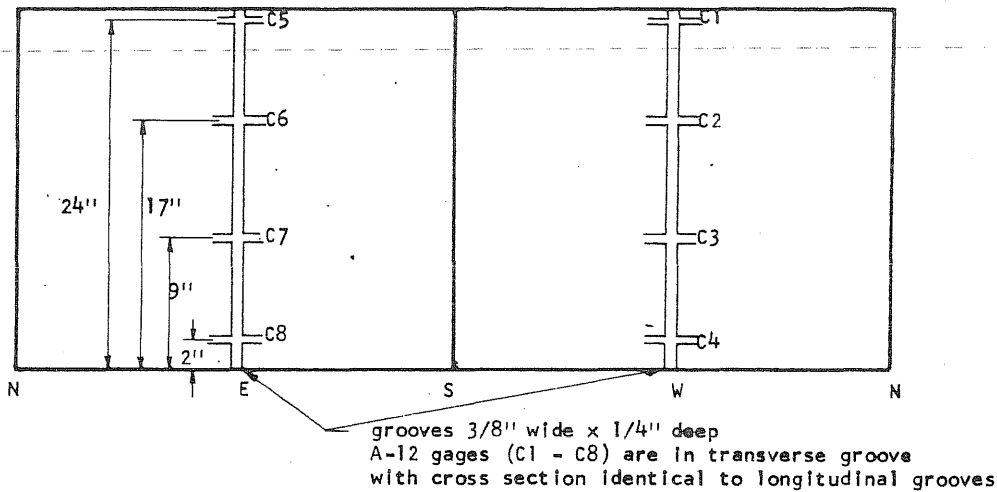


FIG. B14.4 LOCATION OF CONCRETE GAGES ON INSIDE SIDE WALL OF PV14

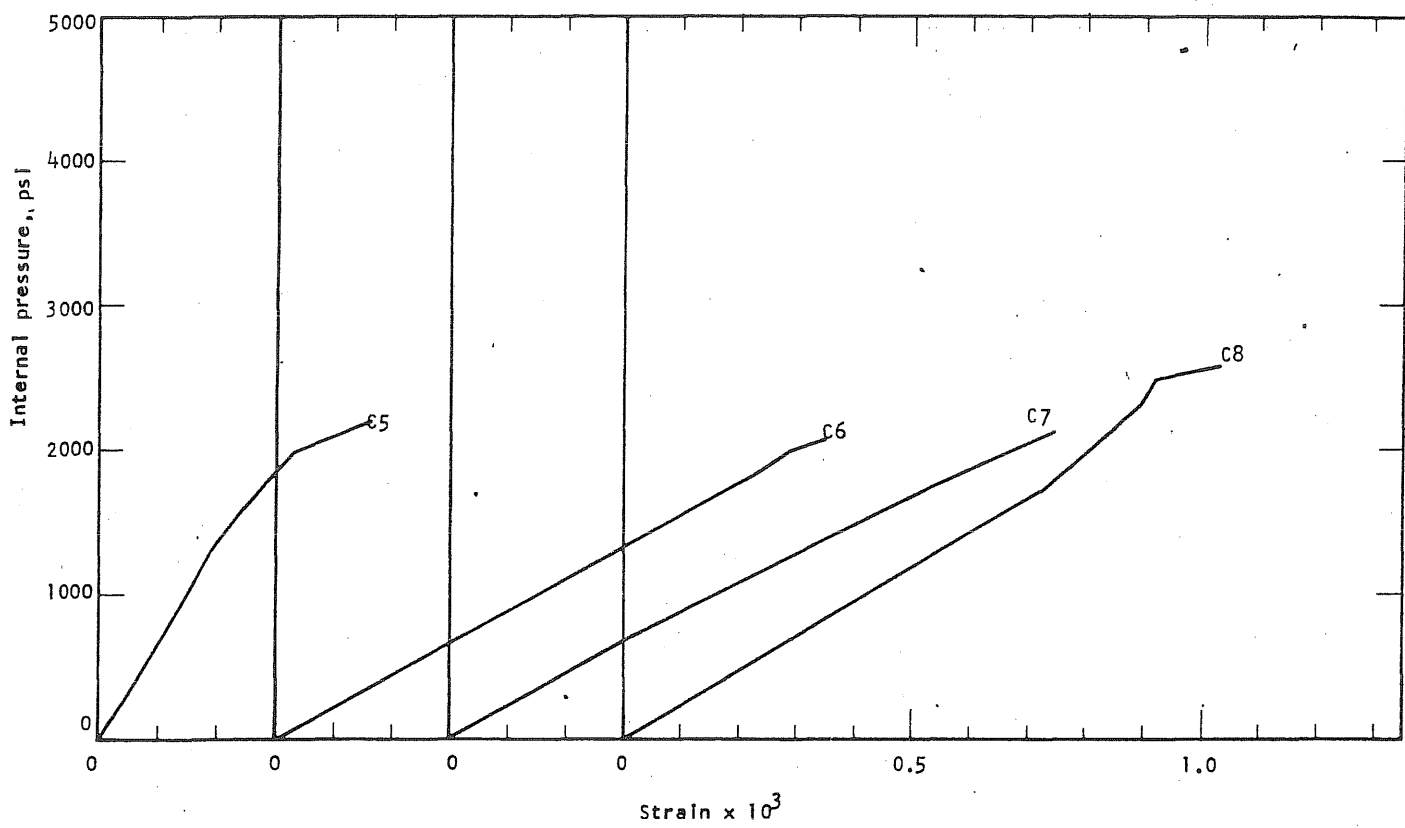


FIG. B14.5 CONCRETE STRAINS, VESSEL PV14

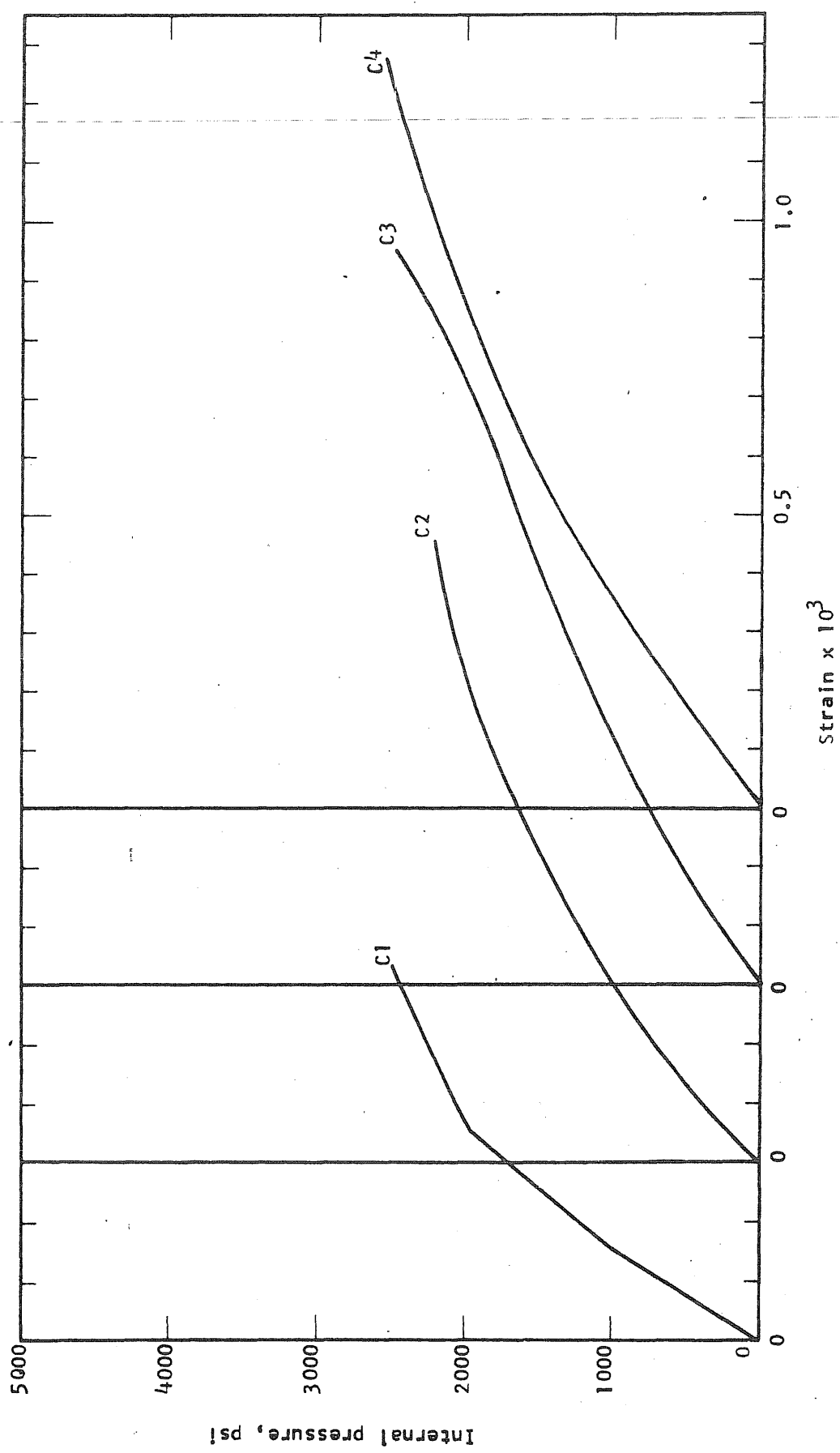


FIG. B14.6 CONCRETE STRAINS, VESSEL PV14

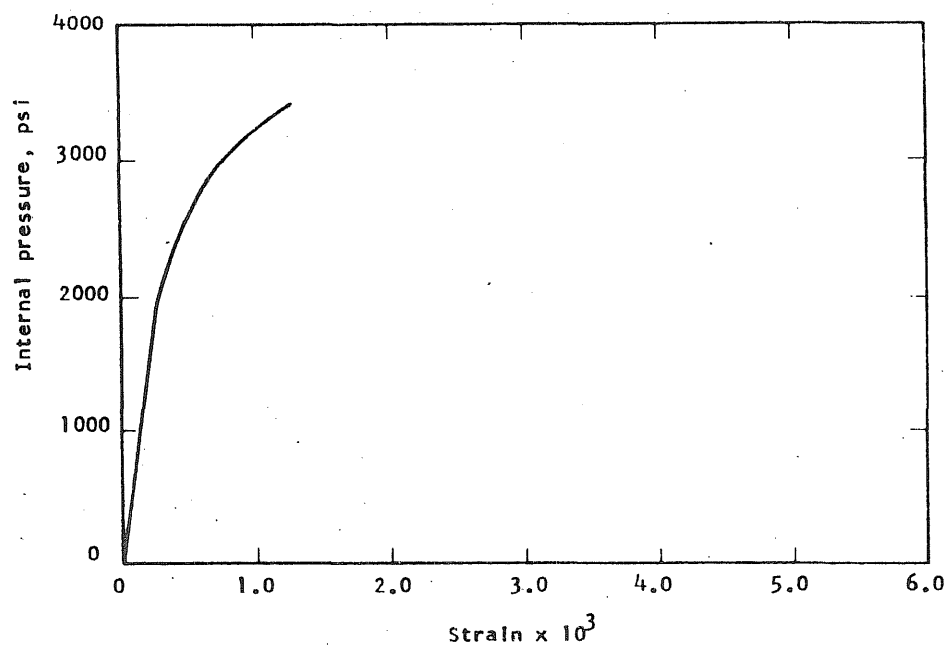


FIG. B14.7 APPLIED PRESSURE vs AVERAGE STRAIN IN CIRCUMFERENTIAL PRESTRESS WIRE AT LEVEL A

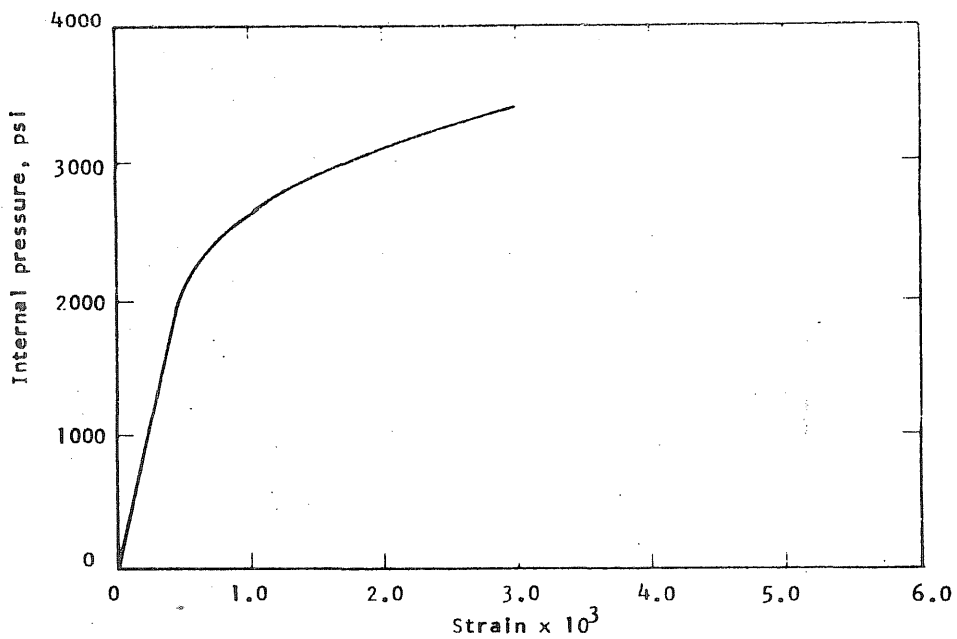


FIG. B14.8 APPLIED PRESSURE vs AVERAGE STRAIN IN CIRCUMFERENTIAL PRESTRESS WIRE AT LEVEL B

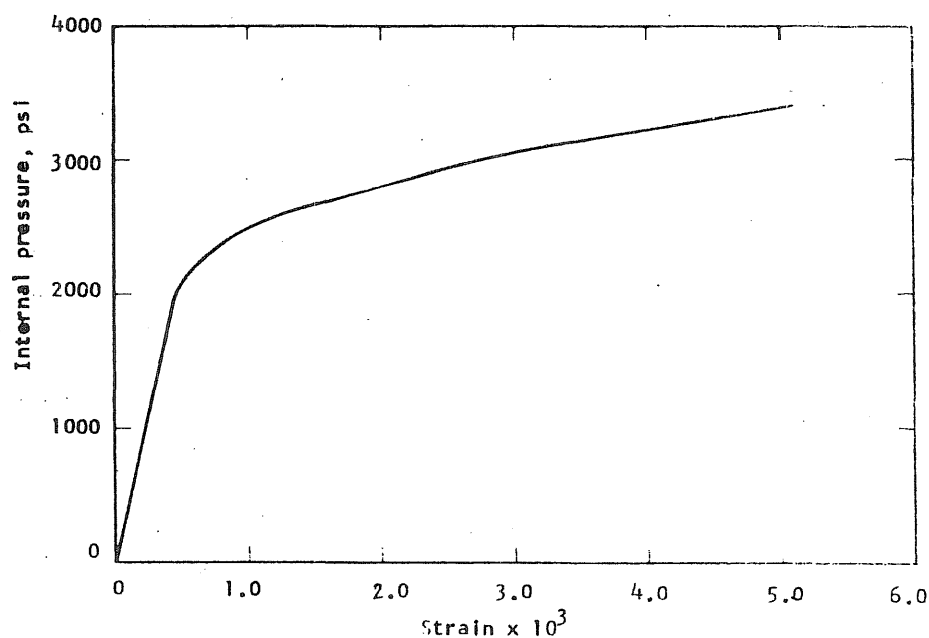


FIG. B14.9 APPLIED PRESSURE vs AVERAGE STRAIN IN CIRCUMFERENTIAL PRESTRESS WIRE AT LEVEL C

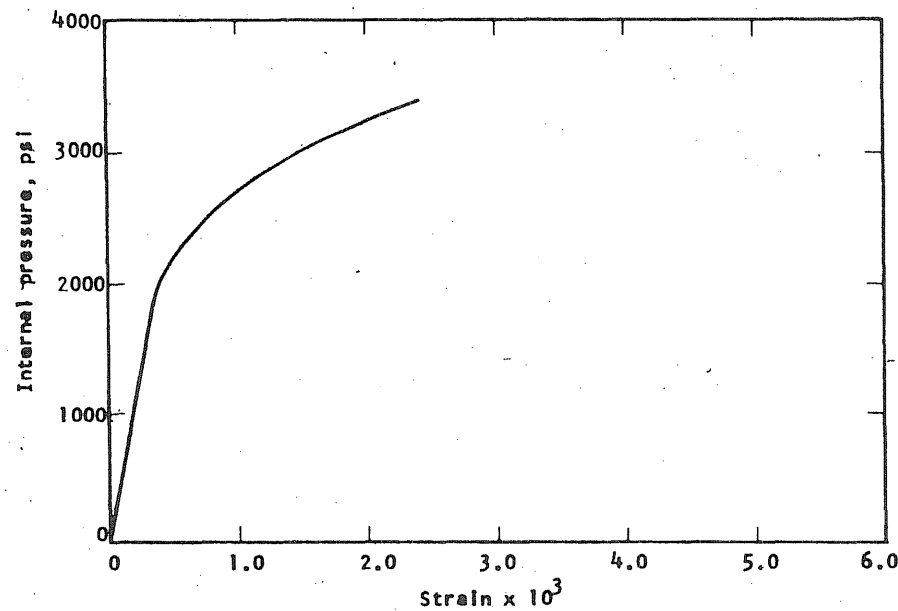


FIG. B14.10 APPLIED PRESSURE vs AVERAGE STRAIN IN CIRCUMFERENTIAL PRESTRESS WIRE AT LEVEL D

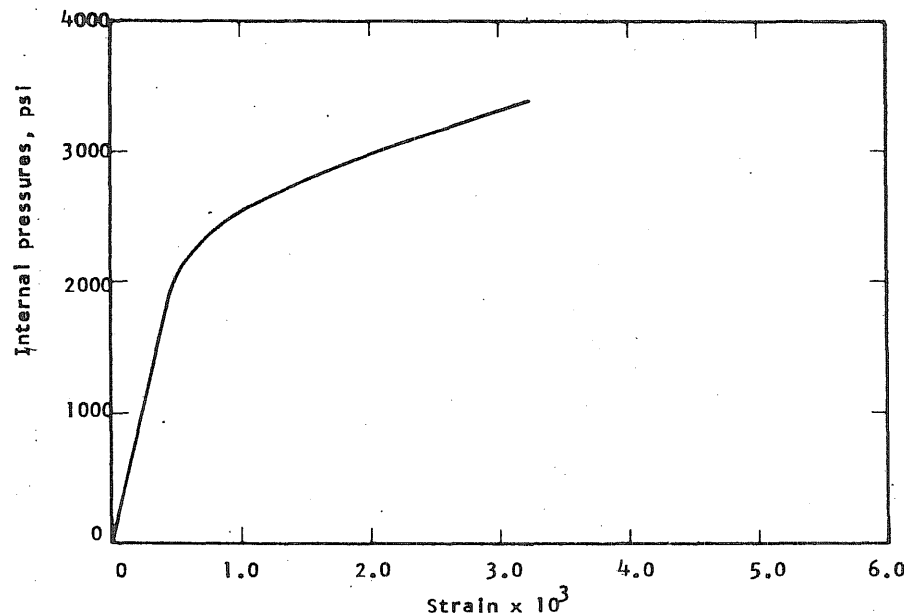


FIG B14.11 APPLIED PRESSURE vs AVERAGE STRAIN IN CIRCUMFERENTIAL PRESTRESS WIRE AT LEVEL E

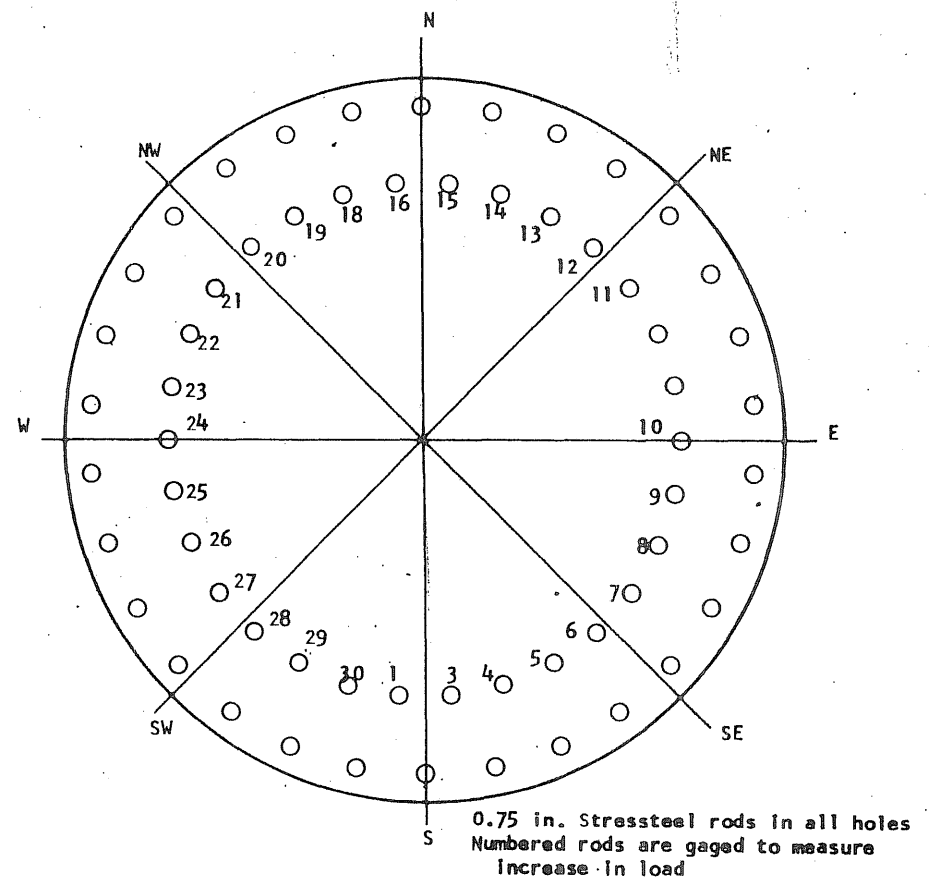


FIG. B14.12 LOCATION OF LONGITUDINAL REINFORCEMENT

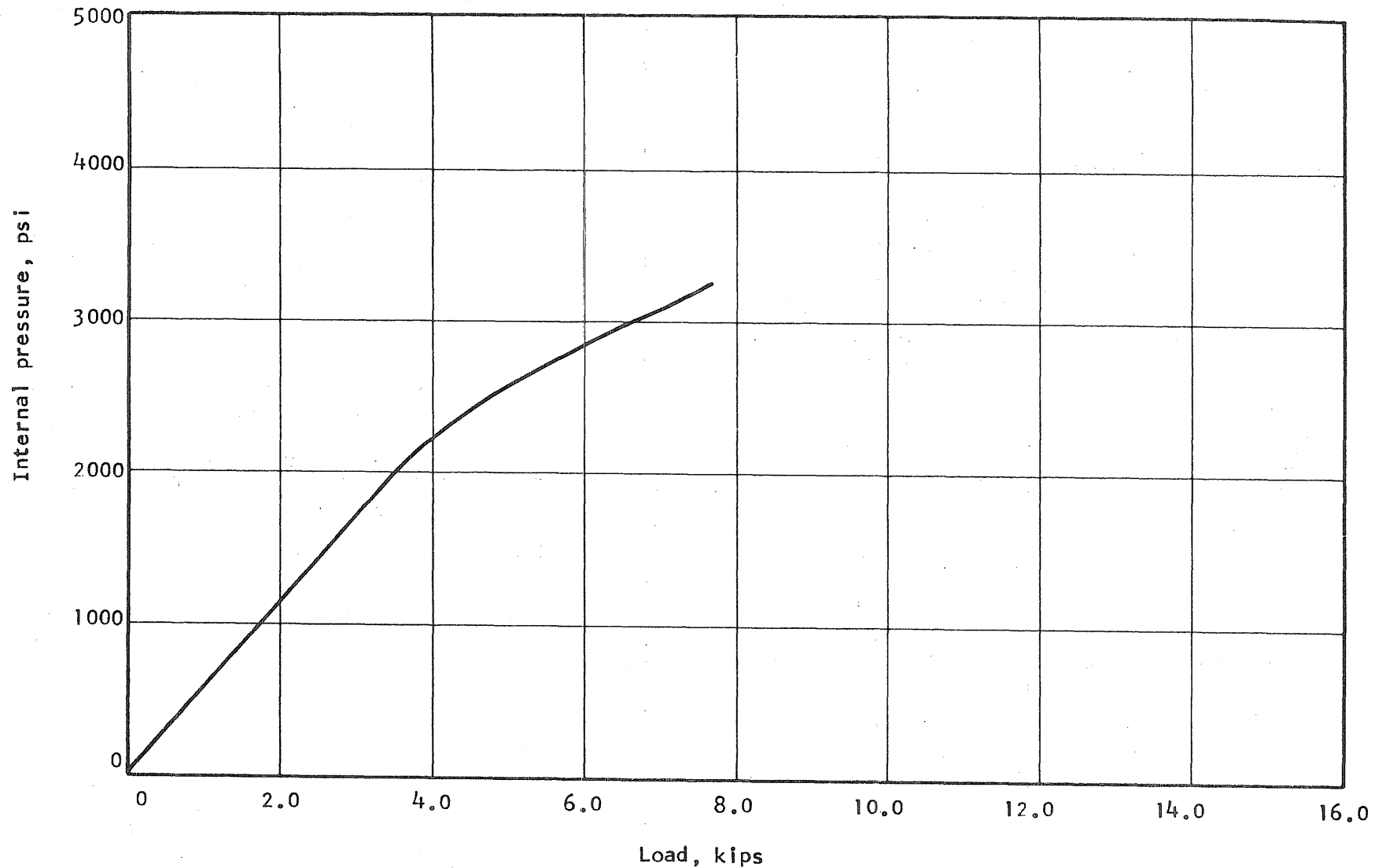


FIG. B14.13 APPLIED PRESSURE vs INCREASE IN LOAD IN STRESSTEEL ROD No. 9

B 179

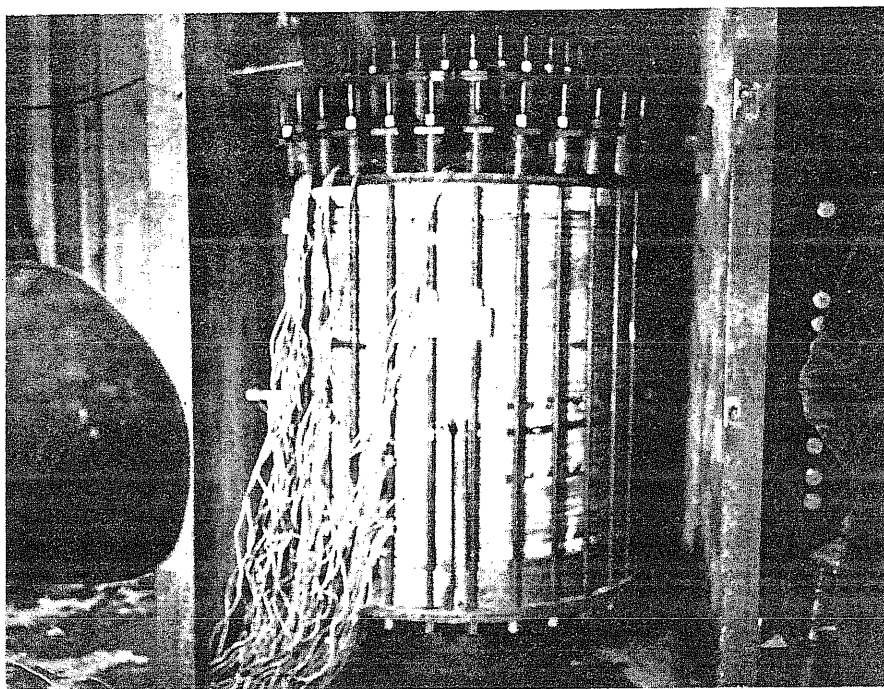


FIG. B14.14 VESSEL PV14 READY TO BE TESTED

B15 Test Vessel PV15 ($t = 7.5$ in., $s = 1/4$ in.)

Test vessel PV15 was cast with two rows of rod holes with diameters of 29 in. and 34 in. Due to the congestion of vertical prestressing on the end slab, it was impossible to use the three in. by three in. bearing plates. Instead, the 1-1/4 in. thick steel plates used for PV13 and PV14 was used. It was necessary to drill another set of holes for the outside set of rods. The top plate was slotted between the rod holes to reduce the radial restraint from the steel ring when the end slab segments rotated.

Sixty stressteel rods were used for the longitudinal prestressing. Dial gages 1 and 7 were omitted. PV15 was sealed in the same manner as the previous three vessels.

The vessel was loaded in 200-psi increments up to a pressure of 1600 psi and then the increments were reduced to 100 psi until failure occurred at 2300 psi. The vessel failed about five minutes after loading had stopped at this pressure. Cracks were clearly visible in the end slab at 1800 psi as seen via the closed circuit TV. The center of the end slab punched out in a shear failure with all three liners in the end slab sheared along the circumference of the hole as shown in Fig. B15.12.

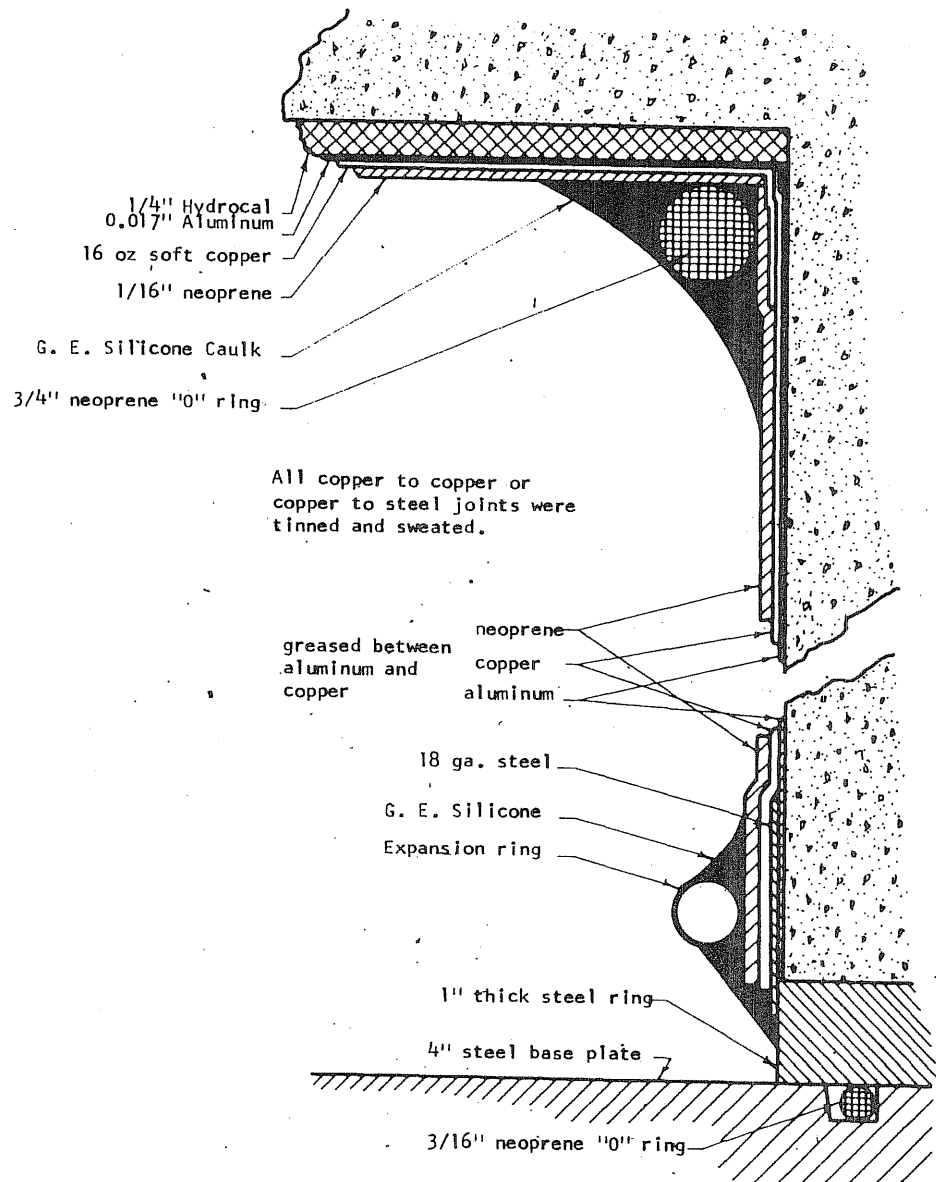


FIG. 15.1 SEALING DETAIL FOR PV15

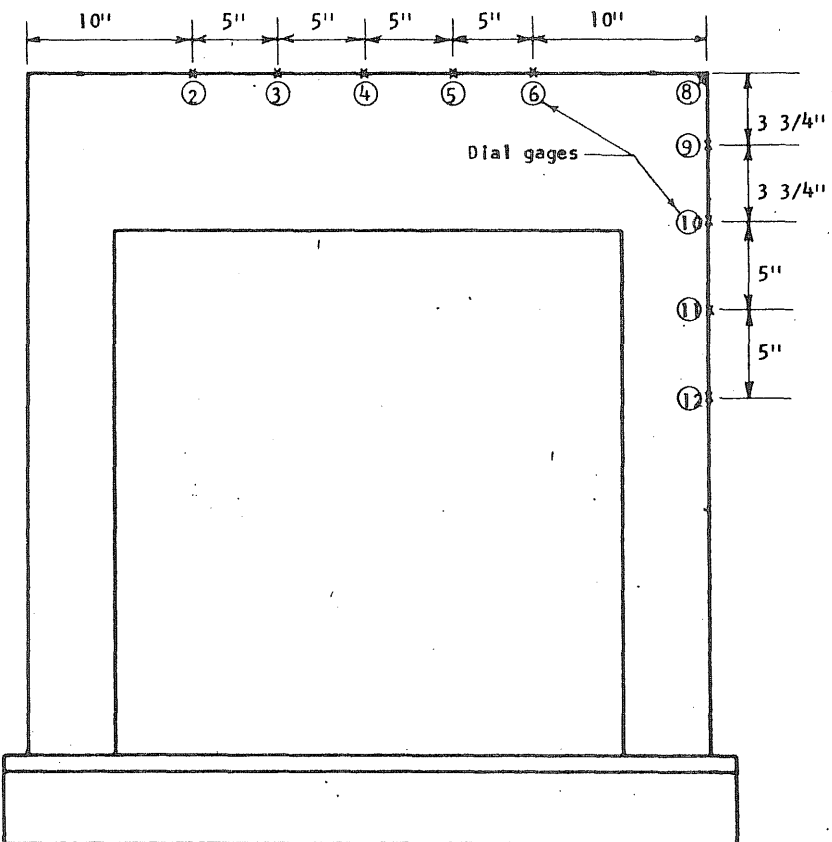


FIG. B15.2 LOCATION OF DEFLECTION GAGES ON PV15

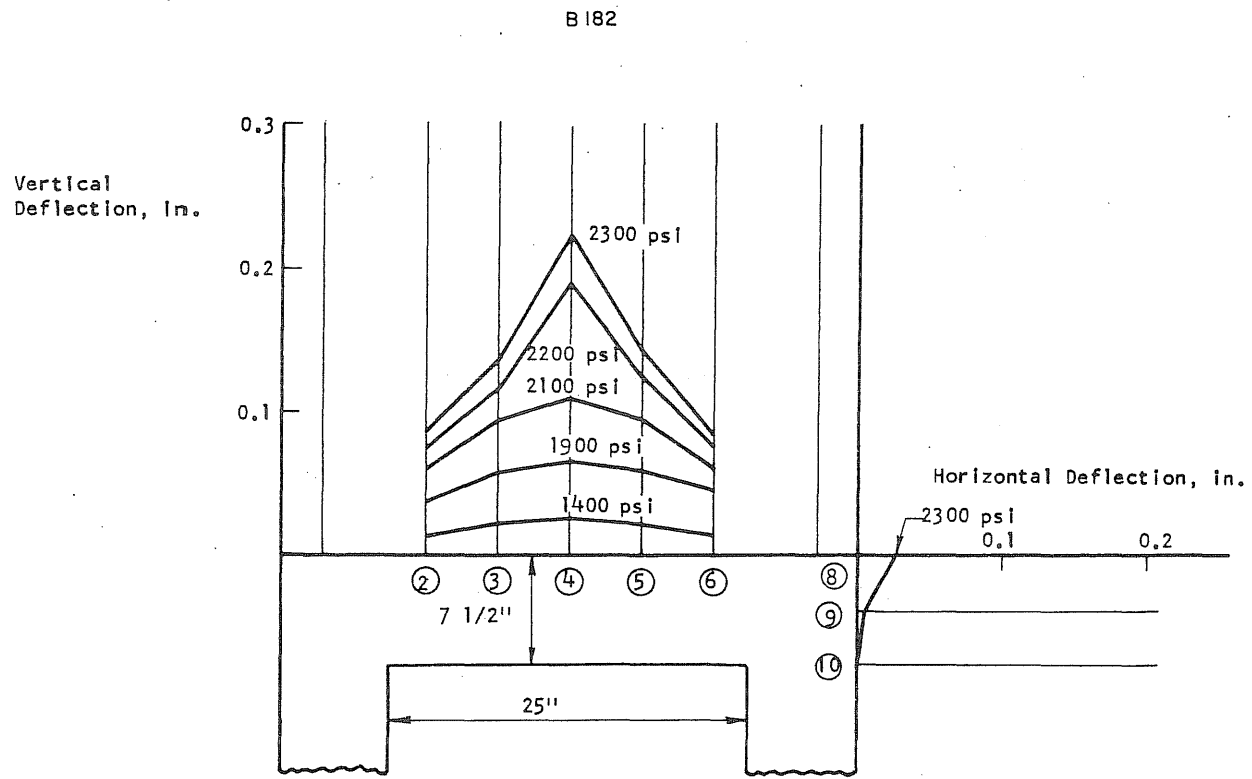


FIG. B15.3 DEFLECTION PROFILES OF THE END SLAB ALONG THE N-S DIAMETER OF PV15

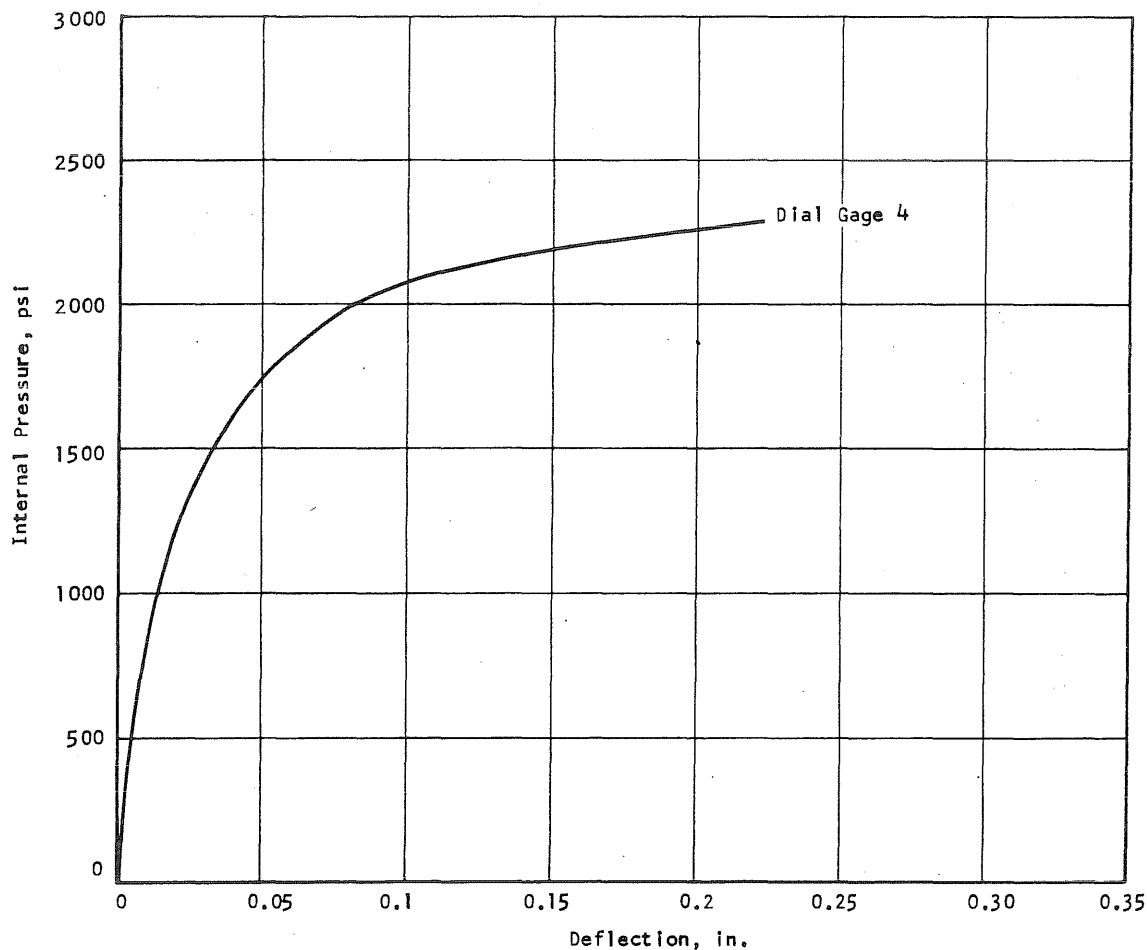
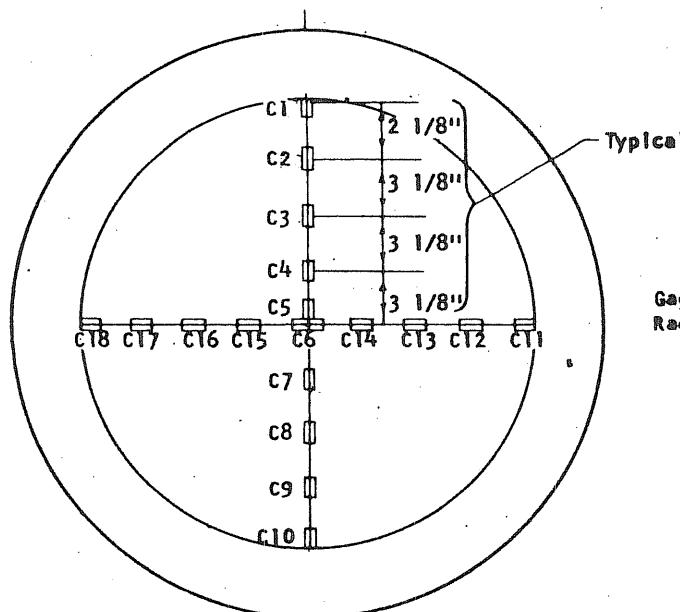
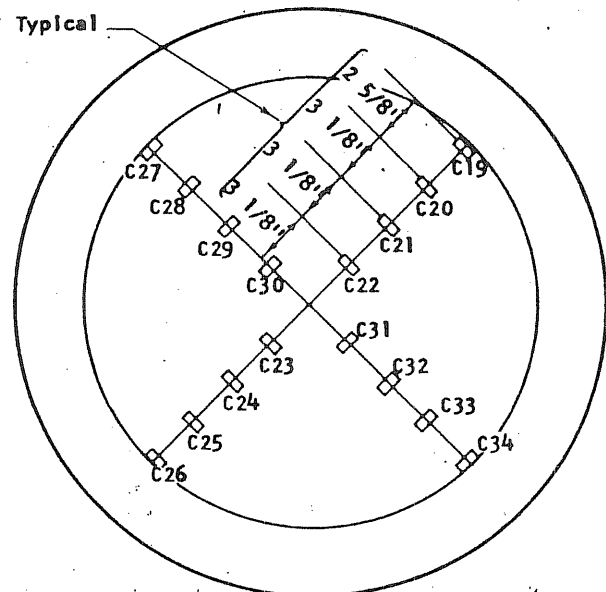
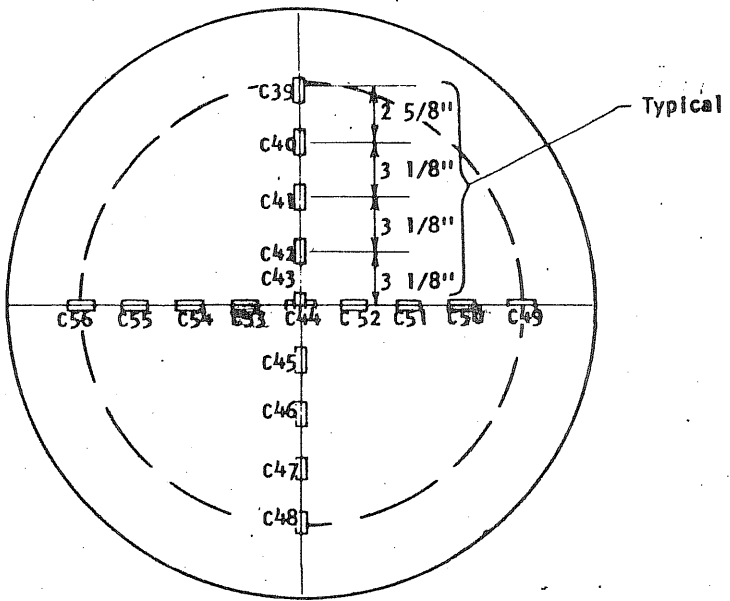


FIG. B15.4 APPLIED PRESSURE vs DEFLECTION AT MIDSPAN OF PV15

Concrete Gages on the Inside of the End Slab



Concrete gages on the Outside of the End Slab



Steel Gages on Circumferential Prestress Wire

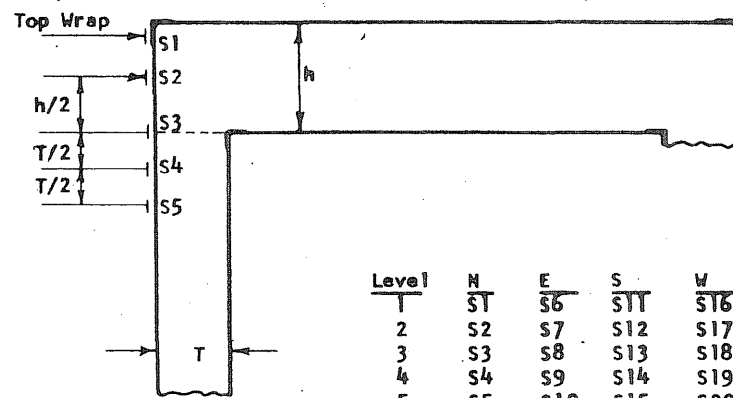


FIG. B15.5 (cont'd) STRAIN GAGE LOCATIONS ON PV15

FIG. B15.5 STRAIN GAGE LOCATIONS ON PV15

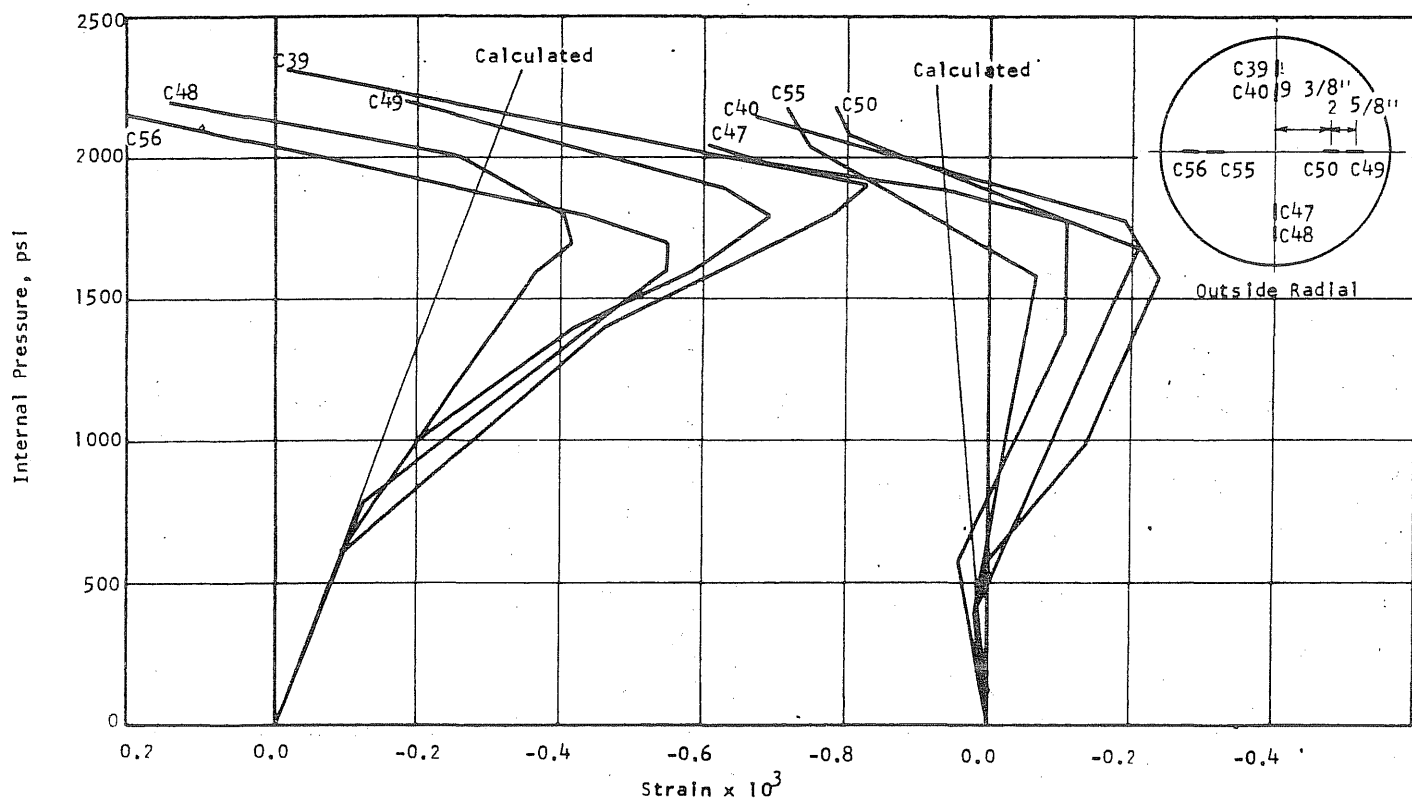


FIG. B15.6 CONCRETE STRAINS, VESSEL PV15

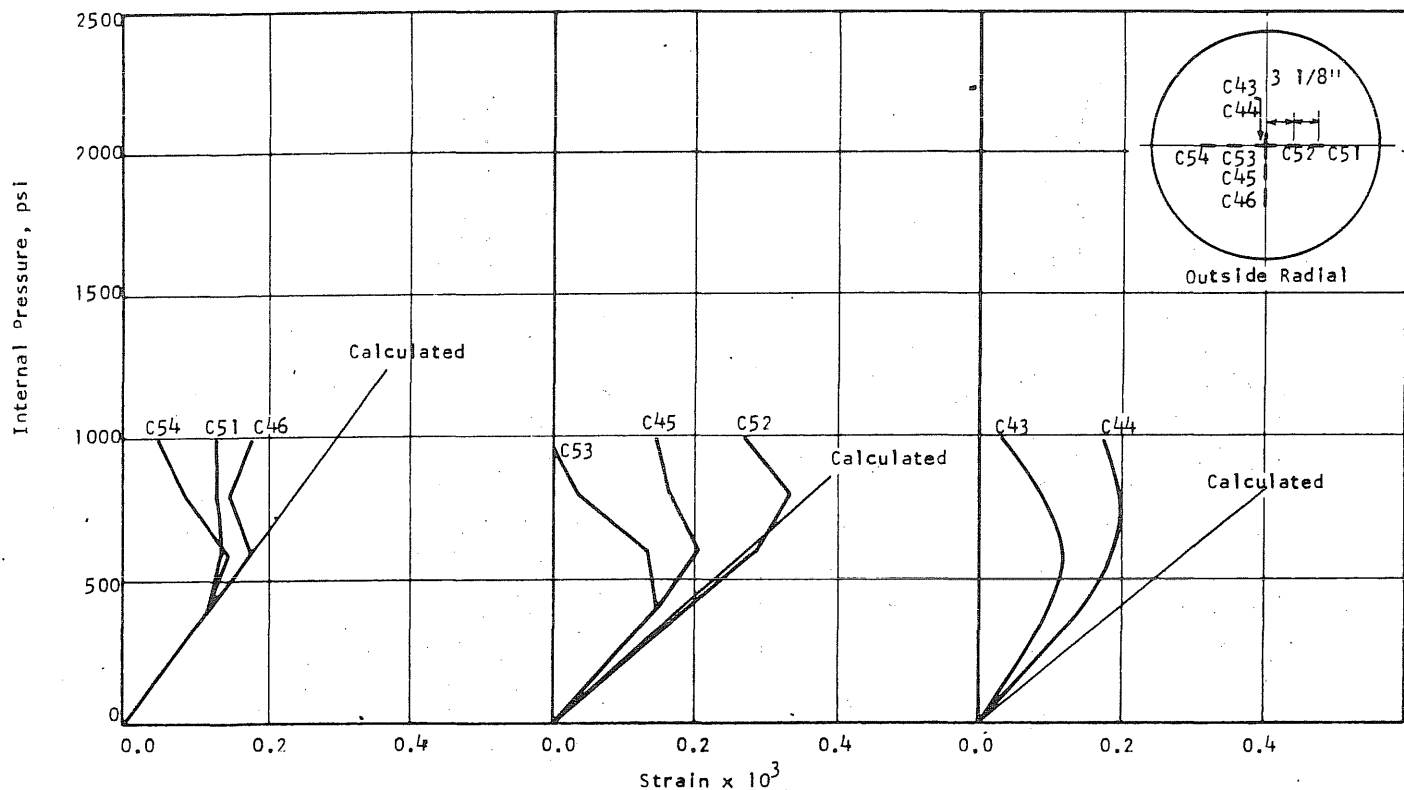


FIG. B15.6 (cont'd) CONCRETE STRAINS, VESSEL PV15

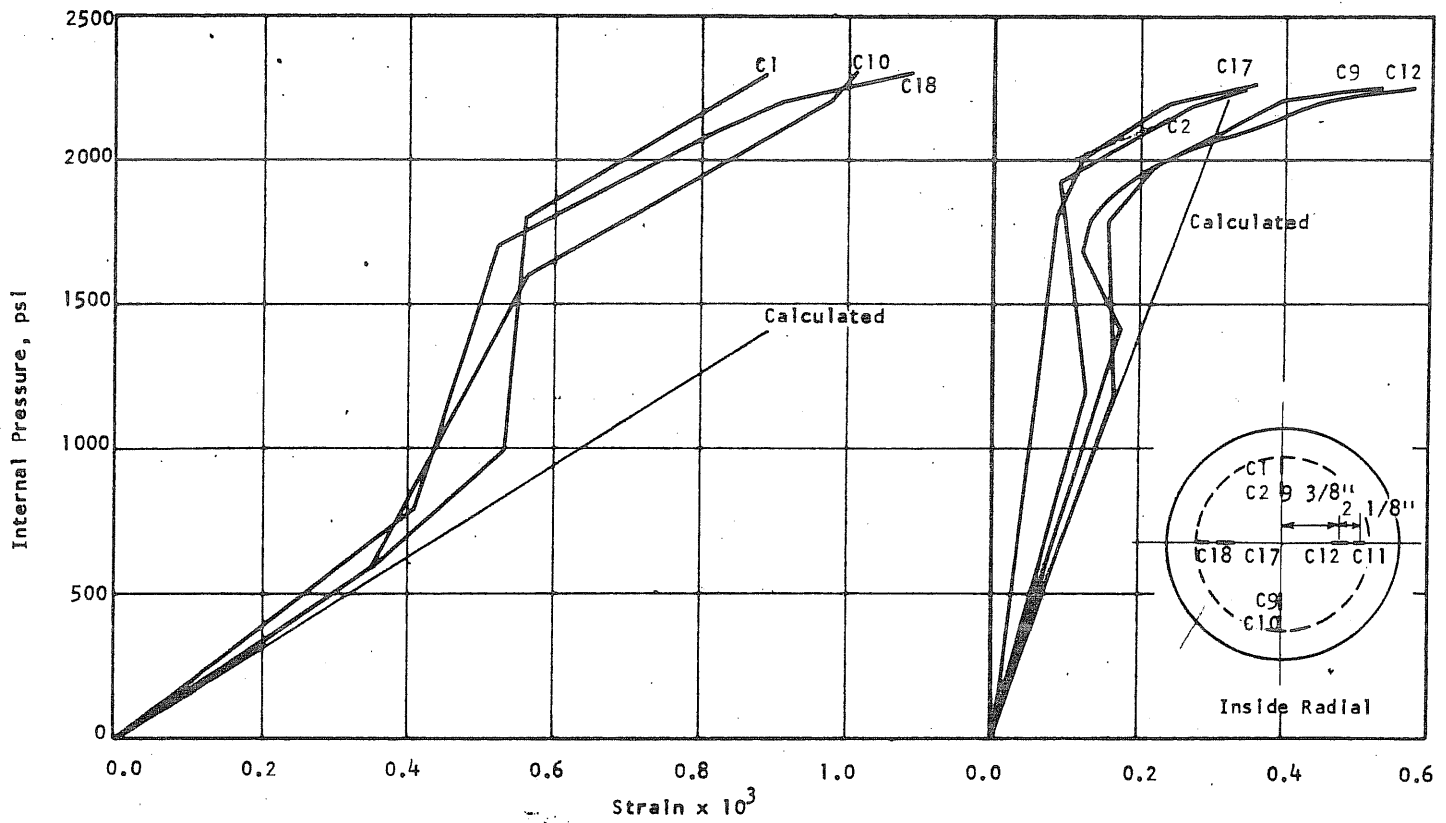


FIG. B15.7 CONCRETE STRAINS, VESSEL PV15

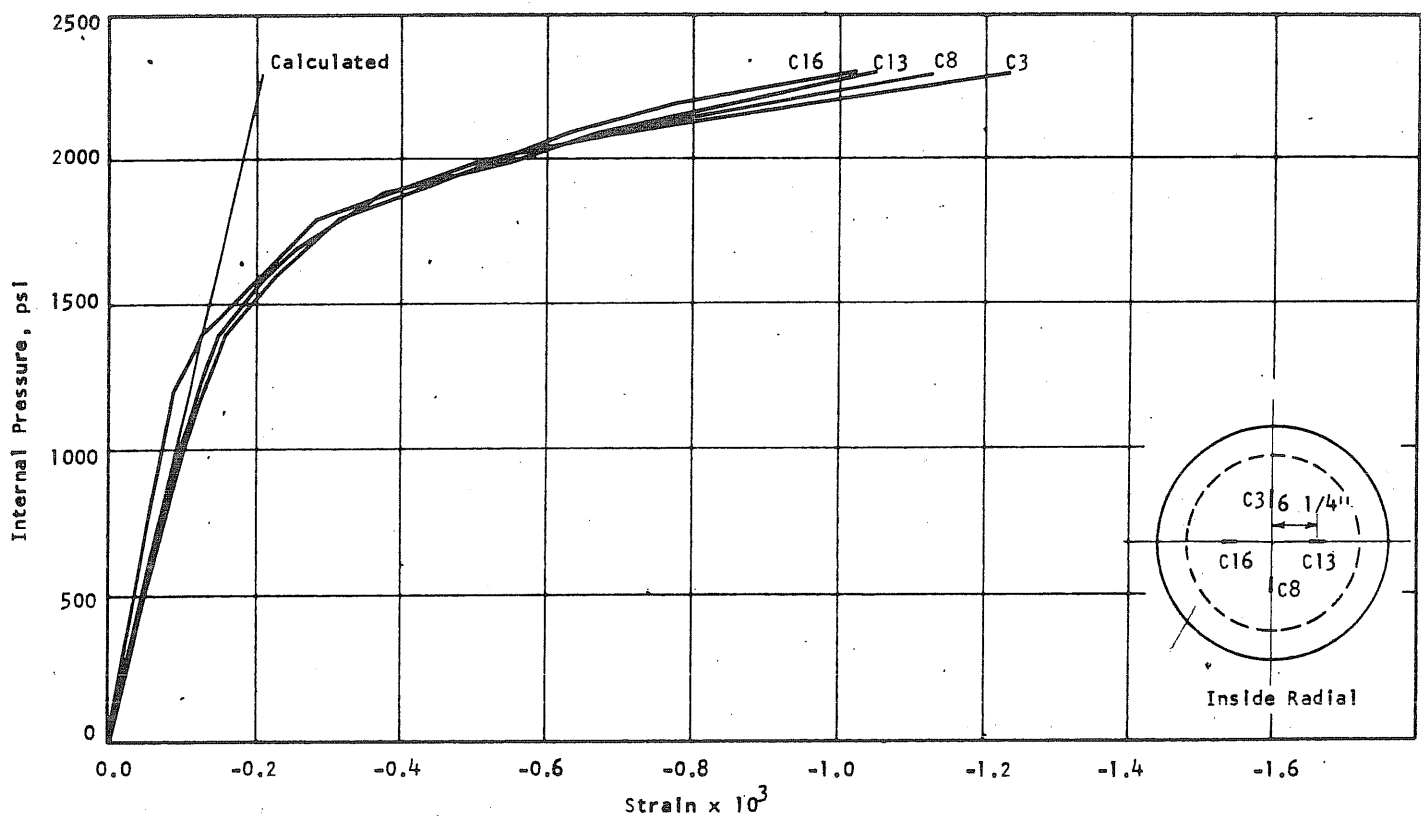
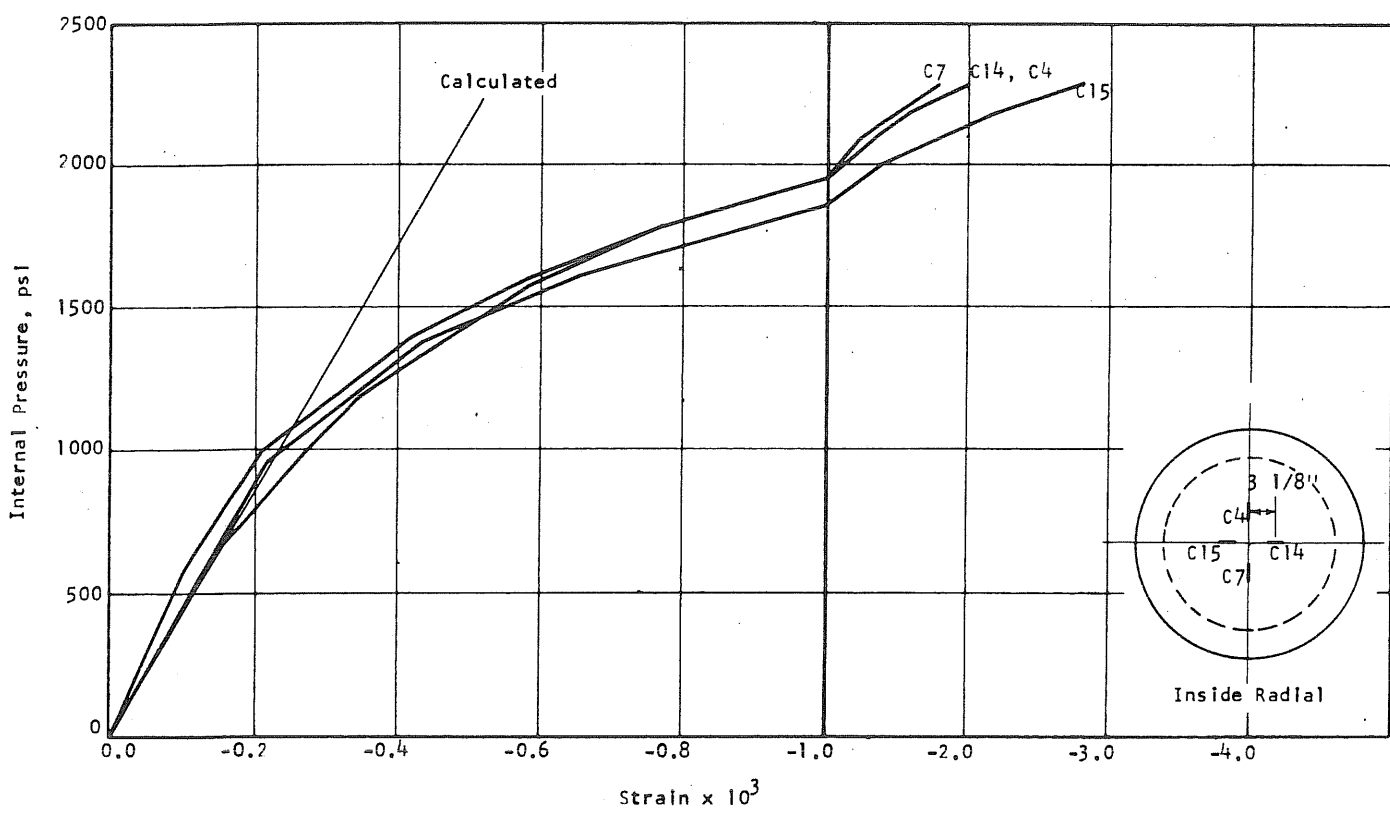
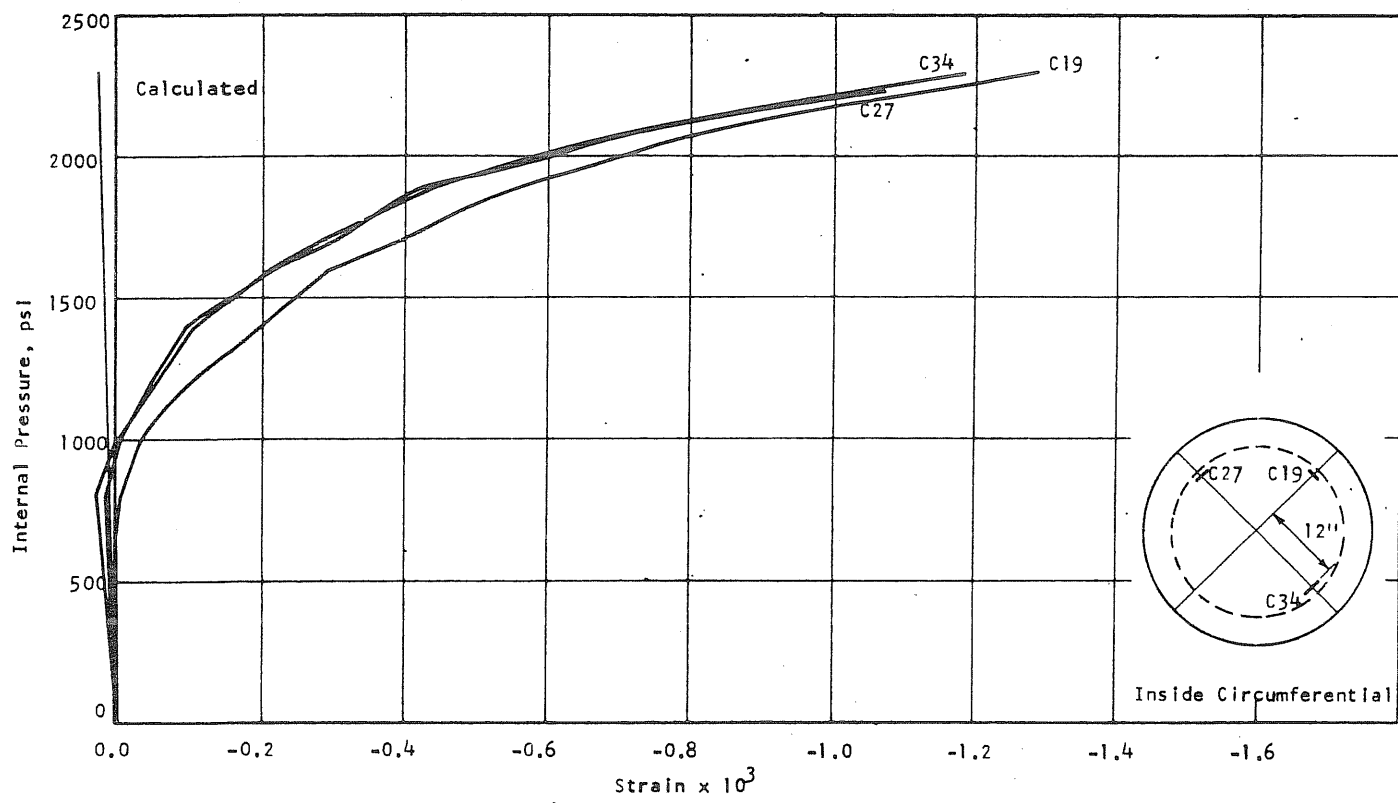


FIG. B15.7 (cont'd) CONCRETE STRAINS, VESSEL PV15



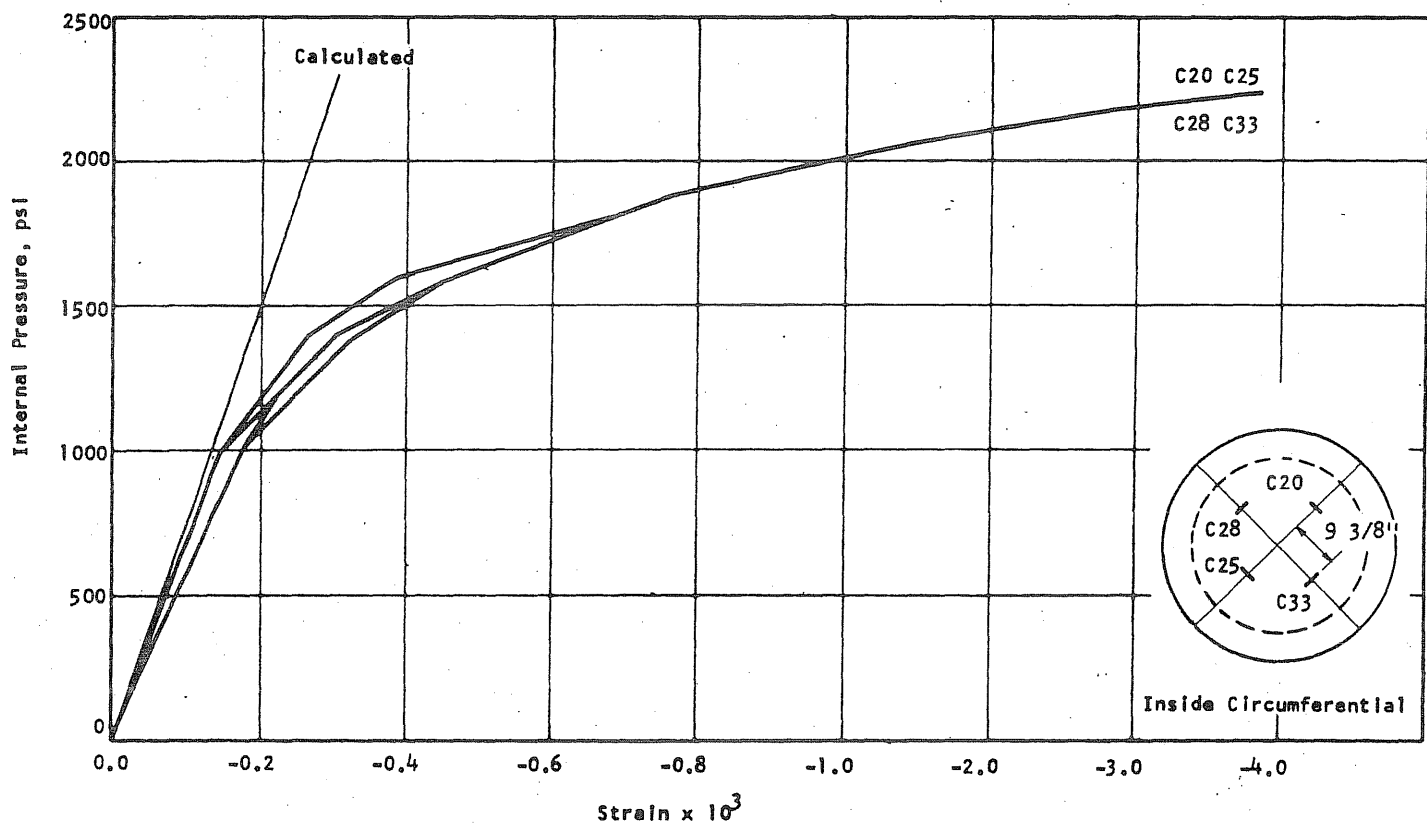


FIG. B15.8 (cont'd) CONCRETE STRAINS, VESSEL PV15

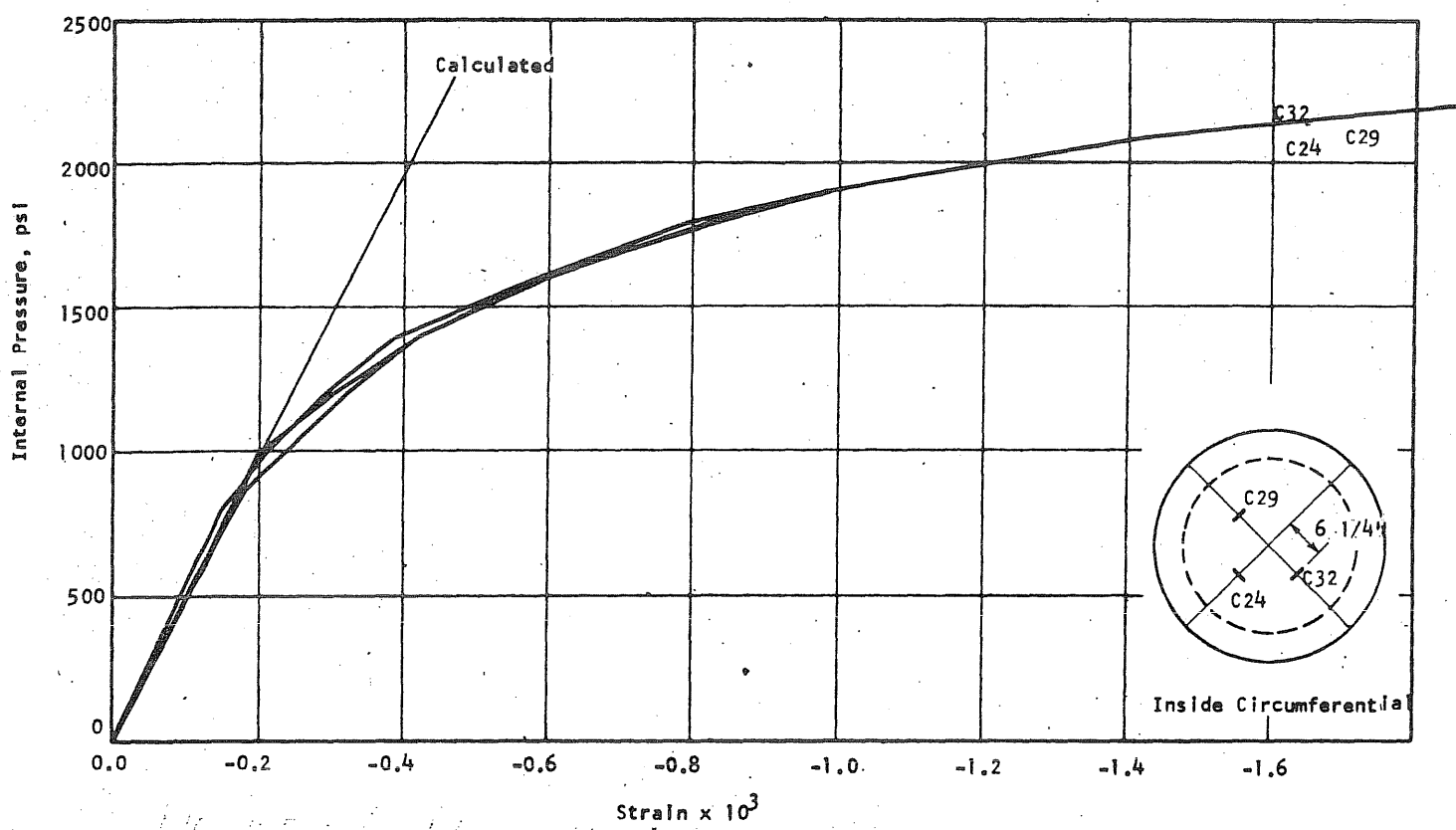


FIG. B15.8 (cont'd) CONCRETE STRAINS, VESSEL PV15

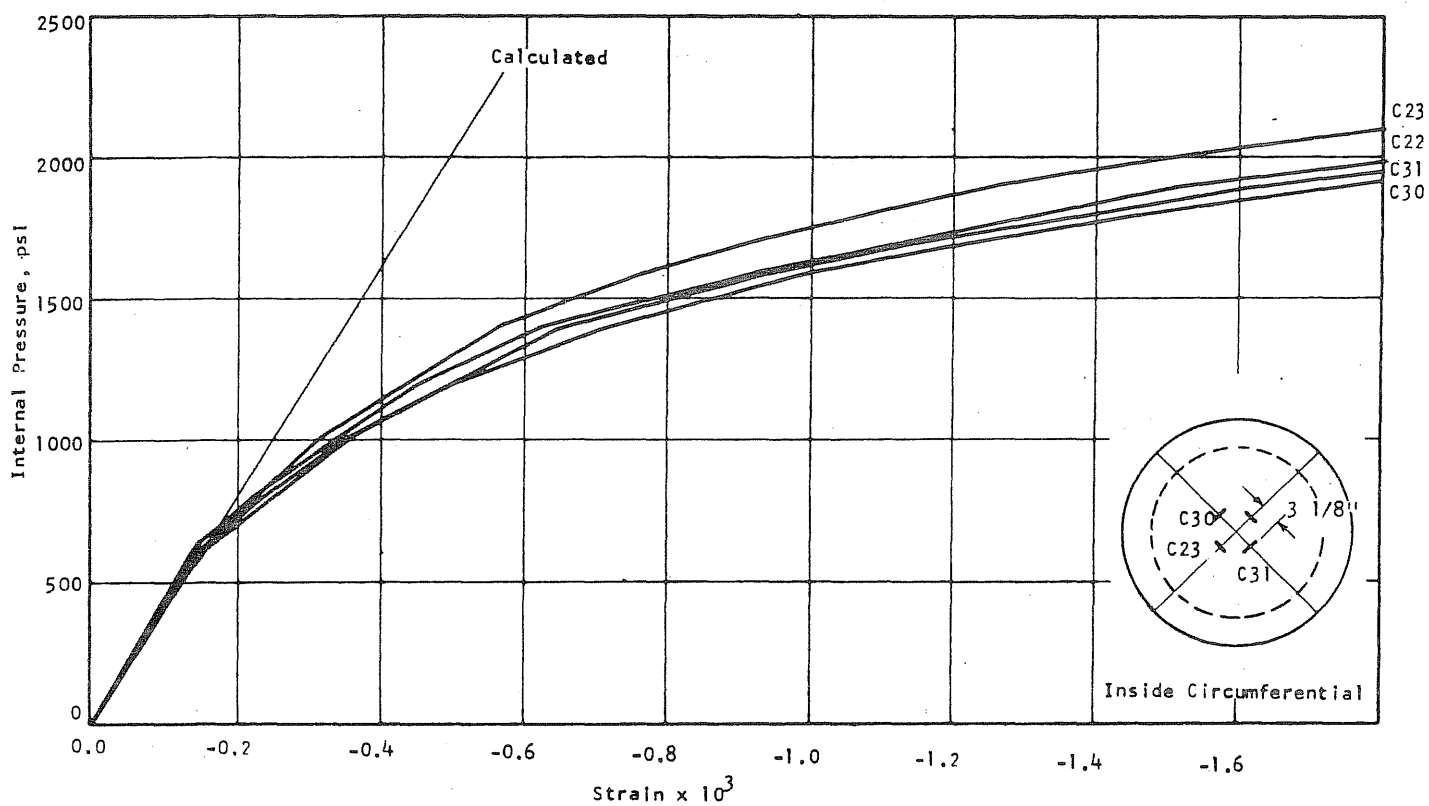


FIG. B15.8 (cont'd) CONCRETE STRAINS, VESSEL PV15

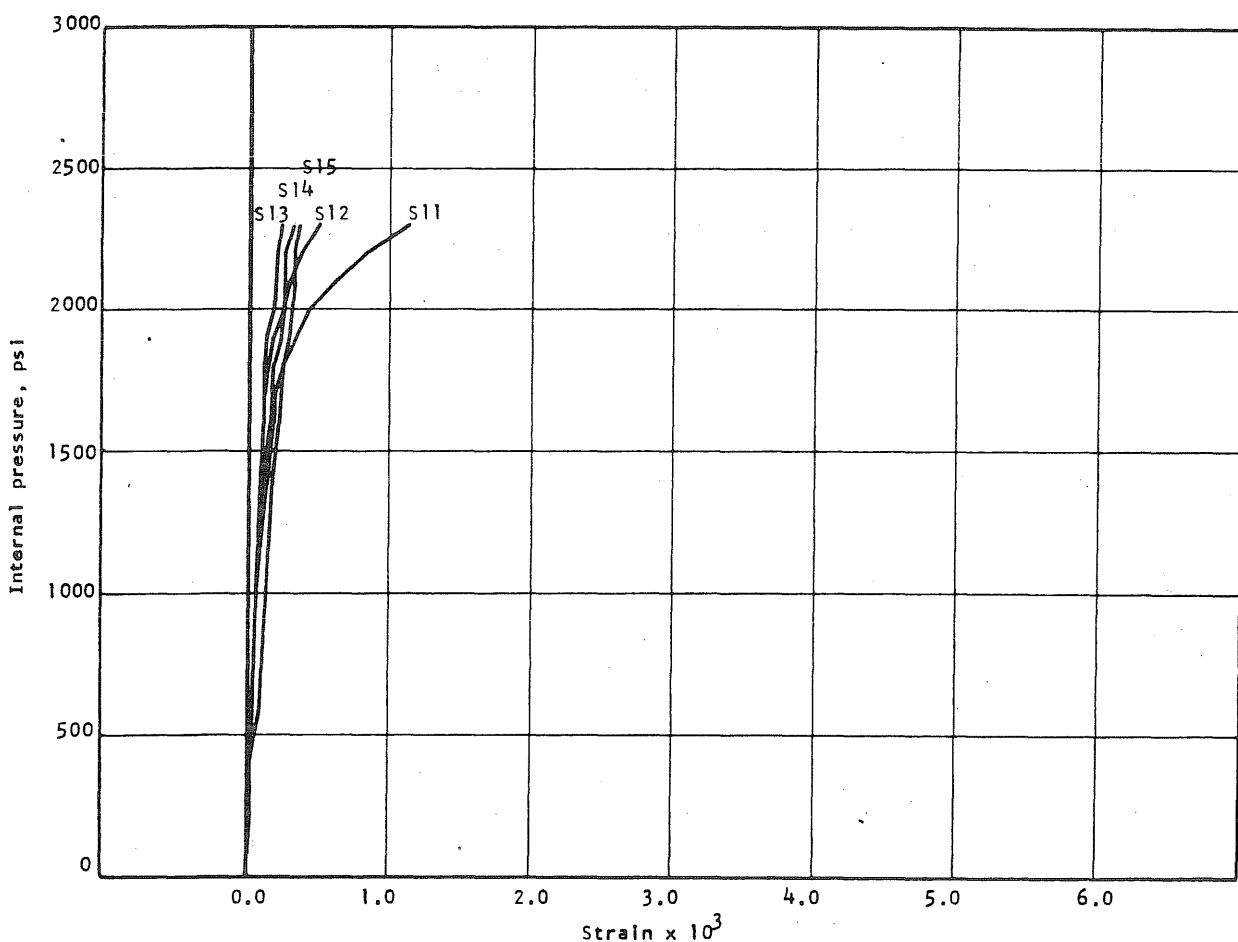


FIG. B15.9 APPLIED PRESSURE VS STRAIN IN CIRCUMFERENTIAL PRESTRESS WIRE AT THE S-END OF THE N-S DIAMETER OF PV15

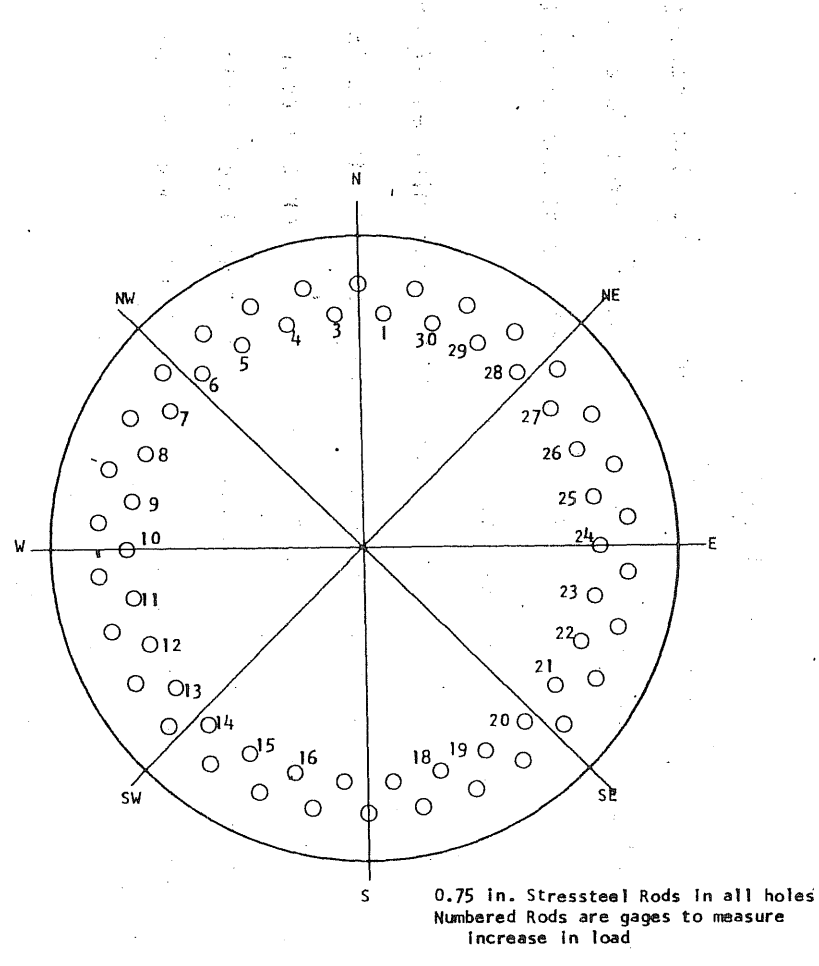


FIG. B15.10 LOCATION OF LONGITUDINAL REINFORCEMENT

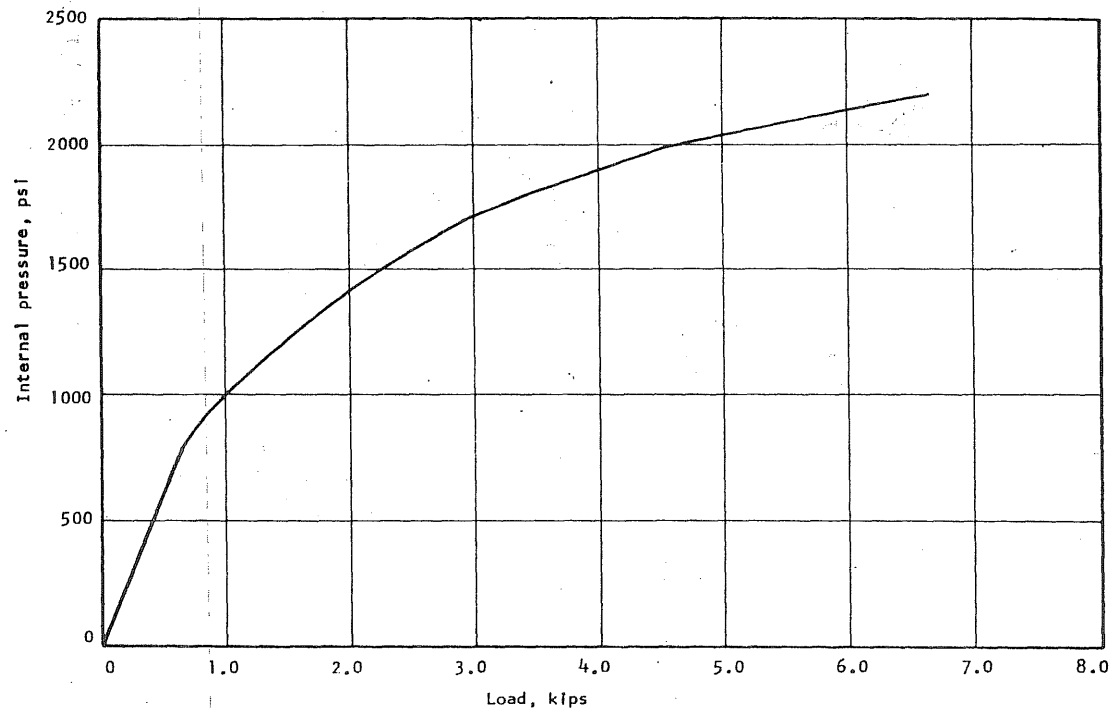


FIG. B15.11 APPLIED PRESSURE vs INCREASE IN LOAD IN STRESSTEEL ROD No. 13

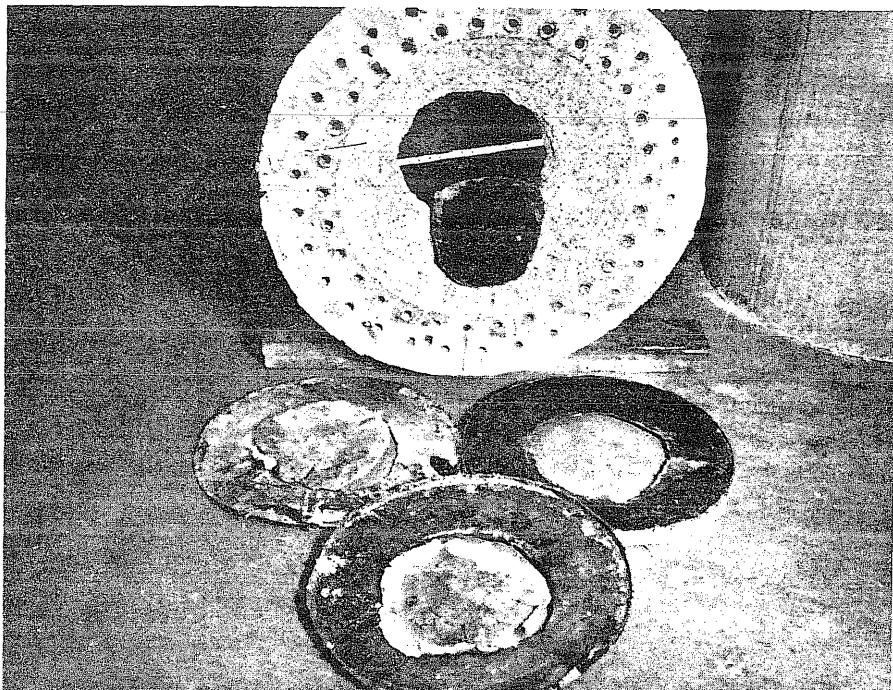


FIG. B15.12 END SLAB AND LINER AFTER FAILURE FOR PV15

B16 Test Vessel PV16 ($t = 10$ in., $s = 1/4$ in.)

Test vessel PV16 was cast in the same manner as PV15. The sealing details and longitudinal prestressing were also the same. Due to unforeseeable delays the vessel was prestressed 25 days before the test was conducted. During that period the vessel was represtressed twice.

The vessel was loaded with gas and failed about five minutes after a load of 3200 psi had been obtained. The creep in the vertical deflection gage at 3200 psi was quite large and increasing in speed. After the test it was noticed that two of the outer circle prestress rods stripped their threads during the latter stages of the test. Figure B16.12 shows the end slab after failure.

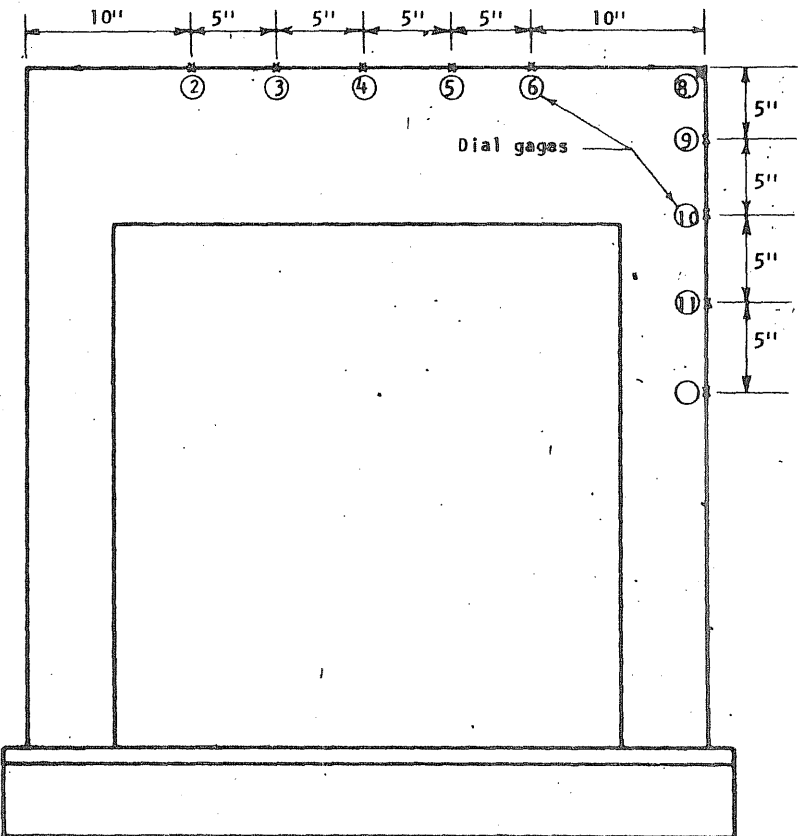
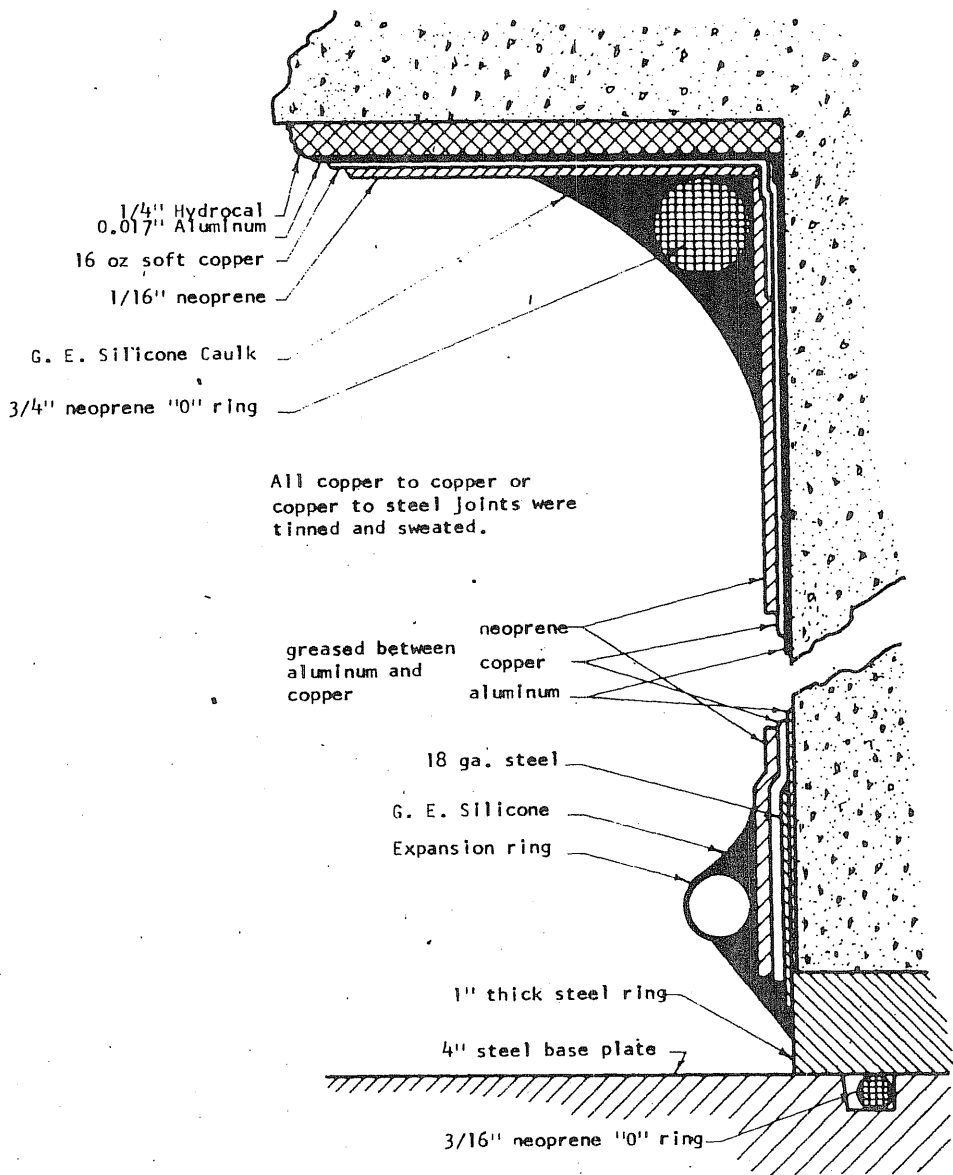


FIG. B16.2 LOCATION OF DEFLECTION GAGES ON PV16

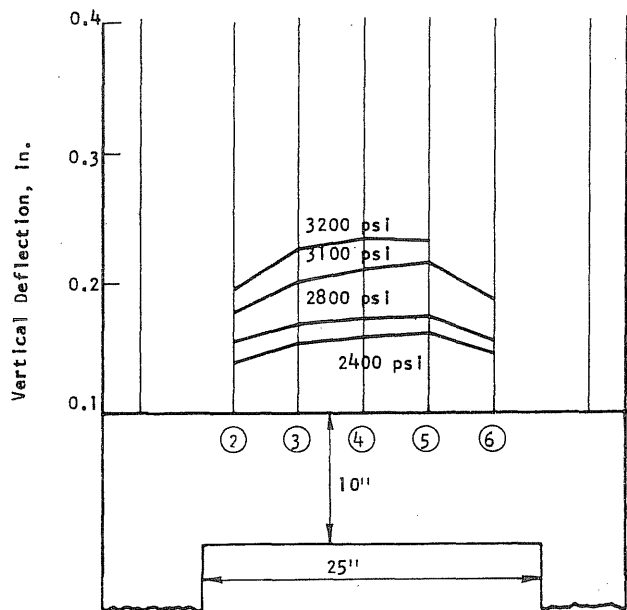


FIG. B16.3 DEFLECTION PROFILES OF THE END SLAB ALONG THE N-S DIAMETER OF PV16

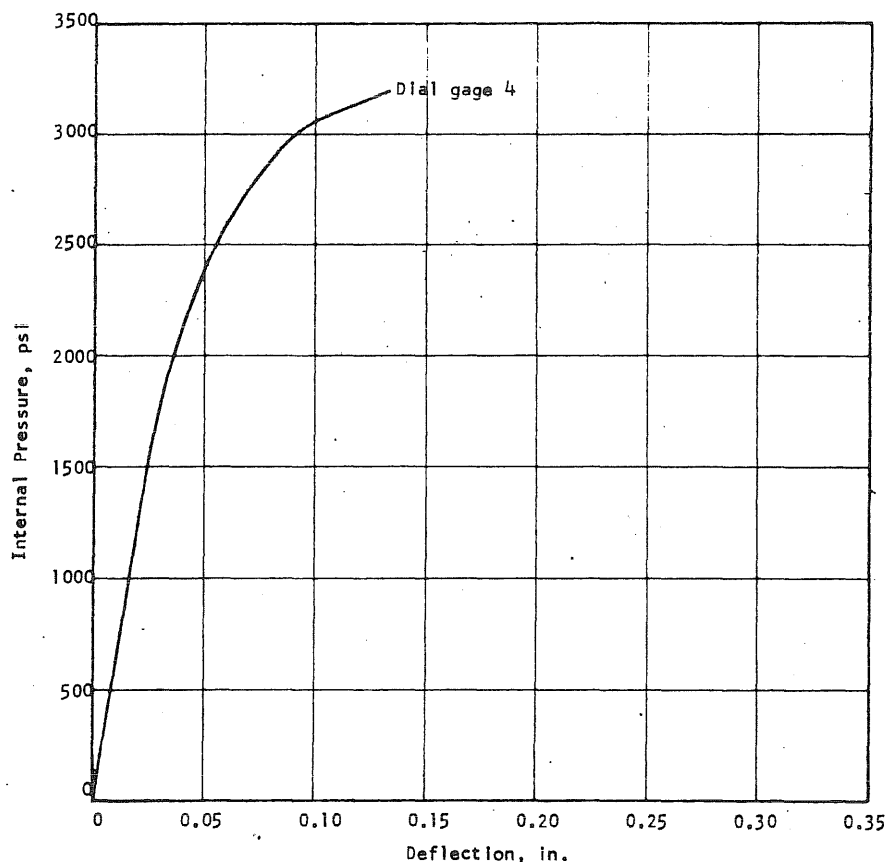
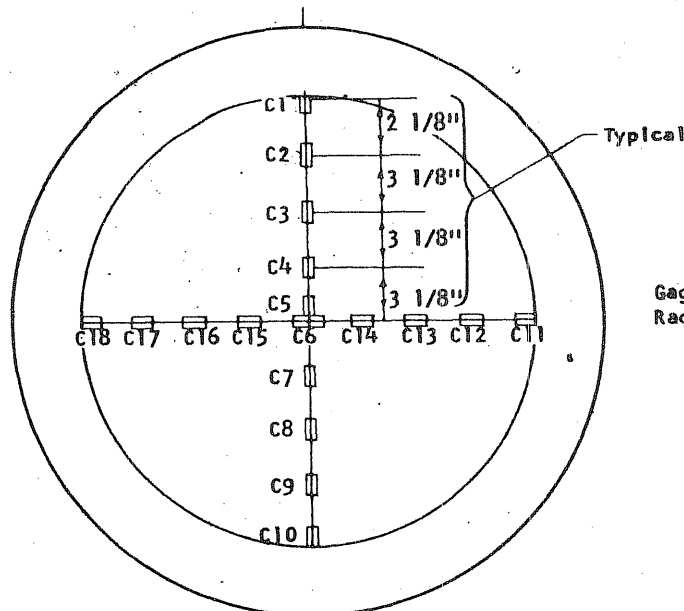
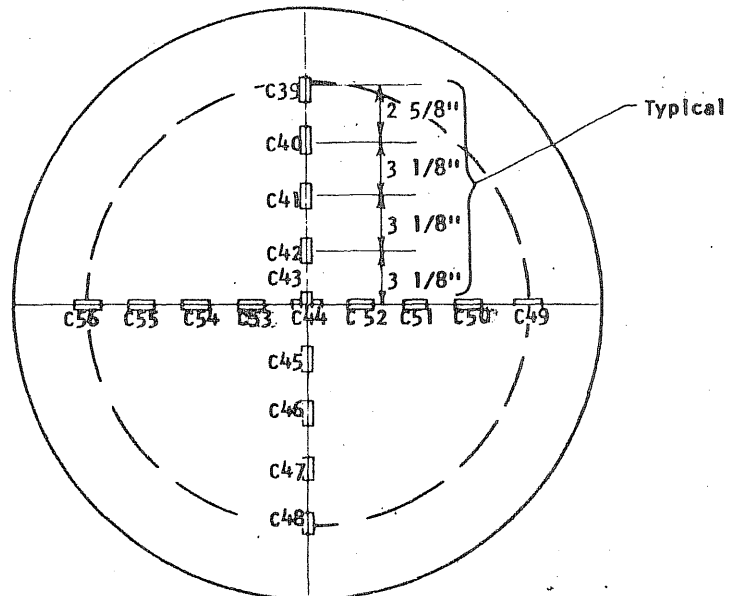


FIG. B16.4 APPLIED PRESSURE vs DEFLECTION AT MIDSPAN OF PV16

Concrete Gages on the Inside of the End Slab



Concrete gages on the Outside of the End Slab



268

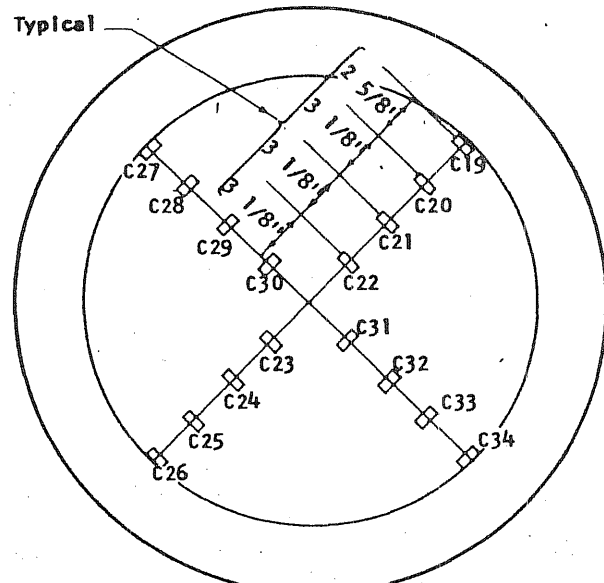


FIG. B16.5 STRAIN GAGE LOCATIONS ON PV16

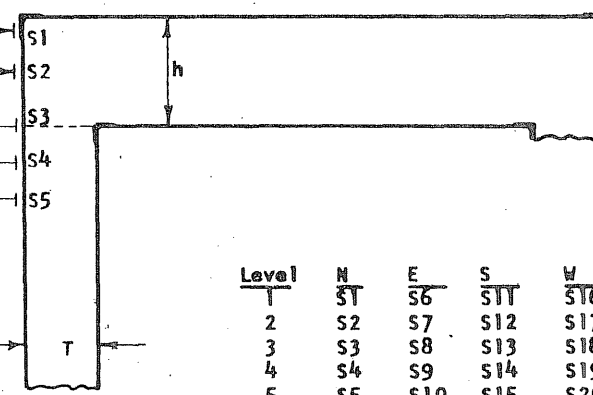


FIG. B16.5 (contd) STRAIN GAGE LOCATIONS ON PV16

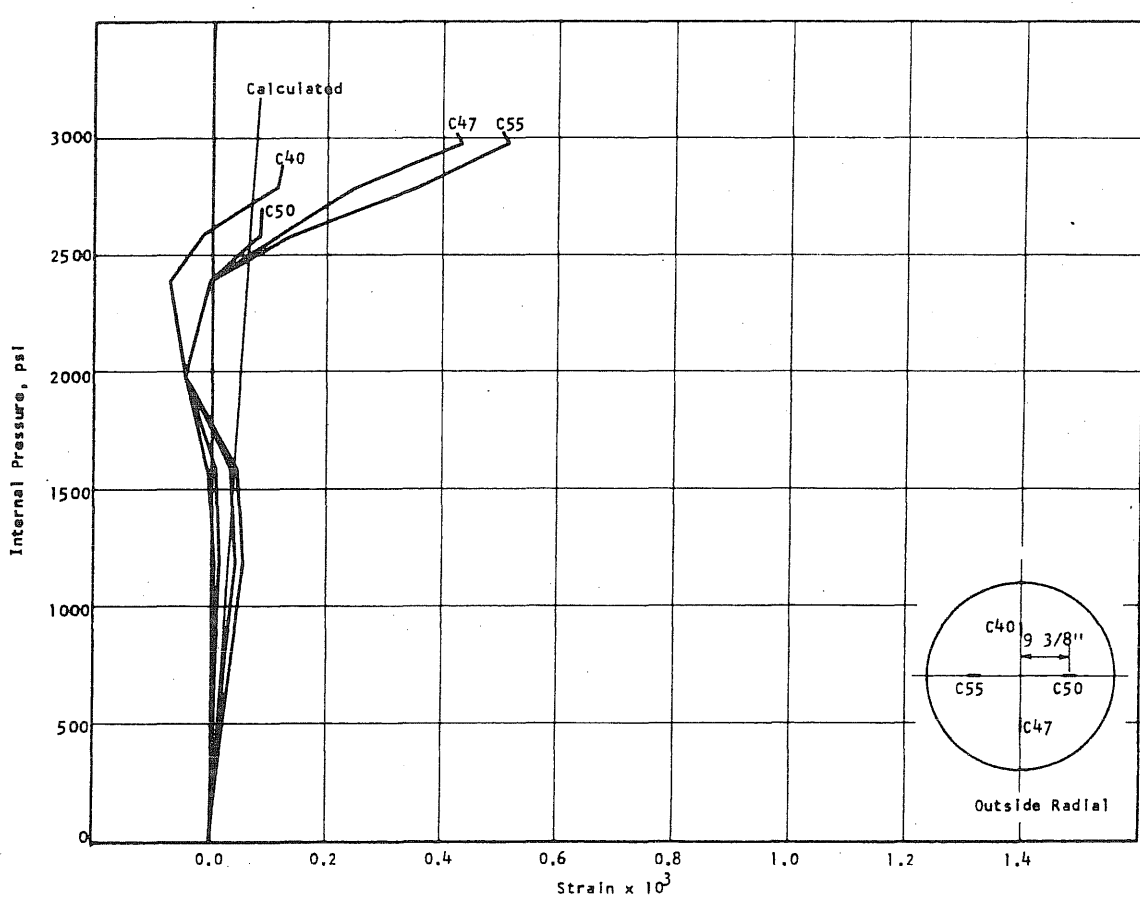
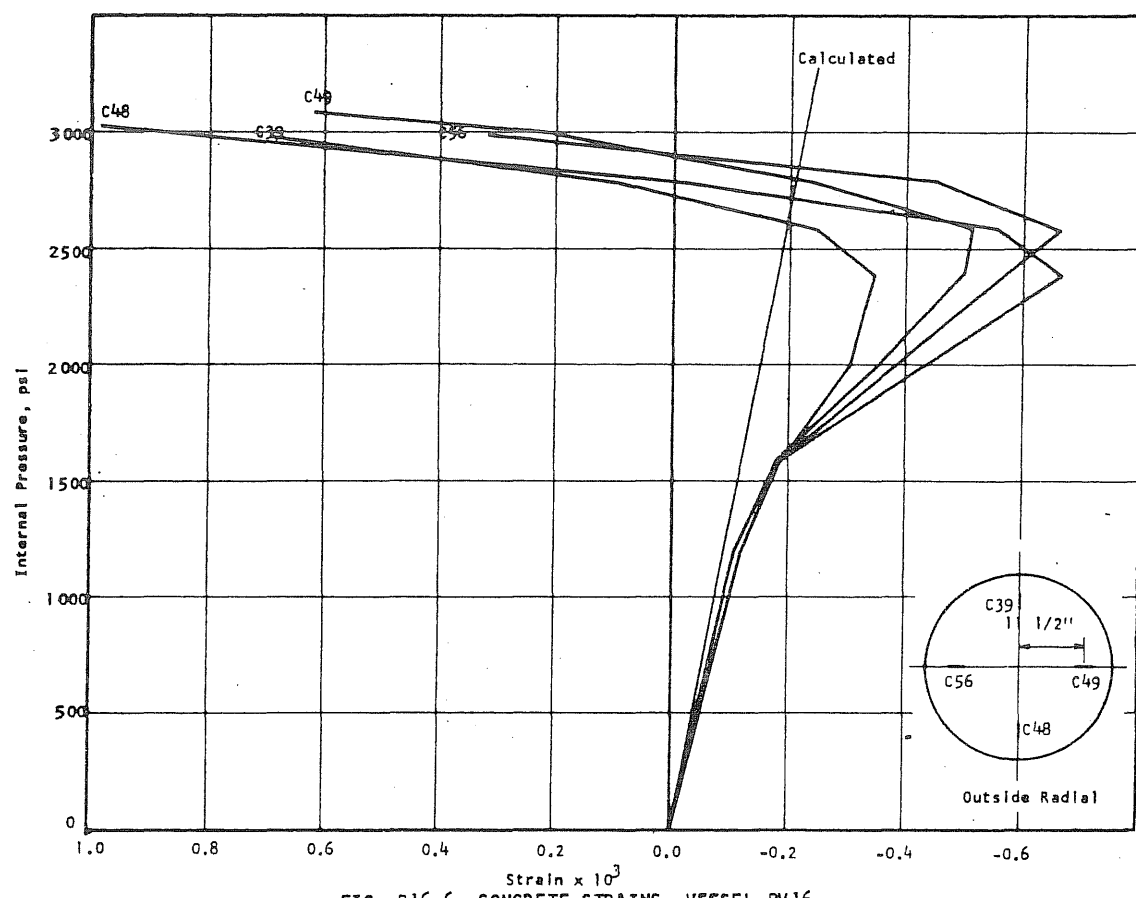


FIG. B16.6 (cont'd) CONCRETE STRAINS, VESSEL PV16

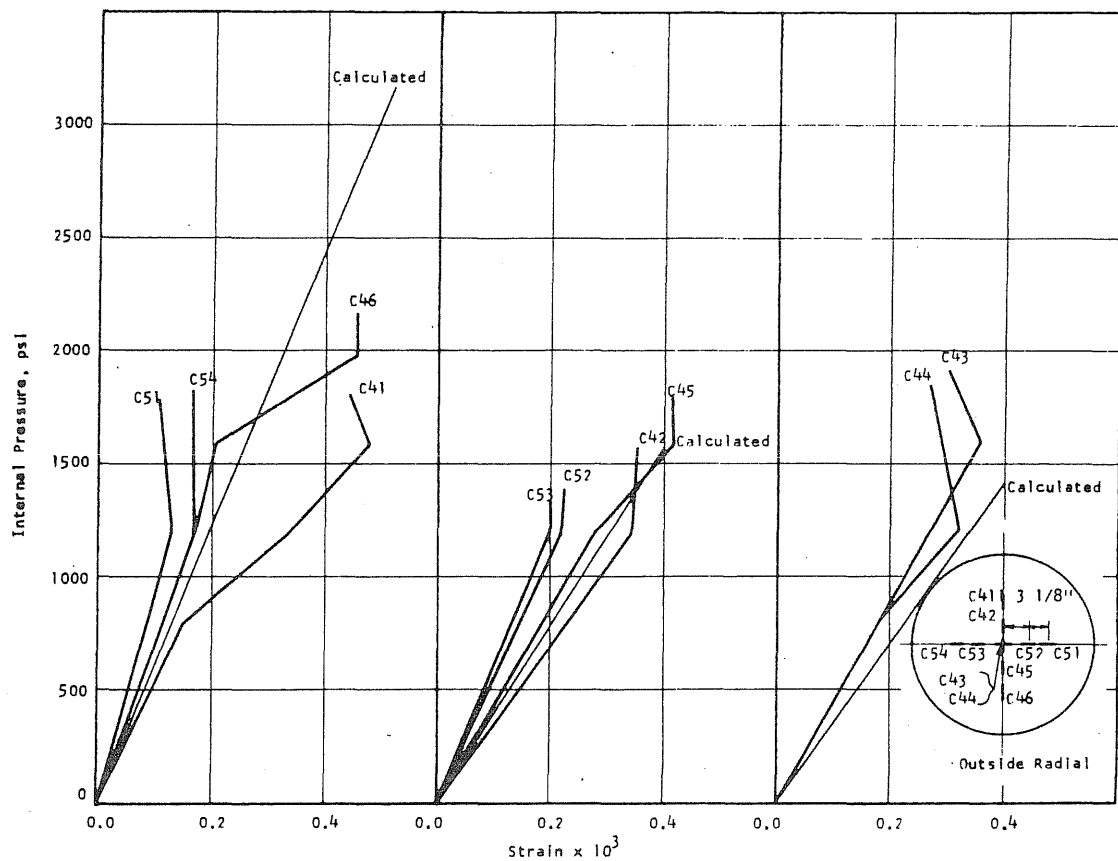


FIG. B16.6 (cont'd) CONCRETE STRAINS, VESSEL PV16

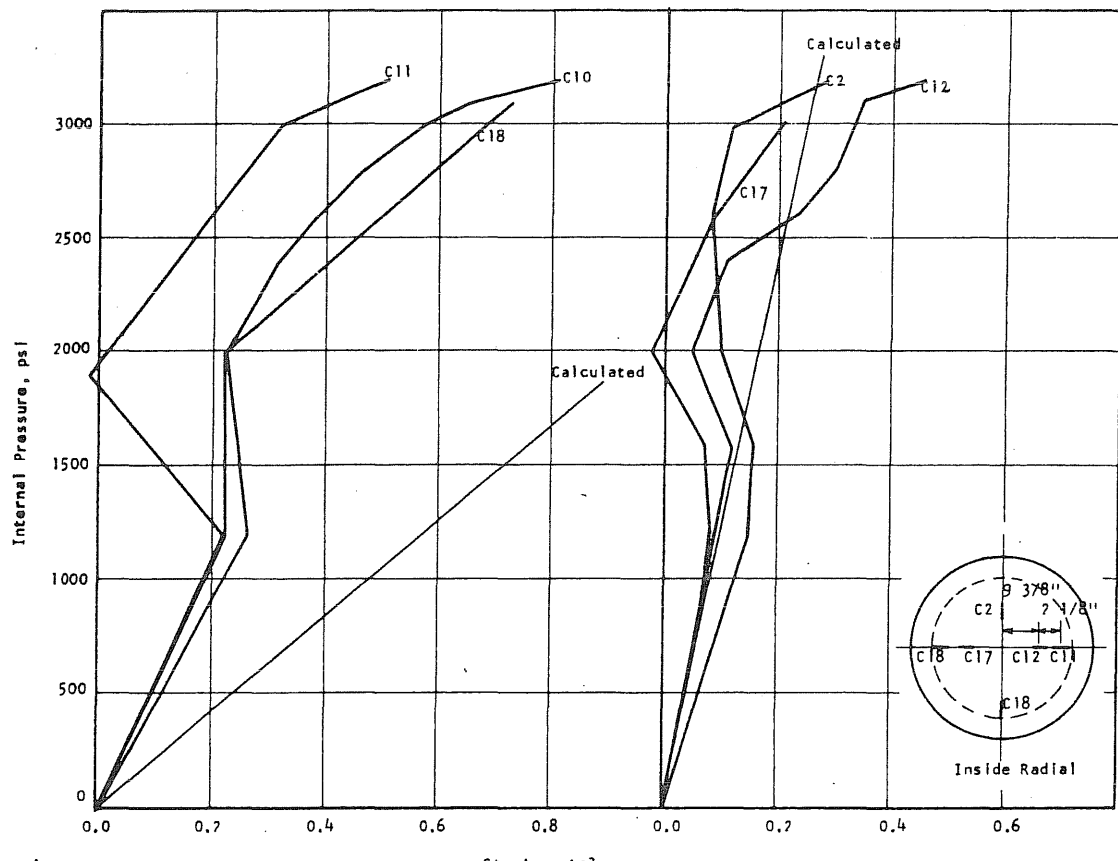


FIG. B16.7 CONCRETE STRAINS, VESSEL PV16

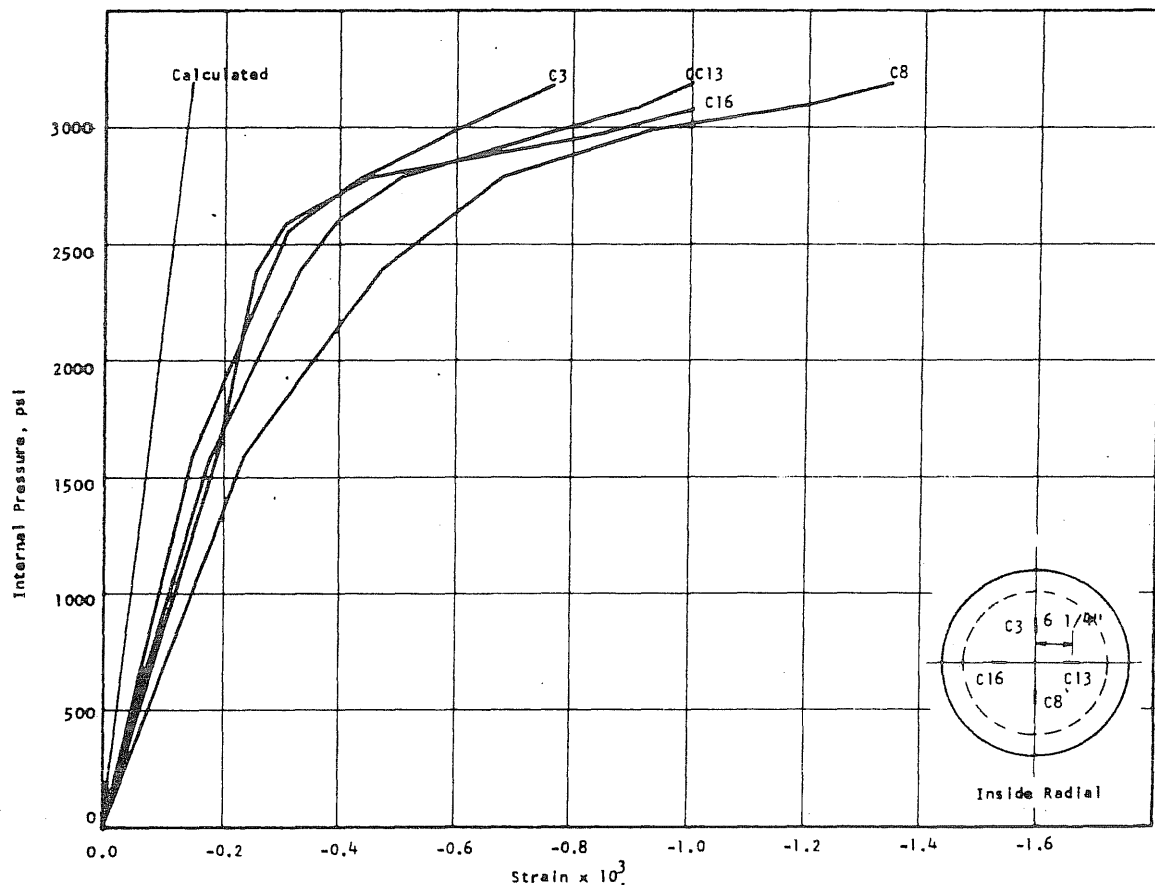


FIG. B16.7 (cont'd) CONCRETE STRAINS, VESSEL PV16

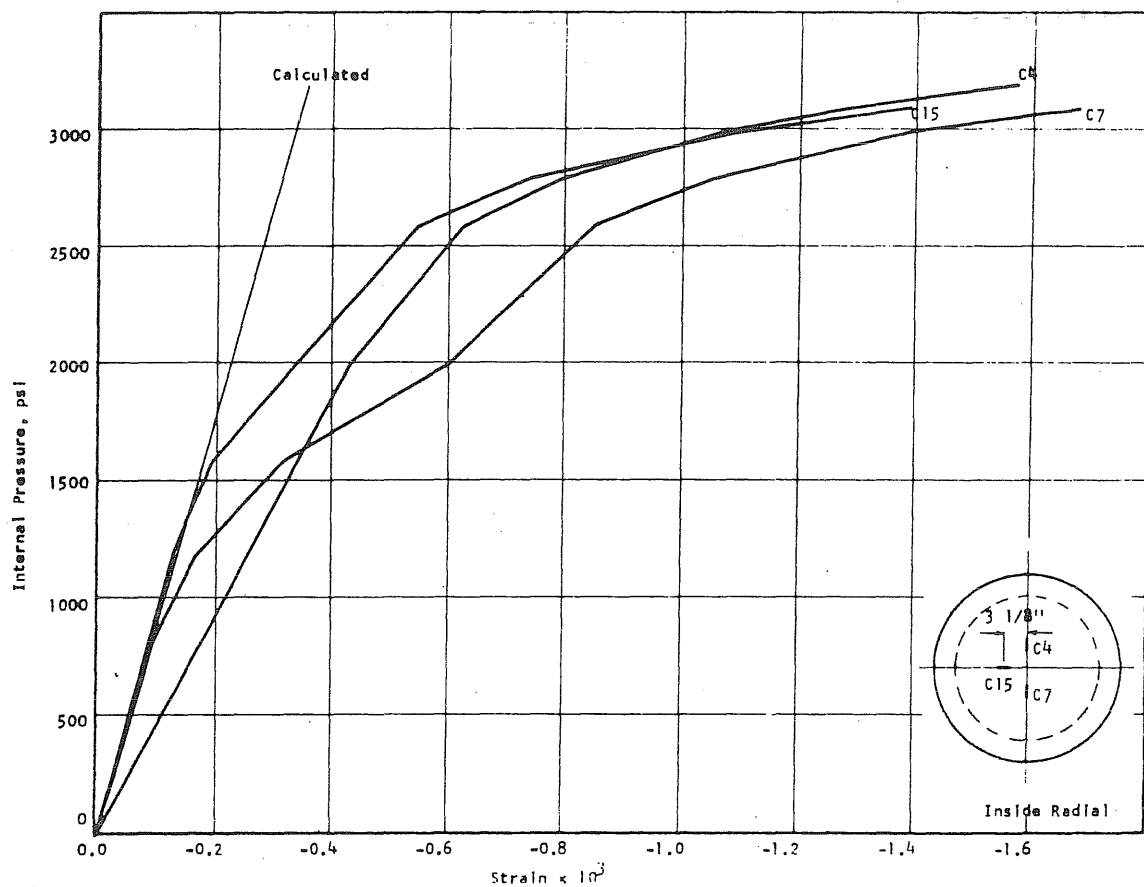


FIG. B16.7 (cont'd) CONCRETE STRAINS, VESSEL PV16

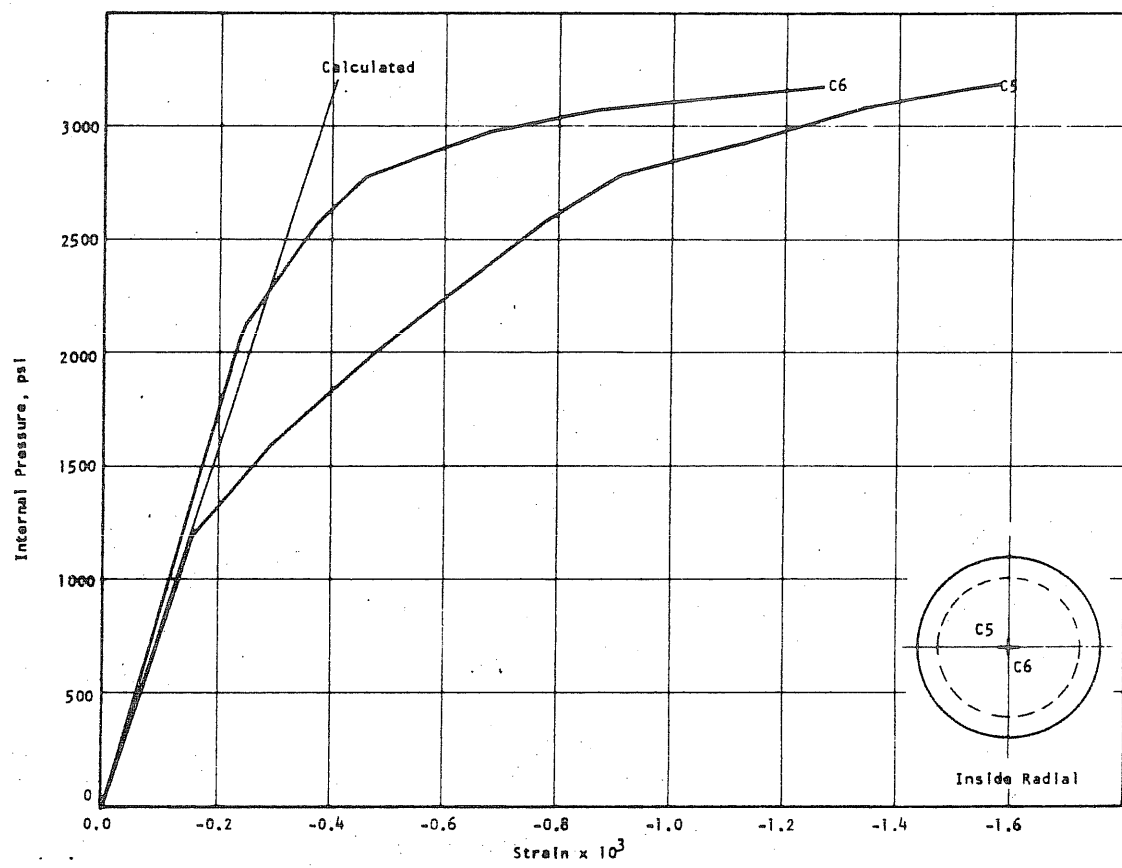


FIG. B16.7 (cont'd) CONCRETE STRAINS, VESSEL PV16

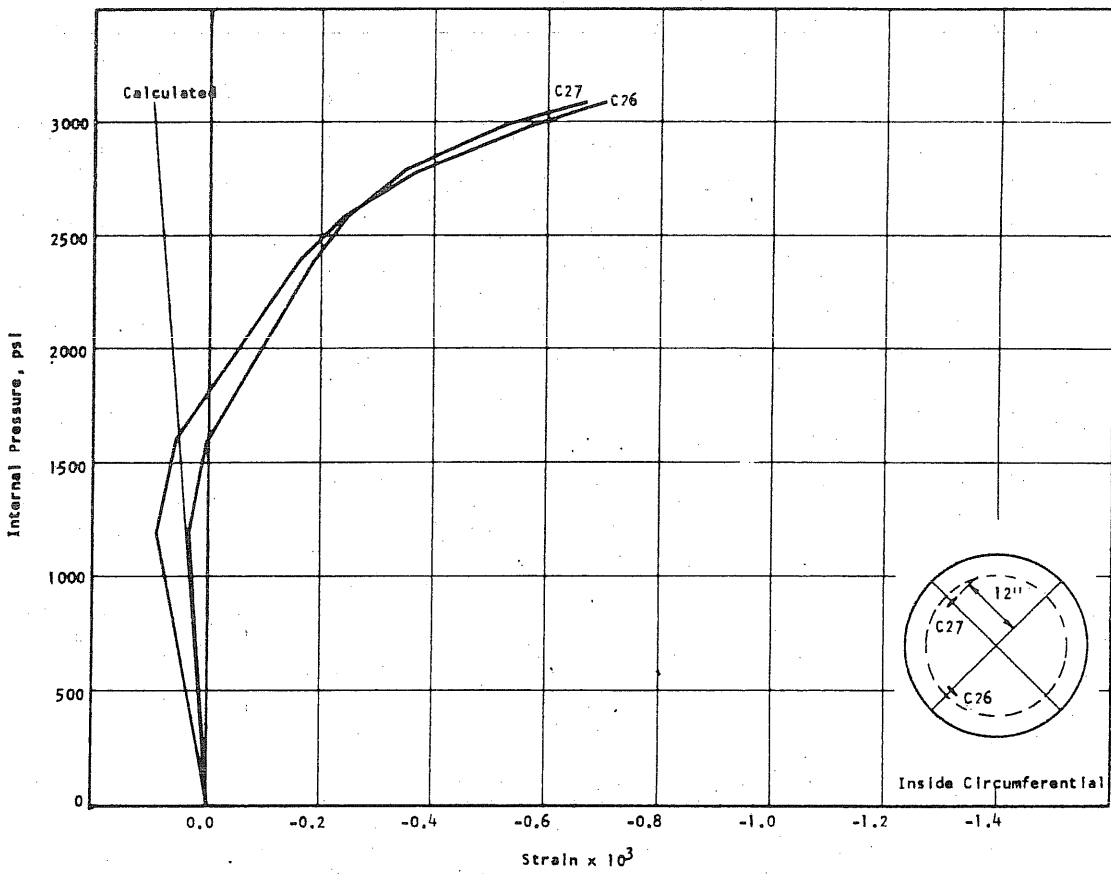


FIG. B16.8 CONCRETE STRAINS, VESSEL PV16

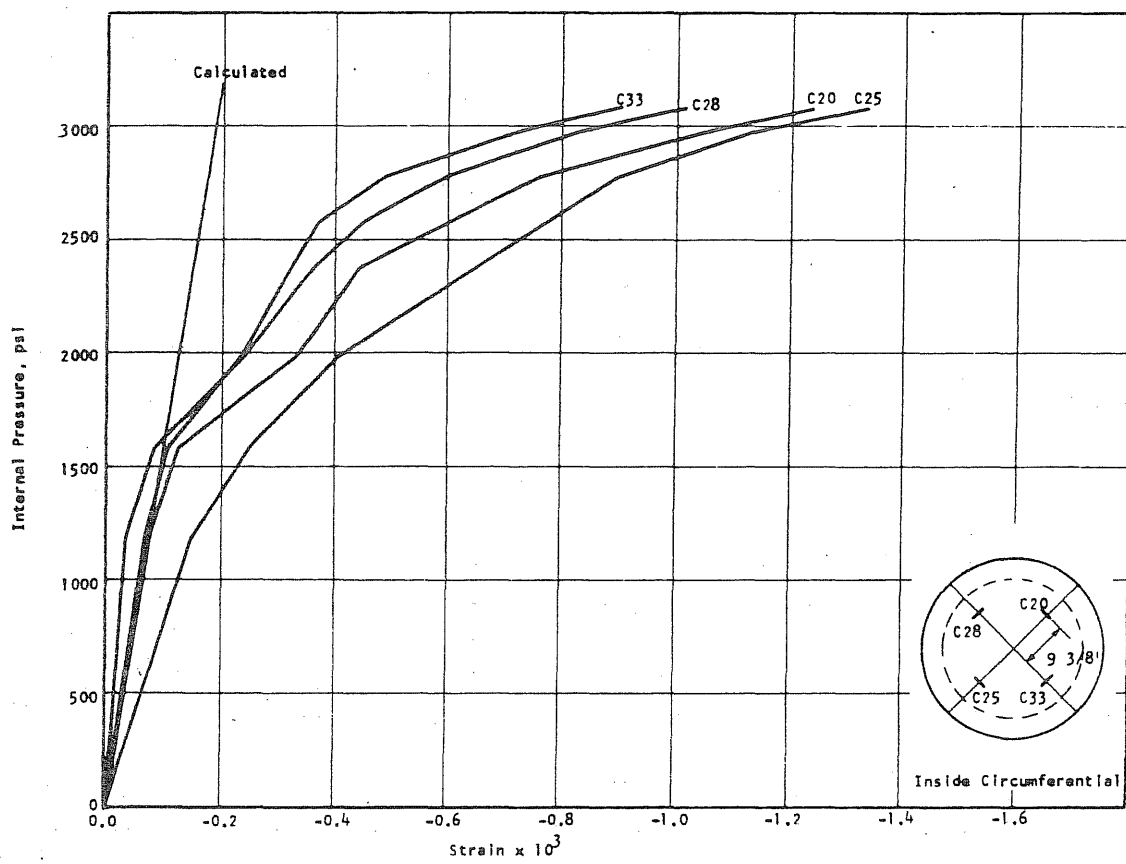


FIG. B16.8 (cont'd) CONCRETE STRAINS, VESSEL PV16

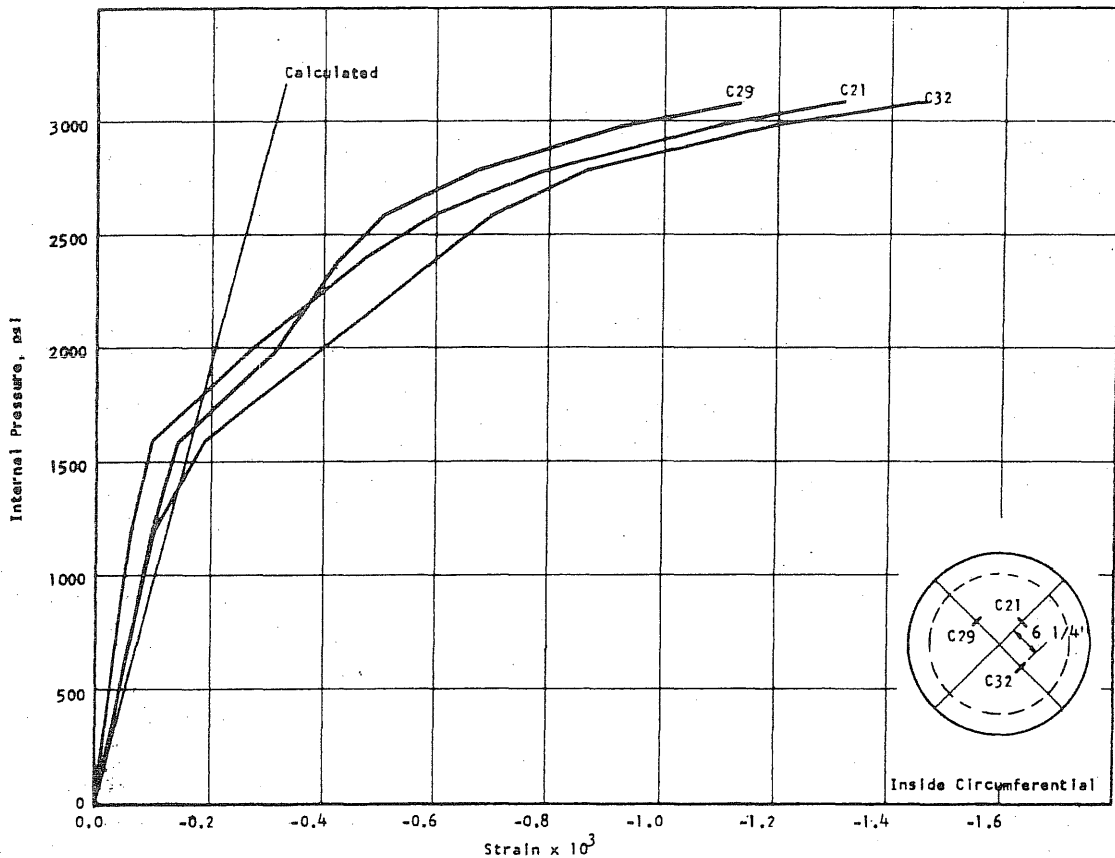


FIG. B16.8 (cont'd) CONCRETE STRAINS, VESSEL PV16

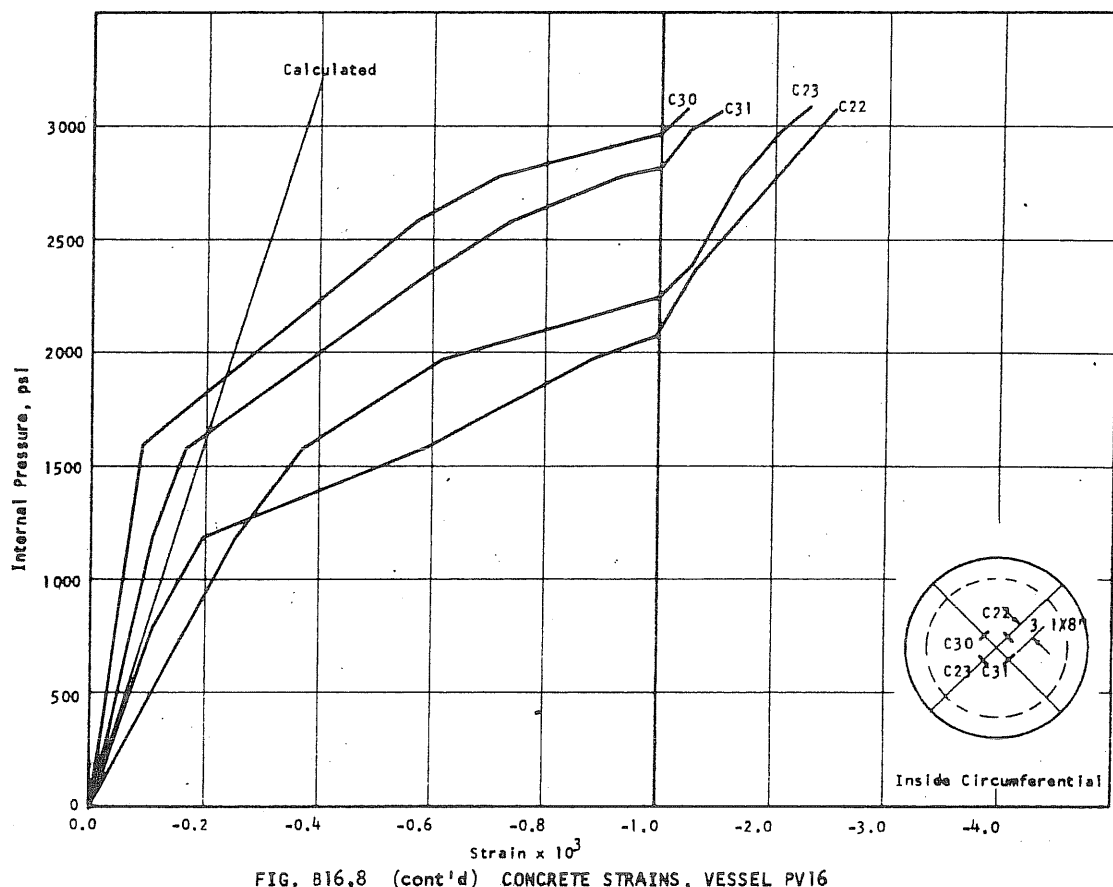


FIG. B16.8 (cont'd) CONCRETE STRAINS, VESSEL PV16

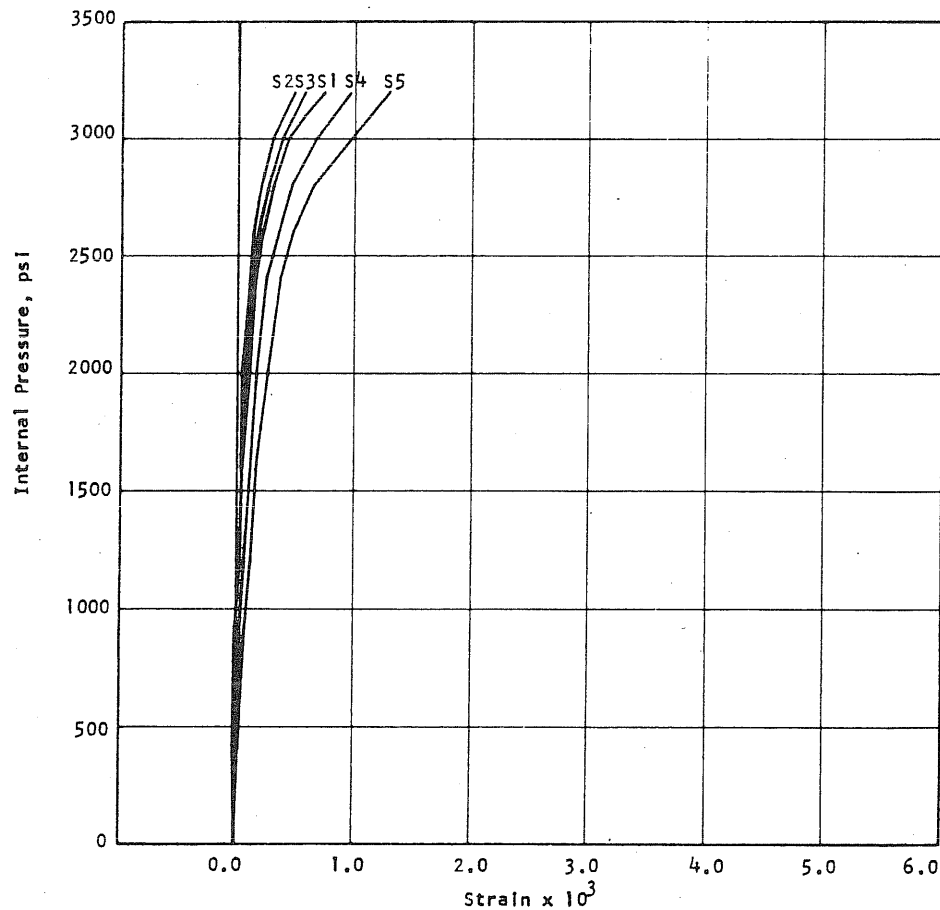


FIG. B16.9 APPLIED PRESSURE VS STRAIN IN CIRCUMFERENTIAL PRESTRESS WIRE AT THE N-END OF THE N-S DIAMETER OF PV16

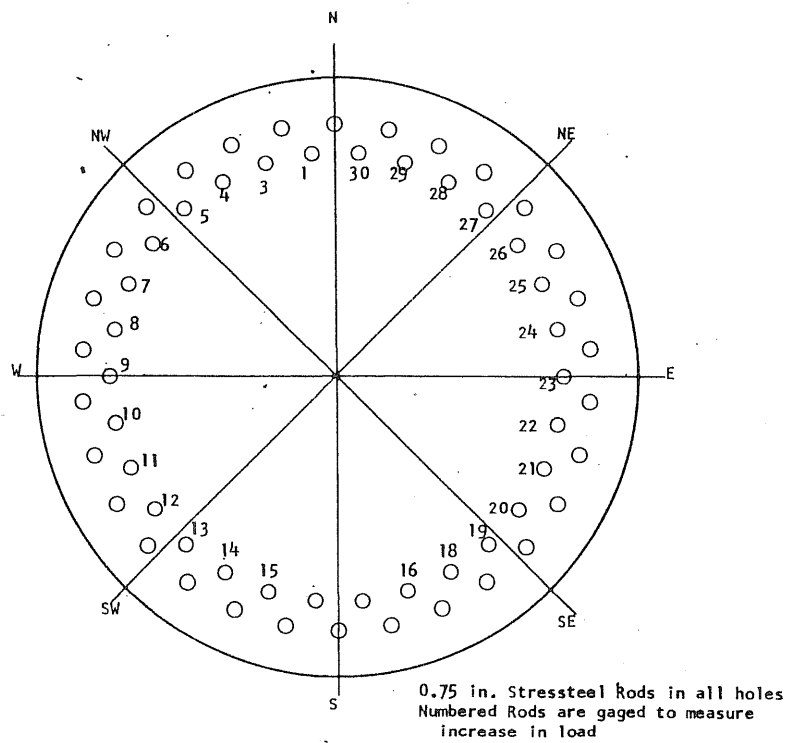


FIG. B16.10 LOCATION OF LONGITUDINAL REINFORCEMENT

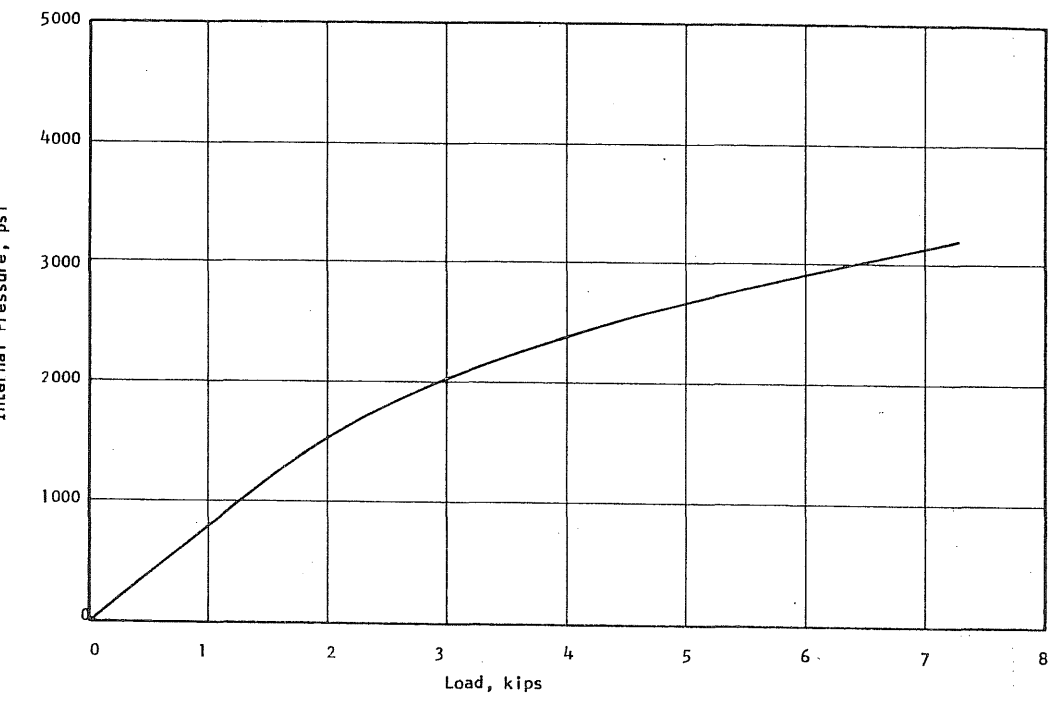


FIG. B16.11 APPLIED PRESSURE vs INCREASE IN LOAD IN STRESSTEEL ROD No. 13

B 201

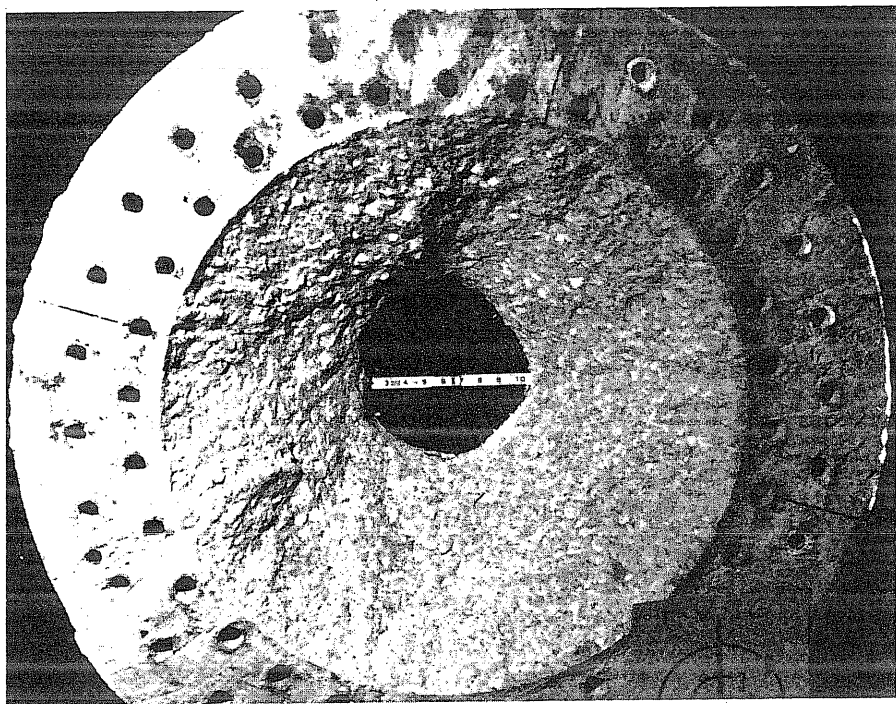


FIG. B16.12 END SLAB AFTER FAILURE

APPENDIX C

STRAIN DISTRIBUTION IN THE CIRCUMFERENTIAL REINFORCEMENT

C1 Description of the Tests

Analysis of the data from pressure tests of the vessels indicated that failure occurred in the circumferential prestress wire at an average strain much less than that which resulted in failure of wire specimens tested in direct tension. This premature wire fracture appeared to be caused by a concentration of strain at cracks in the concrete vessel walls. Tests were performed to check this observation.

A reinforced concrete disk was cast with a joint on a diameter to simulate a crack in the end slab of a test vessel. The concrete disk is shown in Fig. C1. Prestressing wire with a 0.192-in. diameter was wrapped around the disk, and the two halves of the disk were forced apart with a hydraulic jack, forcing the crack to open and at the same time imposing additional strain in the prestressing wire. During the tests the concrete disk lay on three-inch diameter pipe rollers to reduce friction between the disk and floor, and was held parallel to the floor with a steel channel section over the disk and loosely attached to the floor.

Opening of the crack was measured at both ends of the diameter with dial gages and the wire in the vicinity of the crack at one end of the diameter was instrumented with electrical resistance type strain gages. Also the force required to push the halves of the concrete disk apart was measured.

Three tests were performed with this arrangement. There was only one wrap of wire around the disk. A prestressing force was applied to the wire before the halves of the concrete disk were forced apart. This pre-stress force was applied with the arrangement shown in Fig. C2 and a load cell was used under the prestress jack to measure the force applied and the change of force at the ends of the wire during the test. The strain gages were placed on the wire after the prestressing force was applied. The jack used to force the halves of the concrete disk apart was placed off center 1/2 in. to assure that fracture of the wire occurred on the side which was instrumented.

C2. Shear Stress Between the Wire and Concrete

An analysis of the relation between shear force along the wire and variation of stress in the wire may be made if certain simplifying assumptions are made. Assume that there is some prestress in the wire which is applied without obtaining a shear stress between the wire and concrete so that the prestress force is uniform. The equilibrium of a section of wire between a crack and the point one-half the distance to the next crack, as shown in Fig. C3 is then investigated. Distance along the wire, x , is measured from the crack. Let F_x be the force at x in the wire, F_0 the initial force in the wire, μ the coefficient of friction between the wire and concrete, and R_o the radius of the concrete disk about which the wire is wrapped. From Fig. C3 it is apparent that the rate of change in force at some distance x along the wire is

$$\frac{dF_x}{dx} = \mu \frac{F_x}{R_o} \quad (C1)$$

where F_x is a function of x . This expression may be written

$$\frac{dF_x}{F_x} = \frac{\mu}{R_o} dx$$

Integration of this expression yields

$$\log F_x + C = \frac{\mu}{R_o} x$$

At $x = 0$, F_x is equal to the force in the wire at the crack, F_o , which gives $C = -\log F_o$. The above equation may then be written

$$\log \frac{F_x}{F_o} = \frac{\mu}{R_o} x \text{ or } \mu = \frac{R_o}{x} \log \frac{F_x}{F_o} \quad (C2)$$

The wire on the test vessel approaches the conditions assumed in this analysis more nearly than does that in the wire friction tests described in the last section. In the wire friction tests the opening of the cracks was much larger so that the movement between the wire and concrete was greater. One would expect this to affect the friction coefficient between the two surfaces since the movement would alter the surface characteristics of the concrete. The wire in these tests was prestressed by pulling the ends of the wire around the concrete disk as explained earlier. This prestress

caused a friction force between the wire and concrete in the direction opposite to that which would occur when the two halves of the disk are pushed apart on the section of wire which was gaged. As the halves of the disk are pushed apart, this initial shear stress must be relieved before any strain can be applied to the wire. Since the strain gages are applied with this reversed shear stress in the wire, the initial wire strain will appear to be a compression, though it is actually a slight relief of some of the initial tension in the wire.

The difference in force in the wire at a crack and away from the crack must result from friction between the wire and concrete. The maximum value of this force depends upon the coefficient of friction between the two surfaces and the distance between the cracks since the friction force will build up only over one-half the distance to the next crack. If the shear force is sufficient to cause the strain at the crack to be in the plastic range while that away from the crack is still below this range, then additional strain will be concentrated at the crack.

C3 Results of the Tests

Though there are certain basic differences between the conditions at the crack in the wire test and in the vessel tests, the pertinent basic information for understanding the wire behavior at a crack can be obtained from the wire tests. It is seen from Fig. C4, C5, and C6 that there is a definite strain concentration in the vicinity of a crack. In these graphs the variation of strain with distance from the crack is shown for several load increments for the three tests. The magnitude of strain

concentration at the crack recorded in these tests depends to a large measure on whether a strain gage was located very near the failure region in the wire. The magnitude is sufficient, however, to cause failure of the wire to occur at the crack, and in Fig. C6 for example, when the load was maximum the highest strain read near the crack was 0.022 while that read at 7 in. from the crack was 0.0066.

Any numerical value of strain concentration given must be based on an arbitrary definition of what is meant by strain concentration; that is, on what level of strain the concentration is based since the strain is varying continuously along the wire. Also, the concentration of strain will depend on the spacing of cracks, the force in the wire, and on the coefficient of friction between the wire and concrete. In the test vessels the cracks were closely spaced so the results obtained from these friction tests probably represent an upper limit on the concentration factors, but the coefficient of friction should be representative of that in the test vessel.

In Fig. C4, C5, and C6 the curves are labeled with the forces at the crack found from the difference in the load cell forces. If these forces are assumed to be correct and a straight line is drawn to average the points from the crack out to 31 in. to the right for the curve labeled 4400 lb in Fig. C4, the difference in force can be found from this strain difference. This force difference is found to be 2100 lb and the force at 31 in. from the crack is then 2300 lb. Substitution of these forces into Eq. C2 gives

$$\mu = \frac{20 \text{ in.}}{31 \text{ in.}} \log \frac{2300 \text{ lb}}{4400 \text{ lb}} = 0.42$$

This value appears high. In Ref. C1 a value of approximately 0.33 is reported. Figure A7 shows the stress-strain curve for the 0.192 in. prestress wire. A stress of 230 ksi is well within the yield range while 220 ksi is well below the flat portion of the curve. This difference of 10 ksi represents a force difference of 290 lb. If a force of 4400 lb is assumed at the crack (certainly a lower limit) and a value of $\mu = 0.33$, then the distance required to obtain this force difference may be found from Eq. C2

$$0.33 = \frac{20 \text{ in.}}{x} \log \frac{4110}{4400}$$

$$x = 4.1 \text{ in.}$$

It is apparent that sufficient force difference could be developed in the wire to cause an appreciable strain concentration.

C7

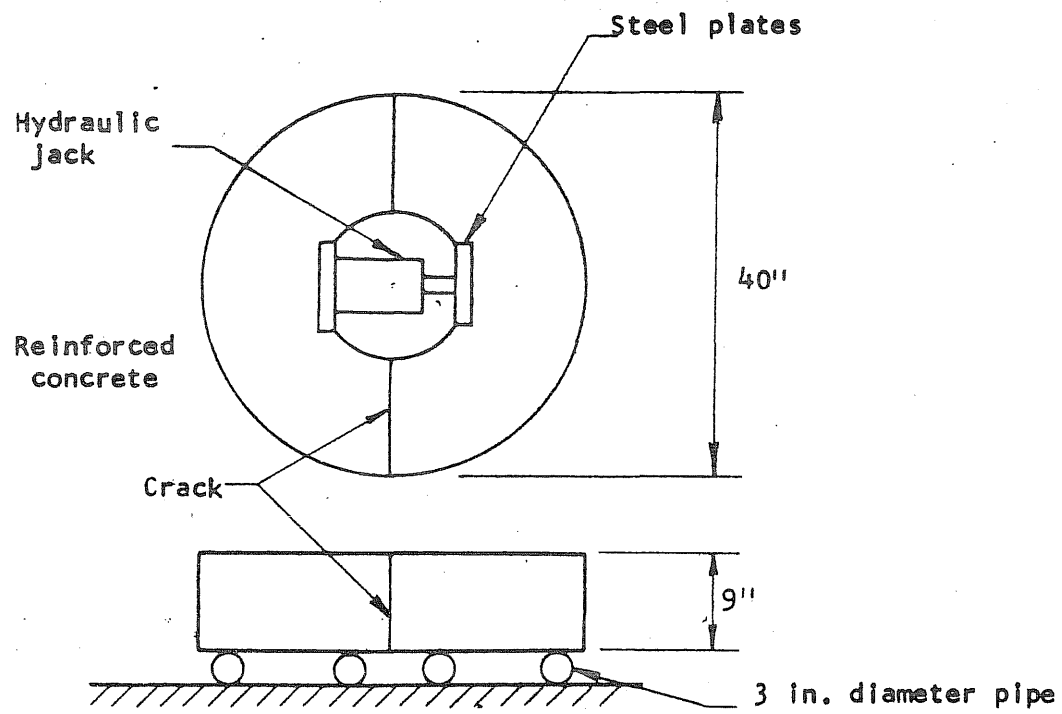


FIG. C1 TEST ARRANGEMENT FOR FRICTION TESTS OF PRESTRESS WIRE

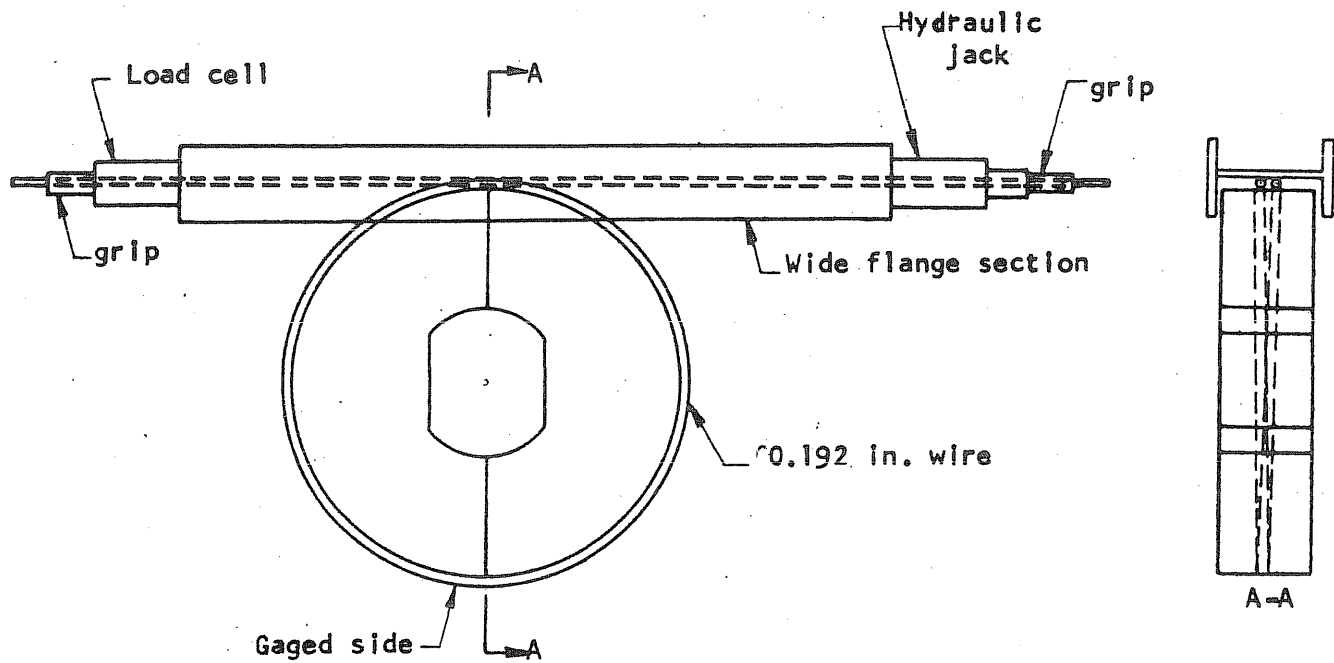


FIG. C2 ARRANGEMENT FOR PRESTRESSING THE WIRE
FOR THE FRICTION TESTS

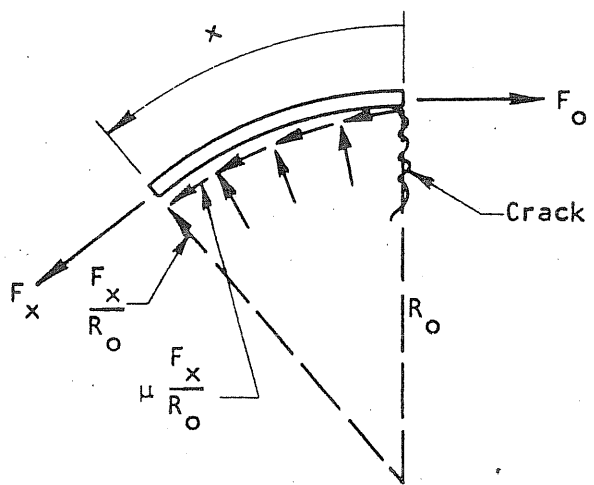


FIG. C3 FORCES ACTING ON A SECTION OF PRESTRESS WIRE AT A CRACK

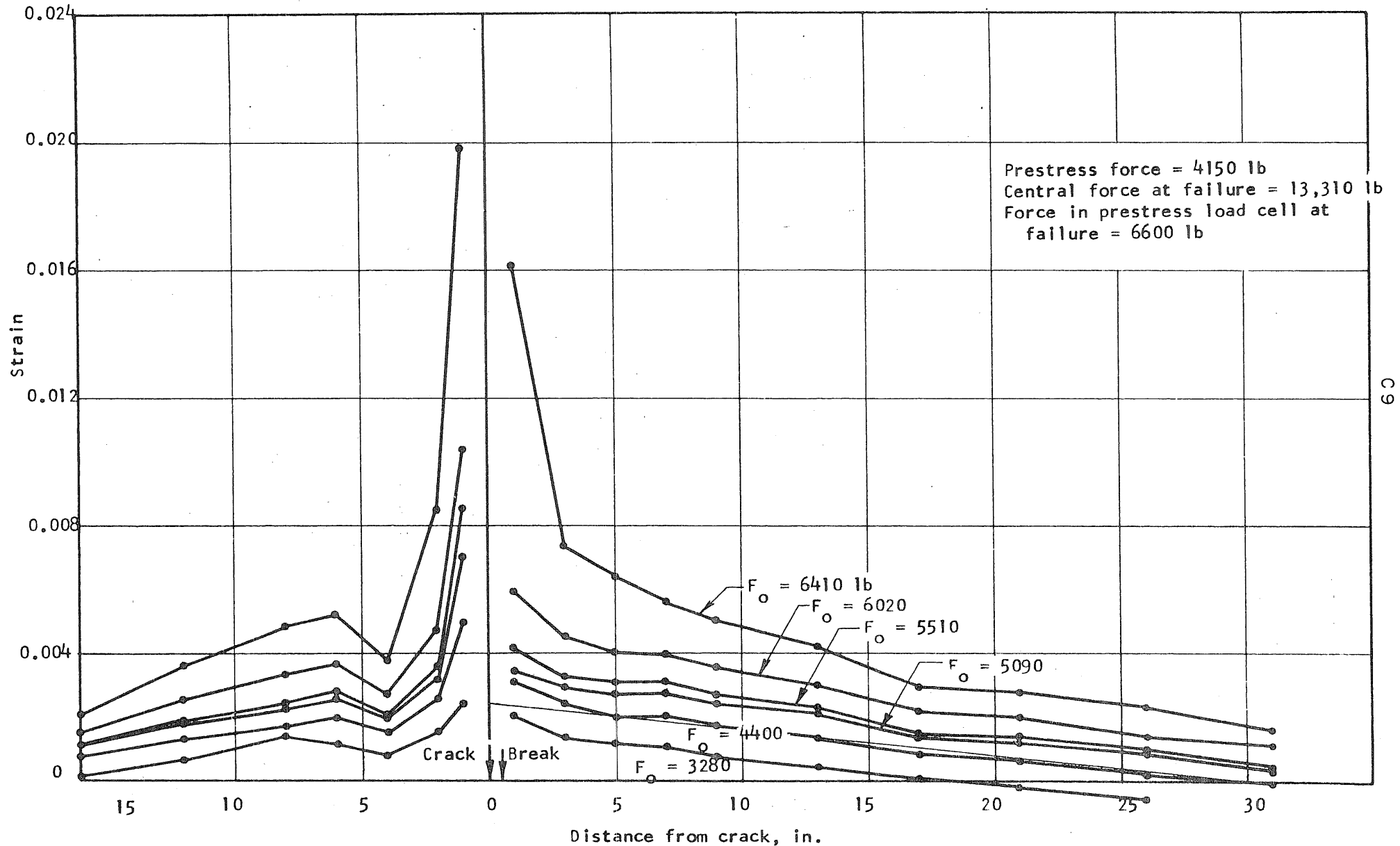


FIG. C4 STRAINS MEASURED ABOVE PRESTRESS STRAINS vs DISTANCE FROM THE CRACK AT SEVERAL LOADS FOR TEST No. 1

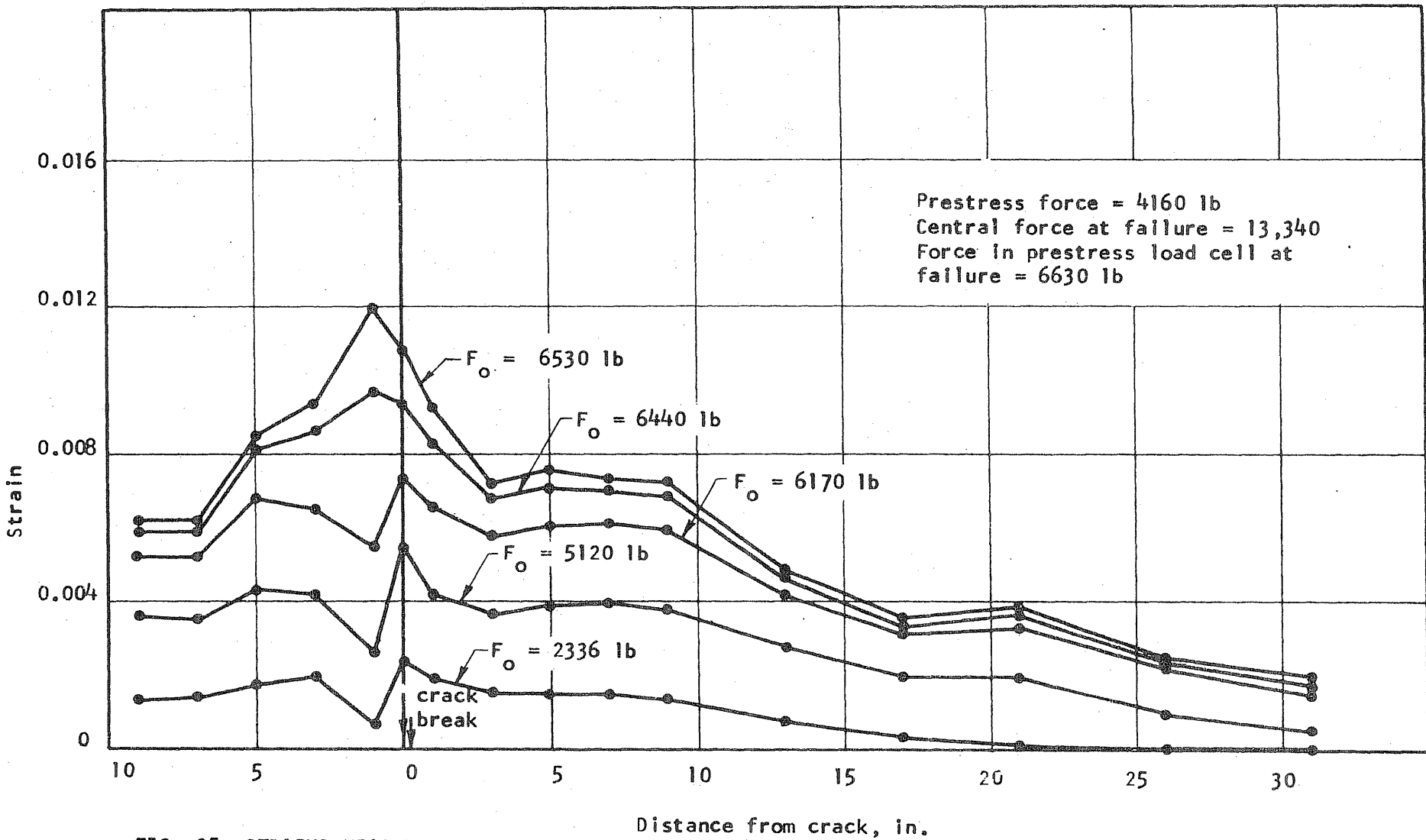


FIG. C5 STRAINS MEASURED ABOVE PRESTRESS STRAINS VS DISTANCE FROM THE CRACK AT SEVERAL LOADS FOR TEST NO. 2

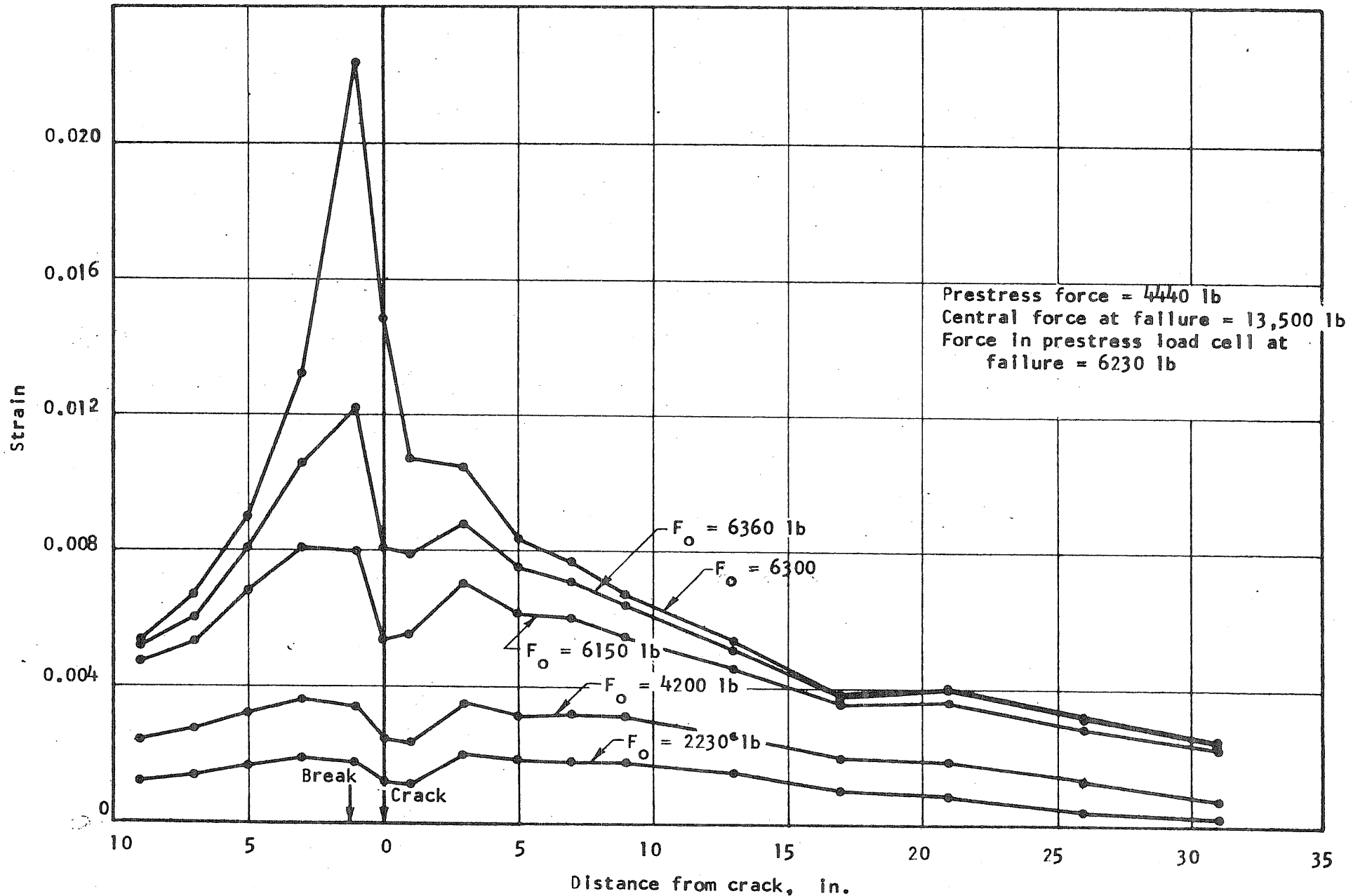
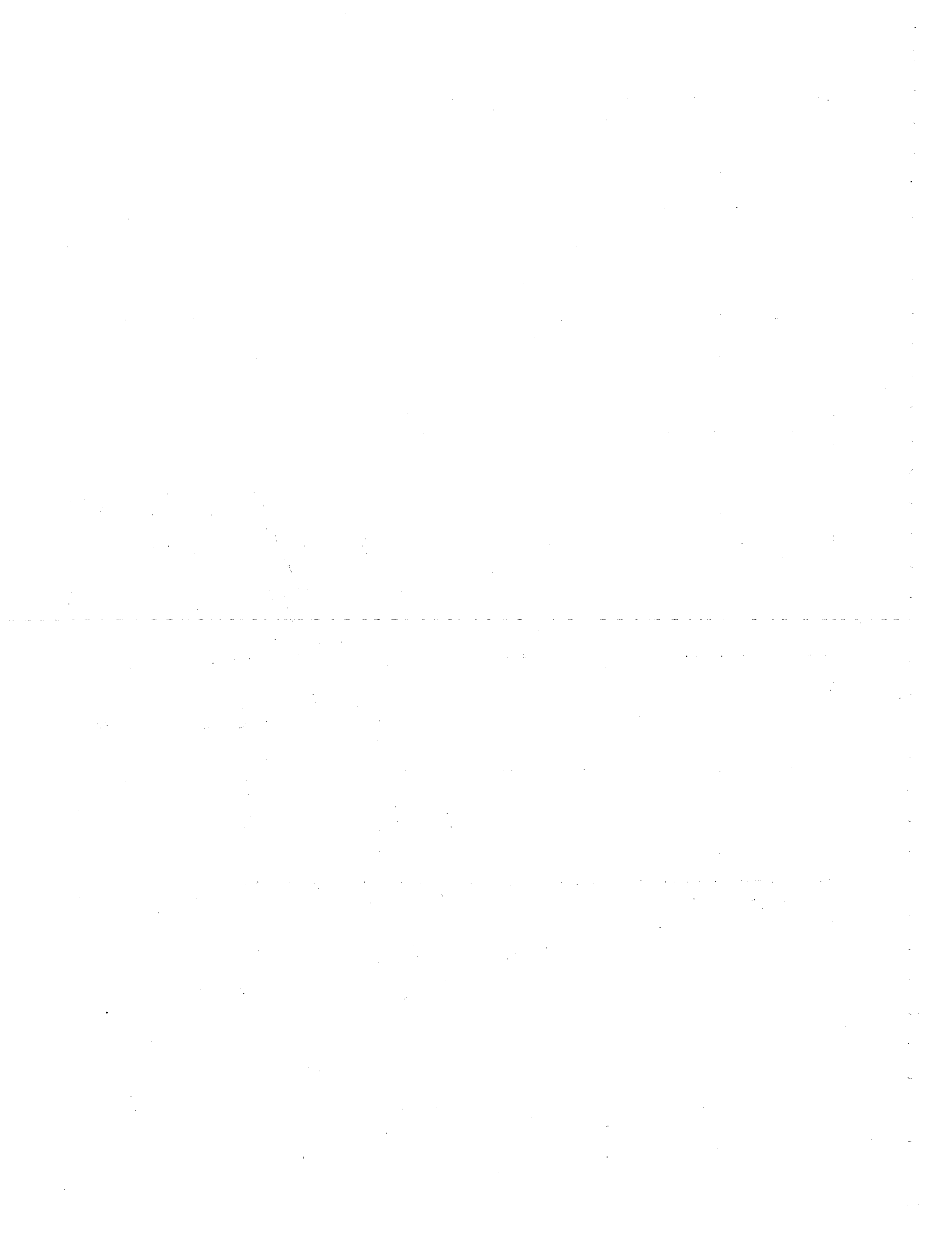


FIG. C6 STRAINS MEASURED ABOVE PRESTRESS STRAINS VS DISTANCE FROM THE CRACK AT SEVERAL LOADS FOR TEST No. 3



APPENDIX D

STIFFNESS MATRIX FOR LUMPED-PARAMETER ELEMENT

The stiffness matrix for a typical node m is

$$[k_m] = 2\pi r_m (L_r L_z / 2) [k_m]$$

The element of the symmetric matrix k_m are given by

$$k_{11} = (1/L_z^2)c_{44}$$

$$k_{21} = 0$$

$$k_{22} = (1/L_z^2)c_{22}$$

$$k_{31} = 0$$

$$k_{32} = (1/L_r L_z)c_{12} - (1/2r_m L_z)c_{23}$$

$$k_{33} = (1/L_r^2)c_{11} - 2(1/2r_m L_r)c_{13} + (1/4r_m^2)c_{33}$$

$$k_{41} = (1/L_r L_z)c_{44}$$

$$k_{42} = k_{43} = 0$$

$$k_{44} = (1/L_r^2)c_{44}$$

$$k_{51} = -k_{11}$$

$$k_{52} = k_{53} = 0$$

$$k_{54} = -(1/L_r L_z) c_{44}$$

$$k_{55} = k_{11}$$

$$k_{61} = 0$$

$$k_{62} = -k_{22}$$

$$k_{63} = -k_{32}$$

$$k_{64} = k_{65} = 0$$

$$k_{66} = k_{22}$$

$$k_{71} = 0$$

$$k_{72} = -(1/L_r L_z) c_{12} - (1/2r_m L_z) c_{23}$$

$$k_{73} = -(1/L_r^2) c_{11} + (1/4r_m^2) c_{33}$$

$$k_{74} = k_{75} = 0$$

$$k_{76} = -k_{72}$$

$$k_{77} = (1/L_r^2) c_{11} + 2(1/2r_m L_r) c_{13} + (1/4r_m^2) c_{33}$$

$$k_{81} = -(1/L_r L_z) c_{44}$$

$$k_{82} = k_{83} = 0$$

$$k_{84} = -(1/L_r^2) c_{44}$$

$$k_{85} = -k_{81}$$

$$k_{86} = k_{87} = 0$$

$$k_{88} = -k_{84}$$

APPENDIX E

COMPUTER PROGRAM LISTING

The computer program used in this study consists of a MAIN routine and a number of SUBROUTINES and FUNCTIONS. The MAIN routine is the control routine of the program in which various SUBROUTINES for reading of input parameters, computation of topological informations, assigning of joint displacement unknown numbers, generation of the stiffness matrix for the complete structure (equilibrium equations), calculation of joint loads for a specified pressure level, solution of equilibrium equations, computation of strains and stresses, etc. are called in. Calculation of various pressure levels corresponding to the cracking stress or the cracking strain at a flexible node is also performed in the MAIN routine.

The computation of the stiffness matrix for the complete structure which is an intermediate major step in the program is performed by the use of several SUBROUTINES. These SUBROUTINES generate the material property matrix (in elastic or in cracking state), the boundary condition matrix (if the node is on the boundary), and the element stiffness matrix for each flexible node. The individual stiffness matrices are then assembled in appropriate manner to obtain the stiffness matrix (equilibrium equations) of the complete structure. The terms in each row of the stiffness matrix between the first and the last non-zero columns are then stored on the DRUM (an auxiliary storage device).

When a crack is initiated at a flexible node or when it is propagated to another node, the equilibrium equations which are affected

by the presence of the crack are regenerated and restored on the DRUM for subsequent use. The program maintains a table of information regarding the state of cracking at the flexible nodes (cracking history). This table is updated at the end of each pressure level and it is printed in order to provide the cracking sequence throughout the study. In addition to this table, the displacements, the strains, and the stresses are also updated at the end of each pressure level.

The program is coded in FORTRAN IV language and it is used on the IBM System 360/75 of the University of Illinois. The number of equilibrium equations which can be solved naturally depends on the storage capacity of the computer. However, due to repeated modification and solution of the equilibrium equations, solution of a large number of equations is not economical.

E3

(a)

(c)

```

***** MAIN *****
***** COMMON *****
COMMON ALR,ALZ,I1C,EC,JIP,JEP,PRFL,PLRC,LR,LG,LPO,LCYC,PR,
1 PHP,MW,NW,KD,I1C,TOT,NG,KD,KLW,KHIG,KHM,KDR,I1C,JIA,
2 JA,NL,CON,ERR,CF,PRFL,PRF2,PRF3,PRF4,LOCAT,LAOD,LCL,SIGN
3 ,C1,C2,C3,C4,CR,JCR,LPRCSS,LCH,P1,TOT,JTOT1,ECRIT,
4 EXCF,SIGCR,TPLATE,TCYLDL,ICM1,I1CP1,L1,JDHUM
COMMON A(150),B(53000),V(53,81),W(53,81),NP(1800),NC(1800),C(4),
1 S(1800),MS(1800),R(53),SUMR(53),DIFFR(53),AR(20),ALP(20),
2 FLP(20),ZP(20),UC(4),WC(4),SRP0(10),ERPO(10),S1P0(10),
3 EZPO(10),STPO(10),ETPO(10),SRZPO(10),ERZPO(10),S1P0(10),
4 EPO(10),S2PO(10),EPR(10),TANP(10),TAN2P(10)
DIMENSION LC(53,81),LG(53,81),V(53,81),W(53,81),NP(53,81),NC(53,81),
1 S(1800),MS(1800),R(53),SUMR(53),DIFFR(53),AR(20),ALP(20),
2 ERPR(53,81),EZPR(53,81),ETPR(53,81),ERZPR(53,81),
3 EPS1(53,81),SIG(53,81),EPS(53,81),DET(53,81)
EQU(VALENCE U(1)),LC(1), (B(1),EPS1(1)),
1 (B(4301),ERPR(1)), (B(4601),EZPR(1)),
2 (B(12901),ETPR(1)), (B(17201),ERZPR(1)),
3 (B(21501),SIGR(1)), (DER(1)), (B(29801),SIGZ(1)), (DERZ(1)),
4 (B(30101),SIGZ(1)), (DE2(1)), (B(34401),SIGT(1)), (DEPS1(1)),
5 (B(38701),SIG(1)), (B(43001),EPS(1)), (B(47301),DET(1))
EXTERNAL DUMP
DEFINE FILE 2(1400,10,IREC)
CALL ERASET (200,1,0,2,DUMP,210)
50 READ (5100) I1C,IEC,JIP,PRFL,N,ICABLE,LRC,LR,LCCY,LG,LPO,LPHCSS,
1 AHP,FNP,ALR,ALZ,D,EST,EC,PR,ECRIT
100 FORMAT (12I4,12F8.5,F12.2,2F30.10,5,2E12.4,2F12.6)
H = (JEP-1)*ALZ/2
TPLATE = (JEP-JIP)*ALZ/2
TCYLDL = (IEC-I1C)*ALR/2
ICBLR = ICABLE-I1C+2
DOE = TCYLDL-(ICBLR-2)*ALR/2
PRF1 = EC/(1.+PR)*(1.-2.*PR)
PRF2 = (1.-PR)*PRF1
PRF3 = PR*PRF1
PRFA = EC/(2.**(1.+PR))
I1CMI = I1C-1
R(1) = 0.
M = IEC-1
DO 1 I=1,M
R(I+1) = R(I)+ALR/2.
SUMR(I+1) = 1./ALR+0.5/R(I+1)
1 DIFFR(I+1) = 1./ALR-0.5/R(I+1)
DIAM = 2.*R(IEC)
CI = 1.+ALR/(R(1)*R(I1C))
CE = 1.-ALR/(R(1)*R(I1C))
PHP=FNP/(DNR(IEC))
MW = JEP-JIP+1
NW = IEC-I1C+
1 TOT1 = 2*((I1C-1)/2)*MW+(2*(I1C/2)-I1C+1)*(MW-I1LRC)/2)
1 TOT = |TOT1+2*((JIP-1)/2)*NW+(2*(JIP/2)-JIP+1)*(NW-I1LRC)/2+1|
(MW/2)*NW+(MW-2*(MW/2)))*(NW+2*(LRC1)/2)-LRC1/2)
1 READ (5101) (ALP(I),FLP(I),I=1,20)
101 FORMAT (5(F8.5,F8.0))
1 IF (JEP>2*(JEP/2)) 24,31,24

```

```

5F CYLINDER = 1,15/6X,1J-LINE CORRESPONDING TO BOTTOM OF PLATE,1,6X,1
6#1+15/6X,1J-LINE CORRESPONDING TO TOP OF PLATE,1,9X,1+15/6X,1J-PLANE,
7L SPACING IN R-DIRECTION = 1,FB0,3+1 IN,1/6X,1PANEL SPACING IN Z-DI
BRECTION = 1,FB0,3+1 IN,1/6X,1
GO TO (3,6),LRC
3 WRITE (6,103)
103 FORMAT (6X,1DISPLACEMENT NODE AT RE-ENTRANT CORNER//)
GO TO 7
6 WRITE (6,104)
104 FORMAT (6X,1STRESS NODE AT RE-ENTRANT CORNER//)
7 WRITE (6,105) EC,PRECIRIT
105 FORMAT (1I ELASTIC CONSTANTS OF MATERIAL//6X,1MODULUS OF ELASTICITY
1, BX,1+1,E13,5,1 PSI,1/6X,1POISSON RATIO,1,6X,1+1,F7,3/6X,1CHACKI
ZNG STRAIN,1,6X,1+1,F9,5//)
WRITE (6,113) AHP,ESTD,FNP,PHP,SUMALP,EST,N,SUMPHZ,DOL
113 FORMAT (1I HOOP PRESTRESSING//6X,1AREA OF CABLE,1,6X,1+1,E13,5,1
2 ,1,6X,1+1,F9,5//)
3LUS OF ELASTICITY,BX=1,E13,5,1 PSI,1/6X,1SPACING,1,22X,1+1,L13,5,1
4 IN,1/6X,1PRESTRESSING LOAD,1,2X,1+1,I3,5,1 L13,5,1/6X,1+1,6X,1+1
SUPPLIED PRESSURE = 1,E13,5,1 PSI,1//1 LONGITUDINAL PRESTRESSING
6//6X,1AREA OF CABLE,1,6X,1+1,E13,5,1 PSI,1/6X,1NUMBER OF CABLES,1,6X,1+1,E13,5,1
7TICITY,1,6X,1+1,E13,5,1 PSI,1/6X,1MODULUS OF ELASTI
8IPRESTRESSING LOAD PER CABLE = 1,E13,5,1 L13,5,1/6X,1+1,6X,1+1
9UTER EDGE = 1,E13,5,1 IN,1//)
GO TO (8,9),LG
8 WRITE (6,106)
106 FORMAT (6X,1LONGITUDINAL PRESTRESSING IS UNROOTED//)
GO TO 10
9 WRITE (6,107)
107 FORMAT (6X,1LONGITUDINAL PRESTRESSING IS GROUDED//)
10 IICP1 = 1IC1+
1ICLP = 1ICP1+16
WRITE (6,108) ((1+1ICP1+1ICLP),(ALP(1),1E3,19)+(FLP(1),1E3,19),
1 LRC(LRL,LCY,C,LGP0,LPRCS5),ITOT
108 FORMAT (6X,1EQUIVALENT PRESTRESSING LOADS AND AMPLS AS THEY APPEAR
1ENE IN THE MODEL//6X,1AT I = 1,17/7//6X,1AREAS 1,17/7//6X,1+1L13,5,1
2 ,1,17/7//0//1 SWITCHES AT START//6X,1LRC = 1,I3,5X,1IN - 1,17/7//6X,1
3LCYC = 1,I3,5X,1LG = 1,I3,5X,1LP0 = 1,I3,5X,1LPRCS5 = 1,I3,5X,1
4OF EQUATIONS 1,15//1)
ITOT = ITOT/2
LRC = LRC+(LRC+1)/2-2*(LRC/2)
JTOT1 = (((1C-1)/2)*MW+(2*(1IC/2)-1IC+1)*((MW-1+LRC)/2)
JTOT = JTOT1+ ((J(P-1)/2)*NW+(2*(J(P/2)-J(P+1))*((NW-1+1C-1)/2)+1
1 (MW/2)*NW+(MW-2)*(MW/2))*(NW+2*((LHC+1)/2)-LHC)/2;
JDRUM = (ITOT+9)/10
ITOT1 = 2*JTOT1
IF (LR) 80,80,81
81 REWIND 3
READ (3) NL,LRC,LPRCS5,LCR,DELPL,P,(CR,JCH,STG)(CR,AN,PHP,AV,+1ZP,U,W
LRC = LRC+(LRC+1)/2-2*(LRC/2)
ITOT1 = 2*((1C-1)/2)*MW+(2*(1C/2)-1C+1)*((MW-1+LRC)/2)
REWIND 4
DO 93 L=1,ITOT1
9Q = 2*L
CALL COORD
93 WRITE (4) U(I,J)+W(I,J)
LRC = LRC+(LRC+1)/2-2*(LRC/2)

```

(b)

```

24 IF ((JIP+LRC-2*( (JIP+LRC)/2)) .LT. 32,33,32
31 LADD = 0
GO TO 37
32 LADD = -1-2*(LRC/2)
GO TO 37
33 LADD = 1-2*(LRC/2)
37 LCL1 = LRC+114*JEP-JIP
IF ((LCL1-2*(LCL1/2)) .LT. 38,39,38
38 LCL = 1
GO TO 40
39 LCL = 0
40 L = 0
K = 1
I = 2+LCL
J = JEP+1
DO 16 II = 1,ITOT
16 NR(II) = 0
13 I = I-1
J = J-1
IF ((I-1)) .LT. 20,20,21,
21 IF ((I-IEC)) 14,14,15
14 L = L+1
CALL NMBR(1,J,L)
IF ((J-1)IP) 17,18,13
20 L = L+1
CALL NMBR(1,J,L)
19 K = K+1
I = 28K+LCL
J = JEP+1
GO TO 13
18 IF ((I-1)IC) 19,19,13
15 I = IEC
J = JEP-(2*K-1)+LCL-IEC)
L = L+1
CALL NMBR(1,J,L)
IF ((IEC-2*(IEC/2)) .LT. 13,11,13
11 IF ((I-IEC)) 13,30,30
30 IF ((J-1)) .LT. 25,25,13
17 IF ((J-1)) .LT. 22,22,23
23 IF ((I-1)IC) 13,19,13
22 IF ((I-2*(IEC/2)) .LT. 19,25,25
25 CONTINUE
DO 28 L=1,ITOT
M = NR(L)
28 NC(M) = L
SUMPZP = 0.
SUMALP = 0.
NLP = IEC-1*IC+2
DO 4 I=1,NLP
SUMALP = SUMALP + ALP(I)
4 SUMPZP = SUMPZP+FLP(I)
WRITE (6,102) TPLATE,TCYLDR,H,DIAM,II
102 FORMAT (1H1,'STRUCTURE DIMENSIONS//'
1 F8.3,1 IN.'//6X,'WALL THICKNESS//'
2 HEIGHT OF VESSEL,BX,I=1,F8.3,1 IN.
3 I=1,F8.3,1 IN.'//','MODEL GEOMETRY//'
4 INTERIOR OF CYLINDER I=1,15/6X,I-LINE

```

```

(d)
1  TOTI = 2*JTOTI
DO 75 K=1,JDRUM
READ (3) ERPO,EZPO,ETPO,ERZPO,EIPO,S1PO,S2PO,L2PO,TANIPO,TAN2PO,
      SRPO,SZPO,STPO,SRZPO
2  NO = 2*(IK-1)*10+L
CALL COORD
DER(I,J) = S2PO(L)
ERPR(I,J) = ERPO(L)
ERPO(L) = ERPR(I,J)+DER(I,J)
DEZ(I,J) = E2PO(L)
EZPR(I,J) = EZPO(L)
EZPO(L) = EZPRI(I,J)+DEZ(I,J)
DET(I,J) = TANIPO(L)
ETPR(I,J) = ETPO(L)
ETPO(L) = ETPR(I,J)+DET(I,J)
ERZP(I,J) = TAN2PO(L)
DERZ(I,J) = ERZPO(L)
ERZPO(L) = ERZPR(I,J)+DERZ(I,J)
EPSI(I,J) = EIPO(L)
DEPSI(I,J) = S1PO(L)
76 CONTINUE
WRITE (21K) SRPO
WRITE (21100+K) ERPO
WRITE (21200+K) SZPO
WRITE (21300+K) EZPO
WRITE (21400+K) STPO
WRITE (21500+K) ETPO
WRITE (21600+K) SRZPO
WRITE (21700+K) ERZPO
78 CONTINUE
GO TO 41
80 NL = 0
DO 83 I=1,NLP
II = I+1+IC-2
AR(I) = 0.
PZP(I) = (N)*PLP(I)/(3.14159*ALR*R(I))
83 CONTINUE
AK = 0.
DELP = 0.
P = 0.
LCR = 0
ICR = IIC
JCR = JIP
DO 2 I=1,IEC
DO 2 J=1,JEP
LC(I,J) = 0
IF (J=JIP) 71,2,2
71 IF (I=IIC) 72,2,2
72 LC(I,J) = 10000
2 CONTINUE
26 CONTINUE
DO 313 I=1,IEC
DO 313 J=1,JEP
SIGR(I,J) = 0.
SIGZ(I,J) = 0.
SIGT(I,J) = 0.

```

(c)

(a)

```

1 GRZ(I,J) = 0.
1 PPR(I,J) = 0.
1 ZPRN(I,J) = 0.
1 FPRN(I,J) = 0.
1 RZPR(I,J) = 0.
11 CONTINUE
1 LRC = LRC+(LRC+1)/2-2*(LRC/2)
1 ITOT1 = 2*((((IC-1)/2)*MW+(2*((IC/2)-1)+(C+1))*((MW-1)+LRC)/2))
1 REWIND 4
1 DO 77 L=1,ITOTH
1 NO = 2*L
1 CALL COORD
1 U(I,J) = 0.
1 W(I,J) = 0.
77 W(I,I,J)=U(I,J)+W(I,J)
78 CONTINUE
1 LNC = LNC+(LNC+1)/2-2*(LNC/2)
1 ITOT1 = 2*JTOT1
1 DO 9 L=1,JTOT1
1 NO = 2*L
1 CALL COORD
1 L= L-(L-1)/10*10
1 SRPO(L) = SIGR(I,J)
1 LRPOL(L) = FRPR(I,J)
1 SZPOL(L) = SIGZ(I,J)
1 EZPOL(L) = EZPR(I,J)
1 STPOL(L) = SIGT(I,J)
1 ETPOL(L) = FTPR(I,J)
1 U1,POU(L) = SIGRZ(I,J)
1 U1,POU(L) = ERZPR(I,J)
1 IF ((L-1)*((L-JTOT1)) .LE. 94*5
74 L10 = (L+9)/10
1 WRITE (21L10) SRPO
1 WRITE (21100+L10) ERPO
1 WRITE (21200+L10) SZPO
1 WRITE (21300+L10) EZPO
1 WRITE (21400+L10) STPO
1 WRITE (21500+L10) ETPO
1 WRITE (21600+L10) SRZPO
1 WRITE (21700+L10) ERZPO
5 CONTINUE
41 LR = LR+1
41 NL = NL+1
41 IF (NL>P) 42,43,44
42 CONTINUE
42 LRC = LRC+(LRC+1)/2-2*(LRC/2)
42 ITOT1 = 2*((((IC-1)/2)*MW+(2*((IC/2)-1)+(C+1))*((MW-1)+LRC)/2))
42 REWIND 1
42 DO 99 L=1,ITOT1
42 NO = NR(L)
42 CALL COORD
42 CALL BAND
42 CALL EQUATN
42 IF (NO>2*(NO/2)) 46,47,48
46 IF (I>11) 48,48,49
48 A(KDR) = 1.
48 GO TO 45

```

(b)

```

47 IF (J>1) 48,48,52
49 CALL SIGRA
CALL SIGRB
CALL SIGRC
CALL SIGRD
CALL SIGTIJ
GO TO 45
52 CALL SIGZC
CALL SIGZD
CALL SIGRZA
CALL SIGRZB
45 WRITE (1) I,J,KLOW,KHIGH,A,CON
99 CONTINUE
60 CALL SOLVER
60 CALL SIGRA
60 DO 53 L=1,ITOT1
60 NO = NR(L)
60 CALL COORD
60 IF (NO>2*(NO/2)) 54,55,54
54 U(I,J) = S(L)
54 GO TO 53
55 W(I,J) = S(L)
53 CONTINUE
LRC = LRC+(LRC+1)/2-2*(LRC/2)
ITOT1 = 2*JTOT1
DO 51 K=1,JDRUM
READ (21K) SRPO
READ (21100+K) ERPO
READ (21200+K) SZPO
READ (21300+K) EZPO
READ (21400+K) STPO
READ (21500+K) ETPO
READ (21600+K) SRZPO
READ (21700+K) ERZPO
DO 51 L=1,10
NO = 2*((K-1)*10+L)
CALL COORD
SIGR(I,J) = SRPO(L)
FRPR(I,J) = ERPO(L)
SIGZ(I,J) = SZPO(L)
EZPR(I,J) = EZPO(L)
SIGT(I,J) = STPO(L)
FTPR(I,J) = ETPO(L)
SIGRZ(I,J) = SRZPO(L)
ERZPR(I,J) = ERZPO(L)
IF (NO>2*JTOT1) 51,95,95
51 CONTINUE
95 CONTINUE
DO 58 L=1,JTOT1
NO = 2*L
CALL COORD
IA = I
JA = J
CALL STRSTR
L1 = L-(L-1)/10*10
CALL SIGEPS
IF ((L-1)*((L-JTOT1)) .LE. 98*58
78 L10 = (L+9)/10

```

(d)

```

DELP = 100.**(EXCF-1.)
LPRCSS = 2
PT = P+DELP
WRITE (6+1141) PT
114 FORMAT (//10THE INTERNAL PRESSURE INCREASES TO*,F8.1,* PSI. REFO
IRE NEXT CRACK DEVELOPS//)
65 P = P+DELP
69 LRC = LRC+(LRC+1)/2-2*(LRC/2)
ITOT1 = 2*((((IC-1)/2)*MW+(2*((IC/2)-1)+(C+1))*((MW-1)+LRC)/2))
GO TO 84
63 ICRT = TABS(ICR)
JCRT = TABS(JCR)
IF (LC(ICRT,JCRT)-1) 201,202,202
201 IF (ICR) 204,204,205
204 LC(ICRT,JCRT) = 2
GO TO 200
202 LC(ICRT,JCRT) = 3
GO TO 200
205 LC(ICR,JCRT) = 1
200 WRITE (6,109) (I,I=1,IEC,2)
109 FORMAT (1H1,50X,ICRACKING TABLE//15X,2B(14)//)
DO 66 J=1,JEP
J1 = JEP-J1
IF (J+LCL-2*((J+LCL)/2)) 67,68,67
68 WRITE (6,111) J1,(LC(I,J))+I=2,IEC,2)
111 FORMAT (10X,I3,2X,2B(14))
GO TO 66
67 WRITE (6,112) J1,(LC(I,J))+I=2,IEC,2)
112 FORMAT (10X,I3+4X,2B(14))
66 CONTINUE
LPRCSS = 3
NL = 1
GO TO 26
64 CALL CHECK
IF (LCR) 87,87,87
59 REWIND 3
WRITE (3) NL,LRC,LPRCSS,LCR,DELP,P,ICR,JCR,SIGCR,AK,PHP,AR,PZP,U,
1      W
DO 73 L=1,JTOT1
NO = 2*L
CALL COORD
L1 = L-(L-1)/10*10
ERPO(L1) = ERPR(I,J)
EZPO(L1) = EZPR(I,J)
ETPO(L1) = ETPR(I,J)
ERZPO(L1) = ERZPR(I,J)
EIP0(L1) = EPS(I,J)
S1PO(L1) = DEPS(I,J)
S2PO(L1) = DER(I,J)
E2PO(L1) = DEZ(I,J)
TAN1PO(L1) = DET(I,J)
TAN2PO(L1) = DERZ(I,J)
IF ((L-1)*((L-JTOT1)) 73,74,73
74 L10 = (L+9)/10
READ (21L10) SRPO
READ (21200+L10) SZPO
READ (21400+L10) STPO

```

(a)

(c)

```

        EXCF1(SIG1,CR1,TPLATE,(ICM1)+(ICP1)+1,JURHM
COMMON A(150),B(53000),U(53+81),W(53+81),NR(1800),NC(1800)+C(44),
1      S(1800)+MS(1800),R(53),SUMR(53),UIFPN(53),AK(20),ALP(20)*
2      FLP(20),PZP(20),W(4),WC(4),SPRPO(10),LWPPO(10),DZPPO(10),
3      EZPO(10),STPO(10),ETPO(10),SHZPO(10),HZKPO(10),DZPO(10),
4      E1PO(10),S2PO(10),E2PO(10),TAN1PO(10),TAN2PO(10)
DIMENSION LC(53+81),SIGR(53+81),SIGZ(53+81),SIGT(53+81),SIGH(53+
1      B1),DER(53+81),DEZ(53+81),DEH(53+81),DEPSI(53+81),
2      ERPR(53+81),EZPR(53+81),ETPR(53+81),EHZPR(53+81),
3      EPS(53+81),SIG(53+81),EPS(53+81)+DET(53+81)
EQUIVALENCE (U(1)),LC(LC(1)),(B(1)),EPS1(1))
1      (B(14301),EPHR(1)),(B(18601),EPZPR(1)),
2      (B(12901),ETPR(1)),(B(17201),ERZPR(1)),
3      (B(21501),SIGR(1)),(DER(1)),(B(25801)),SIGZR(1),DEHZ(1)),
4      (B(30101),SIGZ(1)),(DEZ(1)),(B(34401)),SIGT(1),DEPSI(1)),
5      (B(38701)),SIG(1),(B(43001),EPS(1)),(B(47301),DET(1))

1 IA = [+]
JA = J
IF ((J-1)*(J-IEC+1)*(J-IEC)*(J-1)*(J-2)*(J-J|P-1)*(J-J|P)*(J-JEP))
6      221,202,221
1 CALL STRSTR
TYPICAL NODE
A(KHR=51) = C((11)/ALR+C(13)/(2.*R([IA])))*C1
A(KHR=4) = C(11)*C1/ALR
A(KHR=3) = -C(14)*C1/ALZ
A(KHR=2) = -C(12)*C1/ALZ
A(KDR=2) = C(14)*C1/ALZ
A(KDR=1) = C(12)*C1/ALZ
A(KDR) = -(C(11)/ALR-C(13)/(2.*R([IA])))*C1
A(KDR1) = -C(14)*C1/ALR
GO TO 250
2 IF (J-IEC+1) 203,204,205
AT EXTERIOR FACE OF CYLINDER
5 A(KDR) = -AK/R([1])*C1
CON = CON-PHP*C1
GO TO 250
HALF-SPACE FROM EXT. FACE OF CYLINDER
4 CON = CON-PHP*C1
IF ((J-2)*(J-JEP)) 206,207,207
6 A(KDR=2) = -AK/(2.*R([IA]))*C1
7 A(KHR=3) = -AK/(2.*R([IA]))*C1
GO TO 250
7 IF (J-2) 208,223,209
8 A(KDR=2) = -AK/R([IA])*C1
GO TO 250
9 A(KDR) = -AK/(2.*R([IA]))*C1
GO TO 217
3 A(KDR=2) = -AK/(2.*R([IA]))*C1
A(KHR=1) = A(KDR=2)
GO TO 250
3 IF ((J-1) 210,211,210
EQUATION AT CENTERLINE
1 A(KDR) = 1*
CON = 0*
RETURN
0 CALL STRSTR
IF (J-J|P) 222,213,214,

```

(b)

```

1 (B( 4301)*ERPA(1)), (B( 8601)*ERZPR(1)), *
2 (B(12901),LTPR(1)), (B(17201),ERZPR(1)), *
3 (B(21501),SIGR(1)+DER(1))+(B(29801),SIGRZ(1),DERZ(1)), *
4 (B(30101),SIGZ(1),DEZ(1))+(B(34401),SIGT(1),DEPS(1))+(B(47301),DET(1))
5 (B(38701),SIG(1)),(B(43001),EPS(1))+(B(47301),DET(1))

KHR = KHIGH-KLOW+1
KDR = KD-KLOW+1
DO 10 K=1,KHR
10 A(K) = 0.
CON = 0.
C1 = SUMR(1)
C2 = -DIFFR(1)
C3 = 1./ALZ
C4 = -C3
IF ((I-1)*(I-IEC)) 11+12+12
11 IF ((I-IC)) 13+14+15
13 IF ((J-JP)*(J-JEP)) 200+17+17
16 IF ((I-2) 17,200+17
14 IF ((J-JP)) 18+19+23
23 IF ((J-JP-1)) 24+24+13
24 C4 = 0.5*(1.-ALR/(R(1)*R(1)))/ALZ
GO TO 13
AT INTERIOR FACE OF CYLINDER
18 C1 = 2.*C1
C2 = -2./ALR
C3 = C3*C1
C4 = -C3
IF ((J-1) 200+17+200
17 C3 = 2.*C3
C4 = -C3
GO TO 200
AT RE-ENTRANT CORNER
19 C2 = 0.5*C2
C4 = 0.5*C4*C1
GO TO 200
15 IF ((I-IC-1) 25+26+25
26 IF ((J-JP)) 25+27+25
27 C2 = 0.5*C2
25 IF ((J-1)*(J-JEP)) 200+17+200
12 IF ((I-1) 21+22+21
AT EXTERIOR FACE OF CYLINDER
21 C1 = 2./ALR
C2 = 2.*C2
C3 = C3*CE
C4 = -C3
IF ((J-1)*(J-JEP)) 200+17+17
22 C1 = 8./ALR
IF ((J-JP)*(J-JEP)) 200+17+17
200 RETURN
END

*****SUBROUTINE SIGRA*****
*****COMMON BLOCKS*****
COMMON ALR,ALZ,I,IEC,JIP,JEP,EC,H,DELP,LRC,LR,LG,LPO,LCYC,PR,
1 PHP,MW,NW,AK,I,TOT1,ITOT1,TOT2,KLOW,KHIGH,KHR,KDR,I,J,IA,
2 JA,NL,COM,ERR,CF,PRF1,PRF2,PRF3,PRFA,LLOCAT,LADU,LCL,SIGN
3 ,C1,CE,C1,C2,C3,C4,ICR,JCR,LPRCSS,LCR,P,JTOT,JTOT1,ECRIT,
```

(a)

```

A(5) = -(C(1))/ALR-C(13)/(2.*R((IA)))*C2
A(6) = -C(14)*C2/ALR
A(KDR) = A(KDR)+C(11)/ALR+C(13)/(2.*R((IA)))*C2
A(KDR+1) = A(KDR+1)+C(14)*C2/ALR
A(KDR+2) = -C(14)*C2/ALR
A(KN3+3) = -C(12)*C2/ALR
GO TO 300
267 IF ((J-JP)) 254,255,261
268 IF ((I-IIC-1)) 257,257,258
269 CON = CON-C2*DELP
    GO TO 300
270 A(4) = 2.*C(12)*C2/ALZ
A(KDR) = A(KDR)+C(11)/ALR+C(13)/(2.*R((IA)))*C2
A(5) = -(C(11)/ALR-C(13)/(2.*R((IA)))*C2
    GO TO 300
271 IF ((I-IIC-1)) 260,259,262
272 IF ((I-IIC-1)) 263,263,251
273 CON = CON-C2*DELP
    GO TO 251
274 CON = CON-C2*DELP
    GO TO 266
275 IF ((I-2)) 300,300,266
276 IF ((I-2)) 300,300,256
277 IF ((J-JEP+1)) 251,265,266
278 A(1) = C(14)*C2/ALZ
A(2) = C(12)*C2/ALZ
A(3) = -(C(11)/ALR-C(13)/(2.*R((IA)))*C2
A(4) = -C(14)*C2/ALR
    GO TO 253
279 LOCAT = 2
CF = C(11)*C2
SIGN = 1.
CALL RSTRN
CF = C(12)*C2
CALL ZSTRN
CF = C(13)*C2
SIGN = -1.
CALL RSTRN
CF = C(14)*C2
CALL RZSTRN
300 RETURN
END
*****+
*****+ SUBROUTINE SIGRZC
*****+
COMMON ALR,ALZ,IIC,IEC,JIP,JEP,EC,H,DELP,LRC,LRI,LG,LPO,LCYC,PR,
1 PHP,MW,NW,AK,ITOT1,IOT1,NG,KD,KLOW,KHIGH,KHN,KDR,I,J,IA,
2 JA,NL,CON,ERR,CF,PRF1,PRF2,PRF3,PRF4,LOCAT,LADD,LCL,SIGN
3 ,C1,CE,C1,C2,C3,C4,ICR,JCR,LPRCSS,LCR,P,JTOT,JTOT1,ECRIT,
4 EXCF1,SIG1CR,TPLATE,TCYLDR,|ICM1||ICP1|L1,JDRUM
COMMON A(150),B(153000),U(53,81),W(53,81),NR(1800),NC(1800),C(44),
1 S(1800),MS(1800),R(53),SUMR(53),DFRR(53),AR(20),ALP(20),
2 FLP(20),PZP(20),UC(4),WC(4),SRPO(10),ERPO(10),SZPO(10),
3 EZPO(10),STPO(10),ETPO(10),SRZPO(10),ERZPO(10),S1PO(10),
4 E1PO(10),S2PO(10),E2PO(10),TAN1PO(10),TAN2PO(10)
DIMENSION LC(53,81),SIGR(53,81),SIGZ(53,81),SIGT(53,81),SIGRZ(53,
1 81),DCR(53,81),DEZ(53,81),DERZ(53,81),DEPS1(53,81),

```

(b)

```

2   ERPR(53,81),EZPR(53,81),ETPR(53,81),ERZPR(53,81)
3   EPS1(53,81),SIG(53,81),EPS(53,81),DET(53,81)
EQUIVALENCE (U(1),LC(1)), (B(1),EPS1(1)),
1   (B(4301),ERPR(1)), (B(8601),EZPR(1)),
2   (B(12901),ETPR(1)), (B(17201),ERZPR(1)),
3   (B(21501),SIGR(1),DER(1)), (B(25801),SIGRZ(1),DERZ(1)),
4   (B(30101),SIGZ(1),DEZ(1)), (B(34401),SIGT(1),DEPS1(1)),
5   (B(38701),SIG(1)), (B(43001),EPS(1)), (B(47301),DET(1))
300 IA = 1
JA = J+1
IF (((I-IIC)*(I-IEC)*(J-JEP+1)*(J-JEP)) 301,302,301
302 IF ((J-JEP+1)) 303,350,350
303 IF ((I-IEC)) 304,350,350
304 IF ((J-JEP+1)) 350,301,301
301 CALL STRSTR
A(1) = C(44)*C3/ALZ
A(2) = C(42)*C3/ALZ
A(3) = A(3)-(C(41)/ALR-C(43)/(2.*R((IA)))*C3
A(4) = A(4)-C(44)*C3/ALR
A(KDR-2) = A(KDR-2)-(C(41)/ALR+C(43)/(2.*R((IA)))*C3
A(KDR-1) = A(KDR-1)-C(4)*C3/ALR
A(KDR) = A(KDR)-C(44)*C3/ALZ
A(KDR+1) = A(KDR+1)-C(42)*C3/ALZ
350 RETURN
END
*****+
*****+ SUBROUTINE SIGRZD
*****+
COMMON ALR,ALZ,IIC,IEC,JIP,JEP,EC,H,DELP,LRC,LRI,LG,LPO,LCYC,PR,
1 PHP,MW,NW,AK,ITOT1,IOT1,NG,KD,KLOW,KHIGH,KHN,KDR,I,J,IA,
2 JA,NL,CON,ERR,CF,PRF1,PRF2,PRF3,PRF4,LOCAT,LADD,LCL,SIGN
3 ,C1,CE,C1,C2,C3,C4,ICR,JCR,LPRCSS,LCR,P,JTOT,JTOT1,ECRIT,
4 EXCF1,SIG1CR,TPLATE,TCYLDR,|ICM1||ICP1|L1,JDRUM
COMMON A(150),B(153000),U(53,81),W(53,81),NR(1800),NC(1800),C(44),
1 S(1800),MS(1800),R(53),SUMR(53),DFRR(53),AR(20),ALP(20),
2 FLP(20),PZP(20),UC(4),WC(4),SRPO(10),ERPO(10),SZPO(10),
3 EZPO(10),STPO(10),ETPO(10),SRZPO(10),ERZPO(10),S1PO(10),
4 E1PO(10),S2PO(10),E2PO(10),TAN1PO(10),TAN2PO(10)
DIMENSION LC(53,81),SIGR(53,81),SIGZ(53,81),SIGT(53,81),SIGRZ(53,
1 81),DCR(53,81),DEZ(53,81),DERZ(53,81),DEPS1(53,81),
2   ERPR(53,81),EZPR(53,81),ETPR(53,81),ERZPR(53,81),
3   EPS1(53,81),SIG(53,81),EPS(53,81),DET(53,81)
EQUIVALENCE (U(1),LC(1)), (B(1),EPS1(1)),
1   (B(4301),ERPR(1)), (B(8601),EZPR(1)),
2   (B(12901),ETPR(1)), (B(17201),ERZPR(1)),
3   (B(21501),SIGR(1),DER(1)), (B(25801),SIGRZ(1),DERZ(1)),
4   (B(30101),SIGZ(1),DEZ(1)), (B(34401),SIGT(1),DEPS1(1)),
5   (B(38701),SIG(1)), (B(43001),EPS(1)), (B(47301),DET(1))
350 IA = 1
JA = J-1
IF (((I-IIC)*(I-IEC)*(J-1)*(J-2)*(J-JP)+(J-JP-1)) 351,352,351
352 IF ((I-IEC)) 353,400,400
353 IF ((I-IEC)) 400,354,355
354 IF ((J-JP-1)) 400,356,351
356 CA = +C1/(2.*ALZ)
    GO TO 351
355 IF ((J-2)) 400,400,351

```

```

351 CALL STRSTR
A(KDR) = A(KDR)+C(44)*C4/ALZ
A(KDR+1) = A(KDR+1)*C(42)*C4/ALZ
A(KDR+2) = A(KDR+2)-(C(41)/ALR-C(43)/(2.*R((IA)))*C4
A(KDR+3) = A(KDR+3)-C(44)*C4/ALR
A(KHR=3) = A(KHR-3)-(C(41)/ALR+C(43)/(2.*R((IA)))*C4
A(KHR-2) = A(KHR-2)+C(44)*C4/ALR
A(KHR-1) = -C(44)*C4/ALZ
A(KHR) = -C(42)*C4/ALZ
400 RETURN
END
*****+
*****+ SUBROUTINE SIGT1J
*****+
COMMON ALR,ALZ,IIC,IEC,JIP,JEP,EC,H,DELP,LRC,LRI,LG,LPO,LCYC,PR,
1 PHP,MW,NW,AK,ITOT1,IOT1,NG,KD,KLOW,KHIGH,KHN,KDR,I,J,IA,
2 JA,NL,CON,ERR,CF,PRF1,PRF2,PRF3,PRF4,LOCAT,LADD,LCL,SIGN
3 ,C1,CE,C1,C2,C3,C4,ICR,JCR,LPRCSS,LCR,P,JTOT,JTOT1,ECRIT,
4 EXCF1,SIG1CR,TPLATE,TCYLDR,|ICM1||ICP1|L1,JDRUM
COMMON A(150),B(153000),U(53,81),W(53,81),NR(1800),NC(1800),C(44),
1 S(1800),MS(1800),R(53),SUMR(53),DFRR(53),AR(20),ALP(20),
2 FLP(20),PZP(20),UC(4),WC(4),SRPO(10),ERPO(10),SZPO(10),
3 EZPO(10),STPO(10),ETPO(10),SRZPO(10),ERZPO(10),S1PO(10),
4 E1PO(10),S2PO(10),E2PO(10),TAN1PO(10),TAN2PO(10)
DIMENSION LC(53,81),SIGR(53,81),SIGZ(53,81),SIGT(53,81),SIGRZ(53,
1 81),DCR(53,81),DEZ(53,81),DERZ(53,81),DEPS1(53,81),
2   ERPR(53,81),EZPR(53,81),ETPR(53,81),ERZPR(53,81),
3   EPS1(53,81),SIG(53,81),EPS(53,81),DET(53,81)
EQUIVALENCE (U(1),LC(1)), (B(1),EPS1(1)),
1   (B(4301),ERPR(1)), (B(8601),EZPR(1)),
2   (B(12901),ETPR(1)), (B(17201),ERZPR(1)),
3   (B(21501),SIGR(1),DER(1)), (B(25801),SIGRZ(1),DERZ(1)),
4   (B(30101),SIGZ(1),DEZ(1)), (B(34401),SIGT(1),DEPS1(1)),
5   (B(38701),SIG(1)), (B(43001),EPS(1)), (B(47301),DET(1))
400 CS = -0.5*R(I)
SIGN = 1.
C6 = -1./4.*R(I)*#2
C15 = C6
C25 = C6
C35 = C6
C45 = C6
IF ((I-IIC-1)) 411,412,413
411 IF ((J-JP)) 414,415,416
414 IF ((J-2)) 417,442,442
417 C15 = 2.*C6
C35 = C15
LOCAT = 1
IA = I+1
JA = J
CALL STRSTR
A(KDR) = A(KDR)+C(33)*C15
CF = C(31)*C5
CALL RSTRN
CF = C(32)*C5
CALL ZSTRN
LOCAT = 3
IA = 1
JA = J+1
CALL STRSTR
A(KDR) = A(KDR)+C(33)*C35
CF = C(31)*C5
CALL RSTRN
CF = C(32)*C5
CALL ZSTRN
RETURN
442 C15 = 2.*C6
IA = I+1
JA = J
CALL STRSTR
A(KDR) = A(KDR)+C(33)*C15
443 LOCAT = 3
IA = 1
JA = J+1
CALL STRSTR
CF = C(31)*C5
CALL RSTRN
LOCAT = 4
JA = J-1
CALL STRSTR
CF = C(31)*C5
CALL RSTRN
GO TO 427
445 IF ((I-IIC)) 443,449,419
449 CS = 0.75*C5
C25 = 0.5*C6
C45 = C25
GO TO 421
450 IF ((J-JP-1)*(J-JEP+1)) 420,425,444
420 IF ((I-2)) 425,425,421
421 IF ((J-JP+1)*(J-JEP+1)) 421,422,422
421 IA = 1
JA = J+1
CALL STRSTR
A(KDR) = A(KDR)+C(33)*C35
A(2) = A(2)+C(32)*C5/ALZ
A(KDR+1) = A(KDR+1)-C(32)*C5/ALZ
JA = J-1
CALL STRSTR
A(KDR) = A(KDR)+C(33)*C45
A(KHR) = A(KHR)-C(32)*C5/ALZ
A(KDR+1) = A(KDR+1)+C(22)*C5/ALZ
JA = J
IA = I+1
CALL STRSTR
A(KDR) = A(KDR)+C(33)*C25+C(31)*C5/ALR
A(5) = A(5)-C(31)*C5/ALR
IA = I+1
CALL STRSTR
A(KHR-5) = A(KHR-5)+C(31)*C5/ALR
A(KDR) = A(KDR)+C(33)*C15-C(31)*C5/ALR
RETURN
443 IF ((I-IEC+1)) 423,422,*24
423 IF ((J-2)*(J-JEP+1)) 421,425,426
422 IF ((J-2)*(J-JEP+1)) 425,425,426

```

(a)

```

425 IA = I+1
JA = J
LOCAT = 1
CALL STRSTR
A(KDR) = A(KDR)+C(33)*C15
CF = C(31)*C5
CALL RSTRN
IA = I-1
LOCAT = 2
CALL STRSTR
A(KDR) = A(KDR)+C(33)*C25
CALL RSTRN
427 IA = I
JA = J-1
LOCAT = 4
CALL STRSTR
A(KDR) = A(KDR)+C(33)*C45
CF = C(32)*C5
CALL ZSTRN
JA = J+1
LOCAT = 3
CALL STRSTR
A(KDR) = A(KDR)+C(33)*C35
CF = C(32)*C5
CALL ZSTRN
RETURN
428 IF (J-1) 443,443,444
433 C35 = 2.*C6
IA = I
JA = J+1
CALL STRSTR
A(KDR) = A(KDR)+C(33)*C35
GO TO 445
444 C45 = 2.*C6
IA = I
JA = J-1
CALL STRSTR
A(KDR) = A(KDR)+C(33)*C45
445 LOCAT = 1
IA = I+1
JA = J
CALL STRSTR
A(KDR) = A(KDR)+C(33)*C15
CF = C(31)*C5
CALL RSTRN
CF = C(32)*C5
CALL ZSTRN
428 LOCAT = 2
IA = I-1
JA = J
CALL STRSTR
A(KDR) = A(KDR)+C(33)*C25
CF = C(31)*C5
CALL RSTRN
CF = C(32)*C5
CALL ZSTRN
RETURN

```

(b)

```

424 C25 = 2.*C6
IF (J-JEP), 429,430,430
429 IF (J-2) 431,446,446
446 IA = I-1
JA = J
CALL STRSTR
A(KDR) = A(KDR)+C(33)*C25
GO TO 41B
431 LOCAT = 3
IA = I
JA = J+1
CALL STRSTR
C35 = C25
A(KDR) = A(KDR)+C(33)*C35
CF = C(31)*C5
CALL RSTRN
CF = C(32)*C5
CALL ZSTRN
GO TO 42B
430 LOCAT = 4
IA = I
JA = J-1
CALL STRSTR
C45 = C25
A(KDR) = A(KDR)+C(33)*C45
CF = C(31)*C5
CALL RSTRN
CF = C(32)*C5
CALL ZSTRN
GO TO 42B
END
*****
```

```

***** SUBROUTINE SIGZC *****
COMMON ALR,ALZ,[I]C,[EC]JIP,JEP,EC,H,DELP,LRC,LRL,LG,LPO,LCYC,PR,
1 PHP,Mw,Nw,AK,[TOT],ITOT,NO,KD,KLW,KHIGH,KHR,KDR,I,J,IA,
2 JA,NL,CON,ERR,CF,PRF1,PRF2,PRF3,PRF4,LOCAT,LADD,LCL,SIGN
3 ,C1,CE,C2,C3,C4,[CR],JCR,LPRCSs,LCR,PJ,TOT,JTOT,ECRIT,
4 EXCF,SIGICR,TPlate,TCYLD,|[CMI],[CP],LJ,JDURM
COMMON A(150)+B(53000),U(53,81),W(53,81),NR(1800),NC(1800),C(44),
1 S(1800),MS(1800),R(53),SUMR(53),DIFFR(53),AR(20),ALP(20),
2 FLP(20),PZP(20),UC(4),SRPO(10),ERPO(10),SPZP(10),
3 EZPO(10),STPO(10),ETPO(10),SRZPO(10),ERZPO(10),S1PO(10),
4 E1PO(10),S2PO(10),EZPO(10),TAN1PO(10),TAN2PO(10)
DIMENSION LC(53,81),SIGR(53,81),SIGZ(53,81),SIGT(53,81),SIGZR(53,
1 81),DER(53,81),DEZ(53,81),DERZ(53,81),DEPS(53,81),
2 ERPR(53,81),EZPR(53,81),ETPR(53,81),ERZPR(53,81),
3 EPS(53,81),SIG(53,81),EPS(53,81),DET(53,81)
EQUIVALENCE U(1),LC(1),W(1),EPS1(1),
1 (B(4301),ERPR(1)),(B(18601),EZPR(1)),
2 (B(12901),ETPR(1)),(B(17201),ERZPR(1)),
3 (B(21501),SIGR(1),DER(1)),(B(25801),SIGZR(1),DERZ(1)),
4 (B(30101),SIGZ(1),DEZ(1)),(B(34401),SIGT(1),DEPS(1)),
5 (B(38701),SIG(1)),(B(43001),EPS(1)),(B(47301),DET(1))
EQUivalence U(1),LC(1),W(1),EPS1(1),
1 (B(4301),ERPR(1)),(B(18601),EZPR(1)),
2 (B(12901),ETPR(1)),(B(17201),ERZPR(1)),
3 (B(21501),SIGR(1),DER(1)),(B(25801),SIGZR(1),DERZ(1)),
4 (B(30101),SIGZ(1),DEZ(1)),(B(34401),SIGT(1),DEPS(1)),
5 (B(38701),SIG(1)),(B(43001),EPS(1)),(B(47301),DET(1))
*****
```

(c)

```

511 IF (((I-1)*(J-JEP+1)*(J-JEP)) 514,515,514
514 CALL STRSTR
A(1) = C(2)*C3/ALZ
A(2) = A(2)+C(22)*C3/ALZ
A(3) = -(C(21)/ALR-C(23)/(2.*R([A])))*C3
A(4) = -C(24)*C3/ALR
A(KDR-3) = (C(21)/ALR+C(23)/(2.*R([A])))*C3
A(KDR-2) = C(24)*C3/ALR
A(KDR-1) = -C(24)*C3/ALZ
A(KDR) = A(KDR)-C(22)*C3/ALZ
GO TO 550
515 IF ((J-JEP+1) 516,550,550
516 CALL STRSTR
A(2) = C(22)*C3/ALZ
A(KDR) = -C(22)*C3/ALZ
A(KDR-3) = 2.*C(21)+C(23)*C3/ALR
GO TO 550
512 IF ((J-JIP+1)*(J-JEP+1) 514,514,518
513 IF ((J-1)*(J-JEP+1)*(J-JEP)*(I-IEC)) 517,518,517
517 GO TO (514,510),LG
518 II = I-[I]C2
A(2) = AR([I])*C3/ALZ
A(KDR) = -AC(2)
GO TO 514
519 IF (J-1) 519,519,520
519 A(KDR) = 1.0
CON = 0.
RETURN
520 IF ((J-JEP+1) 521,522,523
521 CALL STRSTR
A(21) = C(22)*C3/ALZ
A(KDR) = -AC(2)
LOCAT = 3
SIGN = 1.
CF = C(21)*C3
CALL RSTRN
SIGN = -1.
CF = C(23)*C3
CALL RZSTRN
GO TO 550
522 II = [I]C2
CON = CON-PZP([I])*C3
GO TO (524,525),LG
524 A(KDR) = -AR([I])*C3/(H-ALZ/2)
GO TO 550
525 CF = AR([I])*C3
CALL STRSTR
CALL ZSTRN
GO TO 550
523 II = [I]C2
CON = CON-PZP([I])*C3
GO TO (526,550),LG
526 A(KDR) = A(KDR)-AR([I])*C3/H
550 RETURN
END

```

(d)

```

***** SUBROUTINE SIGZD *****
***** COMMON ALR,ALZ,[I]C,[EC]JIP,JEP,EC,H,DELP,LRC,LRL,LG,LPO,LCYC,PR,
1 PHP,Mw,Nw,AK,[TOT],ITOT,NO,KD,KLW,KHIGH,KHR,KDR,I,J,IA,
2 JA,NL,CON,ERR,CF,PRF1,PRF2,PRF3,PRF4,LOCAT,LADD,LCL,SIGN
3 ,C1,CE,C2,C3,C4,[CR],JCR,LPRCSs,LCR,PJ,TOT,JTOT,ECRIT,
4 EXCF,SIGICR,TPlate,TCYLD,|[CMI],[CP],LJ,JDURM
COMMON A(150)+B(53000),U(53,81),W(53,81),NR(1800),NC(1800),C(44),
1 S(1800),MS(1800),R(53),SUMR(53),DIFFR(53),AR(20),ALP(20),
2 FLP(20),PZP(20),UC(4),SRPO(10),ERPO(10),SPZP(10),
3 EZPO(10),STPO(10),ETPO(10),SRZPO(10),ERZPO(10),S1PO(10),
4 E1PO(10),S2PO(10),EZPO(10),TAN1PO(10),TAN2PO(10)
DIMENSION LC(53,81),SIGR(53,81),SIGZ(53,81),SIGT(53,81),SIGZR(53,
1 81),DER(53,81),DEZ(53,81),DERZ(53,81),DEPS(53,81),
2 ERPR(53,81),EZPR(53,81),ETPR(53,81),ERZPR(53,81),
3 EPS(53,81),SIG(53,81),EPS(53,81),DET(53,81)
EQUIVALENCE U(1),LC(1),(B(1),EPS1(1)),
1 (B(4301),ERPR(1)),(B(18601),EZPR(1)),
2 (B(12901),ETPR(1)),(B(17201),ERZPR(1)),
3 (B(21501),SIGR(1),DER(1)),(B(25801),SIGZR(1),DERZ(1)),
4 (B(30101),SIGZ(1),DEZ(1)),(B(34401),SIGT(1),DEPS(1)),
5 (B(38701),SIG(1)),(B(43001),EPS(1)),(B(47301),DET(1))
*****
```

```

550 IA = I
JA = J-1
CALL STRSTR
IF ((I-[I]C2) 551,552,553
551 IF ((I-1)*(J-JIP)*(J-JEP-1) 554,555,554
554 A(KDR-1) = A(KDR-1)+C(24)*C4/ALZ
A(KDR) = A(KDR)+C(22)*C4/ALZ
A(KDR+2) = -(C(21)/ALR-C(23)/(2.*R([I])))*C4
A(KHR-3) = (C(21)/ALR+C(23)/(2.*R([I])))*C4
A(KHR-2) = C(24)*C4/ALR
A(KHR-1) = -C(24)*C4/ALZ
A(KHR) = A(KHR)-C(22)*C4/ALZ
GO TO 600
555 IF ((J-JIP-1) 556,556,557
556 CON = CON-DELPH*C4
GO TO 600
557 A(KDR) = A(KDR)+C(22)*C4/ALZ
A(KHR) = -C(22)*C4/ALZ
A(KHR-3) = 2.*C(21)+C(23)*C4/ALR
GO TO 600
558 IF ((J-JIP) 560,561,561
560 LOCAT = 4
SIGN = 1.
CF = C(21)*C4
CALL RSTRN
CF = C(22)*C4
CALL ZSTRN
SIGN = -1.
CF = C(23)*C4
CALL RZSTRN
CF = C(24)*C4
CALL RSTRN
CF = C(25)*C4
CALL ZSTRN
SIGN = 1.
CF = C(26)*C4
CALL RZSTRN
END

```

(a)

E 8

(c)

```

60 GO TO 600
61 CON = CON+(1.-ALR/(B.*RC(1)))*DELP/(2.*ALZ)
62 IF J=600
63 IF C1/(2.*ALZ)
64 JN = CON+(1.-ALR/(B.*RC(1)))*DELP/(2.*ALZ)
65 GO TO 594
66 IF ((J-2)*(1-IFC)) 562,563,562
67 GO TO 565+LG
68 IF I=1-IFC+2
69 A(KHR)= -AR((1))*C4/ALZ
70 A(KHR)= A(KDR)-AKHR
71 GO TO 554
72 IF ((I-IFC)) 566,560,560
73 A(KDR)= A(KDR)+2*C(22)*C4/ALZ
74 A(KHR)= ((C(21)/ALR+C(23))/(2.*R(I)))*C4
75 A(KDR+1)= -(C(21)/ALR-C(23)/(2.*R(I)))*C4
76 RETURN
77 END
***** ****
SUBROUTINE SIGRZA
***** ****
COMMON ALR,ALZ,IIC,IEC,JIP,JEP,EC,H,DELP,LRC,LR,LG,LPO,LCYC,PR,
1 PHP,MW,NW,AK,ITOT,ITOT,NG,KD,KLOW,KHIGH,KHR,KDR,I,J,IA,
2 JA,NL,CON,ERR,CF,PRF1,PRF2,PRF3,PRF4,LOCAT,LADD,LCL,SIGN
3 ,C1,CE,C1,C2,C3,C4,ICR,JCR,LPRCSS,LCR,P,JTOT,JTOT,ECRIT,
4 EXCF,SIGICR,TPLATE,TCYLD,ICM1,ICP1,L1,JDRUM
COMMON A(150),B(53000),W(53,81),NR(1800),NC(1800),C(44),
1 S(1800),MS(1800),R(53),SUMR(53),DIFFR(53),AR(20),ALP(20),
2 FLP(20),PZP(20),UC(4),WC(4),SRPO(10),ERPO(10),SZPO(10),
3 EZPO(10),STPO(10),ETPO(10),SRZPO(10),ERZPO(10),SIP(10),
4 EIP(10),S2PO(10),E2PO(10),TAN(10),TAN2PO(10)
DIMENSION LC(5,81),SIGR(53,81),SIGZ(53,81),SIGT(53,81),SIGRZ(53
1 81),DER(53,81),DEZ(53,81),DEPS1(53,81),
2 ERPR(53,81),EZPR(53,81),ETPR(53,81),ERZPR(53,81),
3 EPS1(53,81),SIG(53,81),EPS(53,81),DET(53,81)
EQUIVALENCE (U(1)),LC(1), (B(1)),EPS1(),
1 (B(4301)),ERPR(1), (B(8601)),EZPR(1),
2 (B(12901)),ETPR(1), (B(17201)),ERZPR(1),
3 (B(21501)),SIGR(1),DER(1),(B(25801)),SIGRZ(1),DERZ(1),
4 (B(30101)),SIGZ(1),DEZ(1),(B(34401)),SIGT(1),DEPS1(1),
5 (B(38701)),SIG(1),(B(43001)),EPS(1),(B(47301)),DET(1)
60 IA = I+1
JA = J
IF ((I-IFC)*(I-IFC)*(J-JEP)) 611,650,611
61 IF ((J-2)*(J-JIP)*(J-JP+1)) 612,614,612
62 CALL STRSTR
A(KHR+3) = (C(41)/ALR+C(43)/(2.*R([IA])))*C1
A(KHR+2) = C(44)*C1/ALR
A(KHR+1) = A(KHR-1)-C(44)*C1/ALZ
A(KHR) = A(KHR)-C(42)*C1/ALZ
513 A(KDR+3) = A(KDR-3)-C(44)*C1/ALZ
A(KDR+2) = A(KDR-2)-C(42)*C1/ALZ
A(KDR+1) = A(KDR-1)-(C(41)/ALR-C(43)/(2.*R([IA])))*C1
A(KDR) = A(KDR-1)-C(44)*C1/ALR
GO TO 650
514 IF (J-JIP) 615,616,617
515 CALL STRSTR

```

(b)

```

A(KHR+3) = (C(41)/ALR+C(43)/(2.*R([IA])))*C1
A(KHR+2) = C(44)*C1/ALR
A(KHR+1) = A(KHR-1)-C(44)*C1/ALZ
A(KHR) = A(KHR)-C(42)*C1/ALZ
GO TO 613
616 IF (I-IFC+1) 650,615,612
617 IF (I-IFC) 615,612,612
650 RETURN
END
***** ****
SUBROUTINE SIGRZB
***** ****
COMMON ALR,ALZ,IIC,IEC,JIP,JEP,EC,H,DELP,LRC,LR,LG,LPO,LCYC,PR,
1 PHP,MW,NW,AK,ITOT,ITOT,NG,KD,KLOW,KHIGH,KHR,KDR,I,J,IA,
2 JA,NL,CON,ERR,CF,PRF1,PRF2,PRF3,PRF4,LOCAT,LADD,LCL,SIGN
3 ,C1,CE,C1,C2,C3,C4,ICR,JCR,LPRCSS,LCR,P,JTOT,JTOT,ECRIT,
4 EXCF,SIGICR,TPLATE,TCYLD,ICM1,ICP1,L1,JDRUM
COMMON A(150),B(53000),W(53,81),NR(1800),NC(1800),C(44),
1 S(1800),MS(1800),R(53),SUMR(53),DIFFR(53),AR(20),ALP(20),
2 FLP(20),PZP(20),UC(4),WC(4),SRPO(10),ERPO(10),SZPO(10),
3 EZPO(10),STPO(10),ETPO(10),SRZPO(10),ERZPO(10),SIP(10),
4 EIP(10),S2PO(10),E2PO(10),TAN(10),TAN2PO(10)
DIMENSION LC(5,81),SIGR(53,81),SIGZ(53,81),SIGT(53,81),SIGRZ(53
1 81),DER(53,81),DEZ(53,81),DEPS1(53,81),
2 ERPR(53,81),EZPR(53,81),ETPR(53,81),ERZPR(53,81),
3 EPS1(53,81),SIG(53,81),EPS(53,81),DET(53,81)
EQUIVALENCE (U(1)),LC(1), (B(1)),EPS1(),
1 (B(4301)),ERPR(1), (B(8601)),EZPR(1),
2 (B(12901)),ETPR(1), (B(17201)),ERZPR(1),
3 (B(21501)),SIGR(1),DER(1),(B(25801)),SIGRZ(1),DERZ(1),
4 (B(30101)),SIGZ(1),DEZ(1),(B(34401)),SIGT(1),DEPS1(1),
5 (B(38701)),SIG(1),(B(43001)),EPS(1),(B(47301)),DET(1)
650 IA = I+1
JA = J
CALL STRSTR
IF ((I-1)*(-2)*(J-JEP)) 651,652,651
651 IF (((I-1)*(I-1-IFC)*(J-JIP)*(J-JEP+1)) 653,654,653
653 CALL STRSTR
A(3) = A(3)+C(44)*C2/ALZ
A(4) = A(4)+C(42)*C2/ALZ
A(5) = -(C(41)/ALR-C(43)/(2.*R([IA])))*C2
A(6) = -C(44)*C2/ALR
655 A(KDR+1) = A(KDR-1)+(C(41)/ALR+C(43)/(2.*R([IA])))*C2
A(KDR) = A(KDR)+C(44)*C2/ALR
A(KDR+2) = A(KDR+2)-C(42)*C2/ALZ
652 RETURN
654 IF (J-JEP+1) 656,657,657
655 IF (J-JIP) 652,658,653
656 IF ((I-1-IFC-1)) 652,653,653
657 CALL STRSTR
A(1) = A(1)+C(44)*C2/ALZ
A(2) = A(2)+C(42)*C2/ALZ
A(3) = -(C(41)/ALR-C(43)/(2.*R([IA])))*C2
A(4) = -C(44)*C2/ALR
GO TO 655
END

```

(d)

```

GO TO 21
27 WC141 = -WC(3)
UC141 = UC(3)
GO TO 21
18 IF (JA-JEP) 28,29,29
28 IF (C(44)) 30,31,30
30 A1 = -C(14)*C(42)/C(44)
A4 = -C(14)*(C(41)/ALR-C(43)/(2.*R([IA])))/C(44)
A5 = -C(14)*(C(41)/ALR+C(43)/(2.*R([IA])))/C(44)
GO TO 32
31 A1 = 0.
A4 = 0.
A5 = 0.
32 A5 = A4+C(11)/ALR+C(13)/(2.*R([IA]))
IF (A5) 33,10,33
33 A4 = A4+C(11)/ALR-C(13)/(2.*R([IA]))
A1 = A1+C(12)
UC(2) = (A4-A5*SIGN)*CF1/A4
WC(3) = -A1*SIGN*CF1/(A4*ALZ)
CON = CON-CF1*DELP*SIGN/A4
25 IF (JA-1) 26,26,27
26 WC131 = 2.*WC(3)
UC131 = 2.*UC(3)
***** ****
SUBROUTINE ZSTRN
***** ****
COMMON ALR,ALZ,IIC,IEC,JIP,JEP,EC,H,DELP,LRC,LR,LG,LPO,LCYC,PR,
1 PHP,MW,NW,AK,ITOT,ITOT,NG,KD,KLOW,KHIGH,KHR,KDR,I,J,IA,
2 JA,NL,CON,ERR,CF,PRF1,PRF2,PRF3,PRF4,LOCAT,LADD,LCL,SIGN
3 ,C1,CE,C1,C2,C3,C4,ICR,JCR,LPRCSS,LCR,P,JTOT,JTOT,ECRIT,
4 EXCF,SIGICR,TPLATE,TCYLD,ICM1,ICP1,L1,JDRUM
COMMON A(150),B(53000),W(53,81),NR(1800),NC(1800),C(44),
1 S(1800),MS(1800),R(53),SUMR(53),DIFFR(53),AR(20),ALP(20),
2 FLP(20),PZP(20),UC(4),WC(4),SRPO(10),ERPO(10),SZPO(10),
3 EZPO(10),STPO(10),ETPO(10),SRZPO(10),ERZPO(10),SIP(10),
4 EIP(10),S2PO(10),E2PO(10),TAN(10),TAN2PO(10)
34 A6 = -(C(14)*C(22)*(C(12)*C(24))/((C(24)*C(42)-C(22)*C(44)))
A6 = -(C(14)*C(21)/ALR-C(23)/(2.*R([IA]))-C(22)*(C(41)/ALR-
1 C(43)/(2.*R([IA])))*A10
A7 = -(C(14)*C(21)/ALR-C(23)/(2.*R([IA]))-C(22)*(C(41)/ALR-
1 C(43)/(2.*R([IA])))*A10
A10 = C(42)*A10
GO TO 36
35 A6 = 0.
A7 = 0.
A10 = 0.
36 A6 = A6+C(22)*(C(11)/ALR+C(13)/(2.*R([IA]))-C(12)*(C(21)/ALR-
1 C(23)/(2.*R([IA])))
IF (A6) 37,10,37
37 I1 = A-1+IC+2
A7 = A7+C(22)*(C(11)/ALR-C(13)/(2.*R([IA]))-C(12)*(C(21)/ALR-
1 C(23)/(2.*R([IA])))
UC(4) = -C(22)*AK*CF1/(A6*2.*R([IA]))
UC(2) = UC(4)*(A-6*SIGN)*CF1/A6
CON = CON-CF1*(C(22)*PHP-(C(12)+A10)*PZP(1))/A6
GO TO 21
END
***** ****
SUBROUTINE ZSTR
***** ****
COMMON ALR,ALZ,IIC,IEC,JIP,JEP,EC,H,DELP,LRC,LR,LG,LPO,LCYC,PR,
1 PHP,MW,NW,AK,ITOT,ITOT,NG,KD,KLOW,KHIGH,KHR,KDR,I,J,IA,
2 JA,NL,CON,ERR,CF,PRF1,PRF2,PRF3,PRF4,LOCAT,LADD,LCL,SIGN
3 ,C1,CE,C1,C2,C3,C4,ICR,JCR,LPRCSS,LCR,P,JTOT,JTOT,ECRIT,
4 EXCF,SIGICR,TPLATE,TCYLD,ICM1,ICP1,L1,JDRUM
COMMON A(150),B(53000),W(53,81),NR(1800),NC(1800),C(44),
1 S(1800),MS(1800),R(53),SUMR(53),DIFFR(53),AR(20),ALP(20),
2 FLP(20),PZP(20),UC(4),WC(4),SRPO(10),ERPO(10),SZPO(10),
3 EZPO(10),STPO(10),ETPO(10),SRZPO(10),ERZPO(10),SIP(10),
4 EIP(10),S2PO(10),E2PO(10),TAN(10),TAN2PO(10)

```

(a)

```

DIMENSION LC(53,81),SIGR(53,81),SIGZ(53,81),SIGT(53,81),SIGRZ(53,
1   81),DER(53,81),DEZ(53,81),DERZ(53,81),DEPS(53,81),
2   ERPR(53,81),EZPR(53,81),ETPR(53,81),ERZPR(53,81),
3   EPS(53,81),SIG(53,81),DEP(53,81)
4   EQUIVALENCE (U(1),LC(1)), (B(1),EPS(1)), (B(4301),EP(1)),
5   (B(12901),ETPR(1)), (B(17201),ERZPR(1)), (B(21501),SIGR(1)*DER(1)),
6   (B(30101),SIGZ(1)*DEZ(1)), (B(34401),SIGT(1)*DEPS(1)),
7   (B(38701),SIG(1)), (B(43001),EPS(1)), (B(47301),DET(1))

DO I K=1,4
UC(K) = 0.
1 WC(K) = 0.
IF ((IA-1)*(JA-JIP)*(JA-JEP)) 11,12,11
11 WC(3) = CF/ALZ
WC(4) = -WC(3)
12 CALL ASSIGN
13 RETURN
12 IF (JA-JIP) 13,14,15
13 WC(3) = P*CF/ALZ
GO TO 14
14 IF (IA-1)[C] 16,11,11
16 IF (C(44)) 19,20,19
17 A2 = C(24)/C(44)
A1 = C(22)-A2*C(44)
GO TO 21
20 A1 = C(22)
A2 = 0.
21 CON = CON-CF*DELP/A1
22 IF ((IA-1) 23,24,23
23 UC(1) = -CF*((C(21)-A2*C(41))/ALR+(C(23)-A2*C(43))/(2.*R([IA]))/A1
UC(2) = CF*((C(21)-A2*C(41))/ALR-(C(23)-A2*C(43))/(2.*R([IA]))/A1
GO TO 18
24 UC(1) = -2.*CF*(C(21)+C(23)-A2*(C(41)+C(43)))/(ALR*A1)
GO TO 18
15 IF (IA-IEC) 25,26,26
25 IF (C(44)) 27,28,27
27 A2 = C(24)/C(44)
A1 = C(22)-A2*C(44)
GO TO 29
28 A1 = C(22)
A2 = 0.
29 IF (IA-IEC) 22,30,30
30 II = IA-1[C]2
GO TO (31,32),LG
31 WC(4) = -CF*AR([1])/(A1*(H=ALZ/2.))
GO TO 33
32 A1 = A1-AR([1])
33 CON = CON-CF*PZP([1])/A1
GO TO 23
34 A1G = (C(14)*C(22)-C(12)*C(24))/(C(24)*C(42)-C(22)*C(44))
A1 = C(22)-C(24)*C(42)/C(44)
A6 = -(C(42)*(C(21)/ALR+C(23)/(2.*R([IA]))-C(22)*(C(41)/ALR+
1   C(43)/(2.*R([IA]))))*A10
A7 = -(C(42)*(C(21)/ALR-C(23)/(2.*R([IA]))-C(22)*(C(41)/ALR-
1   C(43)/(2.*R([IA]))))*A10
35 A9 = A9+C(21)/ALR-C(23)/(2.*R([IA]))
II = IA-1[C]2
CON = CON-CF*PZP([1])/A1
UC(2) = A9*CF/A1
A6 = A6+C(22)*(C(11)/ALR+C(13)/(2.*R([IA]))-C(12)*(C(21)/ALR+
1   C(23)/(2.*R([IA])))*
IF (A6) 37,10,37
37 A7 = A7+C(22)*(C(11)/ALR-C(13)/(2.*R([IA]))-C(12)*(C(21)/ALR-
1   C(23)/(2.*R([IA])))
A8 = A8+C(21)/ALR-C(23)/(2.*R([IA]))
UC(4) = A8*C(22)*AK*CF/(A1*A6*2.*R([IA]))
UC(2) = A8+C(22)*AK*CF/(A1*A6)
CON = CON +A8*CF*(C(22)*PHP-(C(12)+A10)*PZP([1])/(A1*A6)
GO TO 18
END
*****
```

(b)

```

AB = -C(24)*C(41)/ALR+C(43)/(2.*R([IA]))/C(44)
A9 = -C(24)*C(41)/ALR-C(43)/(2.*R([IA]))/C(44)
A10 = C(42)*A10
GO TO 36
35 A1 = C(22)
A6 = 0.
A7 = 0.
A8 = 0.
A9 = 0.
A10 = 0.
36 A9 = A9+C(21)/ALR-C(23)/(2.*R([IA]))
II = IA-1[C]2
CON = CON-CF*PZP([1])/A1
UC(2) = A9*CF/A1
A6 = A6+C(22)*(C(11)/ALR+C(13)/(2.*R([IA]))-C(12)*(C(21)/ALR+
1   C(23)/(2.*R([IA])))*
IF (A6) 37,10,37
37 A7 = A7+C(22)*(C(11)/ALR-C(13)/(2.*R([IA]))-C(12)*(C(21)/ALR-
1   C(23)/(2.*R([IA])))
A8 = A8+C(21)/ALR-C(23)/(2.*R([IA]))
UC(4) = A8*C(22)*AK*CF/(A1*A6*2.*R([IA]))
UC(2) = A8+C(22)*AK*CF/(A1*A6)
CON = CON +A8*CF*(C(22)*PHP-(C(12)+A10)*PZP([1])/(A1*A6)
GO TO 18
END
*****
```

```

SUBROUTINE RZSTRN
*****
COMMON ALR, ALZ, T1[C], IEC, JIP, JEP, EC, H, DELP, LRC, LRL, LGL, LPO, LYCYC, PR,
1   PHP, MW, NW, AK, ITOT1, ITOT, NO, KD, KLOW, KHIGH, KHR, KDR, I, J, IA,
2   JA, NL, CON, ERR, CF, PRF1, PRF2, PRF3, PRF4, LOCAT, LADD, LCL, SIGN
3   , CI, CE, C1, C2, C3, C4, ICR, JCR, LPRCSS, LCR, P, JTOT, JTOT1, ECRIT,
4   EXCF, SIG1CR, TPLATE, TCYLD, ICM1, [ICP1]*L1, JDRUM
COMMON A(150), B(53000), U(53,81), W(53,81), NR(1800), NC(1800), C(44),
1   S(1800), MS(1800), R(53), SUMR(53), DIFFR(53), AR(20), ALP(20),
2   FLP(20), PZP(20), UC(4), WC(4), SRPO(10), ERPO(10), SZPO(10),
3   EZPO(10), STPO(10), ETPO(10), SRZPO(10), ERZPO(10), SIPO(10),
4   EIPO(10), S2PO(10), E2PO(10), TAN1PO(10), TAN2PO(10)
DIMENSION LC(53,81), SIGR(53,81), SIGZ(53,81), SIGT(53,81), SIGRZ(53,
1   81), DER(53,81), DEZ(53,81), DERZ(53,81), DEPS(53,81),
2   ERPR(53,81), EZPR(53,81), ETPR(53,81), ERZPR(53,81),
3   EPS(53,81), SIG(53,81), EPS(53,81), DET(53,81)
EQUIVALENCE (U(1),LC(1)), (B(1),EPS(1)), (B(4301),EP(1)),
1   (B(12901),ETPR(1)), (B(17201),ERZPR(1)),
2   (B(21501),SIGR(1)*DER(1)), (B(25801),SIGZ(1)*DEZ(1)),
3   (B(30101),SIGZ(1)*DEZ(1)), (B(34401),SIGT(1)*DEPS(1)),
4   (B(38701),SIG(1)), (B(43001),EPS(1)), (B(47301),DET(1))
DO I K=1,4
UC(K) = 0.
1 WC(K) = 0.
IF ((IA-1)*(JA-1)*(IA-IEC)*(JA-JIP)*(JA-JEP)) 11,12,11
11 UC(3) = CF/ALZ
UC(4) = -UC(3)
WC(1) = CF/ALR
WC(2) = -WC(1)
GO TO 14
*****
```

E9

(c)

```

12 IF (((IA-1)*(JA-1)) 13,10,13
13 IF ((IA-IEC) 15,16,17
15 UC(1) = C(42) 35,36,35
35 A2 = C(22)/C(42)
A1 = C(24)-A2*C(44)
GO TO 37
36 A1 = C(24)
A2 = 0.
37 IF (A1) 18,10,18
18 UC(1) = -CF*((C(21)-A2*C(41))/ALR+(C(23)-A2*C(43))/(2.*R([IA]))/A1
UC(2) = CF*((C(21)-A2*C(41))/ALR-(C(23)-A2*C(43))/(2.*R([IA]))/A1
IF (JA-JIP) 19,19,14
19 CON = CON+CF*DELP/A1
GO TO 14
16 IF (JA-JIP) 20,11,21
20 A4 = C(64)*C(11)/ALR-C(13)/(2.*R([IA]))-C(14)*(C(41)/ALR-
1   C(43)/(2.*R([IA])))
IF (A4) 22,10,22
22 UC(1) = CF*((C(11)/ALR+C(13)/(2.*R([IA]))*(C(41)/ALR-C(43)/(2.*R([IA]))*
1   R([IA]))*(C(21)/ALR+C(43)/(2.*R([IA]))*(C(11)/ALR-C(13)/(2.*R([IA]))*
2   ))/A4
UC(3) = CF*((C(12)*(C(41)/ALR-C(43)/(2.*R([IA])))*C(42)*(-1)/ALR-
1   C(13)/(2.*R([IA])))/ALZ*A4)
WC(4) = -WC(3)
CON = CON+CF*(C(41)/ALR-C(43)/(2.*R([IA]))*DELP/A4
GO TO 14
21 IF (JA-JIP) 11,23,11
17 IF ((JA-JIP)*(IA-IEC)) 23,24,23
23 IF (C(42)) 38,39,38
38 A2 = C(22)/C(42)
A1 = C(24)-A2*C(44)
GO TO 40
39 A1 = C(24)
A2 = 0.
40 IF (A1) 25,10,25
25 II = IA-1[C]2
CON = CON+CF*PZP([1])/A1
GO TO (26,27),LG
26 WC(4) = CF*AR([1])/(A1*(H=ALZ/2.))
GO TO 18
27 A1 = A1-AR([1])*A2*C(44)/C(22)
GO TO 18
28 IF (IA-IEC) 25,26,26
29 IF (JA-JEP) 29,10,10
29 A5 = C(44)*(C(11)/ALR+C(13)/(2.*R([IA]))-C(14)*(C(41)/ALR+
1   C(43)/(2.*R([IA])))
IF (A5) 31,10,31
31 UC(2) = CF*((C(41)/ALR-C(43)/(2.*R([IA]))*(C(11)/ALR+C(13)/(2.*R([IA]))*
1   R([IA]))*(C(11)/ALR-C(13)/(2.*R([IA]))*(C(41)/ALR+C(43)/(2.*R([IA]))*
1   ))/A5
UC(3) = CF*((C(12)*(C(41)/ALR+C(43)/(2.*R([IA])))*C(42)*(C(11)/ALR-
1   C(13)/(2.*R([IA])))/ALZ*A5)
WC(4) = -WC(3)
UC(3) = CF*(C(41)/ALR+C(43)/(2.*R([IA]))*AK/(A5*2.*R([IA]))
UC(4) = UC(3)
CON = CON + CF*(C(41)/ALR+C(43)/(2.*R([IA]))*PHP/A5
14 CALL ASSIGN
*****
```

(d)

```

10 RETURN
END
*****
SUBROUTINE ASSIGN
*****
COMMON ALR, ALZ, T1[C], IEC, JIP, JEP, EC, H, DELP, LRC, LRL, LGL, LPO, LYCYC, PR,
1   PHP, MW, NW, AK, ITOT1, ITOT, NO, KD, KLOW, KHIGH, KHR, KDR, I, J, IA,
2   JA, NL, CON, ERR, CF, PRF1, PRF2, PRF3, PRF4, LOCAT, LADD, LCL, SIGN
3   , CI, CE, C1, C2, C3, C4, ICR, JCR, LPRCSS, LCR, P, JTOT, JTOT1, ECRIT,
4   EXCF, SIG1CR, TPLATE, TCYLD, ICM1, [ICP1]*L1, JDRUM
COMMON A(150), B(53000), U(53,81), W(53,81), NR(1800), NC(1800), C(44),
1   S(1800), MS(1800), R(53), SUMR(53), DIFFR(53), AR(20), ALP(20),
2   FLP(20), PZP(20), UC(4), WC(4), SRPO(10), ERPO(10), SZPO(10),
3   EZPO(10), STPO(10), ETPO(10), SRZPO(10), ERZPO(10), SIPO(10),
4   EIPO(10), S2PO(10), E2PO(10), TAN1PO(10), TAN2PO(10)
DIMENSION LC(53,81), SIGR(53,81), SIGZ(53,81), SIGT(53,81), SIGRZ(53,
1   81), DER(53,81), DEZ(53,81), DERZ(53,81), DEPS(53,81),
2   ERPR(53,81), EZPR(53,81), ETPR(53,81), ERZPR(53,81),
3   EPS(53,81), SIG(53,81), EPS(53,81), DET(53,81)
EQUIVALENCE (U(1),LC(1)), (B(1),EPS(1)), (B(4301),EP(1)),
1   (B(12901),ETPR(1)), (B(17201),ERZPR(1)),
2   (B(21501),SIGR(1)*DER(1)), (B(25801),SIGZ(1)*DEZ(1)),
3   (B(30101),SIGZ(1)*DEZ(1)), (B(34401),SIGT(1)*DEPS(1)),
4   (B(38701),SIG(1)), (B(43001),EPS(1)), (B(47301),DET(1))
LD = 2*(NO/2)-NO+1
KDR1 = KDR-LO
GO TO (1,2,3,4),LOCAT
RIGHT
1 IF ((J-1)*(J-2)*(J-1)*(J-1)*(J-1)*(J-1)*(J-1)) 11,12,11
11 AKDRI-2 = A(KDRI-2)+UC(3)
A(KDRI-1) = A(KDRI-1)+WC(3)
13 A(KHR-5) = A(KHR-5)+UC(1)
A(KHR-4) = A(KHR-4)+WC(1)
A(KHR-3) = A(KHR-3)+UC(4)
A(KHR-2) = A(KHR-2)+WC(4)
14 A(KDRI) = A(KDRI)+UC(2)
A(KDRI+1) = A(KDRI+1)+WC(2)
RETURN
12 IF (J-JIP) 15,15,13
15 IF ((I-1)[C] 16,17,18
16 IF (J-JIP) 19,19,17
18 IF (J-2) 19,17,11
17 A(KHR-3) = A(KHR-3)+UC(1)
A(KHR-2) = A(KHR-2)+WC(1)
A(KHR-1) = A(KHR-1)+UC(4)
A(KHR) = A(KHR)+WC(4)
GO TO 20
19 A(KHR-1) = A(KHR-1)+UC(1)
A(KHR) = A(KHR)+WC(1)
20 A(KDRI-2) = A(KDRI-2)+UC(3)
A(KDRI-1) = A(KDRI-1)+WC(3)
GO TO 14
C LEFT
2 IF ((J-JEP+1) 31,32,33
31 A(3) = A(3)+UC(3)
A(4) = A(4)+WC(3)
*****
```

(a)

E10

(c)

```

1 A(5) = A(5)+UC(2)
2 A(1) = A(5)+WC(2)
3 A(KDR1) = A(KDR1)+UC(1)
4 A(KDR1+1) = A(KDR1+1)+WC(1)
5 A(KDR1+2) = A(KDR1+2)+UC(4)
6 A(KDR1+3) = A(KDR1+3)+WC(4)
7 RETURN
8 A(1) = A(1)+UC(2)
9 A(2) = A(2)+WC(2)
10 GO TO 74
11 A(1) = A(1)+UC(3)
12 A(2) = A(2)+WC(3)
13 A(3) = A(3)+UC(2)
14 A(4) = A(4)+WC(2)
15 GO TO 74
16 ABORT
17 IF ((J-JEP+1)) 41,42,44
41 A(1) = A(1)+UC(3)
51 A(2) = A(2)+WC(3)
52 A(3) = A(3)+UC(2)
53 A(4) = A(4)+WC(2)
43 A(KDR1-2) = A(KDR1-2)+UC(1)
44 A(KDR1-1) = A(KDR1-1)+WC(1)
45 A(KDR1) = A(KDR1)+UC(4)
46 A(KDR1+1) = A(KDR1+1)+WC(4)
47 RETURN
48 A(1) = A(1)+UC(2)
49 A(2) = A(2)+WC(2)
50 GO TO 47
51 KLOW = NC(NQ)
52 IF ((J-JEP+1)) 51,52,51
53 A(KHR-3) = A(KHR-3)+UC(1)
54 A(KHR-2) = A(KHR-2)+WC(1)
55 A(KHR-1) = A(KHR-1)+UC(4)
56 A(KHR) = A(KHR)+WC(4)
57 A(KDR1) = A(KDR1)+UC(1)
58 A(KDR1+1) = A(KDR1+1)+WC(3)
59 A(KDR1+2) = A(KDR1+2)+WC(2)
60 A(KDR1+3) = A(KDR1+3)+WC(2)
61 RETURN
62 IF ((J-JEP+1)) 54,55,51
63 IF ((I-1C)) 54,51,51
64 A(KHR-1) = A(KHR-1)+UC(1)
65 A(KHR) = A(KHR)+WC(1)
66 GO TO 50
67 END

***** SUBROUTINE COORD *****
COMMON ALR,ALZ,IIC,IEC,JIP,JEP,EC,H,DELP,LRC,LR,LG,LPU,LCYC,PR,
1 PHP,MW,NW,AK,ITOT1,TOT1,NQ,KD,KLOW,KHIGH,KHR,KDR,I,J,IA,
2 JA,NL,CON,ERR,CF,PRF1,PRF2,PRF3,PRF4,LOCAT,LADD,LCL,SIGN
3 ,CI,CE,C1,C2,C3,C4,[CR,JCR,LPRCSS,LCR,P,]JTOT1,JTOT1,ECHR,
4 EXCF,SIGICR,TPPLATE,TCYLDR,[ICM1,][CPI,]L,JDRUM
COMMON A(150),B(55000),U(53,81),W(53,81),NR(1800),NC(1800),C(44),
1 S(1800),MS(1800),R(53),SUMR(53),DIFFR(53),AR(20),ALP(20),
2 FLP(20),PZP(20),UC(4),W(4),SRPO(10),ERPO(10),S2PO(10),
3 EPO(10),STPO(10),ETPO(10),SRZPO(10),EZPR(10),TAN1PO(10),
4 EPO(10),S2PO(10),E2PO(10),TAN2PO(10),

```

(b)

```

3 EZPO(10),STPO(10),ETPO(10),SRZPO(10),EPS(10),S1PO(10),
4 EPO(10),S2PO(10),E2PO(10),TAN1PO(10),TAN2PO(10)
DIMENSION LC(53,81),SIGR(53,81),SIGZ(53,81),SIGT(53,81),SIGRZ(53,
1 81),DER(53,81),DEZ(53,81),DERZ(53,81),DEPS(53,81),
2 ERPR(53,81),EZPR(53,81),ETPR(53,81),ERZPR(53,81),
3 EPS(53,81),SIG(53,81),DET(53,81)
EQUIVALENCE (U(1)),LC(1)),(B(1)),EPS(1),
1 (B(4301)),ERPR(1)),(B(8601)),EZPR(1)),
2 (B(12901)),ETPR(1)),(B(17201)),ERZPR(1)),
3 (B(21501)),SIGR(1),DER(1)),(B(25801)),SIGRZ(1),DERZ(1)),
4 (B(30101)),SIGZ(1),DEZ(1)),(B(34401)),SIGT(1),DEPS(1)),
5 (B(38701)),SIG(1)),(B(43001)),EPS(1)),(B(47301)),DET(1))
IF ((NOTOT1)) 1,1,2
1 I = (NO-1)/MW+1
2 IF ((MW=2*(MW/2))) 3,4,3
3 IF ((IIC+LRC-2*((IIC+LRC)/2))) 7,9,7
4 IF ((IIC+LRC-2*((IIC+LRC)/2))) 5,6,5
5 IF ((NO-MW-(2*MW)*(I-1)/2)) 7,8,7
6 I = I+1
7 J=2*((NO+1)/2)-((I-1)/2)*((2*(MW+1)/2)-1)-(1/2)*((2*(MW/2)+1)+JIP-1)
RETURN
8 IF ((NO-MW-1-(2*MW)*(I-1)/2)) 9,10,9
10 I = I-1
11 J=2*((NO-1)/21-((I/2)*((2*(MW+1)/2)-1))-((I-1)/2)*((2*(MW/2)+1))+JIP
RETURN
12 I = (NO-1)/JEP+1C
13 IF ((JEP-2*(JEP/2))) 11,12,11
14 IF ((JEP+LRC-2*((JIP+LRC)/2))) 13,14,13
15 IF ((JEP+LRC-2*((JIP+LRC)/2))) 17,16,17
16 IF ((NG-(NOTOT1-1)-JEP-(2*JEP)*((I-1)[C])) 14,18,14
18 I = I-1
19 J=2*((NO-(NOTOT1-1)/2)+1-((I-1)[C])/2)*((2*(JEP/2)+1))-((I-1)[C]+1)/2)*(
12*(JEP+1)/2)-1)
RETURN
20 IF ((NOTOT1-JEP-(2*JEP)*((I-1)[C])) 13,15,13
21 I = I+1
22 J = 2*((NO-(NOTOT1+1)/2)-((I-1)[C]+1)*((2*(JEP/2)+1))-((I-1)[C])/2)*(
12*(JEP+1)/2)-1)
RETURN
END

***** SUBROUTINE BAND *****
COMMON ALR,ALZ,IIC,IEC,JIP,JEP,EC,H,DELP,LRC,LR,LG,LPU,LCYC,PR,
1 PHP,MW,NW,AK,ITOT1,TOT1,NQ,KD,KLOW,KHIGH,KHR,KDR,I,J,IA,
2 JA,NL,CON,ERR,CF,PRF1,PRF2,PRF3,PRF4,LOCAT,LADD,LCL,SIGN
3 ,CI,CE,C1,C2,C3,C4,[CR,JCR,LPRCSS,LCR,P,]JTOT1,JTOT1,ECHR,
4 EXCF,SIGICR,TPPLATE,TCYLDR,[ICM1,][CPI,]L,JDRUM
COMMON A(150),B(55000),U(53,81),W(53,81),NR(1800),NC(1800),C(44),
1 S(1800),MS(1800),R(53),SUMR(53),DIFFR(53),AR(20),ALP(20),
2 FLP(20),PZP(20),UC(4),W(4),SRPO(10),ERPO(10),S2PO(10),
3 EPO(10),STPO(10),ETPO(10),SRZPO(10),EZPR(10),TAN1PO(10),
4 EPO(10),S2PO(10),E2PO(10),TAN2PO(10),

```

(d)

```

40 NO1 = NO-2*(JEP/2)-2*((JEP+1)/2)
GO TO 23
38 IF ((I-IEC+1)) 43,42,42
42 KHIGH = KD+1
GO TO 20
43 NO1 = NO+2*(JEP/2)+2*((JEP+1)/2)+1
GO TO 19
300 KD = KDT
NO = NOT
RETURN
END

***** SUBROUTINE STRSTR *****
COMMON ALR,ALZ,IIC,IEC,JIP,JEP,EC,H,DELP,LRC,LR,LG,LPU,LCYC,PR,
1 PHP,MW,NW,AK,ITOT1,TOT1,NQ,KD,KLOW,KHIGH,KHR,KDR,I,J,IA,
2 JA,NL,CON,ERR,CF,PRF1,PRF2,PRF3,PRF4,LOCAT,LADD,LCL,SIGN
3 ,CI,CE,C1,C2,C3,C4,[CR,JCR,LPRCSS,LCR,P,]JTOT1,JTOT1,ECHR,
4 EXCF,SIGICR,TPPLATE,TCYLDR,[ICM1,][CPI,]L,JDRUM
COMMON A(150),B(55000),U(53,81),W(53,81),NR(1800),NC(1800),C(44),
1 S(1800),MS(1800),R(53),SUMR(53),DIFFR(53),AR(20),ALP(20),
2 FLP(20),PZP(20),UC(4),W(4),SRPO(10),ERPO(10),S2PO(10),
3 EPO(10),STPO(10),ETPO(10),SRZPO(10),EZPR(10),TAN1PO(10),
4 EPO(10),S2PO(10),E2PO(10),TAN2PO(10),
DIMENSION LC(53,81),SIGR(53,81),SIGZ(53,81),SIGT(53,81),SIGRZ(53,
1 81),DER(53,81),DEZ(53,81),DERZ(53,81),DEPS(53,81),
2 ERPR(53,81),EZPR(53,81),ETPR(53,81),ERZPR(53,81),
3 EPS(53,81),SIG(53,81),DET(53,81)
EQUIVALENCE (U(1)),LC(1)),(B(1)),EPS(1),
1 (B(4301)),ERPR(1)),(B(8601)),EZPR(1)),
2 (B(12901)),ETPR(1)),(B(17201)),ERZPR(1)),
3 (B(21501)),SIGR(1),DER(1)),(B(25801)),SIGRZ(1),DERZ(1)),
4 (B(30101)),SIGZ(1),DEZ(1)),(B(34401)),SIGT(1),DEPS(1)),
5 (B(38701)),SIG(1)),(B(43001)),EPS(1)),(B(47301)),DET(1))
C(31) = PRF3
C(32) = PRF3
C(33) = PRF2
C(34) = 0
IF ((LC(I,A,JA)=1)) 11,12,13
13 IF ((LC(I,A,JA)=3)) 14,12,16
14 C(31) = 0,
C(32) = 0,
C(33) = 0,
C(34) = 0,
GO TO 11
16 GO TO 11
HERE, VARIOUS TYPES OF CLOSED CRACKS CAN BE TAKEN INTO ACCOUNT
11 C(11) = PRF2
C(12) = PRF3
C(14) = PRF4
C(13) = C(31)
C(14) = 0,
C(21) = C(12)
C(22) = C(11)
C(23) = C(32)
C(24) = 0,
C(41) = 0,
```

(a)

E | I

(c)

```

C(42) = 0.
C(43) = 0.
END SUBROUTINE

10 IF ((I-IIC1) .LT. 21) P1,P1+22
11 I = (J-JIP+1) 23,23,22
12 J = ATAN(W((IA,JA)))-1,2 22+22,24
13 I = LCL((IA,JA))-1, 11,11,14
14 PRF1 = PRF2*SIN(W((IA,JA))**2
15 PRF2 = PRF2*COS(W((IA,JA))**2
16 TCP = C(32)
17 CP = -0.5*PRF2*SIN(2.*W((IA,JA)))
18 WP = SIN(W((IA,JA))**2
19 DP = COS(W((IA,JA))**2
20 WCF = -0.5*W((IA,JA)**2*W((IA,JA)))
21 C(11) = FZCF*SRCF
22 C(12) = FZCF*SRCF
23 C(14) = ERZCF*SRCF
24 C(11) = FRCF*SZCF
25 C(21) = FRCF*SZCF
26 C(24) = FZCF*SZCF
27 C(41) = FZCF*SRZCF
28 C(42) = EZCF*SRZCF
29 C(44) = FZCF*SRZCF
30 IF (LCL((IA,JA))-P1) 17,14,18
31 C(13) = ETCF*SRCF
32 C(21) = ETCF*SZCF
33 C(14) = ETCF*SRZCF
34 GO TO 19
35 C(13) = 0.
36 C(21) = 0.
37 C(14) = 0.
38 C(43) = 0.
39 C(31) = C(13)
40 C(32) = C(21)
41 C(43) = C(34)
42 RETURN
43 END

***** SUBROUTINE EXTRPL *****
***** COMMON ALR,ALZ,IIC,IEC,JIP,JEP,EC,H,DELP,LRC,LR,LG,LPO,LCCY,PR,
1 PHP,MW,NW,AK,ITOT1,KD,KLOW,KHIGH,KKH,KDN,I,J,IA,
2 JA,NL,CON,ERR,CFT,PRF1,PRF2,PRF3,PRF4,LOCAT,LADU,LCL,SIGN,
3 ,CI,CE,(C1,C2,C3,C4,ICR,JCR,LPRCS5,LCR,P,JTOT,JTOT1,ECRIT,
4 EXUF,SIGICH,TPLATE,TCYLD,(IICM1+IICP1),LI,JURUM,
5 COMMON A(150),B(15300),U(53,81),W(53,81),NR(1800),NC(1800),C(44),
6 S(1800),MS(1800),R(53),SUMR(53),DIFFR(53),AR(20),ALP(20),
7 FPL(20),PPZP(20),UC(4),WC(4),SPRO(10),ERPO(10),S2PO(10),
8 EZPO(10),STPO(10),ETPO(10),SRZPO(10),ERZPU(10),S1PO(10),
9 E1PO(10),S2PO(10),E2PO(10),TANPO(10),TANZPO(10)
10 DIMENSION LC(53,81),SIGR(53,81),BZ(53,81),SIGT(53,81),S1GRZ(53,
11 81),DERZ(53,81),DERZ(53,81),DERZ(53,81),DEPSI(53,81),
12 ERPR(53,81),EZPR(53,81),ETPR(53,81),ER2PR(53,81),
13 EPS1(53,81),SIG(53,81),EPS(53,81),DET(53,81)
14 EQUIVALENCE (U(1)),LC(1)), (B(1)),EPS(1)),
15 (B( 401)), (B( 8601)), (EZPR(1)),
16 (B( 12901)), (ETPR(1)), (B(17201)), (ERZPR(1)),

```

(b)

```

3   (B(21501),SIGR(1),DER(1)),(B(25801),SIGRZ(1),DERZ(1)),
4   (B(30101),SIGZ(1),DEZ(1)),(B(34401),SIGT(1),DEPSI(1)),
5   (B(38701),SIG(1),(B(43001),EPS(1)),(B(47301),DET(1)))
EXCF = 100000.
DO 40 L=1, JTOT
  NQ = 2*L
  CALL COORD
  IF ((LC(I,J)-1) 11+10,28
11 IF (DEPSI(I,J)) 10,10,12
12 D = 4.*DER(I,J)*DEZ(I,J)-DERZ(I,J)**2
  F = 4.*ECRIT**2-4.*ECRIT*(ERPR(I,J)+EZPR(I,J))+4.*ERPR(I,J)*EZPR(I,J)
13 E = -2.*ECRIT*(DER(I,J)+DEZ(I,J))+2.*DER(I,J)*EZPR(I,J)+2.*DEZ(I,J)
14 ERPR(I,J)-DERZ(I,J)*ERZP(I,J)
  IF (D) 13,21,13
21 IF (DEZ(I,J)) 22,24,22
22 ROOT = F/(4.*DEZ(I,J)*(ECRIT-ERPR(I,J)))
  GO TO 7
24 ROOT = F/(4.*DER(I,J)*(ECRIT-EZPR(I,J)))
  7 IF (ROOT) 10,9+9
13 IF (ABS(EVD)-1.E 05) 8+8*21
  8 CONTINUE
  DISCR = E**2-D**F
  IF (DISCR) 23,14,14
23 WRITE (6,101) I,J
101 FORMAT ('0CRACK HAS ALREADY PROPAGATED TO NODE AT I = *,I3+*, J = *
1 ,I3/')
  GO TO 10
14 F1 = (-E+SQR(T(DISCR)))/D
  F2 = (-E-SQR(T(DISCR)))/D
  X1 = ERPR(I,J)+F1*DER(I,J)
  Y1 = EZPR(I,J)+F1*DEZ(I,J)
  Z1 = EZPR(I,J)+F1*DERZ(I,J)
  PRSTR1 = 0.5*(X1-Y1)+SQR((X1-Y1)**2+Z1**2)
  X2 = ERPR(I,J)+F2*DER(I,J)
  Y2 = EZPR(I,J)+F2*DEZ(I,J)
  Z2 = EZPR(I,J)+F2*DERZ(I,J)
  PRSTR2 = 0.5*(X2-Y2)+SQR((X2-Y2)**2+Z2**2)
  IF (ABS(PRSTR1-ECRIT)->1E-05) 15,15,16
15 ROOT = F1
  IF (ROOT) 16,25,25
25 CONTINUE
  IF (ABS(PRSTR2-ECRIT)->1E-05) 17,17,9
16 IF (ABS(PRSTR2-ECRIT)->1E-05) 18,18,23
17 IF (F2) 9,26,26
26 IF (F1=F2) 9,9+18
18 ROOT = F2
  IF (ROOT) 10,10,9
  9 IF (ROOT-EXCF) 20,20,10
20 EXCF = ROOT
  ICR = I
  JCR = J
10 IF (I=1) 40,40,29
29 IF (LC(I,J)-1) 27,27,40
27 IF (DET(I,J)) 40,40,31
31 ROOT = (ECRIT-ETPR(I,J))/DET(I,J)
  IF (ROOT) 40,40,38

```

```

38 IF (ROOT-EXCF) 30,32,40
30 EXCF = ROOT
34 ICR = -I
34 JCR = -J
GO TO 40
32 IF (I-ABS(ICR)) 33,34,33
33 WRITE(6,103) I,J,ICR,JCR
103 FORMAT('WE ARE IN THE PRESENCE OF THE RARE CASE WHERE TWO NODES
1 APPART FROM EACH OTHER CRACK SIMULTANEOUSLY I = ',I,' J = ',J,' AN
2 I = ',I3,' J = ',J3//)
GO TO 40
28 IF (LCL(I,J)-3) 11,40,39
39 CONTINUE
HERE - CLOSED CRACKS CAN BE CONSIDERED
40 CONTINUE
RETURN
END
***** SUBROUTINE CHECK *****
***** COMMONS *****
COMMON ALR,ALZ,IIC,IEC,JIP,JEP,EC,H,DELP,LRC,LRL,GLPHU,LCYC,PIN,
1 PHP,MW,NW,AK,ITOT,ITOT,NGKD,KLOW,KHIGH,KH,KCH,I,J,IA,
2 JA,NL,CON,ERR,CF,PRF1,PRF2,PRF3,PRF4,LUCA1,LCL,SLGN
3 ,C1,CE,C1,C2,C3,C4,ICR,JCR,LPKCS5,LCR,P,JUT,JGFI,ECRIT,
4 EXCF,SIGICR,TPLATE,TCYLD,IICM,IICP1,L1,JURUM
COMMON A((150),B((5300)),U((53,81)),NR((1800)),NC((1800)),C((44),
1 S((1800)),MS((1800)),R((53)),SUMR((53)),UF((53)),AV((20)),ALP((5)),
2 FLP((53,81)),PTP((20)),UC((4)),WC((4)),SRPO((10)),EPPO((10)),SZPO((10)),
3 EZPO((10)),STPO((10)),ETPO((10)),SRZPO((10)),ERZPO((10)),IPU((10)),
4 EIPO((10)),S2PO((10)),E2PO((10)),TANIP((10)),TANZPO((10))
DIMENSION LC((53,81)),SIGR((53,81)),SIG((53,81)),SIGT((53,81)),SIGH((53,
1 81)),DER((53,81)),DEZ((53,81)),DEK((53,81)),DOLP((153,81)),
2 EHRP((53,81)),EZPR((53,81)),TPR((53,81)),ENZPH((53,81)),
3 EPS((53,81)),SIG((53,81)),EPS((53,81)),DET((53,81))
EQUivalence U((1)),LC((1)),(B(1)),EPS((1)),
1 (B(4301)),EPRP((1)),(B(4661)),EZPR((1)),
2 (B(12901)),EPR((1)),(B(17201)),ERZPR((1)),
3 (B(21501)),SIGR((1)),DER((1)),(A(25901)),SIGKZ((1)),DET((1)),
4 (B(30101)),SIGZ((1)),DEZ((1)),(A(34401)),SIG((1)),DEPs((1)),
5 (B(38701)),SIG((1)),(B(43001)),EPS((1)),(A(47301)),DET((1))

LCR = 0
ETEMP = 0,
DO 10 L=1,JTOT
NO = 2*L
CALL COORD
ET = ETPR((I,J)+DET(I,J))
IF (LCL(I,J)-1) 31,32,33
31 IF (EPS((I,J))-ECRIT) 34,37,37
34 IF (ET-ECRIT) 10,38,38
38 ICRT = -I
JCRT = -J
ETEMPI = ET
GO TO 39
36 IF (ET-EPS((I,J))) 35,40,40
40 IF (I-1) 35,35,38
37 IF (ET-ECRIT) 35,36,36
35 ICRT = I

```

(d)

```

JCRT = J
ETEMPI = EPS1(I,J)
39 LCR = LCR+1
IF (ETEMPI-ETEMP) 10,11,12
11 WRITE (6+103) I,J,JCRT,JCRT
103 FORMAT ('WE ARE IN THE PRESENCE OF THE RARE CASE WHERE TWO NODES
1 APPART FROM EACH OTHER CRACK SIMULTANEOUSLY I =',I3,' J =',I3,' AND
20 I =',I3,' J =',I3,'//')
GO TO 10
32 IF (ET-ECRIT) 10,42,42
42 IF (I-1) 43,43,38
43 LCI(I,J) = 3
GO TO 10
33 IF (LCI(I,J)-2) 44,44,10
44 IF (EPS1(I,J)-ECRIT) 10,35,35
12 ETEMP = ETEMPI
   ICR = JCRT
   JCR = JCRT
10 CONTINUE
11 IF (LCR) 15,15,16
15 CONTINUE
* WRITE (6+113)
113 FORMAT ('THE CRACK DOES NOT PROPAGATE!//')
DELP = 100.
LPRCSS = 1
NPH = 0
NLP = IEC-I[C+2
DO 90 I=1,NLP
90 PZP(I) = 0
RETURN
16 WRITE (6+114) LCR
114 FORMAT ('THE CRACK SEEKS TO PROPAGATE INSTANTANEOUSLY THROUGH',
1  I , ' STRESS NODES!//')
RETURN
END
***** SUBROUTINE SOLVER *****
COMMON ALR,ALZ,IIC,IEC,JIP,JEP,EC,HDELP,LRC,LR,LG,LPU,LCY,CPR,
1 PHP,MW,NW,AK,ITOT1,ITOT2,NQ,KD,KLOW,KHIGH,KHR,KDR,I,J,IA,
2 JA,NL,CON,ERR,CF,PRF1,PRF2,PRF3,PRF4,LOCAT,LADU,LCL,SIGN,
3 ,CI,CE,C1,C2,C3,C4,ICR,JCR,LPRCSS,LCH,P,JTOT1,JTOT1,ECRIT,
4 EXCF,SIGICR,TPLATE,TCYLDN,I[CM],I[CH],V,LJURUM
COMMON A(150),B(15000),U(53,81),W(53,81),NC(1800),C(44),
1 S(1800),MS(1800)+MR(1800),SUMR(53),DIFFR(53),AR(20),ALP(20),
2 FLP(20),PZP(20),UC(4),WC(4),SRPO(1:C)=ERPL(10)+SPC(10),
3 EZPO(10),STPO(10),ETPO(10),ERZPO(10)=ERZPU(10),SI(1:P(10),
4 EIP(10),SEPO(10),E2PO(10),TANPO(10),TAN2PO(10),
DIMENSION LC(53,81),SIGR(53,81),SIGT(53,81),SIGZR(53,
1 81),DER(53,81),DEZ(53,81),DERZ(53,81),DEPS(53,81),
2 ERPR(53,81),EZPR(53,81),ETPR(53,81),ERZPR(53,81),
3 EPS1(53,81),SIGR(53,81),EPS1(53,81),DET(53,81)
EQUIVALENCE (U(1)),LC(1)) , (B(1)),EPS1(I))
1 (B(4301)),ERPR(1)) ,(B(8601)),EZPR(1)) ,
2 (B(12901)),ETPR(1)) ,(B(17201)),ERZPR(1)) ,
3 (B(21501)),SIGR(1)),DET(1)) ,(B(25801)),SIGHZ(1)),DERZ(1)) ,
4 (B(30101)),SIGZ(1)),DET(1)) ,(A(34401)),SIGT(1)),DEPS(1)) ,

```

(2)

E12

(c)

```

      (B(38701),SIG(1)),(B(43001),EPS(1)),(B(47301),DET(1))
      REWIND 1
      CALL TRI
      IF (ERR) 1, 2, 3
 1  WRITE (6,4) ERR
 2  FORMAT (16H TOO MANY TERMS ,F10.0)
 3  GO TO 6
 2 CALL BACK
      WRITE (6,7) MS((ITOT))
 7  FORMAT (' SIZE OF VECTOR B IS ',I6)
 8  RETURN
 3 WRITE (5,5) ERR
 4  FORMAT (10H ZERO DIAGONAL TERM ,F10.0)
 5  CONTINUE
 6  RETURN
 7  END

*****SUBROUTINE BACK*****
*****COMMONS*****
COMMON ALR,ALZ,IIC,IEC,JIP,JEP,EC,H,DELP,LRC,LRL,GLP0,LCYC,PR,
1 PHP,MW,NW,AK,ITOT1,ITOT,ITOT,NO,KD,KLOW,KHIGH,KHR,KDR,I,J,IA,
2 JA,NL,CON,ERR,CF,PRF1,PRF2,PRF3,PRF4,LOCAT,LADD,LCL,SIGN
3 .C1,CE,C1,C2,C3,C4,ICR,JCR,LPRCSS,LCR,P,JTOT,JTOT1,ECRIT,
4 EXCF,SIGICR,TPLATE,TCYLD,[(CM1,ICP1),L1,JDRUM
COMMON A(150),B(53000),U(53,81),W(53,81),NR(1800),NC(1800),C(44),
1 S(1800),MS(1800),R(53),SUMR(53),DFRR(53),AR(20),ALP(20),
2 FLP(20),PPZ(20),UC(4),WC(4),SRPO(10),ERPO(10),SZPO(10),
3 EZPO(10),STPO(10),ETPO(10),SRZPO(10),ERZPO(10),S1PO(10),
4 E1PO(10),SZP(10),E2PO(10),TAN1PO(10),TAN2PO(10)
DIMENSION LC(53,81),SIGR(53,81),SIGZ(53,81),SIGT(53,81),SIGRZ(53,
1     B11,DER(53,81),DEZ(53,81),DERZ(53,81),DEPS1(53,81),
2     ERPR(53,81),EZPR(53,81),ETPR(53,81),ERZPR(53,81),
3     EPS1(53,81),SIG(53,81),EPS(53,81),DET(53,81)
EQUIVALENCE (U(1,1),LC(1,1),(B(1),EPS1(1)),
1     (B(1,4301),ERPR(1)),(B(1,8601),EZPR(1)),
2     (B(12901),ETPR(1)),(B(17201),ERZPR(1)),
3     (B(21501),SIGR(1),DER(1)),(B(25801),SIGRZ(1),DEWR(1)),
4     (B(30101),SIGZ(1),DEZ(1)),(B(34401),SIGT(1),DEPS1(1)),
5     (B(38701),SIG(1)),(B(43001),EPS(1)),(B(47301),DET(1)))
N2 = ITOT-1
DO I 1 = I, N2
JE = ITOT-I
JL = MS(JE)
JU = MS(JE+1)-1
JZ = JE
DO I J = JL, JU
JZ = JZ+1
1  SIGF1 = S(JE)+R(J)*S(JZ),
RETURN
END

*****SUBROUTINE TRI*****
*****COMMONS*****
COMMON ALR,ALZ,IIC,IEC,JIP,JEP,EC,H,DELP,LRC,LRL,GLP0,LCYC,PR,
1 PHP,MW,NW,AK,ITOT1,ITOT,ITOT,NO,KD,KLOW,KHIGH,KHR,KDR,I,J,IA,
2 JA,NL,CON,ERR,CF,PRF1,PRF2,PRF3,PRF4,LOCAT,LADD,LCL,SIGN
3 .C1,CE,C1,C2,C3,C4,ICR,JCR,LPRCSS,LCR,P,JTOT,JTOT1,ECRIT,
4 EXCF,SIGICR,TPLATE,TCYLD,[(CM1,ICP1),L1,JDRUM
COMMON A(150),B(53000),U(53,81),W(53,81),NR(1800),NC(1800),C(44),
1 S(1800),MS(1800),R(53),SUMR(53),DFRR(53),AR(20),ALP(20),
2 FLP(20),PPZ(20),UC(4),WC(4),SRPO(10),ERPO(10),SZPO(10),
3 EZPO(10),STPO(10),E2PO(10),TAN1PO(10),TAN2PO(10)
DIMENSION LC(53,81),SIGR(53,81),SIGZ(53,81),SIGT(53,81),SIGRZ(53,
1     B11,DER(53,81),DEZ(53,81),DERZ(53,81),DEPS1(53,81),
2     ERPR(53,81),EZPR(53,81),ETPR(53,81),ERZPR(53,81),
3     EPS1(53,81),SIG(53,81),EPS(53,81),DET(53,81)
EQUIVALENCE (U(1,1),LC(1,1),(B(1),EPS1(1)),
1     (B(1,4301),ERPR(1)),(B(1,8601),EZPR(1)),
2     (B(12901),ETPR(1)),(B(17201),ERZPR(1)),
3     (B(21501),SIGR(1),DER(1)),(B(25801),SIGRZ(1),DEWR(1)),
4     (B(30101),SIGZ(1),DEZ(1)),(B(34401),SIGT(1),DEPS1(1)),
5     (B(38701),SIG(1)),(B(43001),EPS(1)),(B(47301),DET(1)))
0  MS(1) = 1
LIMIT = 53000
DO 1 IS=1,ITOT
KD = IS
READ(1) I,J,KLOW,KHIGH+A,CON
NO = NR(IS)
KL = KLOW
KH = KHIGH+1-KLOW
KU = IS-1
IF (KU) 4,4,3
3  K1 = 0
IF (KU=KL) 4,2,2
2  DO 5 K = KL, KU
K1 = K1+1
LL = MS(K)
LU = MS((IS))-1
L1 = K1
DO 6 L = LL, LU
L1 = L1+1
A(L1) = A(L1)+B(L)*A(K1)
IF (L1-KH) 6,6,14
14 IF (A(L1)) 15,6,15
15 KH = L1
6  CONTINUE
5  CON = CON+A(K1)*S(K)
4  K1 = IS+-KLOW
KL = K1+
L = MS((IS))-1
DO 7 K = KL, KH
IF (A(K1)) 10,11,10
11 ERR = IS
RETURN
10 CONTINUE
L = L+1
7  B(L) = -A(K)/A(K1)
MS((IS+1)) = L+1
S((IS)) = -CON/A(K1)
IF (L+-LIMIT) 1,13,13
13 ERR = -IS
RETURN
1  CONTINUE

```

```

ERR = 0
501 RETURN
END
***** SUBROUTINE SIGEPS *****
COMMON ALR,ALZ,I1C,IEC,JIP,JEP,EC,H,DELP,LHC,LH,LGP,LPU,LCYC,PR,
1 PHP,MW,NW,AK,|TOT|,TOT,NO,KD,KLOW,KHIGH,KHR,EDU|I|,JU|A|,
2 JA,NL,CON,ENR,CF,PRF1,PRF2,PRF3,PRF4,LUCAT,LALZ,LCL,IGN
3 ,CI,CE,C1,C2,C3,C4,ICR,JCR,LPHCCS,LCH,LH,J/1/1,JU|T|,ECH1,
4 EXCF,B1G1CK,TPLATE,TCYLP,|CM|,|ICH|,L1,JUH
COMMON A(150),B(5300),U(5300),W(5300),N(1500),NC(1500),C(44),
1 S(150),M(1800),U(5300),W(5300),N(1500),NC(1500),C(44),
2 FLP(20),FPZP(20),UC(4),WC(4),SHD0(10),ERH0(10),ZPZP(10),
3 EZPO(10),STPO(10),SRZPO(10),EZPZP(10),ZPZP(10),
4 EIP0(10),S2PO(10),E2PO(10),TAN,PO(10),TANZP(10)
DIMENSION LC(53*61),SIGR(53*61),SIGZ(53*61),SIGT(53*61),SIGRZ(53*61),
1 B11,DER(53,81),DEZ(53,81),DERZ(53,81),DEPS(53,81),DEPS1(53,81),
2 ERPA(53,81),EZPR(53,81),TRP(53,81),ERZPH(LJ,M1),
3 EPS1(53,81),SIG(53,81),EPS(53,81),DET(53,81)
EQUIVALENCE (U(1),LC(1)), (E(1),EPS(1)),
1 (B(4301),ERPR(1)), (B(4601),EZPR(1)),
2 (B(12901),EZPR(1)), (B(17201),ERZPH(1)),
3 (B(21501),SIGR(1)), DEP(1), (B(25801),SIGRZ(1)), DERZ(1),
4 (B(30101),SIGZ(1)), DEZ(1), (B(34401),SIGT(1)), DET(1),
5 (B(36701),SIG(1)), (A(43001),EPS(1)), ((47301),DEL,F(1))
DEFINE FILE 2(1400+10*VIREC)
IF ((I-1)*(I-1C)*(J-1)*(J-1P) < (J-JP)*(J-JJ-P)) 11,12,13
11 ER = (U(I-1,J)-U(I-1,J))/ALR
EZ = (W(I-1,J+1)-W(I-1,J))/ALZ
ET = (U(I-1,J)+U(I-1,J))/2.*R(1))
ERZ = (U(I-1,J+1)-U(I-1,J))/ALZ+(W(I-1,J)-W(I-1,J))/ALZ
GO TO 300
12 IF (I-1C) 13,14,15
13 IF (I-1) 16,17,16
14 ER = (U(I-1,J)-U(I-1,J))/ALR
ET = (U(I-1,J)+U(I-1,J))/2.*R(1))
EZ = 0.
15 IF (C(42)) 18,19,18
18 A2 = C(22)/C(42)
A1 = C(24)-A2*C(44)
GO TO 20
19 A1 = C(24)
A2 = 0.
20 IF (A1) 21,22,21
21 ERZ = -(C(21)-A2*C(41))*ER+(C(23)-A2*C(43))*LT)/41
IF (J-JP) 23,24,23
23 IF (I-1C) 25,26,26
26 ERZ = ERZ+PZP(11)/A1
GO TO 25
24 ERZ = ERZ+DELP/A1
GO TO 25
17 ER = 2.*U(2,J)/ALR
ET = ER
EZ = 0.
ERZ = 0.
IF ((J-JJ-P)*(J-JEP)) 10,25,25

```

(a)

E13

(c)

```

49 I1 = I-1;C+2
  GO TO 16
47 IF (J-JEP) 50,51,51
50 IF (J=1) 52,52,53
52 FZ = 2.*W(I,2)/ALZ
  GO TO 54
53 EZ = (W(I,J+1)-W(I,J-1))/ALZ
54 IF (C(44)) 55,56,55
55 A1 = -C(14)*C(42)/C(44)
  A4 = -C(14)*(C(41)/ALR-C(43))/(2.*R(I))/C(44)
  A5 = -C(14)*(C(41)/ALR+C(43))/(2.*R(I))/C(44)
  GO TO 57
56 A1 = 0.
  A4 = 0.
  A5 = 0.
57 A5 = A5+C(11)/ALR+C(13)/(2.*R(I))
  IF (A5) 58,59,58
59 ER = 0.
  ET = 0.
  ERZ = 0.
  GO TO 300
58 A4 = A4+C(11)/ALR-C(13)/(2.*R(I))
  A1 = A1+C(12)
  IF (J-1) 60,60,61
60 PHPF = PHP+AK*U(I,J+1)/R()
  ERZ = 0.
  GO TO 62
61 PHPF = PHP+AK*(U(I,J+1)+U(I,J-1))/(2.*R(I))
  ERZ = ((C(11)/ALR-C(43))/(2.*R(I)))*(C(11)/ALR+C(13)/(2.*R(I)))+
  1  *(C(11)/ALR-C(13)/(2.*R(I)))*(C(11)/ALR+C(43)/(2.*R(I)))*
  2  U(I-1,J)*(C(12)*(C(41)/ALR+C(43)/(2.*R(I))-C(42)*(C(11)/ALR+
  3  C(13)/(2.*R(I)))*EZ+(C(41)/ALR+C(43)/(2.*R(I)))*PHPF)/A5
62 UFICT = (A4*U(I-1,J)-A1*EZ-PHPF)/A5
  ER = (UFICT-U(I-1,J))/ALR
  ET = (UFICT+U(I-1,J))/(2.*R(I))
  GO TO 300
61 I1 = I-1;C+2
  IF (C(42)) 63,64,63
63 A11 = C(24)-C(22)*C(44)/C(42)
  A12 = 1./C(24)*C(42)-C(22)*C(44)
  GO TO 65
64 A11 = C(24)
  A12 = 0.
  ERZ = 0.
  IF (A11) 66,67,66
66 ERZ = -RPZ(I1)/A11
67 A9 = C(42)*C(21)/ALR+C(23)/(2.*R(I))-C(22)*(C(41)/ALR+C(43)/
  1  (2.*R(I)))
  A5 = C(42)*(C(21)/ALR-C(23)/(2.*R(I))-C(22)*(C(41)/ALR-C(43)/
  1  (2.*R(I)))
  IF (C(44)) 68,69,68
68 A1 = C(22)*C(24)*C(42)/C(44)
  A10 = -(C(14)*C(22)-C(12)*C(24))/(C(24)*C(42)-C(22)*C(44))
  A6 = -A4*A10
  A7 = -A5*A10
  A8 = -C(24)*(C(41)/ALR+C(43)/(2.*R(I))/C(44)
  A9 = -C(24)*(C(41)/ALR-C(43)/(2.*R(I))/C(44)

```

(b)

```

A10 = C(42)*A10
  GO TO 70
69 A1 = C(22)
  A12 = C(24)*C(42)
  A6 = 0.
  A7 = 0.
  A8 = 0.
  A9 = 0.
  A10 = 0.
70 A9 = A9+C(21)/ALR-C(23)/(2.*R(I))
  EZ = -(PZP(I1)-A9*U(I-1,J))/A1
  A6 = A6+C(22)*(C(11)/ALR+C(13)/(2.*R(I))-C(12)*(C(21)/ALR+
  1  C(23)/(2.*R(I)))
  IF (A6) 71,72,71
72 ER = 0.
  ET = 0.
  GO TO 73
71 A7 = A7+C(22)*(C(11)/ALR-C(13)/(2.*R(I))-C(12)*(C(21)/ALR-
  1  C(23)/(2.*R(I)))
  AB = AB+C(21)/ALR+C(23)/(2.*R(I))
  UFICT = (A7*U(I-1,J)-C(22)*(PHP+AK*(U(I-1,J)+U(I,J-1))/(2.*R(I))+
  1  PZP(I1)*(C(12)+A10))/A6
  ER = (UFICT-U(I-1,J))/ALR
  ET = (UFICT+U(I-1,J))/(2.*R(I))
  EZ = EZ-PZP(I1)*(C(12)+A10)/(A1*A6)
  ERZ = ERZ-A12*(A7*AB+U(I-1,J)+C(22)*(PHP+AK*(U(I-1,J)+U(I,J-1))-
  1  (2.*R(I)))+A6+PZP(I1)*(C(12)+A10))/A6
73 ERZ = ERZ+A12*A58*(I-1,J)
300 DSIGR = C(12)*EZ+C(13)*ET+C(14)*ERZ
  DSIGZ = C(21)*ER-C(22)*EZ+C(23)*ET+C(24)*ERZ
  DSIGT = C(31)*ER-C(32)*EZ+C(33)*ET+C(34)*ERZ
  DSIGRZ = C(41)*ER-C(42)*EZ+C(43)*ET+C(44)*ERZ
  SIGRT = SIG(I,J)+DSIGR
  SIGZT = SIG(I,J)+DSIGZ
  SIGTT = SIG(I,J)+DSIGT
  SIGRZT = SIGR(I,J)+DSIGRZ
  EPSR = ERPR(I,J)*ER
  EPSZ = EZPR(I,J)*EZ
  EPST = ETPR(I,J)*ET
  EPSRZ=ERZPR(I,J)*ERZ
  E1 = 0.5*(ER+EZ+SQRT((ER-EZ)**2+ERZ**2))
  EPS(I,J) = 0.5*(EPSR+EPSZ+SQRT((EPSR-EPSZ)**2+EPSRZ**2))
  EPS2 = 0.5*(EPSR+EPSZ-SQRT((EPSR-EPSZ)**2+EPSRZ**2))
  IF (LC(I,J-1)) 97,520,520
520 IF (I-1;C) 521,521,96
521 IF (J-JP1=1) 523,523,96
523 IF (LC(I,J-2)) 524,524,524
524 IF (ABS(TAN(W(I,J)))>1.2) 96,97,97
96 SIGRT = C(11)*EPSR+C(12)*EPSZ+C(13)*EPST+C(14)*EPSRZ
  SIGZT = C(21)*EPSR+C(22)*EPSZ+C(23)*EPST+C(24)*EPSRZ
  SIGTT = C(31)*EPSR+C(32)*EPSZ+C(33)*EPST+C(34)*EPSRZ
  SIGRZT = C(41)*EPSR+C(42)*EPSZ+C(43)*EPST+C(44)*EPSRZ
  IF (LC(I,J-2)) 200,97,200
200 CONTINUE
  SIG1 = SIGRT*COS(W(I,J))**2+SIGZT*SIN(W(I,J))**2+
  1  SIGRZT*SIN(2.*W(I,J))

```

(d)

```

ETPO(L1) = EPST
SRZPO(L1) = SIGRZT
ERZPO(L1) = EPSRZ
S1PO(L1) = SIG1
E1PO(L1) = EPS1(L1,J)
S2PO(L1) = SIG2
E2PO(L1) = EPS2
TAN1PO(L1) = TAN1
TAN2PO(L1) = TAN2
RETURN
END
***** SUBROUTINE OUTPUT *****
***** COMMONS *****
COMMON ALR,ALZ,I1C,IEC,JEP,EC,H1DEL,P,LRC,LRL,G,LPO,LCYC,PR,
  PHP,MW,NW,AK,ITOT1,TOT,NO,KD,KLOW,KHIGH,KHR,KDR,I,JIA,
  JA,NL,CON,ERR,CF,PRF1,PRF2,PRF3,PRF4,LUCAT,P,JTOT,JTOT1,ECRIT,
  EXCF,SIGICR,THTLATE,TCYLDR,ICM1,I(CP1),L,JDHUM
COMMON A(150),B(5300),U(53,81),W(53,81),NR(1800),NC(1800),C(44),
  S(1800),MS(1800),K(S3),SUMR(S3),DIFFR(S3),AH(20),ALP(20),
  2  FLPO(20),PZP(20),UC(41),WC(41),SRPO(10),ERPO(10),SZPO(10),
  3  EZPO(10),STPO(10),ETPO(10),SRZPO(10),ENZPO(10),S1PO(10),
  4  E1PO(10),ZPPO(10),E2PO(10),TAN1PO(10),TAN2PO(10)
DIMENSION LC(53,81),SIGR(53,81),SIGZ(53,81),SIGT(53,81),SIGRZ(53,
  1  81),DER(53,81),DEZ(53,81),DERZ(53,81),DEPS1(53,81),
  2  ERPR(53,81),EZPR(53,81),ETPR(53,81),ENZPR(53,81),
  3  EPS(53,81),SIG(53,81),EPS(53,81),DET(53,81)
EQUIVALENCE U(I,J),LC(I,J),(B(I,J),EPS1(I,J)),
  1  (B(I,4301),ERPR(I,J)),(B(I,8601),EZPR(I,J)),
  2  (B(I,29001),ETPR(I,J)),(B(I,17201),ENZPR(I,J)),
  3  (B(I,21501),SIGR(I,J),DER(I,J)),(B(I,25801),SIGZ(I,J),DEZ(I,J)),
  4  (B(I,30101),SIGZ(I,J),DEZ(I,J)),(B(I,34401),SIGT(I,J),DEPS(I,J)),
  5  (B(I,38701),SIG(I,J)),(B(I,43001),EPS(I,J)),(B(I,47301),DET(I,J))
DEFINE FILE 2(14001,0,U,REC)
DO 331 KD=1,B
  GO TO 1(2,3,4,5,6,7,B),KD
1 DO 11 I=1,IEC
  DO 11 J=1,JER
  SIG(I,J) = U(I,J)
  11 EPS(I,J) = W(I,J)
  LCL = LCL+1
  LRC = LRC+1
  DO 12 K=1,JDHUM
    READ (2(100+K)) ERPO
    DO 12 L=1,10
      NO = 2*(K-1)*10+L
      CALL COORD
      SIG(I,J) = SRPO(L)
      EPS(I,J) = ERPO(L)
      IF (NO>2*JTOT) 12,12,9
12 CONTINUE
  3 DO 13 K=1,JDHUM

```

(a)

```

READ (21200+K) S2PO
READ (21300+K) E2PO
DO 13 L=1,10
NO = 2*(K-1)*10+L
CALL COORD
SIG(I,J) = S2PO(L)
EPS(I,J) = E2PO(L)
IF (NO-2*JTOT) 13,13,9
13 CONTINUE
4 DO 14 K=1,JDRUM
  READ (21400+K) S1PO
  READ (21500+K) E1PO
  DO 14 L=1,10
  NO = 2*(K-1)*10+L
  CALL COORD
  SIG(I,J) = S1PO(L)
  EPS(I,J) = E1PO(L)
  IF (NO-2*JTOT) 14,14,9
14 CONTINUE
5 DO 15 K=1,JDRUM
  READ (21600+K) SRZPO
  READ (21700+K) ERZPO
  DO 15 L=1,10
  NO = 2*(K-1)*10+L
  CALL COORD
  SIG(I,J) = SRZPO(L)
  EPS(I,J) = ERZPO(L)
  IF (NO-2*JTOT) 15,15,9
15 CONTINUE
6 DO 16 K=1,JDRUM
  READ (21800+K) S1PO
  READ (21900+K) E1PO
  DO 16 L=1,10
  NO = 2*(K-1)*10+L
  CALL COORD
  SIG(I,J) = S1PO(L)
  EPS(I,J) = E1PO(L)
  IF (NO-2*JTOT) 16,16,9
16 CONTINUE
7 DO 17 K=1,JDRUM
  READ (211000+K) S2PO
  READ (211100+K) E2PO
  DO 17 L=1,10
  NO = 2*(K-1)*10+L
  CALL COORD
  SIG(I,J) = S2PO(L)
  EPS(I,J) = E2PO(L)
  IF (NO-2*JTOT) 17,17,9
17 CONTINUE
8 DO 18 K=1,JDRUM
  READ (21200+K) TAN1PO
  READ (212100+K) TAN2PO
  DO 18 L=1,10
  NO = 2*(K-1)*10+L
  CALL COORD
  SIG(I,J) = TAN1PO(L)
  EPS(I,J) = TAN2PO(L)

```

(b)

```

18 CONTINUE
9 CALL TITLES
10 WRITE (6+100) (I,I=1,17)
100 FORMAT (9X,17(17//))
DO 131 J=1,MW
J1 = JEP-J+1
IF (J+LCL-2*((J+LCL)/2)) 132,133,132
133 WRITE (6+101) J1,(SIG(I,J1),I=1,17,2)
101 FORMAT (1H0,1X,12,3X,9E14.5)
WRITE (6+102) (EPS(I,J1),I=1,17,2)
102 FORMAT (7X,9E14.5)
GO TO 131
132 WRITE (6+103) J1,(SIG(I,J1),I=2,17,2)
103 FORMAT (1H0,1X,12,3X,9E14.5)
WRITE (6+104) (EPS(I,J1),I=2,17,2)
104 FORMAT (14X,9E14.5)
131 CONTINUE
11 IF ((IC-18) 129,129,128
128 IF ((IC-34) 127,127,126
127 II = 17
III = IICM1
GO TO 130
126 II = 17
III = 33
130 CALL TITLES
WRITE (6+100) (I,I=II,III)
IIPI = II-1
DO 231 J=1,MW
J1 = JEP-1+1
IF (J+LCL-2*((J+LCL)/2)) 232,233,232
233 WRITE (6+101) J1,(SIG(I,J1),I=IIPI,III,2)
WRITE (6+102) (EPS(I,J1),I=IIPI,III,2)
GO TO 231
232 WRITE (6+103) J1,(SIG(I,J1),I=IIPI,III,2)
WRITE (6+104) (EPS(I,J1),I=IIPI,III,2)
231 CONTINUE
125 II = 33
III = IICM1
GO TO 130
129 CALL TITLES
WRITE (6+100) (I,I=II,IEC)
DO 331 J=1,IEC
J1 = JEP-J+1
IF (J+LRC+MW-2*((J+LRC+MW)/2)) 332,333,332
332 WRITE (6+101) J1,(SIG(I,J1),I=II,IEC,2)
WRITE (6+102) (EPS(I,J1),I=II,IEC,2)
GO TO 331
333 WRITE (6+103) J1,(SIG(I,J1),I=II,IEC,2)
WRITE (6+104) (EPS(I,J1),I=II,IEC,2)
331 CONTINUE
RETURN
END
*****SUBROUTINE TITLES*****
*****
```

(c)

```

COMMON ALR,ALZ,IIC,IEC,JIP,JEP,EC,H,DELPL,RHC,LRL,LRG,LPO,LCCY,PR,
1 PHR,MW,NW,AK,ITOT1,ITOT,NO,KD,KLOW,KHIGH,CHR,CDR,I,J,I+
2 JAI,NL,CON,ERR,CF,PRF1,PRF2,PRF3,PRF4,LOCAT,LAU,LCL,SIGN
3 +C1,CE,C1,C2,C3,C4,ICR,JCR,LPRCSS,LCH,P,ITOT1,ITOT1,ECRITN
4 EXCF,SIGICR,TPLATE,TCYLDR,ICM1,ICP1,L1,JDRUM
COMMON A(150),B(53000),U(53,81),W(53,81),NR(1800),NC(1800),C(44),
1 S(1800),MS(1800),R(53),SUMR(53),DIFFR(53),NR(220),ALP(20),
2 FLP(20),PZP(20),UC(4),MC(4),SRPO(10),ERZPO(10),SIP(10),
3 EZPO(10),STPO(10),ETPO(10),SRZPO(10),ERZPO(10),SIP(10),
4 ETPO(10),STPO(10),ETPO(10),TAN2PO(10),TANPO(10)
DIMENSION LC(53,81),SIG(53,81),SIG2(53,81),SIGT(53,81),SIGZ(53,
1 81),DER(53,81),DEZ(53,81),DCR(53,81),DCR2(53,81),
2 ERPR(53,81),EZPR(53,81),ETPR(53,81),ERZPR(53,81),
3 EPS(53,81),SIG(53,81),EPS(53,81),DET(53,81)
EQUIVALENCE (U(1),LC(1)),(B(1),EPS(1)),
1 (B(1,4301),ERPR(1)),(B(1,8601),EZPR(1)),
2 (B(1,12901),ETPR(1)),(B(1,17201),ERZPR(1)),
3 (B(21501),SIGR(1)),(DER(1)),(B(25801),SIGZ(1),DER(1)),
4 (B(30101),SIGZ(1)),(DEZ(1)),(B(34001),SIGT(1),DEZ(1)),
5 (B(38701),SIG(1)),(B(43001),EPS(1)),(B(47301),DET(1))
WRITE (6,100) TPLATE,TCYLDR
100 FORMAT (1STRUCTURE/11X,F4.1,1N,SLAB,1,F8.1,1N,SKIRT,VESSE
1L/1LOADING/11X,1PRESTRESSING AND INTERNAL PRESSURE 1,F8.1,1P
21,1///)
GO TO (1,2,3,4,5,6,7,8),KD
1 WRITE (6,101) LR
101 FORMAT (1 LR =1,4,45X,1TOTAL DISPLACEMENTS 1N/1///)
RETURN
2 WRITE (6,102)
102 FORMAT (44X,1DIRECT STRESSES/STRAINS IN R-DIRECTION)///
RETURN
3 WRITE (6,103)
103 FORMAT (44X,1DIRECT STRESSES/STRAINS IN Z-DIRECTION)///
RETURN
4 WRITE (6,104)
104 FORMAT (44X,1DIRECT STRESSES/STRAINS IN T-DIRECTION)///
RETURN
5 WRITE (6,105)
105 FORMAT (46X,1SHEAR STRESSES/STRAINS IN RZ-PLANE)///
RETURN
6 WRITE (6,106)
106 FORMAT (45X,1MAXIMUM PRINCIPAL STRESSES/STRAINS -RZ-PLANE-)///
RETURN
7 WRITE (6,107)
107 FORMAT (45X,1MINIMUM PRINCIPAL STRESSES/STRAINS -RZ-PLANE-)///
RETURN
8 WRITE (6,108)
108 FORMAT (23X,1DIRECTION OF PRINCIPAL STRESSES MAXIMUM/MINIMUM GI
1VEN THROUGH TANGENT FNCT OF ANGLE W/R TO R-DIRECTION)///
RETURN
END

```